SECURITY CLASSIFICATION O 5 PAGE *(When Data Entered)*

REPORT DOCUMENTATION PAGE

READ INSTRUCTIONS BEFORE COMPLETING FORM

1. REPORT NUMBER: FINAL	2. GOVT ACCESSION NO.
3. RECIPIENT'S CATALOG NUMBER	
4. TITLE *(and Subtitle)*: The Analysis of Crack Growth Initiation, Propagation, and Arrest in Flawed Ship Structures Subjected to Dynamic Loading	5. TYPE OF REPORT & PERIOD COVERED: Final 1/77 to 9/83
	6. PERFORMING ORG. REPORT NUMBER
7. AUTHOR(s): C. R. Barnes, M. F. Kanninen, and J. Ahmad	8. CONTRACT OR GRANT NUMBER(s): N00014-77
9. PERFORMING ORGANIZATION NAME AND ADDRESS: Battelle Columbus Laboratories, 505 King Avenue, Columbuys, Ohio 43201	10. PROGRAM ELEMENT, PROJECT, TASK AREA & WORK UNIT NUMBERS
11. CONTROLLING OFFICE NAME AND ADDRESS	12. REPORT DATE: August 10, 1984
	13. NUMBER OF PAGES: 432
14. MONITORING AGENCY NAME & ADDRESS *(if different from Controlling Office)*	15. SECURITY CLASS. *(of this report)*: unclassified
	15a. DECLASSIFICATION/DOWNGRADING SCHEDULE

16. DISTRIBUTION STATEMENT *(of this Report)*

Approved for public release; distribution unlimited.

17. DISTRIBUTION STATEMENT *(of the abstract entered in Block 20, if different from Report)*

18. SUPPLEMENTARY NOTES

Final Report

19. KEY WORDS *(Continue on reverse side if necessary and identify by block number)*

Blast-induced fracture
Ship steels
Fracture toughness
Crack tip opening angle
Elastodynamic analyses
Elasto-plastic

20. ABSTRACT *(Continue on reverse side if necessary and identify by block number)*

This work represents a systematic experimental and analytical approach to extend state-of-the-art fracture mechanics treatment of crack initiation, propagation, and arrest in tough ductile materials such as ship steels. A dynamic nonlinear finite element analysis was devised to attack the problem on a step-by-step basis. The program began by work on a high strength 4340 steel under mechanical impact conditions. Then, as a degree of understanding was achieved, more realistic conditions were treated.

DD FORM 1 JAN 73 1473

SECURITY CLASSIFICATION OF THIS PAGE *(When Data Entered)*

In the most recent year of work, experiments were performed on a precracked HY-80 steel weldment under explosive loading conditions. A key finding of the following analysis work was that the crack tip opening angle (CTOA) remained constant during rapid crack propagation. This had not been previously demonstrated.

Battelle
Columbus Laboratories

Report

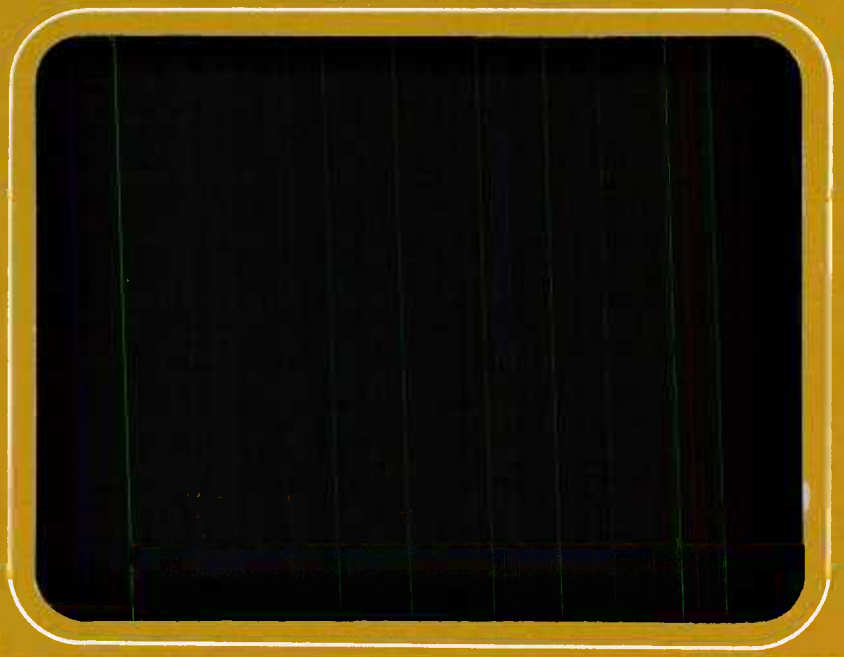

FINAL REPORT

on

THE ANALYSIS OF CRACK GROWTH INITIATION, PROPAGATION, AND ARREST IN FLAWED SHIP STRUCTURES SUBJECTED TO DYNAMIC LOADING.

to

MECHANICS DIVISION
OFFICE OF NAVAL RESEARCH
Arlington, Virginia 22217

August 10, 1984

by

C. R. Barnes, M. F. Kanninen,
and J. Ahmad

Contract No. N00014-77-C-0576

BATTELLE
Columbus Laboratories
505 King Avenue
Columbus, Ohio 43201

SUMMARY

At the beginning of this research program, it was recognized that the study of blast-induced fracture in ship steels and their weldments required the extension of the then available fracture mechanics capabilities in several areas. These included the necessity to (1) admit rapidly applied loading, (2) treat nonsimple flaw-structure geometry, (3) model extensive crack tip plasticity, (4) make reliable crack growth measurements in ductile materials under impact and explosive blast loading conditions, (5) compute weld-induced residual stresses in ship grade steels, and (6) model crack growth in welded joints. The approach adopted was to examine these complications systematically, beginning with the first. In this way, the past 5 years on this contract has produced capabilities to address all of these areas.

The knowledge gained through the research conducted on this contract has resulted in an improved fundamental understanding of dynamic crack growth/arrest phenomena for ship structures. Notable are a number of key conclusions: (1) the neglect of plasticity induced effects remote from the crack tip can produce significant errors in the fracture toughnesses deduced for quasi-static and impact conditions, (2) the critical crack tip opening angle (CTOA) is the most appropriate criterion for predicting dynamic propagation and arrest under elastic-plastic conditions, and (3) weld-induced residual stresses have a significant effect on the behavior of rapidly running cracks. Taken together, this work has, therefore, provided the basis for the assessment of ship structures under blast loading via a crack arrest point of view.

TABLE OF CONTENTS

LIST OF TABLES

LIST OF FIGURES

LIST OF FIGURES
(Continued)

THE ANALYSIS OF CRACK GROWTH INITIATION, PROPAGATION, AND ARREST IN FLAWED SHIP STRUCTURES SUBJECTED TO DYNAMIC LOADING

by

C. R. Barnes, M. F. Kanninen, and J. Ahmad

1.0 INTRODUCTION

The objective of this work has been to develop and validate a nonlinear dynamic analysis methodology that could be applied to determine critical crack sizes in ship hull structures subjected to blast loadings. The point of view taken was that a crack-like flaw could exist in a local low toughness region of a ship material. This flaw would likely initiate under blast loading (e.g., from a depth charge or a remote nuclear explosion). But, catastrophic fracture would not occur if crack arrest intervenes before the rapidly running crack penetrates the wall. The key research issue was then to quantify the conditions under which a run/arrest event could occur in a tough, ductile material subjected to a rapidly varying applied loading.

There were several issues that originally placed the analysis problem beyond the state of the art of fracture mechanics. First, a criterion for rapid crack propagation in elastic-plastic conditions had not been established. Second, crack propagation behavior under rapidly applied loading was not well understood. Third, the effect of weld-induced residual stress and deformation fields on crack propagation was completely unknown. Added to these complexities is the difficulty of obtaining meaningful experimental results on crack propagation and arrest in blast-loaded welded components; particularly of the precise character that is required for a quantitative understanding of the problem.

In view of the many complexities that existed in this problem, a step-by-step procedure was adopted. An integrated program of experimentation coupled with nonlinear dynamic finite element analysis was devised to treat each major uncertainty on an individual basis. More specifically, the research program began by work on a high strength material (AISI 4340 steel)

and mechanical impact conditions. Then, as a degree of understanding was achieved, more realistic conditions were treated. In the most recent year of work, experiments were performed on a precracked HY-80 steel weldment under explosive loading conditions. The accompanying analyses (1) determined the residual stress and deformation state by directly simulating the welding process and (2) calculated the initiation, propagation history, and arrest point of the crack under the pressure history measured in the experiment.

A key finding in this research was the confirmation that rapid crack propagation can be characterized by a constant value of the crack tip opening angle (CTOA) parameter. This criterion is often assumed, but not previously demonstrated. As an expedient, by assuming that, (1) the weldment property is the same as that of the base material, (2) this value is independent of the crack speed, and (3) it is unaffected by large scale plasticity, an estimate of the CTOA was obtained for trial calculations. Using this value, an elastic-plastic dynamic analysis was performed to compare with the experimental run/arrest event. These results were encouraging as they have established the basis for a methodology which can be used to predict the rapid propagation and arrest behavior of cracks in naval structures subjected to blast loads.

Because of the absence of established fracture toughness data for elastic-plastic crack propagation, it was necessary to use crude estimates of the CTOA. These were simply based on the LEFM fracture toughness data for HY-80 weldments available in the literature. Rough agreement was nevertheless obtained with the observed results. Of greater significance, it was found that the presence of weld-induced residual stress strongly affects the prediction of the crack length at arrest.

2.0 REVIEW OF PREVIOUS RESEARCH

2.1 Basis of the Technical Approach

In a flawed ship structure subjected to a blast load, it is important to know whether a flaw of the size likely to be present in the structure would become unstable and, if so, whether it would arrest before catastrophic fracture occurs. For structures made of high toughness materials where considerable crack tip plastic deformation precedes crack initiation, the analysis problem is nonlinear. In addition, because the loading rates can be very high, and also because cracks may propagate at relatively high rates, conventional quasi-static fracture mechanics treatments are generally not applicable. A dynamic elastic-plastic fracture mechanics approach is therefore needed.

A further complicating feature arises from the fact that a structural defect likely resides in or around a weld. In addition to producing defects, the welding process introduces substantial localized changes in material properties and further gives rise to thermally induced residual stresses. Reliable elastic-plastic dynamic fracture mechanics techniques for predicting crack initiation, growth, and arrest of cracks residing in and around welded regions do not currently exist. In order to develop such techniques, a stepwise procedure has been followed. The early work was primarily focused on identifying the appropriate criterion for rapid crack growth; see References (1-8)*. A brief review of the early research that has led to the current stage of development is described next. Then, the experimental and computational developments specifically addressed to the fracture of HY-80 steel weldments subjected to explosive loading conducted in the preceding year are presented in more detail.

2.2 Review of Earlier Research

At the beginning of this research program it was recognized that the study of fracture of ship structures under shock loading required the extension of then current fracture mechanics capabilities in several areas.

---

*References are listed on page 26.

These included the ability to (1) treat rapidly applied loading, (2) treat nonsimple flaw-structure geometry, (3) model extensive crack tip plasticity, (4) make reliable crack growth measurements in ductile materials under impact and explosive blast loading conditions, (5) compute weld-induced residual stresses in ship grade steels, and (6) model crack growth in welded joints. The approach adopted was to examine these complications systematically, beginning with the first. Hence, initial attention was placed upon a well-characterized, high-strength, low-toughness material (AISI 4340 steel) and a relatively simple test specimen (a dynamic tear test specimen) that was amenable to analysis.

The expectation in working with 4340 steel was that the dynamic fracture toughness property, $K_{ID} = K_{ID}(\dot{a})$, for a fast propagating crack initiated from quasi-static loading conditions should also characterize crack propagation due to impact loading. Instead, it was found that, while elastodynamic analyses did provide an excellent description of the impact experiments, the toughness values needed to achieve this agreement were substantially different from those given by the quasi-static initiation experiments[1].

The disparity between the fracture toughness values deduced for quasi-static and impact initiation conditions obviously has great practical importance. If it could be concluded that the elastodynamic fracture characterization is therefore not unique, it follows that the fracture properties deduced for small specimen testing may not provide reliable data for the assessment of ship or other full-scale structures. The potential significance of this finding required a reexamination of the experimental and analysis results that have led to it.

The ensuing effort warranted the development of an elastic-plastic dynamic finite element analysis capability. This resulted in the development of the finite element code FRACDYN, which has since been used to solve a variety of problems related to the Navy, NRC, and several industrial applications. Of more direct interest to this research was the fact that, by using this code, the disparity between the fracture toughness values deduced for quasi-static and impact initiation conditions was finally explained[4]. It was found that the disparity was largely due to the linear elastic

interpretation of the experiments reported in Reference (1). An elastic-plastic dynamic interpretation of the experiments virtually eliminated the disparity. As a by-product of this work, the inertia enhanced version of the J-integral was identified as a viable criterion for crack initiation under elastic-plastic dynamic conditions.

Concurrent with the above, this research effort has resulted in achievements in five other aspects of the problem:

(1) To set the stage for the eventual test of the methodology that is expected to evolve from this program, the known dynamic toughness parameters for the HY-80 grades of steel and their weld metals were collected and analyzed[3] and a crack propagation/arrest analysis for the design of an intermediate-level submerged hull experiment performed[4].

(2) A viscoelastic dynamic treatment of crack propagation/arrest events in photoelastic materials was developed to ascertain whether the neglect of the time-dependent nature of the material is proper in interpreting such results[5].

(3) Impact fracture testing was performed on HY-130 steel (using dynamic tear test specimens instrumented to determine crack length versus time) and a dynamic finite element code was developed to analyze the dynamic tear test results[6,7].

(4) Thermoplastic finite element simulations of weld-induced deformation were performed in order to study crack growth under conditions that would exist in a heat-affected zone around a weld[8].

(5) Detailed examination of the deformation state at the tip of a fast running crack in an elastic-plastic material was made for eventual use in finite element analyses of such events[9,10].

2.3 Recent Computational Research

Of particular importance for the objectives of this work is the progress made in two important areas: the performance of blast loading

experiments and in the analysis of crack growth in welded regions. In the first area, 4340 steel plates were fractured using an explosive detonated at a stand-off distance. Strain gages were fixed on the specimen to determine the time of crack initiation and of complete fracture. Pressure transducers in conjunction with a dummy specimen were used to give the pressure-time history at various points on the plate face for input to the analysis.

In the second area, the analysis of crack growth in the heat-affected zones around welds was made possible by the development of a thermo-plastic finite element analysis capability (under other sponsorship). This model can be used for the direct computation of the inelastic deformation and attendant residual stresses in any welded or weld-related thermal problem as long as the thermomechanical properties of the materials are available. Further, crack growth was introduced into the model to simulate both fatigue and unstable crack propagation. In both instances, a heuristic elastic-plastic crack growth relation was introduced based upon the crack tip opening angle as a measure of the crack driving force.

In the most recent year of work, experiments were performed on a precracked HY-80 steel weldment under explosive loading conditions. The accompanying analyses (1) determined the residual stress and deformation state by directly simulating the welding process and (2) calculated the initiation, propagation history, and arrest point of the crack under the pressure history measured in the experiment. A key finding in this research was the confirmation that rapid crack propagation can be characterized by a constant value of the crack tip opening angle (CTOA) parameter.

The identification of a characterizing parameter for large amounts of crack growth in elastic-plastic conditions is a problem that is currently being addressed by several different investigators. A particularly attractive choice is the CTOA parameter. A number of investigators have found that this parameter remains constant during elastic-plastic stable crack growth--see Reference (9). This fact, together with its ease of application, strongly suggests that the CTOA be explored for dynamic crack propagation also. However, previous to the recently completed work of Ahmad, et al[7], the constancy of the CTOA during rapid crack propagation has not been demonstrated. This key result is shown in Figure 1.

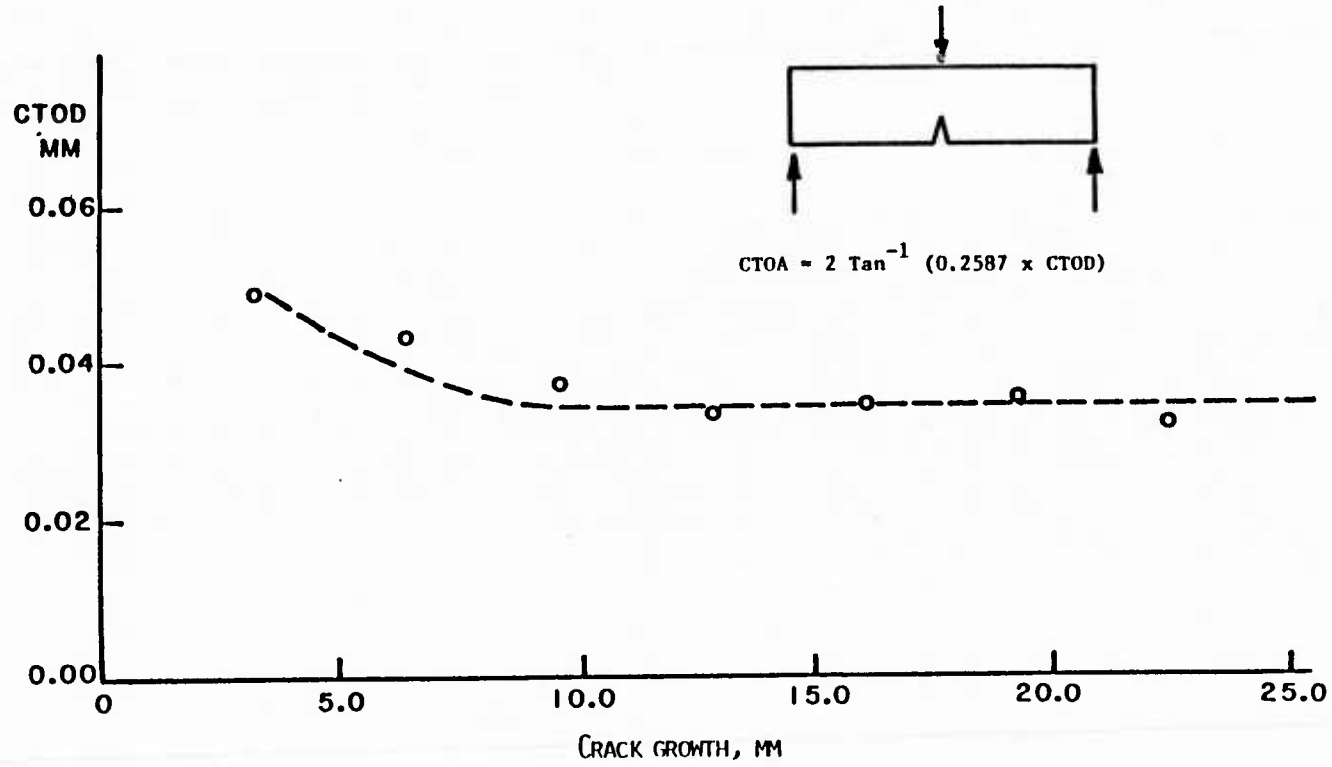

FIGURE 1. CRITICAL CRACK TIP OPENING DISPLACEMENT VALUES INFERRED FROM AN ELASTIC-PLASTIC DYNAMIC ANALYSIS OF DYNAMIC CRACK PROPAGATION IN A SIDE GROOVED AISI 4340 STEEL BEND SPECIMEN SUBJECTED TO A QUASI-STATIC LOAD

The result shown in Figure 1 was obtained by performing a "generation phase" finite element analysis of a fracture experiment. In the experiment, an AISI 4340 steel three-point-bend specimen was quasi-statically loaded to initiate rapid crack propagation. In the companion dynamic elastic-plastic finite element analysis, the crack was made to propagate according to the experimentally measured crack length history. The CTOA values were then obtained from the finite element solution. As shown in Figure 1, these values are based on the crack tip opening displacement (CTOD) values at one element length behind the crack tip, determined at the first instant of node release. It can be seen that, following an initial transient, the CTOA remains virtually constant throughout the rest of the crack growth process. This result reveals--possibly for the first time--that a near constant CTOA value can be used as a criterion for rapid crack propagation. However, possible crack velocity dependence of CTOA needs to be further investigated.

2.4 Recent Experimental Research

The crack initiation and propagation characteristics of engineering structural weldments invariably differ from those of the base material. This is due primarily to the effects of residual stresses induced by the welding process coupled with weld metal inhomogeneity. Although the degree of material inhomogeneity is difficult to quantify, the residual stresses can be determined. Consequently, as a first step, following the preparation of the welded HY-80 specimens, four were sacrificed to obtain weld residual stresses. These determinations were made using the trepanning technique.

The trepanning technique involves the removal of a prism-shaped element of material under a biaxial strain gage applied to the surface of a welded specimen. Upon removal, these gages no longer sense the stresses at that location. Hence, the resulting change in strain is taken to be indicative of the magnitude of the residual stresses that were present at the gage position. Figures 2 and 3 show the gage locations for two sets of residual stress determinations. Figure 4 shows a typical element taken from one of these specimens.

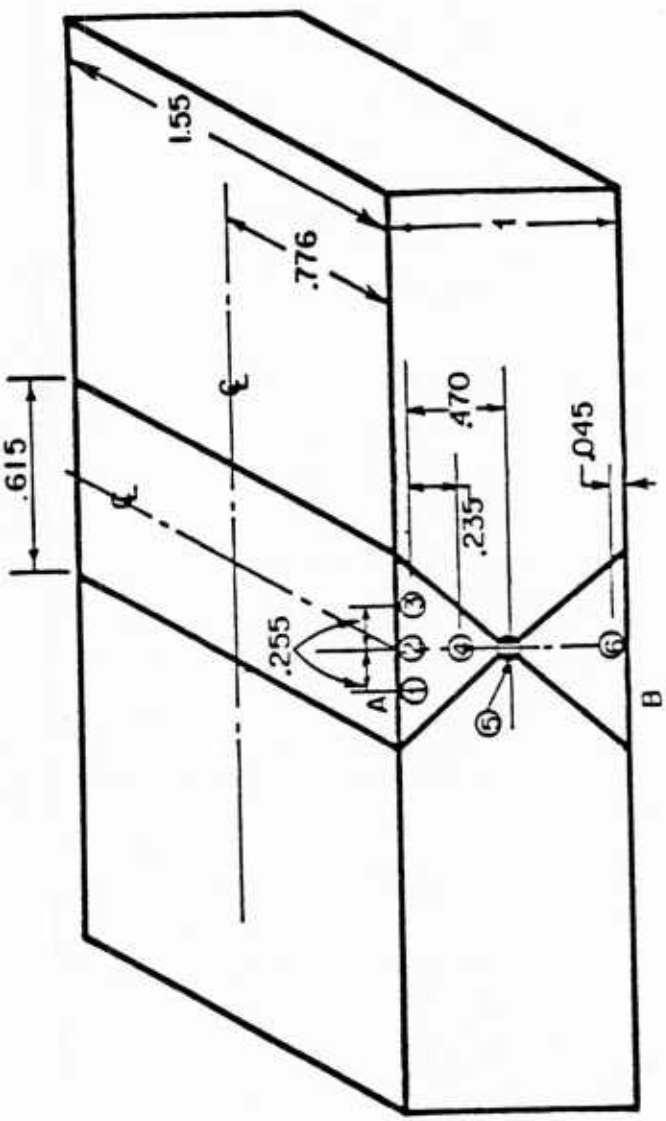

FIGURE 2. STRAIN GAGE LOCATIONS FOR FIRST SERIES OF RESIDUAL STRESS DETERMINATIONS

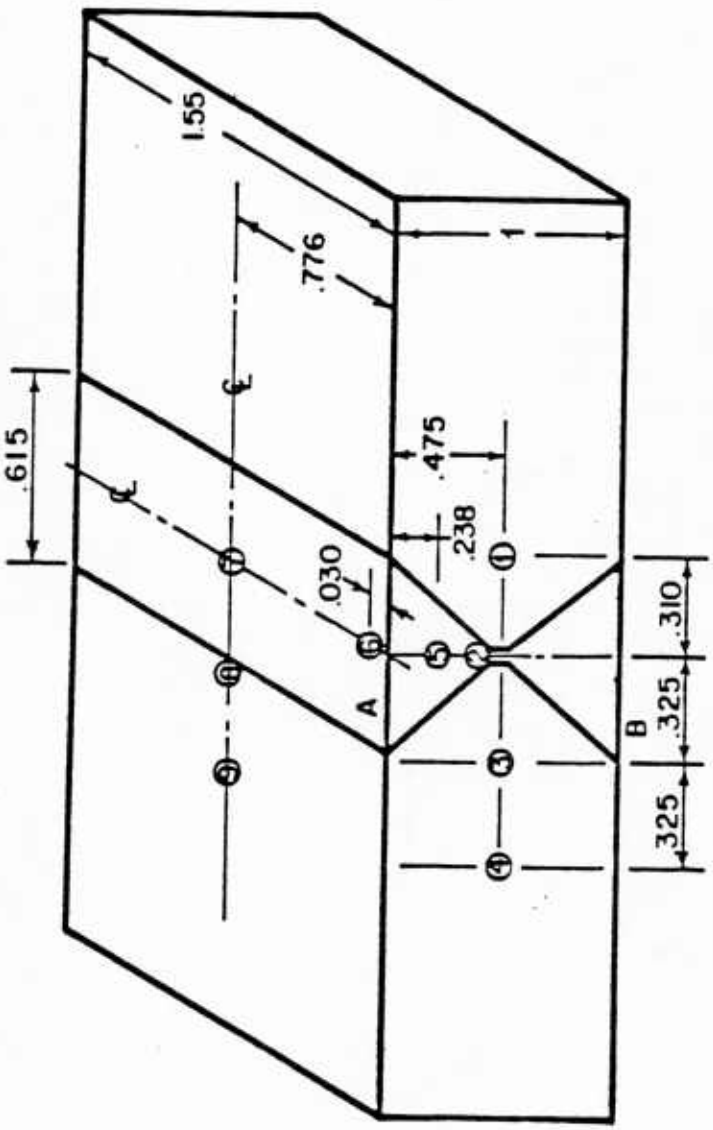

FIGURE 3. STRAIN GAGE LOCATIONS FOR SECOND SERIES OF RESIDUAL STRESS DETERMINATIONS

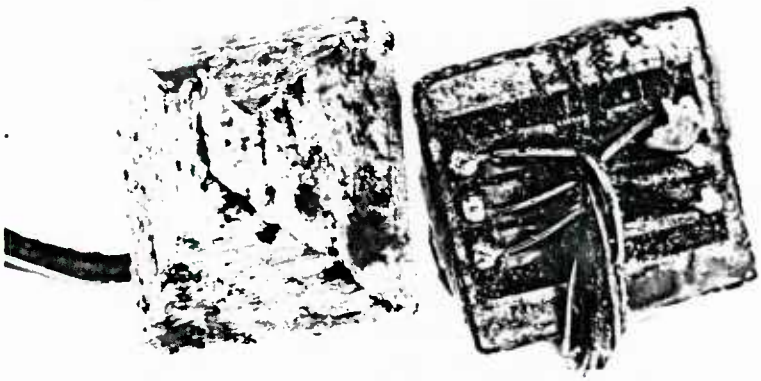

(A) (B)

FIGURE 4. TREPANNING ELEMENT

(A) Bottom surface of residual stress chip
(B) Top surface showing biaxial strain gage

The next step in the experimental effort was to precrack and instrument the remaining specimens, then subject them to blast loading. The precrack was sharpened by EDM to a total depth of 8 mm. The specimen thickness was 25.4 mm. The blast load was provided by a 2.27-kg charge of composition C-4 explosive. The explosive was detonated from a 38-cm standoff, as measured from the center of the the charge to the upper specimen surface. The test configuration is shown in Figure 5. An expanded view of the loading fixture is contained in Figure 6. Figure 7 shows the post-test appearance of a welded specimen.

Each test specimen was instrumented with strain gages to provide the times of crack initiation, propagation, and complete specimen fracture. A diagram of the specimen with these strain gage locations shown is contained in Figure 8. In addition to the strain gages, the specimens were also instrumented to provide an additional indication of time at complete specimen fracture. This was done by integrating the specimen into a simple electrical circuit. In essence, the specimen initially was part of a closed circuit. But, because complete specimen fracture produces an open circuit, a readily detected sharp voltage change is produced. In this way, the time of complete fracture, should it occur, could be accurately determined. A similar concept was used to determine the time of blast arrival on the specimen surface.

For a 4340 steel monolithic specimen used as a trial, the crack mouth gage indicated a crack initiation time of 20 to 29 μs after the blast arrival, with total fracture, as indicated by the upper surface gage, at 71 μs after blast arrival. These readings correspond to an average crack speed of 374 m/s. This is consistent with the crack speeds observed in the 4340 steel fracture experiments conducted earlier with other loading mechanisms. This suggests that these data are reliable. Offsetting this encouraging finding, the side gage and the battery circuit gave readings of 110 μs and 125 μs, respectively. These are obviously contradictory. In view of the fact that the surface gages are highly susceptible to blast and heat effects while the side gage reading will lag behind the crack passage by an indefinite time, these readings are not believed to be useful.

Three replicate experiments were conducted on HY-80 welded specimens. One of these produced questionable results that were inconsistent

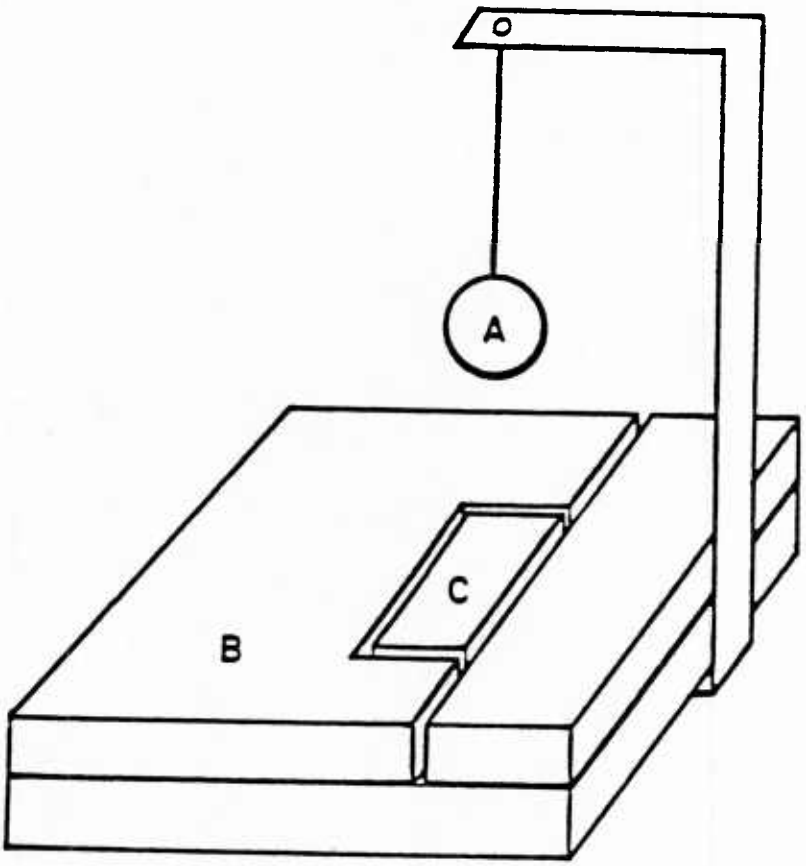

FIGURE 5. SPECIMEN LOADING FIXTURE USED DURING BLAST LOADING EXPERIMENTS

(A) is the explosive charge,
(B) is the loading fixture, and
(C) is the specimen.

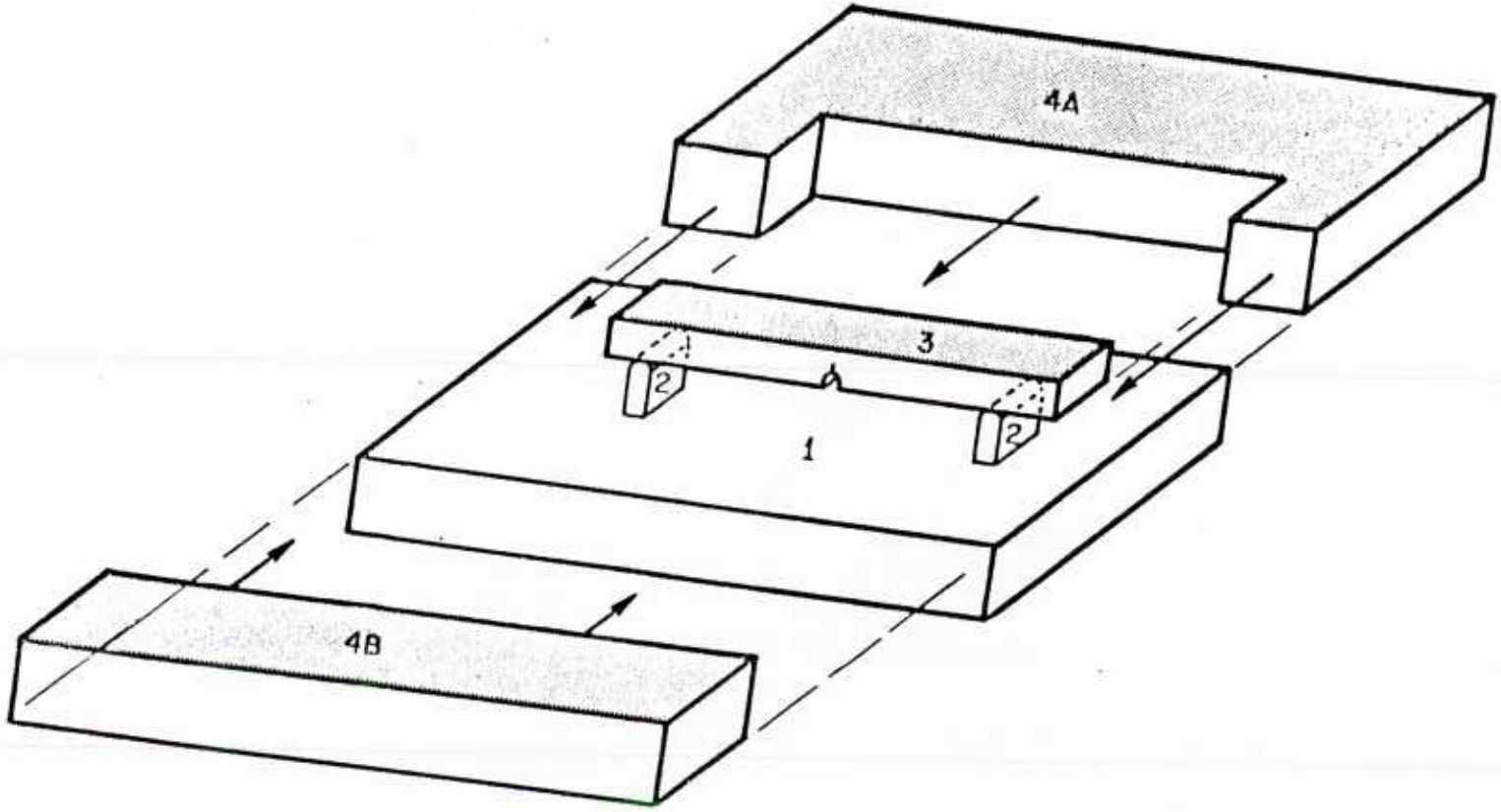

FIGURE 6. EXPANDED REPRESENTATION OF BLAST LOADING FIXTURE

(1) Base plate, (2) Supports, (3) Specimen, (4) Specimen encompassing plates to minimize gas blow by.

FIGURE 7. POST TEST APPEARANCE OF HY-80 WELDED SPECIMEN SHOWING BLAST INDUCED CRACK GROWTH

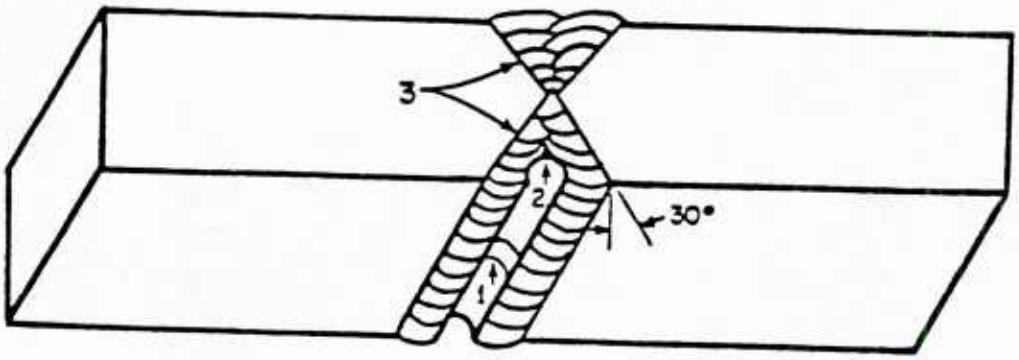

FIGURE 8. SPECIMEN USED FOR BLAST INDUCED FRACTURE

(1) Strain gage mounted within notch, (2) EDM notch, (3) Weld zone (typical of an 18 pass butt-weld in an HY-80 steel ship structure), (4) An additional gage is also bonded to the specimen upper surface to indicate complate specimen fracture.

with the other two, both in terms of the gage readings and the extent of crack propagation. Hence, these data are omitted. The results obtained from the remaining two specimens are shown in Table 1. It can be seen that the crack initiated (as indicated by the crack tip gage) at roughly 85 μs and that crack arrest was achieved after a crack advance of about 14 mm. Because fracture did not occur in these experiments, the upper surface gage readings are not believed to be significant.

TABLE 1. EXPERIMENTAL RESULTS FOR WELDED HY-80 BLAST-LOADED FRACTURE EXPERIMENTS(a)

Crack Lengths (mm)		Crack Extension	Time of Significant Gage Response After Arrival of Blast (μs)	
Initial	Final	(mm)	Crack Tip	Upper Surface
8.0	20.7	12.7	72 - 81	120
8.0	23.2	15.2	90 - 95	176

(a) Initial specimen depth was 25.4 mm.

2.5 Current Status of Crack Propagation Analysis

The analytical effort in this research consisted of two types of analyses, one providing the initial condition for the other. The first type was an elastic-thermoplastic finite element computation to obtain the residual stresses due to welding. The second type of analysis was the finite element solution for dynamic crack propagation under blast loading conditions. The modeling used the weld-induced residual stresses as initial conditions and included direct consideration of crack tip plasticity and of the inertial effects due both to dynamic loading and rapid crack propagation.

In all finite element computations, the equations of motion were solved using a displacement-based finite element method with an isoparametric element formulation and quadratic shape functions in a two-dimensional space. A singular element was not used. A modified Newton-Raphson approach was used

for elastic-plastic analysis with the Von Mises yield condition and isotropic strain hardening assumed. The approach employed the implicit Newmark-Beta time integration scheme. Crack growth was modeled by releasing double-noded elements along a preset crack path. This was done by gradually releasing the crack tip nodes over several time steps.

The welding simulation computation was made using the temperature dependent material properties of HY-80 steel. The heat input and weld-pass sequence used in the analysis were the same as in the actual welding process employed to fabricate the specimens. The multipass simulation of the process was performed as developed by Kanninen, et al[10]. The computed residual stress distribution across the weld centerline is shown in Figure 9. Also shown in Figure 9 are the residual stresses at selected locations as deduced from experimental strain measurements by the trepanning method. The agreement can be seen to be reasonable.

To aid in the design of the blast-loaded specimens, a preliminary elastodynamic finite element analysis was performed. The result is shown in Figure 10. The temporal pressure distribution used in this case was obtained by fitting a least-square curve through the experimentally measured pressure-time record measured for a 2.27-kg explosive charge detonated at a distance of 38 cm from the specimen. This is

$$p(t) = 6.895\ (11.0 - 0.072t + 0.000062t^2)\ H(t)$$

where t is the time from the blast arrival (μs), p is the pressure exerted on the upper surface of the specimen (MPa), and H is a function such that $H(t) = 0$, $t < 0$, and $H(t) = 1$, $t \geq 0$. Note that the specimen configuration used in the blast loading experiments and analyses is also shown in Figure 10.

From the data collected by Hahn and Kanninen[11], the dynamic initiation toughness of an HY-80 weld appears to be about 120 MPa$\sqrt{m}$. Using this number, the analysis shows that the crack should initiate at about 100 μs following the arrival of the blast at the specimen surface. Note that, in this preliminary computation, the effects of crack tip plasticity and residual stresses were totally ignored. The purpose was simply to get a rough estimate of the crack initiation time for pretest design purposes.

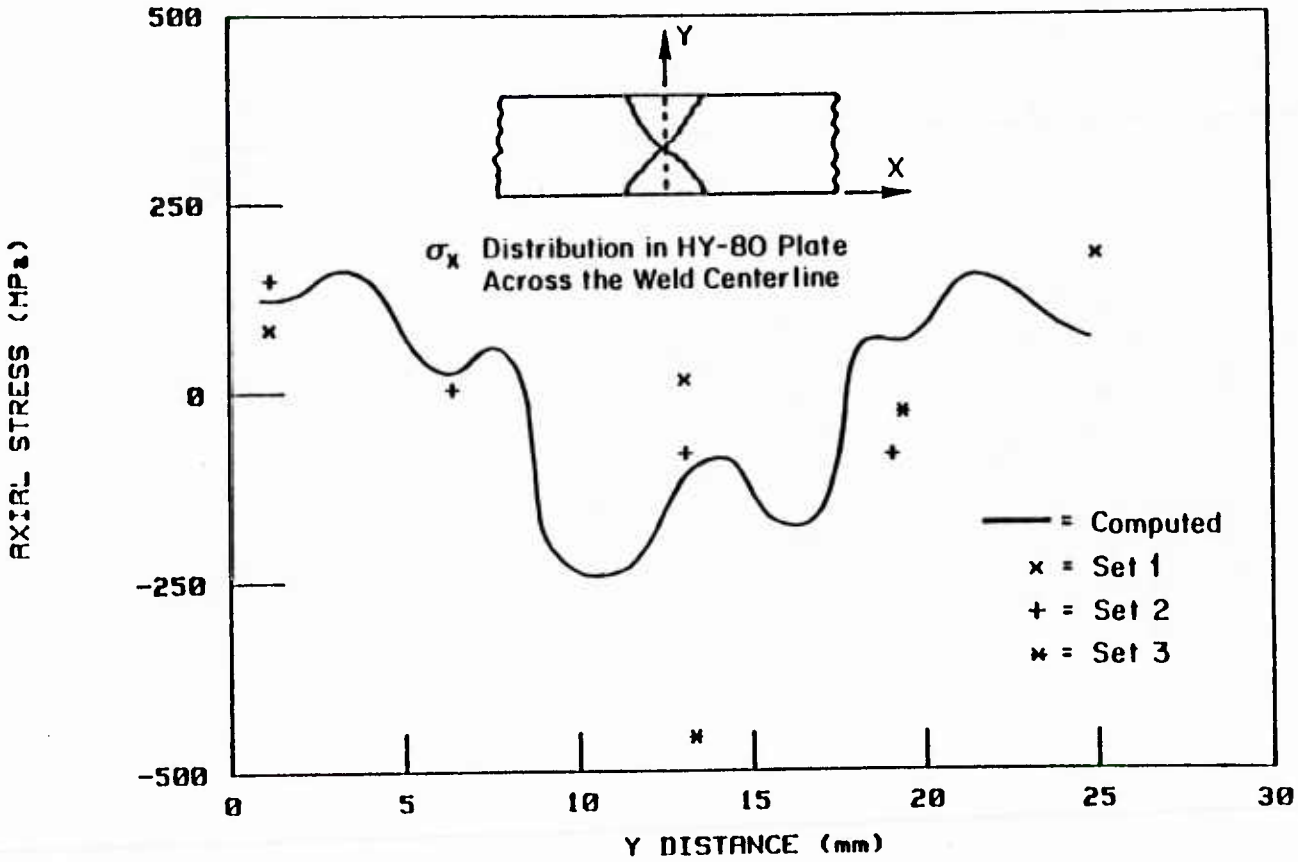

FIGURE 9. COMPARISON OF COMPUTED AND MEASURED WELD-INDUCED RESIDUAL STRESSES IN WELDED HY-80 SPECIMENS

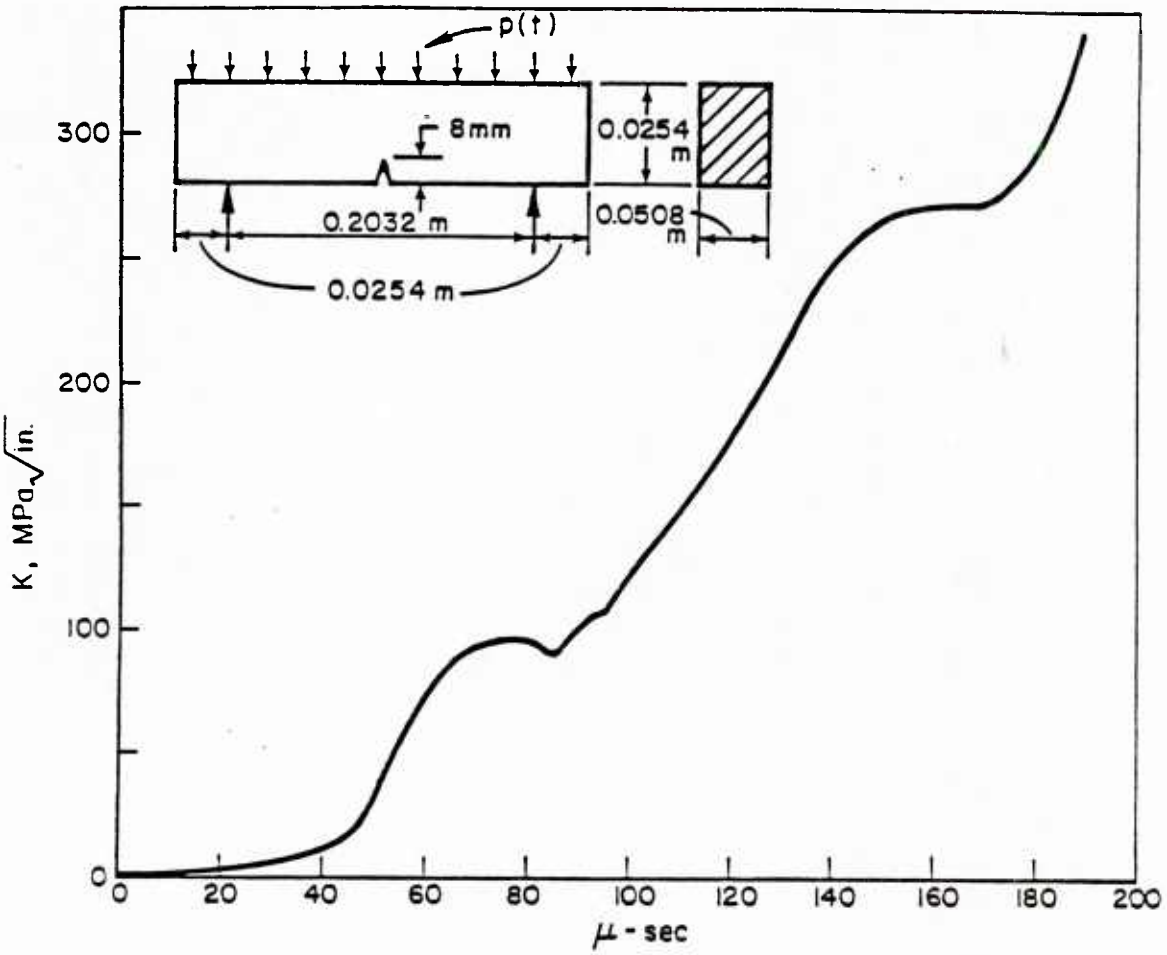

FIGURE 10. ELASTODYNAMIC COMPUTATION OF STRESS INTENSITY FACTOR AS A FUNCTION OF TIME FROM THE BLAST APPRIVAL

The next step in the analysis was to perform an elastic-plastic dynamic finite element analysis to predict the crack propagation history. The input to the finite element analysis included the temporal pressure distribution, the residual stress distribution, and critical CTOA values for crack initiation and propagation. Unfortunately, the fracture toughness values for a rapidly propagating crack in elastic-plastic conditions are not available. As an expedient, estimates were obtained from the existing linear elastic data as follows.

From Hahn and Kanninen[11], the lower bound initiation toughness K_{Ic} and crack arrest toughness K_{Ia} for HY-80 weldments were estimated at 120 MPa$\sqrt{m}$ and 92 MPa$\sqrt{m}$, respectively. It was then assumed that the dynamic fracture toughness K_{ID} is the same as K_{Ia}, and that K_{ID} is independent of crack velocity in the range of crack velocities expected in the experiment. Also, it was assumed that the lower bound K_{Ic} is the same as K_{Id}, the rapid loading fracture toughness. Using these values, the crack opening displacements at one element length (1.933 mm) behind the crack tip were determined from an elastic-plastic finite element computation. For initiation and propagation, these were found to be 0.076 mm and 0.058 mm, respectively. The result of the analysis employing these values is shown in Figure 11.

To help in understanding the effects of elastic-plastic conditions and residual stresses, two additional computations were also performed. As shown in Figure 11, these were an elastodynamic computation and an elastic-plastic dynamic computation without the initial residual stresses. These computations also employed the critical CTOA values just given. It can be seen that, in this instance, both give nearly the same result for the initiation time and for the crack length history. In contrast, the result of the elastic-plastic analysis with residual stresses included is considerably different.

Because the choices of K_{Id} and K_{ID} in the analyses just described was rather arbitrary, a second set of computations was performed. In these, the K_{ID} value (and, hence, the corresponding CTOA value) was specifically selected to obtain better agreement with the experimental crack arrest point. This value was 84 MPa$\sqrt{m}$. The results of the analyses performed with this new value of K_{ID} are shown in Figure 12.

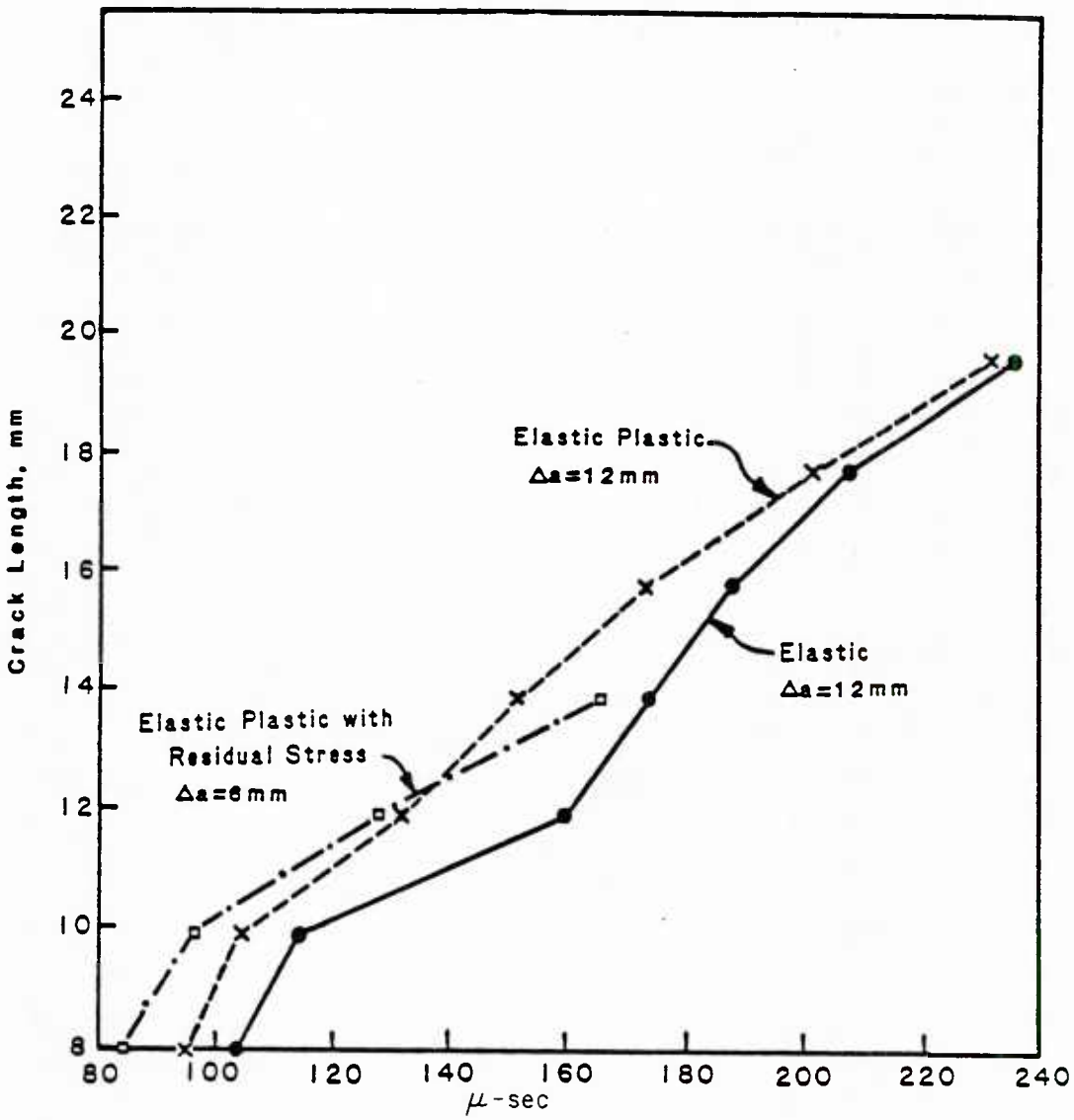

FIGURE 11. PREDICTION OF CRACK LENGTH HISTORY FOR A WELDED HY-80 SPECIMEN UNDER BLAST LOADING WITH K_{Id} = 120 MPa$\sqrt{m}$ AND K_{ID} = 92 MPa$\sqrt{m}$

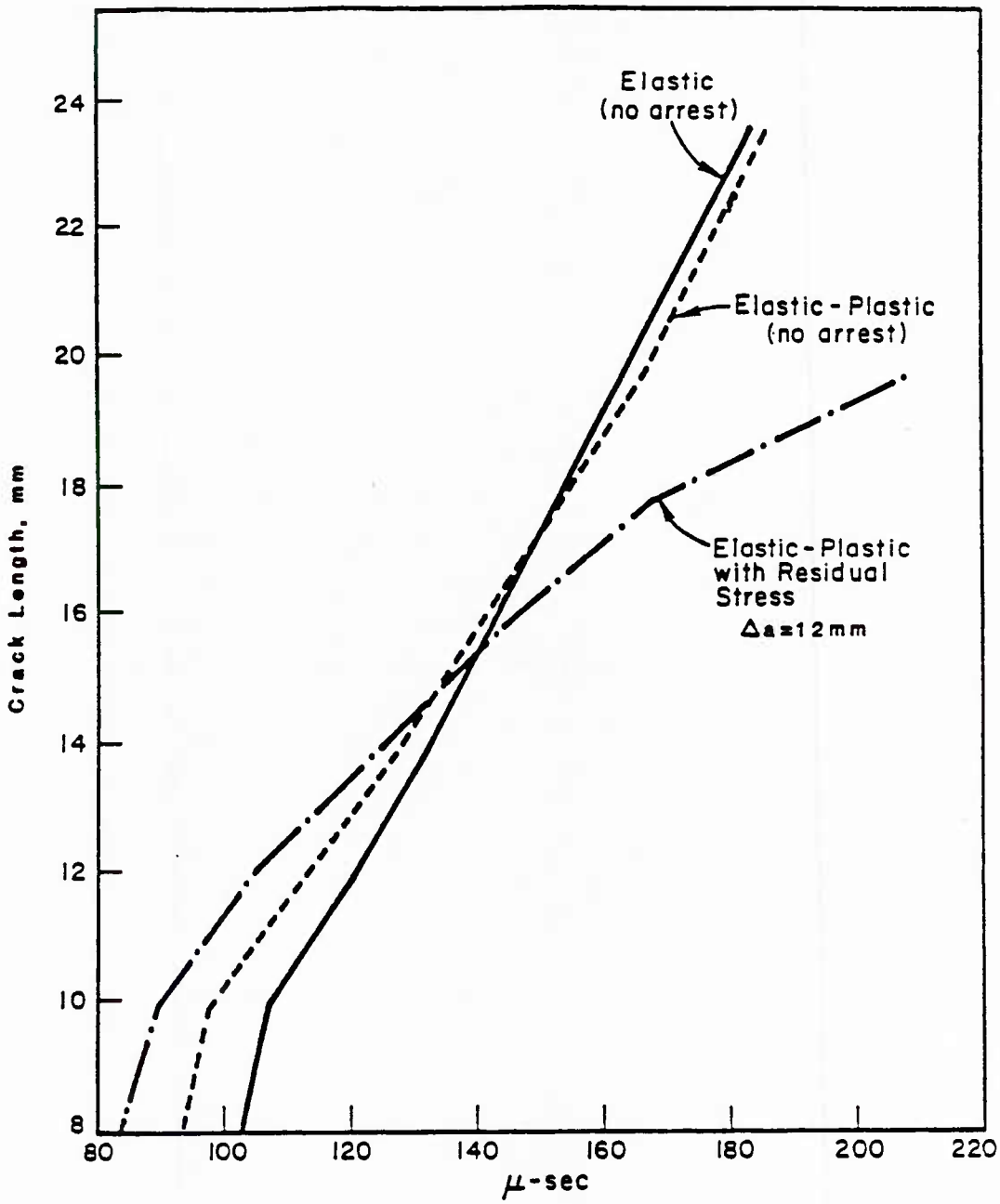

FIGURE 12. PREDICTION OF CRACK LENGTH HISTORY FOR A WELDED HY-80 SPECIMEN UNDER BLAST LOADING WITH K_{Id} = 120 MPa$\sqrt{m}$ AND K_{ID} = 84 MPa$\sqrt{m}$

It can be seen in Figure 12 that, while the elastic-plastic dynamic analysis that includes the residual stresses is now close to the experimental result (see Table 1), the comparison analyses predict that the crack would run through the specimen without arresting. This demonstrates that the analytical predictions are quite sensitive to the accuracy of K_{ID}. Of more significance, it also reveals the importance of considering residual stresses in such analyses.

It might be tempting to conclude from the results shown in Figures 11 and 12 that the neglect of initial residual stresses is conservative; i.e., the inclusion of residual stresses gives a prediction that is less severe than that obtained in their omission. However, it is entirely possible that this result was obtained because of the particular residual stress distribution within these particular specimens. For a residual stress distribution that is highly tensile in the vicinity of the initial flaw, it is conceivable that a different conclusion would be reached. This can only be determined with further computations of the kind described here. However, before this is done, more reliable fracture property values are closely needed.

3.0 SUGGESTED FUTURE RESEARCH

The objective of the future work should be to develop and validate a nonlinear dynamic analysis methodology that can be applied to determine critical crack sizes in structures subjected to blast loadings. The point of view is that a crack-like flaw may exist in a local low toughness region of a weld. But, while such a flaw would likely initiate, catastrophic fracture would still be avoided if the crack arrests. The key research issue is then to quantify the conditions under which a run/arrest event can occur in a tough, ductile material subjected to a rapidly varying applied loading.

A key assumption in the previous work was that rapid crack propagation can be characterized by a constant value of the CTOA parameter. While there is solid evidence for this assumption (see Figure 1), the work that has been performed so far has not allowed the proper value for the CTOA for crack propagation to be determined for Navy grade steels. Hence, further work is needed in which a direct determination of the running fracture toughness of HY-80 and HY-130 steels could be made. This work would also reveal the speed dependence, if any exists, of the CTOA parameter. Regardless, using these data as input, crack initiation/propagation/arrest predictions could be made and compared to the experimental result for more unequivocal assessments of the analysis approach. This could be done in terms of a combination of experimentation and finite element analysis.

4.0 REFERENCES

(1) Kanninen, M. F., et al, "Dynamic Crack Propagation Under Impact Loading", Nonlinear and Dynamic Fracture Mechanics ASME, AMD, Vol. 35, N. Perrone and S. N. Atluri, Editors, The American Society of Mechanical Engineers, New York, 1979.

(2) Kanninen, M. F., Brust, F. W., Ahmad, J., and Abou-Sayed, I. S., "The Numerical Simulation of Crack Growth in Weld-Induced Residual Stress Fields", Residual Stress and Stress Relaxation, edited by E. Kula and V. Wiess, Plenum Press, New York, pp 227-247, 1982.

(3) Kanninen, M. F., "Dynamic Fracture Mechanics and its Application to Material Behavior under High Stress and Loading Rates", Proceedings of the 29th Army Sagamore Materials Research Conference, Lake Placid, New York, July, 1982.

(4) Ahmad, J., Barnes, C. R., and Kanninen, M. F., "Analysis of Crack Initiation and Growth in a Ductile Steel Under Dynamic Loading", ASME Winter Annual Meeting, Phoenix, November, 1982.

(5) Ahmad, J., Jung, J., Barnes, C. R., and Kanninen, M. F., "Elastic-Plastic Finite Element Analysis of Dynamic Fracture", Engineering Fracture Mechanics, Vol. 17, 1983.

(6) Kanninen, M. F., Ahmad, J., and Barnes, C. R., "Dynamic Crack Propagation in Welded Structures Subjected to Explosive Loading", Army Symposium on Solid Mechanics, Army Mechanics and Materials Research Center, Watertown, Massachusetts, September, 1982.

(7) Ahmad, J., Barnes, C. R., and Kanninen, M. F., "Crack Initiation and Propagation Under Dynamic Elastic-Plastic Conditions". To be published.

(8) Barnes, C. R., Ahmad, J., and Kanninen, M. F., "Crack Initiation and Propagation Through Welded HY-80 Plates Under Blast Loading", Fracture Mechanics: Sixteenth Conference, ASTM STP, in press, 1983.

(9) Kanninen, M. F., Popelar, C. H., and Broek, D., "A Critical Survey on the Application of Plastic Fracture Mechanics to Nuclear Pressure Vessels and Piping", Nuclear Engineering and Design, Vol. 67, pp 27-55, 1981.

(10) Kanninen, M. F., Barber, T. E., Brust, F. W., and Mishler, H. W., "Controlling Residual Stresses by Heat Sink Welding", EPRI Report NP-2159-LD, Electric Power Research Institute, Palo Alto, California, December, 1981.

(11) Hahn, G. T., and Kanninen, M. F., "Dynamic Fracture Toughness Parameters for HY-80 and HY-130 Steels and Their Weldments", Engineering Fracture Mechanics, Vol. 14, pp 725-740, 1981.

APPENDIX

DYNAMIC ELASTOPLASTIC CRACK PROPAGATION INITIATED BY IMPACT

by

J. Ahmad

and

M. F. Kanninen

Engineering and Materials Sciences Division

Southwest Research Institute

San Antonio, Texas

January, 1984

Submitted for publication in the International Journal of Fracture.

SECURITY CLASSIFICATION O S PAGE (When Data Entered)

REPORT DOCUMENTATION PAGE

READ INSTRUCTIONS BEFORE COMPLETING FORM

1. REPORT NUMBER

2. GOVT ACCESSION NO.

3. RECIPIENT'S CATALOG NUMBER

4. TITLE (and Subtitle)

Dynamic Elastoplastic Crack Propagation Initiated by Impact

5. TYPE OF REPORT & PERIOD COVERED

Interim

6. PERFORMING ORG. REPORT NUMBER

7. AUTHOR(s)

J. Ahmad
M.F. Kanninen

8. CONTRACT OR GRANT NUMBER(s)

N00014-77C-0576

9. PERFORMING ORGANIZATION NAME AND ADDRESS

Battelle Columbus Laboratories
Columbus, Ohio
Southwest Research Institute
San Antonio, Texas

10. PROGRAM ELEMENT, PROJECT, TASK AREA & WORK UNIT NUMBERS

11. CONTROLLING OFFICE NAME AND ADDRESS

Office of Naval Research
Structural Mechanics Program
Department of the Navy
Arlington, Virginia 22217

12. REPORT DATE

January 1984

13. NUMBER OF PAGES

32

14. MONITORING AGENCY NAME & ADDRESS(if different from Controlling Office)

15. SECURITY CLASS. (of this report)

unclassified

15a. DECLASSIFICATION DOWNGRADING SCHEDULE

16. DISTRIBUTION STATEMENT (of this Report)

Approved for public release; distribution unlimited.

17. DISTRIBUTION STATEMENT (of the abstract entered in Block 20, if different from Report)

18. SUPPLEMENTARY NOTES

Manuscript submitted for publication in the International Journal of Fracture.

19. KEY WORDS (Continue on reverse side if necessary and identify by block number)

crack initiation
quasi-static
impact
analyses
linear elastic
elastic plastic
fracture criterion

20. ABSTRACT (Continue on reverse side if necessary and identify by block number)

Analyses of rapid crack propagation in three-point-bend specimens are presented. Both quasi-statically and impact initiated cracks are considered. Through parallel elastic and elastic-plastic dynamic finite element dynamic finite element computations it is shown that a linear elastic treatment of the problem is inadequate even for a relatively high strength material. For unstable crack propagation under elastic plastic conditions, the critical crack tip opening displacement is identified as a fracture criterion.

DD FORM 1 JAN 73 1473

unclassified
SECURITY CLASSIFICATION OF THIS PAGE (When Data Entered)

ABSTRACT

Analyses of rapid crack propagation in three point bend fracture specimens is presented. Both quasi-statically initiated, and impact initiated cracks are considered. Through parallel elastic and elastic-plastic dynamic finite element computations it is shown that a linear elastic treatment of the problem even for a relatively high strength material is inadequate. For unstable crack propagation under elastic-plastic condition the critical crack tip opening displacement is identified as a fracture criterion.

INTRODUCTION

Most current efforts in elastic-plastic fracture mechanics (EPFM) are focused on initiation and instability of crack growth under quasi-static loading conditions. Analytical treatments of impact loaded structures containing cracks has thus far remained within the regime of linear elasto-dynamic fracture mechanics. However, in many practical problems the material behavior is such that even relatively fast loading may induce considerable plastic deformation, both prior to and following crack growth initiation. Example applications are the blast loading of ship structures, mechanical impact in collisions, seismic water hammer in nuclear plant piping. and gun tubes.

The main reason for the wide neglect of plasticity effects in dynamic fracture mechanics has been the lack of appropriate analysis techniques. Until very recently, almost all numerical work in dynamic fracture mechanics analysis was done with finite difference methods under the constraint of a linear elastic material assumption. The focus of attention then was on how to model the crack tip singularity and on how to adapt the method for complicated crack-structure geometries. Modeling plasticity effects, which had just begun receiving significant attention in the fracture mechanics research community, was not really possible for a moving crack.

Almost coincident with beginning of major advances in EPFM, the finite element method gained recognition as a more versatile technique for analyzing crack problems. The method has virtually eliminated the complexities associated with the analysis of complicated crack-structure geometries. Particularly since the advent of special crack tip elements, the finite element method has essentially replaced the use of finite difference methods, even in

elastic fracture problems. However, progress in finite element analysis techniques for crack problems remained closely tied to the needs of the emerging EPFM technology, which was concerned only with quasi-static loading. Most of the effort in dynamic fracture mechanics remained married to elastodynamic finite difference and finite element techniques. However, in the late 1970's, the need for developing nonlinear numerical techniques in dynamic fracture problems became apparent [1].

Based on the mounting experimental evidence on the non-uniqueness of the K_{ID} parameter reported by Kanninen, A. S. Kobayashi, J. T. Kalthoff and their coworkers (See Reference [1]), Kanninen suggested that many of the puzzling questions in elastodynamic fracture mechanics could be resolved by eliminating the assumption of linear elastic material behavior. This in itself was not an unsurmountable problem. Advances in the finite element method had been made, and could be called upon to develop an analysis procedure for nonlinear dynamic crack growth modeling. The question centered on just what crack tip characterizing parameter should be used to model extended crack propagation under dynamic elastic-plastic conditions. This question has yet to be unequivocally resolved.

While the search for the appropriate dynamic elastic-plastic fracture parameter continues, other efforts in finite element modeling of dynamic crack propagation revolve around developing increasingly sophisticated techniques for representing the crack tip singularity, employing translating mesh algorithms, and improving numerical algorithms in general. Most efforts remained limited to linear elastic material problems and thus were unable to resolve a dilemma brought to light by Kanninen et al. [2]. Basically, this dilemma stemmed from the inability of an elastodynamic finite difference analysis to predict correctly crack initiation under impact loading in a high strength

material (AISI 4340 steel)--a situation for which a linear elastic material assumption should be valid. While the work reported in this paper was focused on the development of an elastoplastic finite element modeling technique for dynamic fracture problems [3,4], use of this technique enabled the dilemma posed by Kanninen et al. to be revisited and resolved.

BACKGROUND

In 1978, Kanninen et al. [2] reported experimental and analysis results on dynamic crack propagation under impact loading. In their investigation two types of experiments were performed. Both types employed three point bend specimens of heat treated AISI 4340 steel (Figure 1). In the first type of experiment, the specimens were quasi-statically loaded until crack initiation occurred. Because the initial crack tip was intentionally blunted, initiation was followed by rapid propagation until the specimen broke into two pieces. The load at crack initiation and the crack length history were recorded. The crack initiation loads are given in Table 1. A typical crack length vs. time record is shown in Figure 2. (The predicted crack length vs. time curve in Figure 2 is discussed later in this section.) Note that, for the various initial notch root radii used in the experiment, the crack length vs. time data were practically the same.

TABLE 1. EXPERIMENTAL RESULTS OF CRACK INITIATED UNDER QUASI-STATIC LOADING

Experiment No.	Notch Root Radius mm	Side Groove Depth %	Load at Initiation kN
1	0.032	25	56.47
2	0.065	0	99.86
3	0.64	0	112.41

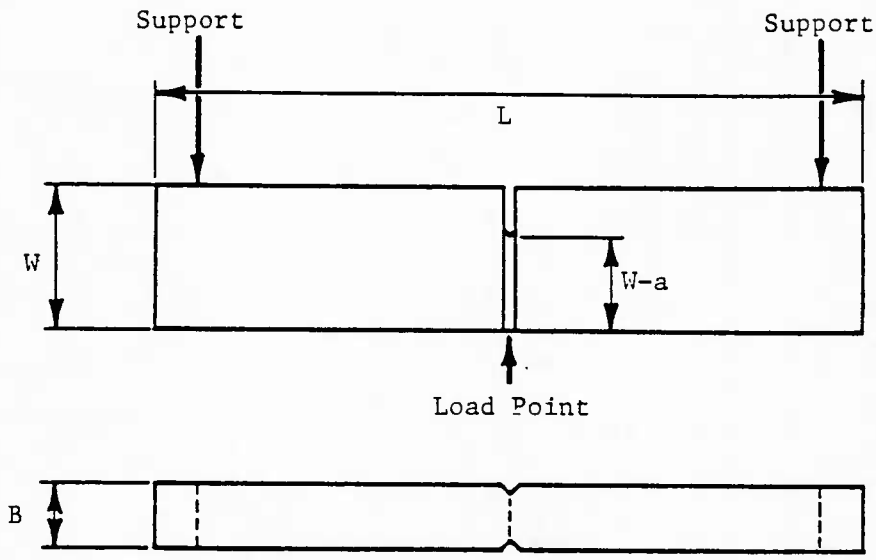

Figure 1. Specimen geometry (L = 181 mm, W = 38mm, B = 15.8 mm, W-a = 28.5 mm). The side groove depth is as shown in Table 1.

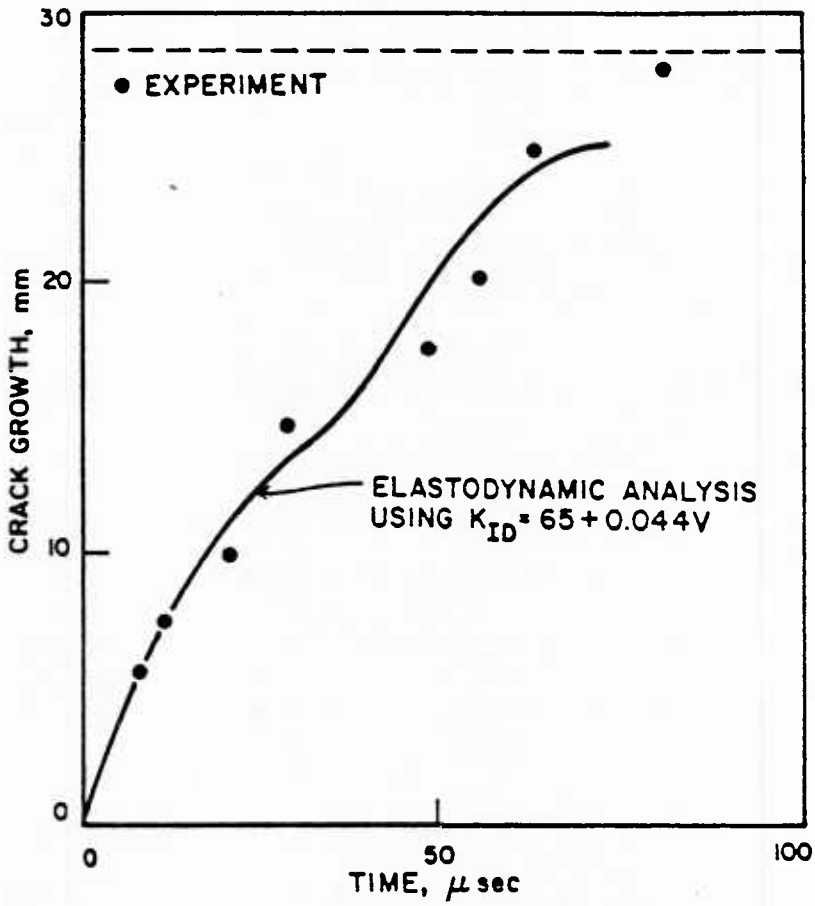

Figure 2. Comparison of measured and predicted dynamic crack propagation in 4340 steel initiated under quasi-static loading.

In the second type of experiment the specimens were loaded by mechanical impact. This was done using a large pendulum machine capable of dissipating 21.7 kJ impact energy. The massive tup of the pendulum moved the load point on the test specimen at a virtually constant velocity of 6.88 m/sec. In these experiments, the crack initiation time (relative to the tup-specimen contact) and crack length vs. time measurements were made. A typical crack length vs. time record for a side grooved specimen is shown in Figure 3. For a smooth-sided (non-side-grooved) specimen the initiation time was about 300 -sec.

The analytical work reported in reference [2] employed the dynamic fracture toughness function, $K_{ID}(\dot{a})$, given by

$$K_{ID} = 65 + 0.044\dot{a} \quad MPam^{1/2} \qquad (1)$$

where $\dot{a}$ is crack velocity in m/sec. This equation was obtained in other work by elastodynamically analyzing data from a series of quasi-statically loaded double cantilever beam (DCB) test specimens. To determine if the K_{ID} relation is geometry independent, Equation (1) was first used to predict the crack velocity in the three point bend experiments conducted under quasi-static loading. In the elastodynamic finite difference analysis, the specimen model was subjected to an applied load equal to the experimentally measured load at initiation. Next, crack growth was modeled according to Equation (1). As shown in Figure 2, the predicted crack length vs. time was in good agreement with the experimental data [2].

The same elastodynamic finite difference code and the same K_{ID} relation were then used to predict crack length as a function of time in the experiments in which crack was initiated by impact loading. The result of such an analysis is contained in Figure 3. As can be seen, if the experimental data

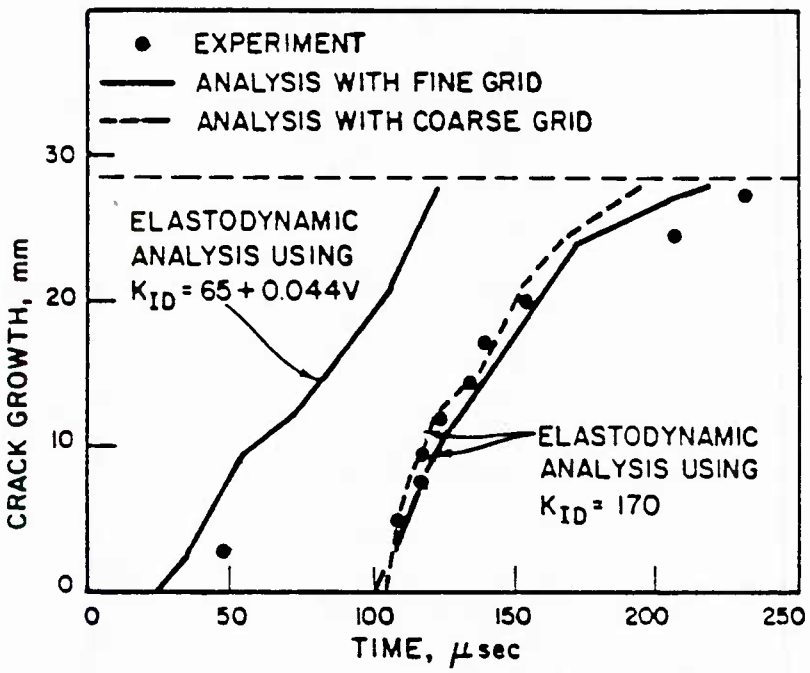

Figure 3. Comparison of measured and predicted dynamic crack propagation in 4340 steel initiated under impact loading. Rigid supports --.064mm initial slot diameter.

point on the extreme left is disregarded, the predicted initiation time is about a factor of four less than the measured value. (As discussed later in this section, this data point was absent in all additional experiments performed since the publication of reference [2].) The value of K_{ID} needed to match the experimental crack length vs. time data was a velocity-independent value of 170 $MPam^{1/2}$. This value, which is roughly double that sampled by the propagating crack in the quasi-statically loaded experiment, cannot be justified.

The only difference between the two types of experiments analyzed was the loading rate. But, this difference presumably was properly accounted for in the solution of the governing equations of motion by the finite difference method. Refusing to believe that the material toughness value could be so much different between the two cases, Kanninen et al. [2] scrutinized the accuracy and convergence characteristics of their finite difference scheme. However, repeated attempts with varying mesh sizes produced essentially the same result as their first analysis. Later, Jung et al. [5] and Ahmad et al. [4] reaffirmed the accuracy of the finite difference results by performing independent checks using an elastodynamic finite element method.

Other attempts have also been made to find the source of error responsible for the difference between the experimental measurements and analytical predictions. First, it was thought that the supporting structure in the impact experiment provided an energy sink. Since this structure was assumed to be perfectly rigid in the analyses, it was thought possible that it could account for the overestimation of the dynamic stress intensity factor. To estimate the energy loss to the supports, an experiment was performed in which the specimen was not supported at all. Using the results of this experiment and a simple energy balance, it was found that the deformation of

supports could not possibly account for the large difference between actual (about 80 $MPam^{1/2}$) and apparent (170 $MPam^{1/2}$) values for K_I or crack propagation. Details of this experiment can be found in references [2] and [5].

Nishioka, Perl, and Atluri [6] reanalyzed the impact-loaded experiments of reference [2] using a hybrid finite element formulation with a moving crack tip singular element. They performed both generation and application phase analyses and obtained results that differed significantly from those of references [2] and [4], although their results still did not adequately agree with the experiments. They initially concluded that the error was in not allowing for the possibility of tup-specimen separation and recontact. But, this conclusion is spurious. Kanninen et al. [2] also allowed for the possibility of recontact and separation and noted that these did indeed occur in their computations.

After repeated experimental evidence that separation and recontact does not actually occur, Ahmad et al. [4] decided that not modeling this phenomenon is more representative of the actual event. They found that the difference in the predictions of Nishioka et al. [6] and those of references [2] and [4] are simply due to an oversight on the part of the former investigators in not accounting for the effect of the side-grooves in the specimens used in the experiments. When the analysis of reference [6] is corrected to account for the side-grooves, the results become almost coincident with those of Ahmad et al. [4], with tup separation allowed. This is shown in Figure 4. Also shown in Figure 4 are the nearly identical results obtained independently by Kobayashi [7].

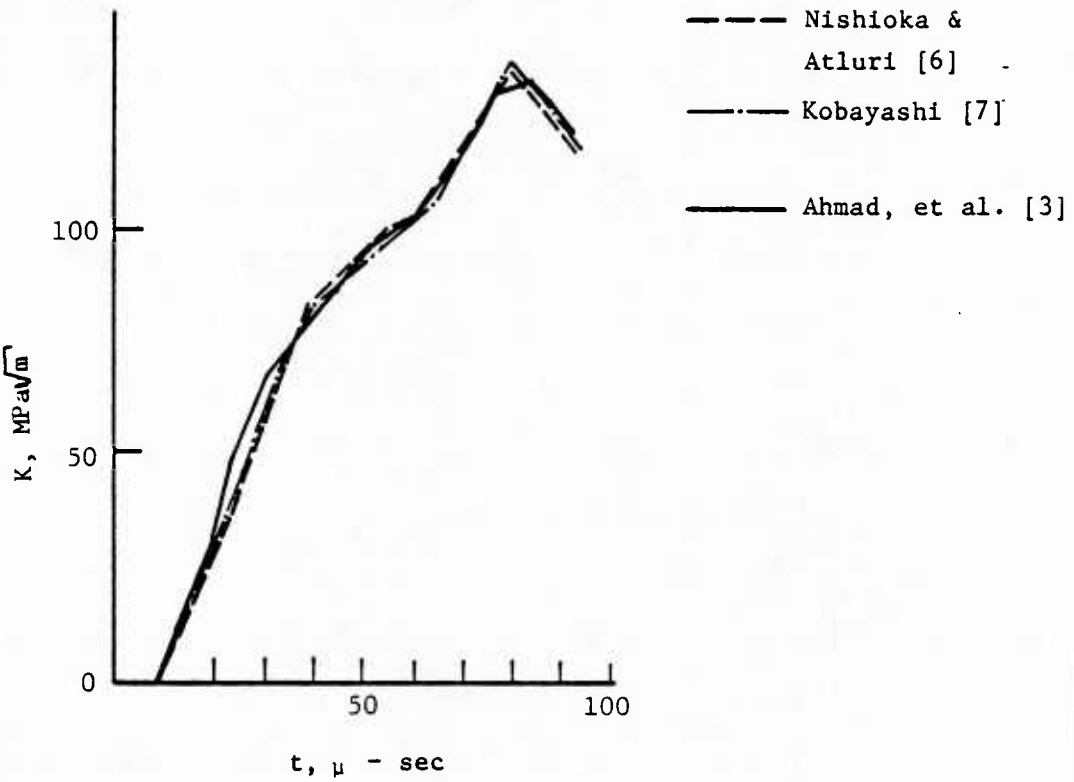

Figure 4. Results of elastodynamic analyses of the impact loaded three-point bend specimen with side grooves.

In his effort to resolve the dilemma, Kobayashi [7] focused on the existence of the single data point that existed at the extreme left of the reference [2] experimental record (see Figure 3). Including this data point as part of the experimental record makes the analytical predictions appear more reasonable, albeit only marginally. However, as already stated, this data point appeared in the experimental record of only one single specimen and was not reproduced in any of the numerous experiments that followed. It must be concluded that this data point is spurious and could not be the key to resolving the dilemma.

All of the analytical efforts that have so far been discussed amount to nothing more than using different numerical techniques, all elastodynamic, to repeat the analysis performed in reference [2]. Not surprisingly, these efforts have produced essentially the same results as those of the original finite difference analysis. Ahmad et al. [4] were the first to attempt an elastic-plastic analysis of the impact test. Using an inertia enhanced version of the J-integral called $\hat{J}$ they assumed that crack initiation should occur when $\hat{J}$ reaches its critical value ($\hat{J}_c = k\, K_{Ic}^2/E$), where E is the Young's modulus and k is the plane strain correction factor. Using the results of this analysis they concluded that including plasticity effects caused only a minimal increase (about 15%) in the computed crack initiation time. This was not nearly enough to account for the wide discrepancy between the analytical and the experimental results.

In using the $\hat{J}$ initiation criterion, Ahmad et al. [4] tacitly assumed that the plastic deformation was confined to the crack tip region, and that it was small. Under small scale yielding conditions J_c (or $\hat{J}_c$) is related to K_{Ic}. For an elastic-plastic analysis in which small scale yielding is not a priori assumed, an elastic-plastic criterion must first be established. In

the present work this was accomplished by first performing a generation phase analysis of the quasi-statically loaded experiment. This analysis identified an elastic-plastic criterion for crack initiation and a criterion for propagation. Next, these criteria were used to predict the crack initiation time, and the crack length history in the impact loading case. These predictions were then compared with the experiments, as described in the following.

DYNAMIC ELASTIC-PLASTIC ANALYSES

Basis of the Computations

The analytical effort involves both generation and application phase analyses of quasi-statically and dynamically initiated crack propagation experiments. In the generation phase analyses, finite element modeling is used as an extension of the actual experiment. Crack initiation and growth is simulated by forcing the finite element model to conform to an experimentally obtained crack length vs. time record. During the computation, the fracture parameters of interest are internally computed. In the application phase analysis, crack initiation and growth are modeled according to a prescribed criterion. Note that in both types of computation the applied loads and other boundary conditions must be specified along with the initial conditions.

A generalization of the path independent contour integral J is used as the criterion for crack initiation under elastic-plastic dynamic conditions. This is the $\hat{J}$ integral proposed by Kishimoto et al. [8]. It is an expression for the energy release rate for a much more general set of conditions than those covered by the common J-integral. It might be noted that $\hat{J}$ contains many other proposed measures of energy release rate as special cases. These include the J-integral itself [9] together with the parameters proposed by

Freund [10], Hellen and Blackburn [11], Neale [12], Bergez [13], Bui [14], and Wilson and Yu [15]. Recently, Ahmad et al. [4,16] have shown by generation-phase computations that the critical value of $\hat{J}$ is a valid criterion for crack initiation under dynamic loading and elastic-plastic material behavior.

For crack propagation, the work reported in this paper identifies the constant crack tip opening displacement (CTOD) as a criterion for rapidly running cracks. This finding substantiates a common assumption that dynamic crack propagation occurs with a constant CTOD, or, equivalently, a constant crack tip opening angle (CTOA).

The computational effort in the work reported in this paper relies upon a strain rate independent plasticity formulation. For dynamic fracture modeling, a time dependent plasticity, or viscoplasticity, formulation would be more appropriate. As this work deals mainly with a relatively strain rate insensitive material (AISI 4340 steel), the simpler rate independent plasticity formulation is palatable. A viscoplastic finite element analysis would have required selecting (and developing the constants for) an appropriate constitutive model for high strain rate applications; e.g., as has been done in a preliminary way by Hoff et al. [17] and Brickstad [18]. This was beyond the scope of the present work. But, future developments in this area of nonlinear dynamic fracture mechanics is definitely appropriate and anticipated.

Computational Procedure

The approach used for the solution of the equations of motion in the analytical procedure presented here employs a displacement-based finite element method. The computer code is based on the isoparametric finite element formulation with linear and quadratic shape functions in a two-dimensional space. General quadrilateral elements with a variable number of nodes in both

the plane-stress and plane-strain conditions may be used. If so desired, the $1/r^{1/2}$ or $1/r$ stress singularity at the crack tip may be imposed by using the quarter point approach [13]. However, this feature was not utilized in any of the analyses presented in this paper.

The modified Newton-Raphson approach is used for elastic-plastic analysis. The von Mises yield condition with isotropic strain hardening is assumed. Also, any strain rate effects on material properties are ignored. The material behavior is described by a single uniaxial stress-strain curve represented in a multilinear fashion. For time integration, either an explicit (central difference) or an implicit (Newmark-Beta) scheme may be used. Because it is inherently more stable, the implicit scheme offers computational advantages in the solution of dynamic fracture problems. All the results included in the present paper therefore were obtained using the Newmark-Beta time integration scheme.

Crack growth is modelled by releasing the force experienced between coupled crack tip nodes in several time steps. Details of the crack growth modeling scheme were described by Jung et al. [5] and will not be repeated here. Suffice to say that the scheme allows for modeling crack growth in both the generation and application-phases of analyses. For application-phase analyses, where the crack tip is advanced according to a selected fracture parameter, a choice of fracture parameters is necessary. Currently, the crack-tip-opening displacement (CTOD), crack-tip-opening angle (CTOA), Mode I and Mode II dynamic stress intensity factors (K_I and K_{II}), and the $\hat{J}$ family of conservation integrals [8] are available. The CTOD and CTOA are obtained directly from the finite element displacement solution while K_I and K_{II} are obtained by first calculating $\hat{J}$ for linear elastic material.

In the elastic-plastic dynamic analyses performed in the present work, a dual $\hat{J}$/CTOD criterion is employed. The $\hat{J}$ integral is computed by using the following expression:

$$\hat{J} = \int_{\Gamma} \left(W n_1 - T_i \frac{\partial u_i}{\partial x} \right) d\Gamma + \iint_{A} \rho \ddot{u}_i \frac{\partial u_i}{\partial x} \, dA \qquad (2)$$

where W is the strain energy density, n_1 is the x-component of the outward normal vector to contour Γ, A is the area enclosed by Γ, ρ is the mass density, and T_i, u_i, and $\ddot{u}_i$ are the traction, displacement, and acceleration components, respectively. The details of this expression can be found in references [3], [4], and [6].

Like the common J-integral, the $\hat{J}$ of equation (2) is valid only if the material behavior can be described by the deformation theory of plasticity. It is well known that, for extended amounts of crack growth, this assumption is severely violated. Consequently, in the present investigation the criterion $\hat{J} = \hat{J}_c$ is taken to be valid only for crack initiation. For extended amounts of crack growth a critical CTOD (or equivalently, CTOA) criterion is used.

Investigation of Crack Initiation

Consider the prediction of crack initiation time in the impact loaded specimen using a J_c value obtained by analyzing a quasi-statically loaded specimen. As shown in Table 1, the quasi-static experiments reported in reference [2] used both side-grooved and smooth-sided specimens with different notch root radii. The experiment using a smooth-sided specimen with a notch root radius of 0.065 mm was first chosen for an elastic-plastic finite element

analysis. The crack initiation load for this specimen was 99.86 KN. In the corresponding impact experiment, the measured time at crack initiation was 300 μ sec.

A smooth-sided specimen was selected because of the uncertainties in treating side-grooves in a two-dimensional elastic-plastic analysis. Note that the effect of side-grooves in an elastic analysis can be accounted for by simple scaling of the results. The reason for choosing the smallest notch root radius was that, in the finite element model, the notch is modeled as a sharp crack.

Finite element analyses were performed first for plane stress, then for plane strain. A simple finite element mesh of eight node isoparametric elements was used (Figure 5). The broken lines in Figure 5 show the $\hat{J}$ (for this static case, same as J) contours used in the analysis. The uniaxial stress-strain curve of the material (AISI 4340 steel), and the multilinear representation used in the analysis, are shown in Figure 6. In the analysis the von Mises yield condition and isotropic hardening was assumed. The Modified Newton Raphson approach was used for the solution of the nonlinear problem.

The results of the quasi-static analysis are shown in Figure 7. These are the average values from the various contours. It was found that the maximum difference between the J values corresponding to different contours was only about 3%. The result of the plane stress analysis can be taken as corresponding to the smooth-sided specimen geometry. If the plane strain results are taken as representing the side-grooved specimen then, using Table 1, the J_c values at crack initiation for the plane-stress (smooth-sided specimen) and plane-strain (side-grooved specimen) are 0.288 MN/m and 0.05 MN/m, respectively.

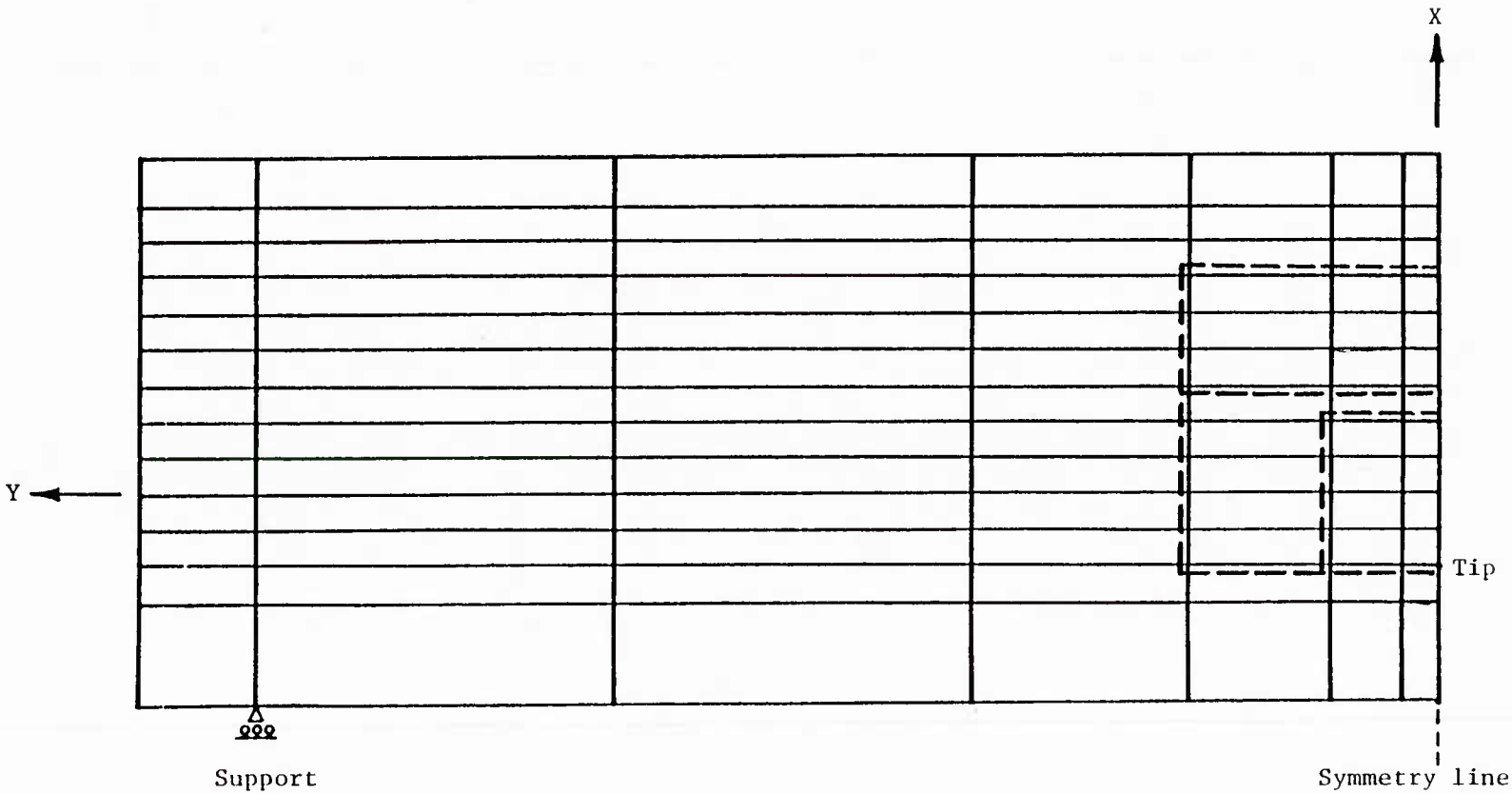

Figure 5. Finite element model used in the analyses.

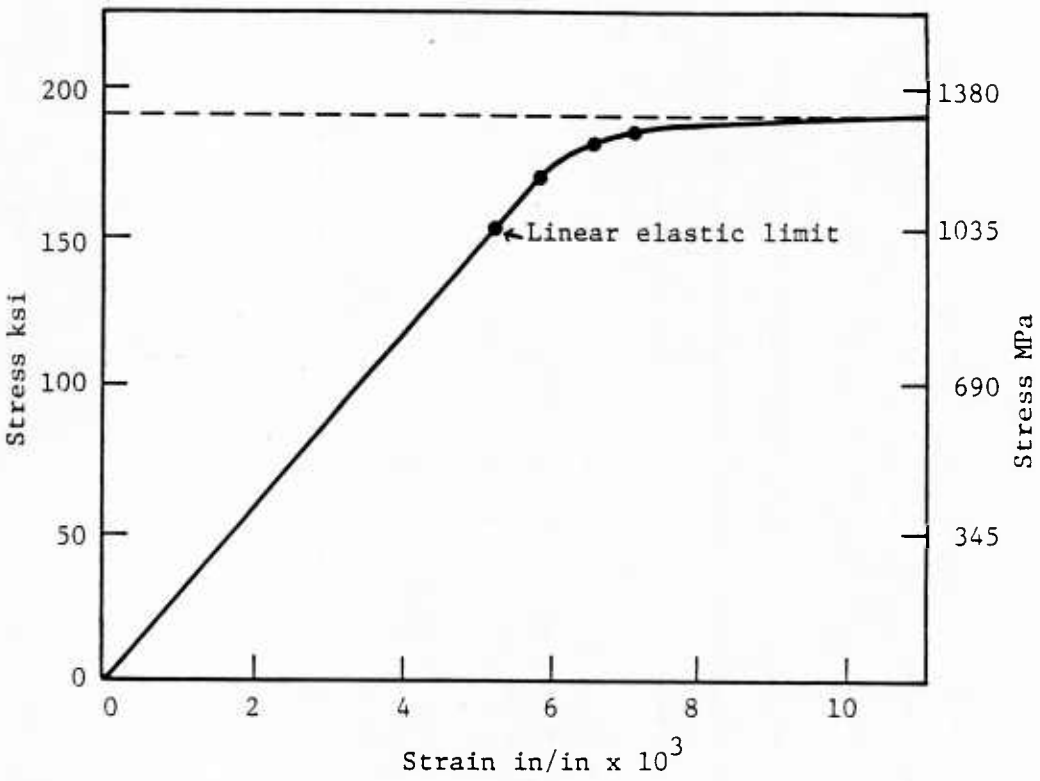

Figure 6. Stress-strain curve for heat treated AISI 4340 steel.

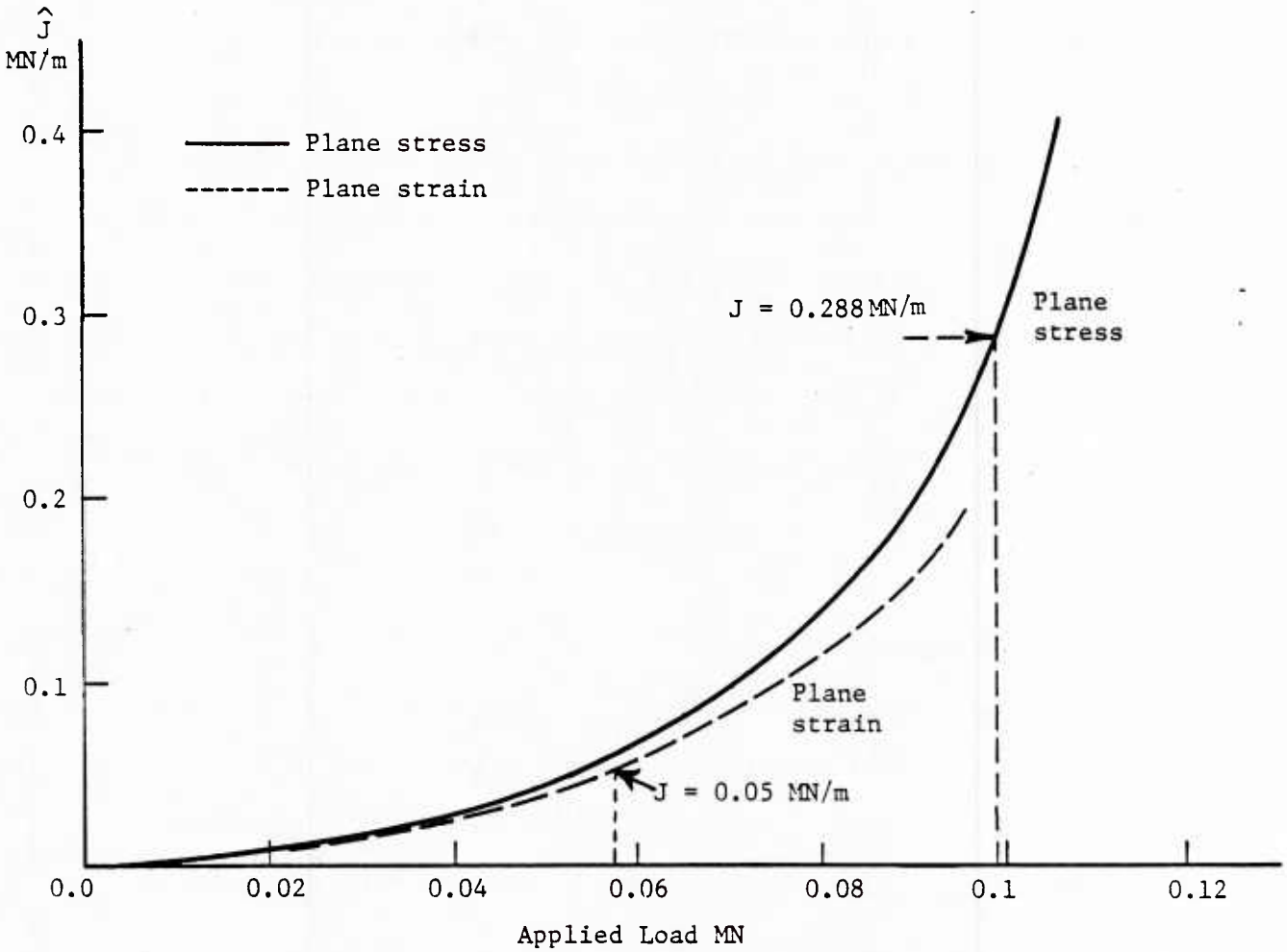

Figure 7. Elastic-plastic finite element analysis results for quasi-static loading of the three point bend specimen.

Next, elastic-plastic dynamic analyses of the impact experiments were performed using the same finite element mesh. The stress-strain behavior was taken to be the same as in the static analysis. The time integration was performed by the Newmark-Beta method using a time step of 1.0 μsec. Again, both plane stress and plane strain analyses were performed. The results are presented in Figure 8.

Consider first the plane stress analysis corresponding to the smooth-sided specimen. The results suggest that crack initiation should occur at 260 sec, the value that corresponds to J_c = 0.288 Mn/m. This is in reasonably good agreement with the measured initiation time of 300 μsec as the roughly 14% difference is certainly within the bounds of experimental measurement error. Similarly, the prediction of initiation time for plane strain conditions is also in good agreement with the measured time. As can be seen from Figure 8, using J_c = .05 MN/m gives an initiation time of 110 μsec. This can be compared with a measured value of 95 μsec for the side grooved experiment.

Investigation of Crack Propagation

The elastic-plastic treatment of crack initiation under impact loading just described has at least partly resolved the dilemma found by Kanninen et al. [2]. It showed that, by using an elastic-plastic fracture mechanics criterion and an elastoplastic dynamic analysis, the initiation time under impact loading could be reasonably well predicted. The next step is to investigate the velocity of rapid crack propagation. However, the consideration of rapid crack propagation in an elastic-plastic medium is complicated by the fact that there is no commonly accepted dynamic crack propagation

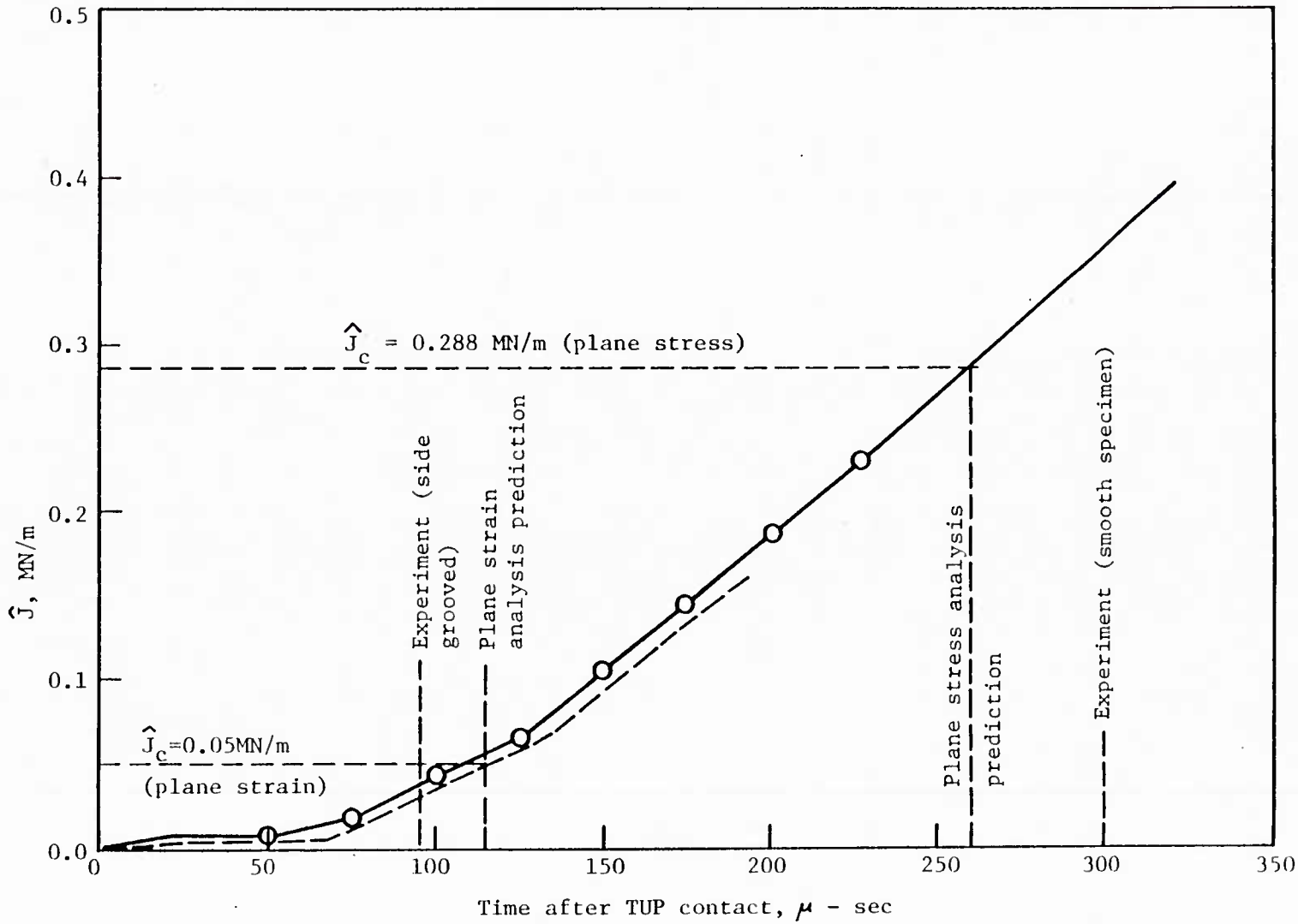

Figure 8. Prediction of time at crack growth initiation in an impact loaded three point bend specimen of AISI 4340 steel by elastoplastic dynamic finite element analysis.

parameter. The conservation integral proposed by Atluri [19] is a possibility, as are those of Dantam and Hahn [20], Achenbach et al. [21], and Freund and Douglas [22]. But, they all await experimental verification.

In the present investigation, the crack tip opening displacement (CTOD) criterion was selected. This choice is not arbitrary. In studies of extended amounts of stable crack growth under elastic-plastic conditions it has been shown by many investigators that crack growth occurs at a practically constant value of CTOD; see, for example, reference [23]. This constant CTOD occurs in a regime where the J-integral has lost both its path independent nature as well as its meaning as a crack tip stress characterizing parameter. The region between J-dominated crack growth and the constant CTOD crack growth is typified by a critical CTOD value that falls to a plateau. The question is whether the constant value of CTOD is mirrored by a constancy after the crack has become unstable. This has simply been assumed to be the case by some investigators. But, it has not previously been proven.

In the present work, such an investigation was made by performing a generation phase elastoplastic dynamic analysis of a quasi-statically loaded fast fracture experiment; specifically, the side-grooved three-point bend specimen of AISI 4340 steel. This was done by using the experimental crack-length vs. time data shown in Figure 2. In the analysis, the load was incrementally applied to reach the initiation value of 56.47 KN (see Table 1). Then, crack growth was modeled according to the experimental record of Figure 2 using a technique described in reference [5].

During the crack growth modeling, both $\hat{J}$ and CTOD were computed. The CTOD corresponded to the opening displacement of the node one element length (3.16 mm) behind the crack tip. It was found that, shortly after crack initiation, the path-independence of $\hat{J}$ was totally lost. The CTOD as a function of crack length is shown in Figure 9. Clearly, following an initial drop, the CTOD seems to attain a constant value.

This result suggests that the crack traveled by maintaining a constant CTOD for the most of its journey. The actual value of the constant CTOD is of course dependent upon the finite element mesh used in the analysis and on the distance behind the crack tip at which the crack opening was monitored. This is a common problem that one faces using the finite element method for crack propagation modeling. The opening, or stretch, at the crack tip can be estimated directly only by using one of the strip yield representation of crack tip plasticity; e.g., the Dugdale model [24], the inclined strip yield model [25]. Further investigations using increasingly refined finite element models may suggest a limiting distance behind the crack tip below which the crack opening displacement and the CTOD may be assumed to be the same. An estimate of this distance can be obtained through the use of the Dugdale model as suggested by Rice [26]. However, this estimate is unrealistic in that the crack tip opening angle is always 90 degrees.

In the present investigation, the need for knowing the unique critical CTOD (or CTOA) was circumvented by using the same finite element mesh in analyzing both the quasi-statically initiated and the impact loaded experiments. The CTOD in both types of analysis corresponded to the same physical point behind the crack tip. The result of the application phase analysis, using J_c = 0.05 MN/m as the initition criterion and the constant CTOD value in Figure 9 as the crack propagation criterion, is shown in

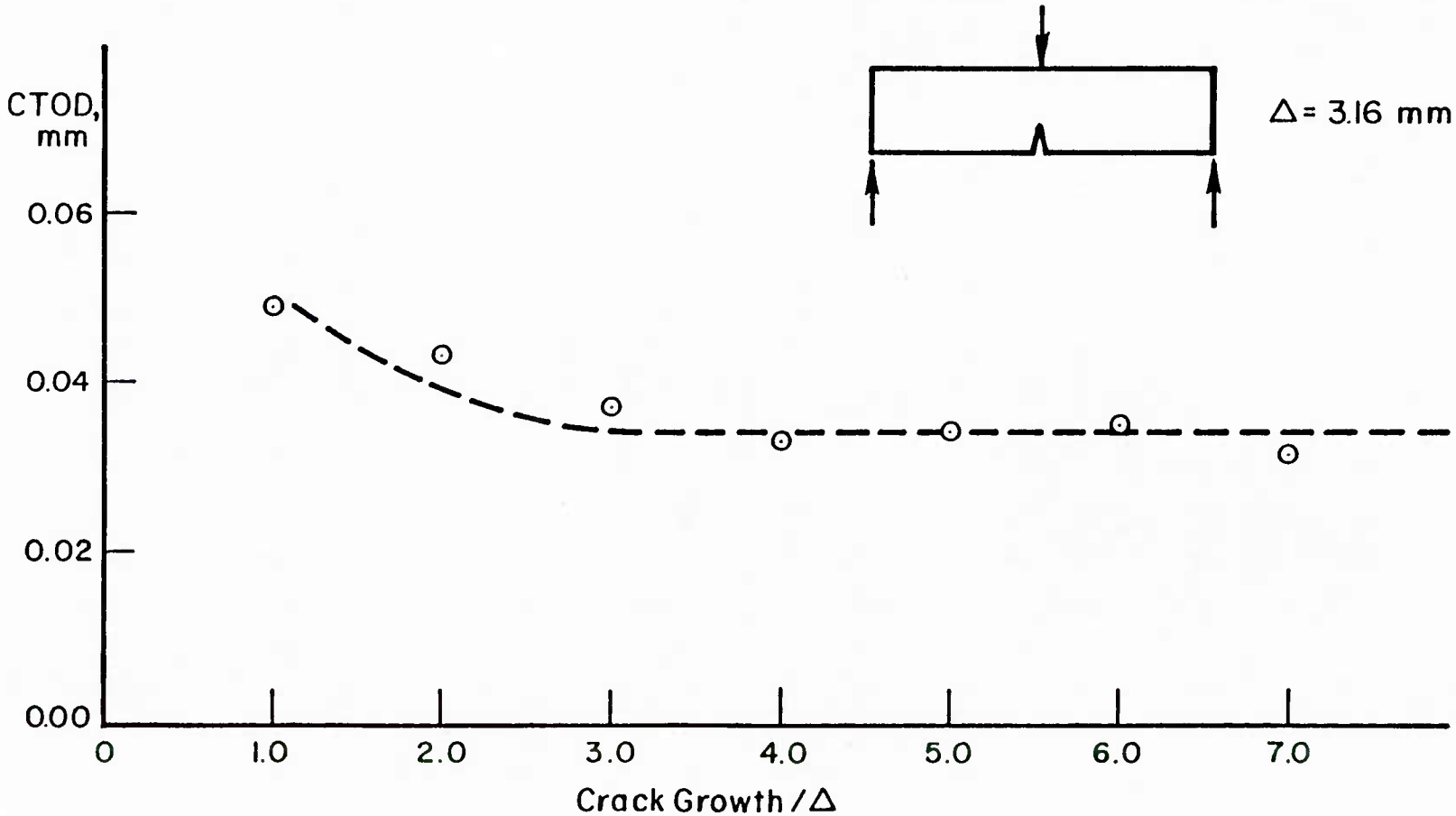

Figure 9. Elastic-plastic dynamic analysis of dynamic crack propagation in side grooved AISI 4340 bend specimen subjected to a quasi-static load.

Figure 10. Also shown in Figure 10 are the results of the elastodynamic analysis and the experimental data points of reference [2]. Clearly, the elastic-plastic analysis gives a much improved prediction.

DISCUSSION OF RESULTS

The work reported in this paper demonstrates the inadequacy of an elastodynamic analysis for a situation where the linear elastic material assumption would commonly be accepted as appropriate. The question is why. To answer this question, consider the elastodynamic analysis of the quasi-statically initiated crack given in reference [2]. Recall that this analysis (Figure 2) gave results that were in good agreement with the measurements made in experiment number 1 of Table 1. However, it should be recognized that, in this analysis, the crack was made to initiate at an applied load of 56.47 N which corresponds to a K_I value of 108 $MPam^{1/2}$ [27].

That the crack was not initiated at K_I = 65 $MPam^{1/2}$, the value corresponding to $\dot{a} = 0$ in equation (1), is reasonable in that, in general, $K_{ID}(0) < K_{Ic}$. However, the K_{Ic} values established for 4340 steel are not as high as 108 $MPam^{1/2}$. Hence, in this respect, the analysis was not truly a predictive application phase analysis. Rather, it was a combination of generation phase (for initiation) and application phase (for propagation) analyses.

If the plastically deformed region is both small and confined to the crack tip region (i.e., if the small scale yielding condition is satisfied), an LEFM-based prediction should be accurate. The difference between the K_I value required for initiation in the quasi-statically loaded three-point bend specimen and accepted K_{Ic} values for the 4340 steel used in these experiments (typically, about 70-80 $MPam^{1/2}$), indicates that other energy losses may be

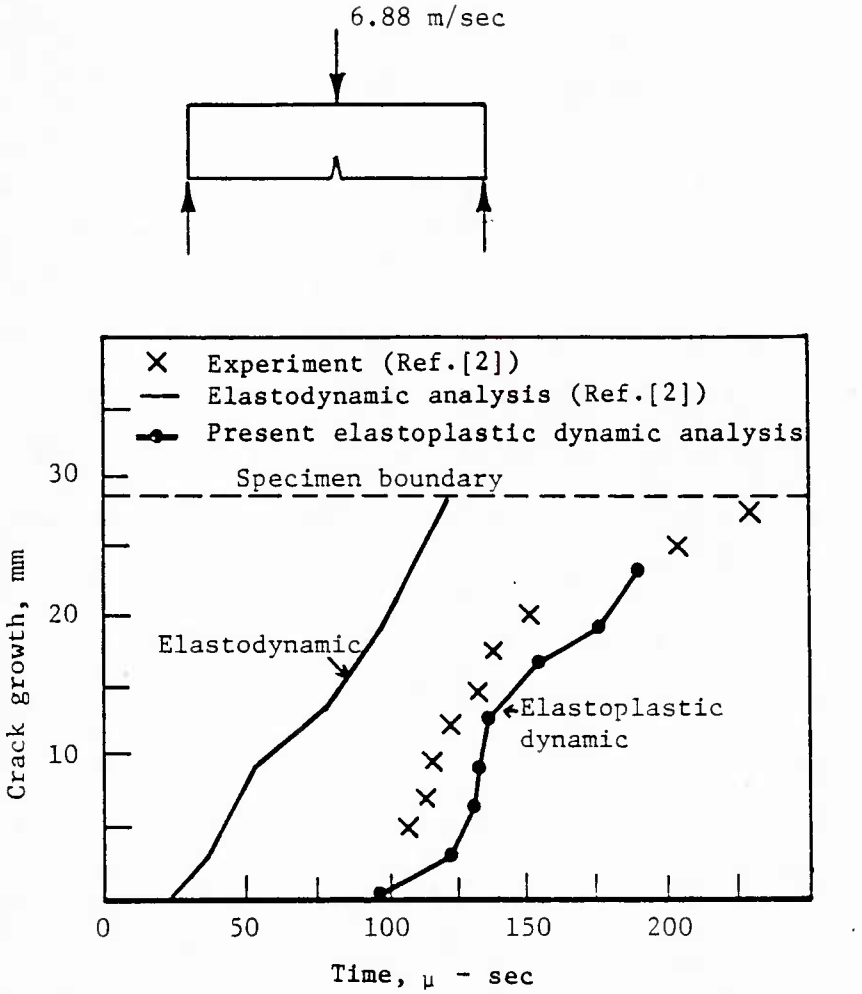

Figure 10. Application phase analysis using 25% side grooved AISI 4340 three point bend specimen.

involved. A detailed study of the elastic-plastic analysis results identified the source of these losses. This result for plane stress is shown in Figure 11(a). It can be seen that, while the crack tip plastic zone is relatively small, there is a sizeable plastically deformed region close to the load application point. (The presence of this plastic deformation is also recognizable on the fracture surface of the specimens used in the experiments.) It must be concluded that this load point plastic zone, which violates the small scale yielding assumption and is therefore unamenable to LEFM, must be the source of disparity between experimental results and elastodynamic analysis prediction.

The plastic deformation zones at the instant of crack initiation under impact loading are shown in Figure 11(b). It can be seen that, while the crack tip plastic zone size is roughly the same as in Figure 11(a), the load point plastic zone is somewhat larger. However, this result can only be accepted with caution in that the analysis ignored strain rate effects. Even though AISI 4340 steel is relatively strain rate insensitive, it is still possible that the impact loading rate raises the yield strength of the material, thus resulting in a smaller plastic zone.

It should be recognized that, for a distributed loading as in blast loading conditions, there will be no comparable energy loss. A problem with blast loading was therefore attempted. It was found that the size of the crack tip plastic zone at initiation is very similar to those of the other cases shown in Figure 11, indicating that the value of the fracture parameter for initiation would be roughly the same in all three instances. This, of course, is a comforting result in view of the virtual strain rate independence of 4340 steel. The absence of remote plastic deformation in the blast loading case

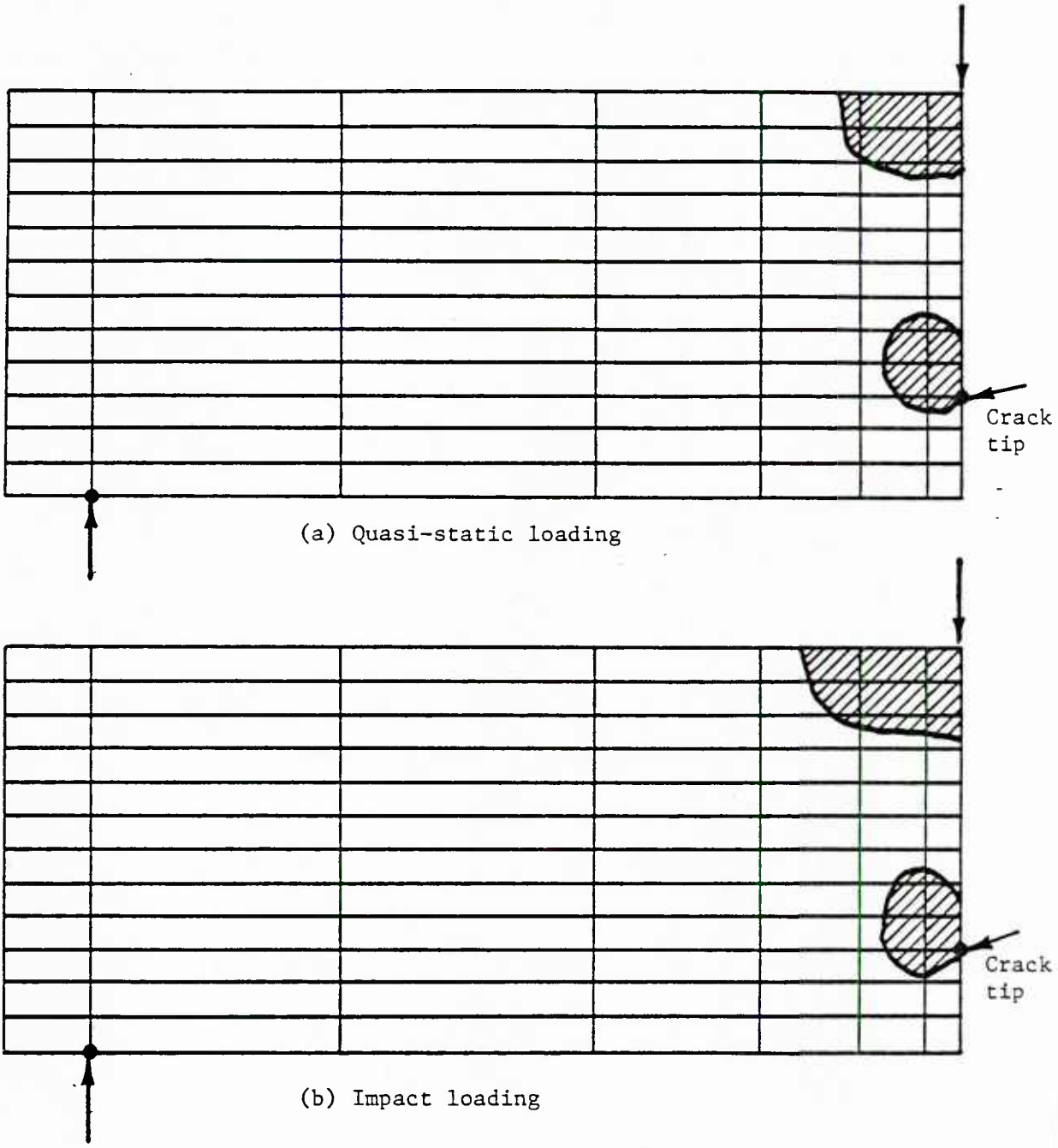

Figure 11. Comparison of plastic zone sizes at crack initiation under the two loading conditions considered.

also suggests that an elastodynamic treatment would be appropriate, and this was indeed found to be so.

CONCLUSIONS

The work described in this paper has resolved a dichotomy concerning the uniqueness of the K_{ID} parameter for characterizing rapid crack propagation and arrest. This was accomplished through the application of a dynamic elastic-plastic analysis procedure. This application revealed that significant plastic deformation can be introduced through the loading procedure. This can confound a strictly linear elastic interpretation of the experimental results even though small-scale yielding conditions are valid at the crack tip. Accounting for the energy dissipated remotely through the use of the dynamic elastic-plastic analyses is therefore essential in such circumstances.

Besides demonstrating the role of plastic deformation in impact loaded fracture experiments, the present work has identified, possibly for the first time, the validity of a critical CTOD (or, equivalently, a CTOA) as a rapid crack propagation criterion. While further work is needed to investigate the possible geometry and crack velocity dependence of the critical CTOD, the result shown in Figure 9 is of clear practical importance. If a constant critical CTOA is the elastic-plastic dynamic crack propagation criterion, a myriad of practical problems so far unamenable to accurate analysis may be addressed. Examples are crack arrest and reinitiation under high upper shelf toughness conditions in nuclear pressure vessel steels, welded ship hull structures and storage tanks, and gas transmission pipelines.

ACKNOWLEDGEMENTS

The research described in this paper was supported by the Structural Mechanics Program of the Office of Naval Research under Contract No. N00014-77-C-0576. The authors would like to express their appreciation to Dr. Yapa Rajapakse of ONR for his encouragement of this work.

REFERENCES

1. Kanninen, M. F., "Whither Dynamic Fracture Mechanics", Numerical Methods in Fracture Mechanics, D.R.J. Owen and A. R. Luxmoore, editors, Pineridge Press, Swansea, United Kingdom, 1980.

2. Kanninen, M. F., Gehlen, P. C., Barnes, C. R., Hoagland, R. G., Hahn, G. T., and Popelar, C. H., "Dynamic Crack Propagation Under Impact Loading", Nonlinear and Dynamic Fracture Problems, N. Perrone, et al., editors, ASME AMD Vol. 35, 1979.

3. Ahmad, J., Jung, J., Barnes, C. R., and Kanninen, M. F., "Elastic Plastic Finite Element Analysis of Dynamic Fracture", Engrg. Fract. Mech., Vol. 17, No. 3, 1983.

4. Ahmad, J., Barnes, C. R., and Kanninen, M. F., "An Elastoplastic Finite Element Investigation of Crack Initiation Under Mixed Mode Static and Dynamic Loading", second ASTM International Symposium on Elastic Plastic Fracture Mechanics, Philadelphia, 1981, to appear in STP.

5. Jung, J., Ahmad, J., Kanninen, M. F., Popelar, C. H., "Finite Element Analysis of Dynamic Crack Propagation", ASME Conference on Failure Prevention and Reliability, 1981.

6. Nishioka, T., Perl, M., and Atluri, S. N., "An Analysis of, and Some Observations on, Dynamic Fracture in an Impact Test Specimen", ASME Paper 81-PVP-18, March, 1981.

7. Kobayashi, A. S., Department of Mechanical Engineering, University of Washington, Seattle, Washington, private communications, 1982.

8. Kishimoto, K., Aoki, S., and Sakata, M., "On the Path Independent Integral J", Engr. Fract. Mech., Vol. 13, p. 841-850, 1980.

9. Rice, J. R., "A Path Independent Integral and the Approximate Analysis of Strain Concentration by Notches and Cracks", Trans. ASME, J. Appl. Mech., June, 1968.

10. Freund, L. B., "Energy Flux into the Tip of an Extending Crack in an Elastic Solid", J. Elasticity, Vol. 2, p. 341-349, 1972.

11. Hellen, T. K., and Blackburn, W. S., "The Calculation of Stress Intensity Factors for Combined Tensile and Shear Loading", Int. J. Fracture, Vol. 11, No. 4, 1975.

12. Neale, B. K., "Elastic Plastic Analysis of Cracked Bodies Using the J-Integral Method", CEGB, Rep. No. RD/B/N3253, Berkely, U.K., 1975.

13. Bergez, D., "Linear Elastic Fracture Mechanics Applied to Cracked Plates and Shells", Int. J. Fract., Vol. 12, No. 4, August, 1976.

14. Bui, H. E., "Stress and Crack-Displacement Intensity Factors in Elastodynamics", ICF4, Waterloo, Canada, Vol. 3, 1977.

15. Wilson, W. K., and Yu, I. W., "The Use of J-Integral in Thermal Stress Crack Problems", Int. J. Fract., Vol. 15, No. 4, August, 1979.

16. Ahmad, J., Jung, J., Barnes, C. R., and Kanninen, M. F., "The Development of a Dynamic Elastoplastic Finite Element Analysis for Fast Fracture Under Impact Loading", ASME PVP Conference, Denver, June, 1981.

17. Hoff, R., Rubin, C. A., and Hahn, G. T., "Strain Rate Dependence of the Deformation at the Tip of a Stationary Crack", Sixteenth ASTM National Symposium on Fracture Mechanics, Columbus, Ohio, 15-17 August 1983.

18. Brickstad, B., "A Viscoplastic Analysis of Rapid Crack Propagation Experiments in Steel", J. Mech. Phys. Solids, Vol. 31, No. 4, p. 307-327, 1983.

19. Atluri, S. N., "Path Independent Integrals in Finite Elasticity and Inelasticity, with Body Forces, Inertia, and Arbitrary Crack Face Conditions", Rep. No. 81-GIT-CACM-8, February, 1981, School of Civil Engineering, Georgia Institute of Technology, Atlanta, GA.

20. Dantam, V., and Hahn, G. T., "Definition of Crack Arrest Performance of Tough Alloys", Fracture Tolerance Evaluation, Kanazawa, et al., editors, Toyoprint Co. Ltd., Japan, 1982.

21. Achenbach, J. D., Kanninen, M. F., and Popelar, C. H., "Crack Tip Fields for Fast Fracture of Elastic Plastic Material", J. Mech. Phys. Solids, Vol. 29, p. 211, 1981.

22. Freund, L. B. and Douglas, A. S., "The Influence of Inertia on Elastic Plastic Anti-plane Shear Crack Growth", J. Mech. Phys. Solids, Vol. 30, p. 59, 1982.

23. Kanninen, M. F., Popelar, C. H., and Broek, D., "A Critical Survey on the Application of Plastic Fracture Mechanics to Nuclear Pressure Vessel and Piping", Nuclear Engineering and Design, Vol. 67, p. 27-55, 1981.

24. Dugdale, D. S., "Yielding of Steel Sheets Containing Slits", J. Mech. & Phys. of Solids, Vol. 8, p. 100, 1960.

25. Atkinson, C., and Kanninen, M. F., "A Simple Representation of Crack Tip Plasticity: The Inclined Strip Yield Model", Int. J. Fract., Vol. 13, p. 151, 1977.

26. Rice, J. R., "Plastic Yielding at a Crack Tip", Proc. First Int. Conf. on Fracture, Vol. 1, Sendai, September 12-17, 1965, Japanese Society for Strength and Fracture of Materials, Tokyo, pp. 283-308, 1966.

27. Tada, H., Paris, P. C., and Irwin, G. R., Stress Analysis of Cracks Handbook, Del Research Corp., Hellertown, PA, 1973.

DYNAMIC CRACK PROPAGATION THROUGH WELDED HY80 PLATES UNDER BLAST LOADING

C. R. BARNES

J. AHMAD*

M. F. KANNINEN*

Battelle Columbus Laboratories

505 King Avenue

Columbus, Ohio 43201

27 August 1983

Manuscript prepared for presentation at the Sixteenth National Symposium on Fracture Mechanics, Columbus, Ohio, 15-17 August 1983, and for publication in the symposium proceedings.

* Present address: Southwest Research Institute, San Antonio, Texas 78284

SECURITY CLASSIFICATION O S PAGE *(When Data Entered)*

REPORT DOCUMENTATION PAGE

READ INSTRUCTIONS BEFORE COMPLETING FORM

1. REPORT NUMBER

2. GOVT ACCESSION NO.

3. RECIPIENT'S CATALOG NUMBER

4. TITLE *(and Subtitle)*

Dynamic Crack Propagation Through Welded HY80 Plates Under Blast Loading

5. TYPE OF REPORT & PERIOD COVERED

Interim

6. PERFORMING ORG. REPORT NUMBER

7. AUTHOR(s)

C. R. Barnes, J. Ahmad, and M. F. Kanninen

8. CONTRACT OR GRANT NUMBER(s)

N00014-77C-0576

9. PERFORMING ORGANIZATION NAME AND ADDRESS

Battelle Columbus Laboratories
Columbus, Ohio 43201

10. PROGRAM ELEMENT, PROJECT, TASK AREA & WORK UNIT NUMBERS

11. CONTROLLING OFFICE NAME AND ADDRESS

Office of Naval research
Structural Mechanics Program
Departmnet of the Navy, Arlington, Virginia 22217

12. REPORT DATE

August 27, 1984

13. NUMBER OF PAGES

29

14. MONITORING AGENCY NAME & ADDRESS*(if different from Controlling Office)*

15. SECURITY CLASS. *(of this report)*

unclassified

15a. DECLASSIFICATION DOWNGRADING SCHEDULE

16. DISTRIBUTION STATEMENT *(of this Report)*

Approved for public release; distribution unlimited.

17. DISTRIBUTION STATEMENT *(of the abstract entered in Block 20, if different from Report)*

18. SUPPLEMENTARY NOTES

Manuscript prepared for presentation at the Sixteenth National Symposium on Fracture Mechanics, Columbus, Ohio, 15-17 August 1983, and for publication in the proceedings.

19. KEY WORDS *(Continue on reverse side if necessary and identify by block number)*

elastic-plastic fracture mechanics
crack propagation and arrest
dynamic
blast loading
ductile
weldment
plastic deformation

20. ABSTRACT *(Continue on reverse side if necessary and identify by block number)*

A systematic approach involving experimental and dynamic elastic plastic finite element analyses was persued to investigate the problem of crack initiation, propagation, and arrest in weldments subjected to rapidly applied loading. The experimental effort included residual stress measurements on HY80 welded HY80 steel specimens together with a series of explosive loading experiments performed after precracking these specimens. Using data from these tests as initial conditions, dynamic elastic-plastic and elastic-thermoplastic computaitons were made to predict crack initiation and growth

DD FORM 1 JAN 73 1473

unclassified

SECURITY CLASSIFICATION OF THIS PAGE *(When Data Entered)*

behavior under the measured explosive loading history. Reasonably good agreement between experimental data and those of the analysis was obtained. Of possible greater significance for subsequent fracture mechanics analyses of weld defect problems, it was found that the presence of weld-induced residual stresses strongly affects the prediction of the crack length at arrest.

ABSTRACT

A systematic approach involving experiments and dynamic elastic-plastic finite element analyses was pursued to investigate the problem of crack initiation, propagation, and arrest in weldments under rapidly applied loading. The aim was to develop a predictive capability that can be used to assess the risk of fracture in welded structures subjected to blast loading. The experimental effort included residual stress measurements on welded HY80 steel specimens together with a series of explosive loading experiments performed after precracking these specimens. Measurements were made of the time of crack growth initiation and on the extent of crack growth at arrest. Elastic-thermoplastic finite element computations were made to obtain the weld-induced residual stresses. With these as initial conditions, dynamic elastic-plastic computations were then performed to predict crack initiation and growth behavior under the measured explosive loading history. These computations used estimates of the running fracture toughness based on fracture toughness data for HY-80 weldments available in the literature. Reasonably good agreement was nevertheless obtained with the observed results. Of possible greater significance for subsequent fracture mechanics analyses of weld defect problems, it was found that the presence of weld-induced residual stresses strongly affects the prediction of the crack length at arrest.

Key Words: dynamic fracture, crack arrest, explosive loading, residual stresses, HY80 steel, HY80 weldments.

DYNAMIC CRACK PROPAGATION THROUGH WELDED HY80 PLATES UNDER BLAST LOADING

by

C. R. Barnes, J. Ahmad and M. F. Kanninen

INTRODUCTION

Elastic-plastic fracture mechanics techniques are now being widely pursued for materials that are ductile and tough. The research reported in this paper extends these developments to provide the basis for elastic-plastic fracture mechanics treatments under dynamic conditions. The work specifically considers the possibility of the arrest of the unstable crack propagation event that results from fracture instability in the weldment of a ductile material subjected to a rapidly applied loading.

There is considerable practical interest in studying the behavior of cracks in rapidly loaded structures. An example application is a flawed ship structure subjected to a blast load. In such situations it is important to know whether a flaw of the size likely to be present in the structure would become unstable and, if so, whether it would arrest before catastrophic fracture occurs. For structures made of high toughness materials where considerable crack tip plastic deformation precedes crack initiation, the analysis problem is nonlinear. In addition, because the loading rates can be very high, and also because cracks may propagate at relatively high rates, conventional quasi-static fracture mechanics treatments are generally not applicable. A dynamic elastic-plastic fracture mechanics approach is therefore needed.

A further complicating feature admitted in this work arises from the fact that most structural defects reside in and around welds. In addition to producing defects, the welding process introduces substantial localized changes in material properties and further gives rise to thermally-induced residual stresses. Reliable elastic-plastic dynamic fracture mechanics techniques for predicting crack initiation, growth, and arrest of cracks residing in and around welded regions treating these complications do not currently exist. In order to develop such techniques, a step wise procedure has been followed by the authors [1-6]. The early work was primarily focused on identifying the appropriate criterion for rapid crack growth. Following a brief description of the previous research that has led to the current stage of development, this paper describes a combined experimental and computational approach specifically addressing the fracture of HY80 steel weldments subjected to explosive loading.

BACKGROUND

Investigation of rapid crack propagation and arrest in the welds of rapidly loaded structures requires a two-fold extension of current elastic-plastic fracture mechanics (EPFM) techniques. As described by Kanninen et al [7], most current efforts in EPFM are focused on the application of the J-resistance curve to predict crack initiation and fracture instability. However, this criterion is limited to small amounts of stable crack growth and quasi-static conditions. In the original derivation of J by Rice [8], the material was taken to be nonlinear elastic. This excludes the effect of the elastic unloading that occurs in the wake of an extending crack. Furthermore, inertia forces, body forces, and initial strains were not considered. Consideration of dynamic loading, rapidly propagating cracks, thermal gradients and residual stresses are therefore excluded from the original formulation.

A number of path independent integrals now exist [9-17] that, like J, are measures of energy flow rate to the crack tip, but are applicable to more general conditions; e.g., dynamic loading, thermal strains, mixed mode loading. Possibly the most general of these formulations is that developed by Kishimoto et al. [17]: the $\hat{J}$ integral. This formulation contains several other extensions of J as special cases. Of more significance, Ahmad et al. [18] have reported experimental and corresponding finite element analysis results to show that $\hat{J}$ provides a realistic criterion for crack initiation under dynamic loading in elastic-plastic conditions.

For rapidly propagating cracks, $\hat{J}$ is still a useful parameter. For elastodynamic treatments, it provides a convenient means to compute dynamic stress intensity factors without the need for movable singular elements or periodic remeshing of the finite element model. But, in elastic-plastic dynamic crack propagation, $\hat{J}$ suffers from the same limitations as J. It loses its path independent character as well as its meaning as a measure of the energy release rate.

The identification of a characterizing parameter for large amounts of crack growth in elastic-plastic conditions is a problem that is currently being addressed by several different investigators. Nishioka and Atluri [19] are pursuing an incrementally computed parameter that maintains the path-independent feature of J for elastic-plastic dynamic crack propagation. However, their approach is complicated and, in addition, critical material-property values of their parameter have not yet been determined for practical applications. Ernst [20] has proposed a modified version of J that allows for extended crack growth while Freund and Douglas [21] simply employ a critical strain criterion. But, both of these may well be related to an alternative crack tip parameter: the crack opening angle (CTOA). A number of investigators have found that this parameter remains constant during elastic-plastic stable crack growth -- see reference [7]. This fact, together with its ease of application, strongly suggests that the CTOA be explored for dynamic crack propagation also.

Because the CTOA is not feasible as an initiation parameter, an expedient such as the dual J/CTOA approach suggested by Kanninen et al. [22] could be implemented. Emery et al. [23] have pursued a similar approach in which, following initiation, they <u>assumed</u> that a constant CTOA value governs rapid crack propagation in their elastic-plastic finite difference

computations for pipes. However, previous to the recently completed work of Ahmad et al. [24], the constancy of the CTOA during rapid crack propagation has not been demonstrated. This key result is shown in Figure 1.

The result shown in Figure 1 was obtained by performing a "generation phase" finite element analysis of a fracture experiment. In the experiment an AISI 4340 steel three-point-bend specimen was quasi-statically loaded to initiate rapid crack propagation. In the companion dynamic elastic-plastic finite element analysis, the crack was made to propagate according to the experimentally measured crack length history. The CTOA values were then obtained from the finite element solution. As shown in Figure 1, these values are based on the crack tip opening displacement (CTOD) values at one element length behind the crack tip, determined at the first instant of node release. It can be seen that, following an initial transient, the CTOA remains virtually constant throughout the rest of the crack growth process. This result reveals - possibly for the first time - that a near constant CTOA value can be used as a criterion for rapid crack propagation.

The region in which the CTOA varies may be a transition region between $\hat{J}$-controlled and CTOA-controlled crack growth. The characterization of crack growth in this region needs to be further investigated. But, for the present work, a simple form of a dual $\hat{J}$/CTOA criterion is used in which a critical $\hat{J}$ value governs initiation and a constant CTOA controls the ensuing rapid propagation. It will further be assumed that the material property values needed to use this criterion can (1) be inferred from measurements made under small-scale yielding conditions, and (2) be directly applied to crack propagation through a weldment with residual stresses and high applied loads. The results of the study, of course, will depend upon these heuristic assumptions.

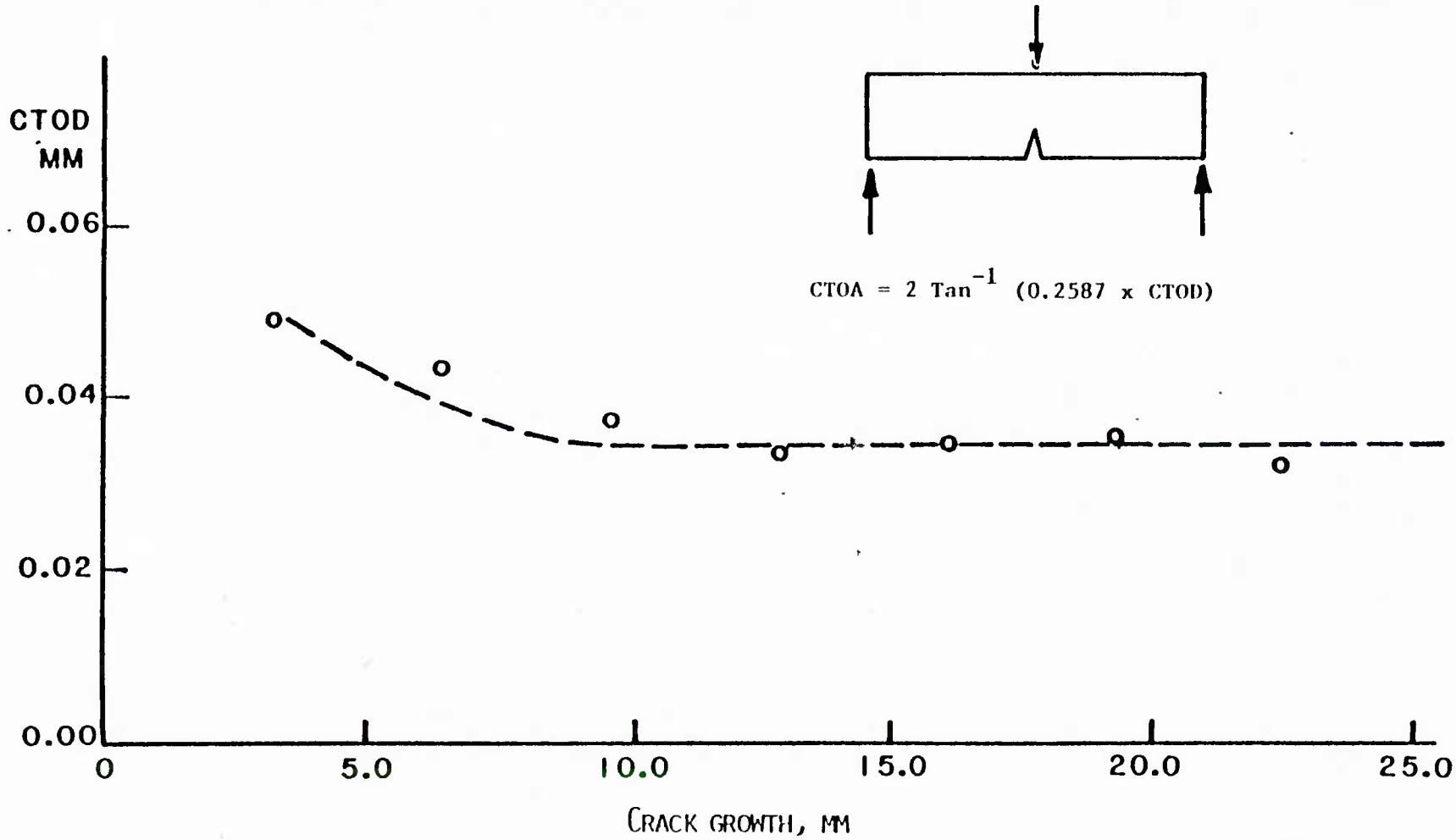

FIGURE 1. CRITICAL CRACK TIP OPENING DISPLACEMENT VALUES INFERRED FROM AN ELASTIC-PLASTIC DYNAMIC ANALYSIS OF DYNAMIC CRACK PROPAGATION IN A SIDE GROOVED AISI 4340 STEEL BEND SPECIMEN SUBJECTED TO A QUASI-STATIC LOAD

EXPERIMENTAL PROCEDURE

The crack initiation and propagation characteristics of engineering structural weldments invariably differ from those of the base material. This is due primarily to the effects of residual stresses induced by the welding process coupled with weld metal inhomogeneity. Although the degree of material inhomogeneity is difficult to quantify, the residual stresses can be estimated. Consequently, as a first step, following the preparation of the welded HY80 specimens, four of these were sacrificed to obtain weld residual stresses. These determinations were made using the trepanning technique.

The trepanning technique involves the removal of a prism-shaped element of material under a biaxial strain gage applied to the surface of a welded specimen. Upon removal, these gages no longer sense the stresses at that location. Hence, the resulting change in strain is taken to be indicative of the magnitude of the residual stresses that were present at the gage position. Figures 2 and 3 show the gage locations for two sets of residual stress determinations. Figure 4 shows a typical element taken from one of these specimens. The residual stress values obtained in this way are given below.

The next step in the experimental effort was to precrack and instrument the remaining specimens, then subject them to blast loading. The precrack was sharpened by EDM to a total depth of 8mm. The specimen thickness was 25.4 mm. The blast load was provided by a 2.27 kg charge of composition C-4 explosive. The explosive was detonated from a 38 cm standoff, as measured from the center of the charge to the upper specimen surface. The test configuration is shown in Figure 5. An expanded view of the loading fixture is contained in Figure 6. Figure 7 shows the post-test appearance of a welded specimen.

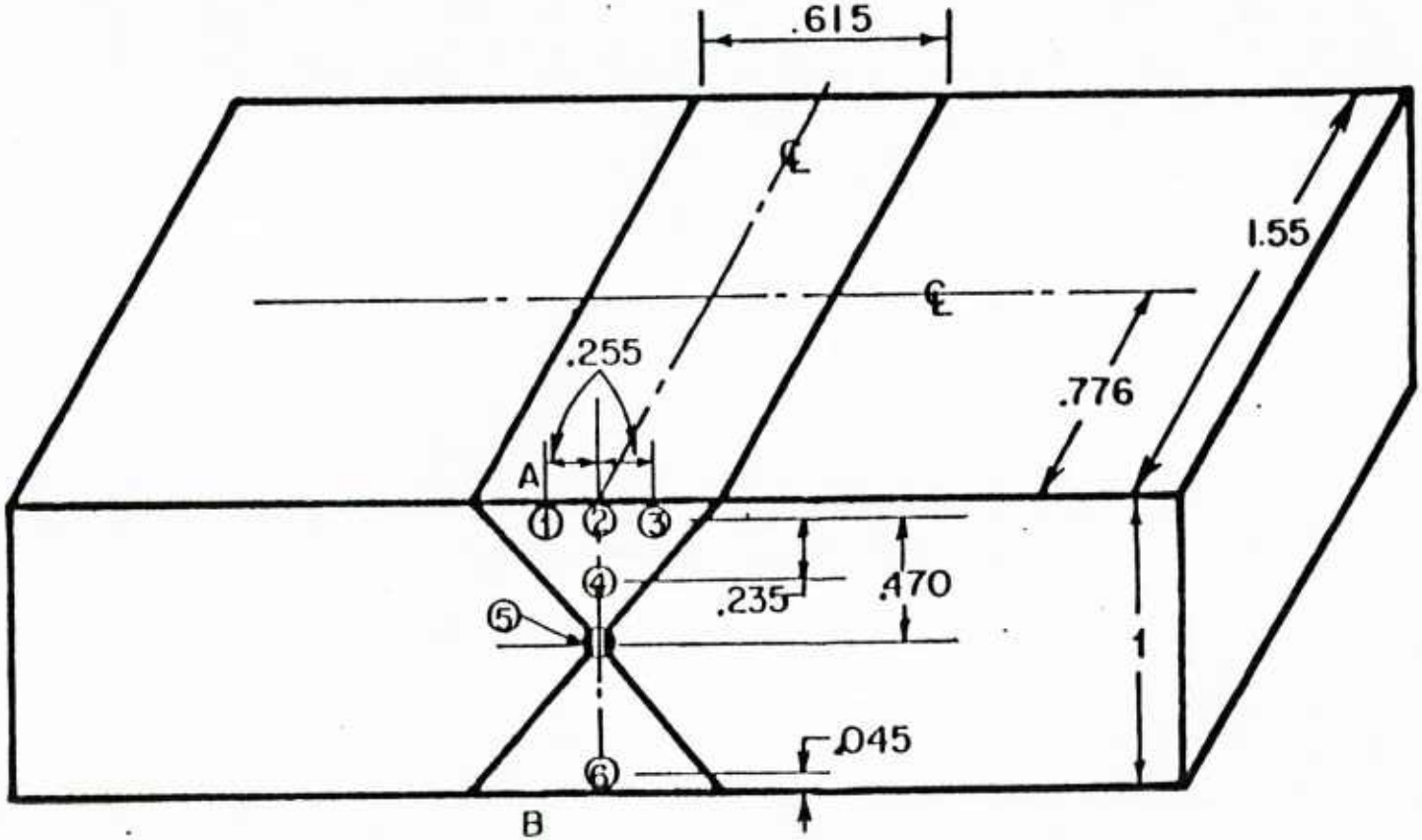

FIGURE 2. STRAIN GAGE LOCATIONS FOR FIRST SERIES OF RESIDUAL STRESS DETERMINATIONS

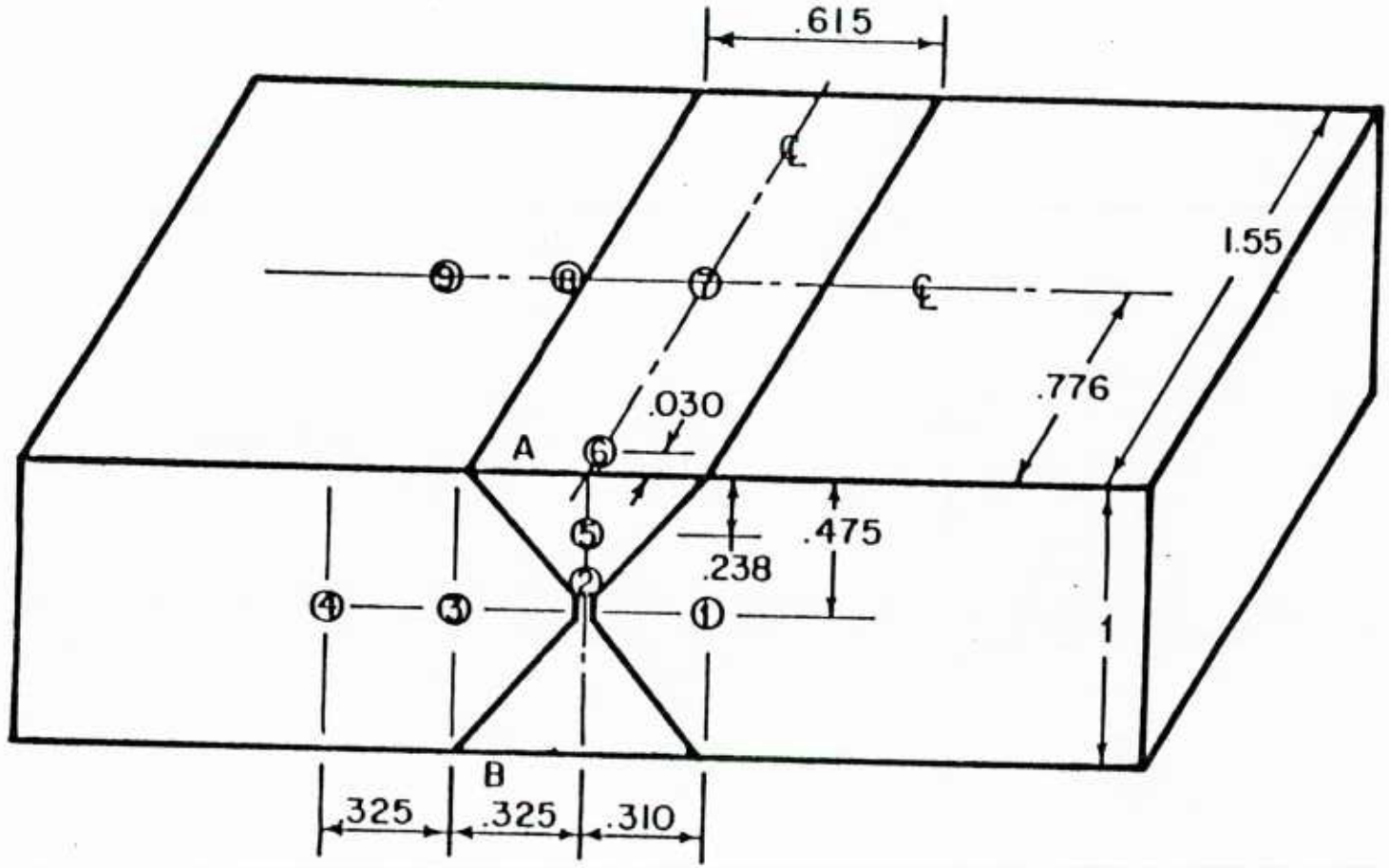

FIGURE 3. STRAIN GAGE LOCATIONS FOR SECOND SERIES OF RESIDUAL STRESS DETERMINATIONS

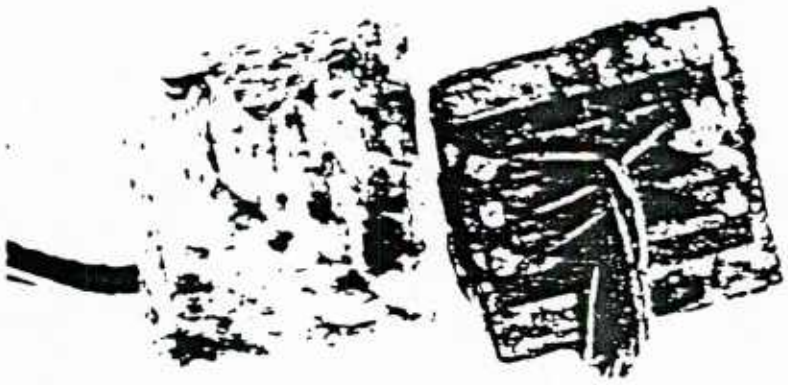

(A) (B)

FIGURE 4. TREPANNING ELEMENT:
(A) Bottom surface of residual stress chip
(B) Top surface showing biaxial strain gage

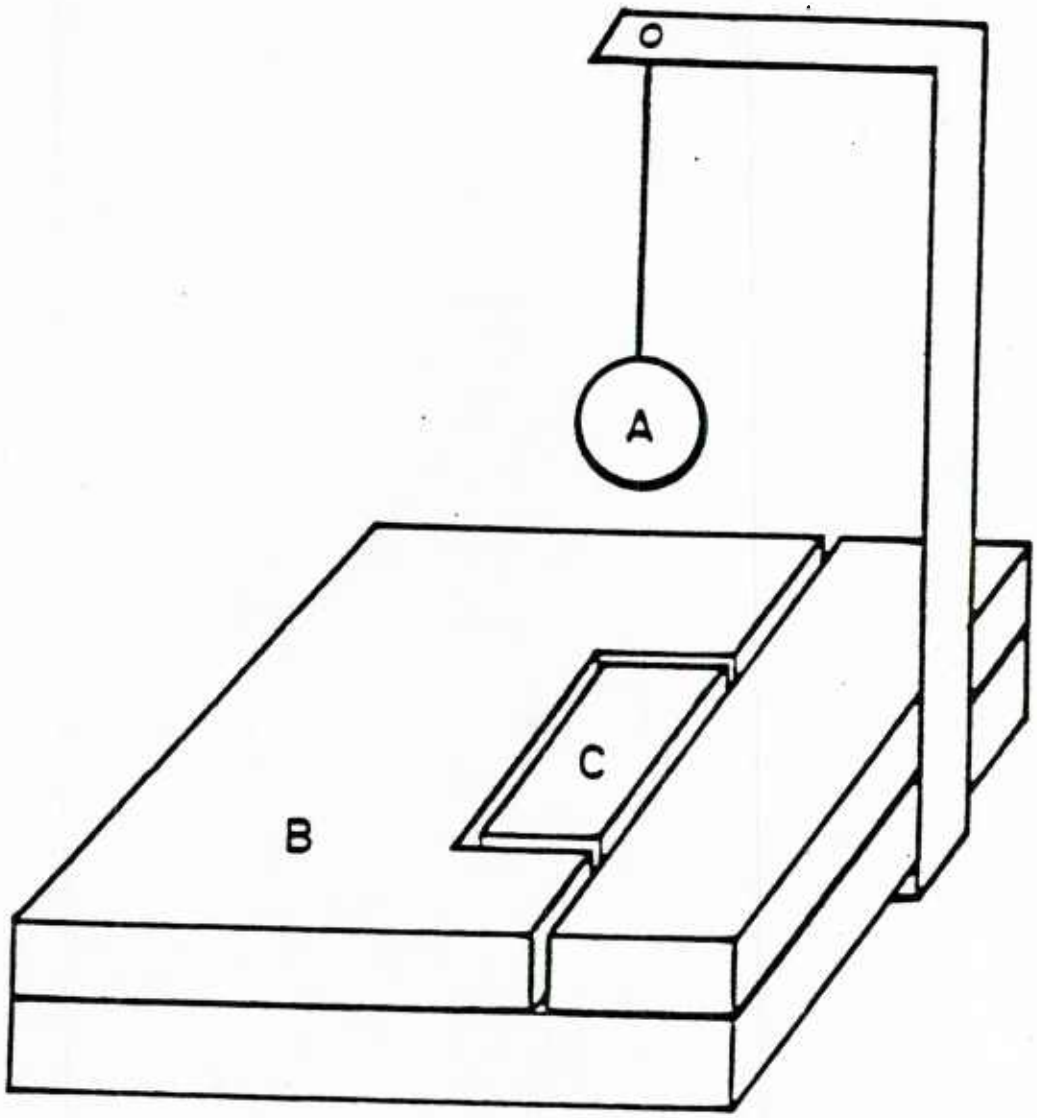

FIGURE 5. SPECIMEN LOADING FIXTURE USED DURING BLAST LOADING EXPERIMENTS (A) is the explosive charge, (B) is the loading fixture, and (C) is the specimen.

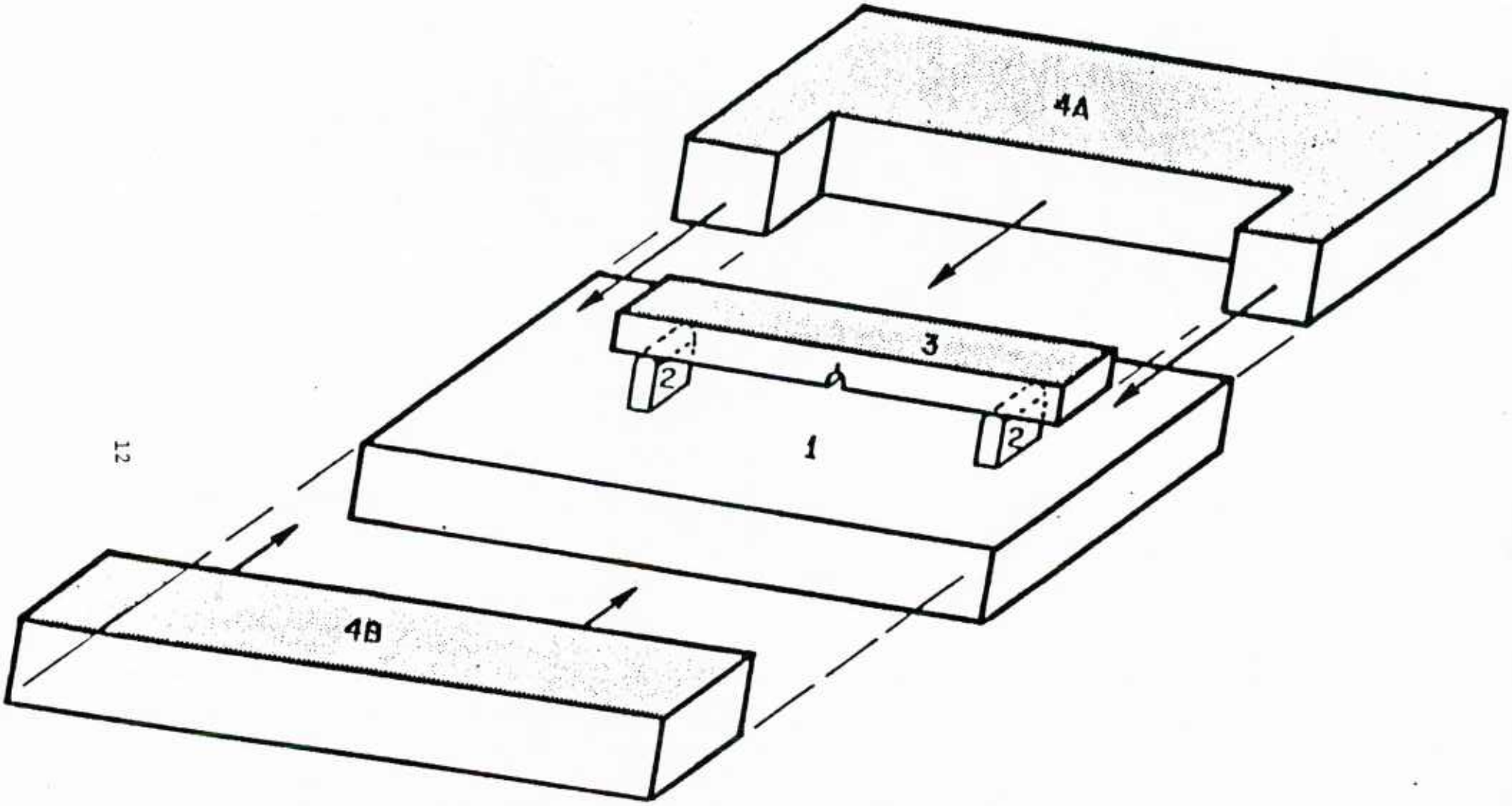

FIGURE 6. EXPANDED REPRESENTATION OF BLAST LOADING FIXTURE
1) Base Plate, 2) Supports, 3) Specimen, 4) Specimen encompassing plates to minimize gas blow by.

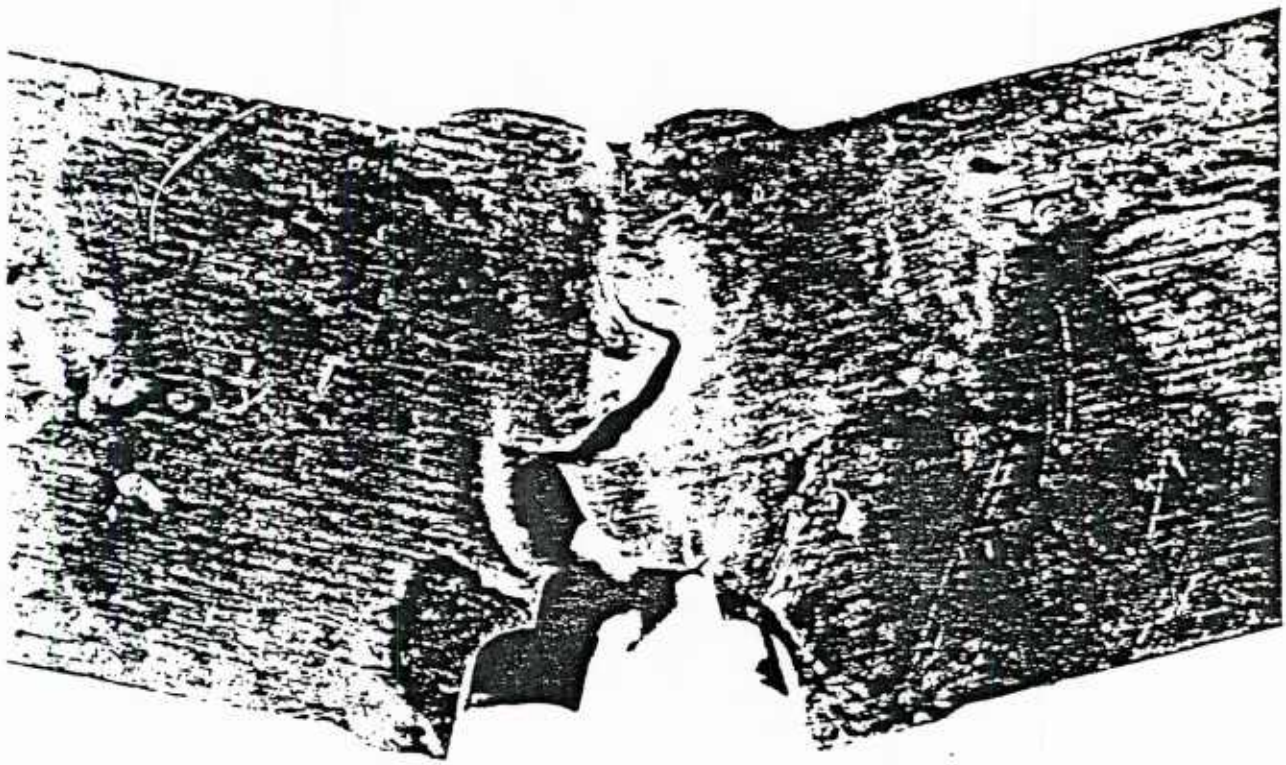

FIGURE 7. POST TEST APPEARANCE OF HY80 WELDED SPECIMEN SHOWING BLAST INDUCED CRACK GROWTH

Each test specimen was instrumented with strain gages to provide the times of crack initiation, propagation, and complete specimen fracture. A diagram of the specimen with these strain gage locations shown is contained in Figure 8. In addition to the strain gages, the specimens were also instrumented to provide an additional indication of time at complete specimen fracture. This was done by integrating the specimen into a simple electrical circuit. In essence, the specimen initially was part of a closed circuit. But, because complete specimen fracture produces an open circuit, a readily detected sharp voltage change is produced. In this way, the time of complete fracture, should it occur, could be accurately determined. A similar concept was used to determine the time of blast arrival on the specimen surface.

To record the output from the specimen instrumentation during blast loading, a redundant systems approach was adopted. Data was recorded using two transient recorders backed up by a high speed FM tape deck. All systems shared a common signal so that the data from each system could be related in real time. Data were recorded on the times of blast arrival, crack mouth gage failure, side gage failure, back gage failure and complete specimen fracture. The development of measurement procedures that retain their integrity under blast loading is felt to be a major accomplishment of this work.

For a 4340 steel monolithic specimen used as a trial, the crack mouth gage indicated a crack initiation time of 20 to 29 μs after the blast arrival, with total fracture, as indicated by the upper surface gage, at 71 μs after blast arrival. These readings correspond to an average crack speed of 374 m/s. This is consistent with the crack speeds observed in the 4340 steel fracture experiments conducted earlier with other loading mechanisms. This suggests that these data are reliable. Offsetting this encouraging finding, the side

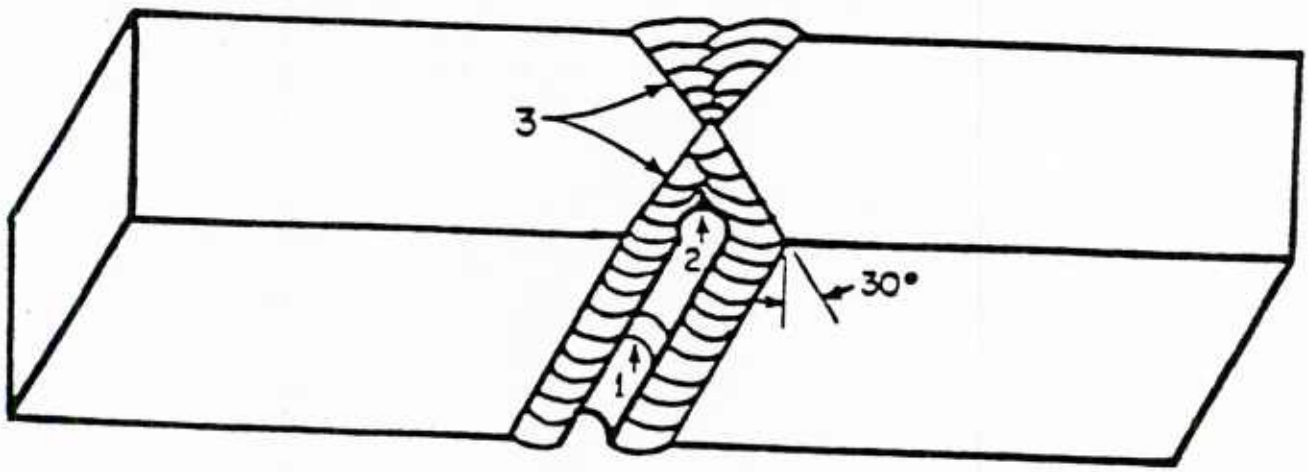

FIGURE 8. SPECIMEN USED FOR BLAST INDUCED FRACTURE
1) Strain gage mounted within notch, 2) EDM Notch, 3) Weld zone (typical of an 18 pass butt-weld in an HY-80 Steel Ship Structure), 4) An additional gage is also bonded to the specimen upper surface to indicate complete specimen fracture

gage and the battery circuit gave readings of 110 μs and 125 μs, respectively. These are obviously contradictory. In view of the fact that the surface gages are highly susceptible to blast and heat effects while the side gage reading will lag behind the crack passage by an indefinite time, these readings are not believed to be useful, therefore.

Three replicate experiments were conducted on HY80 welded specimens. One of these produced questionable results that were inconsistent with the other two, both in terms of the gage readings and the extent of crack propagation. Hence, these data are omitted. The results obtained from the remaining two specimens are shown in Table 1. It can be seen that the crack initiated (as indicated by the crack tip gage) at roughly 85μs and that crack arrest was achieved after a crack advance of about 14mm. Because fracture did not occur in these experiments, the upper surface gage readings are not believed to be significant.

Table 1

Experimental Results for Welded HY80 Blast Loaded Fracture Experiments(a)

Crack Lengths (mm)		Crack Extension	Time of Significant Gage Response After Arrival of Blast (μs)	
Initial	Final	(mm)	Crack Tip	Upper Surface
8.0	20.7	12.7	72-81	120
8.0	23.2	15.2	90-95	176

(a) Total specimen depth was 25.4 mm

CRACK PROPAGATION ANALYSIS

The analytical effort in this research consisted of two types of analyses, one providing the initial condition for the other. The first type was an elastic-thermoplastic finite element computation to obtain the residual stresses due to welding. The second type of analysis was the finite element solution for dynamic crack propagation under blast loading conditions. The modeling took the weld-induced residual stresses as initial conditions and included direct consideration of crack tip plasticity and of the inertial effects due both to dynamic loading and rapid crack propagation.

In all finite element computations, the equations of motion were solved using a displacement-based finite element method with an isoparametric element formulation and quadratic shape functions in a two-dimensional space. A singular element was not used. A modified Newton-Raphson approach was used for elastic-plastic analysis with the Von Mises yield condition and isotropic strain hardening assumed. The approach employed the implicit Newmark-Beta time integration scheme. Crack growth was modeled by releasing double-noded elements along a pre-set crack path. This was done by gradually releasing the crack tip nodes over several time steps.

The welding simulation computation was using the temperature-dependent material properties of HY80 steel. The heat input and weld-pass sequence used in the analysis were the same as in the actual welding process employed to fabricate the specimens. The multipass simulation of the process was performed as developed by Kanninen et al. [25]. The computed residual stress distribution across the weld centerline is shown in Figure 9.

Also shown in Figure 9 are the residual stresses at selected locations as deduced from experimental strain measurements by the trepanning method. While the agreement between the experimental and computed values

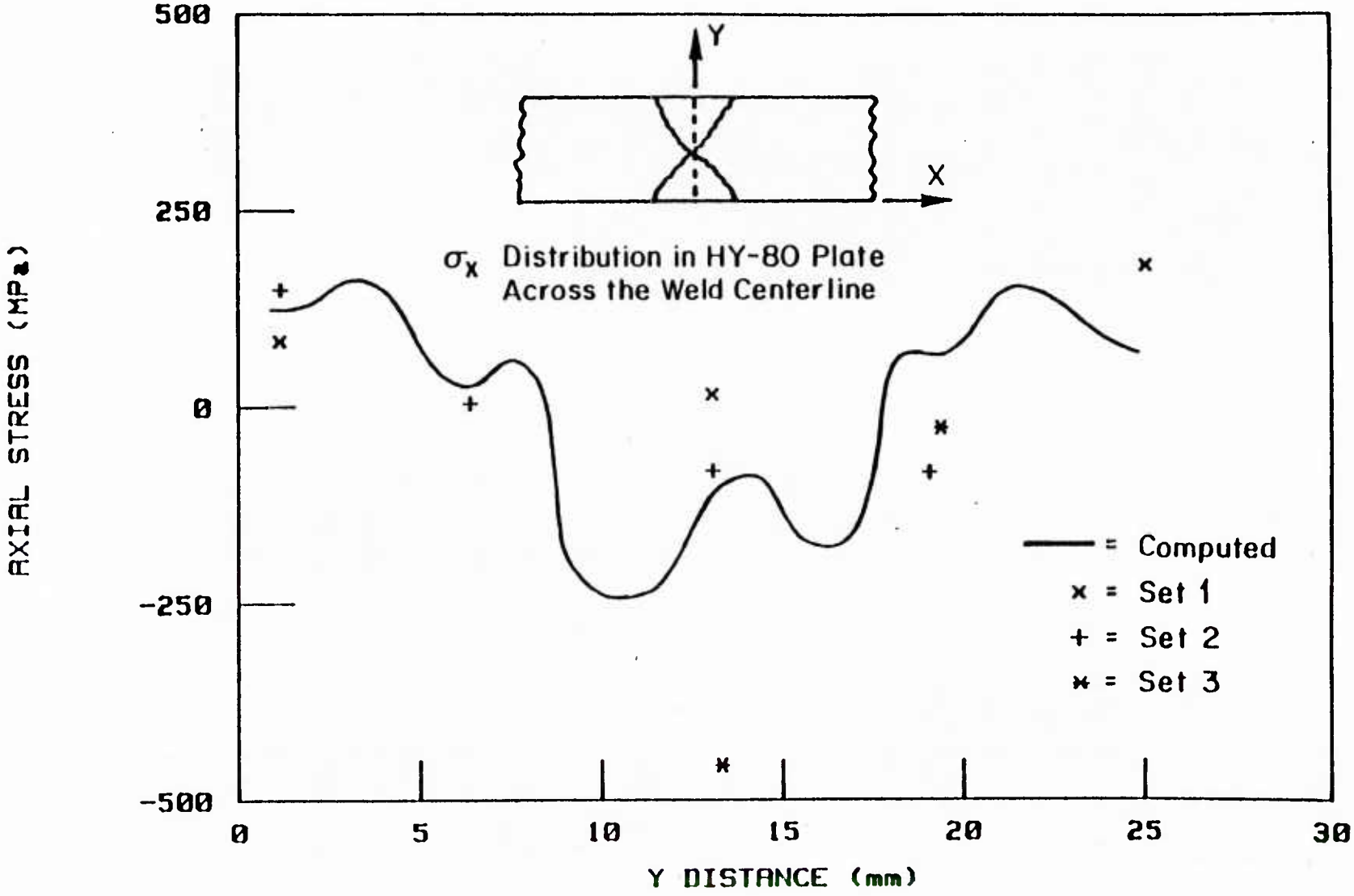

FIGURE 9. COMPARISON OF COMPUTED AND MEASURED WELD-INDUCED RESIDUAL STRESSES IN WELDED HY-80 SPECIMENS

shown in Figure 9 is less than perfect, the disparity is no greater than that between the measured values themselves. In any event, the computation does seem to predict the general trend of the data. Consequently, the residual stress distribution as computed by finite element method was accepted as the basis for further analyses.

To aid in the design of the blast loaded specimens, a preliminary elastodynamic finite element analysis was performed. The result is shown in Figure 10. The temporal pressure distribution used in this case was obtained by fitting a least-square curve through the experimentally-measured pressure-time record measured for a 2.27 kg explosive charge detonated at a distance of 38 cm from the specimen. This is

$$p(t) = 6.895\ (11.0 - .072t + .000062t^2)\ H(t)$$

where t is the time from the blast arrival (μs), p is the pressure exerted on the upper surface of the specimen (Mpa), and H is a function such that $H(t)=0$, $t < 0$, and $H(t) = 1$, $t > 0$. Note that the specimen configuration used in the blast loading experiments and analyses is also shown in Figure 10.

From the data collected by Hahn and Kanninen [26], the dynamic initiation toughness of an HY80 weld appears to be about 120 MPa$\sqrt{m}$. Using this number, the analysis shows that the crack should initiate at about 100 μ-sec following the arrival of the blast at the specimen surface. This was considered short enough for the experimental instrumentation to remain intact to detect the crack initiation time. Note that, in this preliminary computation, the effects of crack tip plasticity and residual stresses were totally ignored. The purpose was simply to get a rough estimate of the crack initiation time for pretest design purposes.

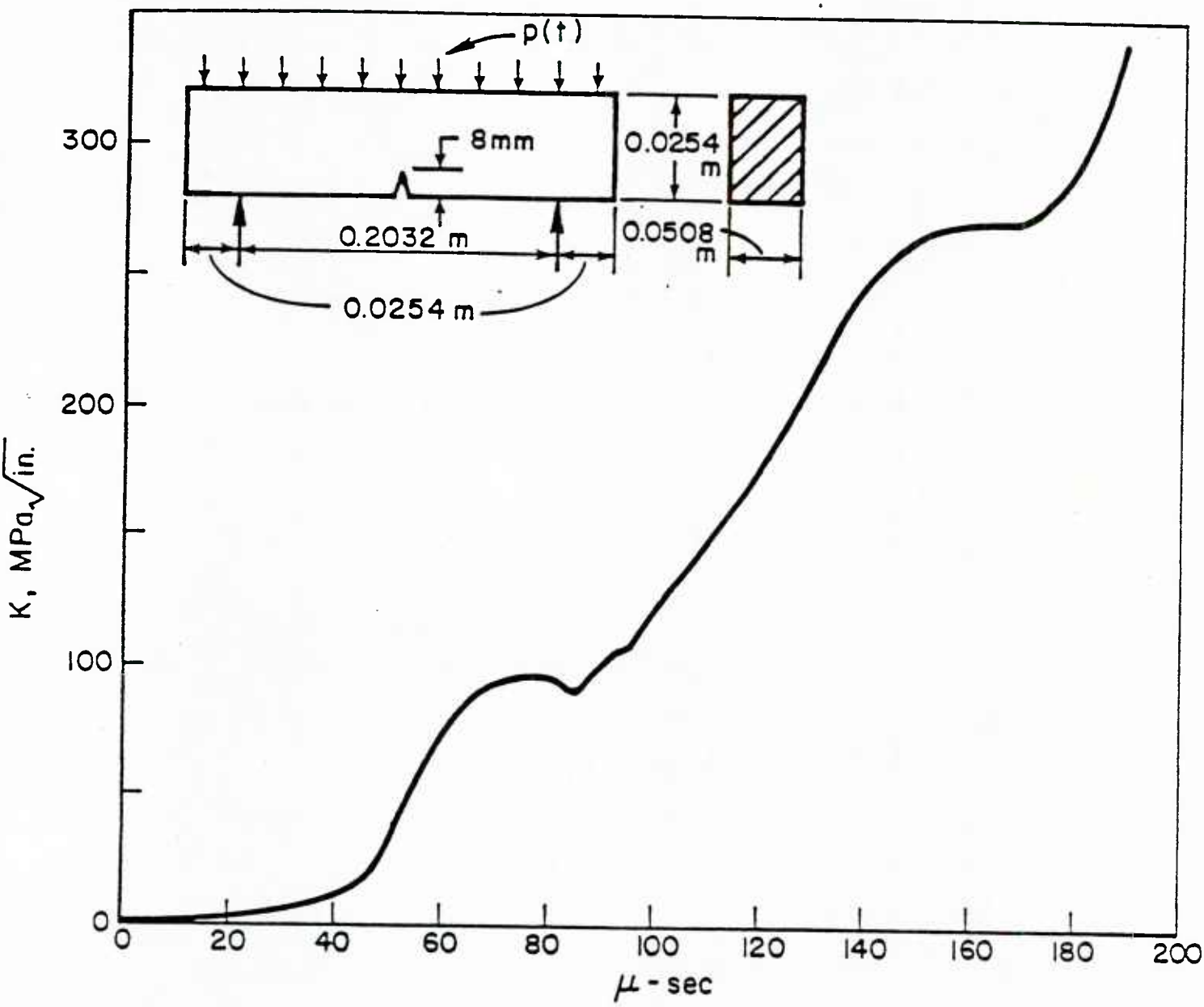

FIGURE 10. ELASTODYNAMIC COMPUTATION OF STRESS INTENSITY FACTOR AS A FUNCTION OF TIME FROM THE BLAST ARRIVAL

The next step in the analysis was to perform an elastic-plastic dynamic finite element analysis to predict the crack propagation history. The input to the finite element analysis included the temporal pressure distribution, the residual stress distribution, and critical CTOA values for crack initiation and propagation. Unfortunately, the fracture toughness values for a rapidly propagating crack in elastic-plastic conditions are not available. As an expedient, estimates were obtained from the existing linear elastic data, as follows.

From Hahn and Kanninen [26], the lower bound initiation toughness K_{Ic} and crack arrest toughness K_{Ia} for HY80 weldments were estimated at 120 MPa$\sqrt{m}$ and 92 MPa$\sqrt{m}$, respectively. It was then assumed that the dynamic fracture toughness K_{ID} is the same as K_{Ia}, and that K_{ID} is independent of crack velocity in the range of crack velocities expected in the experiment. Also, it was assumed that the lower bound K_{Ic} is the same as K_{Id}, the rapid loading fracture toughness. Using these values, the crack opening displacements at one element length (1.933mm) behind the crack tip were determined from an elastic-plastic finite element computation. For initiation and propagation, these were found to be 0.076 mm and 0.058 mm, respectively. The result of the analysis employing these values is shown in Figure 11.

To help in understanding the effects of elastic-plastic conditions and residual stresses, two additional computations were also performed. As shown in Figure 11, these were an elastodynamic computation and an elastic-plastic dynamic computation without the initial residual stresses. These computations also employed the critical CTOA values just given. It can be seen that, in this instance, both give nearly the same result for the initiation time and for the crack length history. In contrast, the result of the elastic plastic analysis with residual stresses included is considerably different.

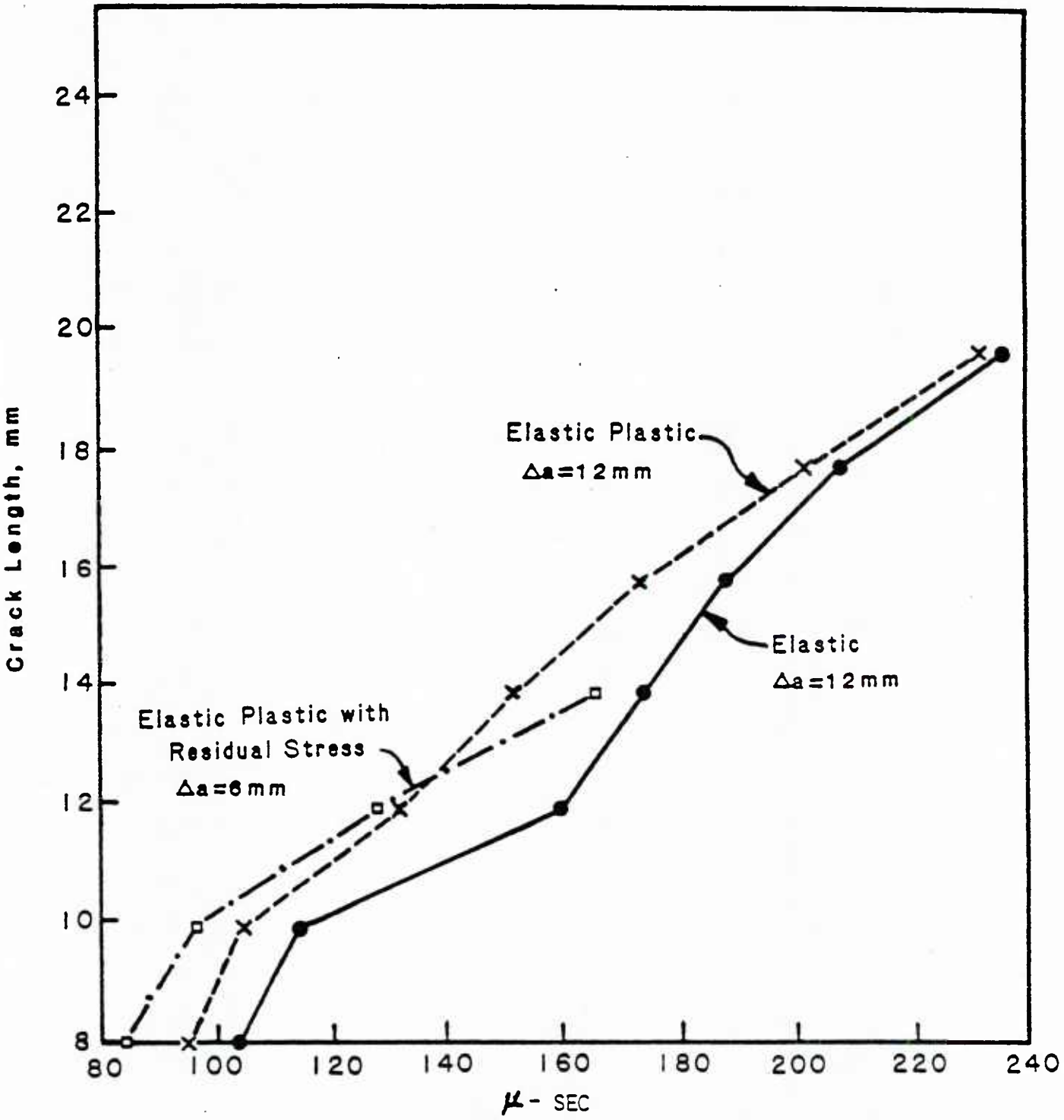

FIGURE 11. PREDICTION OF CRACK LENGTH HISTORY FOR A WELDED HY-80 SPECIMEN UNDER BLAST LOADING WITH K_{Id} = 120 MPa$\sqrt{m}$ and K_{ID} = 92 MPa$\sqrt{m}$

Because the choices of K_{Id} and K_{ID} in the analyses just described was rather arbitrary, a second set of computations was performed. In these, the K_{ID} value (and, hence, the corresponding CTOA value) was specifically selected to obtain better agreement with the experimental crack arrest point. This value was 84 MPa$\sqrt{m}$. The results of the analyses performed with this new value of K_{ID} are shown in Figure 12. It can be seen that, while the elastic-plastic dynamic analysis that includes the residual stresses is now close to the experimental result (see Table 1), the comparison analyses predict that the crack would run through the specimen without arresting. This demonstrates that the analytical predictions are quite sensitive to the accuracy of K_{ID}. Of more significance, it also reveals the importance of considering residual stresses in such analyses.

It might be tempting to conclude from the results shown in Figures 11 and 12 that the neglect of initial residual stresses is conservative; i.e., the inclusion of residual stresses gives a prediction that is less severe than that obtained in their omission. However, it is entirely possible that this result was obtained because of the particular residual stress distribution that pertained. For a residual stress distribution that is highly tensile in the vicinity of the initial flaw, it is conceivable that a different conclusion would be reached. This can only be determined with further computations of the kind described here.

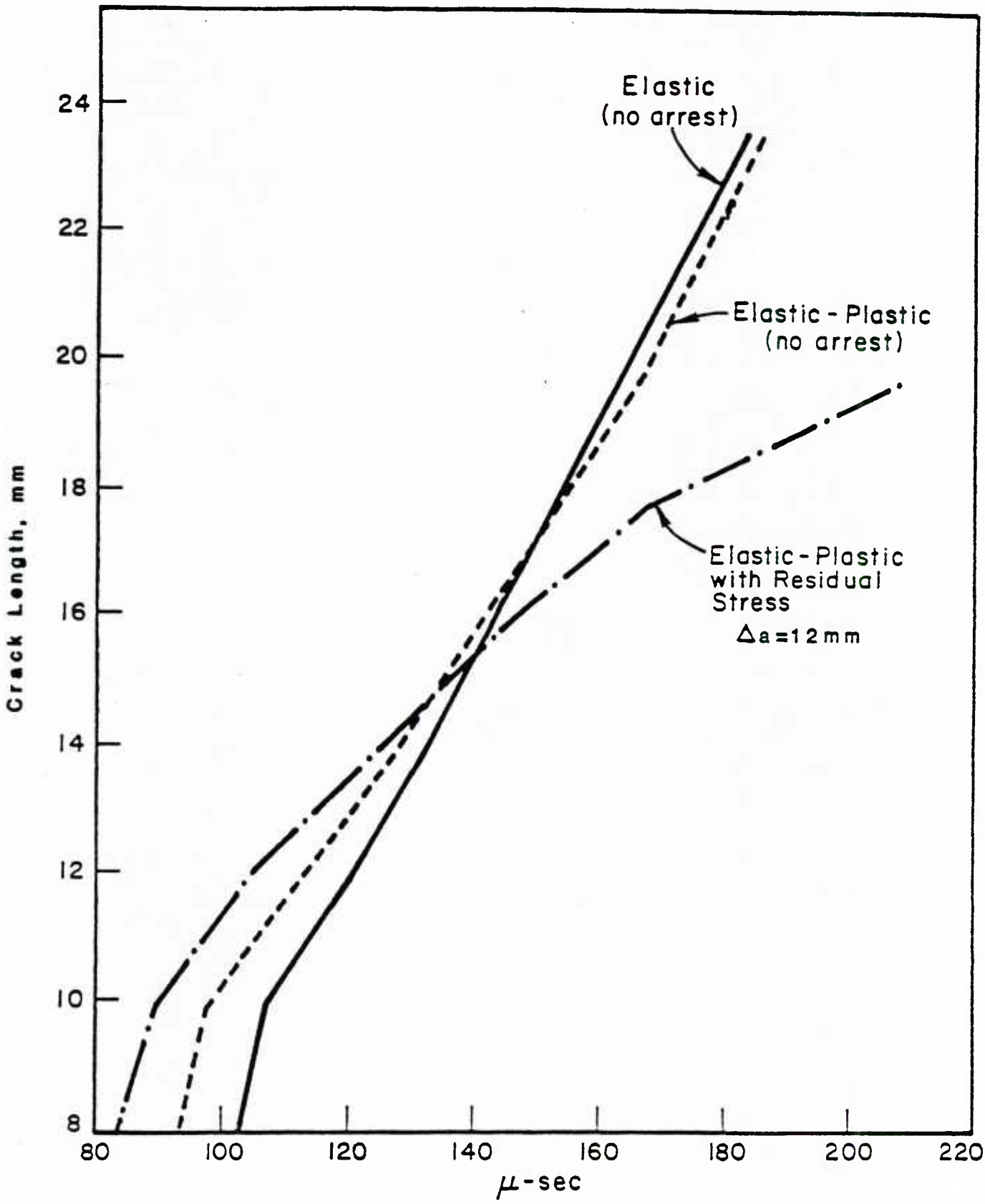

FIGURE 12. PREDICTION OF CRACK LENGTH HISTORY FOR A WELDED HY-80 SPECIMEN UNDER BLAST LOADING WITH K_{Id} = 120 MPa $\sqrt{m}$ and K_{ID} = 84 MPa $\sqrt{m}$

SUMMARY AND CONCLUSIONS

The objective of the present work has been to develop and validate a nonlinear dynamic analysis methodology that could be applied to determine critical crack sizes in welded structures subjected to blast loadings. The point of view that was taken is that a crack-like flaw may exist in a local low toughness region of a weld. But, while such a flaw would likely initiate, catastrophic fracture would still be avoided if the crack arrests. The key research issue is then to quantify the conditions under which a run/arrest event can occur in a tough, ductile material subjected to a rapidly varying applied loading.

There are several issues that place this analysis problem beyond the current state of the art of fracture mechanics. First, a criterion for rapid crack propagation in elastic-plastic conditions has not been previously established. Second, crack propagation initiated under rapidly applied loadings is not well understood. Third, the effect of weld-induced residual stress and deformation fields on crack propagation is virtually unknown. Added to these complexities is the difficulty of obtaining meaningful experimental results on crack propagation and arrest in blast loaded welded components; particularly of the precise character that are required for an assessment of a fracture mechanics analysis.

In view of the many complexities that exist in this problem, an integrated program of experimentation coupled with nonlinear dynamic finite element analysis was devised in which experiments were performed on precracked HY80 steel weldments under explosive loading conditions. The accompanying analyses, (1) determined the residual stress and deformation state by directly simulating the welding process, and (2) calculated the crack propagation history and the crack arrest point under the pressure history measured in

the experiment. These results were compared with measured residual stress values and with observed crack initiation/propagation behavior. The agreement was good in both instances.

A key assumption in the present work was that rapid crack propagation can be characterized by a constant value of the crack tip opening angle (CTOA) parameter. While there is solid evidence for this assumption (see Figure 1), the work that has been performed so far has not allowed the proper value for the CTOA for crack propagation in a weldment to be determined. As an expedient, by assuming that, this value is (1) unaffected by large scale plasticity, and (2) independent of the crack speed, an estimate of the CTOA was obtained for heuristic calculations. Using this value, an elastic-plastic dynamic analysis was performed. These results revealed that the effect of including residual stresses as initial conditions can be significant. A second set of computations in which the critical CTOA value was taken to force close agreement with the experimentally observed crack arrest point reinforces this conclusion.

Further work is planned in which a direct determination of the running fracture toughness of the weldment will be made. This work is also expected to reveal the speed-dependence, if any exists, of the CTOA parameter. Regardless, using these data as input, crack initiation/propagation/arrest predictions will be made and compared to the experimental result for more unequivocal assessments of the analysis approach described herein.

ACKNOWLEDGEMENT

This paper is based upon research performed for the Office of Naval Research under contract number N-00014-77-C-0576. The authors would like to express their appreciation to Dr. Yapa Rajapakske of ONR for his encouragement of this work.

REFERENCES

[1] Kanninen, M.F. et al, "Dynamic Crack Propagation Under Impact Loading", Nonlinear and Dynamic Fracture Mechanics ASME, AMD, vol. 35, N. Perrone and S.N. Atluri, Editors, The American Society of Mechanical Engineers, New York, 1979.

[2] Kanninen, M.F., Brust, F.W., Ahmad, J. and Abou-Sayed, I.S., "The Numerical Simulation of Crack Growth in Weld-Induced Residual Stress Fields", Residual Stress and Stress Relaxation, edited by E. Kula and V. Wiess, Plenum Press, New York, pp 227-247, 1982.

[3] Kanninen, M.F., "Dynamic Fracture Mechanics and its Application to Material Behavior under High Stress and Loading Rates", Proceedings of the 29th Army Sagamore Materials Research Conference, Lake Placid, New York, July, 1982.

[4] Ahmad, J., Barnes, C.R., and M.F. Kanninen, "Analysis of Crack Initiation and Growth in a Ductile Steel Under Dynamic Loading", ASME Winter Annual Meeting, Phoenix, November, 1982.

[5] Ahmad, J., Jung, J., Barnes, C.R., and Kanninen, M.F., "Elastic-Plastic Finite Element Analysis of Dynamic Fracture", Engineering Fracture Mechanics, Vol. 17, 1983.

[6] Kanninen, M.F., Ahmad, J., Barnes, C.R., "Dynamic Crack Propagation in Welded Structures Subjected to Explosive Loading", Army Symposium on Solid Mechanics, Army Mechanics and Materials Research Center, Watertown, Massachusetts, September, 1982.

[7] Kanninen, M.F., Popelar, C.H., and Broek, D., "A Critical Survey on the Application of Plastic Fracture Mechanics to Nuclear Pressure Vessels and Piping", Nuclear Engineering and Design, Vol. 67, pp 27-55, 1981.

[8] Rice, J.R., "A Path Independent Integral and the Approximate Analysis of Strain Concentration by Notches and Cracks", Trans. ASME, J. Appl. Mech., June, 1968.

[9] Hellen, T.K., and Blackburn, W.S., "The Calculation of Stress Intensity Factors for Combined Tensile and Shear Loading", Int. J. Fracture, Vol. 11, No. 4, 1975.

[10] Blackburn, W.S., "Path Independent Integrals to Predict Onset of Crack Instability in an Elastic Plastic Material", Int. J. Fract. Mechanics, No. 8, 1972.

[11] Neale, B.K., "Elastic Plastic Analysis of Cracked Bodies Using the J-Integral Method", CEGB, Rep. No. RD/B/N3253, Berkely, U.K., 1975.

[12] Bergez, D., "Linear Elastic Fracture Mechanics Applied to Cracked Plates and Shells", Int. J. Fract., Vol. 12, No. 4, August, 1976.

[13] Bui, H.E., "Stress and Crack-Displacement Intensity Factors in Elastodynamics", ICF4, Waterloo, Canada, Vol. 3, 1977.

[14] Wilson, W.K., and Yu, I.W., "The Use of J-Integral in Thermal Stress Crack Problems", Int. J. Fract., Vol. 15, No. 4, August, 1979.

[15] Mall, S., "A Finite Element Analysis of Transient Crack Problems with a Path Independent Integral", 5th International Conference on Fracture, Cannes, France, April, 1981.

[16] Miyamoto, H., Kikuchi, M., Sakaguchi, Y., and Takenori, S., "J-Integral Evaluation of a crack in a Reactor Vessel", U.S. Japan Conference on Fracture Mechanics, 1980.

[17] Kishimoto, K., Aoki, S., and Sakata, M., "On the Path Independent Integral J", Engineering Fracture Mechanics, Vol. 13. p 841-850, 1980.

[18] Ahmad, J., Barnes, C.R., Kanninen, M.F., "An Elastic Plastic Finite Element Investigation of Crack Initiation Under Mixed Mode Static and Dynamic Loading", Second Internation Symposium on Elastic Plastic Fracture Mechanics, Philadelphia, PA, October 6-9, 1981, in press, 1983.

[19] Nishioka, T. and Atluri, S.N., "Path-Independent Integrals, Energy Release Rates, and General Solutions of Near-Trip Fields in Mixed-Mode Dynamic Fracture Mechanics", Engineering Fracture Mechanics, Vol 18, pp 1-22, 1983.

[20] Ernst, H.A., "Material Resistance and Instability Beyond J-Controlled Crack Growth", Scientific Paper 81-107-JINF-P6, Westinghouse R. and D. Center, Pittsburgh, December, 1981.

[21] Freund, L.B. and Douglas, A.S., "The Influence of Inertia on Elastic-Plastic Antiplane Shear Crack Growth", J. Mech. Phys. Solids, Vol 30, pp 59-74, 1982.

[22] Kanninen, M.F., Rybicki, E.F., Stonesifer, R.B., Broek, D., Rosenfield, A.R., Marschall, C.W., and Hahn, G.T., "Elastic-Plastic Fracture Mechanics for Two-Dimensional Stable Crack Growth and Instability Problems", Elastic-Plastic Fracture, J.D. Landes et al., editors, ASTM STP 668, pp 121 - 150, 1979.

[23] Emery, A.F., Kobayashi, A.S., Love, W.J. and Jain, A., "Dynamic Propagation of Circumferential Cracks in Two Pipes with Large-Scale Yielding", J. Pressure Tech., Vol 102, pp 28-32, 1980.

[24] Ahmad, J., Barnes, C.R., and Kanninen, M.F., "Crack Initiation and Propagation Under Dynamic Elastic-Plastic Conditions". To be published.

[25] Kanninen, M.F., Barber, T.E., Brust, F.W. and Mishler, H.W., Controlling Residual Stresses by Heat Sink Welding, EPRI report NP-2159-LD, Electric Power Research Institute, Palo Alto, California, December, 1981.

[26] Hahn, G.T. and Kanninen, M.F., "Dynamic Fracture Toughness Parameters for HY80 and HY130 Steels and Their Weldments", Engineering Fracture Mechanics, Vol 14, pp 725-740, 1981.

CRACK INITIATION AND GROWTH UNDER EXPLOSIVE LOADING

by

C. R. Barnes

J. Ahmad

M. F. Kanninen

BATTELLE COLUMBUS LABORATORIES
505 King Avenue
Columbus, Ohio 43201

May 1983

Presented and published in the proceedings of the Spring Conference of Society for Experimental Stress Analysis, Cleveland, Ohio, May 15-20, 1983.

CRACK INITIATION AND GROWTH UNDER EXPLOSIVE LOADING

C. R. BARNES
J. AHMAD
M. F. KANNINEN
Battelle Columbus Laboratories
505 King Avenue
Columbus, Ohio 43201

ABSTRACT

A combined experimental and analytical approach designed to address the problem of crack initiation, propagation and arrest in ductile materials is outlined. A series of the explosive loading experiments on AISI 4340 steel were performed. A generalized version of the J-integral valid for dynamic conditions known as $\tilde{J}$ was employed in the analysis. The predicted time at crack growth initiation was in reasonable agreement with the measured values. The resulting crack propagation speed was also found to be in accord with measurements.

INTRODUCTION

The fracture mechanics techniques needed for materials that fracture in a highly ductile manner must give explicit attention to the extensive plastic deformation surrounding the crack tip. Large-scale crack-tip plasticity has two effects. First, because of crack tip blunting, crack growth initiation tends to occur under conditions for which conventional linear elastic fracture mechanics analyses are invalid. Second, significant amounts of stable crack growth can occur prior to fracture instability. To cope with these essentially inelastic processes, elastic-plastic fracture mechanics techniques are now being widely pursued (1). The research reported in this paper builds on these developments to provide the basis for fracture mechanics treatments under the more general conditions involved in dynamic loading.

For some Navy applications there is considerable interest in studying the behavior of cracks in rapidly loaded structures. For example, if a naval structure is subjected to a blast load, it is of interest to know whether an inherent flaw of certain size present in the material would initiate, and if so, whether it will arrest before catastrophic failure occurs. Because the loading rates in such cases are rather high, and also because cracks may propagate at relatively high rates, conventional quasi-static fracture mechanics is, in general, not applicable. A dynamic fracture mechanics treatment is usually warranted. A further complicating factor in these problems is due to the fact that naval structures are made of high toughness materials. Therefore, considerable crack tip plastic deformation may precede crack initiation, thus making the analysis problem nonlinear.

Another complicating feature appears due to the fact that a large majority of defects in naval structures (as in other large structures) reside in or around welds. Usually the welding process introduces substantial localized changes in material properties besides giving rise to thermally induced residual stresses in and around the welded region. However, reliable elastoplastic dynamic fracture yielding mechanics techniques for predicting crack initiation, growth, and arrest of cracks residing in and around welded regions do not currently exist. In order to develop such techniques a step wise procedure was followed to extend analytical procedures from quasi-static loading to intermediate loading rates and, eventually, to the high rate loading produced by an explosive. A first step is described in this paper.

GENERAL APPROACH

In a critical survey of progress in elastic-plastic fracture mechanics, Kanninen, et al (1) found that most efforts are focussed on the J-resistance curve approach. Despite the fact that such approaches are inherently limited to small amounts of crack growth prior to fracture instability, they do provide a significant improvement over the conventional linear-elastic fracture mechanics techniques. However, the current approaches are largely restricted to quasi-static loading. A generalization of the J-integral valid for dynamic loading conditions, the $\tilde{J}$-integral, has been developed by Kishimoto, et al (2). But, it has not previously been critically examined. Nevertheless, in view of the success that has been achieved with J and the complete lack of a viable alternative, this parameter was selected for use in this study. The mathematical basis for $\tilde{J}$ and the manner in which it can be applied to elasto-plastic dynamic fracture problems has been described by Ahmad, et al (3,4).

The experimental work employed AISI 4340 three-point-bend specimens containing crack starters as shown. This configuration has a number of advantages for this research. First, crack initiation and propagation can be obtained for both quasi-static and dynamic loading in the same specimen geometry. Second, this specimen can be economically analyzed with a finite element method. Third, because of constraint that arises in bending, the $\tilde{J}$-resistance curves obtained may be lower bound values that will provide conservative predictions when utilized for structural integrity assessments.

A dynamic elastic-plastic finite element analysis was used in the analysis portion of the research. The objective was to learn if crack growth initiation in AISI 4340 is governed by critical values of $\tilde{J}$. The $\tilde{J}$ values were determined by finite element analyses of the experiments. In essence, by calculating the $\tilde{J}$ parameter as a function of load, and using the load level at initiation, critical values for crack initiation and propagation were determined. This provided a tentative elastic-plastic fracture criterion in terms of a single material fracture parameter.

Analyses were also performed for impact loading. Here, the fracture criterion deduced under quasi-static loading was used as input to a finite element simulation of the impact loaded experiment. In this way a prediction of the initiation time was made for comparison with an experiment. The quite reasonable accuracy of this predition then gave an indication of the usefulness of the approach for the general conditions of interest in this research. Details of the experimental and analytical effort for the quasi-static and impact loading are given by Kanninen, et al (5). The modified analytical procedures that have resulted in improved predictive capability have been outlined by Ahmad, et al (6).

THE EXPERIMENTAL RESEARCH

The explosive tests were performed at Battelle's remote facility at West Jefferson, Ohio. It consists of a bomb proof building containing instrumentation ports extending into a room containing instrumentation as needed to monitor the blast effects resulting from explosive charges. In this case, the instrumentation was for the most part identical to that used in the quasi-static and impact tests detailed elsewhere(5,6). During these tests the following parameters were measured with respect to time:

- Blast arrival by means of a simple contact switch.
- Crack initiation, propagation, and complete specimen fracture using strain gauges.
- Blast pressure by means of a piezo-electric transducer.
- Specimen displacement by means of piezo-electric pins.

The specimen geometry and loading arrangement used in these tests is shown in Figure 1a and 1b. Note that the original specimen notch contains a root radius considerably larger than most conventional test specimens. This larger radius was adopted to facilitate strain gage application near the notch tip to determine crack initiation. Additional strain gages were mounted slightly below the crack tip and on the back of the specimen surface (normal to the projected crack path) to detect crack growth and complete specimen fracture, respectively. The loading fixture was designed to maintain the specimen in a bend configuration during loading. During each test the wooden arm which supported the explosive charge was completely destroyed.

During the course of these tests, it was necessary to perform preliminary tests on sacrificial specimens since the amount of explosive required to fracture a test specimen was not readily predetermined. Accordingly, uninstrumented specimens were subjected to the blast effects of 2.5, 5, and 10 pounds of C-4 explosive detonated from a 15 inch standoff as shown schematically in Figure 1b. During these preliminaries it was determined that a 5 pound explosive charge was the optimum useful amount as it was sufficient for specimen fracture but not so large as to destroy the piezo-electric transducer used to monitor blast pressure. After the appropriate charge and standoff distance had been decided upon, actual testing began.

In all, three specimens were instrumented and tested with varying degrees of success. During the first test no useful data was recorded due to instrumentation lead wire destruction due to the heat and blast effects generated by the explosive detonation. A slight modification of test procedures resulted in partial data recording during the second test. Additional procedure modifications, consisting mainly of filling all cracks in the specimen loading system with silicone rubber, resulted in full data acquisition for the third test.

ANALYSIS RESULTS

Analyses were performed using Battelle's FRACTDYNEP elastoplastic dynamic finite element code. On the basis of the analytical results of Reference 6, it was concluded that for the blast loaded AISI 4340 specimen used in this work, an elastodynamic analysis procedure was adequate. The finite element model used in the analysis is shown in Figure 2.

Due to the symmetry of the specimen about the crack line, only one half of the geometry was included in the model. The top surface was loaded using the pressure vs. time record obtained from the experiments. The spatial load distribution was assumed to be uniform throughout the length of the specimen. To model crack growth, the following criterion was supplied to the finite element code:

$$K_D = 65 + 0.044\ \dot{a},\ \text{MPa}\sqrt{\text{in.}}$$

where K_D is the dynamic fracture toughness, and $\dot{a}$ is the crack velocity. This is the same criterion which was used in Reference 5 to model crack propagation under quasi-static and impact loading conditions.

The results of the analysis included time at crack initiation, and a prediction of crack velocity. These are shown in Figures 3 and 4 along with the experimental data.

CONCLUSIONS

Experimental and analytical techniques have been developed to address the problem of predicting crack growth behavior under explosive loading. The techniques are now being extended to more ductile materials than used in this work. A research program is also underway to study the problem of crack growth through welded specimens.

ACKNOWLEDGEMENTS

The work reported in this paper was supported by the Office of Naval Research, Structural Mechanics Division, under Contract Number N00014-77-C-0576. The authors would like to thank Dr. Yapa Rajapakse of the ONR for his personal support and encouragement of their work in this area.

REFERENCES

(1) Kanninen, M. F., Popelar, C. H., and Broek, D., "A Critical Survey on the Applications of Plastic Fracture Mechanics to Nuclear Pressure Vessels and Piping", Nuclear Engineering and Desing, 67, p 27-55, 1981.

(2) Kishimoto, K., Aoki, S., and Sakata, M., "On the Path Independent Integral J ", Engineering Fracture Mechanics, Vol. 13, p 841-850, 1980.

(3) Jung, J., Ahmad, J., Kanninen, M. F., and Popelar, C. H., "Finite Element Analysis of Dynamic Crack Propagation", Failure Prevention and Reliability-1981, F.T.C. Loo, Editor, ASME, 1981.

(4) Ahmad, J., Jung, J., Barnes, C. R., and Kanninen, M. F., "The Development of a Dynamic Elastoplastic Finite Element Analysis for Fast Fracture Under Impact Loading", ASME/PVP Conference, Denver, Colorado, June 22-25, 1981.

(5) Kanninen, M. F. et al, "Dynamic Crack Propagation Under Impact Loading", Nonlinear and Dynamic Fracture Mechanics AMD, Vol. 35 N. Perrone and S. N. Atluri, Editors, The American Society of Mechanical Engineers, New York, 1979.

(6) Ahmad, J., Barnes, C. R., and Kanninen, M. F., "Crack Initiation Under Dynamic Elastic-Plastic Conditions", To be published.

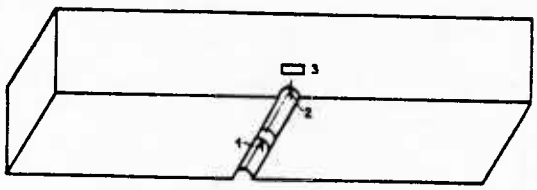

(a)

1 and 3 denote strain gages used to detect crack initiation and crack propagation respectively. 2 denotes the sharpened notch produced by electric discharge machining. Not shown in this view is a page on the back specimen surface used to detect specimen fracture

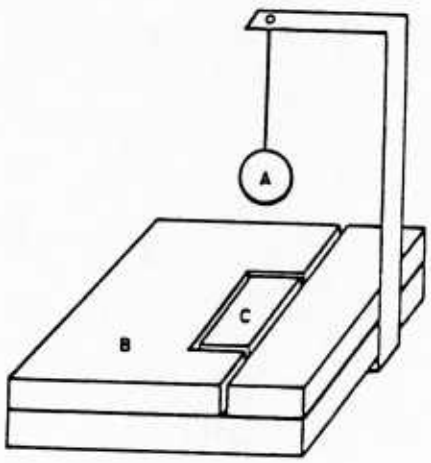

(b)

a denotes explosive charge. b denotes the specimen holder and c denotes the test specimen.

Figure 1. Specimen geometry and loading arrangement

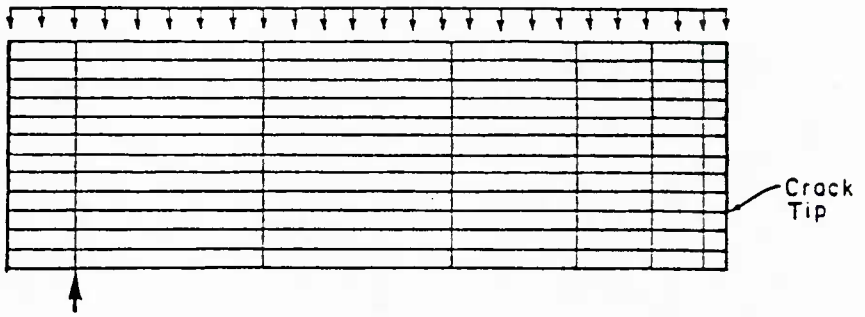

Figure 2. Finite element model used in the analysis

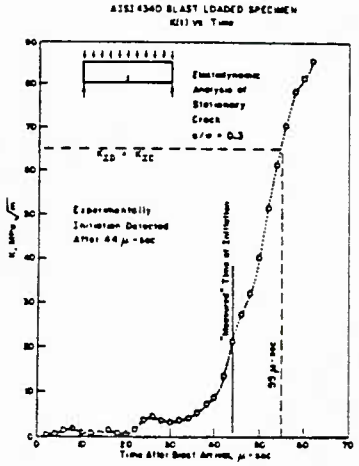

Figure 3. Predictions of crack initiation under explosive loading

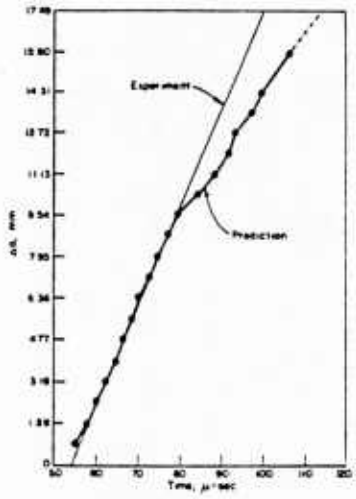

Figure 4. Prediction of crack velocity under explosive loading

ELASTIC-PLASTIC FINITE ELEMENT ANALYSIS OF DYNAMIC FRACTURE

by

J. Ahmad
J. Jung
C.R. Barnes
M.F. Kanninen

BATTELLE
Columbus Laboratories
505 King Avenue
Columbus, Ohio 43201

November, 1981

Submitted for publication in Engineering Fracture Mechanics, November, 1981.

SECURITY CLASSIFICATION O S PAGE (When Data Entered)

REPORT DOCUMENTATION PAGE

READ INSTRUCTIONS BEFORE COMPLETING FORM

1. REPORT NUMBER

2. GOVT ACCESSION NO.

3. RECIPIENT'S CATALOG NUMBER

4. TITLE (and Subtitle)

Elastic-Plastic Finite Element Analysis of Dynamic Fracture

5. TYPE OF REPORT & PERIOD COVERED

Interim

6. PERFORMING ORG. REPORT NUMBER

Battelle

7. AUTHOR(s)

J. Ahmad, J. Jung, C. R. Barnes, and M. F. Kanninen

8. CONTRACT OR GRANT NUMBER(s)

C00014-77-C-0576

9. PERFORMING ORGANIZATION NAME AND ADDRESS

Battelle Columbus Laboratories
Columbus, Ohio 43201

10. PROGRAM ELEMENT, PROJECT, TASK AREA & WORK UNIT NUMBERS

11. CONTROLLING OFFICE NAME AND ADDRESS

Office of Naval Research
Structural Mechanics Program
Department of the Navy, Arlington, Virginia 22217

12. REPORT DATE

November 1981

13. NUMBER OF PAGES

23

14. MONITORING AGENCY NAME & ADDRESS(if different from Controlling Office)

15. SECURITY CLASS. (of this report)

15a. DECLASSIFICATION DOWNGRADING SCHEDULE

16. DISTRIBUTION STATEMENT (of this Report)

Approval for public release; distribution unlimited.

17. DISTRIBUTION STATEMENT (of the abstract entered in Block 20, if different from Report)

18. SUPPLEMENTARY NOTES

Published in Engineering Fracture Mechanics, Vol 17, No. 3, 1982.

19. KEY WORDS (Continue on reverse side if necessary and identify by block number)

elastodynamic crack propagation and arrest
dynamic elastic-plastic finite element analysis
crack tip plasticity
fracture mechanics
high strength materials

20. ABSTRACT (Continue on reverse side if necessary and identify by block number)

Recent evidence indicates that present treatments of elastodynamic crack propagation and arrest are possibly inadequate. The paper describes the development of a dynamic elastic-plastic finite element capability to address this concern by taking direct account of crack tip plasticity. The capability is compared with known dynamic fracture mechanics solutions and with experimental data to verify this approach.

DD FORM 1 JAN 73 1473

unclassified

SECURITY CLASSIFICATION OF THIS PAGE (When Data Entered)

ABSTRACT

Recent evidence has pointed to the possible inadequacy of elastodynamic treatments of rapid crack propagation and crack arrest. This paper describes the development of a dynamic elastic-plastic finite element capability designed to address this concern by taking direct account of crack tip plasticity. Comparisons with known dynamic fracture mechanics solutions and with experimental data are made to demonstrate the fidelity of the approach. A comparison with an elastodynamic solution in an impact loaded 4340 steel bend specimen is also made. This result reveals that a significant effect of crack tip plasticity may exist even for high strength materials.

ELASTIC-PLASTIC FINITE ELEMENT ANALYSIS OF DYNAMIC FRACTURE

by

Jalees Ahmad, J. Jung, C.R. Barnes, and M.F. Kanninen

INTRODUCTION

Fracture mechanics researchers are becoming aware that the applicability of even rigorous dynamic analyses of unstable crack propagation and crack arrest may be more limited than was previously realized.[1] An important contributor to this dilemma is the still unexplained difference in the crack propagation behavior when crack growth is initiated under impact loading rather than under conventional quasi-static conditions. Specifically, as reported by Kanninen et al,[2] the use of the K_{ID} values obtained for 4340 steel in quasi-static initiation gave decidedly poor agreement when used to predict the crack length-time data obtained in an impact test. In fact, the K_{ID} value inferred from the latter test was roughly a factor of two greater! Added to the geometry-dependence that cast doubt on the validity of $K_{ID} = K_{ID}(V)$ as a unique material property, there is some concern about the presently accepted elastodynamic treatments of fast fracture. This paper describes a first step towards a possible resolution of these difficulties via the development of an elastoplastic dynamic finite element model for the future treatment of fast fracture problems.

Besides providing a more realistic model of the specimen geometry and the boundary conditions, a finite element method is particularly suitable for modeling nonlinear material behavior. To avoid the use of an extremely small mesh size in the evaluation of the dynamic stress intensity factor, a conservation integral, $\hat{J}$ [3] can be utilized. The $\hat{J}$-integral is essentially a consequence of several attempts[4-6] aimed at extending the regime of applicability

of the path-independent contour integral J[7] to include dynamic, elastic-plastic, body force, and thermal contributions to the energy release rate under mixed-mode conditions. Then, crack propagation can be simulated via a gradual crack tip nodal-force release technique using either crack-length vs time data (generation-phase analysis) or a given fracture criterion (application-phase analysis). Finally, to obtain more realistic material modelling, a strain-rate independent constitutive relation based on a Von Mises plasticity potential with an isotropic hardening rule has been included.

In this paper, a general background discussion of current problems in dynamic fracture is followed by a description of the salient features of the finite element based computational procedure. The validity of the computational procedure is ascertained by solving problems for which reliable analytical or experimental results are available. Results for both stationary and propagating cracks are presented. Also presented is a comparison of the results of linear elastodynamic vs elastoplastic dynamic analyses performed on a three-point-bend specimen of AISI 4340 steel under impact loading conditions.

BASIS OF THE COMPUTATIONAL PROCEDURE

Background

Until recently there has been a controversy between the use of static or dynamic treatments for the arrest of a rapidly propagating crack. On the basis of results obtained by Hahn et al[8] and Kalthoff[9], it is now widely believed that a dynamic based analysis is the more correct. Nevertheless, workers in dynamic fracture mechanics are now faced with other problems. Analytical studies, which have been until recently based predominantly on linear elastodynamic analyses, have brought increased understanding of the problem. But, they have also brought to light some new problems.

The problem identified by Kanninen et al [2] concerns the marked differences in the initiation and growth of cracks initiated under different loading conditions. Their key result is shown in Figure 1. This experiment was performed on an impact loaded three-point-bend specimen of AISI 4340 steel (yield strength ≈ 200 ksi). It can be seen that, by using K_{ID} values obtained from quasi-static initiation tests (i.e., $K_{ID} = 65 + .044\ V$), a very poor prediction is obtained. Instead, the value $K_{ID} = 170$, which has no apparent connection with the "established" value, is needed for good agreement.

Because the analytical results in this study were obtained by a relatively simple elastodynamic finite difference scheme, one possible reason for the discrepancy would be the analysis procedure itself. Solving the same problem with an entirely different - and preferably improved - analytical procedure should remove any such doubt. For this purpose a finite element computer code with isoparametric element formulation was developed. To further depart from the previously used global energy balance approach for the calculation of stress intensity factor, the $\hat{J}$-integral approach was implemented.

A second possible reason for the discrepancy could be the assumption of linear elastic material behavior. The finite element code was, therefore, enriched to model the material behavior in accordance with a user supplied uniaxial stress-strain curve. This, and other reasons for the discrepancy, will be dealt with in a later section.

Outline of the Solution Procedure

The approach used for the solution of the equations of motion in the analytical procedure presented here employs a displacement-based finite element method. An isoparametric finite element formulation with linear and quadratic shape functions in a two-dimensional space is used.

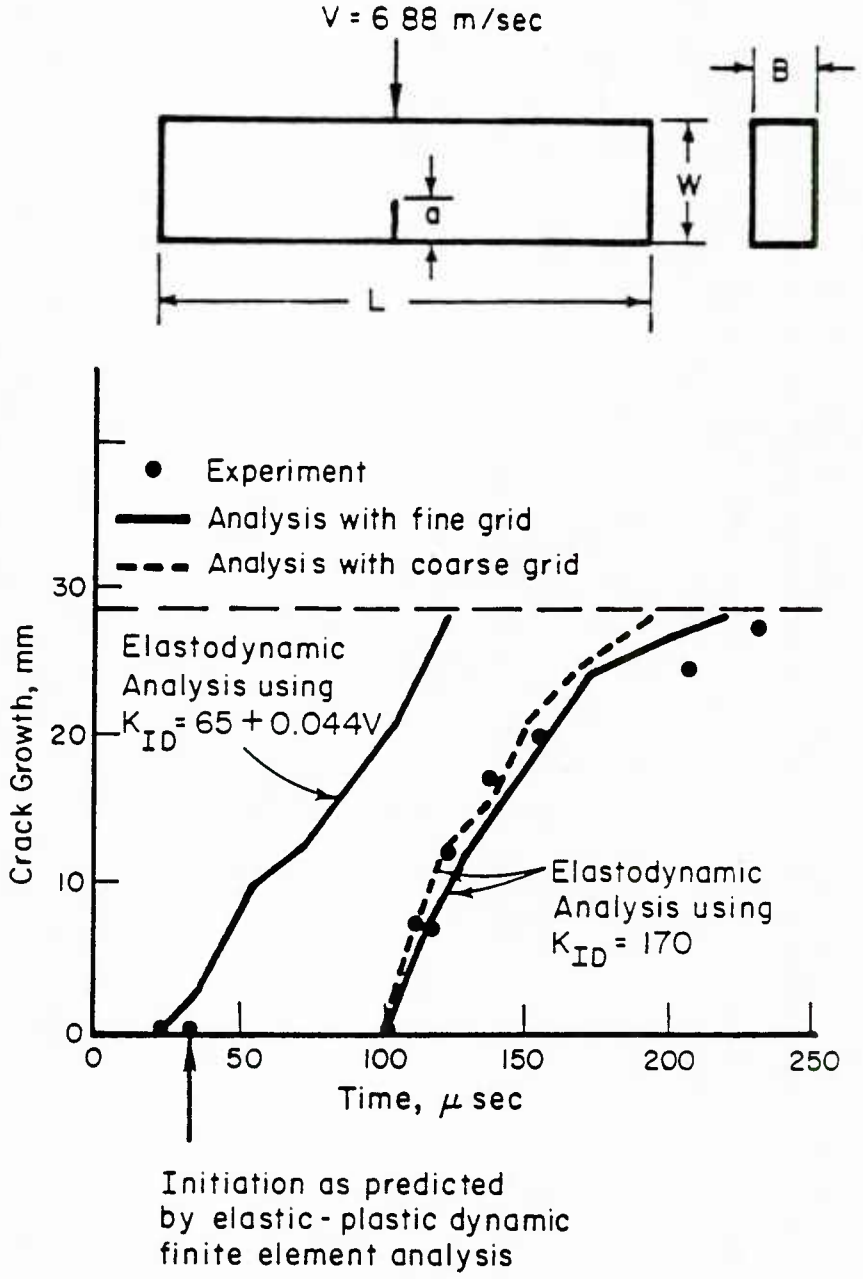

FIGURE 1. CRACK GROWTH IN 4340 STEEL UNDER IMPACT LOADING
L = 0.181 m, a =.0095 m, B = .0158 m, W = .038 m

General quadrilateral elements with a variable number of nodes in both plane-stress and plane-strain conditions may be used. If so desired the $1/\sqrt{r}$ or $1/r$ stress singularity at the crack tip may be imposed by using the quarter point approach[10]. However, this feature was not utilized in any of the analyses presented in this paper.

The modified Newton-Raphson approach[11] is used for elastic-plastic analysis. Von Mises yield condition with isotropic strain hardening is assumed. For time integration, either an explicit (central difference) or an implicit (Newmark-Beta) scheme may be used. Due to it being inherently more stable, the implicit scheme offers computational advantages in the solution of dynamic fracture problems. All the results included in the present paper were obtained by using the Newmark-Beta time integration scheme[12].

Crack growth is modelled by gradually releasing the force experienced by the crack tip at a given instant of time in several steps. Details of the crack growth modelling scheme are described in a paper by Jung, Ahmad, Kanninen, and Popelar[13]. The scheme allows for modelling crack growth in both generation and application phases of analysis. For application-phase analysis where the crack tip is advanced according to a selected fracture parameter, a choice of fracture parameters is necessary. Currently, crack-tip-opening displacement (CTOD), crack-tip-opening angle (CTOA), Mode I and Mode II dynamic stress intensity factors (K_I and K_{II}), and the $\hat{J}$ family of conservation integrals[3] are available. Since CTOD and CTOA are obtained directly from the finite element displacement solution, and K_I and K_{II} are obtained by first calculating $\hat{J}$ for linear elastic material, only a description of the $\hat{J}$-integrals is included in the following.

The $\hat{J}$-Integral

The mathematical details involved in the derivation of $\hat{J}$ are available in a paper by Kishimoto et al[3]. Here, a general expression for $\hat{J}$ is taken in a form which makes the parameter physically more

tractable and convenient to implement in a computational scheme. This is done by defining

$$\hat{J}_k = J_{k_e} + J_{k_d} + J_{k_t} + J_{k_p} + J_{k_b} \qquad (1)$$

Where the lower case letter subscripts stand for the elastic (e), dynamic (d), thermal (t), plastic (p), and body force (b), contributions to the $\hat{J}_k$-integrals and K (=1,2) indicates that each term in Equation (1) is a vector.

Kishimoto et al [3] define $\hat{J}$ as follows:

$$\hat{J} = \hat{J}_1 \text{ Cos } \Theta + \hat{J}_2 \text{ Sin } \Theta \, , \qquad (2)$$

where Θ is the angle of crack extension measured anticlockwise from the crack line (Figure 2). The integrals J_{k_e} thru $\bar{K}_{k_b}$ in Equation (2) may be expressed as follows:

$$J_{ke} = \int_{\Gamma + \Gamma s} \left(W_e n_k - T_i \frac{\partial u_i}{\partial x_k} \right) d\Gamma$$

$$J_{kd} = \iint_A \rho \ddot{u}_i \frac{\partial u_i}{\partial x_k} \, dA$$

$$J_{kp} = \iint_A \sigma_{ij} \frac{\partial \varepsilon^*_{ij}}{\partial x_k} \, dA$$

$$J_{k_t} = \iint_A \alpha \, \varepsilon_{ii} \frac{\partial T}{\partial X_k} \, dA - \int_{\Gamma + \Gamma_s} 1/2 \, \alpha \, T \, \varepsilon_{ii} \, n_k \, d\Gamma$$

$$J_{k_b} = - \iint_A F_i \frac{\partial u_i}{\partial X_k} \, dA$$

$$\alpha = \frac{E}{1-2\nu} \text{ --- Plane Strain} = \frac{E}{1-\nu} \text{ ---Plane Stress}$$

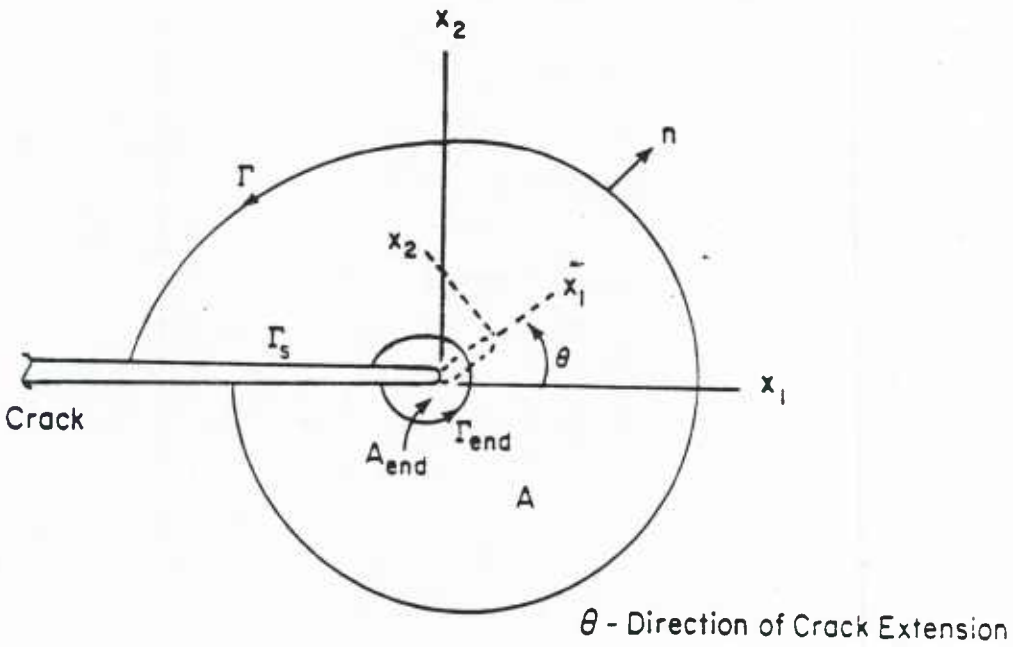

FIGURE 2. CRACK TIP COORDINATES USED IN THE DEFINITION OF $\hat{J}_k$

where

W_e = elastic strain energy density
T_i = traction vector
σ_{ij} = stress tensor
ε^*_{ij} = plastic strain tensor
u_i = displacement vector
$\ddot{u}_i$ = acceleration vector
T = temperature increment
F_i = body force

In Figure 2, A is the area enclosed between contours Γ and Γ_{end} and $\hat{J}$ is defined as the area Aend approaches zero. For running cracks, it is assumed that the so-called "process-region"[3] shown in Aend in Figure 2 remains constant in dimensions and moves with the crack tip.

While there may be some uncertainty regarding the use of $\hat{J}$ as a fracture criterion, it is highly appealing from a computational viewpoint. The strength of the idea is in the fact that other proposed forms of energy release rate expressions such as J of Rice [7], J^* of Blackburn [6], $\tilde{G}$ of Eftis and Liebowitz[14], and expressions proposed by Wilson and Yu[15], Freund [5], and Bui [4], all can be shown to be specialized versions of the $\hat{J}$-integral[3]. Therefore, $\hat{J}$ is at least equally valid as a fracture criterion as any of the above-mentioned parameters.

For a linear elastic material ($J_{k_p} = 0$) and in the absence of body forces ($J_{k_b} = 0$), it can be shown[16] that:

$$\hat{J}_1 = \frac{\kappa+1}{8\mu}\left[K_I^2(t) + K_{II}^2(t)\right] + \frac{1}{2\mu} K_{III}^2(t) \qquad (3)$$

$$\hat{J}_2 = \frac{\kappa+1}{4\mu} K_I(t)\, K_{II}(t) \qquad (4)$$

where μ is the shear modulus, and $\kappa = 3-4\nu$ for plane strain and $(3-\nu)/(1+\nu)$ for plane stress.

In a single mode situation the appropriate stress intensity factor can be readily obtained from Equation (3).

NUMERICAL RESULTS

Solutions to some representative problems solved by using the analytical procedure described above are now presented. The first four problems were chosen primarily for ensuring the validity of the solutions procedure by comparing the results with available analytical solutions and with experimental results. In the second and the fourth problems, comparisons with the previously used finite difference scheme[2] are also made.

The fifth and sixth problems were selected to demonstrate the differences in K_I obtained by using quasi-static analysis vs the dynamic analysis, and to illustrate the effect of plasticity even in a high strength material, AISI 4340 steel. Note that, in all cases involving linear-elastic-material assumption, the stress intensity factors were calculated by the $\hat{J}$ approach.

Problem 1: Stationary Crack in an Impulsively-Loaded Center-Cracked Panel

The problem considered here is of a center-cracked plate (Figure 3) loaded dynamically in a suddenly-applied uniform tension σ. The material was taken to be linear elastic ($E = 200$ GPa, $\nu = 0.3$) having a density of 5000 Kg/m^3. This problem has been solved by a number of other authors. Some of these results are shown in Figure 3 along with the results of the present analysis. The good correlation that is evident indicates that the present finite element procedure with the $\hat{J}$-integral provides sufficiently accurate dynamic stress intensity factors for stationary cracks.

Problem 2: Unrestrained Impact-Loaded Bend Specimen

A bend specimen totally unrestrained (no supports) is considered (Figure 4). In an actual experiment the specimen was struck by a hammer at an average velocity of 6.88 m/sec and was allowed to fly freely. In Figure 4, the variation of the dynamic stress intensity factor with time,

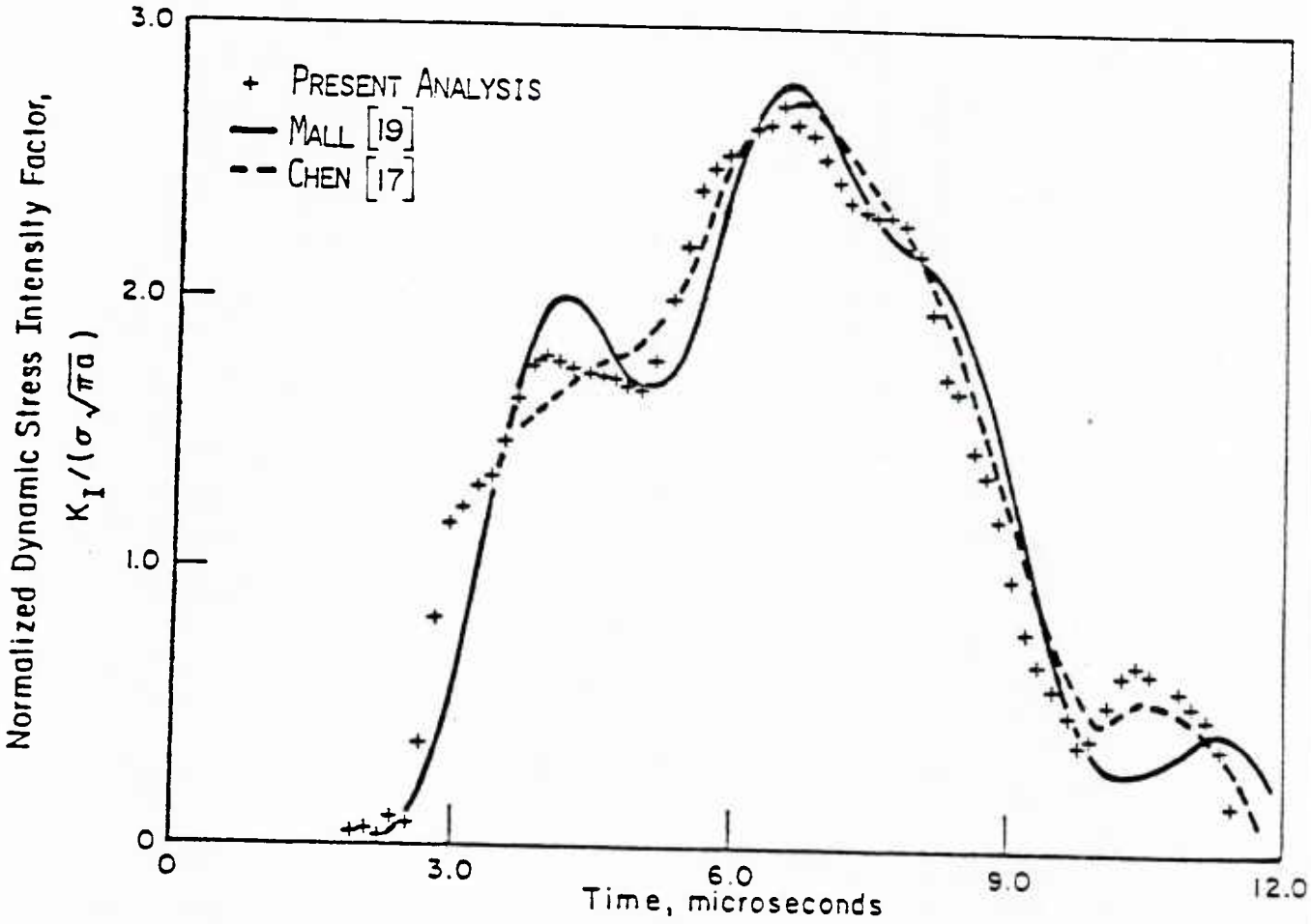

FIGURE 3. DYNAMIC STRESS INTENSITY FACTOR VERSUS TIME FOR AN IMPULSIVELY LOADED CENTER-CRACKED PANEL WITH A STATIONARY CRACK.

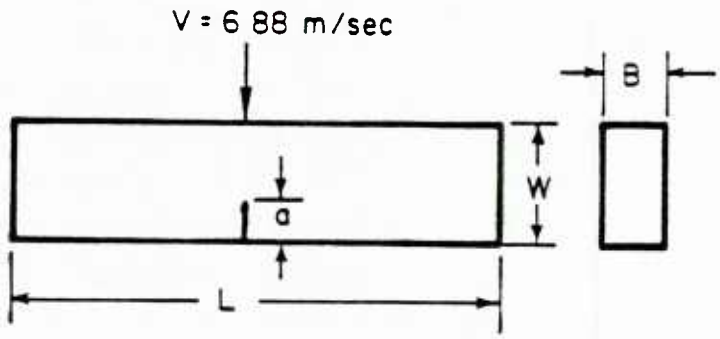

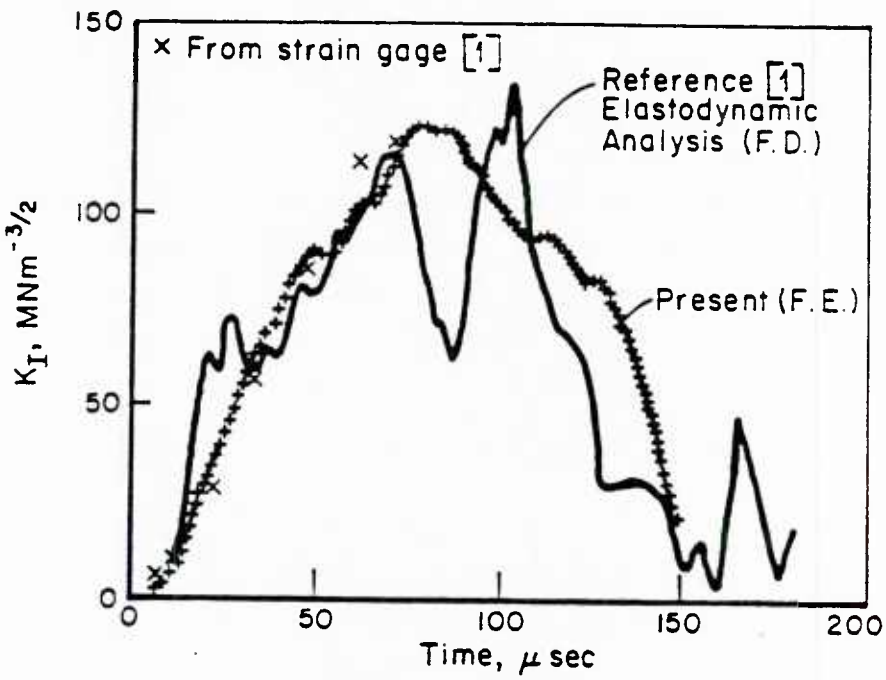

FIGURE 4. RESULTS FOR UNRESTRAINED 1 SPECIMEN

L = 0.181 m, W = 0.038 m,
a = 0.0095 m, B = 0.0158 m

as obtained by the present analysis, is compared with K_I obtained by both the finite difference calculation (2) and with experimental strain measurements. The material properties used in this analysis were those of AISI 4340 steel. Good agreement is obtained which demonstrates that the $\hat{J}$-integral approach provides essentially the same values for dynamic stress intensity factors as the global energy balance approach used in the finite difference scheme and, in view of the agreement with the strain gage data, that both are correct.

Problem 3: Propagating Crack in an Infinite Medium

The problem of a crack propagating at a constant velocity of 0.2 times the shear wave speed (C_s) in a center-cracked panel was analyzed for an initial crack length to specimen width ratio (a/w) of 0.2. The results are compared with analytical solution by Broberg [18] in Figure 5.

The results indicate that the $\hat{J}$-integral provides an effective means of calculating dynamic stress intensity factors for propagating cracks. However, it should be noted that the crack velocity in this comparison was held constant; NB, analytical solutions for a crack propagating at changing velocity do not exist. In the next problem, such a comparison is made with experimental, as well as numerical results, obtained by finite difference method.

Problem 4: Application-Phase Analysis of a Propagating Crack in a Bend Specimen

An elastodynamic crack growth analysis in a three-point-bend specimen of AISI 4340 steel was performed. Experimental as well as finite difference analysis results for this problem were first obtained by Kanninen et al [2] using $K_{I_D} = 65 + 0.044\ V$ as a fracture criterion. In the present finite element computations the same criterion was used. Figure 6 shows the specimen geometry used in the analysis and a comparison of the new results with those of Reference (2).

This application-phase analysis does indicate an equivalence between the $\hat{J}$-integral approach of calculating K_I and the approach used in the finite

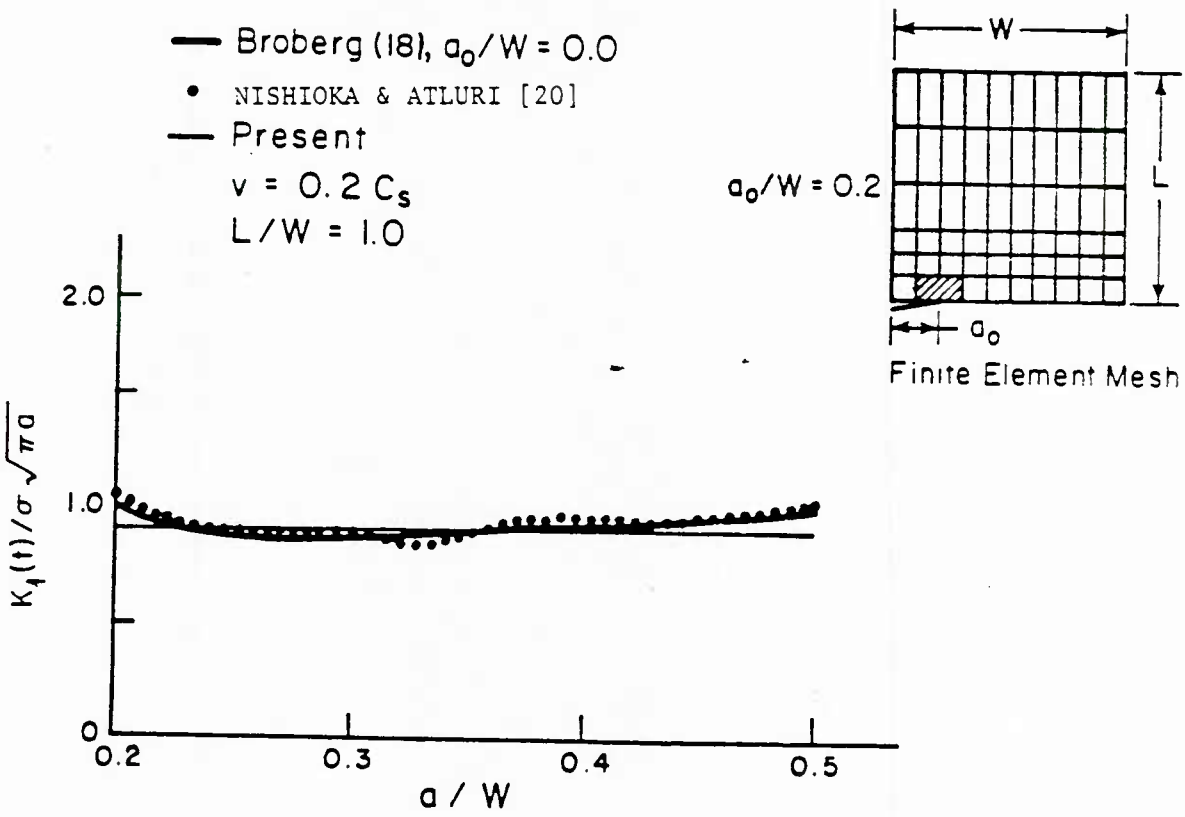

FIGURE 5. ELASTODYNAMIC ANALYSIS OF CONSTANT VELOCITY CRACK PROPAGATION

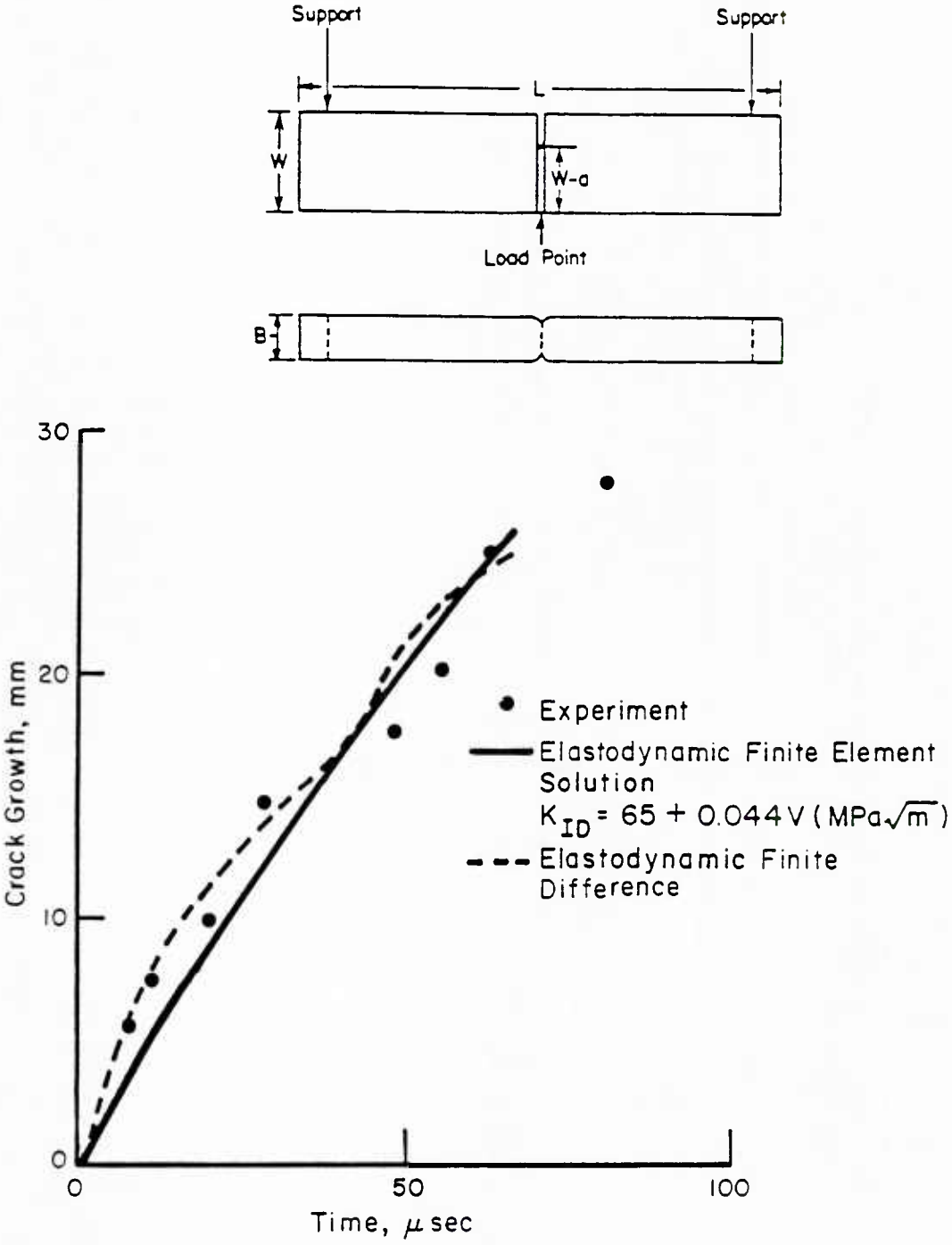

FIGURE 6. A COMPARISON OF FINITE ELEMENT ANALYSIS, FINITE DIFFERENCE ANALYSIS AND EXPERIMENT FOR A QUASI-STATICALLY INITIATED CRACK IN A 4340 DYNAMIC TEAR SPECIMEN.
L = 181 mm, W = 38 mm, B = 15.8 mm, (W-a) = 28.5 mm.

difference scheme even for a crack propagating at a nonconstant speed. The results also provide an increased level of confidence in the accuracy of numerical results.

Problem 5: Generation-Phase Analysis of a Propagating Crack in a Bend Specimen

A generation phase analysis, in which an experimentally obtained crack length vs time record (Figure 7) from a dynamic tear test experiment on HY130 steel was provided as an input to the computer code, was performed. The elastodynamic finite element analysis then gave values of K_D as a function of time. These are plotted in Figure 8. Also shown are K_o values inferred by using a handbook formula for three-point-bend specimen in which inertia forces are ignored. As might be expected, the dynamic values oscillate around a mean value given by the quasi-static solution.

Problem 6: Elastic-Plastic Dynamic Analysis of a Stationary Crack in a Bend Specimen

The three-point-bend specimen of AISI 4340 steel was analyzed under an impact load with and without the elastic material assumption. For the elastic-plastic dynamic analysis, the material behavior was described by an experimentally obtained static stress-strain curve from a uniaxial tension test. Strain rate effects on material property are not included in the analysis.

Figure 9 shows the variation with time of the crack-opening displacement (COD), measured at 0.68 mm behind the crack-tip for both elastic and elastic-plastic analyses. In Figure 10, values obtained are plotted against time. It can be seen that, even in a high-strength material, the effect of plasticity appears to be significant. The effect of plasticity seems to damp-out the oscillations in COD (which is directly proportional to K_I and $\sqrt{J}$ in the linear elastic case); cf, Figure 8.

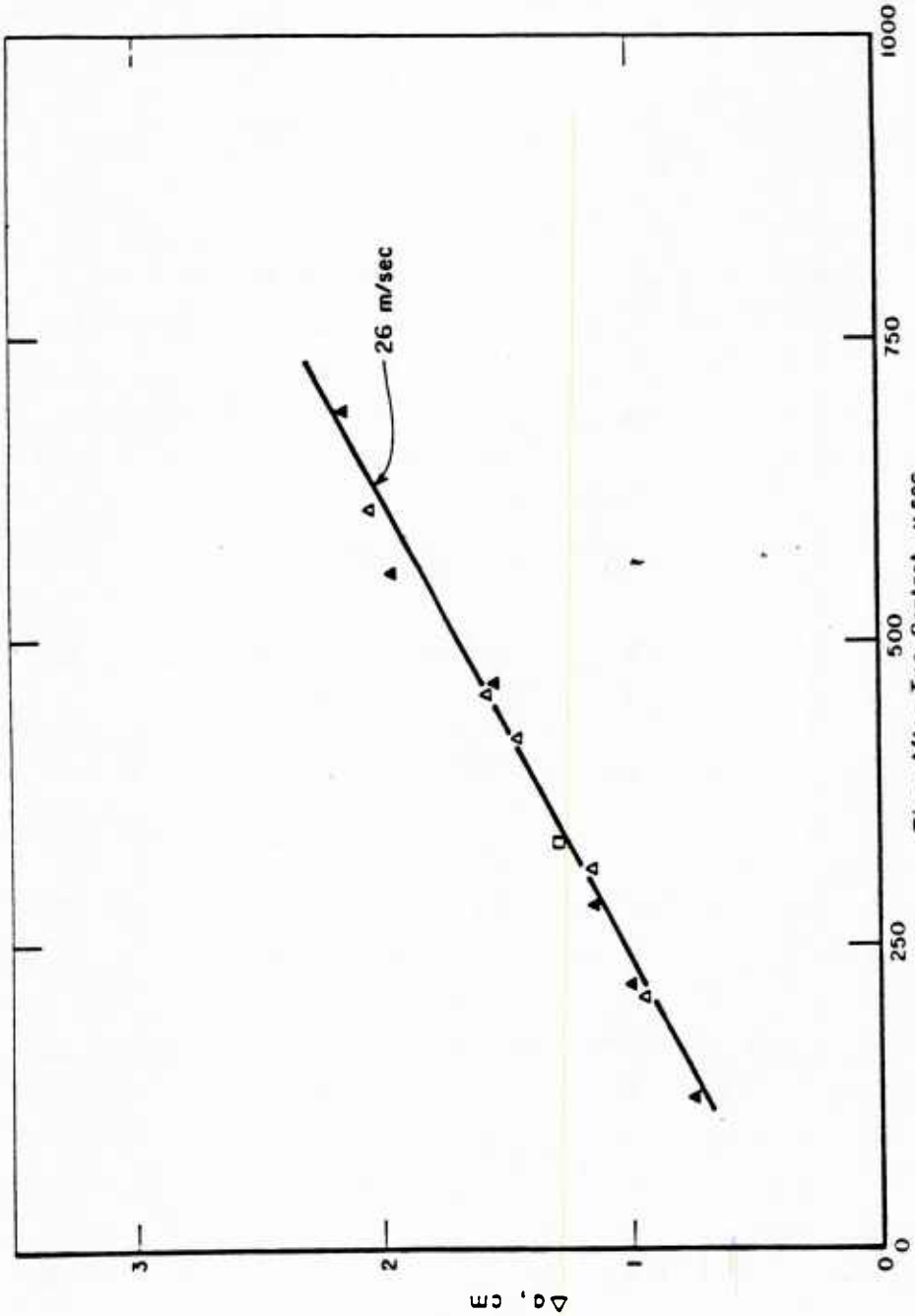

FIGURE 7. MEASURE CRACK EXTENSION-TIME RECORD FOR HY-130 STEEL FROM DYNAMIC TEAR TEST EXPERIMENT.

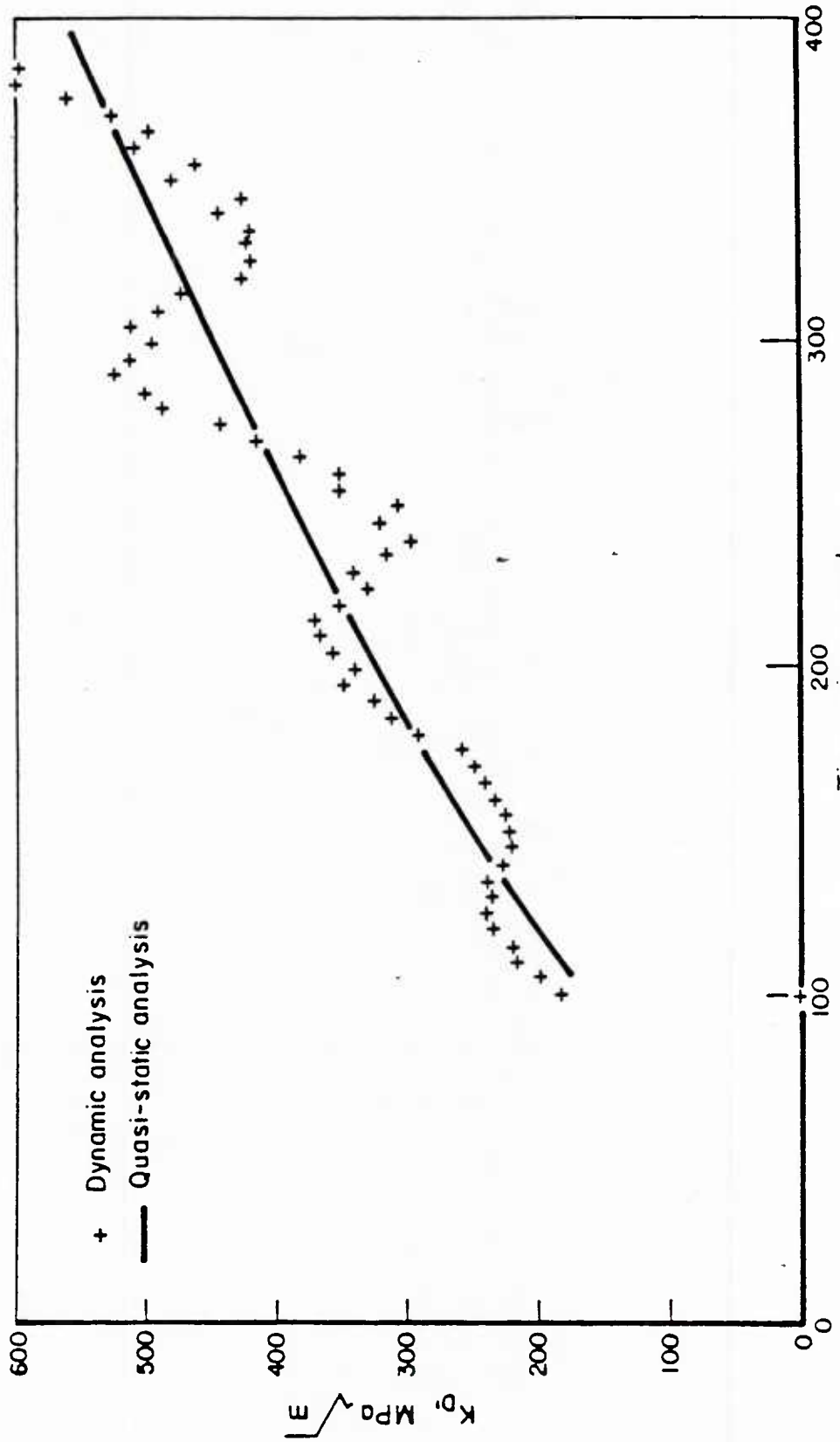

FIGURE 8. COMPARISON OF ELASTIC FRACTURE TOUGHNESS VALUES DEDUCED BY QUASI-STATIC AND DYNAMIC CALCULATIONS FOR A HY-130 DYNAMIC TEAR TEST EXPERIMENT

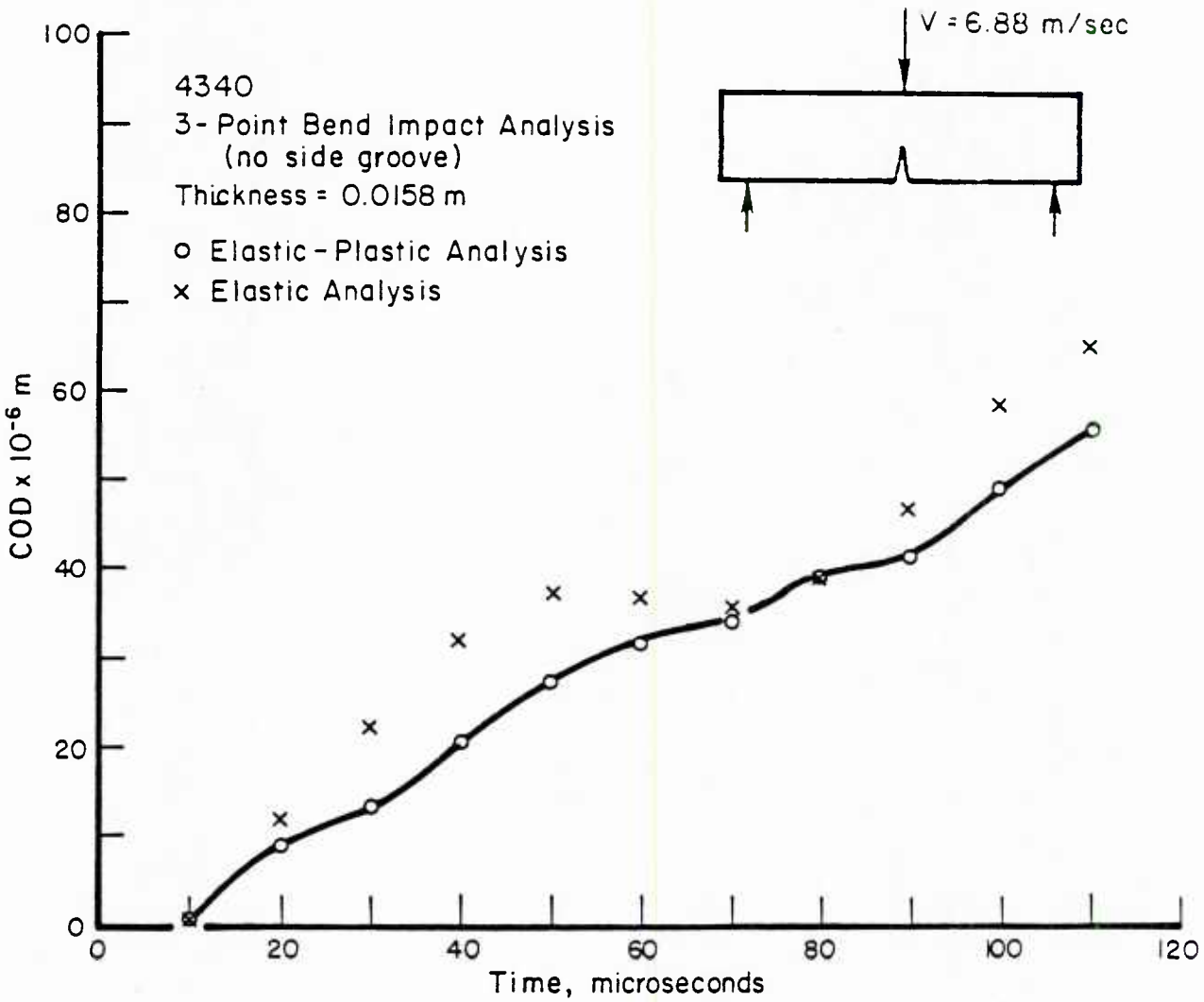

FIGURE 9. CRACK-OPENING DISPLACEMENT (0.00068 m BEHIND THE CRACK TIP) VS TIME.

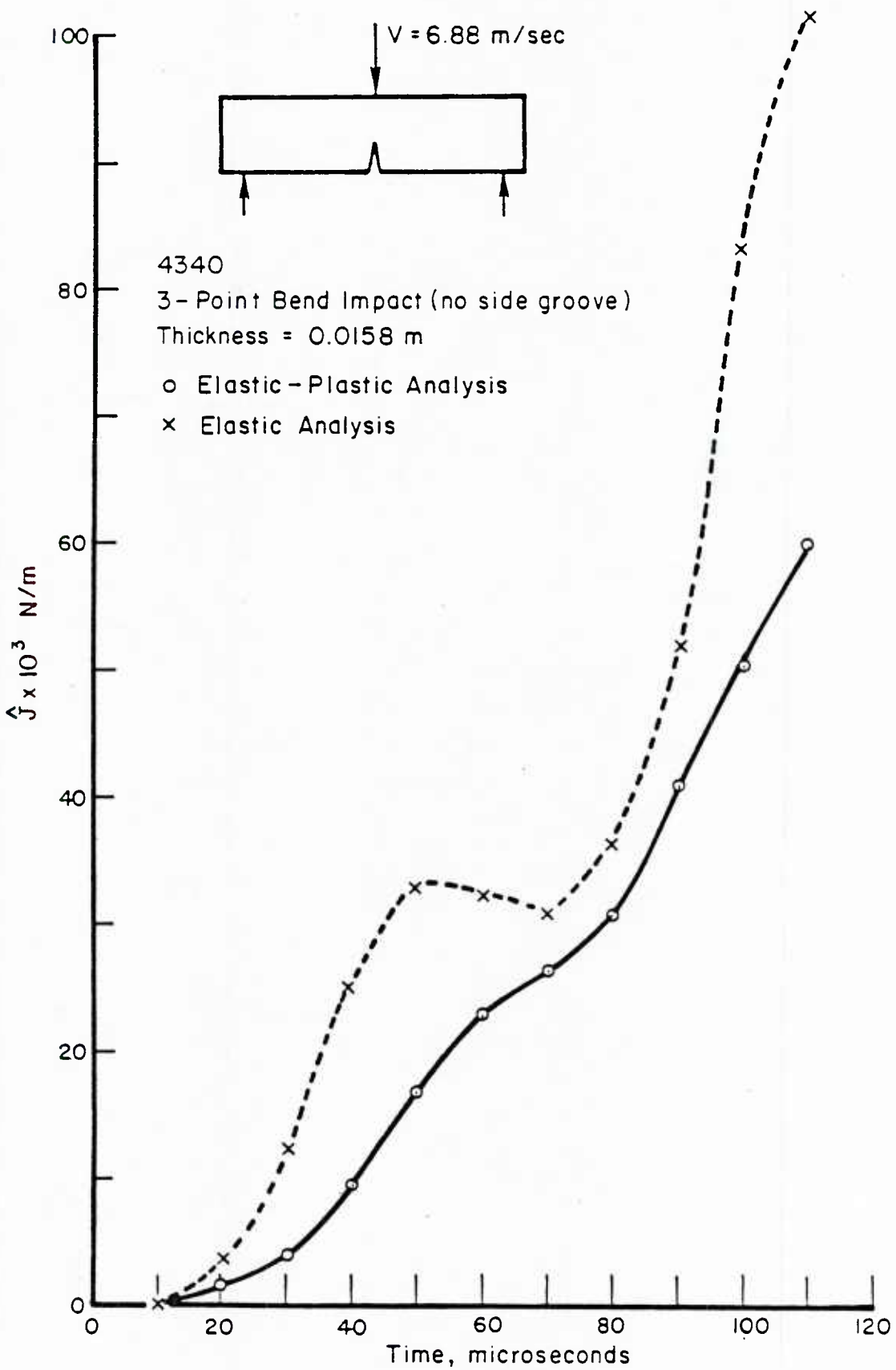

FIGURE 10. $\hat{J}$-INTEGRAL VS. TIME

DISCUSSION AND CONCLUSIONS

Uncertainties now exist concerning the adequacy of elastodynamic solution procedures for unstable crack propagation and crack arrest analyses. The most obvious reason for the existence of these uncertainties is the neglect of crack tip plasticity in such formulations. To address this possibility, an elastic-plastic dynamic finite element capability has been developed. It has been shown in this paper, by comparisons with existing dynamic fracture mechanics solutions and with experimental data, that this capability is more than adequate for its intended purposes.

Some preliminary calculations comparing the elastic and the elastic-plastic predictions for a stationary crack in an impact loaded bend specimen were also obtained. These indicate that the effect of crack tip plasticity is significant even for a high-strength material. The present capability will next be extended to treat a propagating crack whereupon an even more prominent effect is expected to be revealed. But, whether or not taking direct account of crack tip plasticity during rapid crack propagation will resolve the questions that now exist on the geometry and initiation mode dependence of K_{ID} remains to be seen.

ACKNOWLEDGEMENT

The research described in this paper was supported by the Structural Mechanics Program of the Orfice of Naval Research under Contract Number N00014-77-C-0576. The authors would like to express their appreciation to Drs. Nicholas Perrone and Yapa Rajapakse of ONR for their encouragement of this work.

REFERENCES

[1] Kanninen, M.F., "Whither Dynamic Fracture Mechanics?", Numerical Methods in Fracture Mechanics, Proceedings of the Second International Conference held at University College, Swansea, United Kingdom, Eds. D.R.J. Owen, A.R. Luxmoore, July 1980.

[2] Kanninen, M.F., Gehlen, P.C., Barnes, C.R., Hoagland, R.G., Hahn, G.T., and Popelar, C.H., "Dynamic Crack Propagation Under Impact Loading", Nonlinear and Dynamic Fracture Mechanics, Eds. Nicholas Perrone and Satya Atluri, American Society of Mechanical Engineers, AMD-Vol 35, pp 195-200, 1979.

[3] Kishimoto, K., et al., "On the Path Independent Integral - $\hat{J}$", Engineering Fracture Mechanics, Vol. 13, 1980, pp. 841-850.

[4] Bui, H.D., "Stress and Crack-displacement Intensity Factors in Elastodynamics", Proceeding of the Fourth International Conference on Fracture, Waterloo, Canada, June 1977, pp 91-96.

[5] Freund, L.B., "Energy Flux into the Tip of an Extending Crack in an Elastic Solid," J. Elasticity, Vol. 2, 1972, pp 341-349.

[6] Blackburn, W.S., "Path Independent Integrals to Predict Onset of Crack Instability in an Elastic-Plastic Material," International Journal of Fracture Mechanics., Vol. 8, 1972, pp. 343-346.

[7] Rice, J.R., "A Path Independent Integral and the Approximate Analysis of Strain Concentration by Notches and Cracks", Trans. ASME J. Appl. Mech., Vol. 90, 1968, pp. 379-386.

[8] Hahn, G.T., Hoagland, R.G., Kanninen, M.F., and Rosenfield, M.R., "A Preliminary Study of Fast Fracture and Arrest in the DCB Test Specimen", Dynamic Crack Propagation, G.C. Sih, Editor, Noordhoff, Leyden, 1973, pp. 649-662.

[9] Kalthoff, J.F., et al,"Measurements of Dynamic Stress Intensity Factors for Fast Running and Arresting Cracks in Double Cantilever Beam Specimens, Fast Fracture and Crack Arrest, Ed. G.T. Hahn and M.F. Kanninen, ASTM STP 627, 1977, pp 161-176.

[10] Barsoum, R.S., "On the Use of Isoparametric Finite Elements in Linear Elastic Fracture Mechanics:, Int. J. of Num. Meth. In Engrg., Vol. 10, No. 1, 1976.

[11] Cook, R.D., Concepts and Applications of Finite Element Analysis, Publ. John Wiley & Sons, Inc., 1974.

[12] Klaus-Jurgen, Bathe, and Wilson, E.L., Numerical Methods in Finite Element Analysis, Prentice-Hall, Inc., Englewood Cliffs, New Jersey, pp 322-326, 1976.

[13] Jung, J., Ahmad, J., Kanninen, M.F., and Popelar, C.H., "Finite Element Analysis of Dynamic Crack Propagation", to be presented at the 1981 ASME Failure Prevention and Reliability Conference, September 23-26, 1981, Hartford, Conn.

[14] Eftis, J., and Liebowitz, H., "On Fracture Toughness Evaluation for Semi-Brittle Fracture", Engineering Fracture Mechanics, Vol. 7, 1975, pp. 491-503.

[15] Wilson, W.K., and Yu, I.W., "The Use of the J-Integral in Thermal Stress Crack Problems", International Journal of Fracture, Vol. 15, No. 4, 1979, pp. 377-387.

[16] Kishimoto, K., Aoki, S., and Sakata, M., "Dynamic Stress Intensity Factors Using J-Integral and Finite Element Method", Engineering of Fracture Mechanics, Vol. 13, 1980, pp. 387-394.

[17] Chen, Y.M., "Numerical Computation of Dynamic Stress Intensity Factors by a Lagrangian Finite-Difference Method (The Hemp Code)", Engineering of Fracture Mechanics, Vol. 7, 1975, pp. 653-660.

[18] Broberg, K.B., "The Propagation of a Brittle Crack", Arkiv for Fysik, Band 18, No. 10, pp 139-192, 1966.

[19] Mall, S., "Finite Element Analysis of Stationary Cracks in Time Dependent Stress Fields", Numerical Methods in Fracture Mechanics, Eds. A.R. Luxmoore and D.R.J. Owen, University College, Swansea, England, 1980.

[20] Atluri, S.N., and Nishioka, T., "Numerical Modeling of Dynamic and Non-linear Crack Propagation in Finite Bodies by Singular Elements, to be published.

THE NUMERICAL SIMULATION OF CRACK GROWTH IN WELD-INDUCED RESIDUAL STRESS FIELDS

by

M.F. Kanninen, F.W. Brust, J. Ahmad, and I.S. Abou-Sayed

STRESS ANALYSIS AND FRACTURE SECTION

BATTELLE
Columbus Laboratories
505 King Avenue
Columbus, Ohio 43201

July, 1981

Invited paper for the 28th Army Sagamore Research Conference, Lake Placid, New York, July 13-17, 1981. To appear in the Conference Proceedings.

SECURITY CLASSIFICATION OF THIS PAGE (When Data Entered)

REPORT DOCUMENTATION PAGE

READ INSTRUCTIONS BEFORE COMPLETING FORM

1. REPORT NUMBER

2. GOVT ACCESSION NO.

3. RECIPIENT'S CATALOG NUMBER

4. TITLE (and Subtitle)

THE NUMERICAL SIMULATION OF CRACK GROWTH IN WELD-INDUCED RESIDUAL STRESS FIELDS

5. TYPE OF REPORT & PERIOD COVERED

Interim

6. PERFORMING ORG. REPORT NUMBER

7. AUTHOR(s)

M.F. Kanninen, F.W. Brust, J. Ahmad, and I.S. Abou-Sayed

8. CONTRACT OR GRANT NUMBER(s)

N00014-77-C-0576 - Battelle

9. PERFORMING ORGANIZATION NAME AND ADDRESS

Battelle's Columbus Laboratories
505 King Avenue
Columbus, Ohio 43201

10. PROGRAM ELEMENT, PROJECT, TASK AREA & WORK UNIT NUMBERS

11. CONTROLLING OFFICE NAME AND ADDRESS

Office of Naval Research
Structural Mechanics Program
Department of the Navy, Arlington, VA 22217

12. REPORT DATE

March 1981

13. NUMBER OF PAGES

22

14. MONITORING AGENCY NAME & ADDRESS(if different from Controlling Office)

15. SECURITY CLASS. (of this report)

Unclassified

15a. DECLASSIFICATION/DOWNGRADING SCHEDULE

16. DISTRIBUTION STATEMENT (of this Report)

Approved for public release; distribution unlimited

17. DISTRIBUTION STATEMENT (of the abstract entered in Block 20, if different from Report)

18. SUPPLEMENTARY NOTES

Paper was presented at the 28th Army Sagamore Research Conference, Lake Placid, New York, July 13-17, 1981.

19. KEY WORDS (Continue on reverse side if necessary and identify by block number)

Stress Corrosion Cracking; Fracture; Dynamic Crack Propagation, Finite Element Analyses

20. ABSTRACT (Continue on reverse side if necessary and identify by block number)

A marriage of elastic plastic fracture mechanics techniques with thermoplastic finite element analyses is developed to examine crack growth in the presence of weld-induced residual stresses. A hypothetical crack growth relation based on the crack tip opening displacement is used. Three problem areas are studied: stress corrosion cracking in a girth-welded pipe, fatigue crack growth under cyclic loading in a butt-welded plate, and dynamic crack propagation under impact loading in a butt-welded plate. Comparisons with computations carried out under conventional linear elastic assumptions are made. It is found that, in all three

DD FORM 1 JAN 73 1473 EDITION OF 1 NOV 65 IS OBSOLETE

S/N 0102-LF-014-6601

(over)

SECURITY CLASSIFICATION OF THIS PAGE (When Data Entered)

cases, neglect of the plastic deformation caused by the welding process appears to be anti-conservative. It is concluded that more realistic computations for crack growth in and around welds than are commonly used may be needed for realistic structural integrity assessments.

THE NUMERICAL SIMULATION OF CRACK GROWTH IN WELD-INDUCED RESIDUAL STRESS FIELDS

M. F. Kanninen, F. W. Brust,
J. Ahmad, and I. S. Abou-Sayed
Stress Analysis and Fracture Section
Battelle Columbus Laboratories
Columbus, Ohio 43201

ABSTRACT

A marriage of elastic-plastic fracture mechanics techniques with thermoplastic finite element analyses is developed to examine crack growth in the presence of weld-induced residual stresses. A hypothetical crack growth relation based on the crack tip opening displacement is used. Three problem areas are studied: stress corrosion cracking in a girth-welded pipe, fatigue crack growth under cyclic loading in a butt-welded plate, and dynamic crack propagation under impact loading in a butt-welded plate. Comparisons with computations carried out under conventional linear elastic assumptions are made. It is found that, in all three cases, neglect of the plastic deformation caused by the welding process appears to be anti-conservative. It is concluded that more realistic computations for crack growth in and around welds than are commonly used may be needed for realistic structural integrity assessments.

INTRODUCTION

A significant proportion of all structural failures can be traced to cracks emanating in and around welds. Crack growth in welded regions must be strongly affected by the presence of the plastically deformed material indigenous to the welding process. Yet, present day fracture mechanics analysis procedures, which are largely based on linear elastic conditions, do not directly treat such complications. While elastic-plastic fracture mechanics analysis procedures have been developed, they have previously been

applied to account only for crack tip plasticity itself. Recently, a further step has been taken by the authors through the use of postulated elastic-plastic crack growth relations for crack growth in weld-induced plastic deformation fields[1-3]. This work is summarized and assimilated in this paper.

The immediate objective of the work reported in References 1-3 was to critically examine the assumptions of linear elastic material behavior commonly made in analyzing weld cracking problems. Three separate problems were addressed. As shown in Table 1, these included two different welded structures - a girth-welded pipe and a butt-welded plate - and three different crack growth mechanisms - stress corrosion, fatigue and unstable crack propagation. The solution procedure and the individual results are first presented in what follows with general conclusions for future progress in the analysis of crack growth in the presence of weld-induced residual stress drawn from them.

Table 1. Problems Examined

Structure	Material	Applied Loading	Simulated Cracking Mechanism
Girth-welded pipe with circumferential crack (axisymmetry)	Type 304 Stainless Steel	Constant Tension	Stress Corrosion
Butt-welded with edge crack (Plane Strain)	HY-80 Steel	Cyclic Tension	Fatigue
Butt-welded plate with edge crack (Plane Strain)	HY-80 Steel	Impulsively Applied Tension	Dynamic Fracture

THE ANALYSIS PROCEDURE

The analysis procedure followed in this work, which is basically the same for all three problems examined, consists of three main steps:

1. The residual stress field induced in a welding process is computed using an incremental thermoplastic finite element analysis procedure.

2. Crack growth is simulated by sequential node release along a pre-set crack plane located in the weld heat-affected zone.

3. A postulated elastic-plastic crack growth relation is used to infer crack length as a function of time or loading history to simulate a particular crack mechanism.

A comparison with a computational result made using a commonly accepted linear elastic approach is then made to assess the significance of the linear elastic assumption and the essential neglect of residual plasticity inherent in such an approach.

Residual Stress Analysis

The residual stress analysis procedure is one that has been used successfully at Battelle in a variety of applications[4-6]. It consists of two parts. First, a thermal analysis is made to obtain the time-temperature history for each point in the body for each individual welding pass. Then, these histories are used as input to an incremental elastic-plastic finite element model to determine the stress and deformation state of the weld and the base material as the weld is deposited. Because each welding pass is considered on an individual basis, the residual stress and strain state that exists at the completion of one weld pass constitutes the initial condition for the next. The final residual stress state is that which exists at the completion of all of the weld passes.

In the work described here, the finite element models for the welding analysis were designed with a line of double nodes along a pre-set crack plane. This had no effect on the residual stress distribution as it was assumed that an initial (small) crack appeared after the welding process was completed. The potential crack plane was located in the heat-affected zone but was otherwise arbitrary.

The two welded structures examined in the work reported here - a girth-welded pipe and a butt-welded plate - are shown in Figures 1 and 2, respectively. The corresponding finite element models are shown in Figures 3 and 4. It can be seen that a number of simplifications have been introduced for computation convenience. These include:

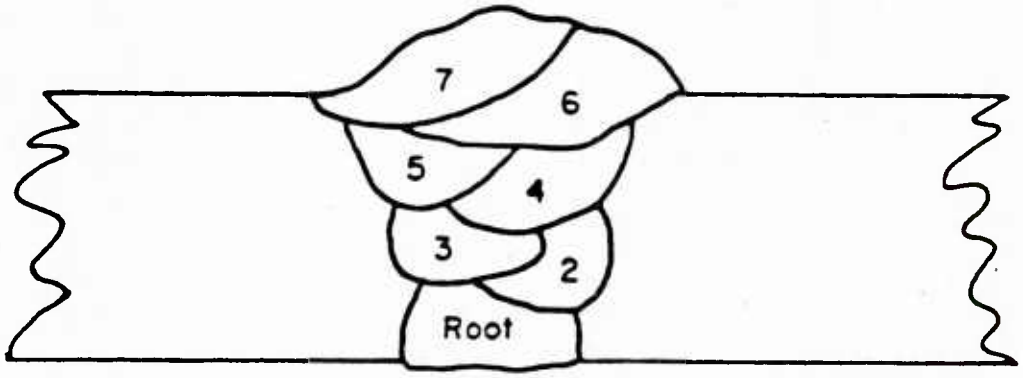

FIGURE 1. CROSS SECTION OF A SEVEN-PASS GIRTH-BUTT WELD IN A 4-INCH DIAMETER SCHEDULE 80 TYPE 304 STAINLESS STEEL PIPE

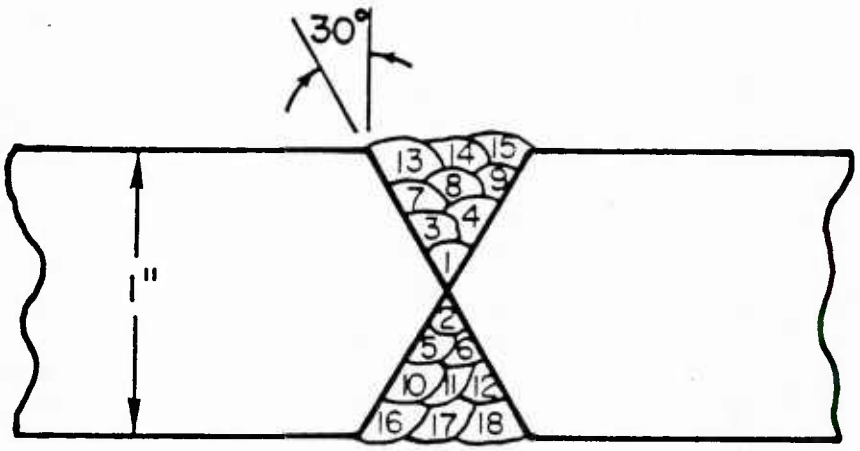

FIGURE 2. CROSS SECTION OF AN 18-PASS BUTT WELD IN AN HY-80 STEEL SHIP STRUCTURE

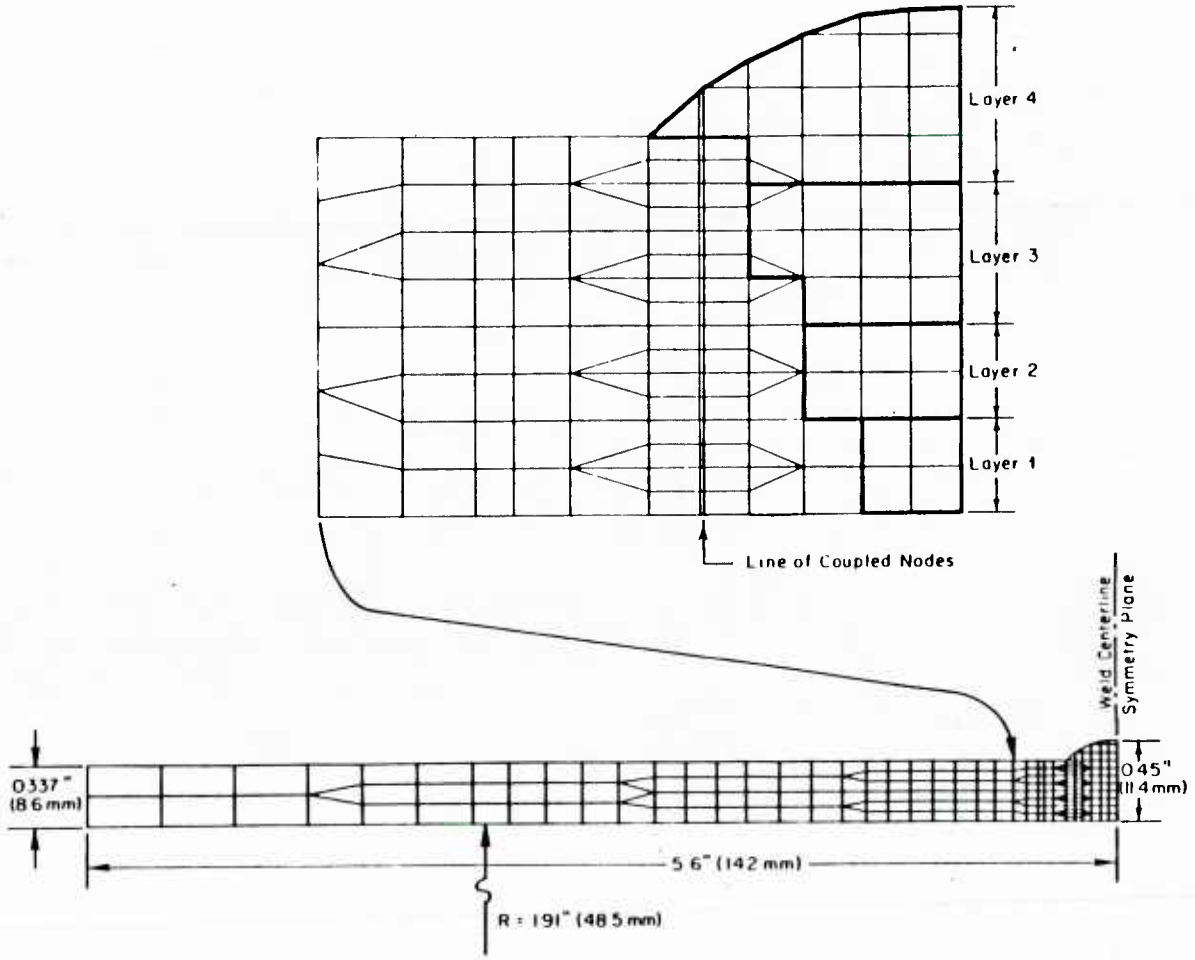

FIGURE 3. FINITE ELEMENT MODEL FOR RESIDUAL STRESS AND CRACK GROWTH ANALYSIS IN A GIRTH-WELDED 4-INCH DIAMETER SCHEDULE 80 TYPE 304 STAINLESS STEEL PIPE

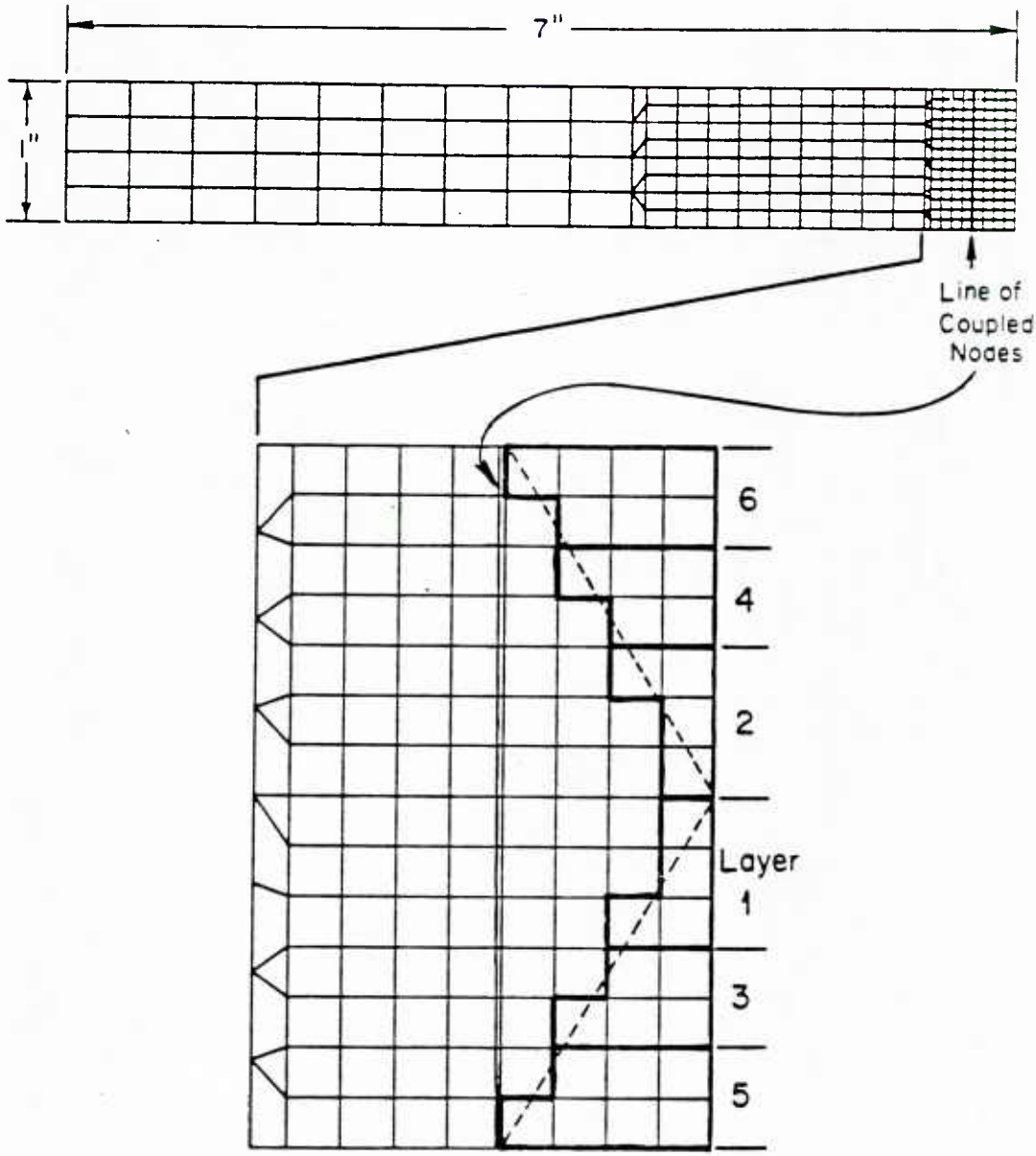

FIGURE 4. FINITE ELEMENT MODEL FOR A BUTT-WELDED PLATE (PLANE STRAIN)

- weld line symmetry
- two-dimensional deformation (i.e., axisymmetry or plane strain)
- one-dimensional crack growth (i.e., concentric or collinear).

Note that, because the cracks are not supposed to be at the center of the weld (cf, Figures 3 and 4), the first of these simplifying assumptions means that two cracks exist in the analysis.

The temperature-dependent material properties used in the analyses of the pipe weld are those of Type 304 stainless steel shown in Figure 5. The properties for the butt-welded plate are those of the ship structure steel HY-80 given in Figure 6. In the first problem, the heat inputs were taken from an actual experience[7] while in the second, typical values were used. These together with the weld pass and structure geometry, suffice to determine the residual stress distribution. The normal stresses acting on the prospective crack plane for the two welded configurations are shown in Figures 7 and 8. It can be seen that, while these are quite different, they share a high tensile stress near the surface. Thus, an edge crack would be likely to grow, particularly when the residual stresses are abetted by a tensile applied stress.

Subcritical Crack Growth Analysis

The equivalence between the crack tip opening displacement (CTOD) and the stress intensity factor in small-scale yielding is well known. Recent progress in elastic-plastic fracture mechanics has further revealed the distinctive role played by the crack tip crack opening displacement in crack initiation and stable growth in large scale yielding conditions[8-10]. Specifically, for the initiation of crack growth, the CTOD can be expressed as

$$\delta = \begin{cases} \alpha \dfrac{K^2}{EY} & \text{small-scale yielding} \\ d_n \dfrac{J}{Y} & \text{deformation plasticity} \end{cases} \qquad (1)$$

where K is the stress intensity factor, J is the J-integral parameter, E is the elastic modulus, Y is the yield stress while α and d_n are numerical constants on the order of unity. In addition, for extended stable crack growth, the CTOD appears to take on a constant value. While certainly not conclusive evidence that the

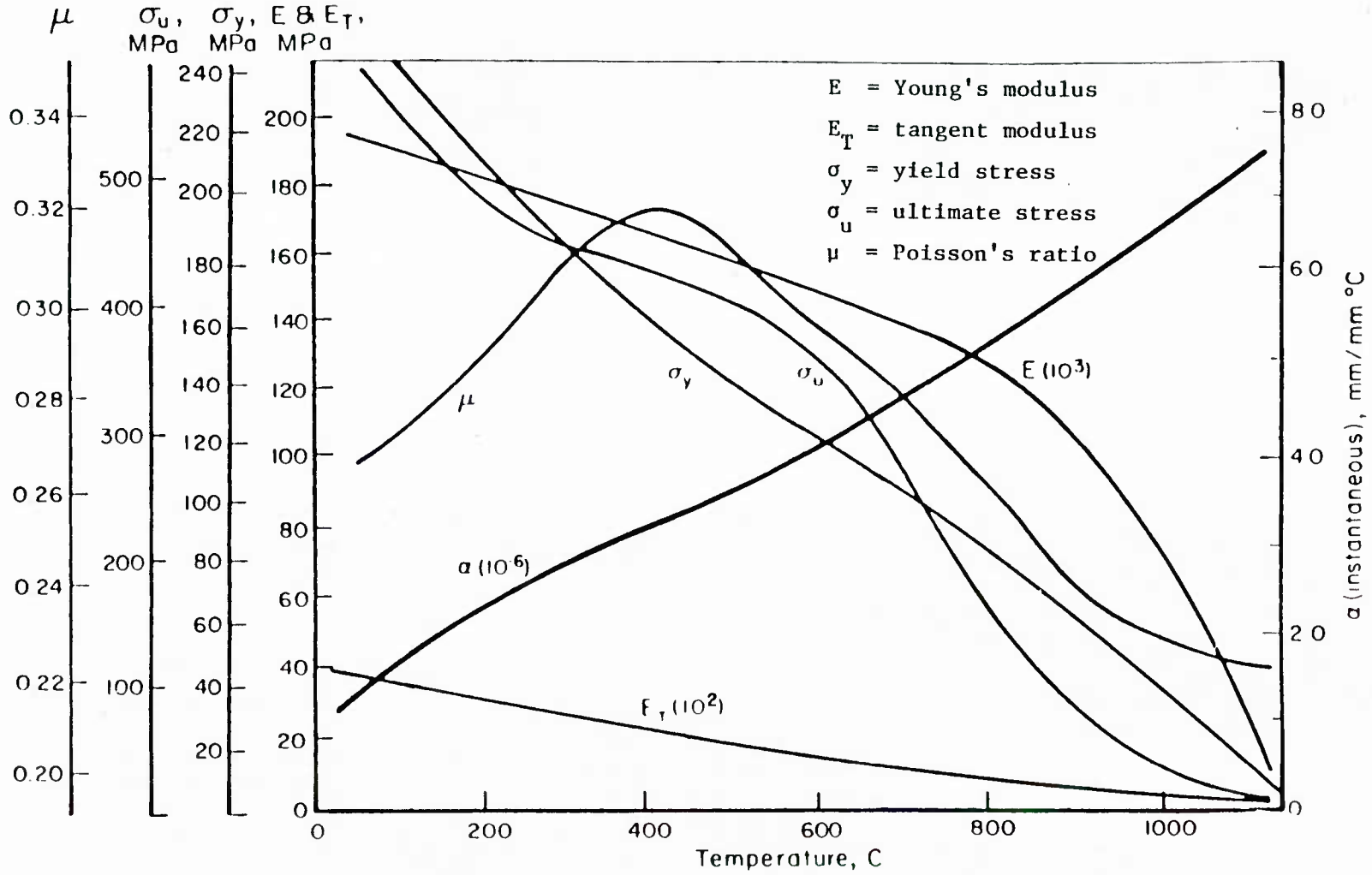

FIGURE 5. TEMPERATURE DEPENDENT PROPERTIES OF TYPE 304 STAINLESS STEEL

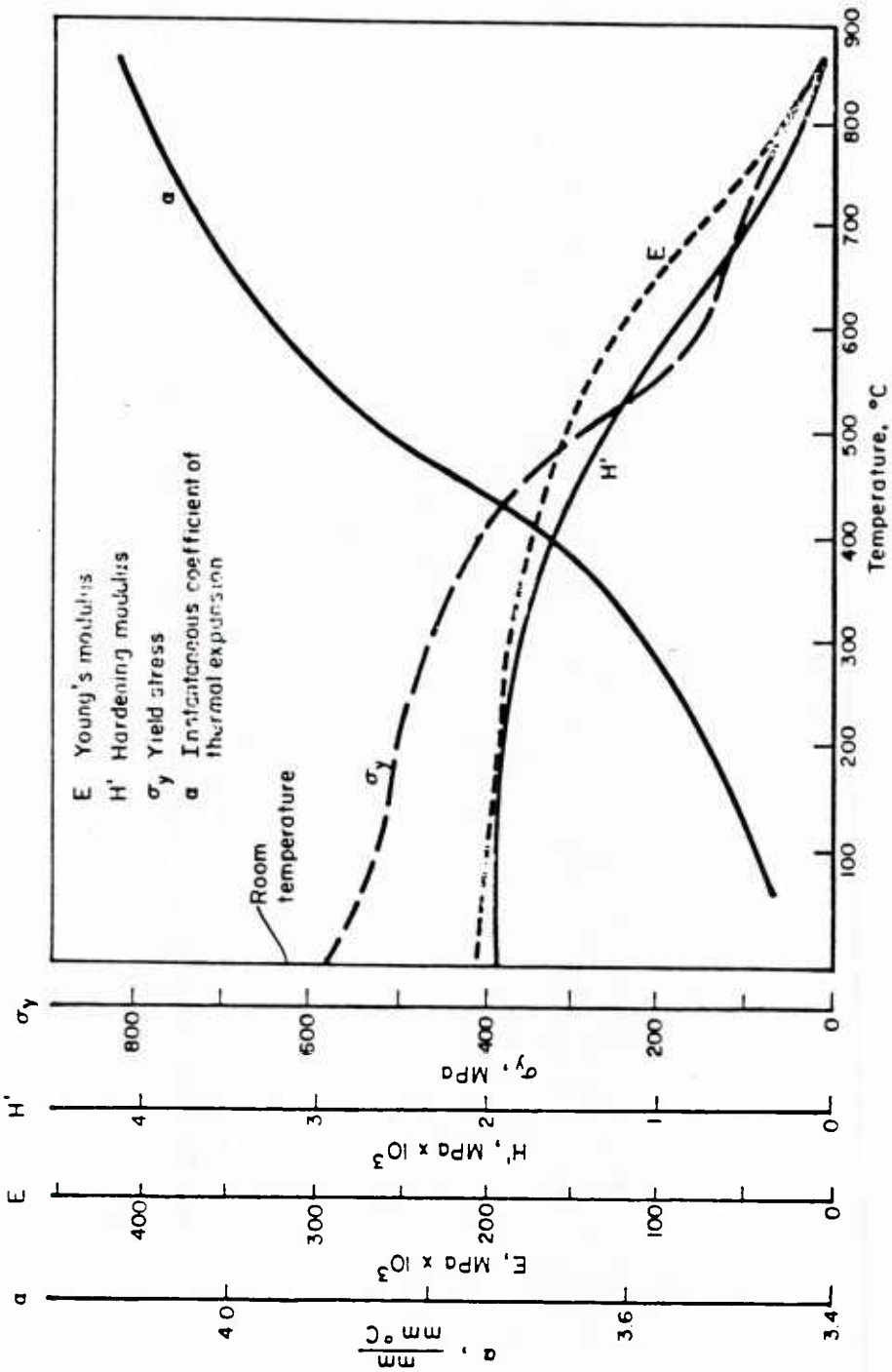

FIGURE 6. TEMPERATURE DEPENDENT MATERIAL PROPERTIES FOR HY-80

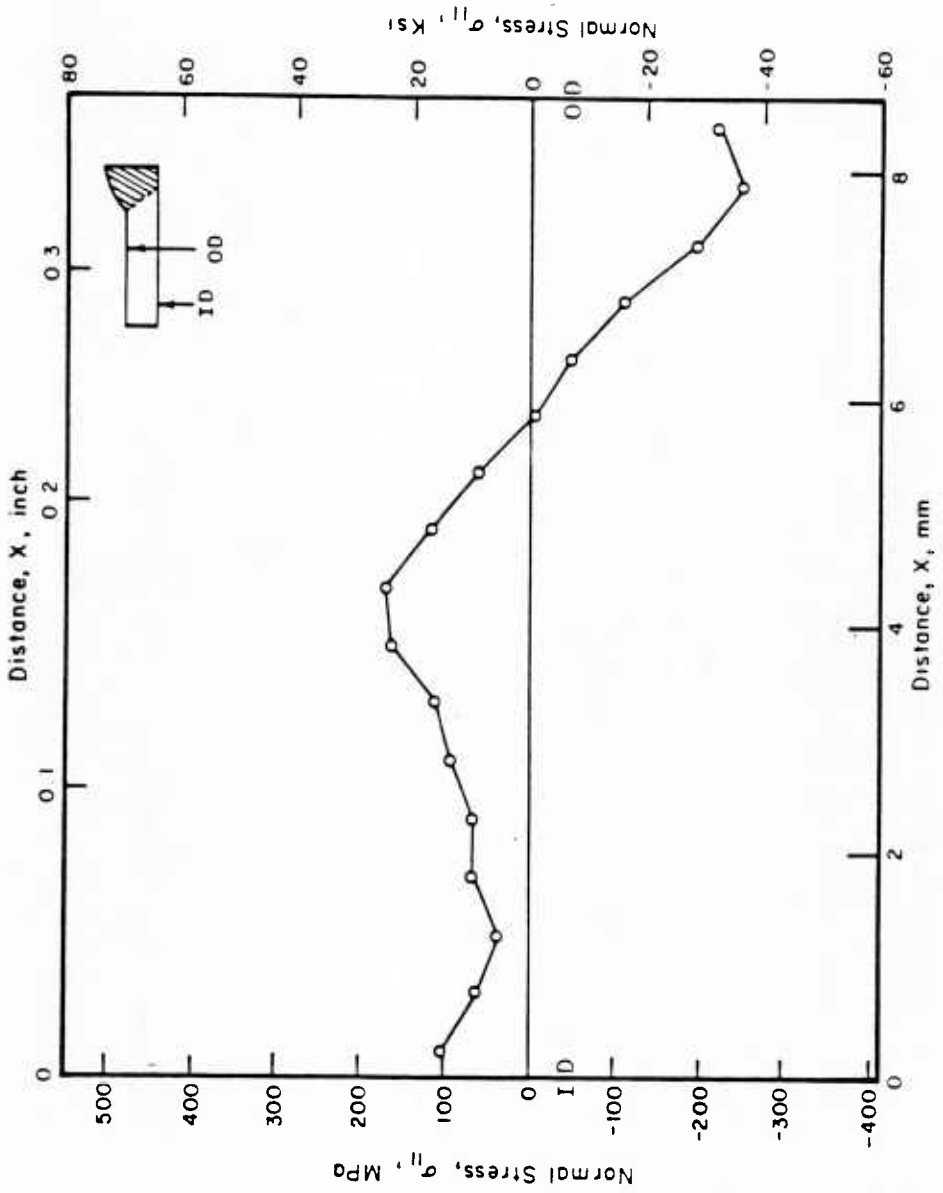

FIGURE 7. THROUGH-WALL RESIDUAL STRESSES ON THE POTENTIAL CRACK LINE IN A GIRTH-WELDED 4-INCH DIAMETER PIPE

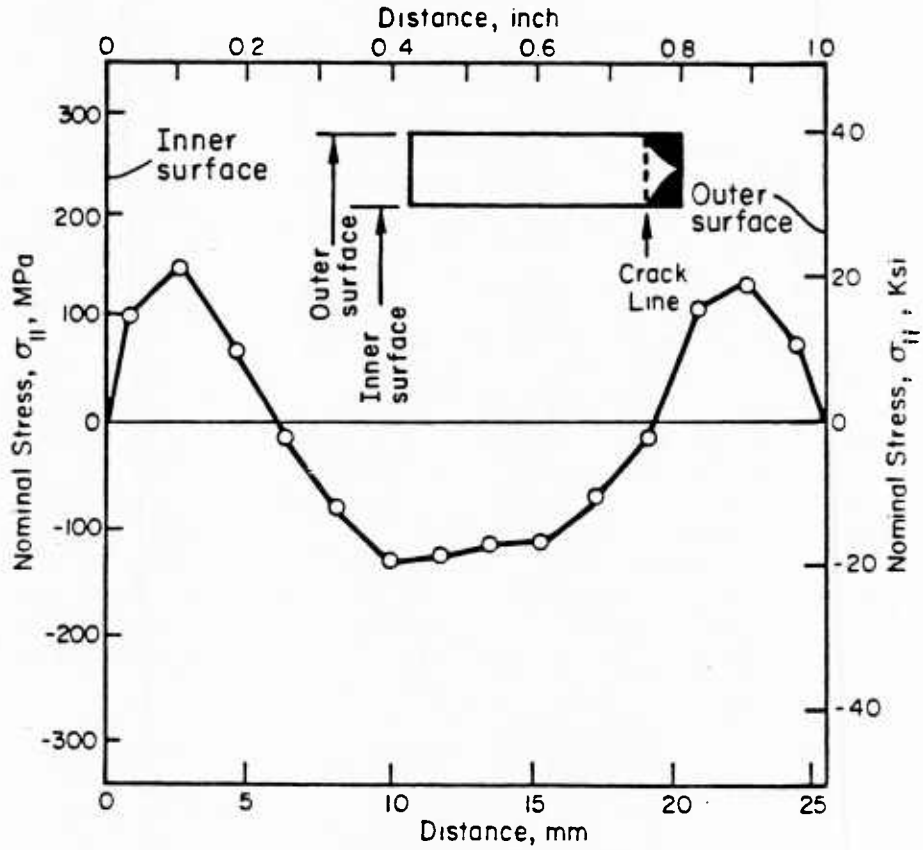

FIGURE 8. RESIDUAL STRESS ON POTENTIAL CRACK LINE IN A 1-INCH THICK BUTT-WELDED PLATE OF HY-80 STEEL

CTOD is the controlling parameter for subcritical crack growth as well, for lack of an alternative, it will be so taken in this work. Note that, because of the equivalence represented by Equation (1), this choice is not inferior to one based on either K or J in any event.

Starting from an assumed initial crack, crack growth is simulated in each of the finite element models by sequential node release along the line of double-noded elements. Each node pair is released by diminishing the initial force that exists between them to zero. This is done over from five to ten load increments. The value of δ for a given crack length is then the value of the CTOD that exists when the load has vanished. Hence, it is a value at one finite element spacing behind the actual crack tip. The results obtained from the finite element models are shown in Figures 9 and 10. Note that in the latter problem two solutions are shown: one with no applied stress, the second with an applied tensile stress normal to the crack plane of 67 percent of the room temperature yield stress of HY-80 steel (80 ksi).

Figures 9 and 10 contrast the CTOD values obtained by advancing the crack through the finite element model under two different conditions. First, the computed weld-induced plastic deformation is left unaltered and an incremental plasticity computation made. This is the elastic-plastic analysis. Second, a simplified approach is followed wherein (1) only the normal component of the residual stress acting on the potential crack plane is retained, and (2) linear elastic behavior is assumed. This is denoted as the simple elastic analysis and typifies that commonly used for this kind of problem.

Stress corrosion cracking is often supposed to occur according to a power law relation of the type

$$\frac{da}{dt} = CK^m \tag{2}$$

where a denotes the crack length, t is time, while C and m are material constants. Because this relation is clearly valid only under small scale yielding conditions, the relation between K and δ expressed by Equation (1) can be used to cast it into the equivalent form

$$\frac{da}{dt} = C'\delta^{m/2} \tag{3}$$

where C' is also a material constant[1]. Having $\dot{\delta} = \delta$ (a) from Figure 9, Equation (3) can be integrated numerically to find the crack length in terms of a dimensionless time t*

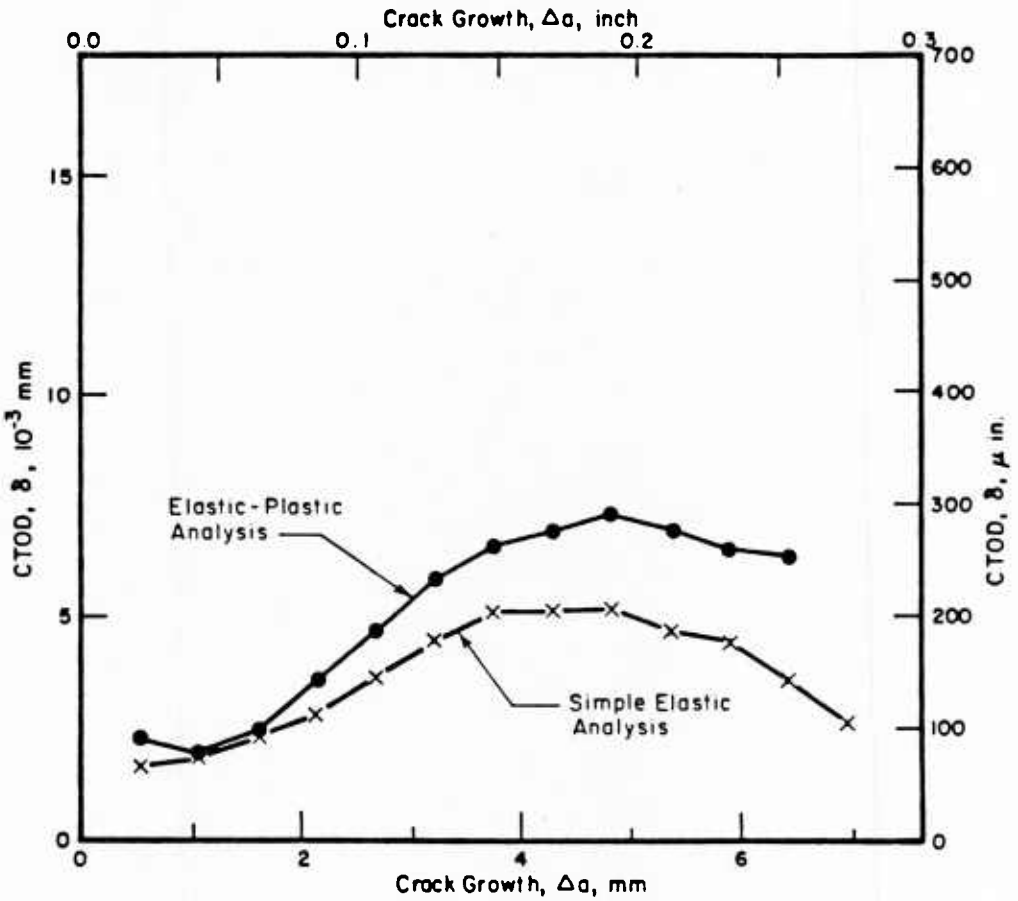

FIGURE 9. CTOD CALCULATED AS A FUNCTION OF CRACK GROWTH (Δa) FOR 4-INCH DIAMETER TYPE 304 STAINLESS STEEL PIPE SUBJECTED TO WELDING INDUCED RESIDUAL STRESSES AND ZERO APPLIED STRESS

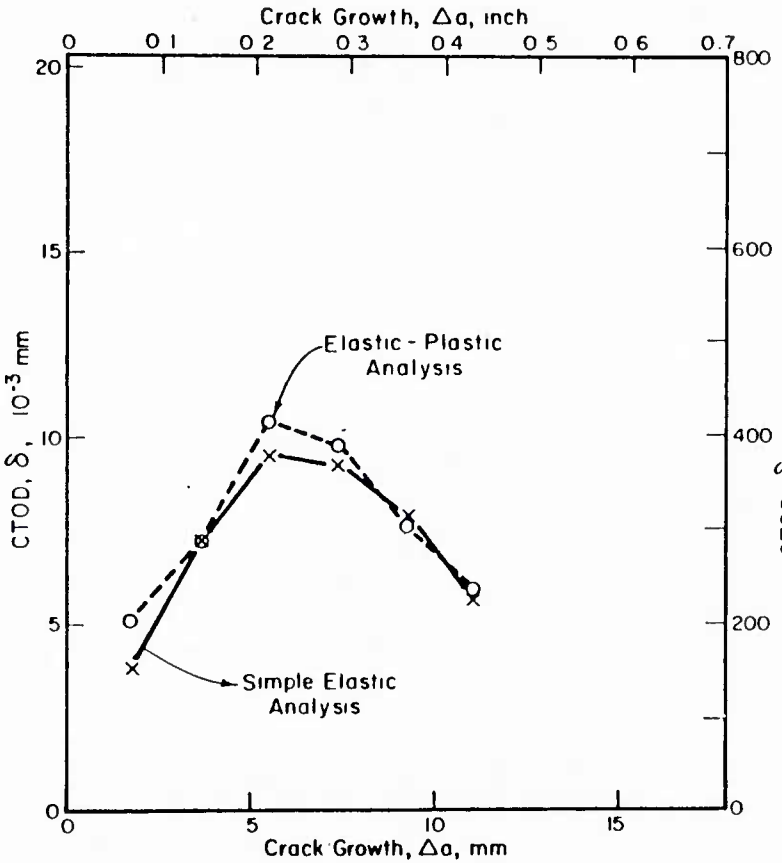

FIGURE 10 (a). ZERO APPLIED LOAD

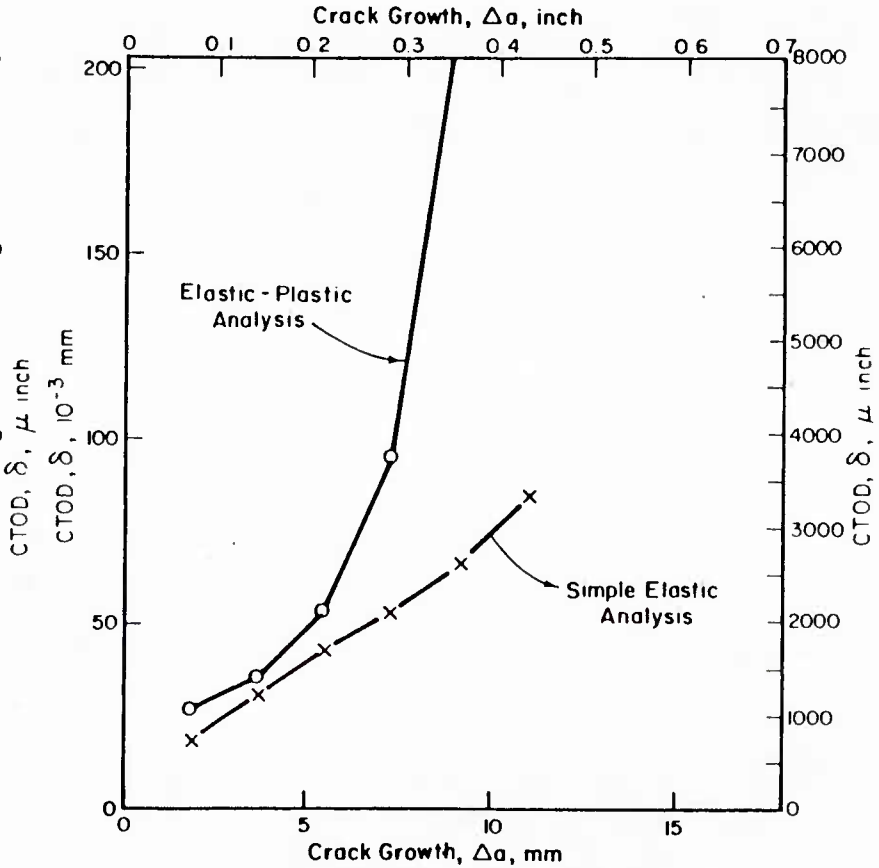

FIGURE 10 (b). APPLIED LOAD = 0.67 σ_o

COMPUTED CRACK TIP OPENING DISPLACEMENT IN A BUTT-WELDED HY-80 PLATE AS A FUNCTION OF CRACK GROWTH

$$t^* = \int_{a_o}^{a} \frac{h^{m/2-1}}{\delta^{m/2}}\, da \tag{4}$$

where h denotes the wall thickness. The result is shown in Figure 11.

Notice that the results given in Figure 11 were obtained without the imposition of an applied stress. Thus, despite the fact that the residual stresses are self-equilibrating, catastrophic crack growth can occur. The reason is that the stresses are redistributed as crack growth occurs and, at least until a net compressive force is freed by the growing crack, a positive crack driving force exists; cf, Figure 9. Of more importance, the results of Figure 11 indicate that the simple elastic analysis predicts an anti-conservative result in that the time-to-failure is greater than in the more rigorous elastic-plastic analysis.

Fatigue crack growth under a uniform cyclic loading can often be adequately characterized in the form

$$\frac{da}{dN} = C\,(K_{max} - K_{min})^m \tag{5}$$

where N denotes a load cycle number and C and m are material constants. Again introducing the CTOD from Equation (1) gives

$$\frac{da}{dN} = C'(\delta_{min}^{1/2} - \delta_{min}^{1/2})^m \tag{6}$$

where δ_{max} and δ_{min} are the CTOD values that would be attained under the maximum and minimum load levels, respectively. Consequently, the number of cycles required to achieve a given crack length can be found by integrating Equation (6) via

$$N = \frac{1}{C'} \int_{a_o}^{a} \frac{da}{(\delta_{max}^{1/2} - \delta_{min}^{1/2})^m} \tag{7}$$

The results, using the CTOD values given in Figure 10, are shown in Figure 12. It can be seen that the simple elastic analysis is once again anti-conservative.

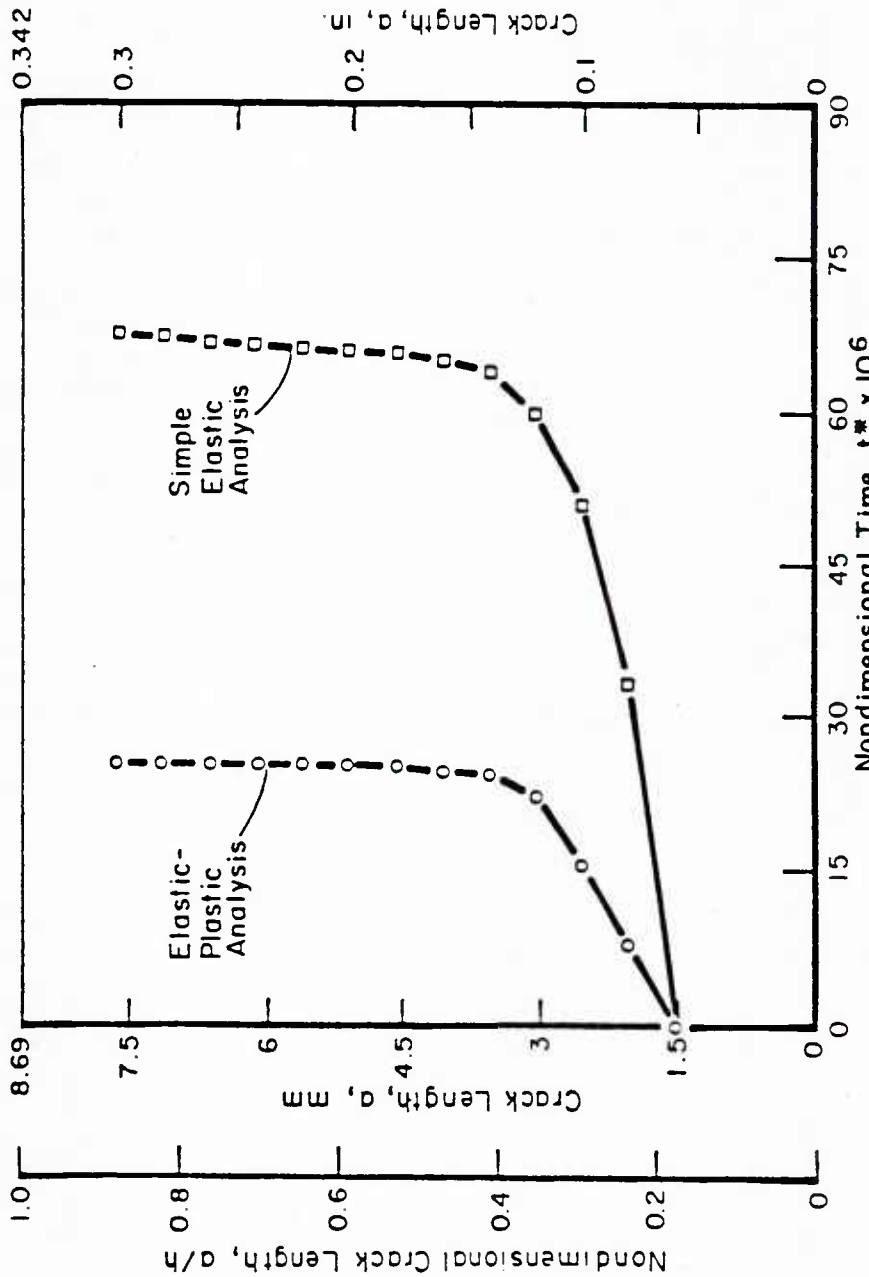

FIGURE 11. NONDIMENSIONAL TIME t* AS A FUNCTION OF CRACK GROWTH FOR 4-INCH DIAMETER TYPE 304 STAINLESS STEEL PIPE SUBJECTED TO WELDING INDUCED RESIDUAL STRESSES

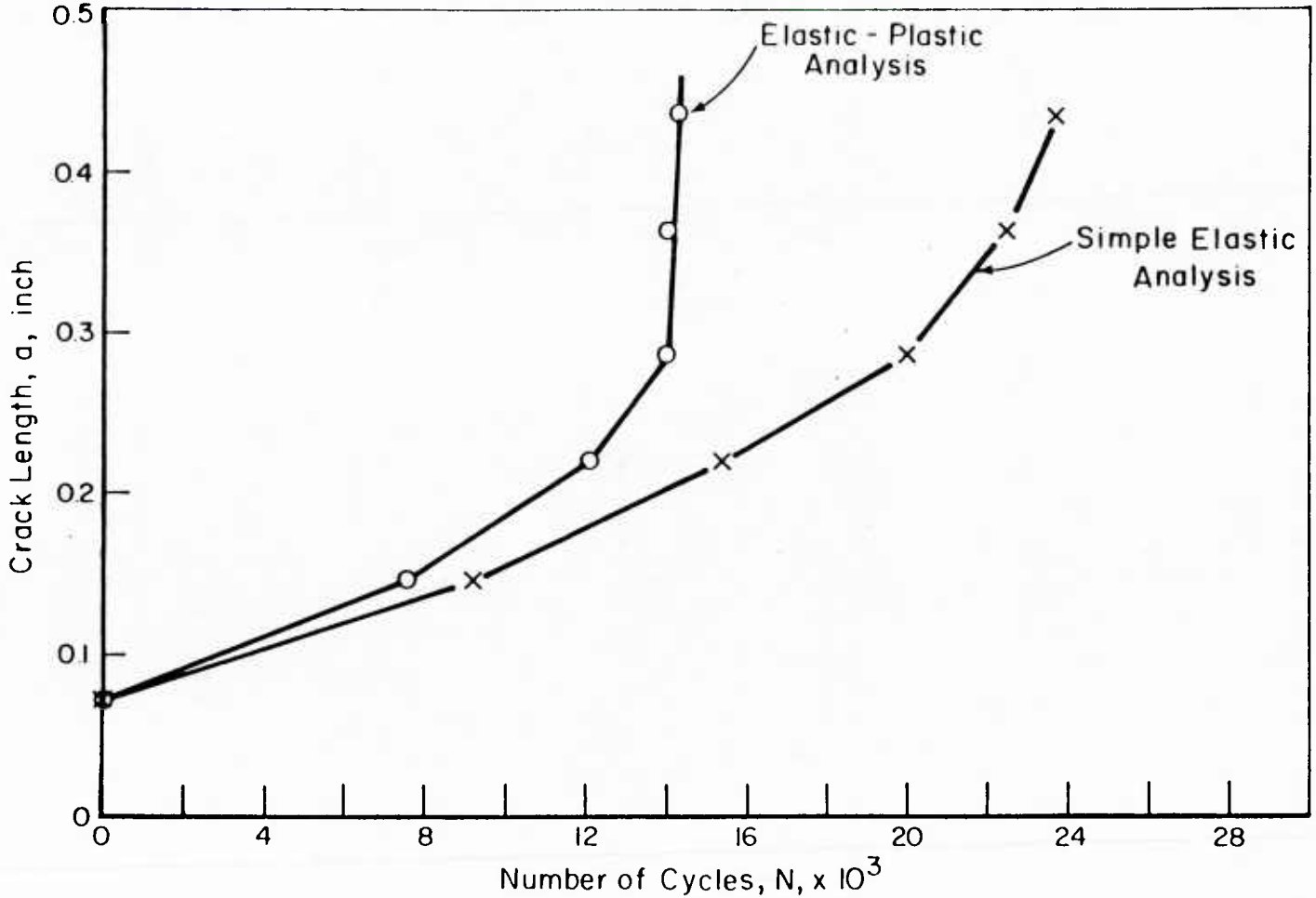

FIGURE 12. COMPARISON OF ELASTIC AND ELASTIC-PLASTIC COMPUTATION OF FATIGUE CRACK GROWTH IN A BUTT-WELDED PLATE

Dynamic Crack Propagation Analysis

The governing relations for unstable crack propagation and arrest in elastodynamic conditions are

$$K = K_D \ , \ \dot{a} > 0$$
$$K < K_D \ , \ \dot{a} = 0 \qquad (8)$$

where K_D is known as the dynamic fracture toughness. Once again, so long as small scale yielding conditions are satisfied, such relations are equivalent to those couched in terms of the CTOD. In particular, the critical CTOD value for dynamic crack propagation would then be simply

$$\delta_D = \alpha \frac{K_D^2}{EY} \qquad (9)$$

Clearly, if a time varying loading is imposed on a cracked body, the CTOD value will also vary. So long as $\delta < \delta_D$, the crack tip will be stationary. If δ becomes equal to δ_D, crack growth will occur at a rate such that the equality is maintained. Arrest occurs when the equality can no longer be satisfied.

A dynamic computation was performed in which the ship structure shown in Figure 2 was subjected to a suddenly imposed load of 42 ksi, about 50 percent of the room temperature yield stress. This load was held for 30 μsec and then dropped to zero. A value of $K_c = 37.9$ ksi$\sqrt{\text{in.}}$ was used to reflect the lower toughness existing in the heat-affected zone. Using Equation (9), this gave a critical CTOD value of 0.0006 inch. Both a linear elastodynamic and an elastic-plastic dynamic calculation were made. The elastic-plastic analysis was based on the entire residual stress and deformation field together with incremental dynamic plasticity. However, in accord with common practice, the residual stresses were completely ignored in the elastic analysis. The computed CTOD values for the two analyses are shown in Figure 13.

It can be seen in Figure 13 that the elastic-plastic analysis predicts that unstable crack growth would quickly occur (at approximately 15 μsec). It also predicts that the crack would penetrate the wall. In contrast, the elastic analysis does not predict initiation of growth until much later (about 40 μsec) and predicts arrest soon thereafter. Consequently, the simpler procedure is once again found to be anti-conservative.

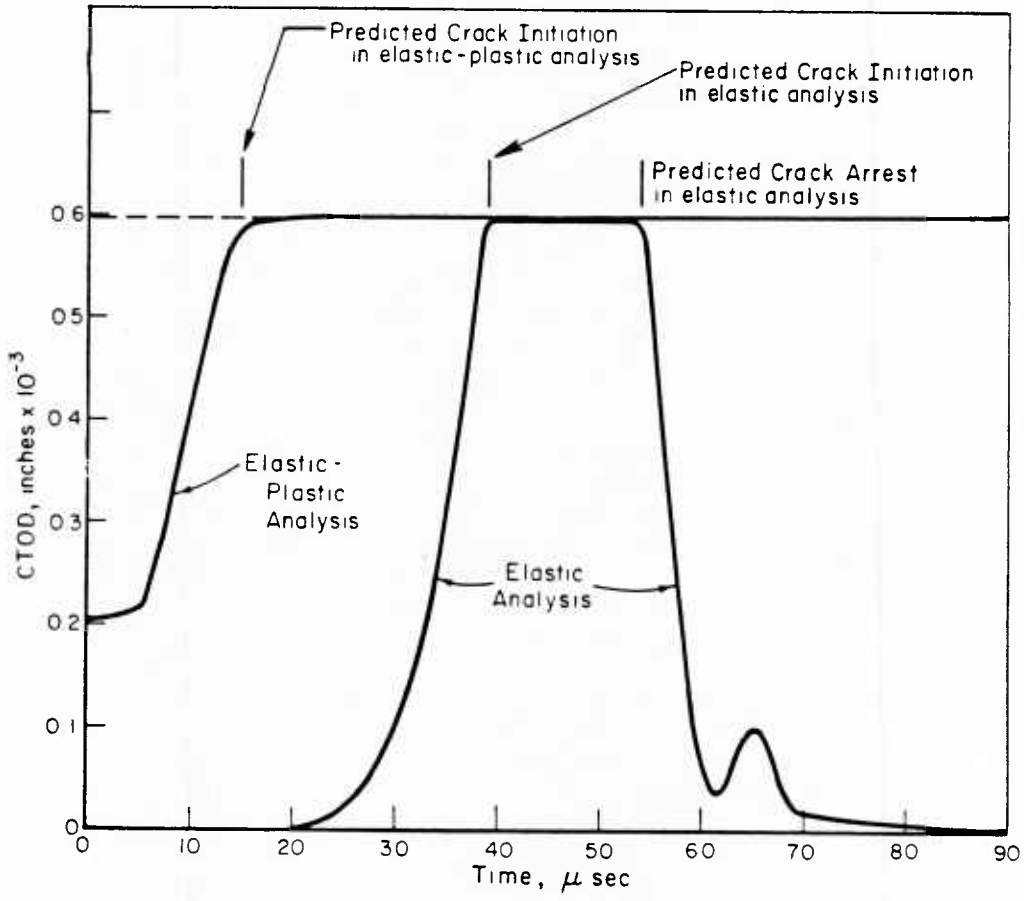

FIGURE 13. COMPARISON OF ELASTIC AND ELASTIC-PLASTIC SOLUTIONS FOR DYNAMIC CRACK PROPAGATION IN THE HEAT AFFECTED ZONE OF AN INITIALLY CRACKED BUTT-WELDED PLATE

DISCUSSION

It is important to recognize that the prime purpose of this work was not to arrive at quantitative results for different types of material behavior. Rather, it was to critically examine a set of assumptions that are commonly used in analyzing a class of problems for given material behavior. The specific materials considered in this study are very ductile and tough (e.g., Type 304 stainless steel, HY-80 steel) which undoubtedly exacerbates the differences that were found. It is quite possible that other materials--and, perhaps more importantly, residual stress fields induced without large-scale plastic deformations--would show considerably less difference. Of equal importance, since the elastic-plastic crack growth criteria needed for the purposes of this study have not been established, a pragmatic approach was taken to obtain comparative results. All of these factors would be borne in mind in interpreting the results given in this paper.

The basic assumption that has been called into question here is the applicability of linear elastic fracture mechanics in the presence of weld-induced residual stress fields. This has been addressed by performing two parallel computations where this assumption has and has not been made. Hence, while there are undeniably many aspects of the calculations that can be improved upon, because the two computations were otherwise performed on exactly the same basis, these cannot be of critical importance. Indeed, the comparison has revealed such wide disparities, that, neglect of the inelastic deformation accompanying welding would appear to be unequivocally incorrect.

Conversely, the work presented in this paper should not be taken as a blanket indictment of LEFM-based crack growth predictions. The mathematical convenience of LEFM is too useful to not play an important part in the assessment of weld cracking. What appears to be needed is some sort of plasticity-enhanced LEFM procedure, possibly calibrated with the more rigorous analyses described in this paper, that can be confidently applied even in the presence of large-scale plasticity and its attendant residual stress fields. How this can best be done is an open question at this time. However, as the work reported herein so strongly suggests, the necessity for it is not.

CONCLUSIONS

Elastic-plastic fracture mechanics research has identified the CTOD as a key crack growth parameter. The use of this finding in conjunction with thermoplastic finite element analysis procedures has enabled more realistic computations of crack growth in the

presence of weld-induced residual deformation and stresses to be made. Comparisons of these results with commonly used approaches based on linear elastic fracture mechanics indicate that the latter could be highly anti-conservative.

ACKNOWLEDGEMENT

This paper was prepared with support from the structural mechanics program of the Office of Naval Research under Contract Number N-00014-77-C-0576. The authors would like to express their gratitude to Drs. N. Perrone and Y. Rajapakse of ONR for supporting their work.

REFERENCES

1. I. S. Abou-Sayed, J. Ahmad, F. W. Brust, and M. F. Kanninen, "An Elastic-Plastic Fracture Mechanics Prediction of Stress Corrosion Cracking in a Girth-Welded Pipe", 14th ASTM National Symposium on Fracture Mechanics, Los Angeles, June 30 to July 2, 1981.
2. F. W. Brust, J. Ahmad, V. Papaspyropoulos, and M. F. Kanninen, "An Elastic-Plastic Fracture Mechanics Prediction of Fatigue Crack Growth in the Heat-Affected Zone of a Butt-Welded Plate", manuscript in preparation (July, 1981).
3. J. Ahmad, F. W. Brust, and M. F. Kanninen, "Dynamic Crack Propagation in the Heat-Affected Zone of an Impact-Loaded Butt-Welded Plate", manuscript in preparation (July, 1981).
4. E. F. Rybicki, D. W. Schmueser, R. G. Stonesifer, J. J. Groom, and H. W. Mishler, "Residual Stresses at Girth-Butt Welds in Pipes and Pressure Vessels", Battelle's Columbus Laboratories Report to the U.S. Nuclear Regulatory Commission, NUREG-0376 (November, 1977).
5. F. W. Brust and R. B. Stonesifer, "Effect of Weld Parameters on Residual Stresses in BWR Piping Systems", Battelle's Columbus Laboratories Report to the Electric Power Research Institute on RP1174 (June, 1980).
6. M. F. Kanninen, T. E. Barber, F. W. Brust, and H. W. Mishler, "Controlling Residual Stresses by Heat Sink Welding", Battelle's Columbus Laboratories Report to the Electric Power Research Institute on RP1576-1 (December, 1980).
7. W. J. Shack, W. A. Ellingson, and L. E. Pahis, "The Measurement of Residual Stresses in Type 304 Stainless Steel Pipe Butt Weldments", Argonne National Laboratory Report to the Electric Power Research Institute on RP449-1 (December, 1978).

8. M. F. Kanninen, et al, "The Development of a Plastic Fracture Methodology", Battelle's Columbus Laboratories Report to the Electric Power Research Institute on RP601-1, EPRI NP-1734 (March, 1981).
9. C. F. Shih, et al, "Methodology for Plastic Fracture", General Electric Company Report to the Electric Power Research Institute on RP601-2, EPRI NP-1735 (March, 1981).
10. M. F. Kanninen, C. H. Popelar, and D. Broek, "A Critical Survey on the Application of Plastic Fracture Mechanics to Nuclear Pressure Vessels and Piping", Battelle's Columbus Laboratories Report to the U.S. Nuclear Regulatory Commission, NUREG CR-2110 (May, 1981).

THE DEVELOPMENT OF A DYNAMIC ELASTOPLASTIC FINITE ELEMENT ANALYSIS FOR FAST FRACTURE UNDER IMPACT LOADING

by

Jalees Ahmad
J. Jung
C. R. Barnes
M. F. Kanninen

BATTELLE
Columbus Laboratories
505 King Avenue
Columbus, Ohio 43201

June, 1981

Submitted for presentation at the ASME/PVP Conference, Denver, Colorado June 22-25, 1981.

SECURITY CLASSIFICATION OF THIS PAGE (When Data Entered)

REPORT DOCUMENTATION PAGE

READ INSTRUCTIONS BEFORE COMPLETING FORM

1. REPORT NUMBER

2. GOVT ACCESSION NO.

3. RECIPIENT'S CATALOG NUMBER

4. TITLE (and Subtitle)

THE DEVELOPMENT OF A DYNAMIC ELASTOPLASTIC FINITE ELEMENT ANALYSIS FOR FAST FRACTURE UNDER IMPACT LOADING

5. TYPE OF REPORT & PERIOD COVERED

Interim

6. PERFORMING ORG. REPORT NUMBER

7. AUTHOR(s)

Jalees Ahmad, J. Jung, C. R. Barnes, M. F. Kanninen

8. CONTRACT OR GRANT NUMBER(s)

N00014-77-C-0576 - Battelle

9. PERFORMING ORGANIZATION NAME AND ADDRESS

Battelle's Columbus Laboratories
505 King Avenue
Columbus, Ohio 43201

10. PROGRAM ELEMENT, PROJECT, TASK AREA & WORK UNIT NUMBERS

11. CONTROLLING OFFICE NAME AND ADDRESS

Office of Naval Research
Structural Mechanics Program
Department of the Navy, Arlington, VA 22217

12. REPORT DATE

June 1981

13. NUMBER OF PAGES

23

14. MONITORING AGENCY NAME & ADDRESS(if different from Controlling Office)

15. SECURITY CLASS. (of this report)

Unclassified

15a. DECLASSIFICATION/DOWNGRADING SCHEDULE

16. DISTRIBUTION STATEMENT (of this Report)

Approved for public release; distribution unlimited

17. DISTRIBUTION STATEMENT (of the abstract entered in Block 20, if different from Report)

18. SUPPLEMENTARY NOTES

Paper was presented at the ASME/PVP Conference, Denver, Colorado, June 22-25, 1981.

19. KEY WORDS (Continue on reverse side if necessary and identify by block number)

Fracture, Dynamic Crack Propagation, Finite Element Analysis

20. ABSTRACT (Continue on reverse side if necessary and identify by block number)

Recent evidence has pointed to the possible inadequacy of elastodynamic treatments of rapid crack propagation and crack arrest. This paper describes the development of a dynamic elastic-plastic finite element capability designed to address this concern by taking direct account of crack tip plasticity. Comparisons with known dynamic fracture mechanics solutions and with experimental data are made to demonstrate the fidelity of the approach. A comparison with an elastodynamic solution in an impact loaded 4340 steel bend specimen is also made. This result reveals that a significant effect (over)

DD FORM 1 JAN 73 1473 EDITION OF 1 NOV 65 IS OBSOLETE

S/N 0102-LF-014-6601

Unclassified

SECURITY CLASSIFICATION OF THIS PAGE (When Data Entered)

20. Abstract (Cont'd)

of crack tip plasticity may exist even for high strength materials.

ABSTRACT

Recent evidence has pointed to the possible inadequacy of elastodynamic treatments of rapid crack propagation and crack arrest. This paper describes the development of a dynamic elastic-plastic finite element capability designed to address this concern by taking direct account of crack tip plasticity. Comparisons with known dynamic fracture mechanics solutions and with experimental data are made to demonstrate the fidelity of the approach. A comparison with an elastodynamic solution in an impact loaded 4340 steel bend specimen is also made. This result reveals that a significant effect of crack tip plasticity may exist even for high strength materials.

THE DEVELOPMENT OF A DYNAMIC ELASTOPLASTIC FINITE ELEMENT ANALYSIS FOR FAST FRACTURE UNDER IMPACT LOADING

by

Jalees Ahmad , J. Jung, C.R. Barnes, and M.F. Kanninen

INTRODUCTION

Fracture mechanics researchers are becoming aware that the applicability of even rigorous dynamic analyses of unstable crack propagation and crack arrest may be more limited than was previously realized [1] An important contributor to this dilemma is the still unexplained difference in the crack propagation behavior when crack growth is initiated under impact loading rather than under conventional quasi-static conditions. Specifically, as reported by Kanninen et al,[2] the use of the K_{ID} values obtained for 4340 steel in quasi-static initiation gave decidedly poor agreement when used to predict the crack length-time data obtained in an impact test. In fact, the K_{ID} value inferred from the latter test was roughly a factor of two greater! Added to the geometry-dependence that cast doubt on the validity of $K_{ID} = K_{ID}(V)$ as a unique material property, there is some concern about the presently accepted elastodynamic treatments of fast fracture. This paper describes a first step towards a possible resolution of these difficulties via the development of an elastoplastic dynamic finite element model for the future treatment of fast fracture problems.

Besides providing a more realistic model of the specimen geometry and the boundary conditions, a finite element method is particularly suitable for modeling nonlinear material behavior. To avoid the use of an extremely small mesh size in the evaluation of the dynamic stress intensity factor, a conservation integral, $\hat{J}$ [3] can be utilized. The $\hat{J}$-integral is essentially a consequence of several attempts[4-6] aimed at extending the regime of applicability

of the path-independent contour integral J[7] to include dynamic, elastic-plastic, body force, and thermal contributions to the energy release rate under mixed-mode conditions. Then, crack propagation can be simulated via a gradual crack tip nodal-force release technique using either crack-length vs time data (generation-phase analysis) or a given fracture criterion (application-phase analysis). Finally, to obtain more realistic material modelling, a strain-rate independent constitutive relation based on a Von Mises plasticity potential with an isotropic hardening rule has been included.

In this paper, a general background discussion of current problems in dynamic fracture is followed by a description of the salient features of the finite element based computational procedure. The validity of the computational procedure is ascertained by solving problems for which reliable analytical or experimental results are available. Results for both stationary and propagating cracks are presented. Also presented is a comparison of the results of linear elastodynamic vs elastoplastic dynamic analyses performed on a three-point-bend specimen of AISI 4340 steel under impact loading conditions.

BASIS OF THE COMPUTATIONAL PROCEDURE

Background

Until recently there has been a controversy between the use of static or dynamic treatments for the arrest of a rapidly propagating crack. On the basis of results obtained by Hahn et al[8] and Kalthoff[9], it is now widely believed that a dynamic based analysis is the more correct. Nevertheless, workers in dynamic fracture mechanics are now faced with other problems. Analytical studies, which have been until recently based predominantly on linear elastodynamic analyses, have brought increased understanding of the problem. But, they have also brought to light some new problems.

The problem identified by Kanninen et al [2] concerns the marked differences in the initiation and growth of cracks initiated under different loading conditions. Their key result is shown in Figure 1. This experiment was performed on an impact loaded three-point-bend specimen of AISI 4340 steel (yield strength ≈ 200 ksi). It can be seen that, by using K_{ID} values obtained from quasi-static initiation tests (i.e., $K_{ID} = 65 + .044\ V$), a very poor prediction is obtained. Instead, the value $K_{ID} = 170$, which has no apparent connection with the "established" value, is needed for good agreement.

Because the analytical results in this study were obtained by a relatively simple elastodynamic finite difference scheme, one possible reason for the discrepancy would be the analysis procedure itself. Solving the same problem with an entirely different - and preferably improved - analytical procedure should remove any such doubt. For this purpose a finite element computer code with isoparametric element formulation was developed. To further depart from the previously used global energy balance approach for the calculation of stress intensity factor, the $\hat{J}$-integral approach was implemented.

A second possible reason for the discrepancy could be the assumption of linear elastic material behavior. The finite element code was, therefore, enriched to model the material behavior in accordance with a user supplied uniaxial stress-strain curve. This, and other reasons for the discrepancy, will be dealt with in a later section.

Outline of the Solution Procedure

The approach used for the solution of the equations of motion in the analytical procedure presented here employs a displacement-based finite element method. An isoparametric finite element formulation with linear and quadratic shape functions in a two-dimensional space is used.

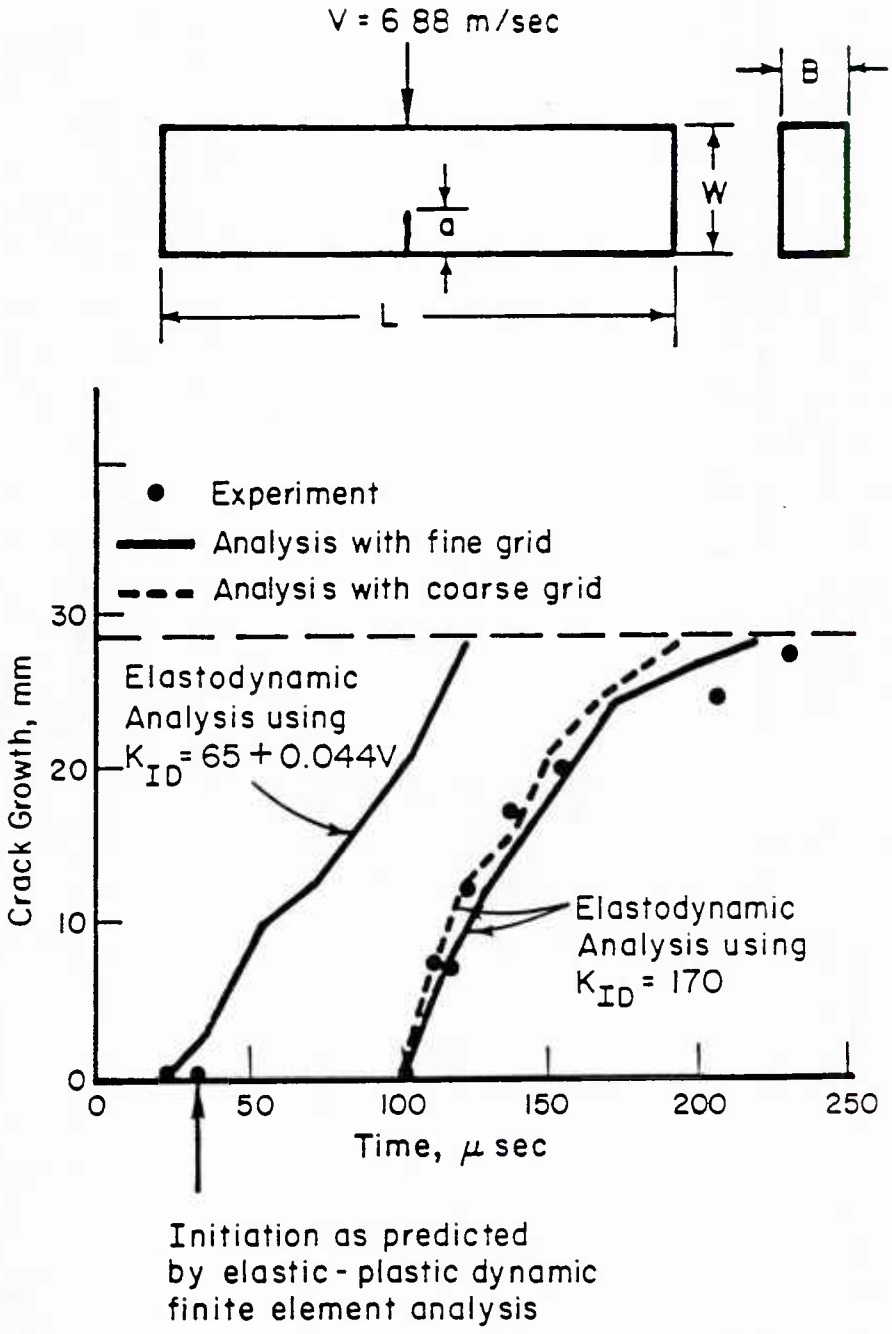

FIGURE 1. CRACK GROWTH IN 4340 STEEL UNDER IMPACT LOADING
L = 0.181 m, a =.0095 m, B = .0158 m, W = .038 m

General quadrilateral elements with a variable number of nodes in both plane-stress and plane-strain conditions may be used. If so desired the $1/\sqrt{r}$ or $1/r$ stress singularity at the crack tip may be imposed by using the quarter point approach[10]. However, this feature was not utilized in any of the analyses presented in this paper.

The modified Newton-Raphson approach[11] is used for elastic-plastic analysis. Von Mises yield condition with isotropic strain hardening is assumed. For time integration, either an explicit (central difference) or an implicit (Newmark-Beta) scheme may be used. Due to it being inherently more stable, the implicit scheme offers computational advantages in the solution of dynamic fracture problems. All the results included in the present paper were obtained by using the Newmark-Beta time integration scheme[12].

Crack growth is modelled by gradually releasing the force experienced by the crack tip at a given instant of time in several steps. Details of the crack growth modelling scheme are described in a paper by Jung, Ahmad, Kanninen, and Popelar[13]. The scheme allows for modelling crack growth in both generation and application phases of analysis. For application-phase analysis where the crack tip is advanced according to a selected fracture parameter, a choice of fracture parameters is necessary. Currently, crack-tip-opening displacement (CTOD), crack-tip-opening angle (CTOA), Mode I and Mode II dynamic stress intensity factors (K_I and K_{II}), and the $\hat{J}$ family of conservation integrals[3] are available. Since CTOD and CTOA are obtained directly from the finite element displacement solution, and K_I and K_{II} are obtained by first calculating $\hat{J}$ for linear elastic material, only a description of the $\hat{J}$-integrals is included in the following.

The $\hat{J}$-Integral

The mathematical details involved in the derivation of $\hat{J}$ are available in a paper by Kishimoto et al[3]. Here, a general expression for $\hat{J}$ is taken in a form which makes the parameter physically more

tractable and convenient to implement in a computational scheme. This is done by defining

$$\hat{J}_k = J_{k_e} + J_{k_d} + J_{k_t} + J_{k_p} + J_{k_b} \qquad (1)$$

Where the lower case letter subscripts stand for the elastic (e), dynamic (d), thermal (t), plastic (p), and body force (b), contributions to the $\hat{J}_k$-integrals and K (=1,2) indicates that each term in Equation (1) is a vector.

Kishimoto et al [3] define $\hat{J}$ as follows:

$$\hat{J} = \hat{J}_1 \text{ Cos } \Theta + \hat{J}_2 \text{ Sin } \Theta \, , \qquad (2)$$

where Θ is the angle of crack extension measured anticlockwise from the crack line (Figure 2). The integrals J_{k_e} thru K_{k_b} in Equation (2) may be expressed as follows:

$$J_{ke} = \int_{\Gamma + \Gamma s} \left(W_e n_k - T_i \frac{\partial u_i}{\partial x_k} \right) d\Gamma$$

$$J_{kd} = \iint_A \rho \ddot{u}_i \frac{\partial u_i}{\partial x_k} \, dA$$

$$J_{kp} = \iint_A \sigma_{ij} \frac{\partial \varepsilon^*_{ij}}{\partial x_k} \, dA$$

$$J_{k_t} = \iint_A \alpha \, \varepsilon_{ii} \frac{\partial T}{\partial X_k} \, dA - \int_{\Gamma + \Gamma_s} 1/2 \, \alpha \, T \, \varepsilon_{ii} \, n_k \, d\Gamma$$

$$J_{k_b} = - \iint_A F_i \frac{\partial u_i}{\partial X_k} \, dA$$

$$\alpha = \frac{E}{1-2\nu} \text{ --- Plane Strain} = \frac{E}{1-\nu} \text{ ---Plane Stress}$$

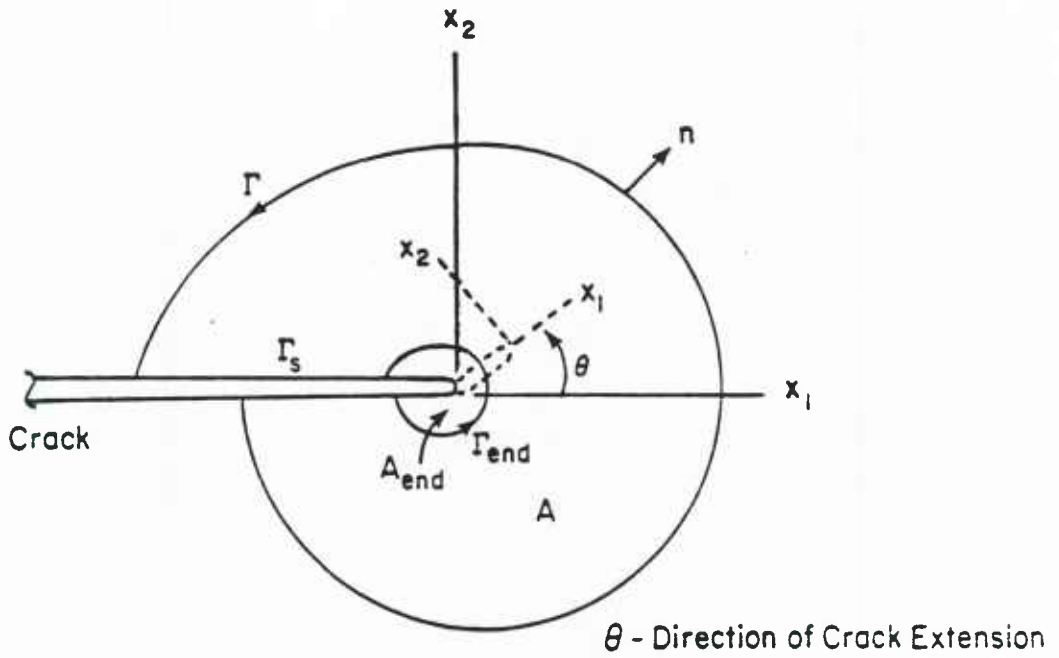

FIGURE 2. CRACK TIP COORDINATES USED IN THE DEFINITION OF $\widehat{J}_k$

where

W_e = elastic strain energy density
T_i = traction vector
σ_{ij} = stress tensor
ε^*_{ij} = plastic strain tensor
u_i = displacement vector
$\ddot{u}_i$ = acceleration vector
T = temperature increment
F_i = body force

In Figure 2, A is the area enclosed between contours Γ and Γ_{end} and $\hat{J}$ is defined as the area Aend approaches zero. For running cracks, it is assumed that the so-called "process-region"[3] shown in Aend in Figure 2 remains constant in dimensions and moves with the crack tip.

While there may be some uncertainty regarding the use of $\hat{J}$ as a fracture criterion, it is highly appealing from a computational viewpoint. The strength of the idea is in the fact that other proposed forms of energy release rate expressions such as J of Rice [7], J^* of Blackburn [6], $\tilde{G}$ of Eftis and Liebowitz[14], and expressions proposed by Wilson and Yu[15], Freund [5], and Bui [4], all can be shown to be specialized versions of the $\hat{J}$-integral[3]. Therefore, $\hat{J}$ is at least equally valid as a fracture criterion as any of the above-mentioned parameters.

For a linear elastic material ($J_{k_p} = 0$) and in the absence of body forces ($J_{k_b} = 0$), it can be shown[16] that:

$$\hat{J}_1 = \frac{\kappa+1}{8\mu}\left[K_I^2(t) + K_{II}^2(t)\right] + \frac{1}{2\mu} K_{III}^2(t) \qquad (3)$$

$$\hat{J}_2 = \frac{\kappa+1}{4\mu} K_I(t)\, K_{II}(t) \qquad (4)$$

where μ is the shear modulus, and $\kappa = 3-4\nu$ for plane strain and $(3-\nu)/(1+\nu)$ for plane stress.

In a single mode situation the appropriate stress intensity factor can be readily obtained from Equation (3).

NUMERICAL RESULTS

Solutions to some representative problems solved by using the analytical procedure described above are now presented. The first four problems were chosen primarily for ensuring the validity of the solutions procedure by comparing the results with available analytical solutions and with experimental results. In the second and the fourth problems, comparisons with the previously used finite difference scheme[2] are also made.

The fifth and sixth problems were selected to demonstrate the differences in K_I obtained by using quasi-static analysis vs the dynamic analysis, and to illustrate the effect of plasticity even in a high strength material, AISI 4340 steel. Note that, in all cases involving linear-elastic-material assumption, the stress intensity factors were calculated by the $\hat{J}$ approach.

Problem 1: Stationary Crack in an Impulsively-Loaded Center-Cracked Panel

The problem considered here is of a center-cracked plate (Figure 3) loaded dynamically in a suddenly-applied uniform tension σ. The material was taken to be linear elastic (E = 200 GPa, ν = 0.3) having a density of 5000 Kg/m^3. This problem has been solved by a number of other authors. Some of these results are shown in Figure 3 along with the results of the present analysis. The good correlation that is evident indicates that the present finite element procedure with the $\hat{J}$-integral provides sufficiently accurate dynamic stress intensity factors for stationary cracks.

Problem 2: Unrestrained Impact-Loaded Bend Specimen

A bend specimen totally unrestrained (no supports) is considered (Figure 4). In an actual experiment the specimen was struck by a hammer at an average velocity of 6.88 m/sec and was allowed to fly freely. In Figure 4, the variation of the dynamic stress intensity factor with time,

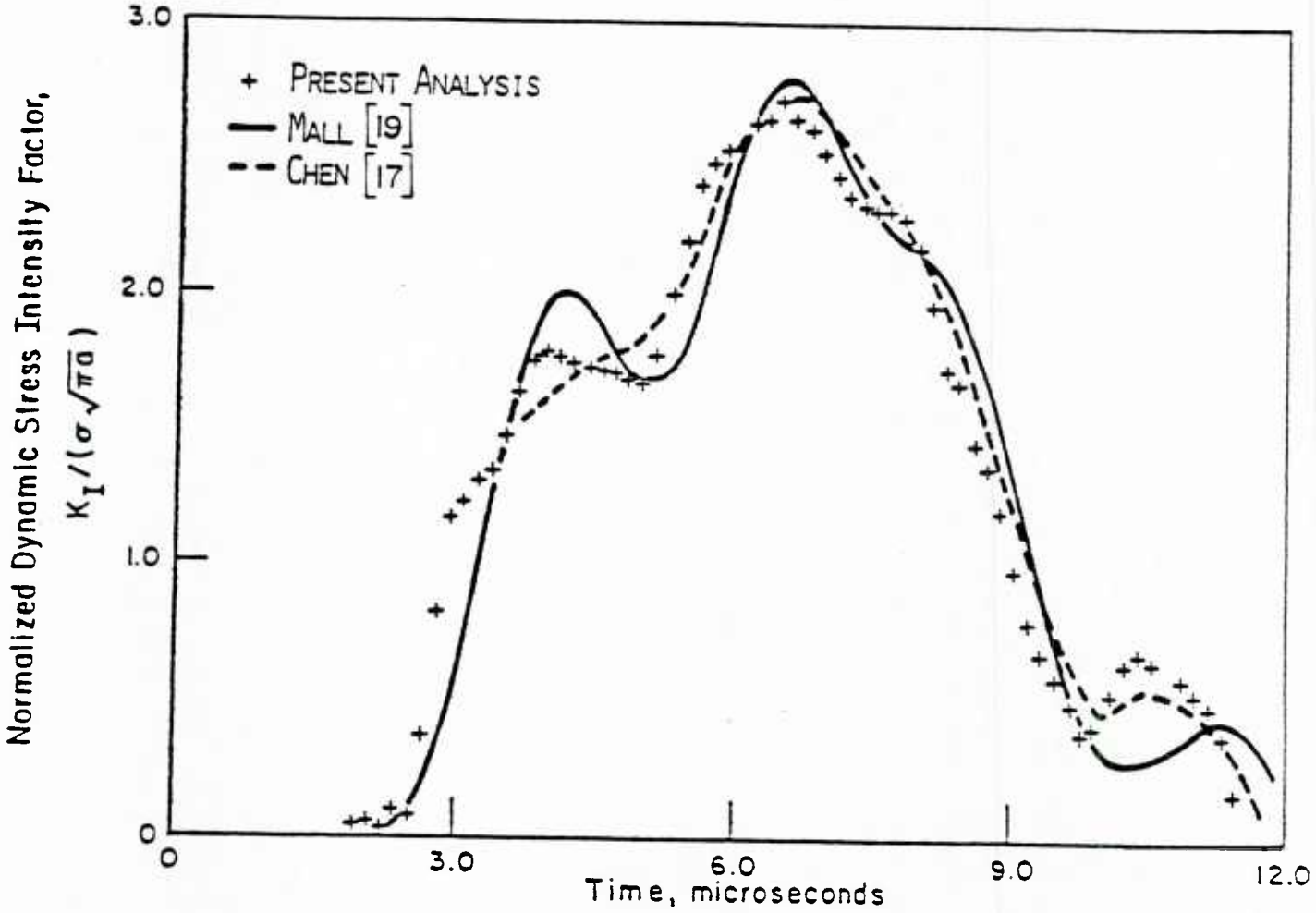

FIGURE 3. DYNAMIC STRESS INTENSITY FACTOR VERSUS TIME FOR AN IMPULSIVELY LOADED CENTER-CRACKED PANEL WITH A STATIONARY CRACK.

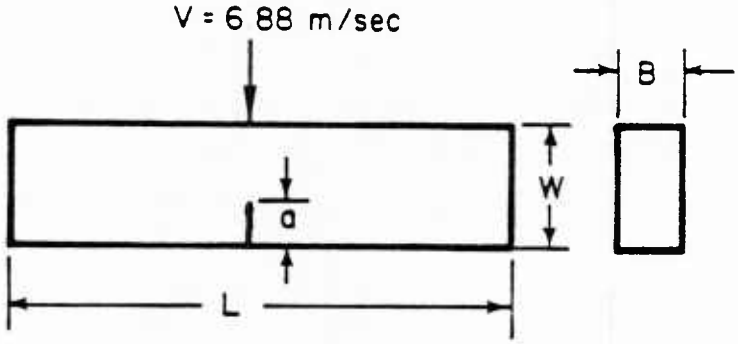

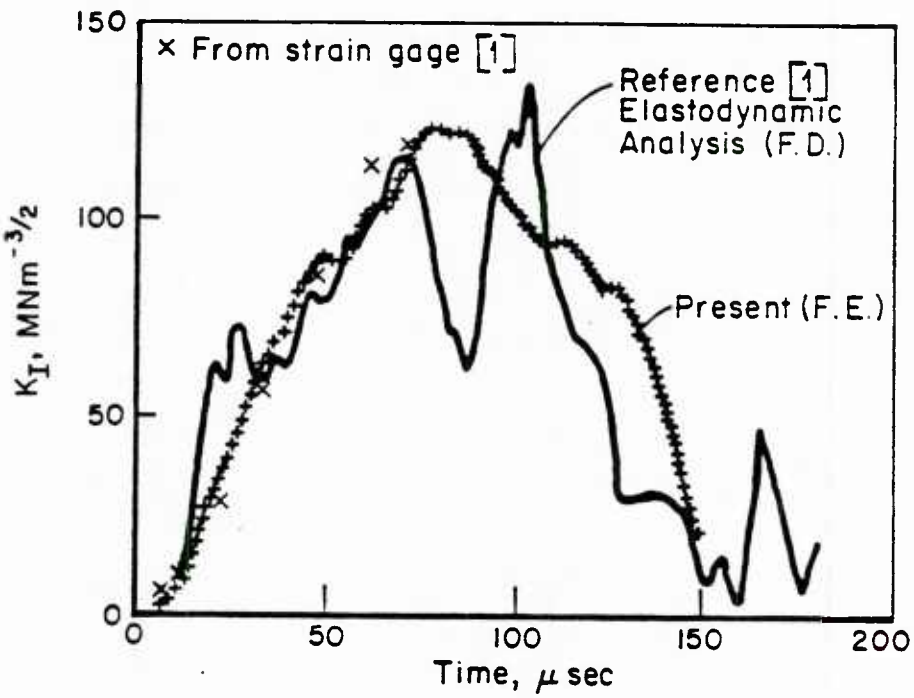

FIGURE 4. RESULTS FOR UNRESTRAINED 1 SPECIMEN

L = 0.181 m, W = 0.038 m,
a = 0.0095 m, B = 0.0158 m

as obtained by the present analysis, is compared with K_I obtained by both the finite difference calculation (2) and with experimental strain measurements. The material properties used in this analysis were those of AISI 4340 steel. Good agreement is obtained which demonstrates that the $\hat{J}$-integral approach provides essentially the same values for dynamic stress intensity factors as the global energy balance approach used in the finite difference scheme and, in view of the agreement with the strain gage data, that both are correct.

Problem 3: Propagating Crack in an Infinite Medium

The problem of a crack propagating at a constant velocity of 0.2 times the shear wave speed (C_s) in a center-cracked panel was analyzed for an initial crack length to specimen width ratio (a/w) of 0.2. The results are compared with analytical solution by Broberg [18] in Figure 5.

The results indicate that the $\hat{J}$-integral provides an effective means of calculating dynamic stress intensity factors for propagating cracks. However, it should be noted that the crack velocity in this comparison was held constant; NB, analytical solutions for a crack propagating at changing velocity do not exist. In the next problem, such a comparison is made with experimental, as well as numerical results, obtained by finite difference method.

Problem 4: Application-Phase Analysis of a Propagating Crack in a Bend Specimen

An elastodynamic crack growth analysis in a three-point-bend specimen of AISI 4340 steel was performed. Experimental as well as finite difference analysis results for this problem were first obtained by Kanninen et al [2] using $K_{I_D} = 65 + 0.044\ V$ as a fracture criterion. In the present finite element computations the same criterion was used. Figure 6 shows the specimen geometry used in the analysis and a comparison of the new results with those of Reference (2).

This application-phase analysis does indicate an equivalence between the $\hat{J}$-integral approach of calculating K_I and the approach used in the finite

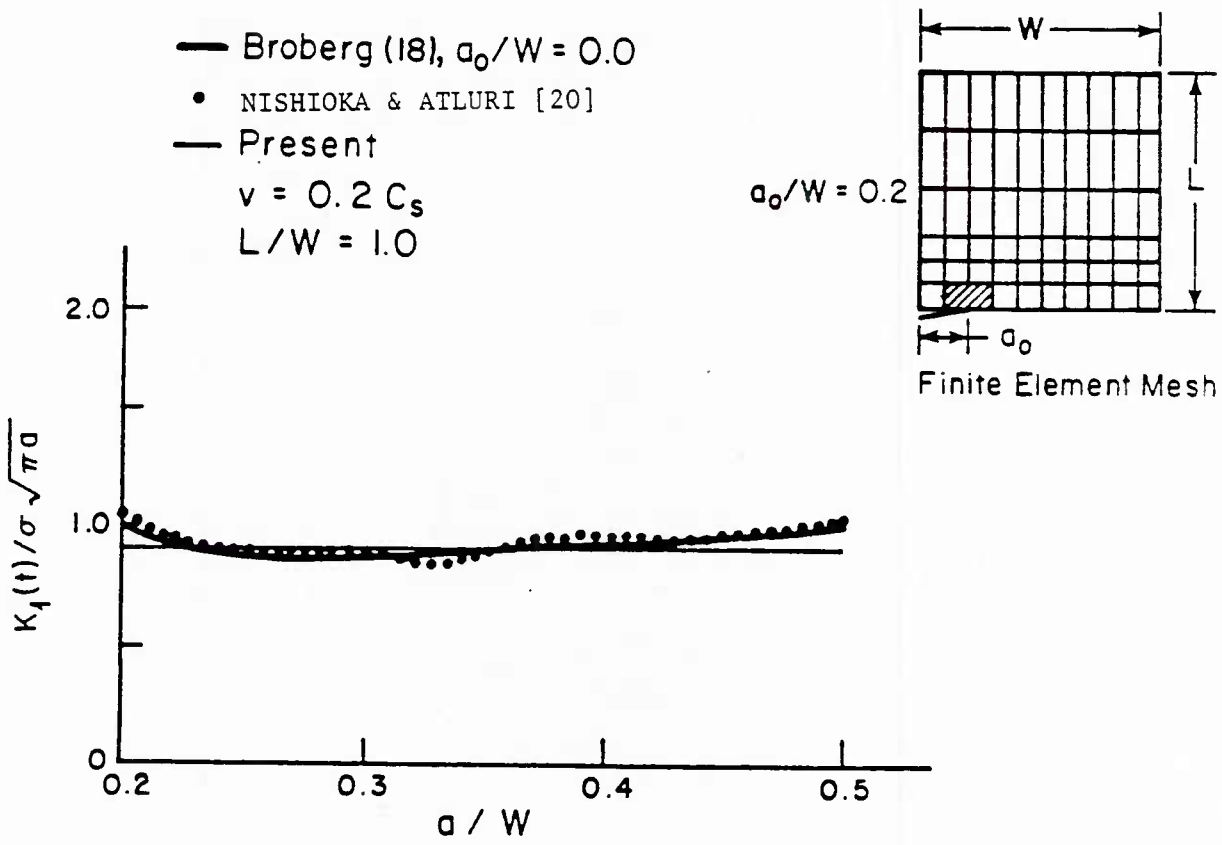

FIGURE 5. ELASTODYNAMIC ANALYSIS OF CONSTANT VELOCITY CRACK PROPAGATION

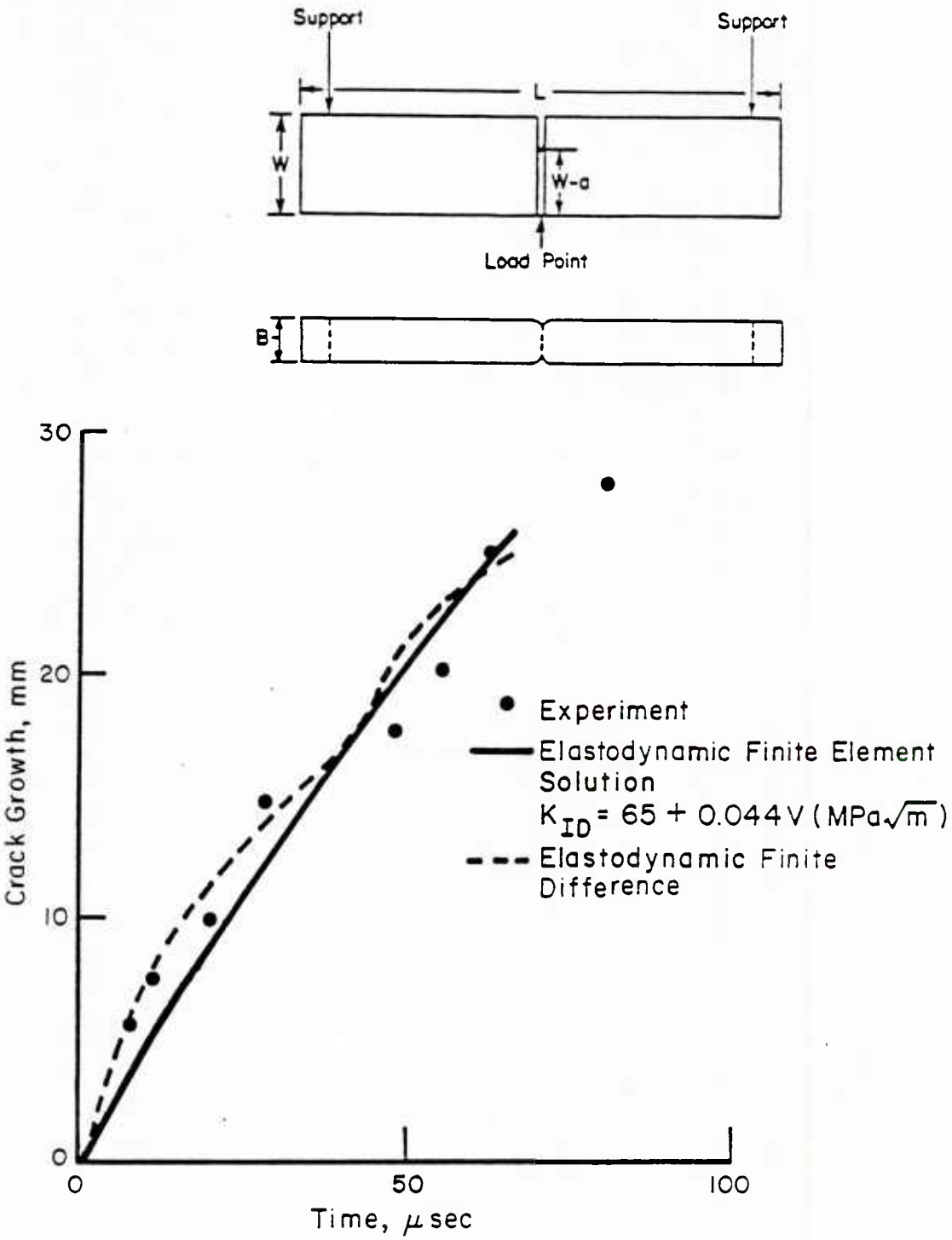

FIGURE 6. A COMPARISON OF FINITE ELEMENT ANALYSIS, FINITE DIFFERENCE ANALYSIS AND EXPERIMENT FOR A QUASI-STATICALLY INITIATED CRACK IN A 4340 DYNAMIC TEAR SPECIMEN.
L = 181 mm, W = 38 mm, B = 15.8 mm, (W-a) = 28.5 mm.

difference scheme even for a crack propagating at a nonconstant speed. The results also provide an increased level of confidence in the accuracy of numerical results.

Problem 5: Generation-Phase Analysis of a Propagating Crack in a Bend Specimen

A generation phase analysis, in which an experimentally obtained crack length vs time record (Figure 7) from a dynamic tear test experiment on HY130 steel was provided as an input to the computer code, was performed. The elastodynamic finite element analysis then gave values of K_D as a function of time. These are plotted in Figure 8. Also shown are K_o values inferred by using a handbook formula for three-point-bend specimen in which inertia forces are ignored. As might be expected, the dynamic values oscillate around a mean value given by the quasi-static solution.

Problem 6: Elastic-Plastic Dynamic Analysis of a Stationary Crack in a Bend Specimen

The three-point-bend specimen of AISI 4340 steel was analyzed under an impact load with and without the elastic material assumption. For the elastic-plastic dynamic analysis, the material behavior was described by an experimentally obtained static stress-strain curve from a uniaxial tension test. Strain rate effects on material property are not included in the analysis.

Figure 9 shows the variation with time of the crack-opening displacement (COD), measured at 0.68 mm behind the crack-tip for both elastic and elastic-plastic analyses. In Figure 10, values obtained are plotted against time. It can be seen that, even in a high-strength material, the effect of plasticity appears to be significant. The effect of plasticity seems to damp-out the oscillations in COD (which is directly proportional to K_I and $\sqrt{J}$ in the linear elastic case); cf, Figure 8.

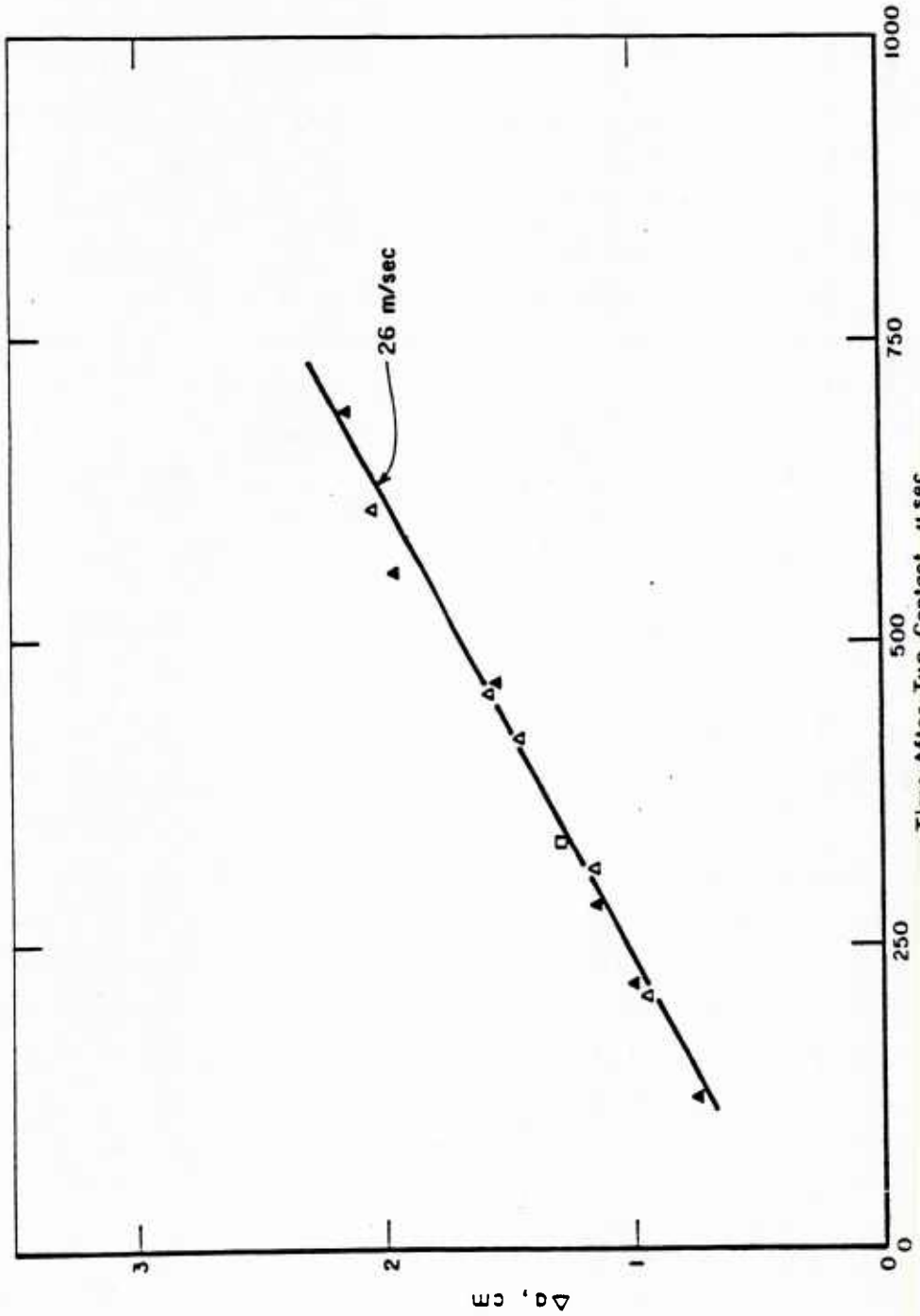

FIGURE 7. MEASURE CRACK EXTENSION-TIME RECORD FOR HY-130 STEEL FROM DYNAMIC TEAR TEST EXPERIMENT.

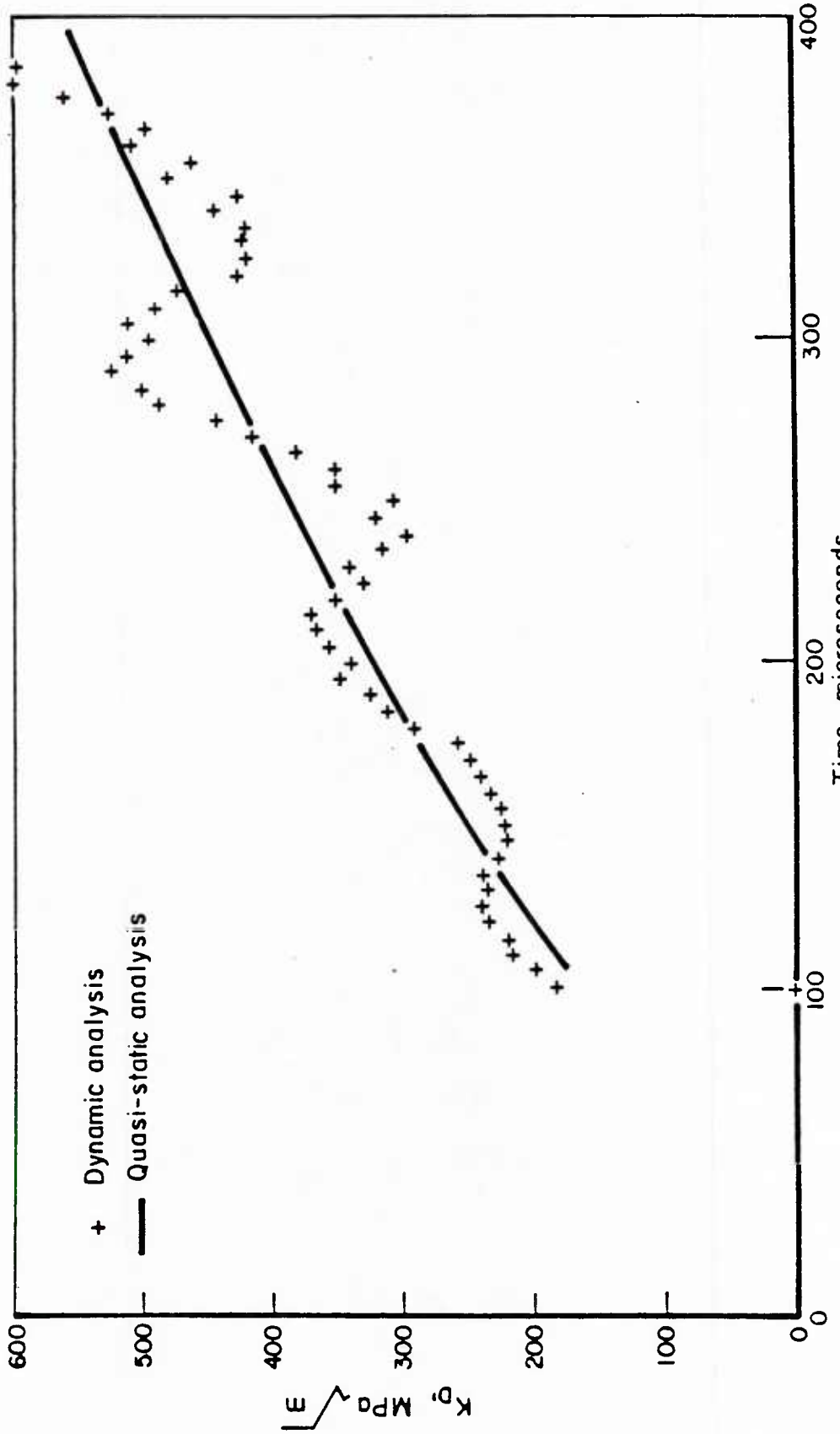

FIGURE 8. COMPARISON OF ELASTIC FRACTURE TOUGHNESS VALUES DEDUCED BY QUASI-STATIC AND DYNAMIC CALCULATIONS FOR A HY-130 DYNAMIC TEAR TEST EXPERIMENT

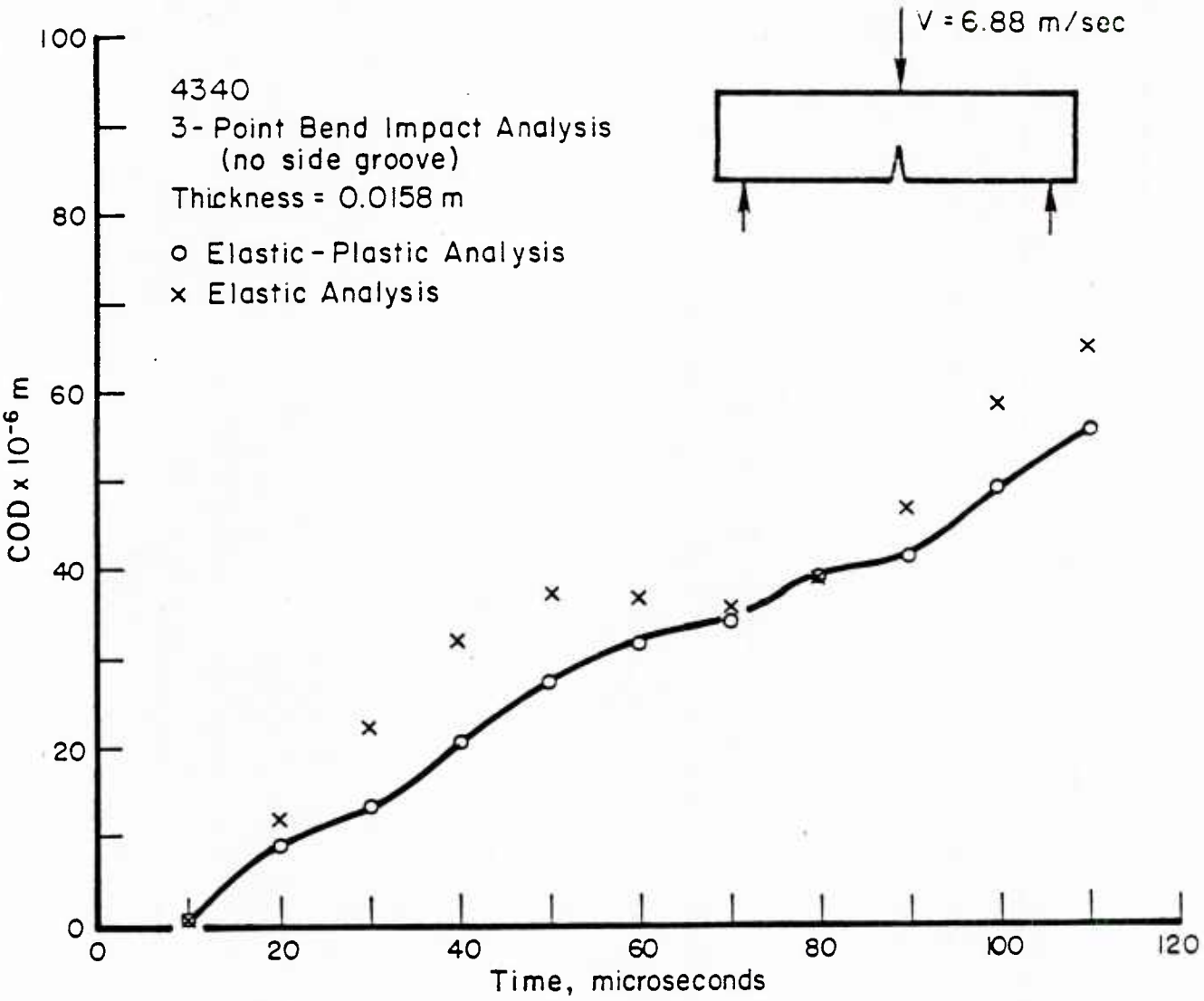

FIGURE 9. CRACK-OPENING DISPLACEMENT (0.00068 m BEHIND THE CRACK TIP) VS TIME.

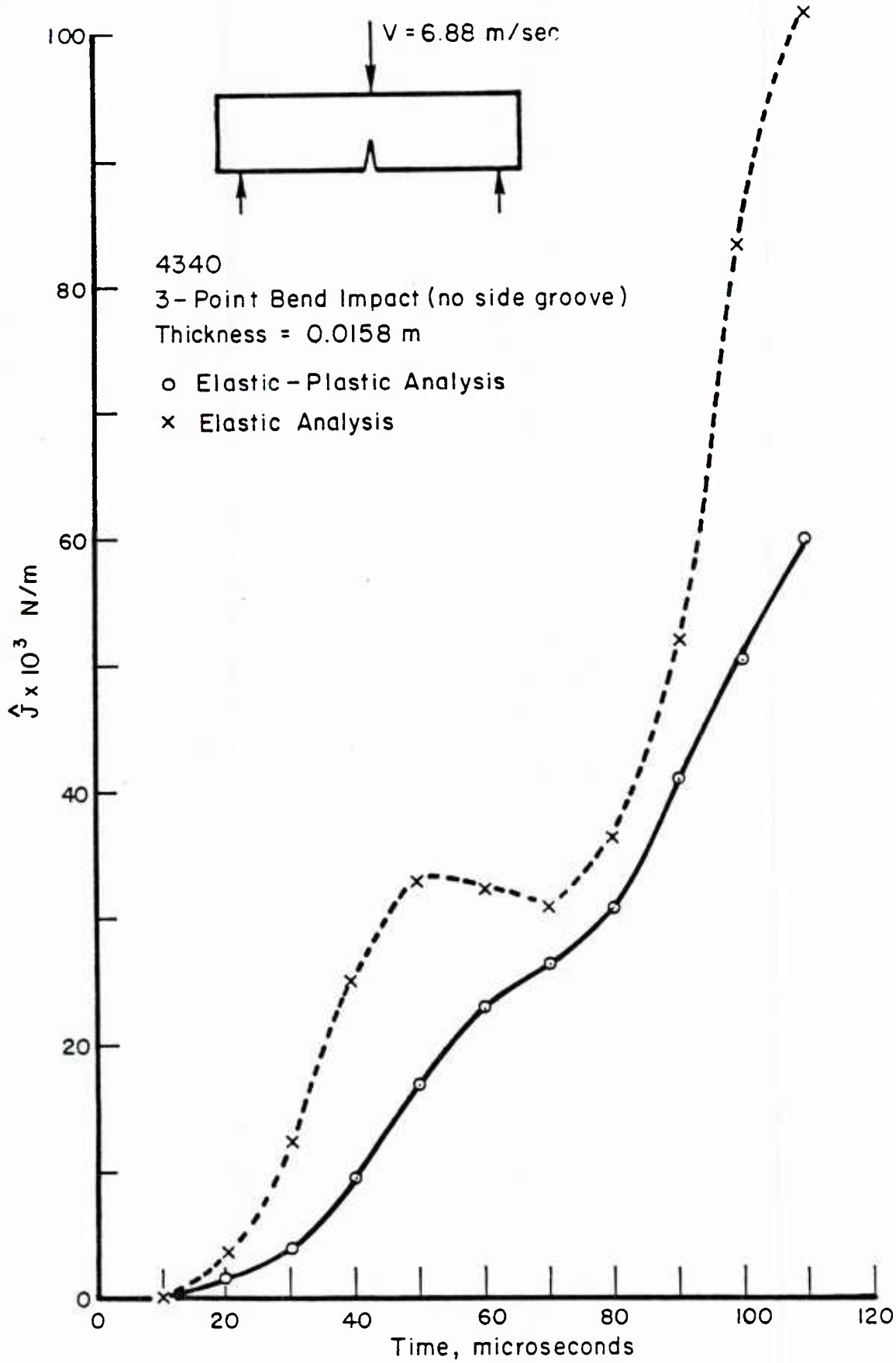

FIGURE 10. $\hat{J}$-INTEGRAL VS. TIME

DISCUSSION AND CONCLUSIONS

Uncertainties now exist concerning the adequacy of elastodynamic solution procedures for unstable crack propagation and crack arrest analyses. The most obvious reason for the existence of these uncertainties is the neglect of crack tip plasticity in such formulations. To address this possibility, an elastic-plastic dynamic finite element capability has been developed. It has been shown in this paper, by comparisons with existing dynamic fracture mechanics solutions and with experimental data, that this capability is more than adequate for its intended purposes.

Some preliminary calculations comparing the elastic and the elastic-plastic predictions for a stationary crack in an impact loaded bend specimen were also obtained. These indicate that the effect of crack tip plasticity is significant even for a high-strength material. The present capability will next be extended to treat a propagating crack whereupon an even more prominent effect is expected to be revealed. But, whether or not taking direct account of crack tip plasticity during rapid crack propagation will resolve the questions that now exist on the geometry and initiation mode dependence of K_{ID} remains to be seen.

ACKNOWLEDGEMENT

The research described in this paper was supported by the Structural Mechanics Program of the Office of Naval Research under Contract Number N00014-77-C-0576. The authors would like to express their appreciation to Drs. Nicholas Perrone and Yapa Rajapakse of ONR for their encouragement of this work.

REFERENCES

[1] Kanninen, M.F., "Whither Dynamic Fracture Mechanics?", Numerical Methods in Fracture Mechanics, Proceedings of the Second International Conference held at University College, Swansea, United Kingdom, Eds. D.R.J. Owen, A.R. Luxmoore, July 1980.

[2] Kanninen, M.F., Gehlen, P.C., Barnes, C.R., Hoagland, R.G., Hahn, G.T., and Popelar, C.H., "Dynamic Crack Propagation Under Impact Loading", Nonlinear and Dynamic Fracture Mechanics, Eds. Nicholas Perrone and Satya Atluri, American Society of Mechanical Engineers, AMD-Vol 35, pp 195-200, 1979.

[3] Kishimoto, K., et al., "On the Path Independent Integral - $\hat{J}$", Engineering Fracture Mechanics, Vol. 13, 1980, pp. 841-850.

[4] Bui, H.D., "Stress and Crack-displacement Intensity Factors in Elastodynamics", Proceeding of the Fourth International Conference on Fracture, Waterloo, Canada, June 1977, pp 91-96.

[5] Freund, L.B., "Energy Flux into the Tip of an Extending Crack in an Elastic Solid," J. Elasticity, Vol. 2, 1972, pp 341-349.

[6] Blackburn, W.S., "Path Independent Integrals to Predict Onset of Crack Instability in an Elastic-Plastic Material," International Journal of Fracture Mechanics., Vol. 8, 1972, pp. 343-346.

[7] Rice, J.R., "A Path Independent Integral and the Approximate Analysis of Strain Concentration by Notches and Cracks", Trans. ASME J. Appl. Mech., Vol. 90, 1968, pp. 379-386.

[8] Hahn, G.T., Hoagland, R.G., Kanninen, M.F., and Rosenfield, M.R., "A Preliminary Study of Fast Fracture and Arrest in the DCB Test Specimen", Dynamic Crack Propagation, G.C. Sih, Editor, Noordhoff, Leyden, 1973, pp. 649-662.

[9] Kalthoff, J.F., et al,"Measurements of Dynamic Stress Intensity Factors for Fast Running and Arresting Cracks in Double Cantilever Beam Specimens, Fast Fracture and Crack Arrest, Ed. G.T. Hahn and M.F. Kanninen, ASTM STP 627, 1977, pp 161-176.

[10] Barsoum, R.S., "On the Use of Isoparametric Finite Elements in Linear Elastic Fracture Mechanics:, Int. J. of Num. Meth. In Engrg., Vol. 10, No. 1, 1976.

[11] Cook, R.D., Concepts and Applications of Finite Element Analysis, Publ. John Wiley & Sons, Inc., 1974.

[12] Klaus-Jurgen, Bathe, and Wilson, E.L., Numerical Methods in Finite Element Analysis, Prentice-Hall, Inc., Englewood Cliffs, New Jersey, pp 322-326, 1976.

[13] Jung, J., Ahmad, J., Kanninen, M.F., and Popelar, C.H., "Finite Element Analysis of Dynamic Crack Propagation", to be presented at the 1981 ASME Failure Prevention and Reliability Conference, September 23-26, 1981, Hartford, Conn.

[14] Eftis, J., and Liebowitz, H., "On Fracture Toughness Evaluation for Semi-Brittle Fracture", Engineering Fracture Mechanics, Vol. 7, 1975, pp. 491-503.

[15] Wilson, W.K., and Yu, I.W., "The Use of the J-Integral in Thermal Stress Crack Problems", International Journal of Fracture, Vol. 15, No. 4, 1979, pp. 377-387.

[16] Kishimoto, K., Aoki, S., and Sakata, M., "Dynamic Stress Intensity Factors Using J-Integral and Finite Element Method", Engineering of Fracture Mechanics, Vol. 13, 1980, pp. 387-394.

[17] Chen, Y.M., "Numerical Computation of Dynamic Stress Intensity Factors by a Lagrangian Finite-Difference Method (The Hemp Code)", Engineering of Fracture Mechanics, Vol. 7, 1975, pp. 653-660.

[18] Broberg, K.B., "The Propagation of a Brittle Crack", Arkiv for Fysik, Band 18, No. 10, pp 139-192, 1966.

[19] Mall, S., "Finite Element Analysis of Stationary Cracks in Time Dependent Stress Fields", Numerical Methods in Fracture Mechanics, Eds. A.R. Luxmoore and D.R.J. Owen, University College, Swansea, England, 1980.

FINITE ELEMENT ANALYSIS OF DYNAMIC CRACK PROPAGATION

by

J. Jung, J. Ahmad, and M. F. Kanninen

BATTELLE
Columbus, Ohio

and

C. H. Popelar
OHIO STATE UNIVERSITY
Columbus, Ohio

Submitted for publication in Engineering Fracture Mecahnics, March 1981.

SECURITY CLASSIFICATION O S PAGE *(When Data Entered)*

REPORT DOCUMENTATION PAGE

READ INSTRUCTIONS BEFORE COMPLETING FORM

1. REPORT NUMBER

2. GOVT ACCESSION NO.

3. RECIPIENT'S CATALOG NUMBER

4. TITLE *(and Subtitle)*
Finite Element Analysis of Dynamic Crack Propagation

5. TYPE OF REPORT & PERIOD COVERED
Interim

6. PERFORMING ORG. REPORT NUMBER

7. AUTHOR(s)
J. Jung, J. Ahmad, M. F. Kanninen, and C. H. Popelar

8. CONTRACT OR GRANT NUMBER(s)
NC00014-77-C-0576
Battelle

9. PERFORMING ORGANIZATION NAME AND ADDRESS
Battelle Columbus Laboratories
Columbus, Ohio 43201

10. PROGRAM ELEMENT, PROJECT, TASK AREA & WORK UNIT NUMBERS

11. CONTROLLING OFFICE NAME AND ADDRESS
Office of Naval Research
Structural Mechanics Program
Department of the Navy, Arlington, Virginia 22217

12. REPORT DATE
March 1981

13. NUMBER OF PAGES
22

14. MONITORING AGENCY NAME & ADDRESS*(if different from Controlling Office)*

15. SECURITY CLASS. *(of this report)*
unclassified

15a. DECLASSIFICATION DOWNGRADING SCHEDULE

16. DISTRIBUTION STATEMENT *(of this Report)*
Approved for public release; distribution unlimited.

17. DISTRIBUTION STATEMENT *(of the abstract entered in Block 20, if different from Report)*

18. SUPPLEMENTARY NOTES
Submitted for presentation at the Failure Prevention and Reliability Conference, ASME Publications 1981.

19. KEY WORDS *(Continue on reverse side if necessary and identify by block number)*
dynamic crack propagation
crack driving force
crack arrest
impact loading
J integral
quasi-static
analytical model

20. ABSTRACT *(Continue on reverse side if necessary and identify by block number)*
A J integral approach is suggested for use in the analytical modeling of stationary and propagating cracks in the presence of inertial forces. A conceptually simple, effective technique has been developed. This scheme eliminates the difficulties associated with the use of moving singular elements.

DD FORM 1 JAN 73 1473

unclassified

SECURITY CLASSIFICATION OF THIS PAGE *(When Data Entered)*

FINITE ELEMENT ANALYSIS OF DYNAMIC CRACK PROPAGATION

by

J. Jung, J. Ahmad and M. F. Kanninen

Battelle
Columbus Laboratories
Columbus, Ohio

and

C. H. Popelar
Engineering Mechanics Department
The Ohio State University
Columbus, Ohio

ABSTRACT

A finite element analysis of stationary and propagating cracks in the presence of inertia forces is presented. An extension of the J-integral approach is employed. To model a propagating crack, a conceptually simple yet effective technique has been developed. The new crack propagation scheme eliminates the difficulties associated with the use of moving singular elements.

INTRODUCTION

It is generally accepted that a crack arrest methodology based on a dynamic view of crack propagation and arrest is more fundamental than the quasi-static approach to the problem [1]. Specifically, when inertia forces, stress-wave reflections, and rate-dependent fracture processes are dominant, quasi-static assumptions will generally underestimate the true crack driving force. In many applications, such as nuclear pressure vessel design and structures subjected to impact loading, dynamic effects can be important. In these cases analytical models based on the quasi-static assumption may lead to erroneous conclusions.

Inclusion of dynamic features in an analytical model undoubtedly leads to complications. In recent years the finite element method has emerged as an important tool that can be used to resolve at least some of the mathematical difficulties associated with the problem. Considerable progress has also been made toward understanding some of the basic concepts.

The purpose of the paper is to present the salient features of a recently developed finite element dynamic crack propagation modeling technique. Results of an elasto-dynamic analyses will be presented for both stationary and running cracks. Comparisons will be made with available experimental results. Through the analyses of test specimens, it will be demonstrated how this analytical model can be used to acquire a better understanding of the dynamic crack propagation phenomenon.

Dynamic Analysis and Numerical Integration

The familiar finite element discretized version of the equations of motion are simply written in the following form:

$$[M]\{\ddot{X}\} + [C]\{\dot{X}\} + [K]\{X\} = \{R\} \tag{1}$$

where

$[M]$ = mass matrix
$[C]$ = damping matrix
$[K]$ = stiffness matrix
$\{R\}$ = the external load vector
$\{\ddot{X}\}, \{\dot{X}\}, \{X\}$ = the displacement, velocity, and acceleration vectors respectively.

There are several methods that could be used to perform the direct numerical integrations of the equations. The method selected for this work was the Newmark implicit scheme [2]. For this method, the following approximations are used:

$$\dot{X}_{t+\Delta t} = \dot{X}_t + [(1-\delta)\ \ddot{X}_t + \delta \ddot{X}_{t+\Delta t}]\ \Delta t \tag{2}$$

$$X_{t+\Delta t} = X_t + \dot{X}_t\ \Delta t + [(1/2 - \alpha)\ \ddot{X}_t + \alpha\ \ddot{X}_{t+\Delta t}]\Delta t^2 \tag{3}$$

where α and δ are parameters that can be varied for accuracy and stability while Δt is the time step. From the above equations it is possible to write the equations of equilibrium for time, $t + \Delta t$, in terms of displacements, velocities, and accelerations at time, t.

$$\begin{aligned}[[K] + a_o[M] + a_1[C]]\ \{X_{t+\Delta t}\} = \{R_{t+\Delta t}\} + [M]\ (a_o\{X_t\} + a_2\{\dot{X}_t\} + a_3\{\ddot{X}_t\}) \\ + [C](a_1\{X_t\} + a_4\{\dot{X}_t\} + a_5\{\ddot{X}_t\})\end{aligned} \tag{4}$$

where

$$\begin{aligned} a_o &= \frac{1}{\alpha\Delta t^2}\ ;\ a_1 = \frac{\delta}{\alpha\Delta t}\ ;\ a_2 = \frac{1}{\alpha\Delta t}\ ;\ a_3 = \frac{1}{2\alpha} - 1 \\ a_4 &= \frac{\delta}{\alpha} - 1\ ;\ a_5 = \frac{\Delta t}{2}\left(\frac{\delta}{\alpha} - 2\right)\ ;\ a_6 = \Delta t\ (1-\delta) \\ a_7 &= \delta\Delta t\ . \end{aligned} \tag{5}$$

Solving Equation (4) yields $\{X_{t+\Delta t}\}$ whereupon the accelerations and velocities at time, $t + \Delta t$, can be calculated using Equations (2) and (3).

Elasto-dynamic Analysis of Stationary Cracks

Consider the problem of determining the stress intensity factor for a stationary crack in a structure subjected to dynamic loadings. Several investigators have solved this problem by employing singular elements around the crack tip [3-5]. While this approach has proved to be successful, it will later require special considerations when the crack is propagating. An alternative to the singular element approach is to derive the stress intensity factors from a path independent J-integral [6]. After accounting for the inertia

effects, the rate of energy release per unit of crack advance in the direction of the crack X_1 is defined as:

$$J = \int_{\Gamma+\Gamma_s} [w dx_2 - \sigma_{ij} n_j \frac{\partial u_i}{\partial x_1} ds] + \iint_A \rho \ddot{u}_i (\frac{\partial u_i}{\partial x_1}) dA \quad , \tag{6}$$

where the first integral is the conventional J-integral over an arbitrary path surrounding the crack tip and the second integral is an integral over the area, A, enclosed by the path, $\Gamma + \Gamma_s$; see Figure 1.

An application of this J-integral is shown in the following example in which a centrally cracked plate in plane strain is impulsively loaded by a uniform stress; see Figures 2 and 3. The finite element model employed 309 nodes and 90 eight noded quadratic isoparametric elements; see Figure 4. The material is linear elastic with a Young's modulus of 200 GPa, Poisson's ratio of 0.3 and density of 5 g/cm^3. Newmark's implicit time integration scheme was used ($\alpha = 0.25$ and $\delta = 0.5$) with a time step of 0.15 microseconds. A consistent mass formulation was used for this analysis.

The results of the present analysis is shown in Figure 5 along with those of other investigators for comparison [7,8]. As the figure shows, the present analysis is in excellent agreement with the other results. It should be mentioned that the path independence of this J-integral has been previously demonstrated [7].

An Analysis of Running Cracks

A technique has been developed that allows for the analysis of running cracks without the need for mesh adjustments or iterations. This technique is based on earlier crack propagation investigations using a finite difference based analysis [9]. It begins by subdividing the element immediately ahead of the crack tip into what can be thought of as subelements, as shown in Figure 6, (in this case, for a mesh composed of four noded linear elements). During propagation, the crack tip will be, in theory, allowed to move in discrete jumps along the crack plane through these subelements; e.g., the crack tip will move from Point "1" to Point "2" in one jump and later move

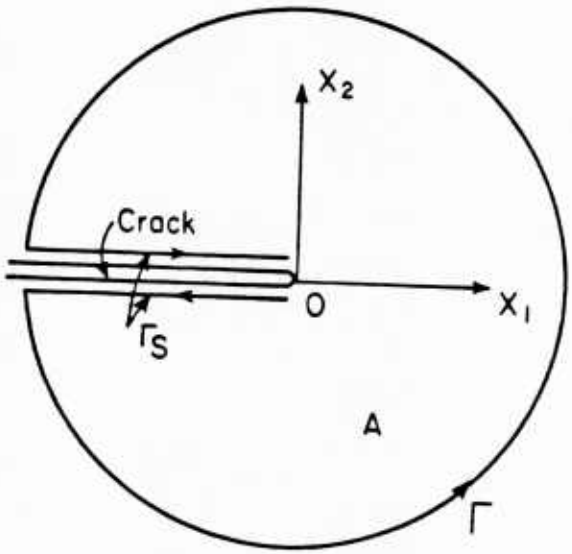

FIGURE 1. COORDINATE SYSTEM AND CURVES Γ and Γ_S.

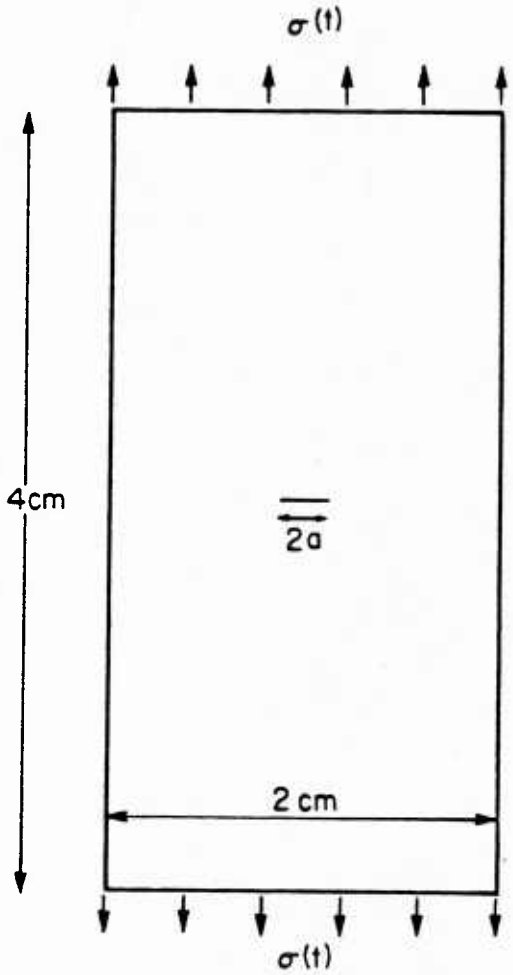

FIGURE 2. GEOMETRY FOR STATIONARY CRACK ANALYSIS; a = 0.24 cm.

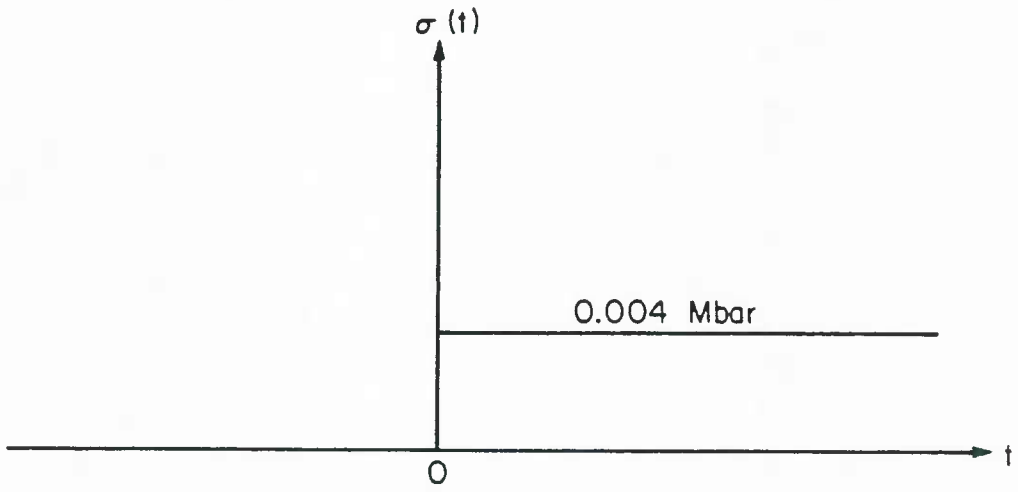

FIGURE 3. LOADING HISTORY FOR STATIONARY CRACK ANALYSIS.

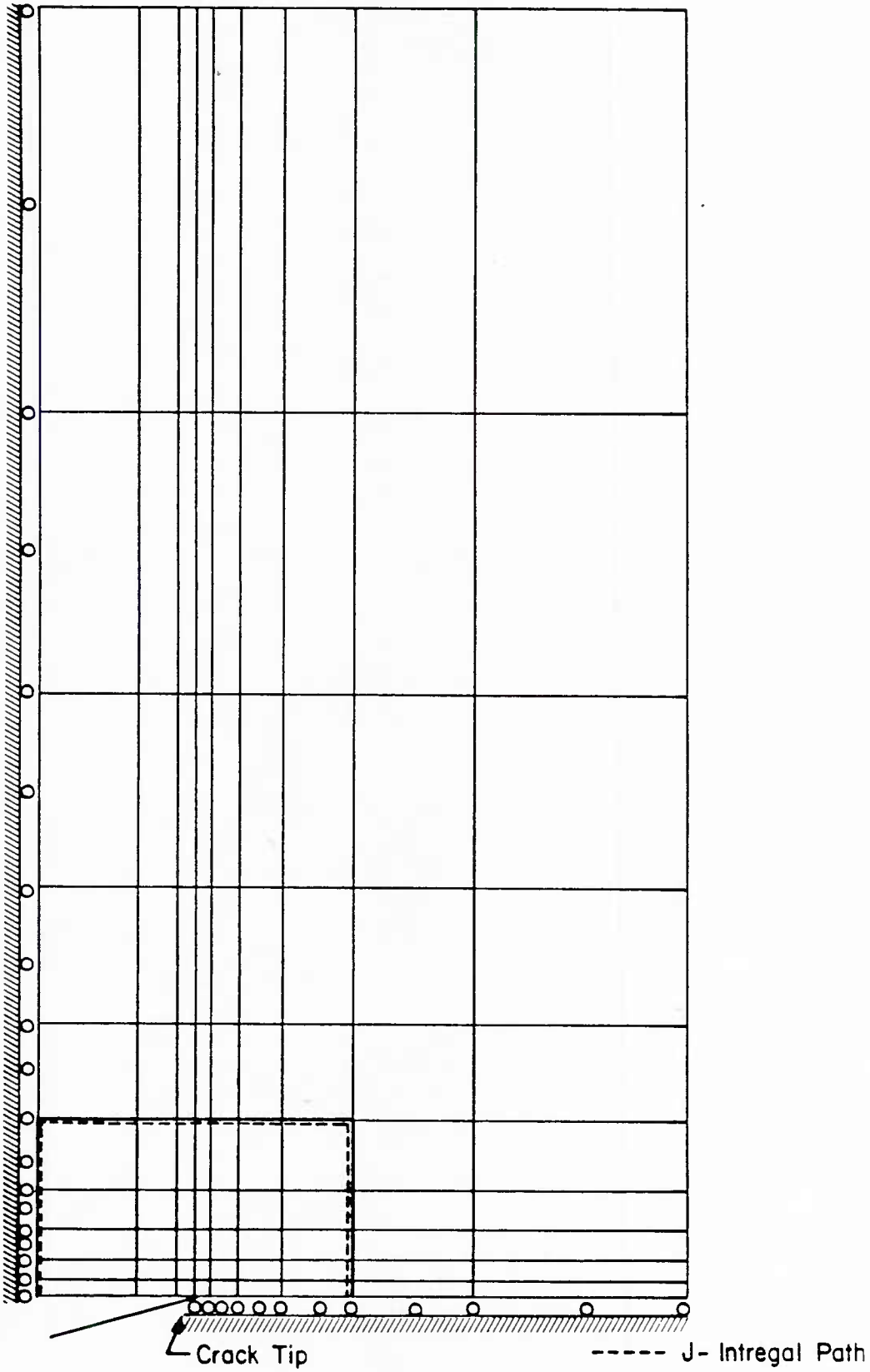

FIGURE 4. FINITE ELEMENT MESH AND J-INTEGRAL PATH FOR A STATIONARY CRACK PROBLEM

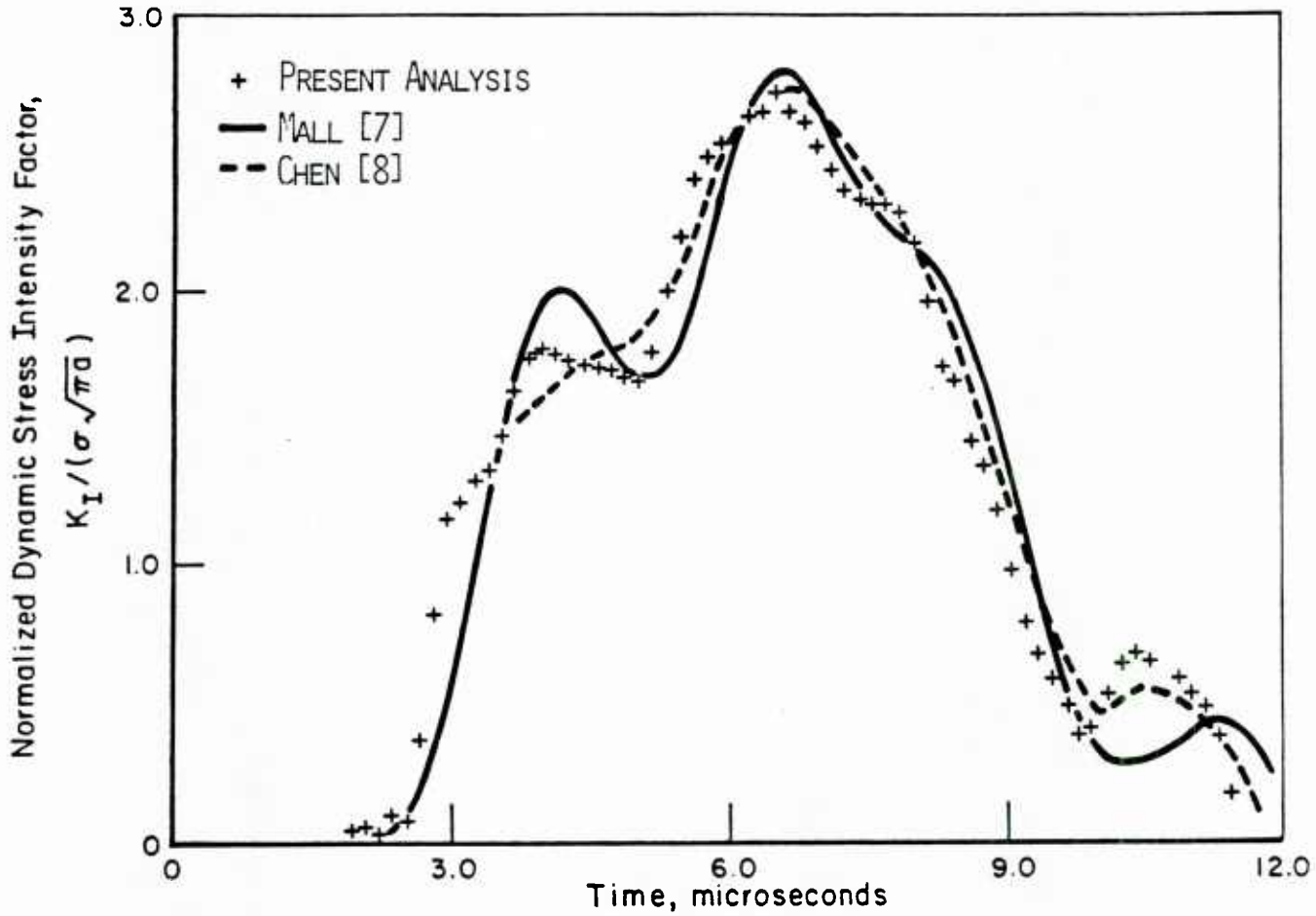

FIGURE 5. DYNAMIC STRESS INTENSITY FACTOR VERSUS TIME FOR AN IMPULSIVELY LOADED CENTER-CRACKED PANEL WITH A STATIONARY CRACK

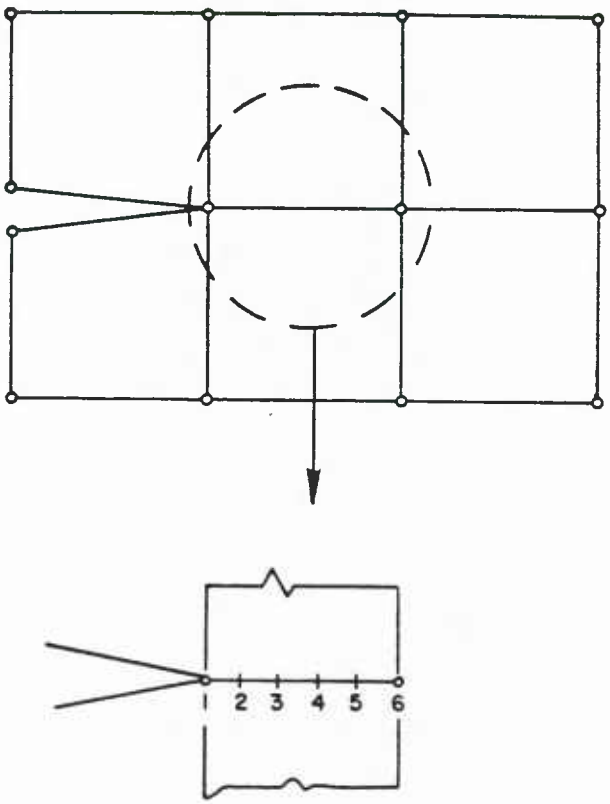

FIGURE 6. ELEMENT SUBDIVISION.

from Point "2" to Point "3" and so on, as the analysis dictates. The stress intensity factor at any crack location will be determined by a J-integral evaluation, Equation (6).

Consider the situation with the crack tip at Point "1". The crack velocity, V, will be estimated by counting the number of time steps, n, which are required until the stress intensity factor, K, is equal to the fracture toughness and performing the simple calculation:

$$V = \frac{|x(2) - x(1)|}{n\Delta t} \tag{7}$$

where Δt is the time step size. This algorithm is repeated as the crack tip moves from Point "1" to "2", "2" to "3", and so on.

This algorithm has the advantage of allowing the calculation of pseudo crack velocities after each time step. This pseudo velocity is equal to the actual crack velocity when the fracture criterion

$$K = K_D\ (V,\ T)$$

is satisfied, where the fracture toughness can be a function of the crack velocity, V, and material temperature, T. Since the crack velocity is calculated first and then the fracture toughness, there are no problems with using a velocity independent fracture toughness relation. This type of criterion would cause problems if the crack was propagating, i.e., $K = K_D$, and the inverse of the K_D relation was used to determine the crack velocity as is done in some codes.

It was then necessary to decide the number of subdivisions to make in each element. This was accomplished by determining the maximum crack velocity to be allowed in the analysis, V_{max}. In this study, V_{max} was taken as the bar wave speed, $\sqrt{E/\rho}$. Once V_{max} is set, the maximum distance the crack can propagate per time step, $\Delta x'$, is

$$\Delta x' = V_{max} \cdot \Delta t \quad . \tag{8}$$

The number of $\Delta x'$ units in an element length, Δx, is, $\frac{\Delta x}{\Delta x'}$. To make the number of subdivisions an integer value and to prevent the crack from traveling more than one element length per time step, the number of subdivisions, N, is taken to be

$$N = \frac{\Delta x}{\Delta x'} + 1 \tag{9}$$

where N is a truncated integer value. Should the crack want to propagate at one subdivision per time step, its propagation speed will be somewhat less than the maximum velocity, V_{max}, set previously due to the truncation. The amount by which the actual maximum crack velocity differs from V_{max} will depend on the value of N.

The last detail was to determine how the crack tip would be placed at the subdivision lines. This was conceptually performed by placing a force on the element to which the crack tip is adjacent. For a four-noded element, the force is placed on the one node on the crack plane behind the crack tip and for an eight-noded element nodal, forces would be placed on the two nodes as shown in Figure 7. The forces were postulated to be linearly related to the crack tip location by the following equation:

$$\frac{F_i}{F_{o_i}} = [1 - \frac{a}{\Delta x}] \tag{10}$$

where F_i is the force at node "i", F_{o_i} is the nodal force at node "i" just prior to the node release, as shown in Figure 7, "a" is the crack length in the element which the crack tip is in, and "Δx" is the length of that element. In the present study, eight-noded quadratic isoparametric elements were used. The midside node was released simultaneously with the trailing vertex node. The force history of each node followed the prescription given in Equation (10). Both nodes were released simultaneously to avoid possible problems discovered in another investigation [10].

A summary of the above algorithm for a quasi-statically initiated event is given in Figure 8.

In the algorithm just described, the location of the "crack tip" is obviously not actually known when there are forces on the crack face. The

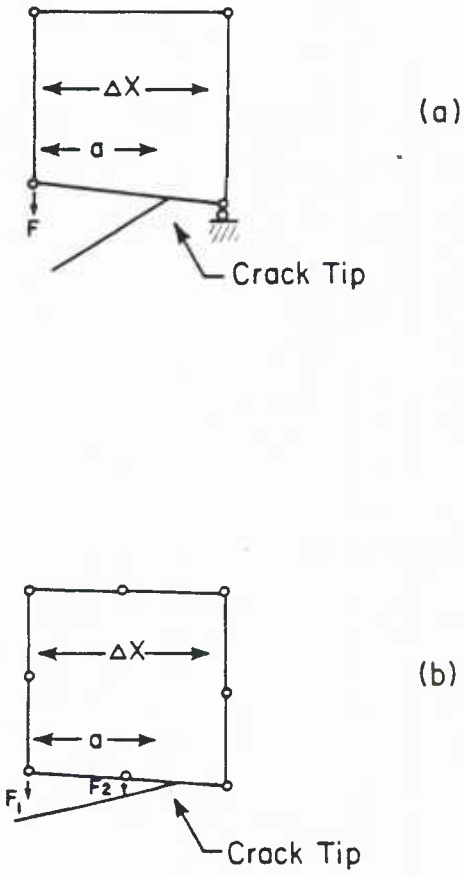

FIGURE 7. PLACEMENT OF NODAL FORCES FOR (a) A FOUR-NODED ELEMENT AND (b) AN EIGHT-NODED ELEMENT.

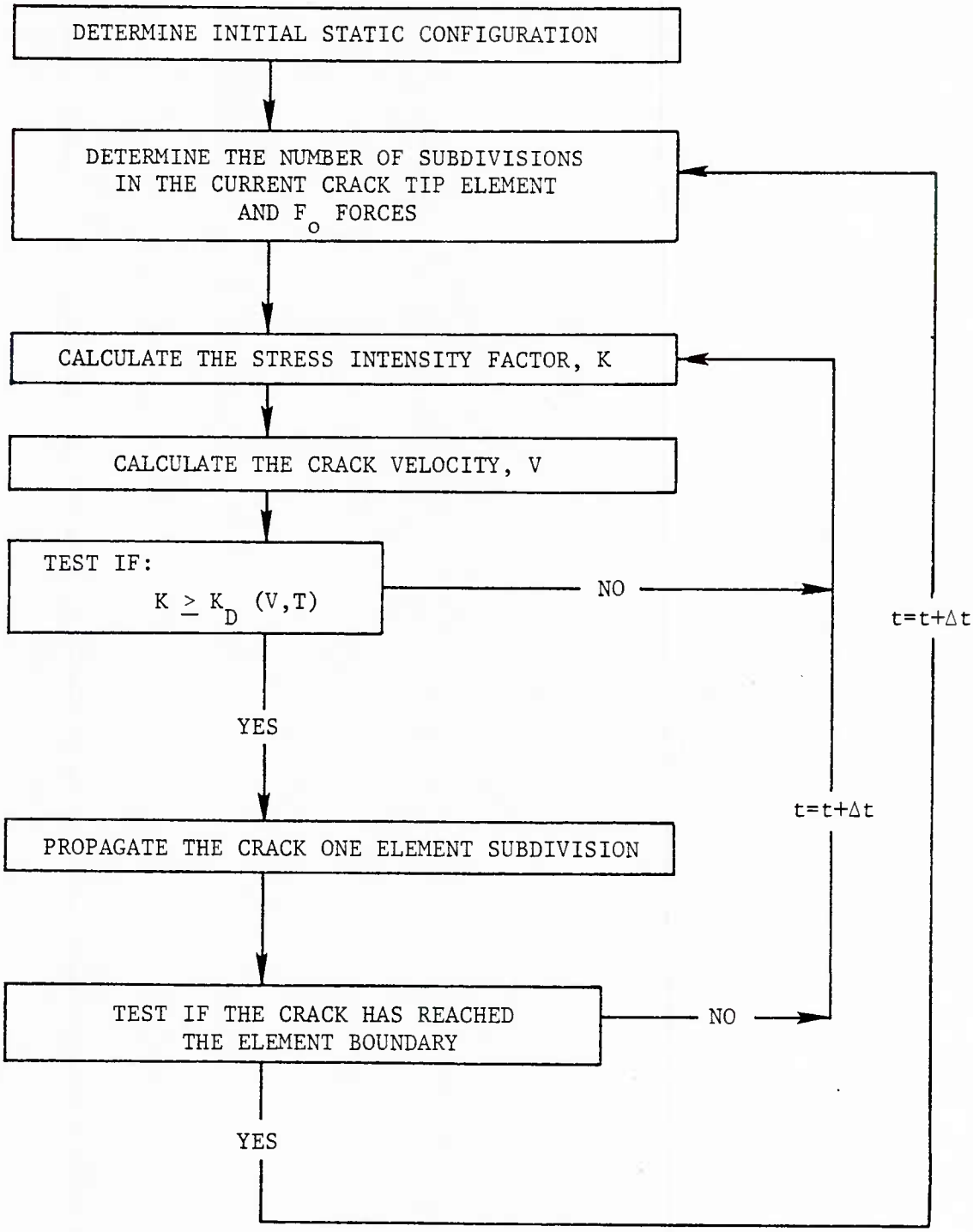

FIGURE 8. FLOW CHART OF PROPAGATION ALGORITHM FOR A QUASI-STATICALLY INITIATED DYNAMIC EVENT

only time when the location of the crack tip is unambiguous is when there are no forces on the crack face. But in order to avoid regeneration of the mesh (which would be necessary to place a node at the desired crack tip location) the interpretation used in the above algorithm was adopted. A similar interpretation has also been used by others [10,11,12].

The applicability of this interpretation can be somewhat tested by performing a constant velocity crack analysis. The problem chosen was a centrally cracked square plate of 40 mm x 40 mm with an initial crack length of 0.2 a/w, where w is the panel width. The panel was initially loaded with a uniform stress in the direction perpendicular to the crack. The properties of the plate were $E = 7716$ kgf/mm^2; $\nu = 0.286$; and $\rho = 2.5 \times 10^{-10}$ kgf $\cdot$ s^2/mm^4. The crack was propagated at a velocity of 0.2 of the shear wave speed of the material which was $C_s = 3.461 \times 10^6$ mm/sec. This problem is similar to that addressed by Broberg [13], except that Broberg treated the crack as opening from a zero initial length. The mesh used for the problem is shown in Figure 9. The model employed 213 nodes and 60 eight-noded isoparametric elements. The time integration employed a time step of 0.2887 microsecond with $\alpha = 0.25$ and $\delta = 0.5$ The results of the analysis is shown in Figure 10 along with the Broberg solution and solutions of Atluri [14]. The figure shows that the two computed solutions are very similar and they converge to the Broberg solution after the initial transient conditions have past. Hence, very reasonable estimates of the stress intensity factor with time can be obtained for the problem of a crack with prescribed velocity.

The inverse of the problem performed above is perhaps of even more importance; i.e., a problem in which the dynamic fracture toughness is specified and the crack length time history is sought. The ability of the proposed procedure to perform such an analysis was tested by comparing computed results with experimental data for a quasi-statically initiated crack in a 4340 steel three-point bend (dynamic tear) specimen; see Figure 11. The finite element mesh used for the analysis used 314 nodes and 91 eight-noded isoparametric elements; see Figure 12. A previously determined dynamic fracture toughness relation given by $K_{ID} = 65 + 0.44\ V$ was used [15].

The results of the analysis given in Figure 13 show excellent agreement with experimental results.

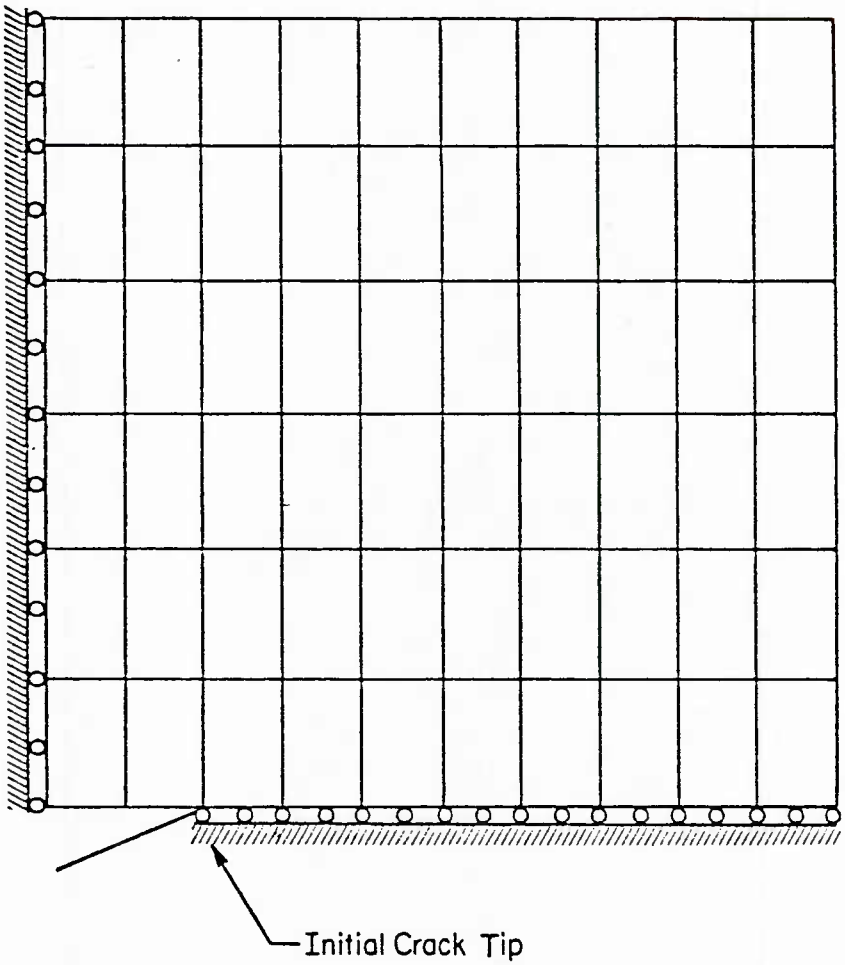

FIGURE 9. MESH FOR A CONSTANT VELOCITY CRACK PROBLEM

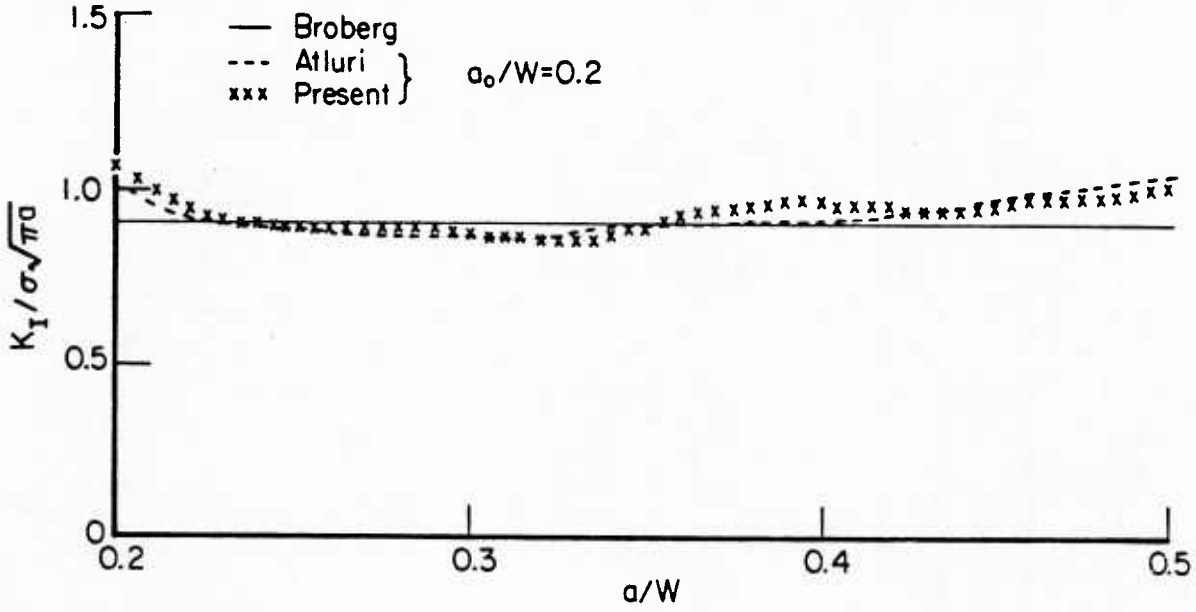

FIGURE 10. STRESS INTENSITY FACTOR FOR A CRACK STARTING AT $a_o/W = 0.2$ AND PROPAGATING AT A CONSTANT VELOCITY OF $V/C_S = 0.2$.

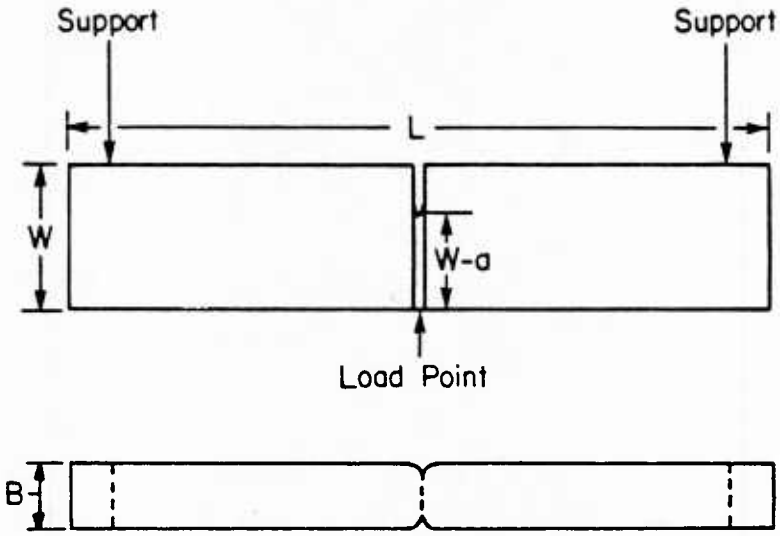

FIGURE 11. SPECIMEN GEOMETRY FOR A QUASI-STATICALLY INITIATED CRACK PROPAGATION TEST L = 181 mm, W = 38 mm, B = 15.8 mm, W-a = 28.5 mm.

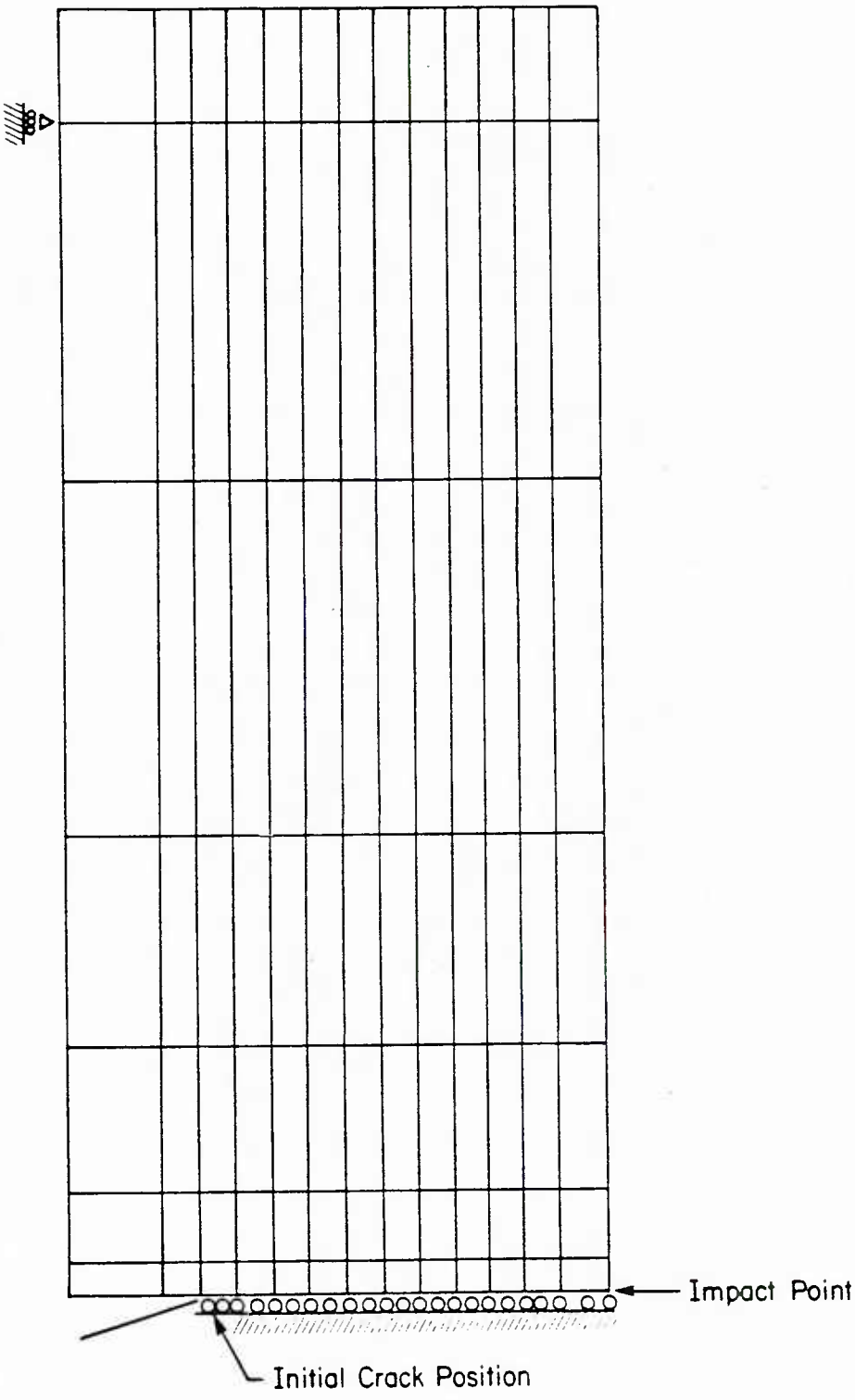

FIGURE 12. MESH FOR IMPACT LOADED THREE-POINT BEND ANALYSIS.

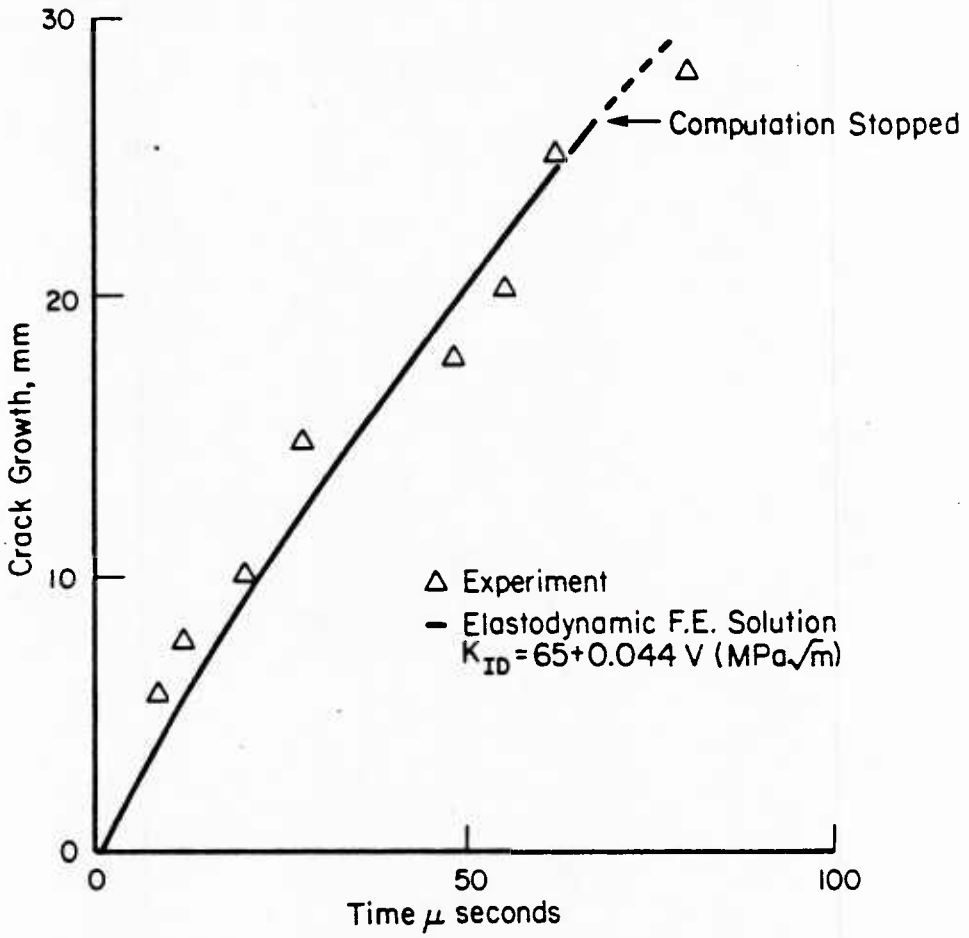

FIGURE 13. A COMPARISON OF ANALYSIS AND EXPERIMENT FOR A QUASI-STATICALLY INITIATED CRACK IN A 4340 DYNAMIC TEAR SPECIMEN.

Conclusions

A simple yet effective technique has been developed to perform dynamic crack propagation problems. The technique does not require using singular elements or updating the finite element mesh during crack propagation. Also, the dynamic fracture criterion need not be velocity dependent. Good agreement has been obtained between analytical results and experimental data.

REFERENCES

[1] Kanninen, M. F., "Whither Dynamic Fracture Mechanics?", Numerical Methods in Fracture Mechanics, Proceedings of the Second International Conference held at University College, Swansea, United Kingdom, Eds. D.R.J. Owen, A. R. Luxmoore, July 1980.

[2] Klaus-Jurgen, Bathe, and Wilson, E. L., Numerical Methods in Finite Element Analysis, Prentice-Hall, Inc., Englewood Cliffs, New Jersey, pp 322-326, 1976.

[3] Aoki, S., Kishimoto, K., Kondo, H., and Sakata, M., "Elastodynamic Analysis of Cracks by Finite Element Method Using Singular Element", Int. J. Fracture, 14, pp 59-68, 1978.

[4] Bazant, Z. O., Glazik, J. L., Jr., and Achenbach, J. D., "Finite Element Analysis of Wave Diffraction by a Crack", Mech. Div. ASCE, 102-EM3, pp 479-496, 1976.

[5] Aberson, J. A., Anderson, J. M., and King, W. W., Dynamic Analysis of Cracked Structures Using Singularity Finite Elements, Elastodynamic Crack Problems, pp 249-294, Ed. G. C. Sih, Noordhoff, 1977.

[6] Kishimoto, K., Aoki, S., and Sakata, M., "Dynamic Stress Intensity Factors Using J-Integral and Finite Element Method", Engineering Fracture Mechanics, 13, pp 387-394.

[7] Mall, S., "Finite Element Analysis of Stationary Cracks in Time Dependent Stress Fields", Numerical Methods in Fracture Mechanics, Eds. A. R. Luxmoore and D.R.J. Owen, University College, Swansea, 1980.

[8] Chen, Y. M., "Numerical Computation of Dynamic Stress Intensity Factors by a Lagrangian Finite-Difference Method (The Hemp Code)", Engineering Fracture Mechanics, 7, pp 653-660, 1975.

[9] Popelar, C. H., and Gehlen, P. C., "Modeling of Dynamic Crack Propagation: II. Validation of Dynamic Analysis", International Journal of Fracture, 15, pp 159-177, 1979.

[10] Mall, S., and Luz, J., "Use of an Eight-Node Element for Fast Fracture Problems", International Journal of Fracture, 16, pp R33-R36, 1980.

[11] Malluck, J. F., and King, W. W., "Fast Fracture Simulated by Conventional Finite Elements: A Comparison of Two Energy-Release Algorithms", Crack Arrest Methodology and Applications, ASTM STP 711, Eds. G. T. Hahn and M. F. Kanninen, American Society for Testing and Materials, pp 138-153, 1980.

[12] Kobayashi, A. S., Urabe, Y., Mark, S., Emery, A. F., and Love, W. J., "Dynamic Finite Element Analysis of Two Compact Specimens", Journal of Engineering Materials and Technology, 100, pp 402-410, October 1978.

[13] Broberg, K. B., "The Propagation of a Brittle Crack", Arkiv for Fysik, Band 18, No. 10, pp 139-192, 1966.

[14] Atluri, S. N., Nishioka, T., and Nakagaki, M., "Numerical Modeling of Dynamic and Nonlinear Crack Propagation in Finite Bodies by Moving Singular Elements", Nonlinear and Dynamic Fracture Mechanics, Eds. Nicholas Perrone and Satya Atluri, American Society of Mechanical Engineers, AMD-Vol 35, pp 37-66, 1979.

[15] Kanninen, M. F., Gehlen, P. C., Barnes, C. R., Hoagland, R. G., Hahn, G. T., and Popelar, C. H., "Dynamic Crack Propagation Under Impact Loading", Nonlinear and Dynamic Fracture Mechanics, Eds. Nicholas Perrone and Satya Atluri, American Society of Mechanical Engineers, AMD-Vol 35, pp 195-200, 1979.

ON THE ENERGY LOSS DURING DYNAMIC CRACK PROPAGATION

by

C.H. POPELAR
DEPARTMENT OF ENGINEERING MECHANICS
THE OHIO STATE UNIVERSITY
155 W. WOODRUFF AVE.
COLUMBUS, OHIO 43210

and

M.F. KANNINEN
STRESS ANALYSIS AND FRACTURE SECTION
BATTELLE COLUMBUS LABORATORIES
505 KING AVENUE
COLUMBUS, OHIO 43201

June, 1981

SECURITY CLASSIFICATION OF THIS PAGE (When Data Entered)

REPORT DOCUMENTATION PAGE		READ INSTRUCTIONS BEFORE COMPLETING FORM
1. REPORT NUMBER	2. GOVT ACCESSION NO.	3. RECIPIENT'S CATALOG NUMBER
4. TITLE (and Subtitle) ON THE ENERGY LOSS DURING DYNAMIC CRACK PROPAGATION		5. TYPE OF REPORT & PERIOD COVERED Interim 6. PERFORMING ORG. REPORT NUMBER
7. AUTHOR(s) C. H. Popelar, M. F. Kanninen		8. CONTRACT OR GRANT NUMBER(s) N00014-77-C-0576 - Battelle
9. PERFORMING ORGANIZATION NAME AND ADDRESS Battelle's Columbus Laboratories 505 King Avenue Columbus, Ohio 43201		10. PROGRAM ELEMENT, PROJECT, TASK AREA & WORK UNIT NUMBERS
11. CONTROLLING OFFICE NAME AND ADDRESS Office of Naval Research Structural Mechanics Program Department of the Navy, Arlington, VA 22217		12. REPORT DATE June 1981 13. NUMBER OF PAGES 19
14. MONITORING AGENCY NAME & ADDRESS(if different from Controlling Office)		15. SECURITY CLASS. (of this report) Unclassified 15a. DECLASSIFICATION/DOWNGRADING SCHEDULE

16. DISTRIBUTION STATEMENT (of this Report)

Approved for public release; distribution unlimited

17. DISTRIBUTION STATEMENT (of the abstract entered in Block 20, if different from Report)

18. SUPPLEMENTARY NOTES

19. KEY WORDS (Continue on reverse side if necessary and identify by block number)

DCB Specimen, Araldite B, Crack Arrest, Energy Damping, Photoelastic Materials.

20. ABSTRACT (Continue on reverse side if necessary and identify by block number)

The amount of energy dissipation that occurs during rapid crack propagation in photoelastic test specimens is examined. The analysis, which is based on a dynamic viscoelastic model for crack propagation in a double cantilever beam specimen, is forced to agree with measured post-arrest behavior observed in Araldite B. The results demonstrate that the energy loss during rapid fracture prior to crack arrest is small compared to the initial stored energy. An error in the procedure of Dally and Shukla, which led to

(over)

20. Abstract (Cont'd)

overestimates of this energy loss from experiments in Homalite 100, is identified. It is concluded that linear elastodynamic analyses can be used for the analysis of run-arrest events, even in polymeric materials.

ABSTRACT

The amount of energy dissipation that occurs during rapid crack propagation in photoelastic test specimens is examined. The analysis, which is based on a dynamic viscoelastic model for crack propagation in a double-cantilever-beam-specimen, is forced to agree with measured post-arrest behavior observed in Araldite B. The results demonstrate that the energy loss during rapid fracture prior to crack arrest is small compared to the initial stored energy. An error in the procedure of Dally and Shukla, which led to overestimates of this energy loss from experiments in Homalite 100, is identified. It is concluded that linear elastodynamic analyses can be used for the analysis of run-arrest events, even in polymeric materials.

INTRODUCTION

Optical techniques are frequently used to study dynamic crack propagation and crack arrest. The purposes of such investigations have been to develop fundamental insights into the physical phenomenon of crack propagation and arrest and/or to verify analytical predictions of such events. The most frequently used materials in these tests are the photoelastic materials Homalite 100 and Araldite B. Because these are polymeric materials, they exhibit rate effects and a degree of viscosity not commonly found in structural metals like steel. For example, Shukla et al [1], using a Hopkinson bar test, reported a value of 0.23 for the logarithmic decrement in Homalite 100, but only 0.0066 for the corresponding value in steel.

Because of the rate effects exhibited by photoelastic materials, an important question arises - can the experimental results attained employing these materials be used to infer the behavior of unstable crack propagation and arrest in steel? Popelar and Kanninen [2] provided a preliminary attempt to answer this question. Modeling these materials as standard linear viscoelastic solids, they found that the viscous energy dissipated during the period of unstable crack growth in a double-cantilever-beam (DCB) specimen was negligible compared to the initial stored energy. Furthermore, it was shown that correlations between elastic and viscoelastic dynamic crack propagation/arrest can be made with elastic analyses using only the long-and short-time properties of the viscoelastic materials. However, the material constants that were used in their calculations may not have properly reflected the behavior of the material during the extremely short time duration associated with a run-arrest event.

Recently Dally and Shukla [3] have used modified compact-tension (MCT) specimens to study the energy losses during crack propagation and after crack arrest in Homalite 100. They report that a total of 35 to 45% of the initial strain energy is lost in damping. By analyzing their post-arrest data, Dally and Shukla concluded that from 45 to 65% of the total damped energy is lost during the period of unstable crack propagation. In complete contradiction to the predictions of Popelar and Kanninen, they therefore concluded that 20% or more of the initial strain energy could be lost due to damping prior to crack arrest.

If Dally and Shukla are correct, their finding has far reaching implications. Surely, with this much energy being dissipated during the relatively short propagation event, the use of Homalite 100 to simulate behavior in steel or other rate-independent materials is highly questionable. Furthermore, the use of linear elastic fracture mechanics analyses to interpret dynamic crack propagation in Homalite 100 specimens would appear to be extremely questionable.

The purpose of this paper is to lay to rest these trepidations and to restore confidence in the elastic interpretation of dynamic crack propagation and arrest. To this purpose, use is made of experimental results obtained by Kalthoff [4] on crack propagation and arrest in Araldite B DCB specimens to improve the dynamic-viscoelastic analysis model developed previously [2]. The results essentially confirm the original findings. The dichotomy is resolved by identifying an error in the analysis of Dally and Shukla [3] which is primarily responsible for their erroneous conclusion.

FORMULATION OF THE ANALYSIS MODEL

Within the confines of conventional linear elastic fracture mechanics (LEFM) and its assumption of small scale yielding, the only source of energy loss during unstable crack growth is the fracture process. But, other forms of energy losses due to internal and external influences also exist even though they are seldom considered. While there are various sources of internal energy dissipation, the one of primary concern here is due to the viscous character of the material. External sources of energy losses due to the interaction of the body with its environment are manifold and must also be considered.

Because both sources of energy dissipation are frequently nonlinear, linear modeling along the lines initiated in the earlier work [2] will necessitate simplification. The internal dissipation will again be modeled by considering the material to be a linear viscoelastic solid. A linear model for external losses will then be added in the form of a viscous damper. Thus, both the internal and external energy losses will be included in the analysis and may be viewed as due to damping.

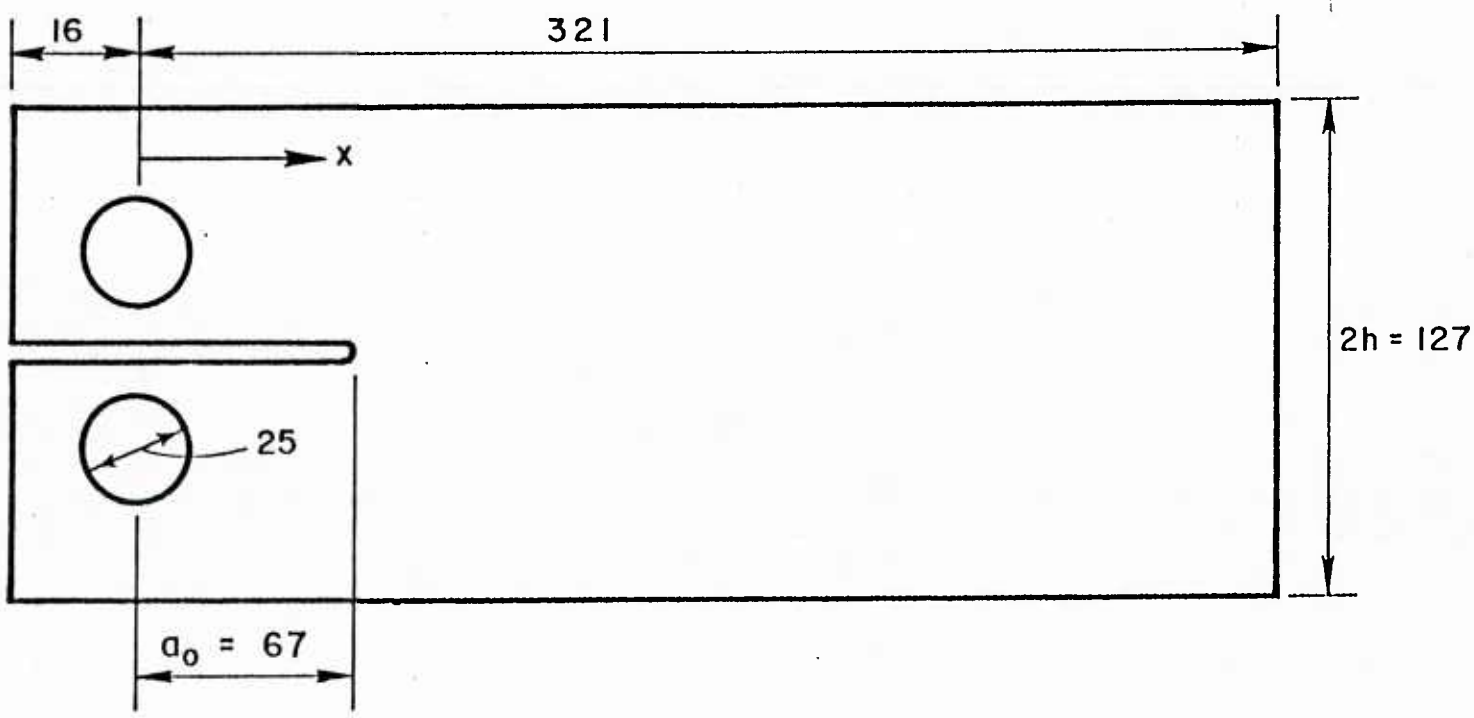

Dimensions are in mm.

FIGURE 1. DCB FRACTURE SPECIMEN

The present analysis is made for the wedge-loaded DCB specimen depicted in Figure 1. The reasons for selecting the DCB specimen are threefold. First, it has been demonstrated repeatedly that this specimen lends itself to a simple analysis which yields reliable predictions [5]. Second, Kalthoff et al [6] have reported that the DCB specimen is the most "dynamic" of the test specimens commonly used in studies of dynamic crack propagation and arrest. Therefore, with everything else being equal, one would anticipate that this specimen will exhibit a proportionally greater amount of damping during unstable crack growth. Thirdly, this formulation can be used in conjunction with the recent experimental results of Kalthoff [4] to deduce the correct mechanical properties for fast fracture in a photoelastic material.

The equations of motion for the DCB specimen derived by Kanninen, et al [5] reflect the symmetry of the specimen with respect to the crack plane and the beam-like character of the specimen. However, for application to a rate-dependent material, insufficient knowledge about the sources of external energy losses in the tests to be analyzed now exists. Hence, only an extensional damper will be used to model external energy dissipation; i.e., rotational damping is ignored. When supplemented by this external damper, the equations of motion of Popelar and Kanninen [2] for the one-dimensional model of the DCB specimen become

$$\frac{\partial S}{\partial x} - pH(x-a) - f = \rho A \frac{\partial^2 w}{\partial t^2} \tag{1}$$

$$\frac{\partial M}{\partial x} - S = \rho I \frac{\partial^2 \psi}{\partial t^2} \tag{2}$$

where the deformation is described by the transverse displacement w and rotation ψ of the cross-section while the internal stress resultants are the transverse shear S, bending moment M, and crack plane tension p per unit length. The external damping force per unit length is denoted by f which represents the basic difference between the present formulation and that of Reference [2]. Properties of the DCB specimen are reflected by the cross-sectional area A of each arm, moment of inertia I, crack length a, thickness b, half height h and mass density ρ. Also in Equation (1), H(x-a) is the Heaviside step function.

A linear three parameter (standard linear) viscoelastic solid is used to model the material. For a relaxation modulus $E(\tau)$ of the form

$$E(t) = E_\infty + (E_o - E_\infty) \exp\left(-\frac{t}{\tau}\right) \tag{3}$$

the constitutive relations are

$$\left(\frac{\partial}{\partial t} + \frac{1}{\tau}\right) M = E_o I \left(\frac{\partial}{\partial t} + \frac{1}{\tau}\frac{E_\infty}{E_o}\right) \frac{\partial \psi}{\partial x} \tag{4}$$

$$\left(\frac{\partial}{\partial t} + \frac{1}{\tau}\right) S = \frac{5}{6} G_o A \left(\frac{\partial}{\partial t} + \frac{1}{\tau}\frac{E_\infty}{E_o}\right) \left(\frac{\partial w}{\partial x} - \psi\right) \tag{5}$$

$$\left(\frac{\partial}{\partial t} + \frac{1}{\tau}\right) p = \frac{2E_o b}{h} \left(\frac{\partial}{\partial t} + \frac{1}{\tau}\frac{E_\infty}{E_o}\right) w\, H(x-a) \tag{6}$$

where E_o and E_∞ denote, respectively, the short and long-time moduli, τ is the relaxation time and $G_o = E_o/2(1 + \nu)$ in which ν is Poisson's ratio. For linear damping

$$f = 2\eta\rho b c_o \frac{\partial w}{\partial t} \tag{7}$$

where η is a dimensionless damping factor and $c_o = (E_o/\rho)^{1/2}$ is the instantaneous bar wave speed of the material.

The fracture criterion is based upon a balance between the energy release rate G and the fracture resistance R which may depend upon crack speed; i.e., for crack propagation

$$G = R(\dot{a}) \qquad \dot{a} > 0 \tag{8}$$

It can be shown that the energy release rate for a DCB specimen having a relaxation modulus given by Equation (3) is

$$G = \left\{\frac{2pu}{b} - \frac{2E_o}{h} w^2 + \frac{h}{2(E_o - E_\infty)} \left[\frac{p}{b} - \frac{2E_o}{h} w\right]^2\right\}_{x=a} \tag{9}$$

In most instances fracture data are presented in terms of the dynamic fracture toughness $K_D = K_D(\dot{a})$ instead of R. However, Kostrov and Nikitin [7] showed that

$$R = \frac{1 - \nu^2}{E_o} A(\dot{a}) K_D^2 \tag{10}$$

where $A(\dot{a})$ is a universal function of crack speed that is identical to the Freund-Nilsson relation provided the short-time modulus replaces the elastic modulus.

For a given pin displacement, or, equivalently, an initial stress intensity factor K_Q, Equations (1), (2), and (4) through (7) can be integrated using a finite difference technique. At each time step, Equation (9) is also evaluated. An increment of crack growth is then permitted whenever the fracture criterion given by Equation (8) is satisfied. In this manner, the crack history can be computed. It is also a straightforward procedure to compute the stored energy U, kinetic energy T, dissipative or damping energy D and the fracture energy F, all per unit thickness of the specimen, throughout the fracture event.

DETERMINATION OF MATERIAL CONSTANTS FROM POST-ARREST BEHAVIOR IN ARALDITE B

Because of some rather unique experimental results that have been made available by Kalthoff [4], the computations will be directed at an Araldite B double-cantilever-beam specimen. In Kalthoff's experiments a 1-mm diameter hole sufficient to arrest a propagating crack was drilled through the thickness of the specimen at a known distance ahead of the initial crack tip. In this manner it was possible to control when and where the crack would arrest. This permitted rather extensive measurements of the post-arrest history of the stress intensity factor.

The results of three replicate experiments for a DCB specimen with a hole located 43 mm ahead of the initial crack tip are shown in Figure 2. In these experiments the crack propagated at an average speed of 190 m/s before reaching the hole at approximately 210 μsec after initiation. The oscillatory decay after-arrest of the stress intensity factor with time is readily apparent. (Similar measurements have been made by Dally and Shukla [3] for naturally arrested cracks in Homalite 100, MCT specimens.) Kalthoff et al [4] have found that the post- arrest behavior of the stress intensity factor in Araldite B and Homalite 100 to be qualitatively similar.

The short- and long-time moduli of Araldite B are 3660 MN/m^2 and 3380 MN/m^2, respectively, with Poisson's ratio being 0.39. The damping coefficient η and relaxation time τ that are representative of these tests are unknown. Therefore, for the measured dynamic fracture toughness - crack speed relation for Araldite B depicted in Figure 3 -computations were performed for various assumed values of τ and η until a combination was found that gave relatively good agreement between the computed and the measured stress intensity factor after arrest. These values were $\eta = 0.01$ (dimensionless) and $\tau = 10^{-4}$ sec.

The computed history for $\eta = 0.01$ and $\tau = 10^{-4}$ is indicated by the solid curve in Figure 2. Aside from a slight difference in the period of oscillation, the agreement is quite good. The computed response seems to decay slightly more rapidly than do the measurements, indicating that the damping losses are, if anything, somewhat overestimated by the model.

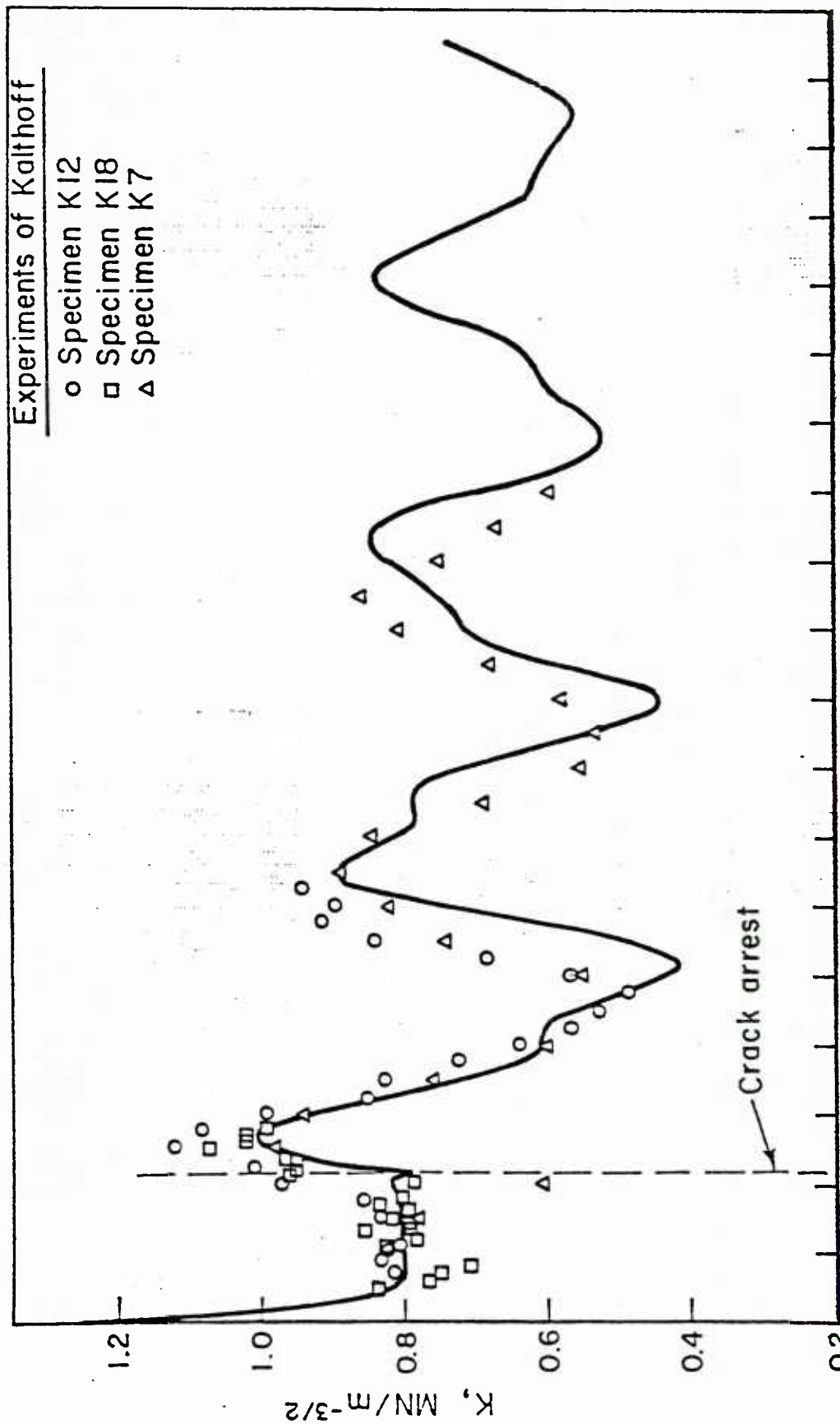

FIGURE 2. STRESS INTENSITY FACTOR VERSUS TIME FOR AN ARTIFICIALLY ARRESTED CRACK.

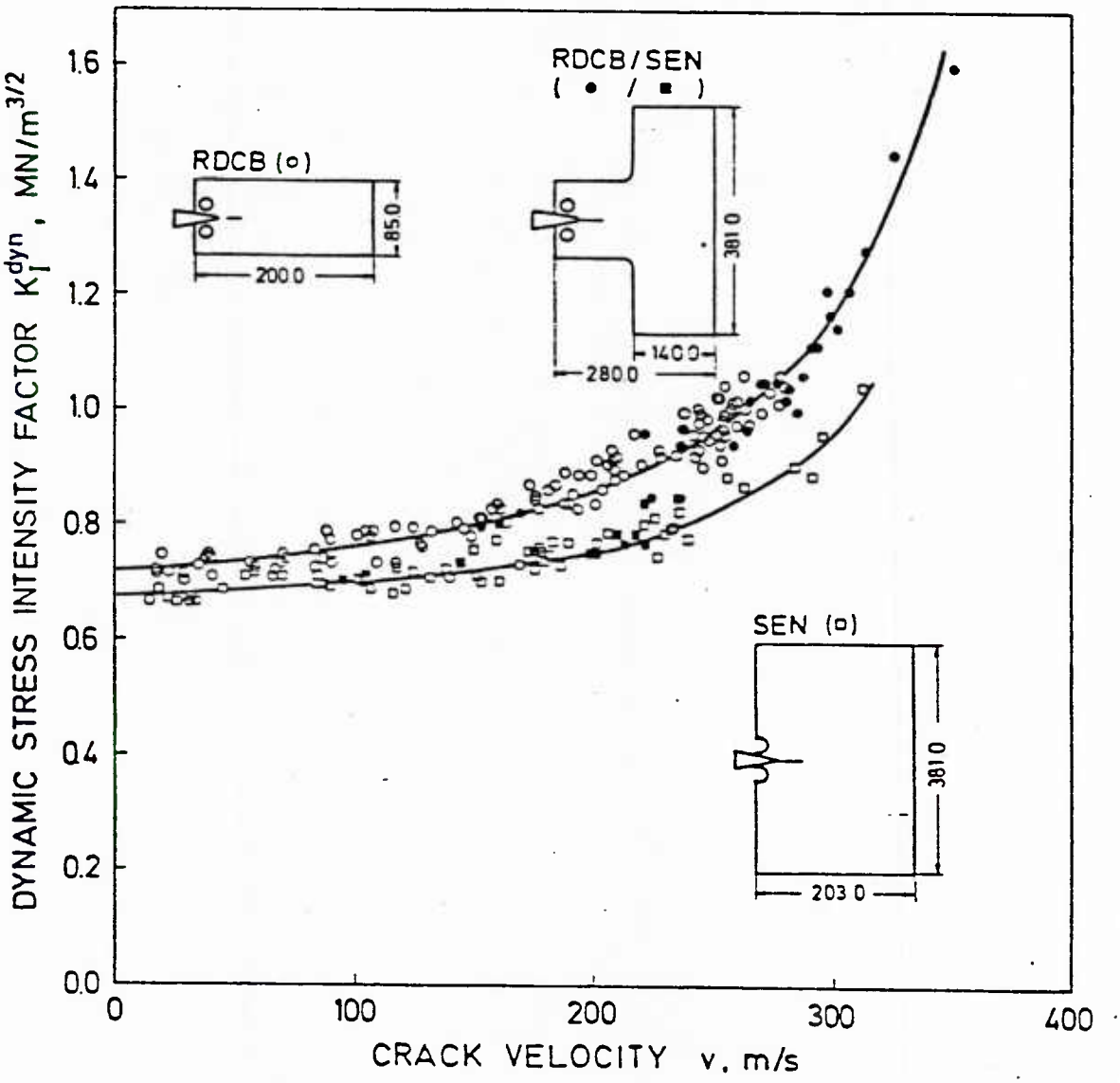

FIGURE 3. DYNAMIC FRACTURE TOUGHNESS AS A FUNCTION OF CRACK SPEED, KALTHOFF [8].

The post-arrest behavior is obviously very dependent upon the conditions existing in the specimen at the instant before arrest. Close post-arrest agreement demands that rather precise computations be made during the period of unstable crack propagation. The value of K_Q = 1.25 $MNm^{-3/2}$ which was used to achieve these results is slightly higher than the value of 1.17 $MNm^{-3/2}$ reported by Kalthoff. The average computed crack speed was 185m/s compared to the measured speed of 190m/s. The reported stress intensity factor after ring down was 0.66 $MNm^{-3/2}$ compared to the computed value of 0.715 $MNm^{-3/2}$. Clearly, while the experiment is not perfectly matched, the one-dimensional model of the DCB specimen provides a quite good simulation.

The time histories of the energy components are shown in Figure 4. These have been made dimensionless with respect to U_i, the initial stored energy in the specimen. These computations reveal that approximately 49% of the initial strain energy was consumed by the fracture process with 40% of the initial energy remaining as stored energy after arrest and 11% lost due to damping. Of perhaps most significance, only about 2.5% of the initial energy was lost due to damping during the period of unstable crack growth, the remainder being lost after crack arrest.

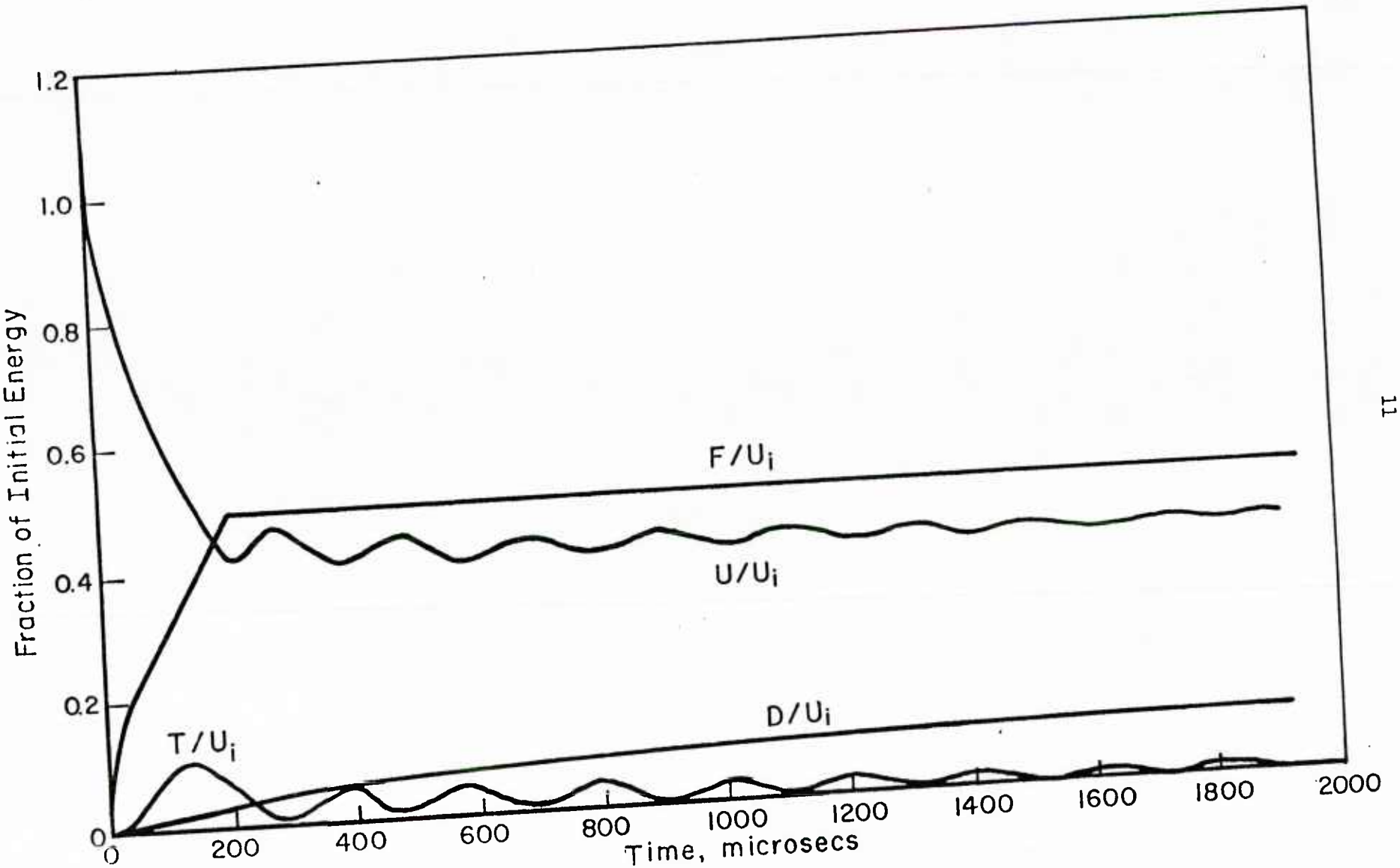

FIGURE 4. ENERGY HISTORIES FOR AN ARTIFICIALLY ARRESTED CRACK.

THE ESTIMATION PROCEDURE OF DALLY AND SHUKLA

Dally and Shukla [3] estimated the energy losses for crack propagation and arrest experiments in Homalite 100 MCT specimens. Their estimates were based upon measurements of the initial and final load and load-point displacements along with determinations of the stress intensity factor as a function of time. From these measurements, they computed the initial stored energy U_i, the final stored energy U_f and the total fracture energy F_t. Then, from a simple energy balance, they found the total dissipated or damped energy D_t to be

$$D_t = U_i - U_f - F_t \tag{11}$$

Next, in an effort to determine the energy loss during propagation D_p, Dally and Shukla argued that the post-arrest energy loss is just equal to the kinetic energy T_a available in the specimen at the instant of crack arrest. Hence,

$$D_p = D_t - T_a \tag{12}$$

Equivalently, this assumes that the stored energy at the instant of crack arrest is equal to the final stored energy.

By the principle of minimum strain energy, the stored energy at crack arrest is an upper bound to the equilibrium state that exists long after crack arrest; i.e., the final value. The present computations indicate that it is a good bound for the DCB specimen. As the computations show, the kinetic energy is subsequently converted to stored energy and vice versa. The energy is not conserved due to damping during this post-arrest period.

Dally and Shukla write that

$$T_a = \frac{U_i}{K_Q^2} \left(K_p^2 - K_s^2\right) \tag{13}$$

where K_p is the peak stress intensity factor after crack arrest and K_s is the final stress intensity factor after ring down of the oscillations. Equation (13) is obtained by arguing that the stored energy is proportional to K^2. While this is correct for LEFM conditions, it should be clear that the proportionality factor depends upon the crack length. Therein lies the source of the error in Equation (13). In particular, for the static case

$$U = g(a) \frac{K^2}{E} \tag{14}$$

where

$$g(a) = C/(Dc/da) \tag{15}$$

in which C denotes the compliance of the specimen. Therefore, the correct form of Equation (13) is

$$T_a = \frac{U_i}{K_Q^2} (K_p^2 - K_s^2) \frac{g(a_f)}{g(a_o)} \tag{16}$$

where a_f is the final length of the crack. Clearly, because $g(a_f)/g(a_o)>1$, T_a as given by Equation (13) is an underestimate. Hence, if it is used in Equation (12), an overestimate of D_p is obtained.

Also implied in this method of estimating the damped energy is the assumption that the excited mode of oscillation in the specimen is identical to the final static deflected shape; i.e., the specimen is modeled as a single-degree-of-freedom system. This can be a rather severe oversimplification as the following computations demonstrate.

For the results depicted in Figures 2 and 4, $g(a_f)/g(a_o) = 1.22$. With $K_p = 1.05$ MNm$^{-3/2}$ and $K_s = 0.715$ MNm$^{-3/2}$, Equation (16) yields $T_a/U_i = 46\%$ for $K_Q = 1.25$ MNm$^{-3/2}$. By contrast, Figure 4 shows that the maximum kinetic energy is only about 10 percent of the initial stored energy. From Figure 4, $D_t/U_i = 11\%$ and Equation (12) yields the absurd result that $D_p/U_i = -35\%$. This apparent paradox is due to the fact that when a rapidly propagating crack is abruptly arrested, the many high frequency modes of oscillation that are excited are ignored in arriving at Equation (16).

If the propagating crack is not artificially arrested but permitted to come to a natural arrest, then for $K_Q = 1.25$ MNm$^{-3/2}$, the computed crack jump was 58 mm, the duration of the period of crack propagation was 320 μsec, the average crack speed was approximately 180 m/s and the stress intensity after ring down was $K_s = 0.59$ MNm$^{-3/2}$. For purposes of comparison, Kalthoff et al [8] reported a measured crack jump of 63 mm and an average speed of approximately 195 m/s for $K_Q = 1.33$ MNm$^{-3/2}$. The computed stress intensity factor-time history is depicted in Figure 5 and the energy histories are shown in Figure 6. In this case, the damped energy during the period of crack propagation is about 5 percent, compared to the total value of 6 percent of the initial stored energy.

For this case $g(a_f)/g(a_o) = 1.35$. However, it is not clear here what value should be used for K_p. If the value of K after crack arrest is taken for K_p, then Equation (16) yields $T_a/U_i = 9\%$ and Equation (12) gives $D_p/U_i = -3\%$. Again, this absurd value is obtained because the mode of oscillation at arrest is not the same as the static deflected shape. If the peak value of K at approximately 760 μsec, nearly 450 sec after arrest, is taken for K_p, then the procedure yields $D_p/U_i = 2\%$ which underestimates the damped energy.

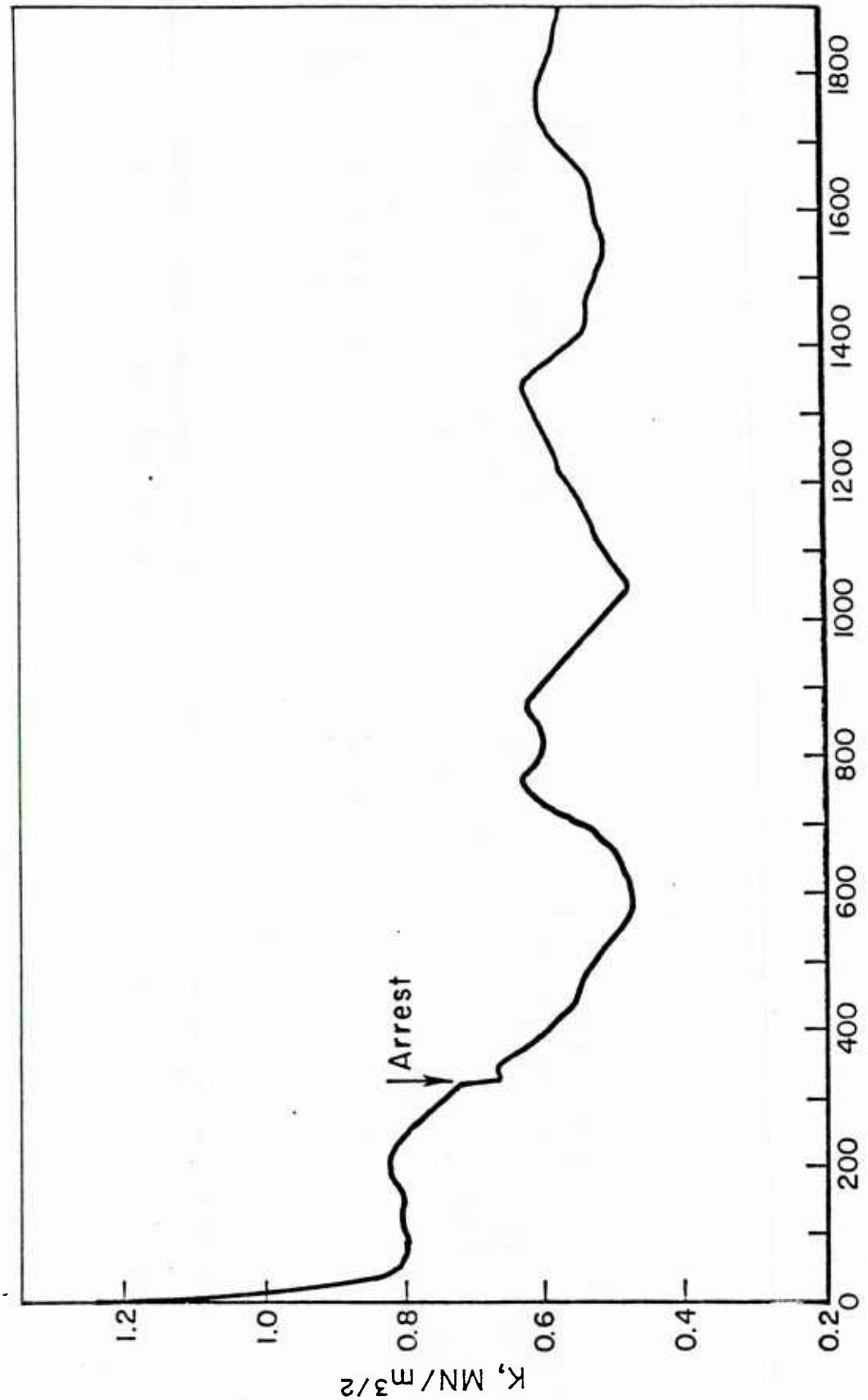

FIGURE 5. STRESS INTENSITY FACTOR VERSUS TIME FOR A NATURALLY ARRESTED CRACK.

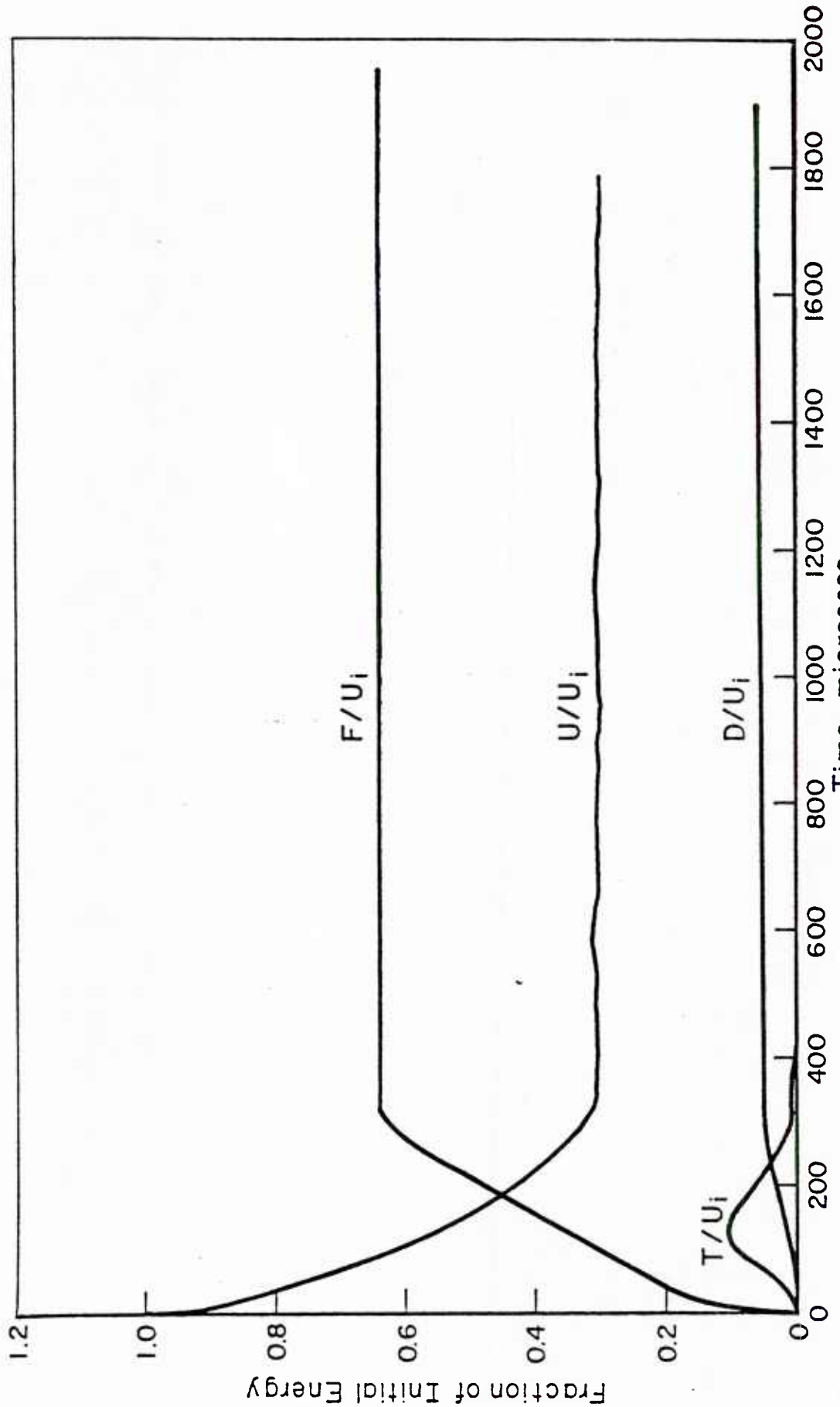

FIGURE 6. ENERGY HISTORIES FOR A NATURALLY ARRESTED CRACK.

DISCUSSION

The post-arrest behavior of the stress intensity factor produced by abruptly arresting a dynamically propagating crack in an Araldite B double-cantilever-beam specimen was used to fix two viscous damping parameters in a dynamic-viscoelastic analysis model of the event. Having fitted the post-arrest behavior, the model was used to determine the energy loss due to internal and external damping during the relatively shorter period of unstable crack growth. The computations demonstrated that a small amount, approximately 2.5 - 5% of the initial stored energy, was lost due to damping prior to arrest. This small value of energy loss is in contrast to the 20 percent or more estimated by Dally and Shukla [3] for a Homalite 100, MCT specimen. It has been demonstrated that these large values reported by Dally and Shukla are due to an error in their analysis.

When the procedure of Dally and Shukla is corrected and applied to the results of the present model, which have been shown to be in very good agreement with measured results, then negative values for the damping energy during crack propagation are predicted. These absurd results are due to an oversimplification by Dally and Shukla which in essence reduces the specimen to a single-degree-of-freedom system, or equivalently, treats the problem quasi-statically. Clearly, such a system cannot properly model the complex phenomenon of dynamic crack propagation and arrest. Furthermore, it should be recalled that the stress intensity factor is simply a measure of the local behavior at the crack tip. To use it to infer global quantities requires an analysis. The present paper demonstrates the dangers of applying a quasi-static analysis to dynamic crack propagation and arrest.

CONCLUSIONS

If the loading fixture is sufficiently stiff, then the energy loss during dynamic crack propagation and arrest in polymers commonly used in experimental studies is a small portion of the initial stored energy. Consequently, correlations between elastic dynamic and viscoelastic dynamic crack propagation and arrest can be made, as Popelar and Kanninen [2] showed, using only the short-and long-time moduli.

ACKNOWLEDGMENTS

The authors are indebted to Dr. J. F. Kalthoff for making available his unique experimental data which played an instrumental part in this paper. This work was supported by the Office of Naval Research Structural Mechanics Program under Contract Number N00014-77-C-056. The authors wish to thank Drs. N. Perrone and Y. Rajapakse for their encouragement of this work.

REFERENCES

1. Shukla, A., Fourney, W. L. and Dally, J. W., "Mechanisms of Energy Loss During a Fracture Process", Proceedings of the Society of Experimental Stress Analysis, June 1-4, 1981, Dearborn, Michigan, pp. 259-267.

2. Popelar, C. H. and Kanninen, M. F., "A Dynamic Viscoelastic Analysis of Crack Propagation and Crack Arrest in a Double-Cantilever-Beam Test Specimen", Crack Arrest Methodology and Applications, ASTM STP 711, G. T. Hahn and M. F. Kanninen, Eds. Philadelphia, 1980, pp 5-23.

3. Dally, J. W. and Shukla, A., "Energy Loss in Homalite 100 During Crack Propagation and Arrest", Engineering Fracture Mechanics, 13, 1980, pp. 807-817.

4. Kalthoff, J. F., Private Communication, June 10, 1980.

5. Kanninen, M. F., Popelar, C. and Gehlen, P.C., "Dynamic Analysis of Crack Propagation and Arrest in the Double-Cantilever-Beam Specimen", Fast Fracture and Crack Arrest, G. T. Hahn and M. F. Kanninen, Eds., ASTM STP 627, pp. 19-38, 1977.

6. Kalthoff, J. F., Beinert, J., Winkler, S. and Klemm, W., "Experimental Analysis of Dynamic Effects in Different Crack Arrest Test Specimens", Crack Arrest Methodology and Applications, ASTM STP 711, G. T. Hahn and M. F. Kanninen, Eds., Philadelphia, 1980, pp. 109-127.

7. Kostrov, B. V. and Nikitin, L. V., "Some General Problems of Mechanics of Brittle Fracture", Archiwum Mechaniki Stosowanej. 22, 1970, pp. 749-775.

8. Kalthoff, J. F., "Influence of Dynamic Effects on Crack Arrest", EPRI-RP-886-4, Monthly Report No. 6, October, 1979.

9. Kalthoff, J. F., Beinert, J., and Winkler, S., "Measurements of Dynamic Stress Intensity Factors for Fast Running and Arresting Cracks in Double-Cantilever-Beam Specimens", Fast Fracture and Crack Arrest, ASTM STP 627, G. T. Hahn and M. F. Kanninen, Eds., Philadelphia, 1977, pp. 161-176.

WHITHER DYNAMIC FRACTURE MECHANICS?

By

M. F. Kanninen
Applied Solid Mechanics Section
Battelle
Columbus Laboratories
Columbus, Ohio

May, 1980

Submitted for presentation at the Second International Conference on Numerical Methods in Fracture Mechanics, Swansea, United Kingdom, July 6-11, 1980

Unclassified

SECURITY CLASSIFICATION OF THIS PAGE (When Data Entered)

REPORT DOCUMENTATION PAGE		READ INSTRUCTIONS BEFORE COMPLETING FORM
1. REPORT NUMBER	2. GOVT ACCESSION NO.	3. RECIPIENT'S CATALOG NUMBER
4. TITLE (and Subtitle) WHITHER DYNAMIC FRACTURE MECHANICS?		5. TYPE OF REPORT & PERIOD COVERED Interim 6. PERFORMING ORG. REPORT NUMBER
7. AUTHOR(s) M. F. Kanninen		8. CONTRACT OR GRANT NUMBER(s) N00014-77-C-0576
9. PERFORMING ORGANIZATION NAME AND ADDRESS Battelle Columbus Laboratories Columbus, OH 43201		10. PROGRAM ELEMENT, PROJECT, TASK AREA & WORK UNIT NUMBERS
11. CONTROLLING OFFICE NAME AND ADDRESS Office of Naval Research Structural Mechanics Program Dept. of the Navy, Arlington, VA 22217		12. REPORT DATE May 1980 13. NUMBER OF PAGES 24
14. MONITORING AGENCY NAME & ADDRESS(if different from Controlling Office)		15. SECURITY CLASS. (of this report) Unclassified 15a. DECLASSIFICATION/DOWNGRADING SCHEDULE

16. DISTRIBUTION STATEMENT (of this Report)

Approved for public release; distribution unlimited

17. DISTRIBUTION STATEMENT (of the abstract entered in Block 20, if different from Report)

18. SUPPLEMENTARY NOTES

To be presented at the Second International Conference on Numerical Methods in Fracture Mechanics on July 6-11, 1980, in Swansea, United Kingdom

19. KEY WORDS (Continue on reverse side if necessary and identify by block number)

crack propagation	one dimensional model	polymeric materials
crack arrest	compact tension specimen	viscoelasticity
DCB test specimen	loss-of-coolant accident	AISI 4340 steel
blunted initial crack tip	homolite-100	three point bend specimen
fracture toughness	elastodynamic analyses	

20. ABSTRACT (Continue on reverse side if necessary and identify by block number)

The experimental basis for the necessity of a dynamic characterization of crack run/arrest events is reviewed. Current anomalies in the use of linear elastodynamic treatments--apparent geometry and load rate dependence of the dynamic fracture toughness property--are discussed. A review of concurrent work in plastic fracture mechanics is given as a possible basis for circumventing these anomalies.

DD FORM 1 JAN 73 1473 EDITION OF 1 NOV 65 IS OBSOLETE

S/N 0102-LF-014-6601

Unclassified

SECURITY CLASSIFICATION OF THIS PAGE (When Data Entered)

WHITHER DYNAMIC FRACTURE MECHANICS?

M. F. Kanninen[(i)]

SUMMARY

The experimental basis for the necessity of a dynamic characterization of crack run/arrest events is reviewed. Current anomalies in the use of linear elastodynamic treatments--apparent geometry and load rate dependence of the dynamic fracture toughness property--are discussed. A review of concurrent work in plastic fracture mechanics is given as a possible basis for circumventing these anomalies.

INTRODUCTION

At the first conference on Numerical Methods in Fracture Mechanics, the author presented an extensive appraisal of the numerical solution techniques used to analyze dynamic fracture mechanics problems [1]. The techniques reviewed were exclusively based on elastodynamic behavior coupled with loading rate dependent (for crack growth initiation) and crack speed dependent (for unstable crack propagation) fracture toughness values. While some new work has appeared in the interim, it is the author's feeling that this does not make a marked departure from the previous trends in the field. Therefore, a reassessment of elastodynamic computational techniques per se is not warranted at this time. The reader interested in this background material can refer to the earlier paper.

An important concern at the time of the first conference was whether a quasi-static or a fully dynamic characteriza-

---

(i) Research Leader and Manager
Fracture Mechanics Projects Office
BATTELLE
Columbus, Ohio U.S.A.

tion of the arrest of a rapidly propagating crack is the more correct. Now, while most workers in the field believe that the dynamic view of crack arrest is more basic, a pragramatic accommodation has been reached with the quasi-static point of view. Hence, this is no longer a critical issue. New issues have emerged to take the place of this controversy, however. These are calling into question basic concepts in dynamic fracture mechanics that were largely taken for granted earlier. A discussion of these with suggestions for possible remedies will form the focal point of this paper. The title chosen for this paper reflects the fact that basic questions about the subject do indeed exist and that further work--possibly in new directions--is called for.

DYNAMIC FRACTURE MECHANICS

Crack Propagation Theories

Until very recently the controversy concerning the proper treatment of the arrest of a rapidly propagating crack dominated work in the field of dynamic fracture mechanics. This controversy centered on whether a dynamic treatment (i.e., one incorporating inertial forces in the equation of motion for the cracked body, stress wave interactions with boundaries, and a crack motion dependent fracture toughness property) or a static post-arrest characterization is basically correct. In a dynamic approach, crack arrest occurs as the terminaton of crack propagation. If this is correct, it follows that, in principle, there can be no direct connection between crack arrest and the quasi-static condition that exists at some long time after arrest. Conversely, if the static condition that corresponds to conditions at the time of arrest (e.g., crack length, applied stresses) uniquely characterizes the arrest process, no consideration of the crack propagation process per se is needed.

Figure 1 shows schematically results obtained by Hahn, et al [2] at Battelle's Columbus Laboratories which revealed clearly the importance of a dynamic-based analysis, at least for the DCB test specimen. As indicated in the figure, crack propagation from an initially blunted crack tip under slowly inserted wedge loading proceeds at an ostensibly constant velocity. This fact, albeit unexpected, made possible a decisive comparison of various possible analysis approaches. The simplest of these possibilities supposes that the crack propagates under quasi-static conditions with a fracture toughness that is always equal to the initiation toughness,

K_{IC}.(ii) As shown in the lower part of Figure 1, for quasi-static conditions with $K_{ID} = K_{IC}$, a higher crack speed is predicted. Also, the crack jump length is considerably underestimated. Hence, this approach is clearly invalid.

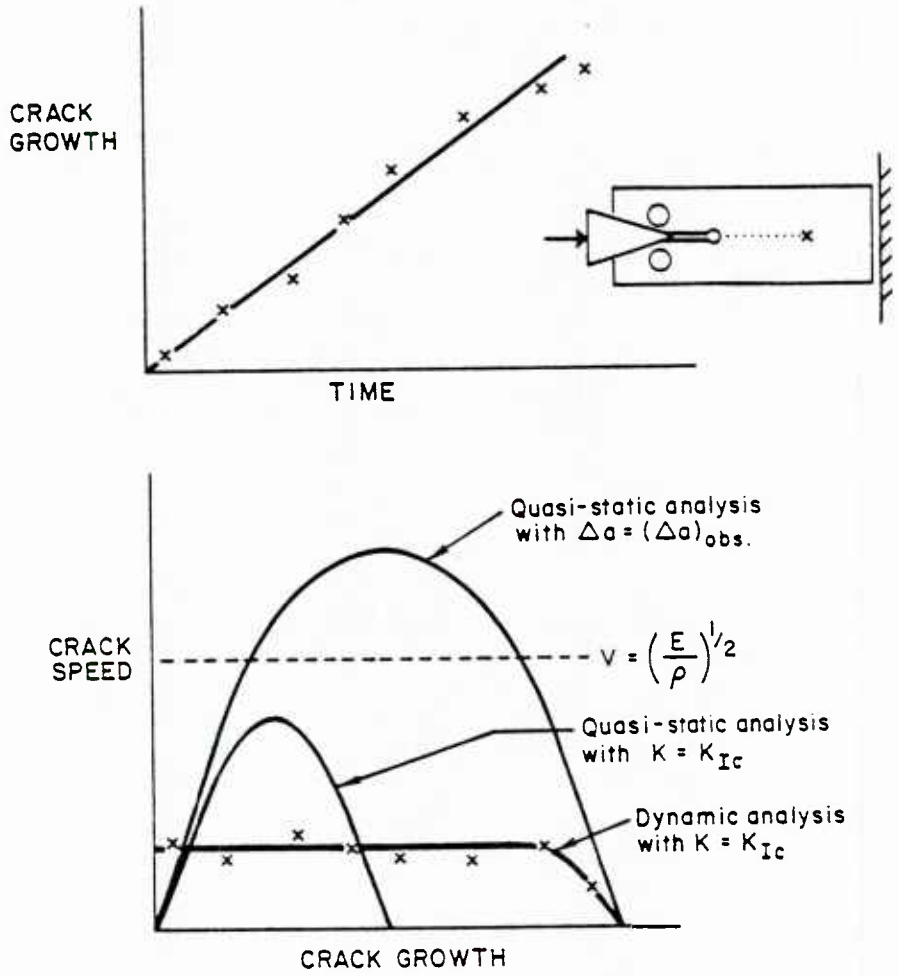

FIGURE 1. QUASI-STATIC VERSUS DYNAMIC ANALYSES OF RAPID CRACK PROPAGATION AND ARREST

(ii) Because of the blunted initial crack tip, the stress intensity factor at the onset of crack growth, K_Q, can be made arbitrarily greater than K_{IC} so that the crack speed and the crack jump length can be systematically varied. Note that with wedge loading the crack propagates into a diminishing stress field and, hence, the arrest of a fast moving crack within a DCB specimen is possible. Moreover, because these can be controlled by the bluntness of the initial crack the DCB specimen is ideally suited to an elucidation of crack arrest principles.

If instead a value of the fracture toughness of the running crack is selected in order to match the observed crack arrest point, much higher crack speeds are obtained. It usually happens that, as indicated in the figure, the predicted crack speeds can exceed the elastic wave speeds for the material. Clearly, therefore, the resolution of this difficulty does not lie in the choice of a fracture toughness property.

Results of the kind shown schematically in Figure 1 provided strong evidence that extended amounts of unstable crack propagation could not be characterized with a quasi-static computational approach. This fact led to the development of a simple dynamic analysis model to study crack propagation in the DCB specimen [3]. A typical result using this approach is also shown in Figure 1 where, to a quite good approximation, the experimental results were reproduced both qualitatively (i.e., a linear crack length-time record virtually from the onset of crack growth to just prior to arrest) and quantitatively.(iii)

The success of the dynamic analysis in predicting crack run/arrest events in DCB specimens exemplified in Figure 1, coupled with the unrealisticness of quasi-static analyses, led to questioning of the then widely accepted static post-arrest characterization of crack arrest. For example, Kanninen [5] performed a series of computations for different initiation conditions in the DCB specimen which showed that the static condition following arrest was a very definite function of the crack jump length in the test. This means that the post-arrest condition--conventionally characterized by the "arrest toughness" K_{Ia}--cannot be related to the material properties controlling the propagation event. Clearly, these two approaches are theoretically incompatible, and on the basis of the foregoing, it appears to be the dynamic approach that is the correct one.

Present Crack Arrest Assessments

Although the work of Hahn, et al [6] accumulated a substantial amount of evidence in support of the dynamic view of

(iii) The equations of the one-dimensional model for dynamic crack propagation in the DCB test specimen that were used for the early work in this area were subsequently modified as a result of a more rigorous derivation. This work, together with numerical verifications using a two-dimensional analysis model, can be found in the paper of Gehlen, et al [4]. The correction, it might be noted, is just that anticipated in footnote (vi) of reference [1].

crack propagation and arrest, wide spread acceptance of this view awaited more direct experimental evidence. This was eventually forthcoming in the work of Kalthoff, et al [7]. Their results were obtained using the shadow pattern (or method of caustics) technique which, coupled with flash photography, enables a direct measurement of the stress intensity factor of a fast running crack to be made. If, as assumed in the dynamic point of view, crack propagation occurs only when

$$K_I = K_{ID}(V) \qquad (1)$$

then experimental results such as those of Kalthoff, et al can be used to determine directly the material property K_{ID} as a function of crack speed V. Figure 2 shows their results for DCB specimens using four different K_Q values.

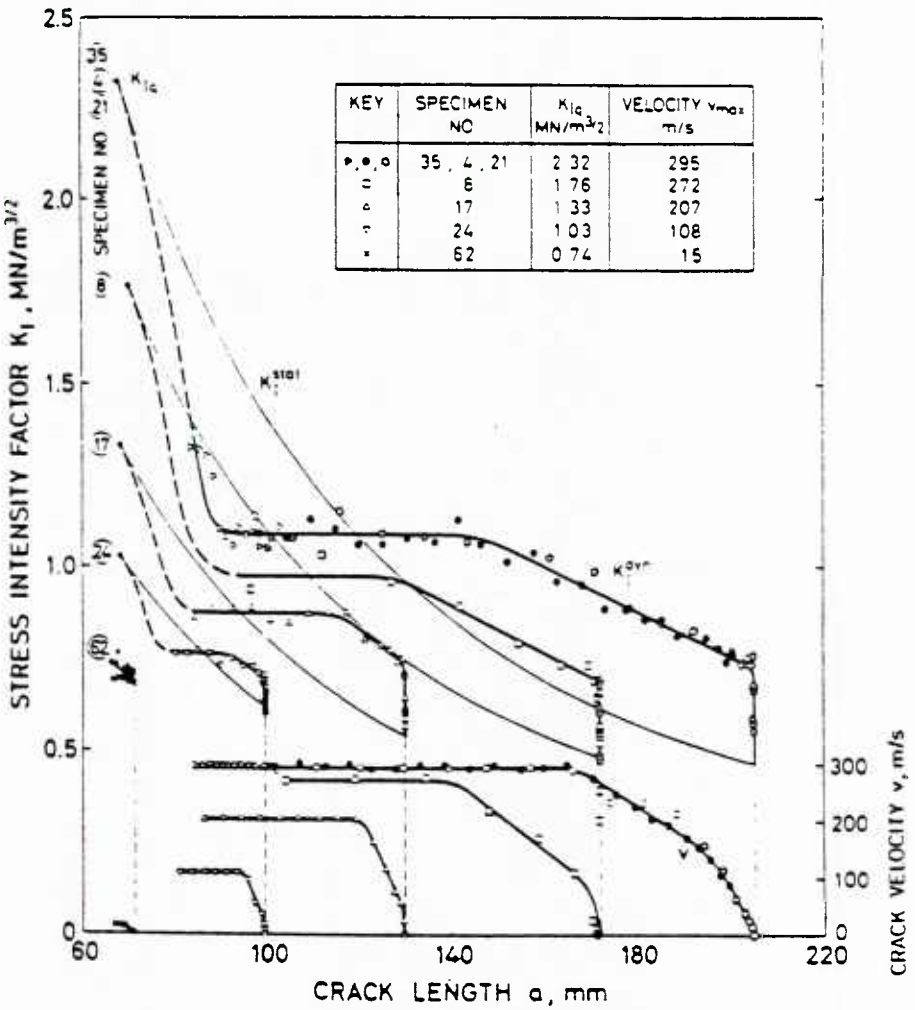

FIGURE 2. STRESS INTENSITY FACTORS FOR CRACK PROPAGATION IN A DCB TEST SPECIMEN FOR VARIOUS DIFFERENT K_Q VALUES - RESULTS OF KALTHOFF, et al [7]

The most important result shown by Figure 2 is that, while the dynamic value of the stress intensity factor at arrest is very nearly the same for all four experiments, the statically computed post-arrest value varies systematically with the crack jump length. This is completely consistent with the dynamic point of view and, of course, at odds with the static arrest characterization. However, it is now generally realized that the DCB specimen is perhaps the most dynamic of all possible structural configurations. Figure 3 illustrates this by comparing a finite difference solution taking into account the finite dimensions of the specimen with Freund's dynamic solution for an infinite medium.(iv)

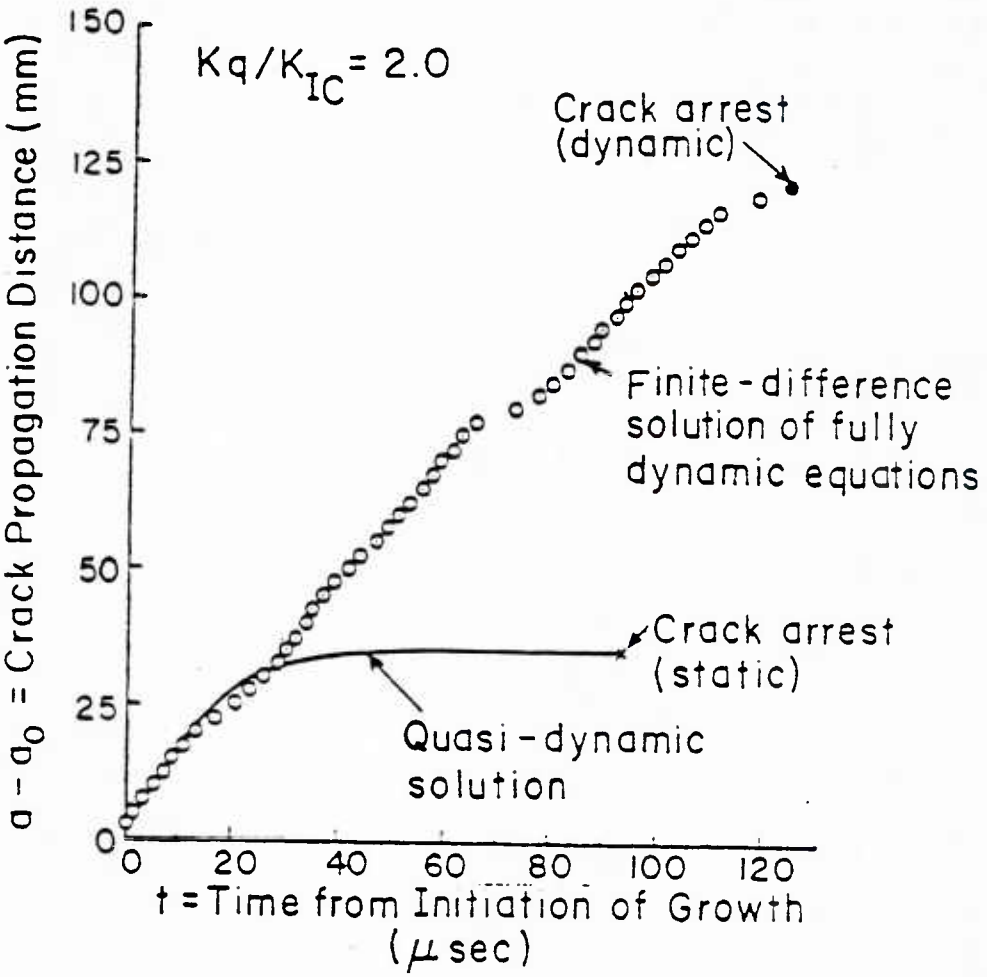

FIGURE 3. COMPARISON OF CALCULATED CRACK LENGTH VERSUS TIME IN A DCB TEST SPECIMEN WITH A DYNAMIC SOLUTION FOR AN INFINITE MEDIUM

(iv) The latter solution was obtained with Equation(11) in reference [1].

The result shown in Figure 3 reveals that the kinetic energy that is reflected back to the crack tip (and is therefore available for use in providing the material's resistance to crack growth) plays a crucial role in crack propagation in a DCB test specimen. That is, the time required for an elastic stress wave to travel from the crack tip to the specimen boundary and return is 26 μsec. It can be seen in Figure 3 that this is just where the infinite medium solution departs and, in fact, predicts arrest. Figure 4 which shows the partitioning of the initial strain energy contained in the specimen during the run-arrest event, further bears this out. It can be seen that the kinetic energy rises to a maximum at about the statically predicted arrest point (i.e., $a - a_o$ = 35 mm). The subsequent decrease indicates the kinetic energy

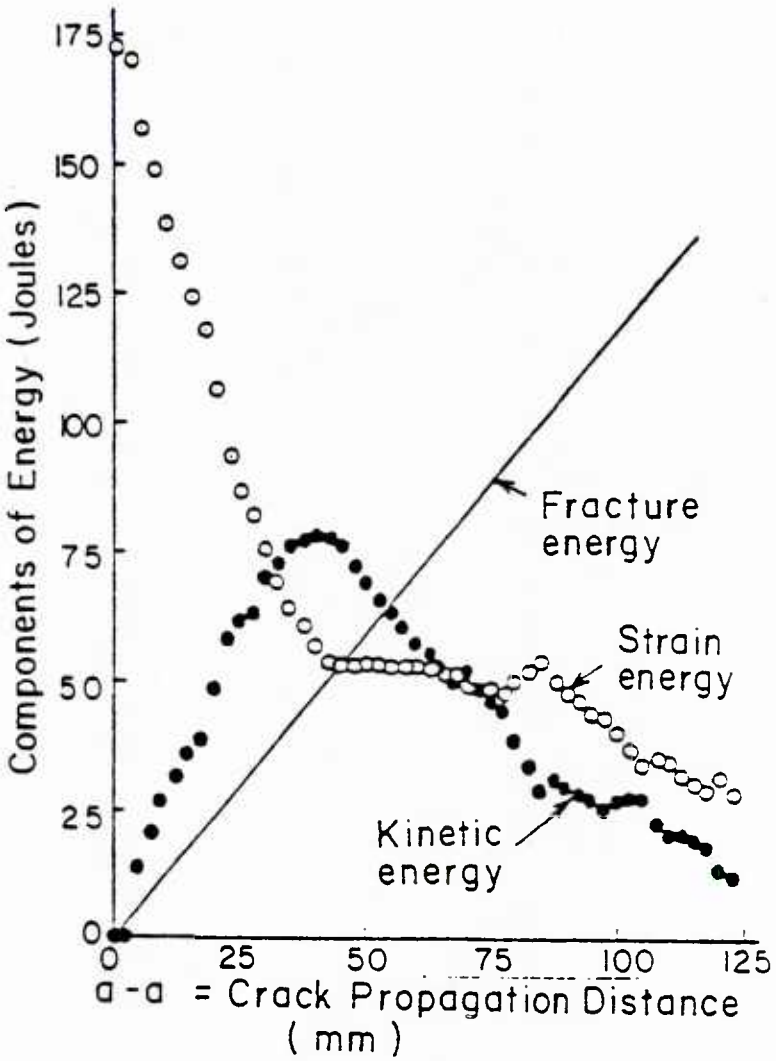

FIGURE 4. DISTRIBUTION OF ENERGY DURING CRACK PROPAGATION IN A DCB TEST SPECIMEN

reflected from the specimen boundaries is being utilized to continue the crack propagation event. Figure 5 shows a result obtained by Kobayashi, et al [8] which indicates that similar behavior occurs in a compact tension specimen.

The accommodation with regard to a static post-arrest characterization mentioned above has been on a pragmatic basis. As examples, Crosley and Ripling [9] and Witt [10] recognize that, because dynamic effects exist in crack arrest, the

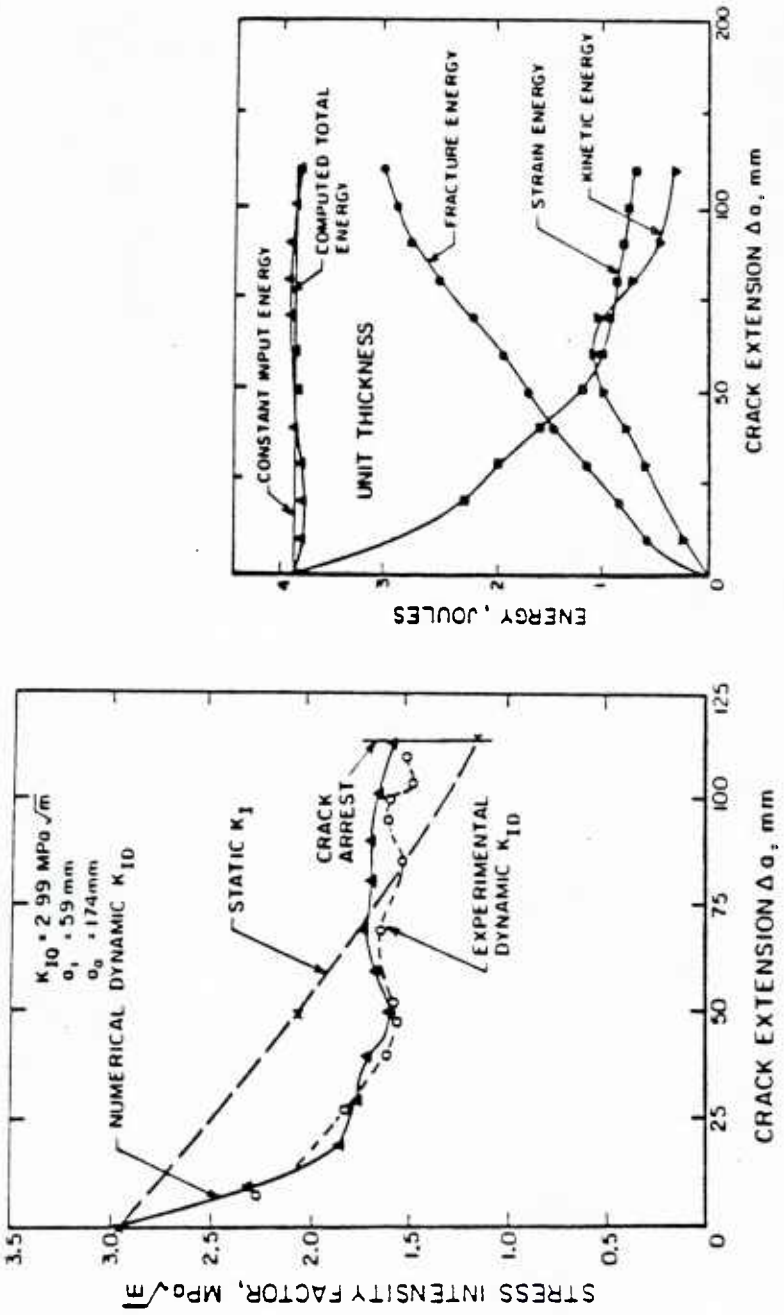

FIGURE 5. COMPARISON OF CALCULATED AND MEASURED RESULTS FOR DYNAMIC CRACK PROPAGATION IN POLYCARBONATE MODIFIED COMPACT TENSION SPECIMENS Results of Kobayashi, et al [8]

quasi-static approach is an over-simplification. Nevertheless, as they assert, reasonably constant statically determined arrest values can be determined experimentally that will suffice for practical purposes if the crack jump length that is allowed is kept small. Moreover, in actual structures,the return of kinetic energy to the crack tip is likely to be small so that the static approach will not be unreasonable.

This same point of view was adopted by Marston, et al [11] in applying a quasi-static approach to assess crack propagation and arrest in a nuclear pressure vessel subjected to thermal stresses in a hypothetical loss-of-coolant accident (LOCA). They concluded that, while dynamic analyses may in general be necessary for crack arrest problems, because of the geometry of the vessel and the anticipated short jump length, a quasi-static analysis should suffice. This assumption is corroborated by the dynamic analysis of the short-jump LOCA event reported by Cheverton, et al. [12] But, as Cheverton, et al also point out, for a hypothetical long crack jump, a dynamic analysis predicts a much deeper penetration than would a quasi-static analysis.

To summarize, while the dynamic approach to crack arrest is clearly the basically correct one, it is also clear that the not inconsiderable computational and experimental complexity required for a fundamentally correct analysis is not always necessary for practical applications. Indeed, for small crack jump lengths, a dynamic fracture mechanics treatment will be indistinguishable from a simpler quasi-static analysis. But, when the two approaches differ, it must be that the dynamic approach is more nearly correct. And, because it generally predicts that the crack will propagate faster and further than will a static analysis, it may be dangerous to assume a priori that quasi-static conditions prevail in any given circumstance.

Adequacy of Elastodynamic Fracture Mechanics

As described in the foregoing, dynamic fracture mechanics has advanced and, in doing so, new critical issues have emerged to replace the crack arrest controversy. Of more prominence is the growing realization that the applicability of even the most rigorous analysis procedures that have been developed may be much more limited than was previously realized. That is, virtually all mathematical solutions and interpretations of experimental results are now made in terms of linear elastic fracture mechanics (LEFM) treatments. However, most work is done on either ductile tough materials like the nuclear pressure vessel steel A533B or on viscoelastic polymeric materials like Homolite 100. While these materials do not satisfy the basic assumptions of LEFM, for lack of an alternative, elastodynamic analyses have been used. Hahn, et al [13] present a crack arrest data base from crack

propagation and arrest measurements on various pressure vessel steels. Similar data are given by Francois [14].

A tacit assumption in the collection of a crack arrest data base is that the elastodynamically inferred property $K_{ID} = K_{ID}(V)$ is a material property. As such, it clearly must be independent of the crack/structure geometry and of the manner in which the load is applied. At least two pieces of evidence exist, however, which casts some doubt on this assumption. The first is exemplified by the results of Kalthoff [15] shown in Figure 6. In these experiments cracks were propagated in both rectangular DCB specimens (RDCB) and single edge notch specimens (SEN). It can be seen that the values determined by the method of caustics (see above) were found to be distinctly different in the specimens.

To determine if batch-to-batch material property variations were influencing their results, Kalthoff also used a tee-shaped specimen (RDCB/SEN). In this specimen cracks propagate for a time in each a DCB-like geometry and, later, in a SEN-like geometry (see Figure 6). He found that the results from each portion of the event correlated quite well with the simple specimen results of the corresponding geometry. Hence, material property variations are not important and, he concludes, there is a definite geometry effect.

Other investigators have also reported results which indicate that the K_{ID} property exhibits some geometry dependence; see, for example, Kobayashi, et al [8]. Dahlberg, et al [16] have argued that geometry-dependence and even a dependence on higher order time derivatives must be accepted to avoid the necessity for nonlinear dynamic analyses. They point out that, even if K-dominance (see below) of the inelastic region around the crack tip exists, a dependence of the dynamic fracture toughness on the second and higher order derivatives of the crack length cannot be excluded by any theoretical argument.

While the geometry dependence exhibited in Figure 6 is certainly significant from a conceptual point of view, the practical limitation imposed by these results is probably not debilitating. It can be argued that, in view of the many other uncertainties that are present in any structural analysis problem, this relatively small difference is not significant. One would simply take a lower bound of such results and thereby impose only a modest penalty on the structure.

Of possibility greater significance, therefore, are the results obtained by Kanninen, et al [17] in a study of dynamic crack propagation initiated by impact loading. Specifically, they used AISI 4340 steel three point bend specimens which were instrumented to measure crack length versus time. First,

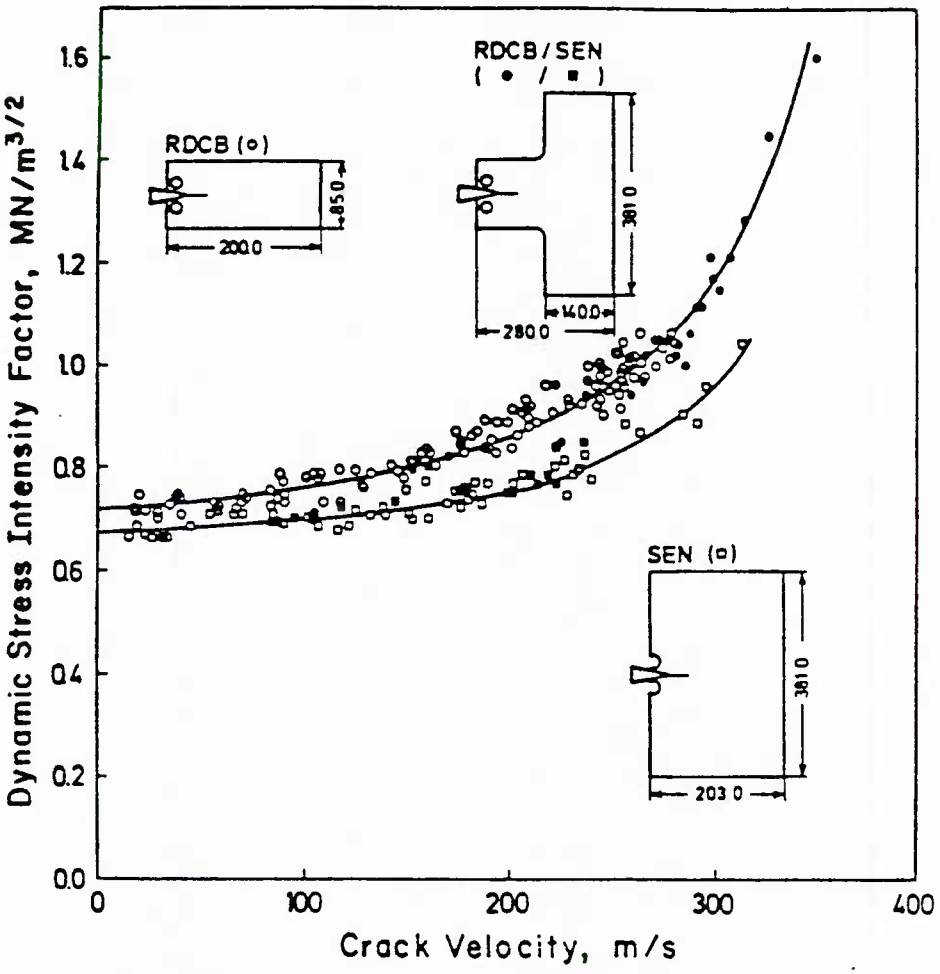

FIGURE 6. DYNAMIC FRACTURE TOUGHNESS VALUES IN ARALDITE B AS DETERMINED BY THE METHOD OF CAUSTICS
Results of Kalthoff [15]

to assess any possible material property variations and to determine the effect of geometry-dependence of the fracture toughness property determined in an earlier program using the DCB test specimen, dynamic crack propagation was initiated under quasi-static loading. A comparison between the experimental results and those predicted with an elastodynamic finite difference calculation using this property is shown in Figure 7. It can be seen that the agreement is excellent.

Because of the agreement shown in Figure 7 and the belief that the material used very well satisfies the basic requirements of a linear elastic fracture theory, it might be logical to expect that the same K_{ID} value would also apply in impact loading. However, as shown in Figure 8, the calculation seriously underestimates the material's resistance to fast

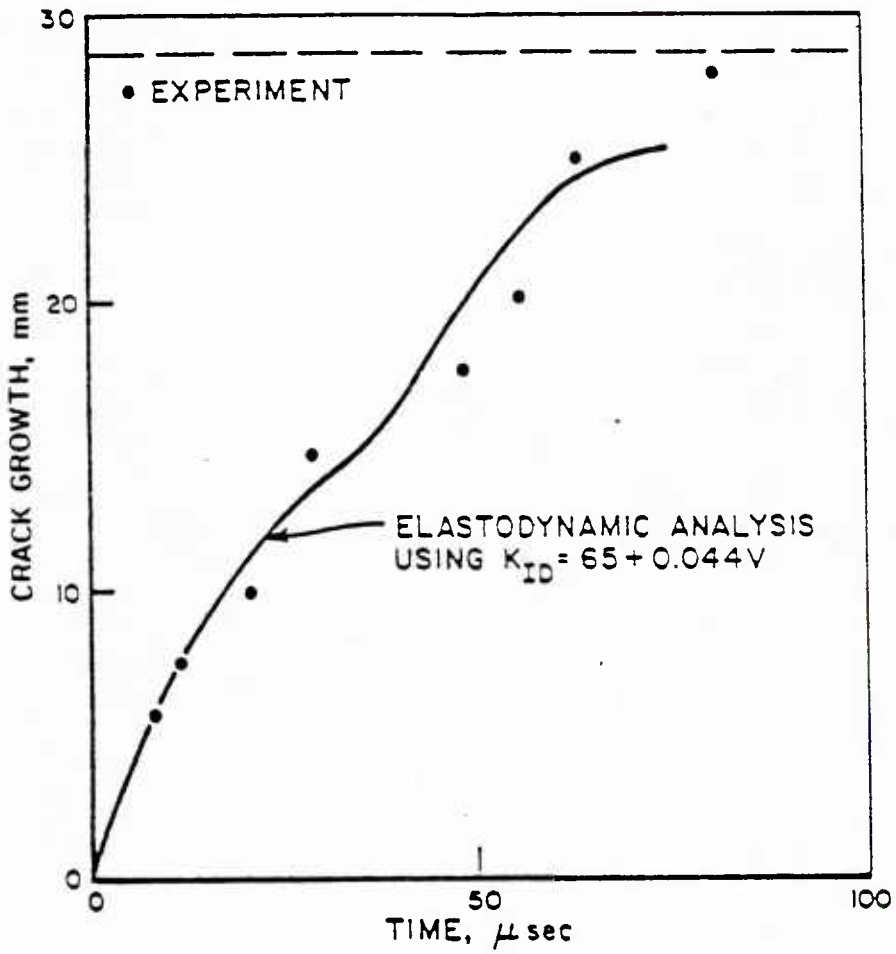

FIGURE 7. COMPARISON OF MEASURED AND CALCULATED CRACK GROWTH VERSUS TIME IN A QUASI-STATICALLY LOADED THREE-POINT BEND SPECIMEN

fracture.(v) A prediction much more in agreement with the experimental results was obtained by back calculating a toughness value from the experimentally determined throw energy (i.e., by deducting the kinetic and strain energy in the

(v) In contrast to the quasi-static loading results shown in Figure 7, where zero time corresponds to the initiation of crack growth, zero time in Figure 8 is the time that the striker contacts the specimen. Clearly, in an impact event, a time lapse is required for the crack tip stress intensity to build up to a critical value.

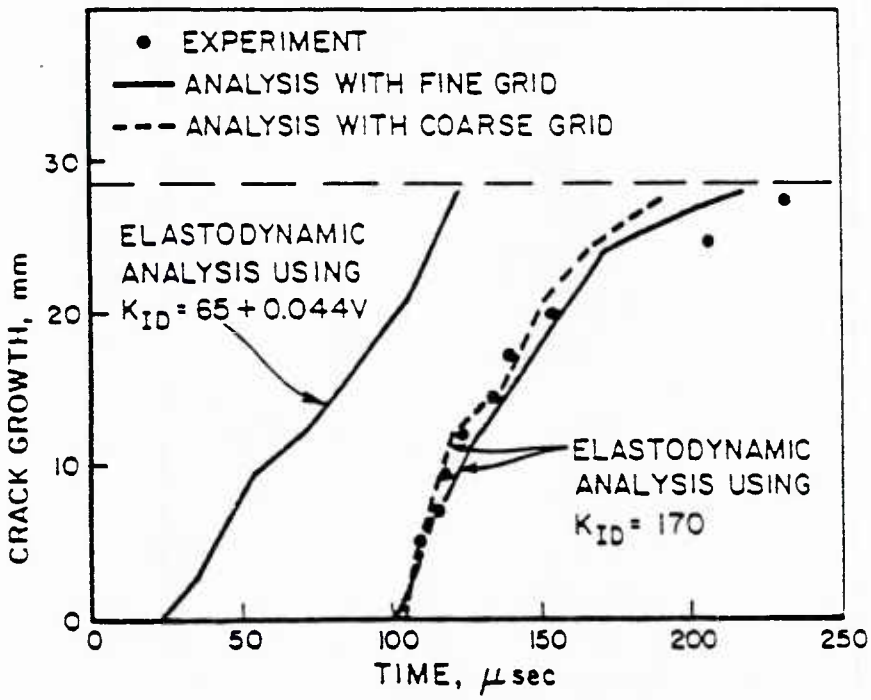

FIGURE 8. COMPARISON OF MEASURED AND CALCULATED CRACK GROWTH VERSUS TIME IN AN IMPACT LOADED THREE-BEND SPECIMEN

broken specimen from the energy supplied by the striker). This gave a value of $K_{ID} = 170$ MNm$^{-3/2}$, a value roughly double that of the quasi-statistically initiated event. Figure 8 shows that excellent agreement is obtained using this value.

There were several artifacts involved in the impact testing that could possibly cause this anomolous result. As described in reference [17], however, none were found to be significant. In addition, as shown in Figure 8, two different finite difference mesh sizes were used without appreciably altering the result. It was therefore concluded that the difference exhibited between quasi-statically initiated and dynamically-initiated rapid crack propagation does seem to proceed with a markedly different toughness property.(vi)

(vi) It can be seen from the results shown in Figure 7 and 8 that the crack speeds in the two events were similar. Regardless, AISI 4340 steel is not greatly rate-dependent. Thus, there is no simple explanation for the quite different toughness values that seem to be required as a speed-dependence.

The disparity exhibited by the impact testing results, when coupled with the geometry-dependence assessments made by Kalthoff and others, appears to cast serious doubt on the general applicability of linear elasticity-based crack propagation/arrest procedures. At the same time it should be recognized that, in any use of experimental observations to assess the basis of mathematical analysis procedures, no direct measurement of the stress intensity factor is possible. While observations of fringe and shadow patterns associated with a propagating crack can be made, the relation of these measurements to fracture mechanics parameters always requires the use of some mathematical model. And, any such model must be based upon a constitutive relation and other presumptions about the interaction between the propagating crack and the component that contains it.

To assess the possible effects of polymeric materials, Popelar and Kanninen [18] have devised a dynamic visoelastic representation for polymer DCB test specimens. Their results indicated that differences do exist but they can be accounted for by using the correct choice of the modulus--the static or long-term viscoelastic modulus, at least for cracks initiated under quasi-static conditions. However, they were unable to substantiate the finding of Fourney [19] that a substantial portion of the initial strain energy is lost by viscous damping prior to crack arrest in the photoelastic polymer Homolite 100. It is entirely possible that a more appropriate viscoelastic model is needed (Popelar and Kanninen used a three-parameter solid representation) before this can be done.

PLASTIC FRACTURE MECHANICS

Crack Tip Fracture Criteria

While the initial work in fracture mechanics was based upon an energy balance criterion, later work identified more esoteric fracture parameters--principally, the stress intensity factor, the crack opening displacement, and the J-integral parameter. In LEFM, these are all interrelated. Specifically, for plane strain conditions in the "opening" mode

$$G = J = \frac{1-\nu^2}{E} K^2 = Y \cdot \delta \qquad (2)$$

where G is the strain energy release rate, J is the value of the J-integral, K is the stress intensity factor, and δ is the crack tip crack opening displacement while E, ν, and Y are, as usual, the elastic modulus, Poisson's ratio, and yield stress, respectively.

Which of the four basic parameters involved in LEFM is the "most basic" may be thought to be a purely academic question. However, it assumes considerably more importance when it becomes necessary to select a crack tip fracture parameter as

the basis of a plastic fracture methodology capable of treating stable crack growth accompanied by extensive crack tip plasticity. Many different choices have been made, all having their origins in one of the LEFM parameters. But, because a set of equalities like (2) for conditions more general than LEFM does not exist, it is important to determine which criterion is on the firmest footing. This, in turn, suggests a more careful study of LEFM.

The modern view of LEFM is contained in Figure 9. It can be shown that, if the body everywhere obeys a linear elastic stress-strain law (see insert in Figure 9), then the stresses at the crack tip can be expressed in terms of a polar coordinate (r,θ) system with origin at the crack tip as

$$\sigma_{ij} = \frac{K}{\sqrt{2\pi r}} F_{ij}(\theta) + ... \qquad (3)$$

where the omitted terms are of higher order in r. For small values of r (i.e., very near the crack tip), only the first term is significant. Then, the remote stresses, the crack length, and the external dimensions of the cracked body will affect the stresses at the crack tip only through the parameter K, the stress intensity factor. More definitely, there will be a region--the "K-dominant" region--having the characteristic dimension D in which the first term of the series is a sufficiently good approximation.

To continue this argument, let R denote the size of the inelastic region surrounding the crack tip where the assumption of linear elastic behavior is invalid. It is in this region that the fracture event takes place. While it is not possible to directly characterize the fracture process using a linear elastic formulation, this is not necessary provided the inelastic region is contained in the K-dominant region. That is, if $R<D$, then any event occurring within the inelastic region is controlled by the deformation in the surrounding K-dominant region. Consequently, if crack growth occurs, it must do so at a critical value of the stress intensity factor.

The importance of this result is not for its own sake but rather for the generalization that is suggested for elastic-plastic conditions. In particular, using a power law hardening solution, an analogous argument to that given above can be followed. As illustrated in Figure 10, the crack tip stresses in this situation can be expressed as

$$\sigma_{ij} = J^{\frac{1}{n+1}} r^{\frac{1}{n+1}} F_{ij}(\theta,n) + ... \qquad (4)$$

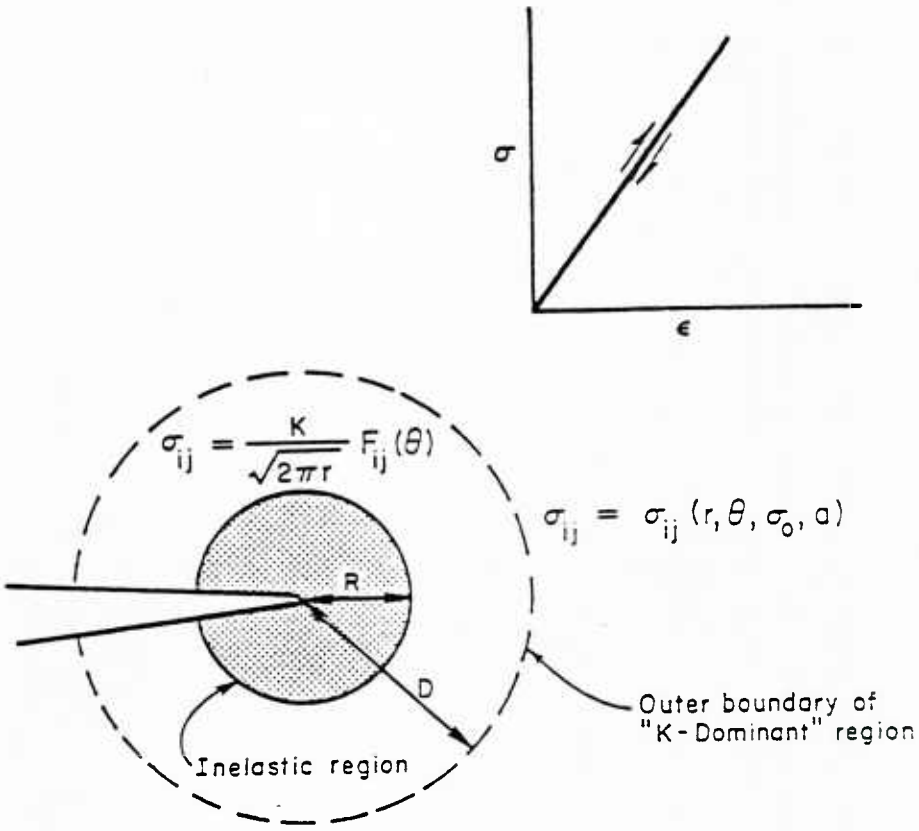

FIGURE 9. BASIS OF LINEAR ELASTIC FRACTURE MECHANICS

where n is a property of the material's stress-strain curve. Now, the effect of the remote stresses, the crack length, and the external dimensions of the body on the stresses within a "J-dominant" region depend only on the parameter J. If this region surrounds the inelastic region, then the conditions governing the fracture event must correspond to a critical value of J. The crack growth criterion can therefore be expressed as

$$J(a,\sigma_o) = J_c \qquad (5)$$

where a denotes the crack length and σ_o the applied stresses.

Notice that, in contrast to the LEFM argument, the inelastic region is not the plastic region here. It is instead the much smaller region in which the deformation plasticity approach (see insert in Figure 10) is invalid. That is, the region in which the hole growth and coalescence processes involved in ductile crack extension are occurring--processes that clearly cannot be taken into account directly in a continuum mechanics approach. However, where J-dominance exists,

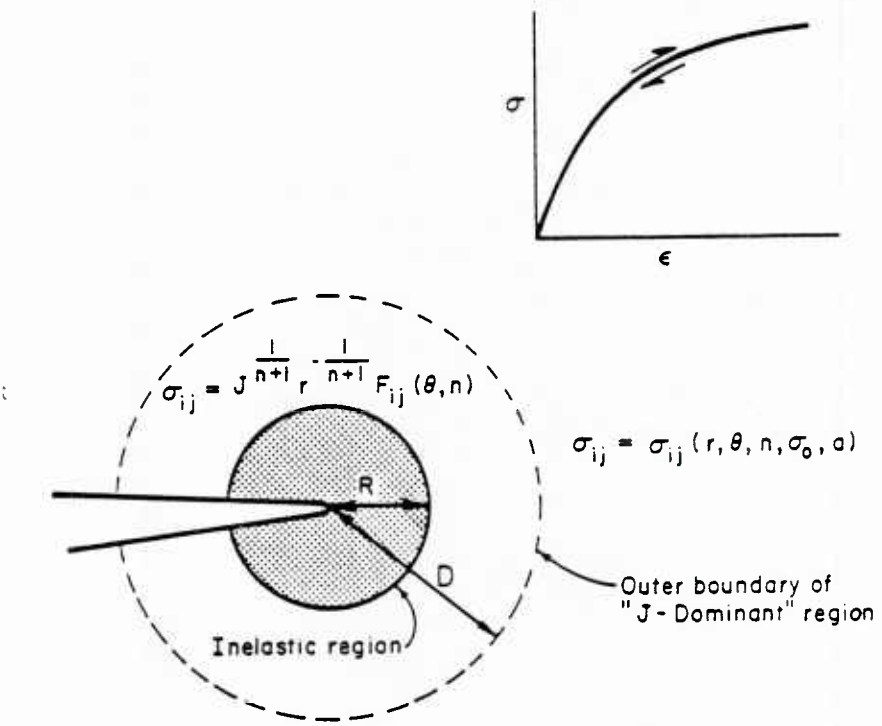

FIGURE 10. BASIS FOR THE USE OF THE J-INTEGRAL IN PLASTIC FRACTURE MECHANICS

the initiation and growth of a crack can be expected to be governed by a material property--the J-resistance curve--which gives critical J values as a function of crack growth.

For a growing crack, elastic unloading takes place in the "wake" plastic region left behind the crack tip. This is also an inelastic process that cannot be addressed within the deformation plasticity-based approach just described. Consequently, it is to be expected that the size of the inelastic region becomes larger and inexorably overtakes the limits of the J-dominant region. At this point the J parameter also becomes invalid. Precise delineations of the amount of crack growth possible before the loss of J-dominance occurs do not now exist. This will depend upon the dimensions of the body and the rate of change of the J-resistance curve. For example, as suggested by Hutchinson and Paris [20], J-dominance will exist provided

$$\omega \equiv \frac{b-a}{J}\frac{dJ}{da} >> 1 \qquad (6)$$

where a denotes the crack length and b is the dimension of the body nearest the crack tip.

Status of Plastic Fracture Mechanics

The key to developing an analysis procedure for plastic fracture is to identify an appropriate crack tip fracture criterion. Work performed by Kanninen, et al [21] has encompassed three main stages. First, center cracked panels were tested to obtain data on crack growth initiation and stable growth. Second, "generation-phase" analyses were performed in which the experimentally observed applied stress/stable crack growth behavior was reproduced in a finite element model with each of a number of candidate crack initiation and stable growth criteria being evaluated for the material tested. In the third stage, "application-phase" finite element analyses were performed using one of the candidate criteria to determine applied stress/crack growth behavior for a given specimen geometry.

The fracture criteria examined included the J integral, the local and average crack opening angles, the conventional LEFM R curve, and various generalized energy release rates. Each of the candidate criteria is attractive in one way or another. Hence, the task of selecting the best criterion for application to nuclear steels is not an easy one. Clearly, geometry independence is a crucial test of the acceptability of a plastic fracture criterion. Physical relevance is another. Practicality is a third. With these as primary qualifications, some assessments can be drawn from progress made so far.

The advantages of the J integral are its virtual independence of finite element type and element size, the computational ease involved in evaluating it, and, because of its history-independence, its catalogability. However, while the J integral is widely acceptable as a criterion for crack growth initiation, as already noted, it is valid only for a limited amount of stable crack growth. A J integral-based approach is unable to cope with large amounts of stable crack growth attended by large-scale plasticity because it is based upon deformation plasticity. Deformation plasticity (nonlinear elasticity) requires small plastic strains and precludes material unloading. This manifests itself in pronounced specimen dependence after a small amount (e.g., 10% of the remaining ligament size) of stable growth.

The crack opening angle is appealing because of its rapidly grasped physical significance and the opportunity that it offers for direct measurement. However, it should be recognized that there are two different definitions of the crack opening angle: a crack tip value that reflects the actual slope of the crack faces (CTOA), and an average value based on the original crack position (COA). While the critical value of the COA can be measured, it is difficult to see how its value has any direct connection with the fracture process.

Conversely, while the critical value of the CTOA can likely be associated with the fracture process, it presents a formidable measurement task. In addition, there are clearly some difficulties in making either value apply to mixed character shear/flat crack growth.

A proper stable crack growth criterion must differentiate between the energy dissipated in direct fracture-related processes near the crack tip and energy dissipated in geometry-dependent plastic deformation remote from the crack tip. With this in mind, a number of investigators have opted for a generalization of the LEFM energy release rate as the basic plastic fracture methodology. But, there is a basic difficulty inherent in this approach. There is a theoretical basis for expecting a computational step size dependence in an energy release rate parameter that is based on the work of separating the crack faces. It can be argued that this can be handled by appealing to micromechanical considerations. Regardless, it appears that the necessity to arbitrarily circumvent the inherent step size difficulty with any energy release rate parameter makes its use somewhat unattractive.

Dynamic Plastic Crack Propagation

Work in dynamic elastic-plastic crack propagation has been performed by Achenbach, et al [22,23]. The material model used in the work was based on Prandtl-Reuss incremental plasticity and a bi-linear stress-strain relation with irreversible material unloading behind the crack tip. Results have been obtained for crack propagation in plane stress, plane strain and in anti-plane strain conditions. These results show that the order of the crack tip singularity and the position of the plastic unloading interface, while highly dependent on the slope of the stress-strain curve in the plastic regime, are only moderately dependent on the crack speed. Results for plane stress conditions are shown in Figure 11, where $\alpha = E_t/E$.

These findings are important primarily in that they demonstrate that a fundamentally correct elastic-plastic dynamic formulation of a propagating crack can be achieved for use in a finite element program. In addition, because for specified material stress-strain behavior, the crack tip characterizing parameters will be essentially unaffected by modest changes in the crack speed, this work shows that it will be possible to devise an efficient computational model.

Further work will be needed to identify a plastic fracture criterion for dynamic crack propagation. This parameter must be one whose critical values are geometry-independent material property values over a wide range of geometries and crack growth lengths. A strong possibility that has been identified during the course of experiments and

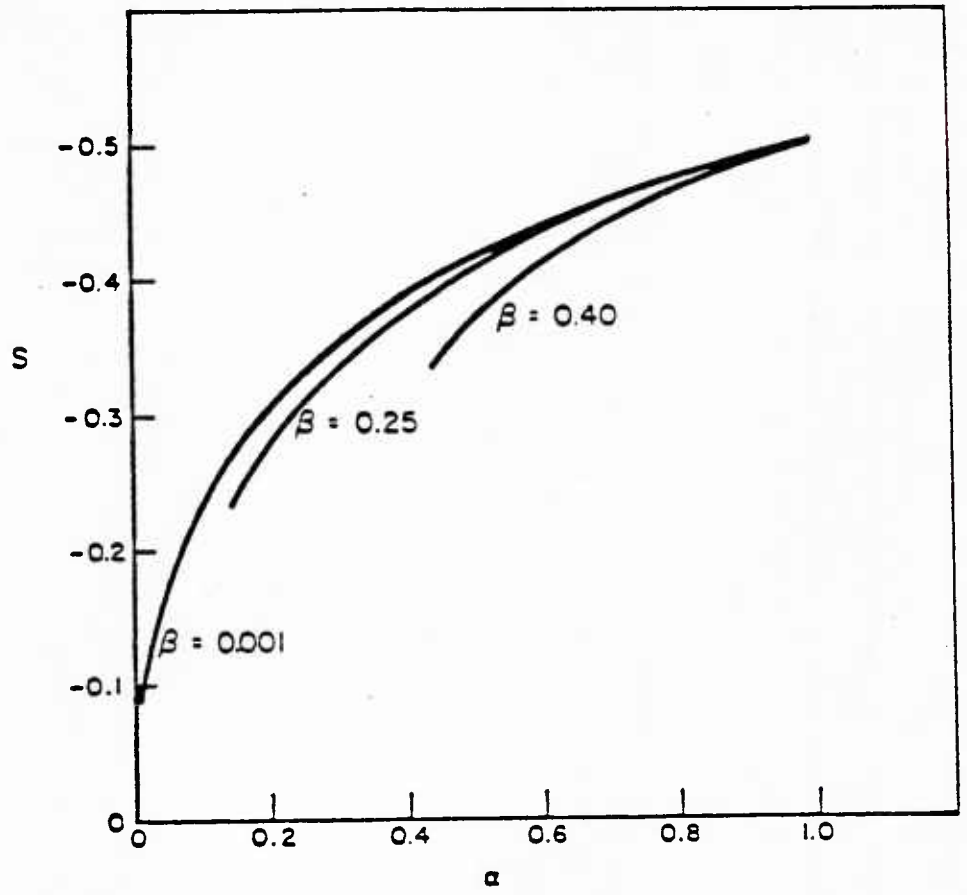

FIGURE 11. ORDER OF THE CRACK TIP SINGULARITY IN PLANE STRESS DYNAMIC CRACK PROPAGATION

generation-phase analyses on compact tension specimens and center-cracked tension panels is the crack tip crack opening angle (CTOA). Kobayashi, et al [8] have shown how effectively this parameter can be used in their analysis of circumferential crack propagation in a pipe.

DISCUSSION

Most potential fracture problems involve cracks emanating from flaws in or near a weld where it is difficult to apply a fracture mechanics assessment for several reasons. First, residual stresses probably exist of unknown magnitude. Second, the toughness of the material in the heat affected zone is uncertain. Third, welding processes generally cause plastic deformation which invalidates the currently available linear elastic fracture mechanics capabilities. These difficulties suggest the use of a crack arrest strategy whereby, even if unstable crack propagation occurs, it will be arrested in the base material. This is the rationale for the dynamic fracture mechanics analysis discussed here.

The schism between the dynamic and the quasi-static characterizations of crack arrest is no longer a critical issue. It is generally agreed that there are conditions where a quasi-static interpretation of a laboratory test result can give an appropriate measure of the arrest toughness property and, under certain types of loading and crack-structure geometries, dynamic effects in crack arrest will indeed be negligible. Specifically, when inertia forces, stress wave reflections, and rate-dependent fracture processes are negligible, then the two approaches will give exactly the same prediction. There appears to be a fairly wide range of conditions in which, because the predictions are not greatly different, for practical purposes, the extra effort required to obtain a dynamic solution is unwarranted. However, where the two predictions are significantly different, it is the dynamic solution which is the more accurate.

It is important to recognize that a quasi-static calculation will generally underestimate the true crack driving force. Consequently, in extracting an arrest toughness value from an experiment, a value that is lower than the actual material property will be obtained. This will be conservative. Applying a quasi-static analysis using a given toughness value to assess the possiblity of crack arrest, on the other hand, will over-estimate the likelihood of crack arrest. While these two errors do tend to offset each other, it would always be prudent in addressing new situations to check the possibility that dynamic effects could be important.

The basic assumption in elastodynamic analyses of crack propagation has been that the dynamic fracture toughness is a unique geometry-independent material property that can, at most, depend upon crack speed, temperature, and plate thickness. However, results presented by several investigators are beginning to seriously question the legitimacy of this assumption. Some investigations indicate that the external dimensions of the component can affect values inferred for the toughness property. Others suggest that unstable crack propagation emanating from impact loading occurs with a toughness which differs markedly from that corresponding to conventional quasi-static loading. Whether or not residual plasticity or other nonlinear effects could play a key role in mollifying this seeming lack of uniqueness cannot presently be determined.

CONCLUSIONS

1. Crack propagation accompanied by significant plastic deformation cannot be rigorously treated at present--only elastodynamic solutions can now be applied. However, these appear to give reasonable predictions even for tough ductile materials (e.g., nuclear vessels, gas pipelines), under certain conditions.

2. Quasi-static predictions of crack arrest can be valid in some circumstances--e.g., when crack jump length is small in comparison to component dimensions--but will give an underestimate when dynamic effects are significant.

3. Controversy now exists on the validity of $K_{ID} = K_{ID}(V)$ as a unique material property. Some geometry dependence has been cited. Also, comparisons of slow versus impact loading have revealed unexplainable differences.

ACKNOWLEDGEMENT

This paper was written in conjunction with a research program on unstable crack propagation in elastic-plastic materials supported by the Office of Naval Research under contract number N00014-77-C-0576. The author would like to thank Dr. Nicholas Perrone, Director of Structural Mechanics Research at ONR for his encouragement of this work. The portion of the paper on plastic fracture mechanics was based in part on research performed at Battelle with support from the Electric Power Research Institute, Palo Alto, California, under RP 601-1, Dr. T. U. Marston, Program Manager.

REFERENCES

[1] KANNINEN, M.F. - A Critical Appraisal of Solution Techniques in Dynamic Fracture Mechanics, Numerical Methods in Fracture Mechanics, Ed. A. Luxmoore and R. Owen, U. Swansea Press, pp. 612-633, 1978.

[2] HAHN, G.T., HOAGLAND, R.G., KANNINEN, M.F. and ROSENFIELD, A.R. - A Preliminary Study of Fast Fracture and Arrest in the DCB Test Specimen, Dynamic Crack Propatation, G. C. Sih, editor, Noordhoff, Leyden, pp. 649-662, 1973.

[3] KANNINEN, M.F. - A Dynamic Analysis of Unstable Crack Propagation and Arrest in the DCB Test Specimen, Int. J. Fracture, Vol. 10, pp. 415-430, 1974.

[4] GEHLEN, P.C., POPELAR, C.H. AND KANNINEN, M.F. - Modeling of Dynamic Crack Propagation: I. Validation of One-Dimensional Analysis, International Journal of Fracture, Vol. 15, pp. 281-294, 1979.

[5] KANNINEN, M.F. - An Analysis of Dynamic Crack Propagation and Arrest for a Material Having a Crack Speed Dependent Fracture Toughness, Prospects of Fracture Mechanics, Ed. G.C. Sih, et al, Noordhoff International Publishing, Leyden, The Netherlands, pp. 251-266, 1974.

[6] HAHN, G.T., et al - Critical Experiments, Measurements and Analyses to Establish a Crack-Arrest Methodology for Nuclear Pressure Vessel Steels, Battelle's Columbus Laboratories Reports to the U.S. Nuclear Regulatory Commission, 1974-1979.

[7] KALTHOFF, J.F., BEINART, J. and WINKLER, S. - Measurements of Dynamic Stress Intensity Factors for Fast Running and Arresting Cracks in Double-Cantilever-Beam Specimens, Fast Fracture and Crack Arrest, Ed. G. T. Hahn and M. F. Kanninen, ASTM STP 627, pp. 161-176, 1977.

[8] KOBAYASHI, A.S., SEO, K., JOU, J.Y., and URABE, Y. - A Dynamic Analysis of Modified Compact-Tension Specimens Using Homolite - 100 and Polycarbonate Plates, Experimental Mechanics, Vol. 20, pp. 73-79, 1980.

[9] CROSLEY, P.B. and RIPLING, E.J. - Comparison of Crack Arrest Methodologies, Crack Arrest Methodology and Applications, Ed. G. T. Hahn and M.F. Kanninen, ASTM STP 711, pp. 211-209, 1980.

[10] WITT, F.J. - Crack Arrest Methodology for Pressurized Water Nuclear Reactor Pressure Vessel Applications, Westinghouse Electric Corporation, Report No. WCAP - 9627, 1979.

[11] MARSTON, T.U., SMITH, E. and STAHLKOPF, K.E. - Crack Arrest in Water-Cooled Reactor Pressure Vessels During Loss-of-Coolant Accident Conditions, Crack Arrest Methodology and Applications, Ed. G. T. Hahn and M. F. Kanninen, ASTM STP 711, pp. 422-431, 1980.

[12] CHEVERTON, R.D., GEHLEN, P.C., HAHN, G.T. and ISKANDER, K. - Application of Crack Arrest Theory to a Thermal Shock Experiment, Crack Arrest Methodology and Applications, Ed. G. T. Hahn and M. F. Kanninen, ASTM STP 711, pp. 392-417, 1980.

[13] HAHN, G.T., ROSENFIELD, A.R., MARSCHALL, C.W., HOAGLAND, R.G., GEHLEN, P.C., KANNINEN, M.F. - Crack Arrest Concepts and Applications, Fracture Mechanics, Ed. N. Perrone, et al, University of Virginia Press, pp. 205-228, 1978.

[14] FRANCOIS, D. - Dynamic Crack Propagation and Arrest, Developments in Pressure Vessel Technology - Flaw Analysis, Ed. R. W. Nichols, Applied Science Pub, pp. 151-167, 1979.

[15] KALTHOFF, J.F. Institut fur Festkorpermechanik, private communication, 1980.

[16] DAHLBERG, L., NILSSON, F. and BRICKSTAD, B. - Influence of Specimen Geometry on Crack Propagation and Arrest Toughness, Crack Arrest Methodology and Applications, Ed. G. T. Hahn and M. F. Kanninen, ASTM STP 711, pp. 89-108,1980.

[17] KANNINEN, M.F., GEHLEN, P.C., BARNES, C.R., HOAGLAND, R.G., HAHN, G.T. and POPELAR, C.H. - Dynamic Crack Propagation Under Impact Loading, Nonlinear and Dynamic Fracture Mechanics, Ed. N. Perrone and S. Atluri, ASME AMD Vol. 35, pp. 185-200, 1979.

[18] POPELAR, C.H. and KANNINEN, M.F. - A Dynamic Viscoelastic Analysis of Crack Propagation and Crack Arrest in a Double Cantilever Beam Test Specimen, Crack Arrest Methodology and Applications, Ed. G. T. Hahn and M. F. Kanninen, ASTM STP 711, pp. 3-21, 1980.

[19] FOURNEY, W.L., University of Maryland, private communication, 1980.

[20] HUTCHINSON, J. and PARIS, P.C. - The Theory of Stability Analysis of J-Controlled Crack Growth, Elastic-Plastic Fracture, Ed. J. D. Landes, et al, ASTM 668, pp. 37-64, 1979.

[21] KANNINEN, M.F., RYBICKI, E.F., STONESIFER, R.B., BROEK, D., ROSENFIELD, A.R., MARSCHALL, C.W. and HAHN, G.T. - Elastic-Plastic Fracture Mechanics for Two-Dimensional Stable Crack Growth and Instability Problems, Elastic-Plastic Fracture, Ed. J. D. Landes, et al, ASTM STP 668, pp. 121-150, 1979.

[22] ACHENBACH, J.D. and KANNINEN, M.F. - Crack Tip Plasticity in Dynamic Fracture Mechanics, Fracture Mechanics, Ed. N. Perrone, et al, University of Virginia Press, pp. 649-670, 1978.

[23] ACHENBACH, J.D., KANNINEN, M.F. and POPELAR, C.H. - An Asymptotic Analysis of Dynamic Elastic-Plastic Crack Propagation, Journal of the Mechanics and Physics of Solids, in press, 1980.

CRACK-TIP FIELDS FOR FAST FRACTURE OF AN ELASTIC-PLASTIC MATERIAL

by

J. D. Achenbach
Department of Civil Engineering
Northwestern University
Evanstown, Illinois

M. F. Kanninen
Applied Solid Mechanics Section
Battelle
Columbus, Ohio

and

C. H. Popelar
Engineering Mechanics Department
The Ohio State University
Columbus, Ohio

December, 1979

Submitted for publication in the Journal
of the Mechanics and Physics of Solids

Unclassified

SECURITY CLASSIFICATION OF THIS PAGE *(When Data Entered)*

REPORT DOCUMENTATION PAGE		READ INSTRUCTIONS BEFORE COMPLETING FORM
1. REPORT NUMBER	2. GOVT ACCESSION NO.	3. RECIPIENT'S CATALOG NUMBER
4. TITLE *(and Subtitle)* CRACK-TIP FIELDS FOR FAST FRACTURE OF AN ELASTIC-PLASTIC MATERIAL		5. TYPE OF REPORT & PERIOD COVERED Interim 6. PERFORMING ORG. REPORT NUMBER
7. AUTHOR(s) J. D. Achenbach, M. F. Kanninen, and C. H. Popelar		8. CONTRACT OR GRANT NUMBER(s) N00014-76-C-0063(Northwestern) N00014-77-C-0576(Battelle)
9. PERFORMING ORGANIZATION NAME AND ADDRESS Northwestern University, Evanston, Ill, 60201 and Battelle, Columbus, Ohio 43201 and The Ohio State University, Columbus, Ohio 43201		10. PROGRAM ELEMENT, PROJECT, TASK AREA & WORK UNIT NUMBERS
11. CONTROLLING OFFICE NAME AND ADDRESS Office of Naval Research Structural Mechanics Program Dept. of the Navy, Arlington, VA 22217		12. REPORT DATE December, 1979 13. NUMBER OF PAGES 33
14. MONITORING AGENCY NAME & ADDRESS*(if different from Controlling Office)*		15. SECURITY CLASS. *(of this report)* Unclassified 15a. DECLASSIFICATION/DOWNGRADING SCHEDULE

16. DISTRIBUTION STATEMENT *(of this Report)*

Approved for public release; distribution unlimited

17. DISTRIBUTION STATEMENT *(of the abstract entered in Block 20, if different from Report)*

18. SUPPLEMENTARY NOTES

Submitted for publication in the Journal of the Mechanics and Physics of Solids

19. KEY WORDS *(Continue on reverse side if necessary and identify by block number)*

near tip stress field
rapid crack propagation
fracture toughness
elastic-plastic material
crack arrest

20. ABSTRACT *(Continue on reverse side if necessary and identify by block number)*

An asymptotic analysis of the near-tip fields is given for transient crack propagation in an elastic-plastic material. The material is characterized by J_2 flow theory together with a bilinear effective stress-strain curve. Both plane stress and plane strain conditions have been considered. Explicit results are given for the order of the crack-tip singularity, the angular position at which unloading occurs, and the angular variation of the near-tip stresses, all as functions of the crack-tip speed and the ratio of the slopes of the two portions of the bilinear stress-strain relation.

DD FORM 1 JAN 73 1473 EDITION OF 1 NOV 65 IS OBSOLETE

S/N 0102-LF-014-6601

Unclassified

SECURITY CLASSIFICATION OF THIS PAGE *(When Data Entered)*

SUMMARY

An asymptotic analysis of the near-tip fields is given for transient crack propagation in an elastic-plastic material. The material is characterized by J_2 flow theory together with a bilinear effective stress-strain curve. Both plane stress and plane strain conditions have been considered. Explicit results are given for the order of the crack-tip singularity, the angular position at which unloading occurs, and the angular variation of the near-tip stresses, all as functions of the crack-tip speed and the ratio of the slopes of the two portions of the bilinear stress-strain relation.

CRACK TIP FIELDS FOR FAST FRACTURE OF AN ELASTIC-PLASTIC MATERIAL

by

J. D. Achenbach, M. F. Kanninen, and C. H. Popelar

INTRODUCTION

An expanding interest is developing in the analysis of rapid unstable crack propagation in which dynamic (inertia) effects may not be negligible. While this interest has been motivated in part by intellectual curiosity in a new and fertile applied mechanics research area, there is also a growing realization that many engineering applications for this technology exist. There are many practical situations in which the result of large scale unstable crack growth is completely unacceptable. To preclude such catastropic occurrences, it is important to develop treatments for the arrest of rapid crack propagation. Because crack arrest must logically be viewed as the termination of fast fracture, attention must be focused on the dynamic crack propagation process.

For the most part, dynamic fracture mechanics is now based upon elastodynamic solutions; for example, see Kanninen (1978). Yet, most structural components where fracture is a concern employ tough ductile materials where it is unlikely that the basic assumptions of linear elastic fracture mechanics (LEFM) are valid. In addition, recent work has begun to raise serious questions about the extent to which the dynamic fracture toughness is truly a material property, even when LEFM conditions are satisfied. Thus, it is necessary to develop nonlinear dynamic elastic-plastic fracture mechanics treatments.

Because unloading may take place in dynamic crack propagation, a deformation theory formulation is undesirable. A flow theory approach is required to account for the elastic unloading in the wake of the crack tip. An asymptotic solution near the tip of a crack propagating dynamically in antiplane strain (Mode III) conditions using such an approach has already been given by Achenbach and Kanninen (1978). Their results determined the form of the crack tip singularity and the angular position at which elastic unloading commences. Clearly, this kind of information is needed in order to devise a finite element or other solution procedure for dynamic crack propagation and arrest analyses.

The work described in this paper extends the Achenbach-Kanninen approach to Mode I crack growth. Results for both plane stress and plane strain conditions are given. These solutions are based upon J_2 flow theory with a bilinear stress-strain relation which allows elastic unloading. The problem formulation leads to a nonlinear eigenvalue problem which is solved using an iterative numerical solution procedure. Confidence in the results was attained by comparisons with the results obtained by Amazigo and Hutchison (1977) for the special case of quasi-static crack growth at low crack-tip speeds when the dynamic effects are negligible.

THE SOLUTION PROCEDURE

Problem Formulation

The fields of stress and deformation are referred to a coordinate system whose origin is attached to the moving crack tip. The system of coordinates is shown in Figure 1. The crack is located in the (x_1x_3)-plane where the x_3 axis coincides with the crack front and x_1 is the direction of crack advance. The relevant displacement components are $u_1(x_1,x_2,t)$ and $u_2(x_1,x_2,t)$, where t is time.

In the following the material derivatives with respect to time will frequently be needed. These are defined as

$$(\dot{}) = \frac{\partial}{\partial t} - v(t)\,\frac{\partial}{\partial x_1} \tag{1}$$

$$(\ddot{}) = \frac{\partial^2}{\partial t^2} - \dot{v}(t)\,\frac{\partial}{\partial x_1} - 2v(t)\,\frac{\partial^2}{\partial x_1 \partial t} + [v(t)]^2\,\frac{\partial^2}{\partial x_1^2} \tag{2}$$

where v(t) is the speed of the crack tip. Notice that v need not be constant and is only subject to the conditions that v(t) and dv/dt are continuous functions.

For the case of plane stress, the non-vanishing stress components are σ_{11}, $\sigma_{12} = \sigma_{21}$, and σ_{22}. The equations of motion are of the form

$$\sigma_{\gamma\delta,\delta} = \rho\ddot{u}_\gamma \quad ; \qquad \gamma,\delta = 1,2 \tag{3}$$

where the second-order material time-derivative is defined by (2)*.

The constitutive equations in the elastic-plastic material take into account strain-hardening characterized by J_2 flow theory and a bilinear effective

*In the following, Greek minuscules have the values 1,2 whereas Latin minuscules have the values 1,2,3.

stress-strain curve. This curve is shown in Figure 2. Let σ_o denote the yield stress in tension, E Young's modulus, and $\alpha = E_t/E$, where E_t is the slope of the bilinear stress-strain relation in tension for stresses in excess of σ_o. The effective stress is defined as

$$\sigma_e = (\frac{3}{2} s_{ij} s_{ij})^{1/2} \tag{4}$$

where s_{ij} is the stress deviator. The constitutive relations for an elastically isotropic solid may then be written following Amazigo and Hutchinson (1977):

loading ($\sigma_e \geq o$):

$$E_t \dot{\varepsilon}_{ij} = \alpha[(1 + \nu)\dot{\sigma}_{ij} - \nu\dot{\sigma}_{kk}\delta_{ij}] + (\frac{3}{2} \sigma_e)(1 - \alpha)s_{ij}\dot{\sigma}_e \tag{5}$$

unloading ($\dot{\sigma}_e < o$):

$$E_t\dot{\varepsilon}_{ij} = \alpha[(1 + \nu)\dot{\sigma}_{ij} - \nu\dot{\sigma}_{kk}\delta_{ij}] \tag{6}$$

where ν is Poisson's ratio.

Field Equations for a Near-Tip Analysis

In this paper, certain a-priori assumptions are made with respect to the general nature of the deformation in the immediate vicinity of the crack tip. Explicit expressions for the near-tip fields will be derived using these assumptions. It will then be shown that the required boundary and continuity conditions are satisfied.

It is assumed that ahead of the crack tip a plastic loading zone exists which is bounded in the near-tip region by radial lines emanating from

the crack tip at angles $\theta = \pm\theta_p$. This is shown in Figure 1. An elastic unloading zone is assumed for $|\theta| > \theta_p$. The possible presence of a plastic reloading zone for $|\theta|$ near π is neglected in this paper. Conceptually, it is possible to include such a reloading zone. But, just as for the quasi-static case investigated by Amazigo and Hutchinson (1977), it is expected that the influence of reloading is not significant enough to justify the computational complications that would be required to treat it.

In the plastic loading zone, asymptotic solutions near the crack tip of the general form

$$\dot{u}_\gamma = Kv\dot{U}_\gamma(\theta)\, r^s \tag{7}$$

are sought. Here, K is an amplitude factor, while $\dot{U}_\gamma(\theta)$ and s are to be determined. In an asymptotic analysis, only the lowest orders in r need to be retained. This means that $\partial/\partial t$ can be neglected compared to $-v(t)\partial/\partial x_1$ in (1). Thus

$$(\dot{}) \sim - v(t) \frac{\partial}{\partial x_1} \tag{8}$$

By using the relations

$$\frac{\partial}{\partial x_1} = \cos\theta \frac{\partial}{\partial r} - \frac{\sin\theta}{r} \frac{\partial}{\partial \theta} \tag{9}$$

and

$$\frac{\partial}{\partial x_2} = \sin\theta \frac{\partial}{\partial r} + \frac{\cos\theta}{r} \frac{\partial}{\partial \theta} \tag{10}$$

the strain rates corresponding to (7) are then computed as

$$\dot{\varepsilon}_{11} = K\, v\, [s\, \dot{U}_1 \cos\theta - \dot{U}_1' \sin\theta]\, r^{s-1} \tag{11}$$

$$\dot{\varepsilon}_{22} = K\, v\, [s\, \dot{U}_2 \cos\theta + \dot{U}_2' \cos\theta]\, r^{s-1} \tag{12}$$

$$\dot{\varepsilon}_{12} = \frac{1}{2} K\, v\, [s\, \dot{U}_1 \sin\theta + \dot{U}_1' \cos\theta + s\, \dot{U}_2 \cos\theta - \dot{U}_2' \sin\theta]\, r^{s-1} \tag{13}$$

where $(\,)' = d/d\theta$. Also by definition

$$\{\sigma_{ij},\ \sigma_e,\ s_{ij}\} = K\, E\, \{\Sigma_{ij}(\theta),\ \Sigma_e(\theta),\ S_{ij}(\theta)\}\, r^s \tag{14}$$

and

$$\{\dot{\sigma}_{ij},\ \dot{\sigma}_e,\ \dot{s}_{ij}\} = K\, E\, v\, \{\dot{\Sigma}_{ij}(\theta),\ \dot{\Sigma}_e(\theta),\ \dot{S}_{ij}(\theta)\}\, r^{s-1} \tag{15}$$

By virtue of (8) and (9), the following relation holds

$$\dot{\Sigma}_{ij} = s\Sigma_{ij} \cos\theta + \Sigma_{ij}' \sin\theta \tag{16}$$

Analogous relations hold for $\dot{\Sigma}_e(\theta)$ and $S_{ij}(\theta)$. Also

$$S_{ij} = \Sigma_{ij} - \frac{1}{3} \Sigma_{kk}\, \delta_{ij} \tag{17}$$

$$\Sigma_e = \left(\frac{3}{2} S_{ij}\, S_{ij}\right)^{1/2} \tag{18}$$

By substituting (7) and the first of (14) into the equations of motion (3), we obtain in the plastic loading zone near the crack-tip

$$s\, \Sigma_{11} \cos\theta - \Sigma_{11}' \sin\theta + s\, \Sigma_{21} \sin\theta + \Sigma_{21}' \cos\theta = \beta^2\, (-s\, \dot{U}_1 \cos\theta + \dot{U}_1' \sin\theta) \tag{19}$$

$$s\, \Sigma_{12} \cos\theta - \Sigma_{12}' \sin\theta + s\, \Sigma_{22} \sin\theta + \Sigma_{22}' \cos\theta = \beta^2\, (-s\, \dot{U}_2 \cos\theta + \dot{U}_2' \sin\theta) \tag{20}$$

where

$$\beta = v/c\ , \qquad c = (E/\rho)^{1/2}\ . \tag{21}$$

Substitution of (11) through (18) into the constitutive relations (5) and (6) yields

$$\alpha\left[s\,\dot{U}_1\cos\theta - \dot{U}_1'\sin\theta\right] = \alpha\left[(1+\nu)\,\dot{\Sigma}_{11} - \nu\dot{\Sigma}_{kk}\right] + \frac{3}{2}(1-\alpha)\,\Sigma_e^{-1}\,S_{11}\,\dot{\Sigma}_e \tag{22}$$

$$\alpha\left[s\,\dot{U}_2\sin\theta + \dot{U}_2'\cos\theta\right] = \alpha\left[(1+\nu)\,\dot{\Sigma}_{22} - \nu\dot{\Sigma}_{kk}\right] + \frac{3}{2}(1-\alpha)\,\Sigma_e^{-1}\,S_{22}\,\dot{\Sigma}_e \tag{23}$$

$$\alpha\left[s\,\dot{U}_1\sin\theta + \dot{U}_1'\cos\theta + s\,\dot{U}_2\cos\theta - \dot{U}_2'\sin\theta\right] = 2\,\alpha\,(1+\nu)\,\dot{\Sigma}_{12} + 3\,(1-\alpha)\,\Sigma_e^{-1}\,\Sigma_{12}\,\dot{\Sigma}_e \tag{24}$$

The unknowns in these equations are U_γ and $\dot{\Sigma}_{\gamma\delta}$.

The above formulation was derived for plane stress conditions. For the case of plane strain, we have the condition $\dot{\varepsilon}_{33} = 0$ and the nonvanishing stress σ_{33}. It follows from (5) and (14) that the additional relation required for determining Σ_{33} is

$$\alpha\left[(1+\nu)\,\dot{\Sigma}_{33} - \nu\dot{\Sigma}_{kk}\right] + \frac{3}{2}(1-\alpha)\,\Sigma_e^{-1}\,S_{33}\,\dot{\Sigma}_e = 0 \tag{25}$$

No other changes are needed.

Corresponding equations for the elastic unloading region can be obtained from the work of Achenbach and Bazant (1975). In the elastic region the displacement rate must satisfy for plane strain the equation

$$(\lambda+\mu)\dot{u}_{\gamma,\gamma\delta} + \mu\dot{u}_{\delta,\gamma\gamma} = \rho\ddot{u}_\delta \tag{26}$$

where λ and μ are Lame's elastic constants. We introduce the displacement-rate potentials $\dot{\phi}$ and $\dot{\psi}$ through

$$\dot{u}_1 = \frac{\partial \dot{\phi}}{\partial x_1} + \frac{\partial \dot{\psi}}{\partial x_2} ; \qquad \dot{u}_2 = \frac{\partial \dot{\phi}}{\partial x_2} - \frac{\partial \dot{\psi}}{\partial x_1} \tag{27}$$

It is then not difficult to show that $\dot{u}_1$ and $\dot{u}_2$ will satisfy (26) if $\dot{\phi}$ and $\dot{\psi}$ are solutions of the wave equations

$$\dot{\phi}_{,\gamma\gamma} = \frac{1}{c_L^2} (\dot{\phi})^{\cdot\cdot} ; \qquad c_L^2 = (\lambda + 2\mu)/\rho \tag{28}$$

$$\dot{\psi}_{,\gamma\gamma} = \frac{1}{c_T^2} (\dot{\psi})^{\cdot\cdot} ; \qquad c_T^2 = \mu/\rho \tag{29}$$

In the near-tip region, the stresses in the elastic unloading zone may be expressed in terms of $\dot{\phi}$ and $\dot{\psi}$ by

$$-v\mu^{-1}\sigma_{22} = \beta_T^2 \frac{\partial \dot{\phi}}{\partial x_1} - \left(\frac{\partial \dot{\phi}}{\partial x_1} + \frac{\partial \dot{\psi}}{\partial x_2}\right) \tag{30}$$

$$-v\mu^{-1}\sigma_{21} = 2 \frac{\partial \dot{\phi}}{\partial x_2} + (\beta_T^2 - 2) \frac{\partial \dot{\psi}}{\partial x_1} \tag{31}$$

where we have used (8).

Let us now consider solutions of (28) and (29) of the general forms

$$\dot{\phi} = K\, v\, \dot{\Phi}(\beta_L, \varepsilon) r^p, \qquad \beta_L = v(t)/c_L \tag{32}$$

$$\dot{\psi} = K\, v\, \dot{\Psi}(\beta_T, \theta) r^p, \qquad \beta_T = v(t)/c_T \tag{33}$$

Solutions of this kind follow immediately as a slight generalization of Equations (22) and (23) of Achenbach and Bazant (1975) as

$$\dot{\Phi}(\beta_L^2, \theta) = (1 - \beta_L^2 \sin^2\theta)^{p/2} \left[A \sin\rho(\varepsilon - \pi) + B \cos\rho(\varepsilon - \pi)\right] \tag{34}$$

$$\dot{\Psi}(\beta_T^2, \theta) = (1 - \beta_T^2 \sin^2\theta)^{p/2} \left[C \sin p(\omega - \pi) + D \cos p(\omega - \pi)\right] \tag{35}$$

where

$$\tan \omega = (1 - \beta_L^2)^{1/2} \tan\theta \tag{36}$$

$$\tan \varepsilon = (1 - \beta_T^2)^{1/2} \tan\theta \tag{37}$$

Defining

$$\dot{u}_\gamma = K v \dot{U}_\gamma^{el}(\theta) r^{p-1} \tag{38}$$

we find the following relations on the basis of (27) and (9-10)

$$\dot{U}_1^{el} = p \cos\theta \dot{\Phi} - \sin\theta \dot{\Phi}' + p \sin\theta \dot{\Psi} + \cos\theta \dot{\Psi}' \tag{39}$$

$$\dot{U}_2^{el} = p \sin\theta \dot{\Phi} + \cos\theta \dot{\Phi}' - p \cos\theta \dot{\Psi} + \sin\theta \Psi' \tag{40}$$

The governing equations for conditions of plane stress in the elastic region can be obtained from the above by replacing λ by $\mu/(1 - \nu)$.

Boundary Conditions

The governing equations in the plastic loading zone, (19) through (24), and the general forms of the solutions in the elastic unloading zone, (34) through (40), must be supplemented by boundary conditions at $\theta = 0$ and $\theta = \pi$, and continuity conditions at $\theta = \theta_p$. By virtue of symmetry, the following conditions hold at $\theta = 0$.

$$\dot{U}_2 = 0 \tag{41}$$

$$\Sigma_{12} = 0 \tag{42}$$

$$\dot{U}_1' = 0 \tag{43}$$

Equations (30) and (31) together with the conditions that σ_{21} and σ_{22} vanish at $\theta = \pi$ yield the following relations

$$(\beta_T^2 - 2)\, pB - 2p\,(1 - \beta_T^2)^{1/2}\, C = 0 \tag{44}$$

$$2p\,(1 - \beta_L^2)^{1/2}\, A + (\beta_T^2 - 2)p\, D = 0 \tag{45}$$

Thus, the displacements and the stresses in the elastic unloading zone can be expressed in terms of two unknown constants, say A and B.

Now, consider the conditions at $\theta = \theta_p$. An obvious condition follows by comparison of (7) and (38) as

$$s = p - 1 \tag{46}$$

Since $\theta = \theta_p$ separates the plastic loading zone from the elastic unloading zone, $\dot{\sigma}_e$ must vanish there. This implies that $\dot{\Sigma}_e$ vanishes at $\theta = \theta_p$; i.e.,

$$-s\,\Sigma_e \cos\theta + \Sigma_e' \sin\theta = 0 \tag{47}$$

Continuity of traction-rates across $\theta = \theta_p$ requires that

$$[\dot{\Sigma}_\theta] = 0 \text{ and } [\dot{\Sigma}_{\theta r}] = 0 \tag{48}$$

Here the following notation has been used

$$[\ ] = \lim_{\theta \to \theta_p^+}(\ ) - \lim_{\theta \to \theta_p^-}(\ ) \tag{49}$$

Displacement-rates are also continuous at $\theta = \theta_p$. Consequently,

$$[\dot{U}_r] = [\dot{U}_\theta] = [\dot{U}_1] = [\dot{U}_2] \equiv 0 \tag{50}$$

Since $[\dot{U}_r] = 0$, we have $[\dot{\varepsilon}_r] = 0$. Then, since $\dot{\Sigma}_e = 0$ and $[\dot{\Sigma}_\theta] = 0$, it follows

from (5) and (6) that $[\dot{\Sigma}_r] = 0$. This result, together with (48), implies $[\dot{\sigma}_{\gamma\delta}] = 0$. From this it follows that $[\dot{\varepsilon}_{\gamma\delta}] = 0$. Since the strain rates and the displacement-rates are continuous, it follows from (11) through (13) that

$$[\dot{U}_1'] = [\dot{U}_2'] = 0 \tag{51}$$

at $\theta = \theta_p$.

Since explicit expressions for the fields in the elastic unloading zone are available, the continuity conditions (50) and (51) can be used to generate boundary conditions for the domain $0 \leq \theta \leq \theta_p$. The two unknown constants in the unloading zone, A and B, can be expressed in terms of $\dot{U}_1(\theta_p^-)$ and $\dot{U}_2(\theta_p^-)$ by the use of (49). Next, the quantities $(\dot{U}_1^{el})$ and $(\dot{U}_2^{el})$, which are now in terms of $\dot{U}_1(\theta_p^-)$, $\dot{U}_2(\theta_p^-)$, s, θ_p, β_L and β_T are computed and the continuity conditions (50) imposed. This yields general relations of the forms

$$\dot{U}_1'(\theta_p^-) = a_{11}(s,\theta_p)\, \dot{U}_1(\theta_p^-) + a_{12}(s,\theta_p)\, \dot{U}_2(\theta_p^-) \tag{52}$$

$$\dot{U}_2'(\theta_p^-) = a_{21}(s,\theta_p)\, \dot{U}_1(\theta_p^-) + a_{22}(s,\theta_p)\, \dot{U}_2(\theta_p^-) \tag{53}$$

The functions $a_{\gamma\delta}(s,\theta_p)$, which also depend on β_L and β_T, are rather lengthy, and they are not reproduced here.

Numerical Solution

Equations (47), (52), and (53) provide a set of boundary conditions for the domain $0 \leq \theta \leq \theta_p$. The governing equations for this domain are given by (19) through (24). The boundary conditions at $\theta = 0$ are given by (41) through (43). The unknowns are the functions depending on θ, such as $\dot{U}_1(\theta)$, etc, as well as the values of θ_p and s. The problem defined in this manner is

like a nonlinear eigenvalue problem, similar to, but more complicated than the one discussed for the anti-plane case by Achenbach and Kanninen (1978). The problem must be solved numerically as discussed in this section.

When (16) is used to eliminate $\dot{\Sigma}_{ij}$ in (19) through (24) and (47), the latter can be written in matrix form as

$$\underline{D}(S_{ij})\ \underline{y} + \underline{R}\ \underline{y} = 0 \tag{54}$$

where

$$\underline{y}^T = [\dot{U}_1,\ \dot{U}_2,\ \Sigma_{11},\ \Sigma_{22},\ \Sigma_{12},\ \Sigma_{33}] \tag{55}$$

in which the superscript T denotes the transpose. The elements of the symmetric, square matrices $\underline{D}(S_{ij})$ and $\underline{R}$ are given in the Appendix.

In preparation for integrating (54) numerically, it is convenient to normalize the θ-variations by taking $\Sigma_e(0) = 1$ and defining

$$q = \Sigma_{11}(0)/\Sigma_{22}(0) \tag{56}$$

The nonlinear two-point boundary value problem defined by (40) through (43), (50) and (54) through (56) is solved by the shooting method. For prescribed values of α and β and assumed values of s and q, (54) is numerically integrated over $\theta > 0$ until (47) is satisfied at a certain θ_p. A check is made to determine whether or not the continuity conditions, Equation (51), are satisfied for this θ_p. If not, Newton's method is used to establish new values of s and q and the procedure is repeated until (51) is satisfied.

A predictor-corrector method was used to integrate Equation (54). If $\underline{y}_i$ denotes the solution at $\theta = i\Delta\theta$, then $\underline{y}_{i+1}$ at $\theta = (i+1)\Delta\theta$ can be written as

$$\underline{y}_{i+1} = \underline{y}_i + \underline{y}_i'\ \Delta\theta + \underline{c}\ \Delta\theta^2/2 \tag{57}$$

and

$$\underset{\sim}{y}'_{i+1} = \underset{\sim}{y}'_{i} + \underset{\sim}{c}\,\Delta\theta \quad . \tag{58}$$

The coefficient vector $\underset{\sim}{c}$ is determined by numerical iterations; i.e., for an assumed $\underset{\sim}{c}$ (57) is substituted into (54) to determine $\underset{\sim}{y}'_{i+1}$ and a new estimate for $\underset{\sim}{c}$ is found from (58). This procedure is repeated until $\underset{\sim}{y}_{i+1}$ agrees with its previous iterant to six significant figures. Typically two iterations were sufficient and the method proved to be stable for α as small as 0.005 whereas the finite difference technique used by Achenbach and Kanninen (1978) was found to be unstable for $\alpha < 0.1$. To commence the numerical integration $\underset{\sim}{y}_o$ and $\underset{\sim}{y}'_o$ are required. These can be obtained by introducing Taylor series expansions about $\theta = 0$ for $\underset{\sim}{D}$, $\underset{\sim}{R}$ and $\underset{\sim}{y}$ into (54) and equating coefficients of θ^0 and θ^1 to zero. For the boundary conditions (41) through (43) and condition (56), $\underset{\sim}{y}_o$ and $\underset{\sim}{y}'_o$ are given in Appendix.

RESULTS AND DISCUSSION

The numerical solution was checked by comparing it with the known elastic solution and the quasi-static, linear strain-hardening solution of Amazigo and Hutchinson (1977). For this comparison it is not possible to consider numerically the limiting case $\beta = 0$ instead, $\beta = 0.001$ was used. The computed values of s and θ_p were found to agree with Amazigo and Hutchinson's values through four significant figures for all of the values of α that they reported; i.e. from $\alpha = .005$ to 1.0.

For a given value of α, there exists a limiting crack speed above which the numerical integration algorithm failed to converge to a non-positive value of s. This occurred whenever the crack speed was greater than the Rayleigh wave speed based upon the tangent modulus; i.e. whenever

$$\beta > 0.57\ \alpha^{1/2}; \qquad \nu = 0.3 \quad . \tag{59}$$

where β is given by Equation (21).

Numerical values of s and θ_p for the condition of plane stress are given in Table 1 for selected values of α and β and for $\nu = 0.3$. Plots of s versus α appear in Figure 3. It is apparent from this figure that if the crack speed is less than approximately one-half of the Rayleigh wave speed based upon the tangent modulus; i.e., if

$$\beta < 0.3\ \alpha^{1/2} \quad , \tag{60}$$

the order of the stress and strain singularity does not differ significantly from that for the quasi-static condition. The stress distributions in the loading region for $\beta = 0.25$ and $\alpha = 0.3$ are shown in Figure 4. These may be

compared with the quasi-static distributions for $\alpha = 0.3$ depicted in Figure 5. While the differences are not great, the largest difference occurs for Σ_{11}.

Numerical values of s and θ_p are summarized in Table 2 and plots of s versus α appear in Figure 6 for conditions of plane strain and $\nu = 0.3$. A comparison of Figures 3 and 6 reveals that inertia effects have a more pronounced influence upon the order of the singularity for plane strain than they do for plane stress. The plane strain distribution of stresses in the loading region are shown in Figures 7 and 8. Here differences between the quasi-static distributions of Figure 7 and the dynamic counterparts of Figure 8 are more perceptible. In both instances the high triaxiality in the loading region is readily apparent.

CONCLUSIONS

A basis for the analysis of rapid crack propagation taking direct account of crack-tip plasticity has been provided in this work. Explicit determination of the crack tip singularity and the angular position at which unloading takes place has been made for both plane stress and plane strain conditions. It was found that, in both conditions, the results are much more sensitive to the ratio of the slopes of the two portions of the bilinear stress-strain relation used then to the crack speed. This indicates that, for a singular finite element dynamic crack propagation solution procedure, only modest adjustments in the crack tip element formulation will be necessary to accommodate changes in the crack speed.

ACKNOWLEDGEMENTS

This work was supported by the Office of Naval Research Structural Mechanics Program, under Contract Number N0014-76-C-0063 (Northwestern University) and N00014-77-C-0576 (Battelle's Columbus Laboratories). The authors would like to thank Dr. Nicholas Perrone, for his encouragement of their work in this field and Professor J. W. Hutchinson for supplying unpublished details of the quasi-static solution.

REFERENCES

Achenbach, J. D. and Kanninen, M. F.	1978	Fracture Mechanics (edited by Perrone, N. et al.) p. 649, U. Virginia Press, Charlottesville, Va.
Achenbach, J. D. and Bazant, Z.P.	1975	J. Appl. Mech. 42, 183.
Amazigo, J. C., and Hutchinson, J. W.	1977	J. Mech. Phys. Solids 25, 81.
Kanninen, M. F.	1978	Numerical Methods in Fracture Mechanics (edited by Luxmoore, A. R. and Owen, D. R. J.), U. College of Swansea Press, Swansea, U.K.

APPENDIX

The nonzero elements of the symmetric matries $\underset{\sim}{D}$ (S_{ij}) and $\underset{\sim}{R}$ for plane strain are as follows. Note, for plane stress, the last column in $\underset{\sim}{R}$ and $\underset{\sim}{D}$ (S_{ij}) and the last row in $\underset{\sim}{R}$, $\underset{\sim}{y}$, $\underset{\sim}{y}_o$, and $\underset{\sim}{D}$ (S_{ij}) are deleted.

$$D_{11} = D_{22} = \beta^2 \sin\theta \tag{A1}$$

$$D_{13} = D_{31} = D_{25} = D_{52} = \sin\theta \tag{A2}$$

$$D_{15} = D_{51} = D_{24} = D_{42} = -\cos\theta \tag{A3}$$

$$D_{33} = \left[1 + \frac{9(1-\alpha)}{4\alpha} \frac{S_{11}^2}{\Sigma_e^2}\right] \sin\theta \tag{A4}$$

$$D_{44} = \left[1 + \frac{9(1-\alpha)}{4\alpha} \frac{S_{22}^2}{\Sigma_e^2}\right] \sin\theta \tag{A5}$$

$$D_{55} = \left[2(1+\nu) + \frac{9(1-\alpha)}{\alpha} \frac{S_{12}^2}{\Sigma_e^2}\right] \sin\theta \tag{A6}$$

$$D_{66} = \left[1 + \frac{9(1-\alpha)}{4\alpha} \frac{S_{33}^2}{\Sigma_e^2}\right] \sin\theta \tag{A7}$$

$$D_{34} = D_{43} = -\left[\nu - \frac{9(1-\alpha)}{4\alpha} \frac{S_{11}\, S_{22}}{\Sigma_e^2}\right] \sin\theta \tag{A8}$$

$$D_{35} = D_{53} = \frac{9(1-\alpha)}{2\alpha} \frac{S_{11}\, S_{12}}{\Sigma_e^2} \sin\theta \tag{A9}$$

$$D_{36} = D_{63} = -\left[\nu - \frac{9(1-\alpha)}{4\alpha} \frac{S_{11}\, S_{33}}{\Sigma_e^2}\right] \sin\theta \tag{A10}$$

$$D_{45} = D_{54} = \frac{9(1-\alpha)}{2\alpha} \frac{S_{22}\, S_{12}}{\Sigma_e^2} \sin\theta \tag{A11}$$

$$D_{46} = D_{64} = -\left[\nu - \frac{9(1-\alpha)}{4\alpha} \frac{S_{22}\, S_{33}}{\Sigma_e^2}\right] \sin\theta \tag{A12}$$

$$D_{56} = D_{65} = \frac{9(1-\alpha)}{2\alpha} \frac{S_{33} S_{12}}{\Sigma_e^2} \sin\theta \tag{A13}$$

$$R_{11} = R_{22} = - s\beta^2 \cos\theta \tag{A14}$$

$$R_{13} = R_{31} = R_{25} = R_{52} = - s \cos\theta \tag{A15}$$

$$R_{15} = R_{51} = R_{24} = R_{42} = - s \sin\theta \tag{A16}$$

$$R_{33} = R_{44} = R_{66} = - \frac{s}{\alpha} \cos\theta \tag{A17}$$

$$R_{34} = R_{43} = R_{36} = R_{63} = R_{46} = R_{64} = s\left(\frac{1-\alpha}{2\alpha} + \nu\right) \cos\theta \tag{A18}$$

$$R_{55} = - s \left[2(1+\nu) + \frac{3(1-\alpha)}{\alpha}\right] \cos\theta \quad . \tag{A19}$$

The values of $\underset{\sim}{y}$ and $\underset{\sim}{y}'$ at $\theta = 0$ are

$$\underset{\sim}{y}_o^T = \Sigma[a, o, q, 1, o, g] \tag{A20}$$

and

$$\underset{\sim}{y}_o'^T = \Sigma[o, b, o, o, c, o] \tag{A21}$$

where

$$\Sigma = (1 + q^2 + g^2 - q - qg - g)^{-1/2} \tag{A22}$$

$$a = (g+1)\left[\frac{1-\alpha}{2\alpha} + \nu\right] - \frac{q}{\alpha} \tag{A23}$$

$$b = s(g+q)\left[\frac{1-\alpha}{2\alpha} + \nu\right] - \frac{s}{\alpha} \tag{A24}$$

$$c = -s\ (\beta^2 a + q) \tag{A25}$$

$$g = \alpha(a+1)\left[\frac{1-\alpha}{2\alpha} + \nu\right] \quad . \tag{A26}$$

TABLE 1. PLANE STRESS RESULTS

$\alpha\backslash\beta$	0.1	0.25	0.40	0.5
		s		
1.0	-0.500	-0.500	-0.500	-0.500
0.7	-0.460	-0.457	-0.439	
0.5	-0.419	-0.411	-0.371	
0.3	-0.355	-0.339		
0.2	-0.306	-0.282		
0.1	-0.232			
		θ_p		
1.0	1.408	1.496	1.706	0.750
0.7	1.426	1.516	1.712	
0.5	1.425	1.517	1.719	
0.3	1.401	1.498		
0.2	1.370	1.475		
0.1	1.304			

TABLE 2. PLANE STRAIN RESULTS

$\alpha\backslash\beta$	0.1	0.25	0.40	0.5
		s		
1.0	-0.500	-0.500	-0.500	-0.500
0.7	-0.472	-0.468	-0.445	
0.5	-0.440	-0.426	-0.336	
0.3	-0.369	-0.320		
0.2	-0.292	-0.161		
0.1	-0.180			
		θ_p		
1.0	1.550	1.630	1.771	0.602
0.7	1.624	1.699	1.798	
0.5	1.718	1.768	1.834	
0.3	1.871	1.847		
0.2	1.967	1.802		
0.1	2.091			

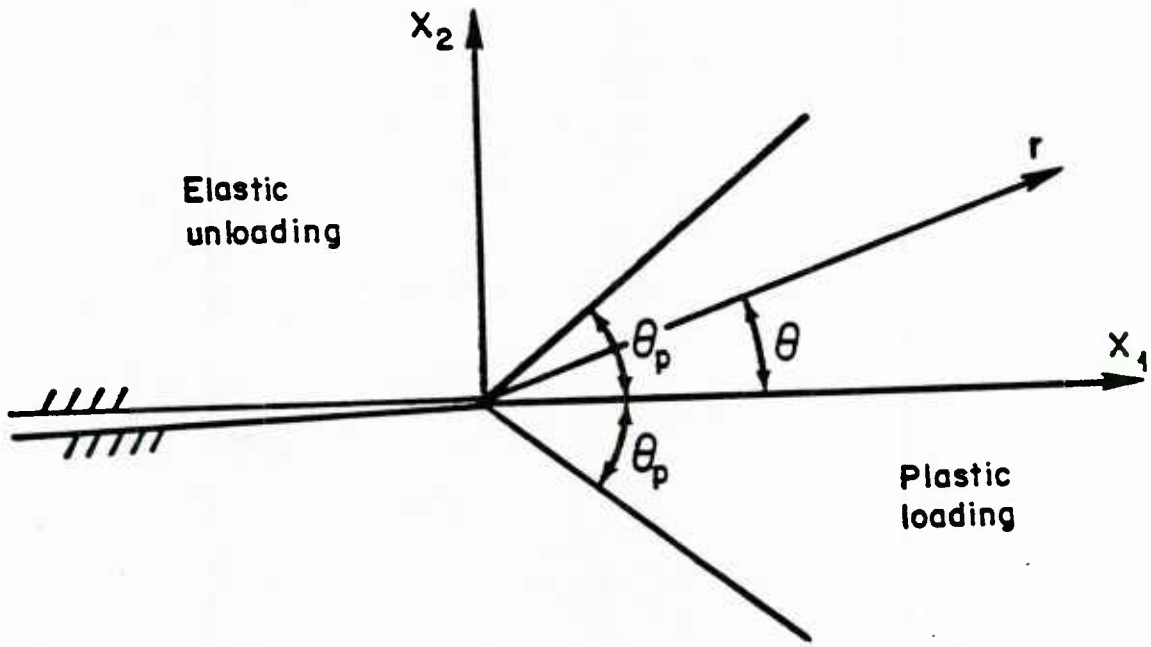

FIGURE 1. CRACK TIP GEOMETRY

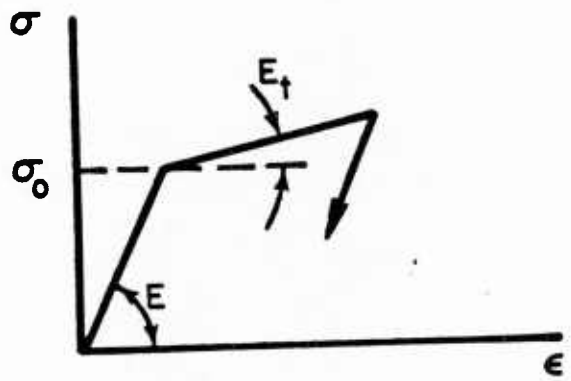

FIGURE 2. BILINEAR STRESS-STRAIN CURVE

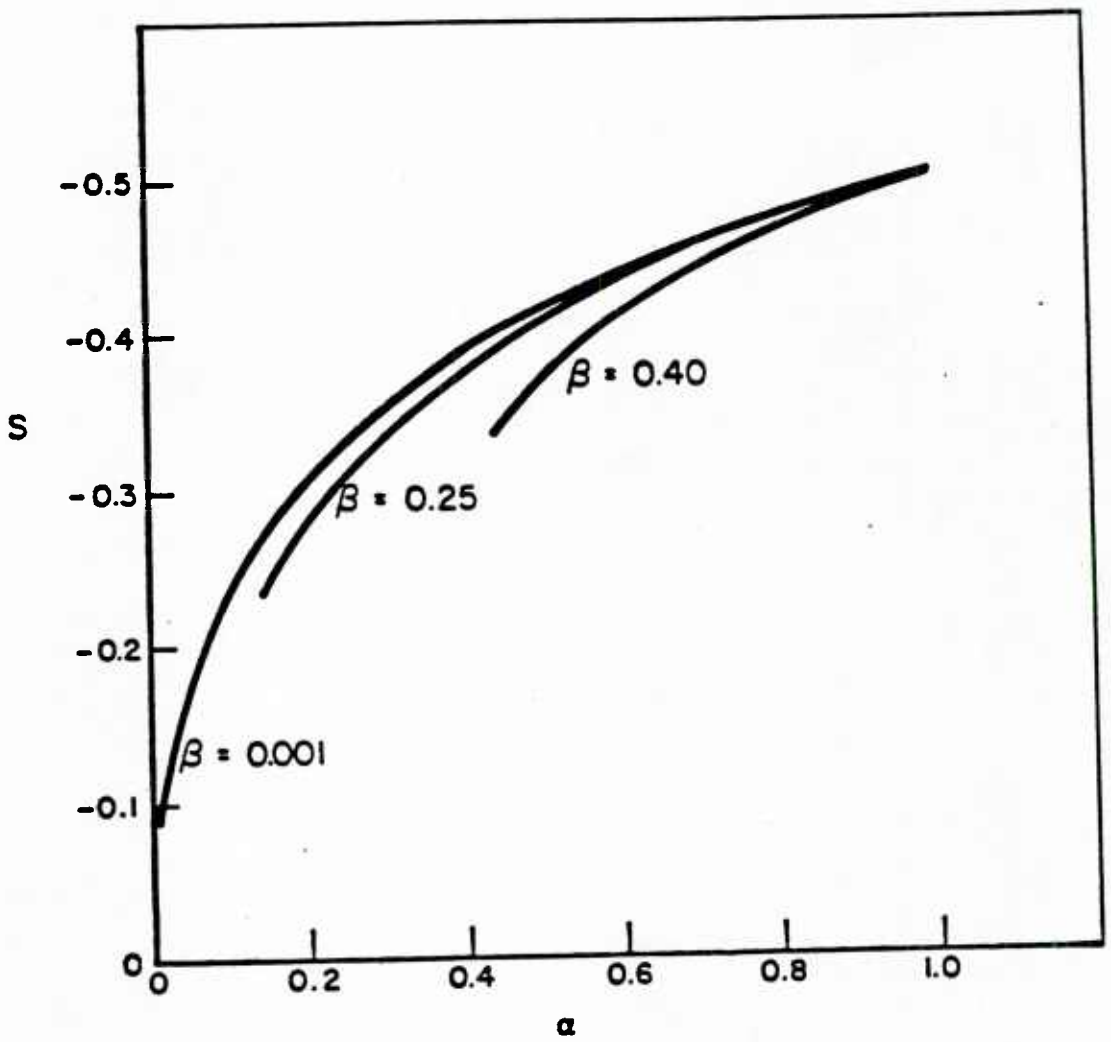

FIGURE 3. ORDER OF THE CRACK TIP SINGULARITY IN PLANE STRESS

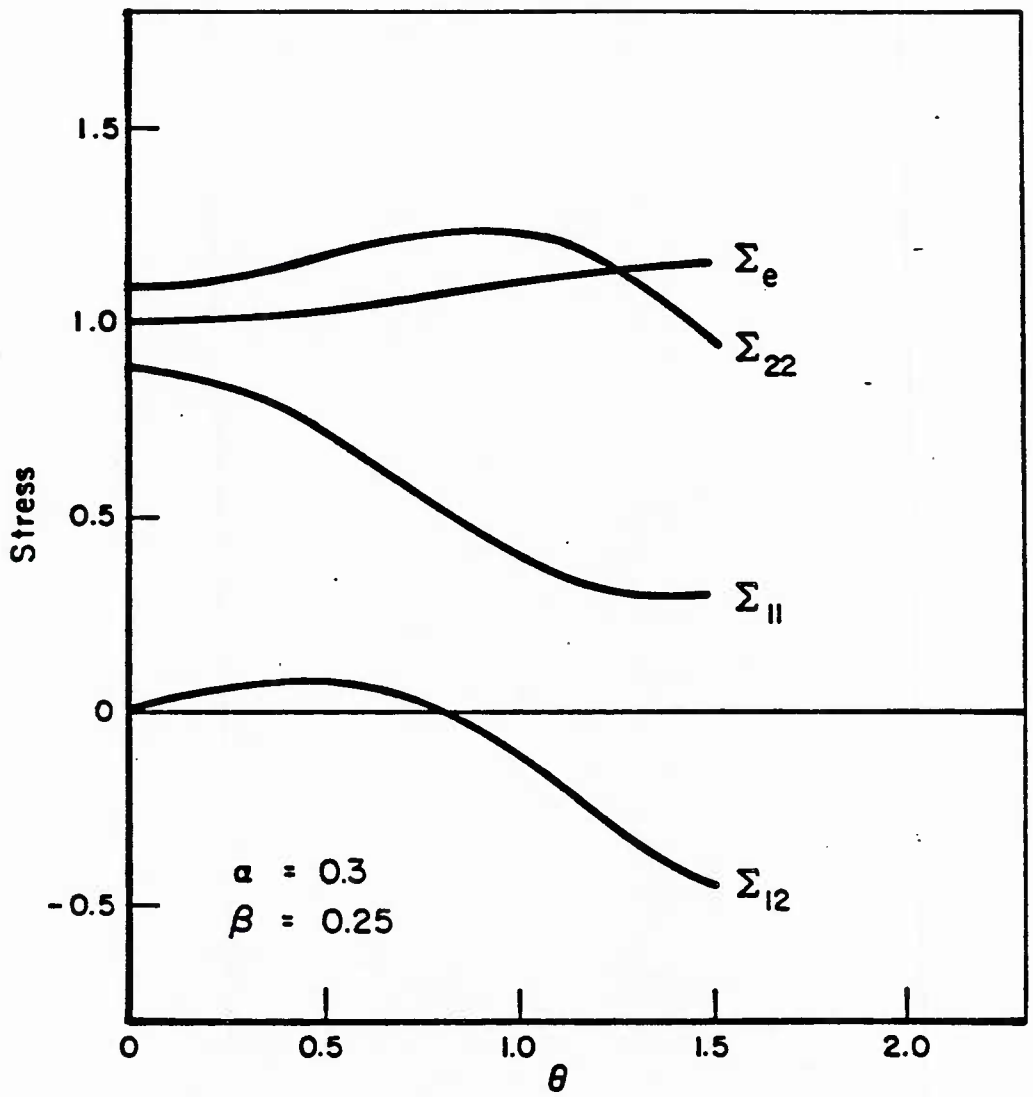

FIGURE 4. DYNAMIC CRACK TIP STRESSES IN PLANE STRESS

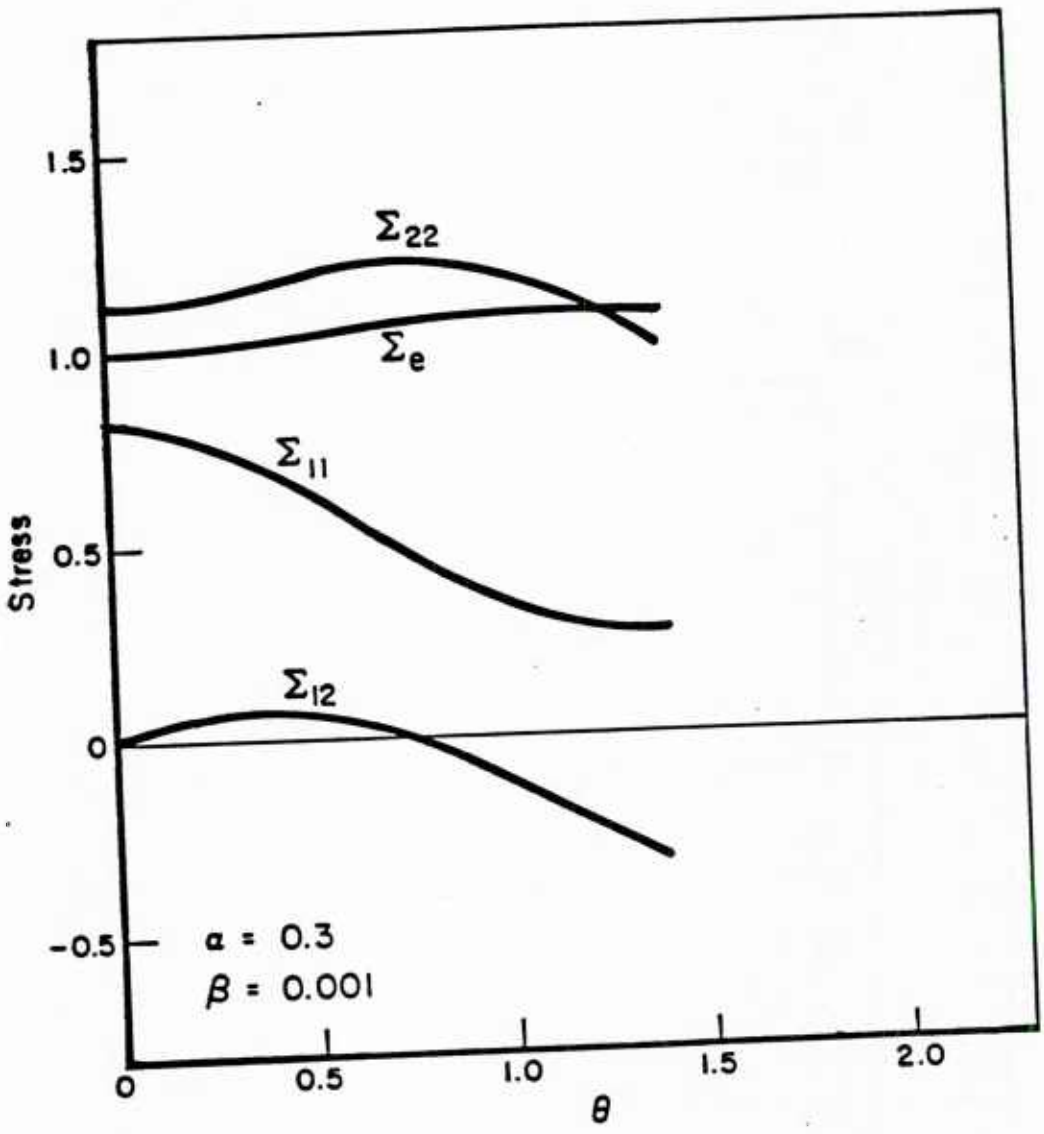

FIGURE 5. QUASI-STATIC CRACK TIP STRESSES IN PLANE STRESS

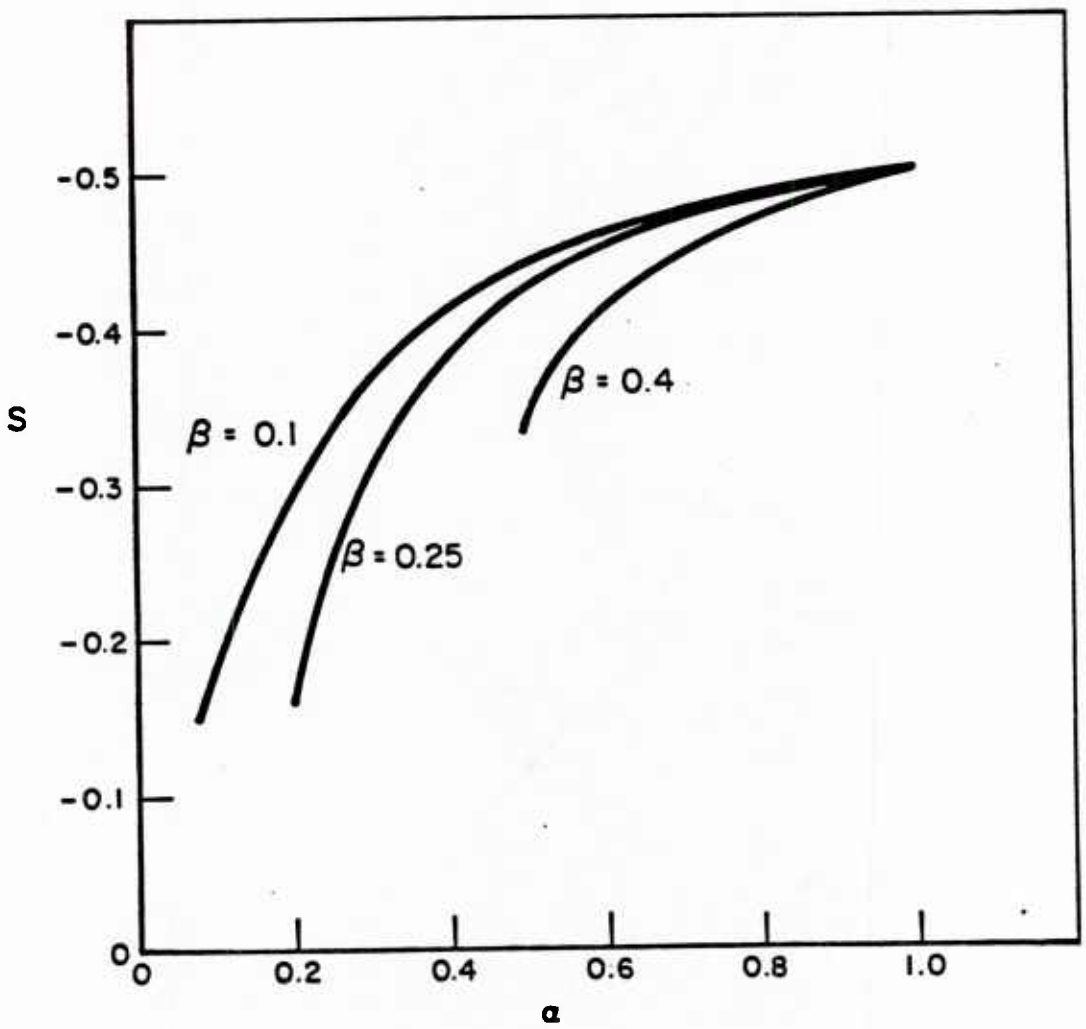

FIGURE 6. ORDER OF THE CRACK TIP SINGULARITY IN PLANE STRAIN

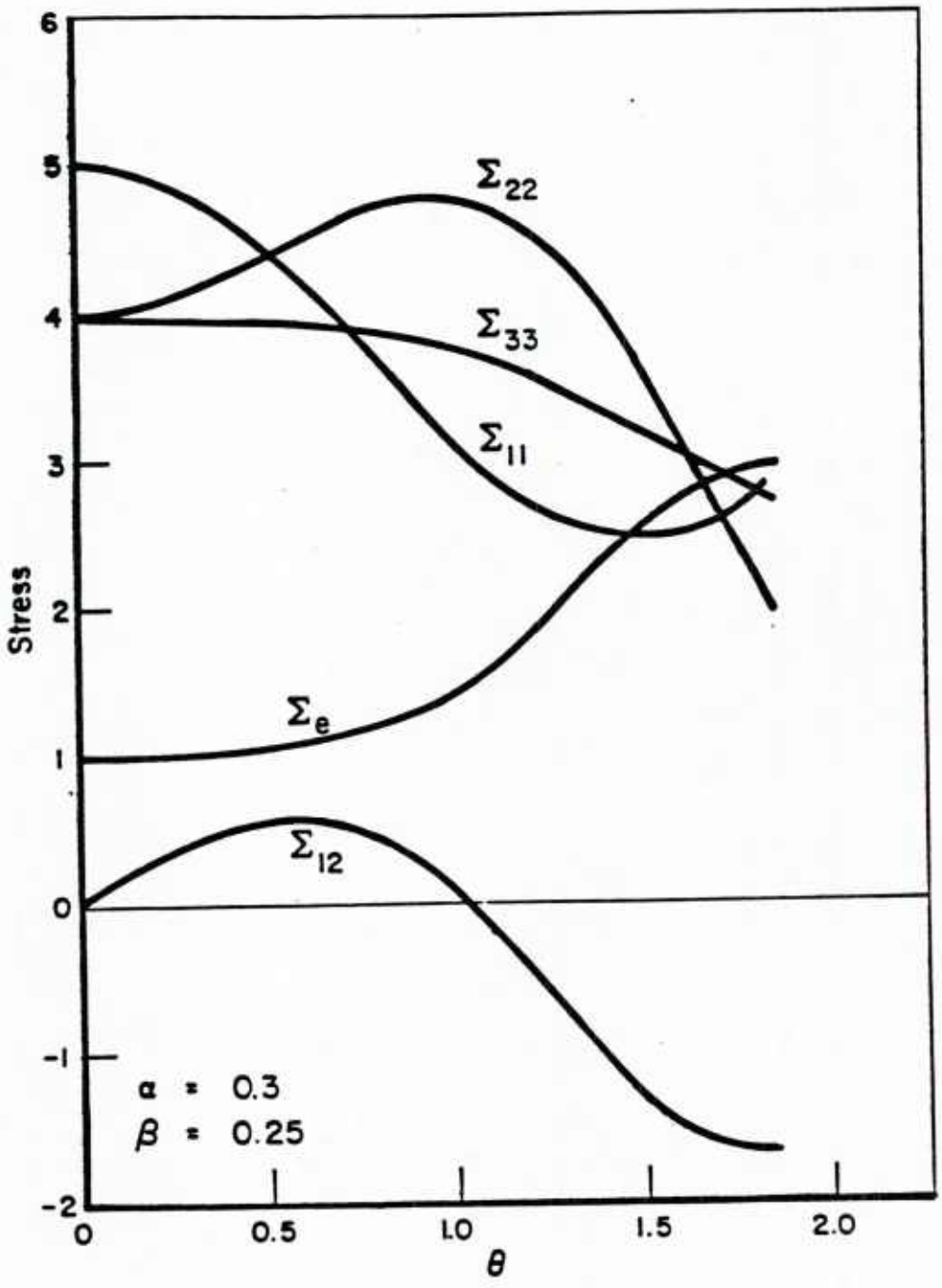

FIGURE 7. DYNAMIC CRACK TIP STRESSES IN PLANE STRAIN

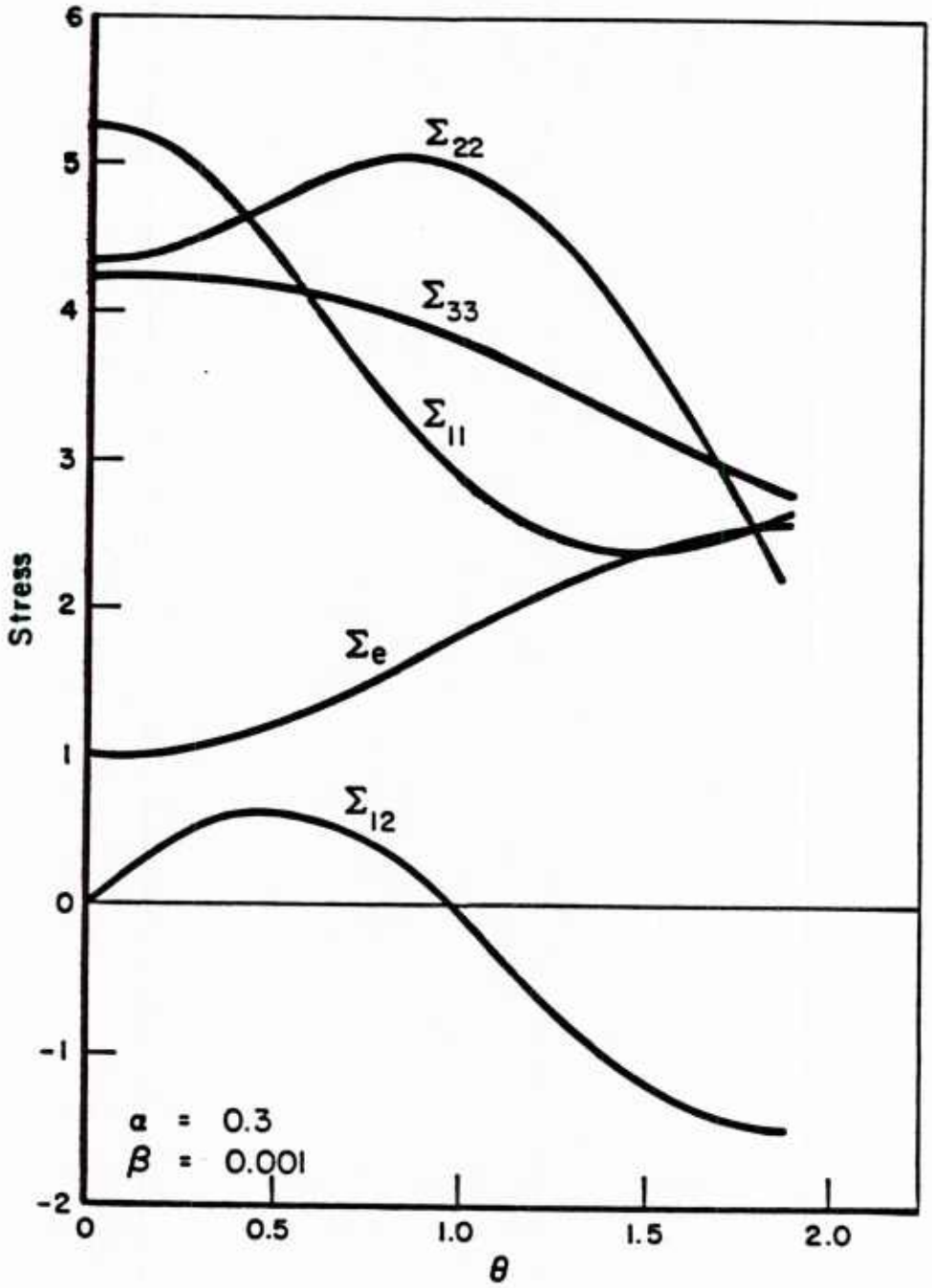

FIGURE 8. QUASI-STATIC CRACK TIP STRESSES IN PLANE STRAIN

DYNAMIC FRACTURE TOUGHNESS PARAMETERS FOR HY-80 AND HY-130 STEELS AND THEIR WELDMENTS

by

G. T. Hahn
Department of Mechanical Engineering and Material Science
Vanderbilt University
Nashville, Tennessee

and

M. F. Kanninen
Applied Solid Mechanics Section
Battelle
Columbus, Ohio

August, 1979

Office of Naval Research, Structural Mechanics Program,
Report on Contract Number N00014-77-C-0576.

Unclassified

SECURITY CLASSIFICATION OF THIS PAGE (When Data Entered)

REPORT DOCUMENTATION PAGE		READ INSTRUCTIONS BEFORE COMPLETING FORM
1. REPORT NUMBER	2. GOVT ACCESSION NO.	3. RECIPIENT'S CATALOG NUMBER
4. TITLE (and Subtitle) DYNAMIC FRACTURE TOUGHNESS PARAMETERS FOR HY-80 AND HY-130 STEELS AND THEIR WELDMENTS		5. TYPE OF REPORT & PERIOD COVERED Interim 6. PERFORMING ORG. REPORT NUMBER
7. AUTHOR(s) G. T. Hahn and M. F. Kanninen		8. CONTRACT OR GRANT NUMBER(s) N00014-77-C-0576 Battelle
9. PERFORMING ORGANIZATION NAME AND ADDRESS Vanderbilt University, Nashville, Tennessee and Battelle, Columbus, Ohio		10. PROGRAM ELEMENT, PROJECT, TASK AREA & WORK UNIT NUMBERS
11. CONTROLLING OFFICE NAME AND ADDRESS Office of Naval Research Structural Mechanics Program Dept. of the Navy, Arlington, VA 22217		12. REPORT DATE August, 1979 13. NUMBER OF PAGES 37
14. MONITORING AGENCY NAME & ADDRESS(if different from Controlling Office)		15. SECURITY CLASS. (of this report) Unclassified 15a. DECLASSIFICATION/DOWNGRADING SCHEDULE

16. DISTRIBUTION STATEMENT (of this Report)

Approved for public release; distribution unlimited

17. DISTRIBUTION STATEMENT (of the abstract entered in Block 20, if different from Report)

18. SUPPLEMENTARY NOTES

Will be submitted for publication in the Engineering Fracture Mechanics Journal

19. KEY WORDS (Continue on reverse side if necessary and identify by block number)

crack propagation
crack arrest
elastodynamic analysis
dynamic fracture toughness
Charpy V-notch specimen
HY-80 and HY-130 steel

20. ABSTRACT (Continue on reverse side if necessary and identify by block number)

Lower bound dynamic fracture toughness parameters for HY-80 and HY-130 steel and their weld metals are identified. Specific values of the parameters K_{Id} and K_{Im} obtained from direct measurements are reported together with estimates inferred from the large body of Charpy energy, nil ductility transition temperature and dynamic tear energy measurements. The emphasis is on reasonable lower bound values at 30 F, the lowest anticipated service temperature, for use in elastodynamic analyses of crack growth initiation, propagation, and arrest in ship structures. For these conditions, it has been found that the ratio K_{Id}/σ_Y is

DD FORM 1 JAN 73 1473 EDITION OF 1 NOV 65 IS OBSOLETE

S/N 0102-LF-014-6601

Unclassified

SECURITY CLASSIFICATION OF THIS PAGE (When Data Entered)

approximately 1 inch$^{1/2}$. Consequently, HY-80 plate appears to be substantially more resistant to fracture under dynamic loading than are the other three grades examined.

TABLE OF CONTENTS

LIST OF TABLES

LIST OF FIGURES

LIST OF FIGURES

(Continued)

ABSTRACT

Lower bound dynamic fracture toughness parameters for HY-80 and HY-130 steel and their weld metals are identified. Specific values of the parameters K_{Id} and K_{Im} obtained from direct measurements are reported together with estimates inferred from the large body of Charpy energy, nil ductility transition temperature and dynamic tear energy measurements. The emphasis is on resonable lower bound values at 30° F, the lowest anticipated service temperature, for use in elastodynamic analyses of crack growth initiation, propagation, and arrest in ship structures. For these conditions, it has been found that the ratio K_{Id}/σ_Y is approximately equal to 2 inches$^{1/2}$ for HY-80 steel. For HY-130 steel and the HY-80 and Hy-130 weld metals under these same conditions, K_{Id}/σ_Y is approximately 1 inch$^{1/2}$. Consequently, HY-80 plate appears to be substantially more resistant to fracture under dynamic loading than are the other three grades examined.

DYNAMIC FRACTURE TOUGHNESS PARAMETERS FOR HY-80 AND HY-130 STEELS AND THEIR WELDMENTS

by

G. T. Hahn and M. F. Kanninen

INTRODUCTION

Applications of dynamic fracture mechanics to treat crack growth initiation, unstable propagation, and arrest can now only be made in conditions where an elastodynamic analysis is applicable. Successful analyses have already been made of impact experiments [1, 2], nuclear pressure vessels under thermal shock conditions [3, 4] and gas transmission pipelines [5, 6]. However, the ability to perform an elastodynamic analysis alone is not enough to obtain results of practical interest. Values of the materials's resistance to crack propagation--the dynamic fracture toughness parameters--must also be available. Unfortunately, for the tough ductile materials used in most engineering structures, these values are not easy to obtain.

The work reported here is part of a larger effort aimed at providing a basis for crack propagation analyses in flawed ship hulls subjected to shock loading. Previous work in this program has shown that elastodynamically derived stress intensity factors can be used to predict crack growth initiation and propagation under impact loads [1]. Hence, while further development of the approach is still needed--e.g., to take direct account of crack tip plasticity--it is possible to provide preliminary estimates to evaluate ship hull performance by coupling these analyses with the material toughness parameters for the HY-grade steels. This report takes a first step toward the acquisition of suitable values for such analyses by means of a literature survey of the fracture properties of HY-80 and HY-130 and their weld metals.

BACKGROUND DISCUSSION

The analysis of crack growth initiation from a preexisting crack in a structure and its subsequent rapid unstable propagation and arrest can now only be effectively treated using elastodynamically determined stress intensity factors. The stress intensity factor arises in the computed stress field attending a crack tip. In general, it depends on time, the crack propagation speed, the crack length, the external geometry of the cracked body, and the applied loads. For a crack propagating in opening made conditions under fixed external loading, an elastodynamic solution can generally be made, albeit numerically, to determine the stress intensity factor in the form $K_I = K_I\ (t,\dot{a})$ where $\dot{a}$ denotes the instantaneous crack speed and t is time.

The criteria governing crack growth initiation and propagation can be expressed in terms of K_I and experimentally determined critical values that are taken as material properties. First, for the onset of growth for a rapidly loaded stationary crack

$$K_I\ (t,\ o) = K_{Id}\ (\dot{K}) \qquad (1)$$

where $\dot{\sigma}$ denotes the time rate of change of the applied loading through the consequent variation in the stress intensity factor. Like K_{Ic}, the conventional fracture toughness, K_{Id} will also be a function of temperature. Of course, for quasi-static loading, K_{Id} is identical with K_{Ic}.

The deformation state ahead of a propagating crack is generally different from that of a stationary crack. Consequently, the fracture property associated with a moving crack will differ from one that is not. The criterion for a rapidly propagating crack takes the form

$$K_I\ (t,\ \dot{a}) = K_{ID}\ (\dot{a}) \qquad (2)$$

where K_{ID}, in addition to being a function of temperature, is assigned a crack speed-dependence to take account of the rate dependence. It is of some importance to recognize that the entire $K_{ID} = K_{ID}\ (\dot{a})$ need not be known to perform

an effective calculation. The minimum value of this function at a given temperature - conventionally designated as K_{Im} - will suffice in many instances.

Equations (1) and (2), respectively, give quantitative criteria for crack growth initiation and subsequent unstable propagation. A third such relation is sometimes used for crack arrest which involves a statically computed value of K_I and an "arrest toughness" parameter K_{Ia}. However, while this approach can be useful as an approximation in some conditions, it is not logically correct. Within the context of an elastodynamic approach, crack arrest will occur when Equation (2) can no longer be satisfied. That is, a propagating crack will arrest at a time t_a when $K_I > K_{Im}$ for all $t > t_a$. While it is true that under some conditions K_{Ia} is about equal to K_{Im}, it does not follow that such an approach is widely applicable. Rather, crack arrest is properly viewed as the termination point of a general dynamic crack propagation event for which the relevant fracture property is K_{Im}.

Methods of measuring K_{Id} ($\dot{K}$), K_{ID} ($\dot{a}$), and K_{Im} have been devised and efforts to produce ASTM standards for these tests are underway[9]. However, very few measurements of this type have so far been performed on the HY-80, HY-100 and HY-130 grades of steel and their weldments. The main reason for this is that the high toughness values displayed by these materials at service temperatures call for prohibitively large LEFM-type test pieces*.

The bulk of the evaluations performed by the NRL (Naval Research Laboratory) and by industry rely on less costly measures of toughness: CVN-(Charpy V-notch) energy, NDT-(Nil Ductility Transition) temperature and DTE (Dynamic Tear Energy). These relative measures of toughness can be used to obtain more-or-less approximate estimates of K_{IC}, K_{Id}, and K_{Im} by way of a number of empirical correlations identified in Table 1 and Appendix A. Of these, the NRL DTE-K_{IC} correlation, (Correlation No. 1 in Table 1) is probably the most important because NRL relies on it to establish material toughness requirements.

---

*The logical extension of the ASTM E-399 fracture toughness test standard size requirements to dynamic loading would call for the crack length and thickness requirement a, $B \geq 2.5\ (K_{Id}/\sigma_{Yd})^2$, where σ_{Yd} is the dynamic yield stress. Accordingly, a test piece about 20 in. x 20 in. x 10 in. is needed to measure shelf level toughness values, i.e., $K_{Id} \approx 200$ ksi $\sqrt{\text{in}}$ of HY-80 steel ($\sigma_{Yd} \approx 100$ ksi $\sqrt{\text{in}}$).

TABLE 1. SUMMARY OF TOUGHNESS CORRELATIONS

No.	Toughness Measured	Property Inferred	Method	Formulation[a]	Reference
1	DTE	K_{Ic}	Empirical Correlation	(See Figure A1)	NRL, 10-13
2	K_{Ic}	K_{Id}[b]	Temperature Shift	T_s (°F) = 215 ksi - 1.5 σ_y	Barsom & Rolfe (14) and Barsom (15)
3	K_{Ic}	K_{Id}[c]	Empirical Correlation	$K_{Id} \geq K_{Ic}$	Barsom & Rolfe (14)
4	CVN	K_{Id}	Empirical Correlation	$K_{Id} = [5(E)(CVN)]^{1/2}$	Barsom & Rolfe (14) and Barsom (15)
5	CVN	K_{Ic}[c]	Empirical Correlation	$K_{Ic} = 2.24\sigma_y[\frac{CVN}{\sigma_y} - 0.05]^{1/2}$	Barsom & Rolfe (14)
6	CVN	K_{Ic}[b]	Temperature Shift and Correlation	$T(K_{Ic} = 100\ MPa\ m^{1/2}) = 9 + 1.37T(CVN=28J)$ $K_{Ic} = 19(CVN)^{1/2}$	Marandet (2) Sanz (16)
7	NDT	K_{Id}/T=NDT	Approximate Analysis	K_{Id}/T=NDT = 0.7 σ_{yd} 0.5 σ_{yd}	Irwin (17) Pellini (18)
8	DTE	NDT	Empirical Correlation	DTE (ft lbs) T = NDT - 0.36σ_{ys} (ksi) + 55	Lange (19)
9	NDT	K_{Id}[b]	Reference Curve	(See Figure A2)	Pellini (20)
10	NDT	K_{Im}[b]	Reference Curve	(See Figure A2)	Halmetal (4)
11	J_{Ic}	K_{Ic}	Theory	$K_{Ic} = [\frac{J_{Ic}E}{1-\nu^2}]^{1/2}$	Rice (21)
12	J_{Ic}	K_{Im}[c]	Approximate Analysis	$K_{Ic} = 1.5\ [\frac{J_{Ic}E}{1-\nu^2}]^{1/2}$	Hahn (22)
13	COD	K_{Ic}	Theoretical Analysis	$K_{Ic} = [2E\sigma y(COD]^{1/2}$	Rice & Johnson (23)

(a) Formulations for Correlation 2, 4 and 5, are in ksi, ksi$\sqrt{in.}$, and ft lb units, for Correlation 6, in J, MPa $m^{1/2}$

(b) Transition

(c) Shelf

This report takes a first step toward defining the K_{Id} and K_{Im} values for the HY-80 and HY-130 steels and their weld metals appropriate for dynamic LEFM analyses of submerged hull structures. The relative importance of base metal, weld metal and HAZ (heat affected zone) is touched on in Appendix B. The report surveys the limited number K_{Id} values obtained from direct measurements, but draws the bulk of its K_{Id} and K_{Im} estimates from the larger body of CVN-, NDT-, and DTE-measurements. Since LEFM calculations are likely to be concerned with "worst-case" conditions, the emphasis is plased on reasonable, lower bound toughness values at the LAST (lowest anticipated service temperature) which is 30° F for submerged shiphull structure. These lower bound values are based on the specified minimum CVN- and DTE-values listed in Table 2, and the trends displayed by representative heats. In addition, the need for J_{Ic} and K_{Im} measurements for base and weld metals and further verification of the NRL-DTE-KIC correlation are identified.

TABLE 2. TOUGHNESS SPECIFICATIONS FOR HY-GRADE STEEL AND WELDMENT

Grade or Type	Spec. No.	CVN	5/8 DTE
HY-80 Plate	MIL-S-16216H	Longitudinal 50 ft lbs @ -120°F(a)	Transverse 400 ft lbs @ 0°F(b)
HY-100 Plate	MIL-S-16216H	Longitudinal 50 ft lbs @ -120°F(c)	Transverse 450 ft lbs @ 0°F(b)
HY-802 HY-100 Weldments			
11018 Stick electrrode	MIL-E-22200/10	50 ft lbs @ 0°F & 70°F	450 ft lbs @ 0°F(b)
12018	MIL-E-22200/1E	20 ft lbs @ -60°F(d)	
MIL-100S, 110S 120S Wire	MIL-E-23765	50 ft lbs @ -60°F	450 ft lbs @ 0°F(b) for 120S only
Type MI88 Submerged arc electrode	MIL-E-24355	20 ft lbs @ -60 50 ft lbs @ 30°F	
HY-130	MIL-E-24355	Transverse 60 ft lbs @ 0°F & 70°F	Transverse 500 ft lbs @ 0°F(b)
HY-130 Weldmental			
Type MIL-4105	MIL-E-24355A		500 ft lbs @ 30°F(e)
Bare, Solid Wire			
14018 Stick electrode	MIL-E-22200/9A		475 ft lbs @ 30°F(e)

(a) 30 ft lbs for sections of 6 inches thick

(b) optional

(c) 30 ft lbs for sections over 4 inches thick

(d) for yield strength 95 ksi - 107 ksi

(e) for yield strength 135 ksi - 150 ksi

DYNAMIC FRACTURE TOUGHNESS PROPERTIES

HY-80 Base Plate

Existing direct measurements and estimates of K_{Id} ($K_I \sim 10^5$ ksi $\sqrt{in.}$ sec^{-1}) derived from K_{IC}-, CVN-, and DTE-measurements are summarized in Figure 1. The CVN curves in Figure 2 illustrate that the NDT temperature for this grade corresponds roughly with the midpoint of the CVN energy transition. An estimate of the lower bound, the curve LB, just satisfies the specified minimum CVN value (50 ft lbs at -120° F) and reflects the likely temperature variation.

The CVN curves and the K_{Id} values inferred form them in Figure 1 (of the Correlations 4 and 5 in Table 1), illustrate that HY-80 displays ductile, upper shelf-level behavior at the LAST. The K_{Id} estimates at the LAST are derived from CVN and DTE measurements (Correlations 3, 1, and 5 in Table 1). No crack arrest toughness (K_{Im}) measurements have so far been performed on HY-80; the estimates in Table 3 are based on the highest NDT temperature and the $\frac{K_{Im}}{\sigma_{Yd}}$ reference curve in Figure A-2.

HY-130 Base Plate

Direct measurements of K_{Id} are produced in Figure 3, together with K_{Id} estimates based on K_{Ic} (Correlation 2), CVN (Correlation 4) and DTE (Correlation 1). Representative CVN and DTE transition curves are reproduced in Figures 4 and 5. These curves illustrate that HY-130 grade, like the HY-80, displays ductile shelf behavior at the LAST.

The specified minimum CVN for this material (60 ft lbs at 30° F) provides one basis for estimating the lower bound K_{Ic} and K_{Id} values. The corresponding DTE provides another. Since the correlation between CVN and DTE is approximate, it further reduces the lower bound value of DTE associated with the LAST to 300 ft lbs. This is illustrated in Figure 6. No crack arrest toughness measurements have so far been performed on HY-130 steel. The estimate of K_{Im} quoted in Table 3 are based on the $\frac{K_{Im}}{\sigma_{Yd}}$ reference curve in Figure A-2.

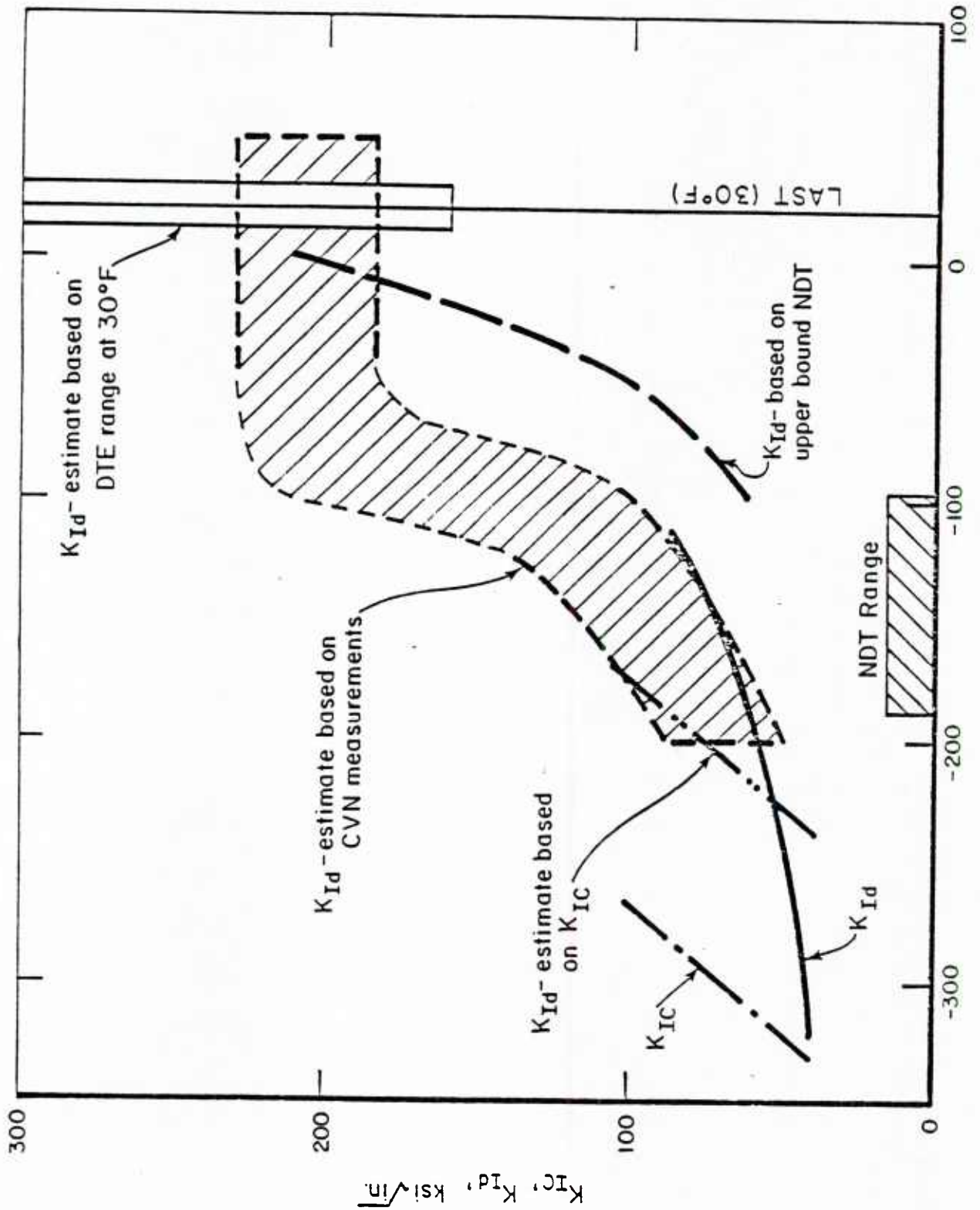

FIGURE 1. SUMMARY OF K_{Id} MEASUREMENTS FOR HY-80 STEEL AND K_{Id} ESTIMATES BASED ON K_{Ic}, CVN, AND DTE MEASUREMENTS, ATTER, SHOEMAKER AND ROLFE(24), BARSON(25), PUZAK(26), AND GOODE ET AL.(27). THE SOURCE OF CVN AND NDT DATA ARE IDENTIFIED IN FIGURE 2.

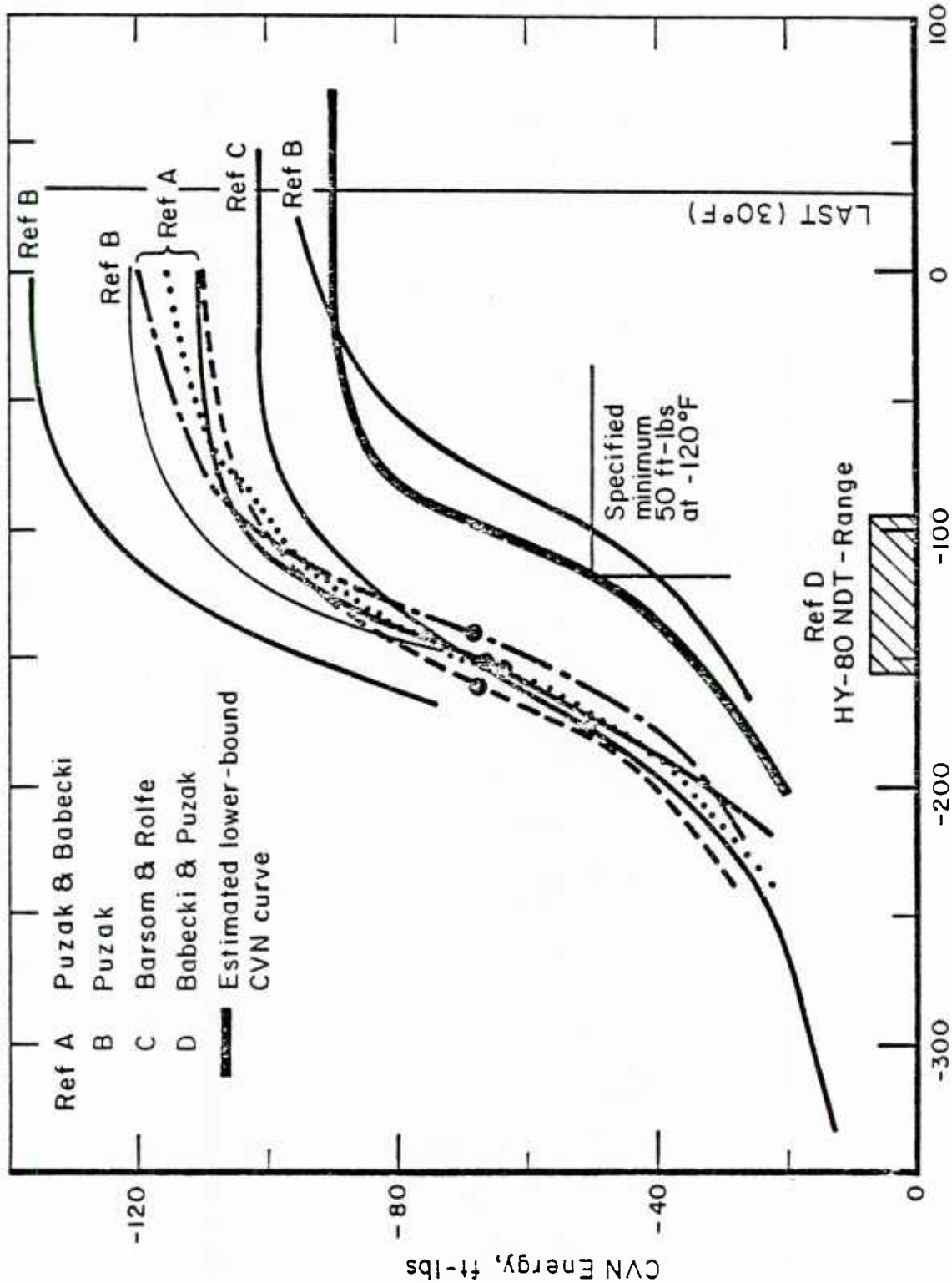

FIGURE 2. CVN ENERGY AND NDT VALUES FOR HY-80 STEEL AFTER PUZAK AND BABECKI(29), PUZAK(28) BARSOM AND ROLFE(14), AND BABECKI AND PUZAK(30)

TABLE 3. SUMMARY OF ESTIMATES OF TYPICAL AND LOWER BOUND TOUGHNESS PARAMETERS FOR HY-80 AND HY-130 STEEL AND WELDMETALS AT THE LAST (30°F)

Material	Toughness Parameter	Typical Value	Lowerbound Estimate
HY-80	NDT, °F	-150	-100
	CVN, ft lbs	110	90
	5/8 in. DTE, ft lbs	~ 800	420
	K_{Ic}, ksi in.	200-250	160[a]
	K_{Id}, ksi in.	$\geq$ 200-250	$\geq$ 160[a]
	K_{Im}, ksi in.	~ 174	~143
MIL-11018 Type	NDT, °F	-	-20
HY-80 Weldmetal	CVN, ft lbs	-	42
	5/8 in. DTE, ft lbs	~ 450	260
	K_{Ic}, ksi in.	~ 160	120
	K_{Id}, ksi in.	-	~ 80
	K_{Im}, ksi in.	-	~ 92
HY-130	NDT, °F	-120	-60
	CVN, ft lbs	~ 80	60
	5/8 in. DTE, ft lbs	550	330
	K_{Ic}, ksi in.	~185[a]	135[a]
	K_{Ia}, ksi in.	~185[a]	$\geq$ 135[a]
	K_{Im}, ksi in.	~229	~ 174
MIL-1405, GMA Type HY-130 Weldmetal	NDT, °F	-110	-60
	CVN, ft lbs	-	-
	5/8 in. DTE, ft lbs	~ 550	340
	K_{Ic}, ksi in.	~ 175	140[a]
	K_{Id}, ksi in.	~ 175	140[a]
	K_{Im}, ksi in.	~220	~ 174

(a) based on DTE

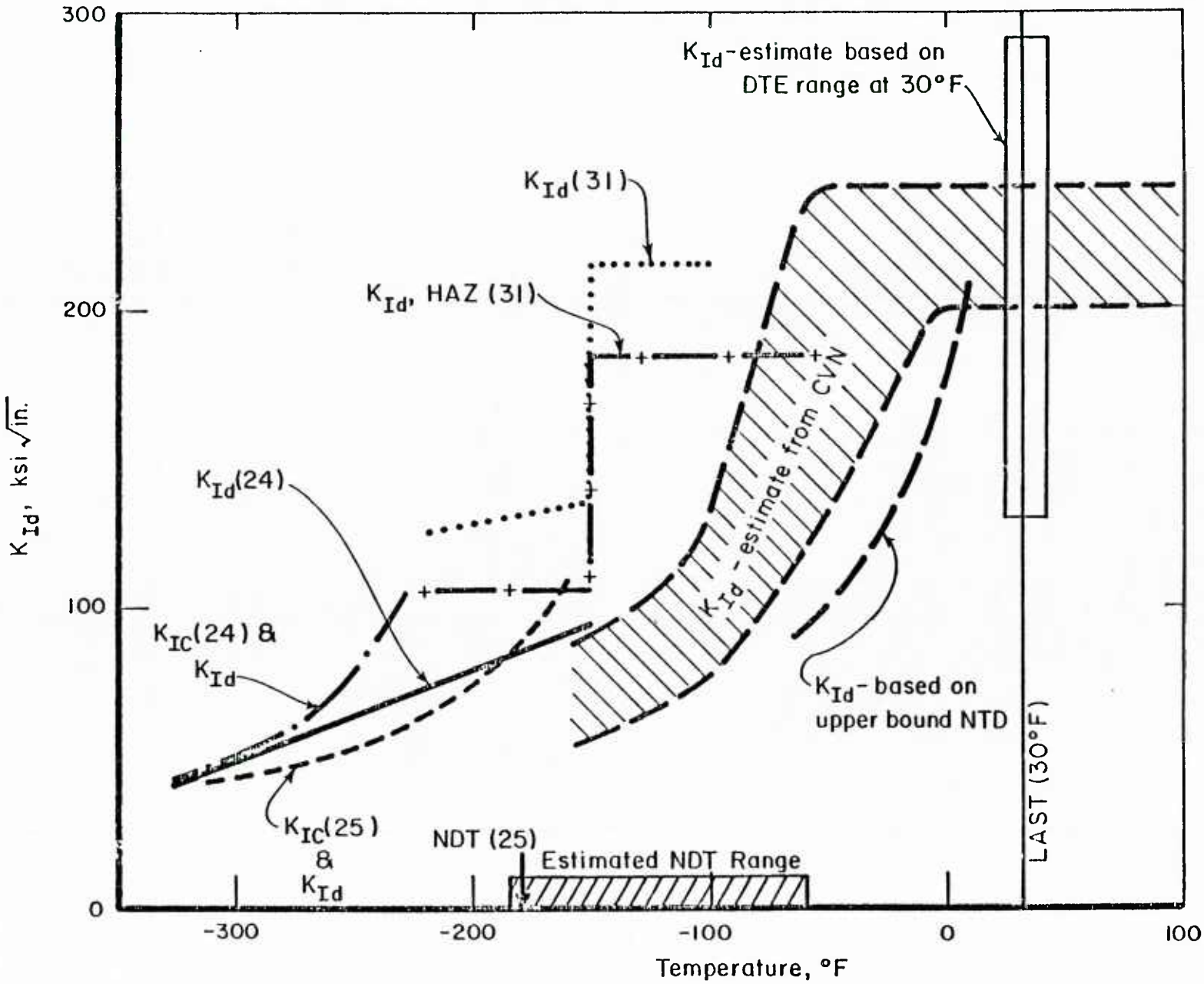

FIGURE 3. SUMMARY OF K_{Id} MEASUREMENTS FOR HY-130 STEEL AND K_{Id} ESTIMATES BASED ON K_{IC}, CVN, AND DTE MEASUREMENTS, ATTER, SHOEMAKER AND ROLFE(24), BARSOM(25) AND PENSE(31), AND PUZAK(32)

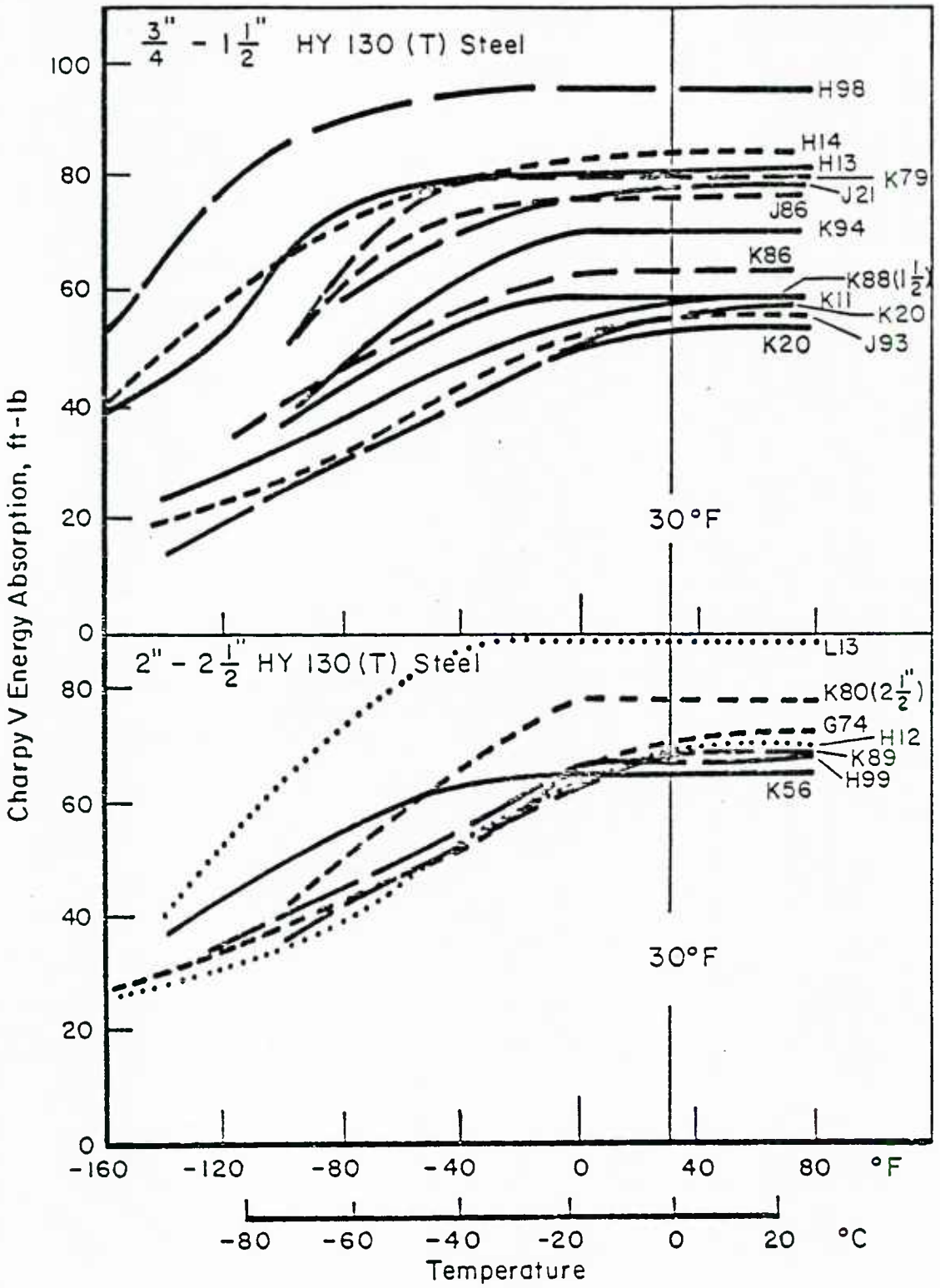

FIGURE 4. CVN ENERGY VALUES FOR HY-130 STEEL PLATES IN THE "WEAK" (WR) ORIENTATION AFTER PUZAK(32)

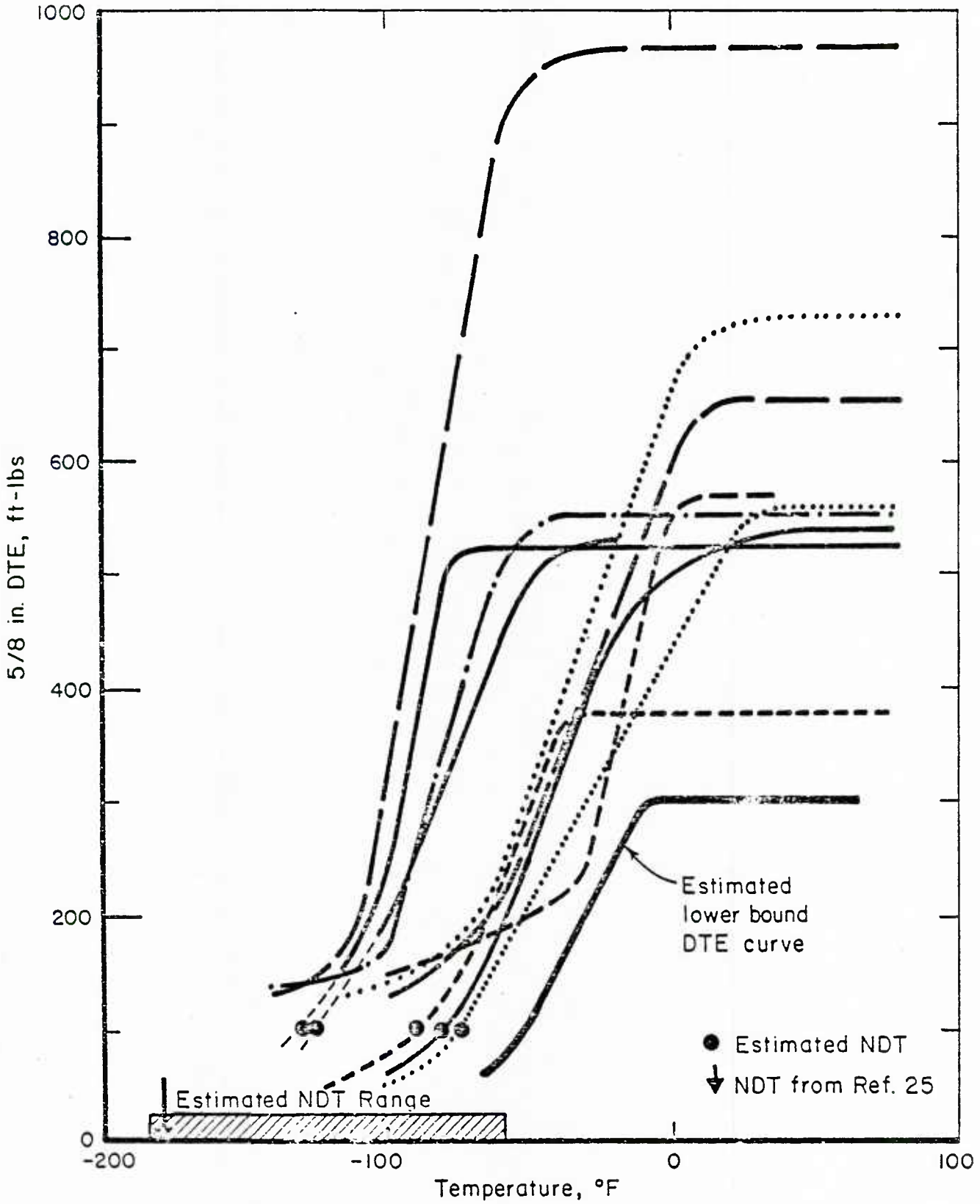

FIGURE 5. DTE ENERGY VALUES FOR HY-130 STEEL PLATES OF DIFFERENT THICKNESSES AFTER PUZAK(32). THE 1 IN., 1.5 IN., 2 IN., AND 2.5 IN. DTE VALUES HAVE BEEN REDUCED BY FACTORS OF 8, 15, 22.6, AND 29 TO MAKE THEM COMPARABLE TO 5/8 IN. DTE VALUES. THE ESTIMATED NDT TEMPERATURES ARE OBTAINED BY RELATING IT TO THE TEMPERATURE CORRESPONDING TO A 5/8 IN. DTE OF 100 FT LBS(19).

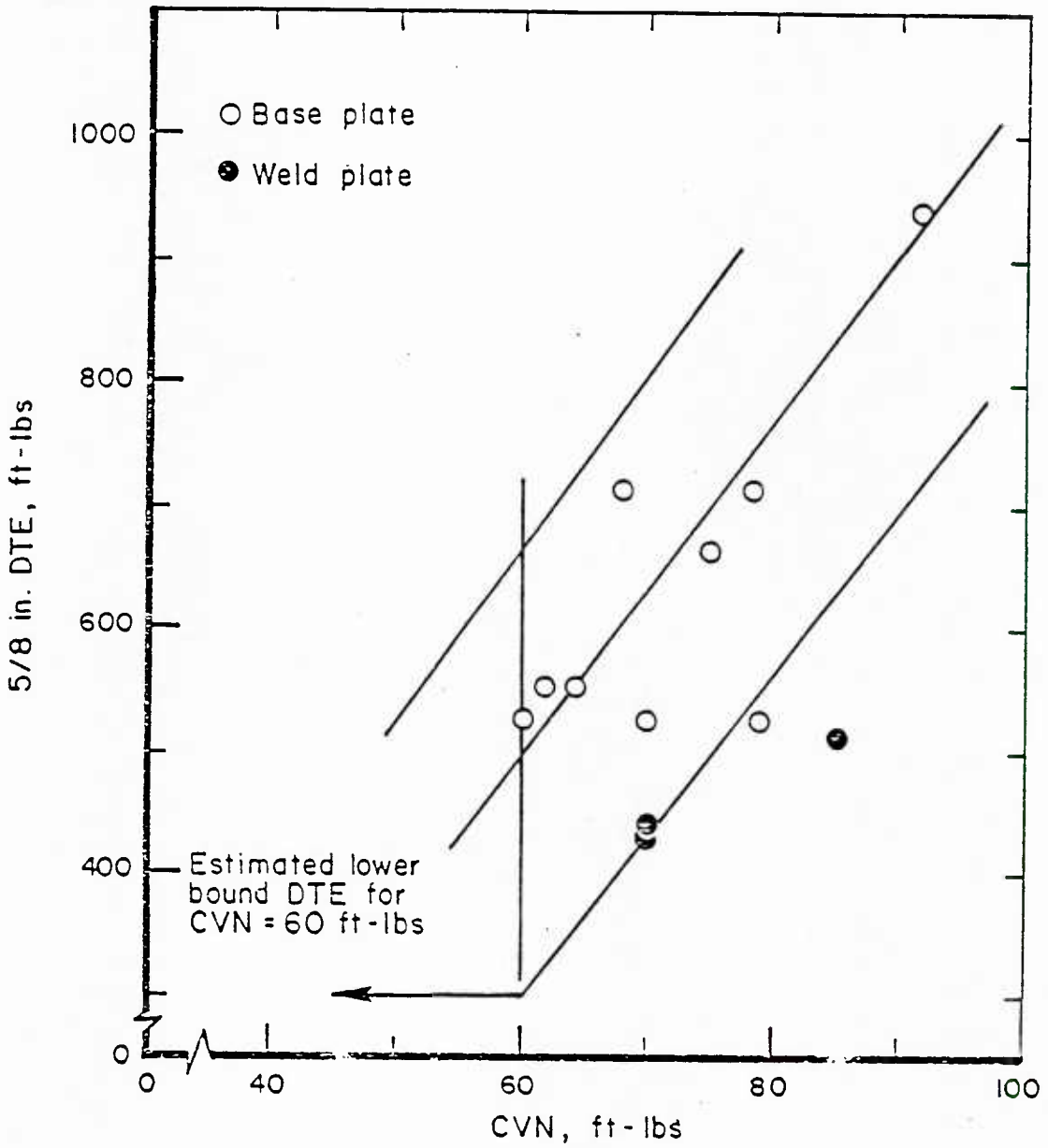

FIGURE 6. CORRELATION BETWEEN CORRESPONDING CVN AND 5/8 IN. DTE VALUES MEASURED ON THE DUCTILE SHELF FOR THE HY-130 STEELS [DATA OF FIGURES 4 AND 5 AFTER PUZAK(32)]. THE SCATTERBAND REFLECTS THE APPROXIMATE NATURE OF THE CVN DTE CORRELATION AND INDICATES THAT A DTE VALUE MAYBE AS LOW AS 300 FT LBS FOR A CVN OF 60 FT LBS

Weld Metals

The most telling toughness evaluations of HY grade weld metal--weld metal and HAZ--are obtained using the explosion bulge test[28,29,36,37]. While this is a very severe test of performance, it has not been correlated with absolute measures of toughness like K_{Ic} or K_{Id}. The only direct LEFM-type tests are the few measurements of the COD for a HY-130 plate and HAZ that have recently been reported by Pense(31). These are converted to K_{Id} estimates in Figure 3 (Correlation 13). Estimates of K_{Id} must be drawn from the body of CVN and DTE measurements of weld metal which have been developed by NRL. These studies show that, while HY-80 and HY-130 display near ductile shelf-level behavior on the average, some lower bound values fall in the transition range.

Figure 7 reproduces lower bound 1 inch DTE curves from a limited sampling of welds produced by the Portsmouth and NSRDC-A facilities. This set of results shows that the lowest value at the LAST is 260 ft lbs (5/8 inch DTE) for a vertical position weld. The CVN curves for this class of weld metal, shown in Figure 8, indicate a lower bound CVN value of 42 ft lbs at the LAST for weldment just meeting the 20 ft lbs at -60° F minimum specification. Figure A-3 indicates that 42 ft lbs (CVN) corresponds with about 2000 ft lb inches, 1 inch DTE, or 250 ft lbs -5/8 inch DTE. This is in agreement with the 260 ft lb value mentioned above. Corresponding K_{Id} estimates are listed in Table 3. The K_{Im} value is based on the NDT estimate of Figure 7 and the K_{Im}/σ_{Yd} reference curve of Figure A-2.

Results for a large number of HY-130 welds of the Mil-140S weld metal GMA type are summarized in Figure 9. The lower bound is an indication of the poorest quality encountered in practice. These results are for 2 inch DT specimens. Estimates of the corresponding 5/8 inch DT behavior are obtained by shifting the curve about 40° F(33) and reducing the energy by a factor of 22.6. These results suggest a lower bound of 340 ft lbs 5/8 inch DTE at the LAST and a maximum NDT temperature of about -60° F. The 340 ft lbs value is significantly lower than 500 ft lbs @ 30° F specified minimum for this type of weld metal (see Table 2). The corresponding K_{Id} estimate (Correlation 1) and K_{Im} estimate (Figure A-2) are listed in Table 3.

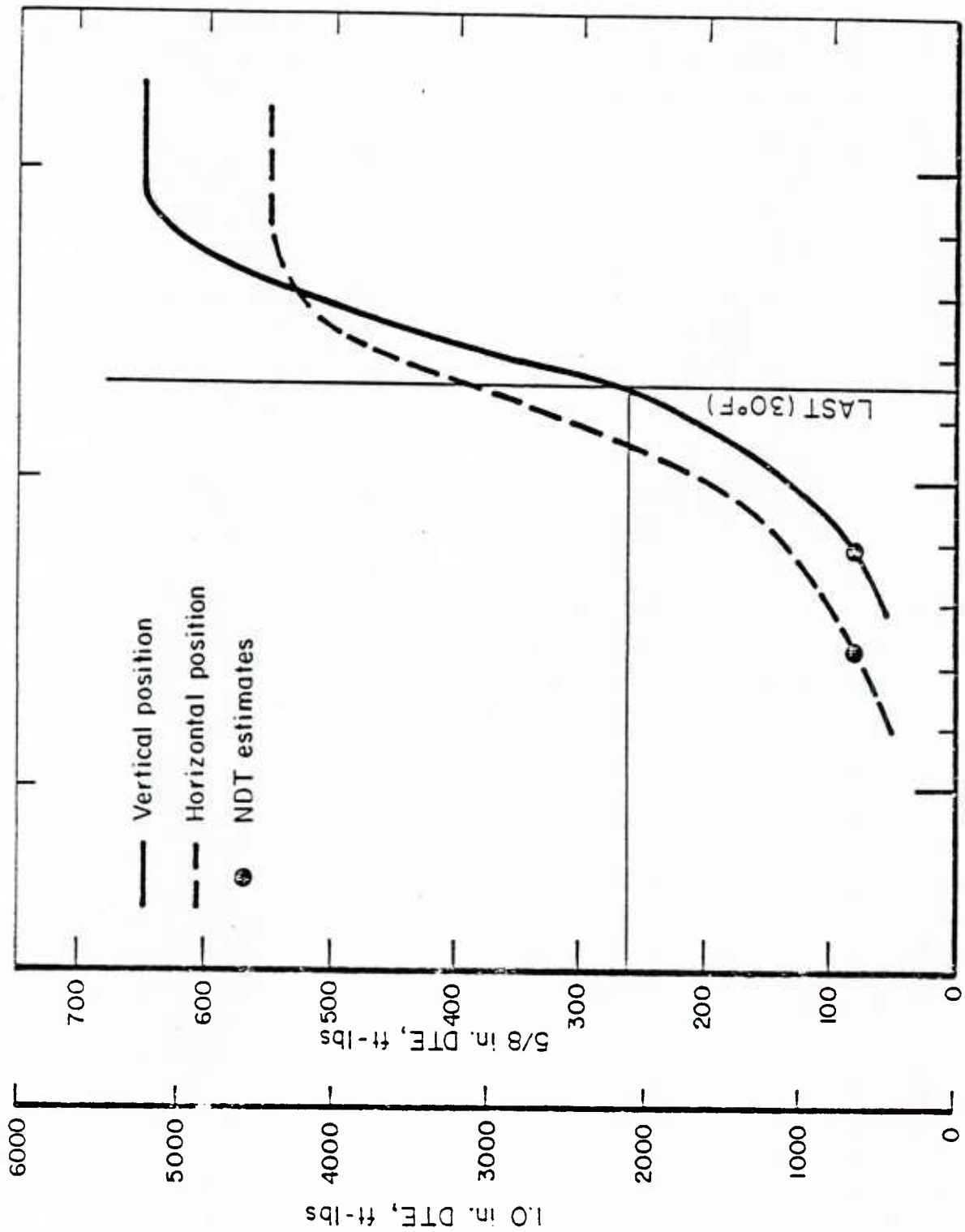

FIGURE 7. LOWER BOUND (IN TERMS OF TOUGHNESS) 1 IN. DTE CURVES FROM A LIMITED SAMPLING OF MIL 11018 WELDS PRODUCED BY THE PORTSMOUTH AND NSRDC-A FACILITIES AFTER PELLINI(33). THE NDT ESTIMATES ARE BASED ON CORRELATION 8 (TABLE 1).

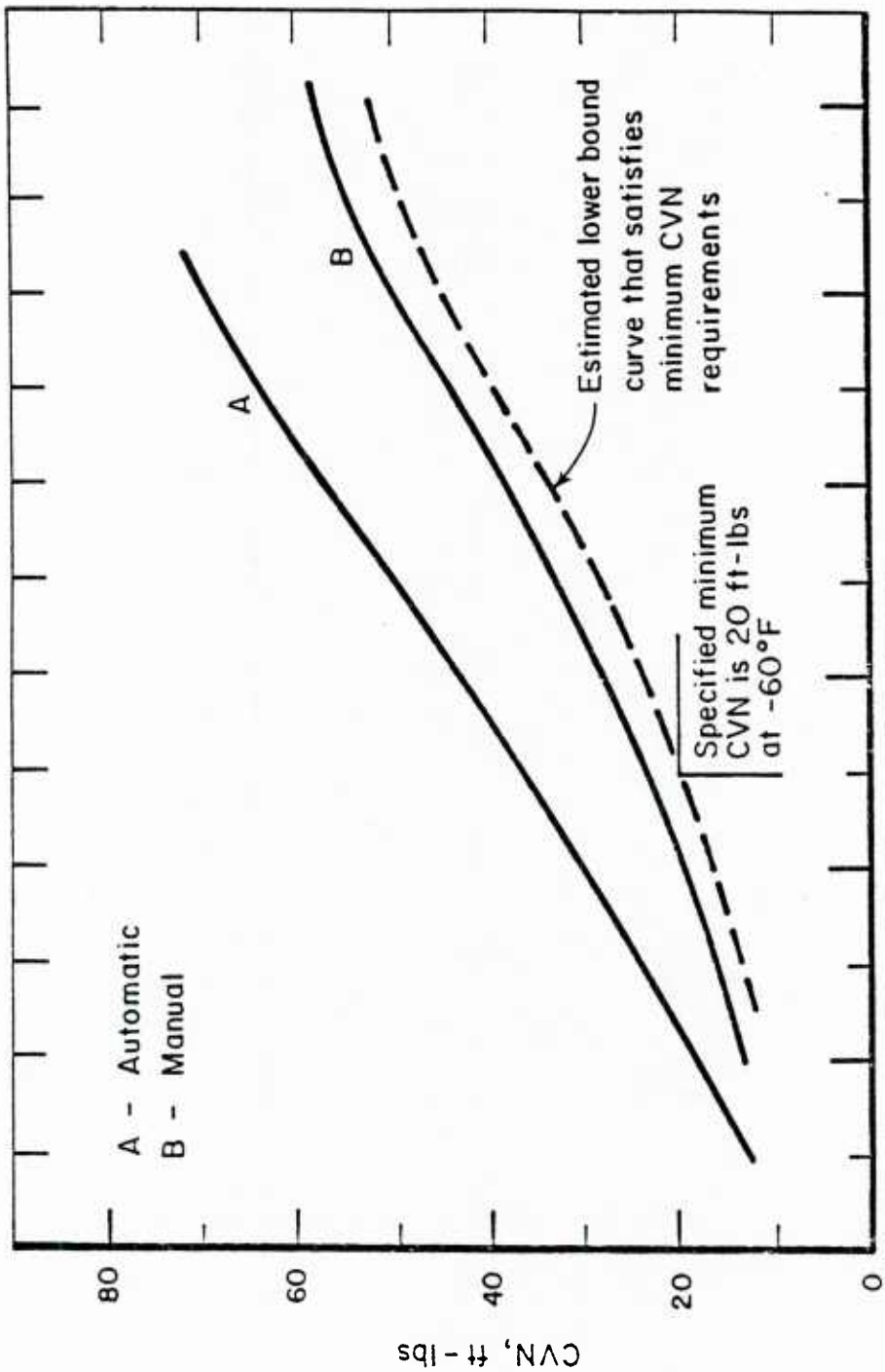

FIGURE 8. CVN CURVES FOR HY-80 WELD D METAL FOR (A) MIL-B-88 AUTOMATIC INERT-GAS-SHIELDED METAL ARC WELD AND (B) MIL-11018 MANUAL WELD DEPOSITS

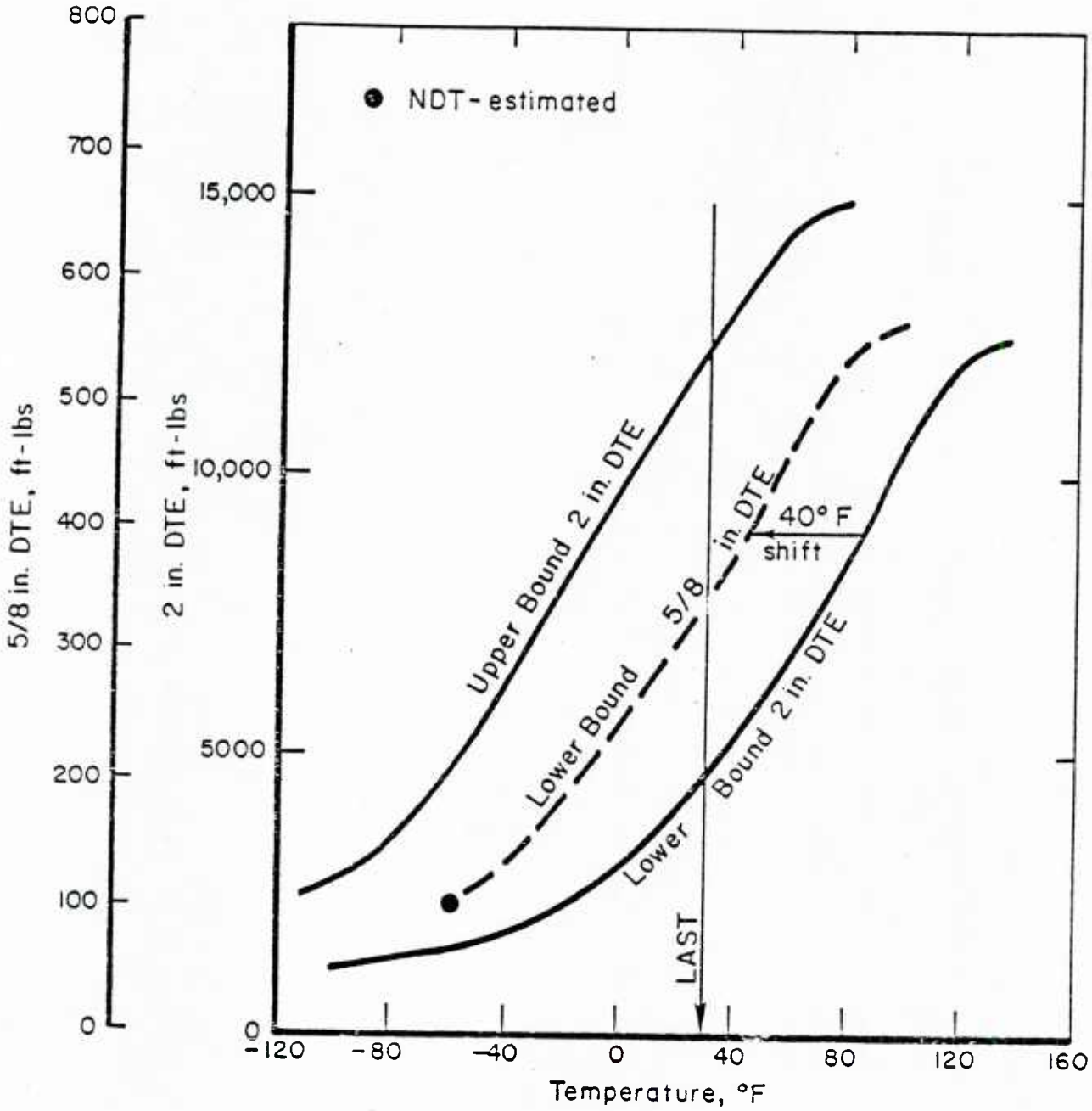

FIGURE 9. ENVELOPE OF 2 IN. DTE VALUES FOR HY-130 TYPE GMA WELDS AFTER LANGE(34,35). THE NDT ESTIMATE IS BASED ON CORRELATION 8 IN TABLE 1

DISCUSSION OF FINDINGS

The lower bound K_{Id} values for the HY-80 and HY-130 steel and weld metals, listed in Table 3, tend to fall short of the toughness levels of 200 $MPam^{1/2}$ - 300 $MPam^{1/2}$ that are usually associated with ductile, shelf-level performance. This may be a consequence of the lack of direct measurements for these materials near the LAST, which forces reliance on approximate (and possibly conservative) DTE and CVN correlations, whose precision for HY-grades and steels under high toughness levels is not well established. Some indication of the uncertainty connected with the NRL-DTE-K_{Ic} correlation can be found in Appendix A.

Where minimum toughness levels are specified in terms of CVN-values, the approximate nature of the CVN-DTE correlation tends to reduce lower bound estimates of K_{Id} via DTE even further. The K_{Im} estimates in Table 3 are particularly uncertain and speculative. No K_{Im} measurements are available for HY-grades that can be used to test the reference curve procedure. In addition, the K_{Id} estimates do not reflect the rising resistance to fracture with crack extension (R-curve behavior). The positive $\dot{K}$-dependence, which adds significantly to load carrying capacity when such extension proceeds with shelf-level toughness values, is also not included. Finally, the present lower bound estimates were obtained without: (i) the precise criteria, (ii) the statistical treatments of the data, and, in some cases, (iii) the sufficiently large data base, which is essential for critical structural analyses.

Bearing those limitations in mind, it is still instructive to note that approximate lower bound values of K_{Id}/σ_Y are $2\sqrt{in.}$ for HY-80 steel and $1\sqrt{in.}$ for HY-130 steel and the two weld metals. The $2\sqrt{in.}$ K_{Id}/σ_Y value indicates that a 4 inch thick plate of HY-80 satisfies the (YC) criterion (essentially, leak-before-break at general yield), while a $1\sqrt{in.}$ value indicates this criterion is only satisfied by HY-130 and the two weldments for 1 inch thick plate. It would therefore appear that the HY-80 plate is substantially more resistant to fracture under dynamic loading than the other three material grades.

The reliability of future calculations of hull-structure fracture behavior under dynamic loading will be enhanced by a better resolution of the K_{Id} and K_{Im} toughness parameters. This will require direct measures of K_{Id} and K_{Im} that can be used to calibrate DTE and CVN values at the LAST. The task of measuring the very large K_{Id} and K_{Im} values is now greatly reduced because K_{Ic} values can be derived from J_{Ic} measurements. These measurements use small test pieces under an ASTM procedure which is close to standardization. Since shelf level K_{Id} values are likely to be 15-25% larger than K_{Ic}*, J_{Ic} values also offer lower bound estimates of K_{Id}.

More research is needed to define the $\dot{K}_I$ dependence of these values, but this should not be a formidable problem. Crack arrest toughness values can also be obtained from J_{Ic} since $K_{Im} \doteq K_{Ic}$ on the shelf. Finally, J_{Ic} determinations can be combined with measurements of the R-curve which offer the possibility of describing stable growth and instability in addition to the onset of crack extension. For weld metal, the existing test procedures make it possible to measure 100 ksi $in.^{1/2} \lesssim K_{Im} \lesssim$ 150 ksi $in.^{1/2}$ in the transition range. Such measurements are needed to establish the reliability of a K_{Im} reference curve based on NDT or other procedures for estimating K_{Im} from more easily measured properties.

---

* Compare shelf-level CVN values for statistically and dynamically loaded specimens in Reference (14).

CONCLUSIONS

A survey of dynamic fracture toughness properties suitable for analyses of crack propagation in submerged ship hulls has been conducted. This survey has concentrated on HY-80 and HY-130 steels and their weld metals at 30° F, the lowest anticipated service temperature (LAST) for these materials. The key findings of the survey are:

1. The HY-80 and HY-130 grades satisfying specified minimum toughness requirements display ductile, shelf-level behavior at the LAST. Weld metals of these grades satisfying minimum toughness requirements operate closer to the lower part of the transition region.
2. A lower bound value of the ratio K_{Id}/σ_Y is estimated to be 2 inches$^{1/2}$ for HY-80 at the LAST. For HY-130 and both the HY-80 and HY-130 weld metals, a lower bound value of this ratio is about 1 inch$^{1/2}$*. It appears from these figures that HY-80 steel is substantially more resistant to fracture under dynamic loading than are the other three grades examined.
3. Lower bound K_{Id} estimates in Table 3 may underestimate the toughness of the HY-steels and weld metals because of the dearth of direct measurements of these quantities and consequent uncertainties in the correlations on which the estimates are based. Lower bound estimates of the crack arrest toughness, K_{Im} in Table 3 are particularly uncertain and speculative because no measurements of this quantity are available for any HY-grades. Direct measurements of K_{Id} and K_{Im} are teasible and should be attempted.

It can be concluded that criteria for "worst-case" lower bound toughness values should be established. These should be applied to statistical treatments of the measurements to improve the definition of lower bound toughness values.

---

* This value is based upon plate purchase to a CVN-60 ft-lb requirement and the CVN-DT Correlation in Figures 6 and A3. If the optional DTE 500 ft-lb at 0°F requirement is used, the minimum K_{Id}/σ_Y ratio for the plate would be 1.6 which is close to a general yield condition for 2 in.-plate.

Also, measurements of shelf value J_{IC} and J_R curves should be performed with the aim of improving and validating the NRL DTE-K_{IC} correlation and to provide more reliable, lower bound estimates of K_{Id} and K_{Im}. Finally, the crack arrest toughness properties of weld metals with toughness levels close to the specified minimum should be measured at the LAST with the aim of establishing a suitable estimation scheme.

REFERENCES

[1] Mall, S., Kohayashi, A. S., and Urabe, Y., "Dynamic Photoelastic and Dynamic Finite Element Analysis of Polycarbonate Dynamic Tear Test Specimens", ASTM STP (To be published)

[2] Kobayashi, A. S., Seo, K., Jou, J. Y., and Urabe, Y., "Dynamic Analyses of Homalite-100 and Polycarbonate Modified Compact-Tension Specimens", Technical Report No. 35 or ONR Contract N00014-76-C-0060 NR 064-478, March, 1979.

[3] Cheverton, R. D., Iskander, S. K., Gehlen, P. C., and Hahn, G. T., "Application of Crack Arrest Theory to a Thermal Shock Experiment, ASTM STP, (To be published).

[4] Hahn, G. T., Hoagland, R. G., Leveim, J., Markworth, A. J., and Rosenfield, A. R., "Fast Fracture and Crack Arrest Toughness of Reactor Pressure Vessel" ASTM STP (To be published).

[5] Kanninen, M. F., "A Critical Appraisal of Solution Techniques in Dynamic Fracture Mechanics", Numerical Methods in Fracture Mechanics A. R. Luxmoore and D. R. J. Owen Eds. Univ. College Swansea, 1978, p. 612.

[6] Popelar, C., Rosenfield, Kanninen, M. F., Pressure Vessel Tech., Vol. 99, p 112, 1977.

[7] Hoagland, R. G., Rosenfiled, A. R., Gehlen, P. C., and Hahn, G. T., "A Crack Arrest Measuring Procedure for K_{Im}, K_{ID}, and K_{IA} Properties ASTM STP 627, p 177, 1977.

[8] Crosley, P. B., Ripling, E. J., "Toward Development of a Standard Test for Measuring K_{IA}", ASTM STP 627, p 372, 1977.

[9] Minutes of the Meetings of the ASTM Task Group, E-24.01.06 on K_{Id} and K_{Ia} Testing.

[10] Low, J. R., Jr., et al, "Rapid Inexpensive Tests for Determining Fracture Toughness, NMATS, 1976.

[11] Judy, R. W., Jr., Freed, C. N., and Goode, R. J., "Characterization of the Fracture Resistance of Thick Section Titanium Alloys", Proceed. Second Int. Conf. on Titanium Science and Technology, Vol. 2 p 1393, 1973.

[12] Freed, C. N., and Goode, R. J., "Correlation of Two Fracture Toughness Tests for Titanium and Ferrous Alloys, NRL Report 6740, 1969.

[13] Freed, C. N., Goode, R. H., and Judy, R. W., Jr., "Comparison of Fracture Toughness Test Procedures for Aluminum Alloys", Eng'g Fract. Mech., Vol. 2, p 359, 1971.

[14] Baosom, J. M., and Rolte, S. T., "Correlation Between K_{Ic} and Charpy V-Notch Test Results in the Transition-Temperature Range", ASTM STP-466, p 281, 1970.

[15] Barson, J. M., Development of the AASHTD Fracture Toughness Requirements for Bridge Steels, Eng'g. Fracture Mech., Vol. 7, p 605, 1975.

[16] Marandet, B., and Sanz, G., Evaluation of the Toughness of Thick Medium Strength Steels by Using Linear Elastic Fracture Mechanics and Correlations Between K_{Ic} and CVN, ASTM STP, 1977.

[17] Irwin, G. R., "Linear Fracture Mechanics, Fracture Transition, and Fracture Control", Eng'g. Fract. Mech., Vol. 1, p 241, 1968.

[18] Pellini, W. S., "Advances in Fracture Toughness Characterization Procedures and in Quantitative Interpretations to Fracture-Safe Design for Fracturesafe Design for Structural Steels, NRL Report 6713, Apr., 1968.

[19] Lange, E. A., "Dynamic Fracture Resistance Testing and Methods for Structural Analysis, NRL Report 7979, Apr., 1976.

[20] Pellini, W. S., "Introduction to AAR Guidelines for Fracture-Safe Design Involving Temperature-Transition Sensitive Steels", Report to AAR on Project No. H-001, Apr., 1979.

[21] Rice, J. R., "A Path Independent Integral and the Approximate Analysis of Strain Concentration by Notches and Cracks", J. App. Mech., Vol. 35, p 379, 1968.

[22] Hahn, G. T. (Unpublished work)

[23] Rice, J. R., and Johnson, M. A., "The Role of Large Crack Tip Geometry Changes in Plane Strain Fracture", Inelastic Behavior of Solids, ed. M. F. Kanninen, et al, McGraw Hill, p 641, 1970.

[24] Shoemaker, A. K., Rolfe, S. T., "The Static and Dynamic Low-Temperature Crack-Toughness Performance of Seven Structural Steels", Eng'g. Fract. Mech., Vol. 2, p 319, 1971.

[25] Barsom, J. M., "Relationship Between Plane Strain Ductility and K_{Ic} for Various Steels", Paper No. 71-PVP-13, 1st National Congress on Pressure Vessels on Piping, San Francisco, 1971.

[26] Puzak, P. P., "Comments and Justifications for Proposed Changes for MIL-S-16216H (SHIPS), NRL Memo, 31 July, 1971.

[27] Goode, R. J., Huber, R. W., Howe, D. G., Judy, R. W., Jr., Puzak, P. P., Lloyd, K. B., Crooker, T. W., Morey, R. E., Lange, E. A., and Freed, C. W., "Metallurgical Characteristics of High Strength Structural Materials NRL Report 6405, Nov., 1965.

[28] Puzak, P. P., "Explosion-Bulge Test Performance of Machine Welded 1-inch thick HY-80 Steel, NRL Memo Report 691, Apr. 1957.

[29] Puzak, P. P. and Babecki, A. J., Explosion Bulge Test Performance of HY-80 Weldments, NRL Memo Report 878, Dec., 1958.

[30] Babecki, A. J., and Puzak, P. P., "Notch Toughness Evaluations of Modified HY-80 Steel in Heavy Gauge Plates, NRL Memo Report 995, Dec., 1959.

[31] Pense, A. W., "Fracture Toughness of Bridge Steels, Phase III Report: State of the Art of Fracture Toughness Testing of Weldments", Report FHWA-RD-760-109, Aug., 1973.

[32] Puzak, P. P., "Summary of Transition Temperature Data for the HY-130 Steel Weldment System", NRL Memorandum Report 2154, July, 1970.

[33] Pellini, W. S., Summary of DT Test Data for HY-130/140 Welds and 11018 Welds, NRL Memo, 5 April, 1973.

[34] Lange, E. A., Characterization of 2-In., HY-130 Welds, NRL Program Report, Mid. FY 1976, 27, 29, Jan., 1976.

[35] Lange, E. A., Characterization of 2-In. Thick HY-130 Welds, NRL Program Report, FY-76 and FY-Q, 2 Dec., 1976.

[36] Pellium, W. S., and Puzak, P. P., "Factors that Determine the Applicability of High Strength Quenched and Tempered Steels to Submarine Hull Construction, NRL Report 5892, Dec. 5, 1962.

[37] Babecki, A. J., and Puzak, P. D., Explosion Test Performance of Small-Scale Submarine Hull Weldments, NRL Memorandum Report 996, Dec. 1959.

[38] Loss, F. J., and Pellium, "Dynamic Teat Test Definition of the Temperature Transition from Linear Elastic to Gross Strain Fracture Conditions", NRL Report 6787, Nov. 1968.

APPENDIX A

CORRELATIONS BETWEEN FRACTURE TOUGHNESS PARAMETERS AND DTE, NDT, AND CVN

APPENDIX A

CORRELATIONS BETWEEN FRACTURE TOUGHNESS PARAMETERS AND DTE, NDT, AND CVN

The reliability of different correlations between LEFM fracture toughness parameters and DTE, NDT, and CVN values is examined in detail in Reference 10. Some points, which are not treated in that reference, but are important in the context of this report are discussed below.

Correlations with DTE

The data, which were used to construct the NRL DTE-K_{Ic} correlation are identified in Figure A-1. Relatively few measurements were originally performed on medium strength steels in the transition range. The K_{Id} portion of the curve was constructed later, and is based on DTE values at the NDT, and the assumed relation $K_{Id}/\sigma_{Yd} = 0.5$ in.[19], which is approximate. The curve for the A533B steel is based on 5/8 in.-DTE measurements performed at NRL[37], and K_{Ic} measurements on a number of (different) heats of [533B in Reference 7. The K_{Ic} values predicted by the A533B curve are about 20-30% smaller than the one obtained from the NRL curve. To be conservative, the A533B curve is used to estimate K_{Ic} and K_{Id} values on this report.

Correlation with NDT

The concept of indexing the toughness transition curve to the NDI temperature, which has been championed by Pellini, is widely used. Recently, Pellini has proposed a K_{Id} reference curve for medium strength steels indexed to the NDT[20]. Pellini's curve relates the absolute toughness, K_{Id}, to the relative temperature (T-TNDT). Since the fracture toughness at the NDT-temperature is believed to vary with yield strength[18], an attempt has been made here to make it more general by expressing the relation in terms of K_{Id}/σ_{Yd}, with the value of this ratio $(K_{Id}/\sigma_{Yd})NDT = 0.6\sqrt{in}$. The resulting reference curve is shown in Figure A-2. Estimates of K_{Id} based on the upper bound NDI

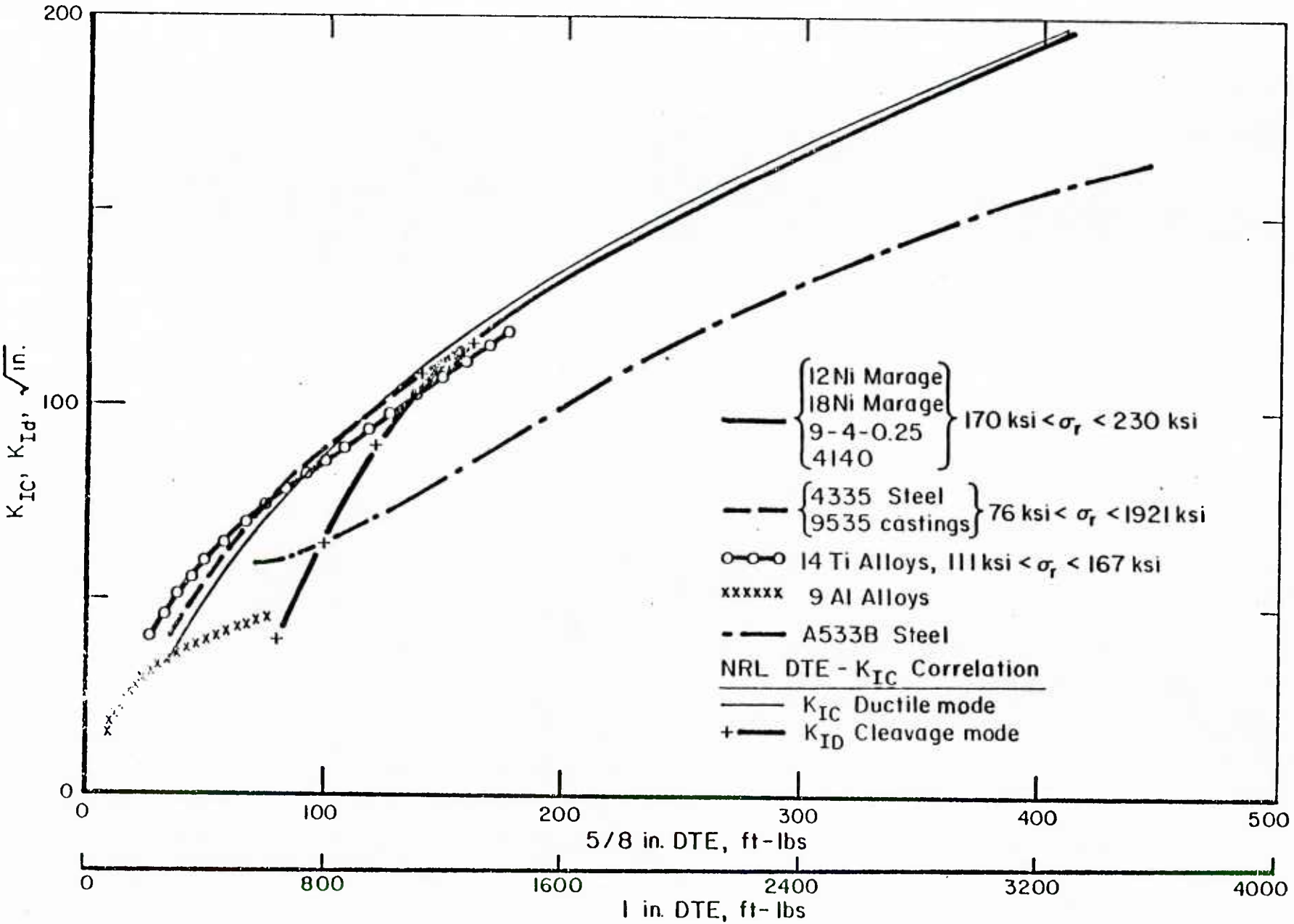

FIGURE A1. SUMMARY OF DATA COMPARING THE NRL DTE K_{IC} CORRELATION(10-13). RESULTS FOR A533B ARE FROM REFERENCE 7 AND 37

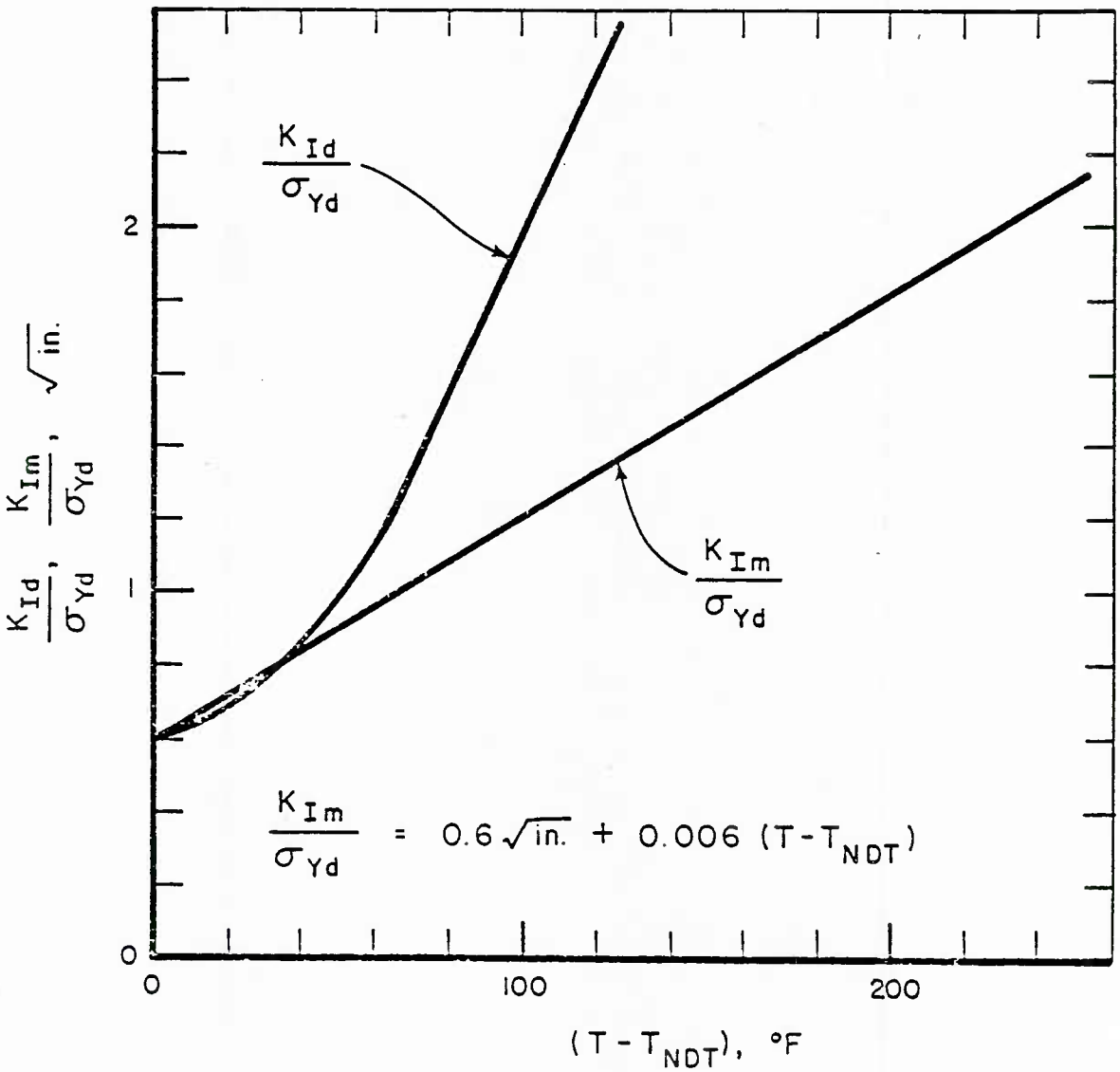

FIGURE A2. PROPOSED "REFERENCE" CURVES RELATING K_{Id} AND K_{Im} TO THE TEMPERATURE RELATIVE TO THE NDT AFTER PELLINI(20) AND HAHN ET AL(7)

and obtained in this way are included in Figures 1 and 3. The same reasoning has been used to generalize K_{Ia} measurements performed on A533B[7]. The K_{Im}/σ_{Yd} reference curve shown in Figure A-2 is based on K_{Ia} values one standard deviations below the average[7]. It should be noted that while this method of estimating K_{Im} is unproven, and speculative, it is the only approach currently available for estimating crack arrest toughness values.

Estimates of σ_{Yd} were obtained using the approximation $\sigma_{Yd} = \sigma_Y +$ 25 ksi, where σ_Y is the conventional yield stress and σ_{Yd} is the yield stress for rates of straining $\varepsilon p \approx 10^3$ sec $^{-1}$.

Correlation with CVN

A correlation between shelf level CVN and DTE values developed at NRL[27] is reproduced in Figure A-3.

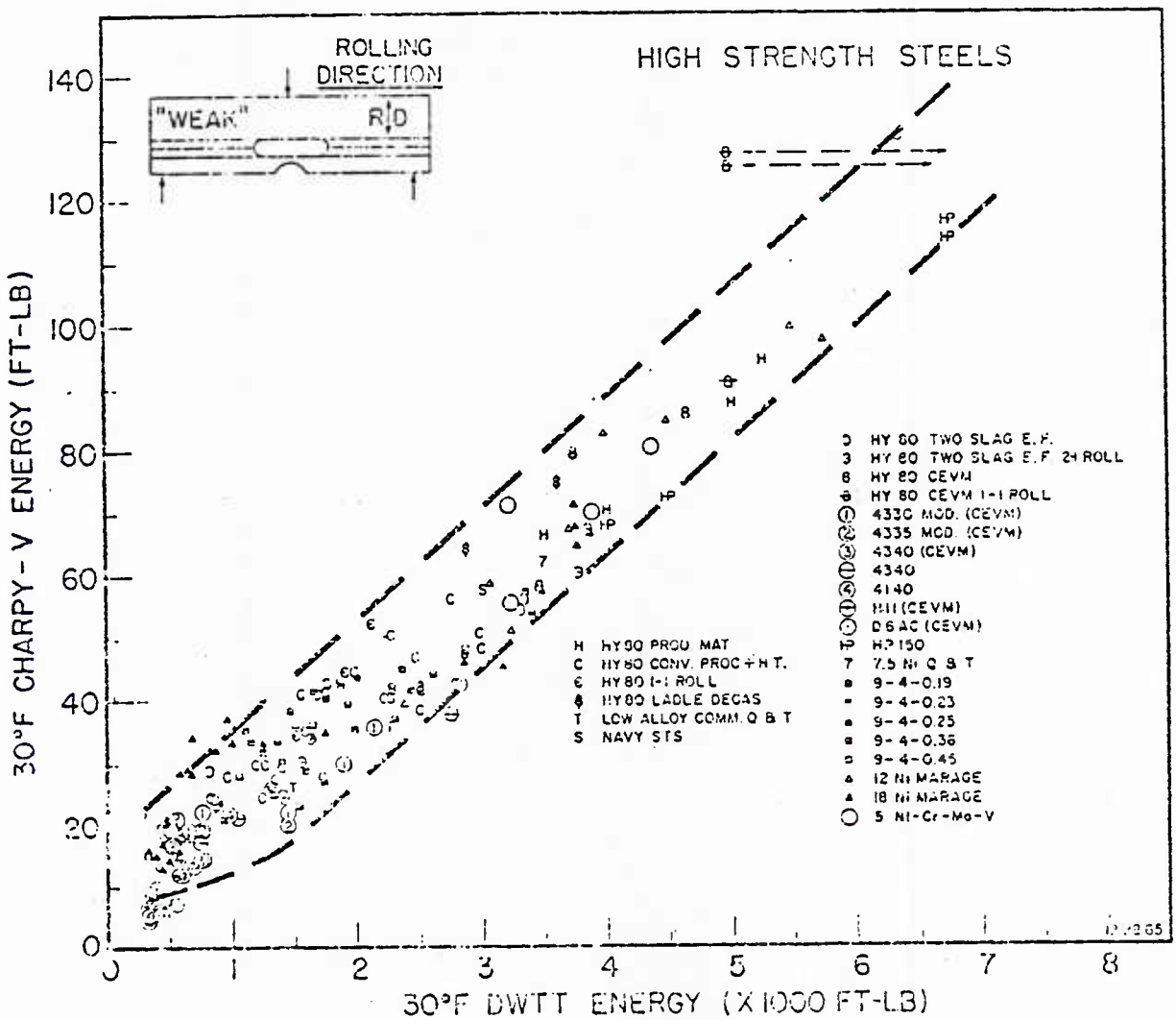

FIGURE A3. CORRELATION OF DWTT AND C_V DATA FOR ALL HIGH STRENGTH STEELS TESTED. THE DATA IS FOR "SHELF ENERGIES" I.E., AT TEST TEMPERATURES WHERE THE FRACTURES ARE FULLY DUCTILE, AFTER GOODE ET AL(27)

APPENDIX B

WELD STRUCTURE

APPENDIX B

WELD STRUCTURE

The toughness of the HAZ (Heat Affected Zone) of a weld (B-1) can be lower than that of the base metal or the weld metal (see Figure B-1). However, because the HAZ is usually narrow, and the weld tapered, a crack initiated in the HAZ of the butt weld will tend to propagate into the base metal or the weld metal. Examples of this for a T-frame attachment are illustrated in Figure B-2. Explosion bulge tests provide further verification that the HAZ does not provide an easy path for a fracture. These considerations provide justification for focusing on the base metal and the weld metal and neglecting the HAZ in lower bound toughness assessments of welded structure.

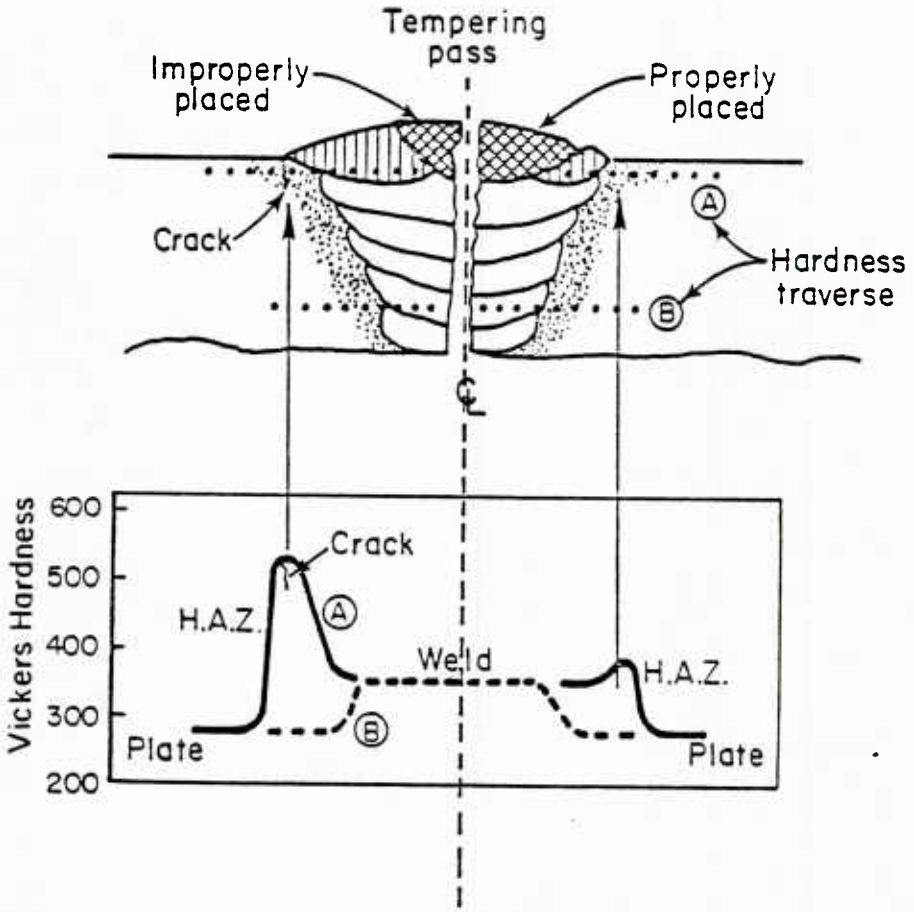

FIGURE B1. SCHEMATIC OF THE STRUCTURE OF A BUTT WELD AFTER PELLINI AND PUZAK(35)

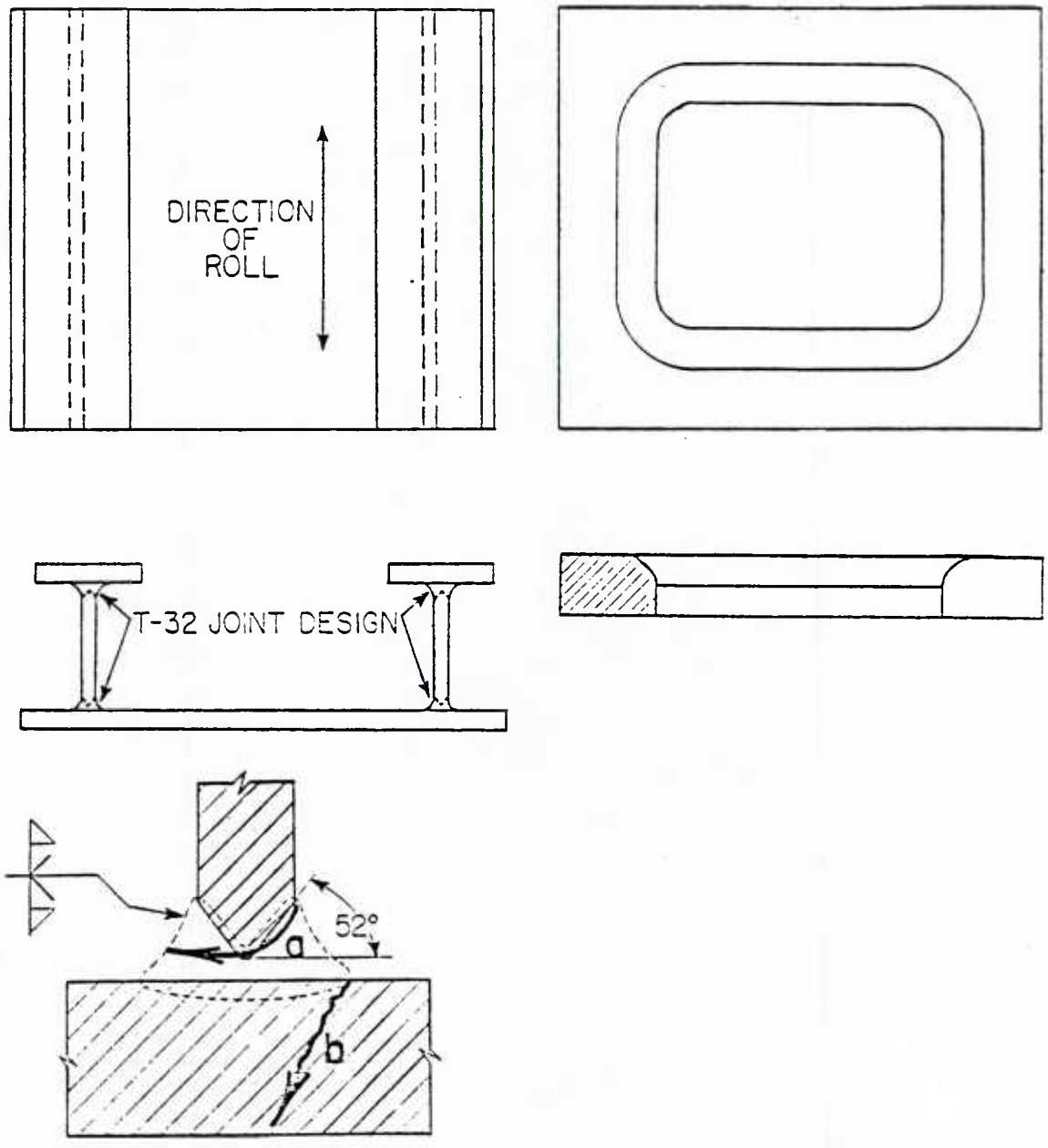

FIGURE B-2. EXPLOSION TEST OF MODEL SIMULATING RESTRAINT OF EXTERNAL FRAMING: SPECIMENS AND WELD JOINT DESIGN (LEFT); CONFIGURATION OF EXPLOSION TEST DIE (RIGHT), AND OBSERVED FRACTURE PATHS ARE IDENTIFIED IN THE LOWER SECTION BY THE LETTER A AND B. THE EXPLOSIVE WAS DETONATED ON THE T-FRAME SIDE OF THE MODEL. AFTER BABECKI AND PUZAK(36)

DYNAMIC CRACK PROPAGATION IN PRECRACKED CYLINDRICAL VESSELS SUBJECTED TO SHOCK LOADING

by

C. H. Popelar
Department of Engineering Mechanics
The Ohio State University
Columbus, Ohio

P. C. Gehlen and M. F. Kanninen
Applied Solid Mechanics Section
Battelle
Columbus Laboratories
Columbus, Ohio

August, 1979

Submitted for presentation in the Computer Technology Session, ASME Pressure Vessels and Piping Conference, San Francisco, August 12-15, 1980

Unclassified

SECURITY CLASSIFICATION OF THIS PAGE *(When Data Entered)*

REPORT DOCUMENTATION PAGE		READ INSTRUCTIONS BEFORE COMPLETING FORM
1. REPORT NUMBER	2. GOVT ACCESSION NO.	3. RECIPIENT'S CATALOG NUMBER
4. TITLE *(and Subtitle)* DYNAMIC CRACK PROPAGATION IN PRECRACKED CYLINDRICAL VESSELS SUBJECTED TO SHOCK LOADING		5. TYPE OF REPORT & PERIOD COVERED Interim 6. PERFORMING ORG. REPORT NUMBER
7. AUTHOR(s) C. H. Popelar, P. C. Gehlen, and M. F. Kanninen		8. CONTRACT OR GRANT NUMBER(s) N00014-77-C-0576- Battelle
9. PERFORMING ORGANIZATION NAME AND ADDRESS The Ohio State University, Columbus, OH 43210 Battelle Columbus Laboratories, Columbus, OH 43201		10. PROGRAM ELEMENT, PROJECT, TASK AREA & WORK UNIT NUMBERS
11. CONTROLLING OFFICE NAME AND ADDRESS Office of Naval Research Structural Mechanics Program Dept. of the Navy, Arlington, VA 22217		12. REPORT DATE August 1979 13. NUMBER OF PAGES 7
14. MONITORING AGENCY NAME & ADDRESS*(if different from Controlling Office)*		15. SECURITY CLASS. *(of this report)* Unclassified 15a. DECLASSIFICATION/DOWNGRADING SCHEDULE

16. DISTRIBUTION STATEMENT *(of this Report)*

Approved for public release; distribution unlimited

17. DISTRIBUTION STATEMENT *(of the abstract entered in Block 20, if different from Report)*

18. SUPPLEMENTARY NOTES

Submitted for presentation in the Computer Technology Session, ASME Pressure Vessels and Piping Conference, San Francisco, August 12-15, 1980

19. KEY WORDS *(Continue on reverse side if necessary and identify by block number)*

dynamic fracture toughness
elastodynamic crack propagation
crack arrest
finite difference grid

20. ABSTRACT *(Continue on reverse side if necessary and identify by block number)*

Previous work has shown that a speed-independent dynamic fracture toughness property can be used in an elastodynamic analysis to describe crack initiation and unstable propagation under impact loading. In this paper, a further step is taken by extending the analysis from simple laboratory test specimens to treat more realistic crack-structure geometries. A circular cylinder with an initial part-through wall crack subjected to an impulsive loading on its inner surface is considered. The crack is in a radial-axial plane and has its length in the axial direction long enough that a state of plane strain exists at the center of

DD FORM 1 JAN 73 1473 EDITION OF 1 NOV 65 IS OBSOLETE
S/N 0102-LF-014-6601

Unclassified

SECURITY CLASSIFICATION OF THIS PAGE *(When Data Entered)*

the crack. Crack growth initiation and propagation through the wall is then calculated. It is found that, once initiated, crack propagation will continue until the crack penetrates the wall. Crack arrest within the wall does not appear to be possible under the conditions considered in this paper.

ABSTRACT

Previous work has shown that a speed-independent dynamic fracture toughness property can be used in an elastodynamic analysis to describe crack initiation and unstable propagation under impact loading. In this paper, a further step is taken by extending the analysis from simple laboratory test specimens to treat more realistic crack-structure geometries. A circular cylinder with an initial part-through wall crack subjected to an impulsive loading on its inner surface is considered. The crack is in a radial-axial plane and has its length in the axial direction long enough that a state of plane strain exists at the center of the crack. Crack growth initiation and propagation through the wall is then calculated. It is found that, once initiated, crack propagation will continue until the crack penetrates the wall. Crack arrest within the wall does not appear to be possible under the conditions considered in this paper.

NOMENCLATURE

a	crack length, mm
c_R	Rayleigh wave speed, m/sec
c_o	bar wave speed, m/sec
E	elastic modulus, Pa
G	dynamic strain energy release rate, J/m^2
h	cylinder wall thickness, mm
K_I	dynamic stress intensity factor, $MPam^{1/2}$
K_{Ia}	static crack arrest toughness, $MPam^{1/2}$
K_{ID}	dynamic fracture toughness, $MPam^{1/2}$
K_{Id}	dynamic initiation toughness, $MPam^{1/2}$
K_{Im}	minimum value of K_{ID}, $MPam^{1/2}$
R	cylinder mean radius, mm
T	period of oscillation, μ sec
t	time, μ sec
U	total energy per unit length, J/mm
V	crack speed, m/sec

INTRODUCTION

Fracture mechanics offers significant opportunities for developing failure-safe structures. By relating the fracture-critical flaw sizes at various locations in the structure to the expected applied stresses, more accurate specification of both material toughness requirements and of non-destructive inspection limits will be possible. This must lead towards an effective use of materials without compromising the integrity of the structure. But, first, an extension of the relatively simple fracture mechanics techniques that are now available must be made to treat the materials, geometries, and loading conditions arising in real engineering application.

The specific objective of this work is the development of fracture mechanics analysis procedures for crack growth initiation, unstable propagation and arrest in ship structures subjected to blast loading. Because there are several different aspects of this problem that are beyond current analysis capabilities, a multi-step approach is being followed. A first step was to assess the effect of impact loading in a combined experimental and mathematical analysis program using simple laboratory test specimens. The work reported in this paper extends this work to more complex structures. The results are expected to permit the effects of structural geometry on dynamic crack propagation to be assessed and, in addition, will assist in the design of a critical experimental test of the validity of dynamic fracture mechanics predictions under shock loading conditions.

PRELIMINARY DISCUSSION

Dynamic fracture mechanics encompasses all problems involving crack growth initiation and subsequent unstable propagation up to and including crack arrest. The methodology was developed to treat problems where, for an acceptable solution, inertia forces must be included in the equations of motion of the cracked body. At present, dynamic fracture mechanics treatments are limited to problems where the basic

assumptions of linear elastic fracture mechanics (LEFM) are valid. The essential assumption in this approach is that the plastic deformation attending the propagating crack tip is small enough to be "dominated" by the elastic deformation in the field surrounding the crack tip. In these conditions, the plastic energy absorbed in the fracture process can be taken as characteristic of the material with the body being treated as completely elastic. Problems of crack growth initiation and subsequent rapid unstable crack propagation can then be solved by using elastodynamically computed stress intensity factors coupled with experimentally determined dynamic fracture toughness values.

The stress intensity factor K_I enters in the computed elastodynamic stress field in the immediate vicinity of the crack tip. It can depend on time t, the crack tip speed, V, the crack length, the external geometry of the cracked body, material constants, and on the applied loads. The conditions governing crack motion in a body can be expressed in terms of $K_I(t,V)$ and experimentally determined critical values that are taken to be properties of the material. Thus, for a propagating crack

$$K_I(t,V) = K_{ID}(V), \qquad (1)$$

where K_{ID} is known as the dynamic fracture toughness. Ordinarily, K_{ID} values will be greater than K_{IC}, although it is possible that K_{Im}, the minimum value of K_{ID}, can be less than K_{IC}.

An equality is sometimes used for crack arrest. This is expressed in terms of K_I and an "arrest toughness" parameter, K_{Ia}. However, while the concept can be useful as an approximation, crack arrest is more rigorously defined as occurring only when Equation (1) cannot be satisfied. That is, the crack will arrest at a time t_a when $K_I < K_{Im}$ for all $t > t_a$. Thus, crack arrest is properly viewed as the termination of a general dynamic crack propagation process, not as a unique event governed solely by material properties. This is the way in which the methodology will be applied here.

Because of the equivalence that exists between them, applications of LEFM can be made either in terms of the stress intensity factor or the energy release rate parameter G. That is, for plane strain conditions

$$G = \frac{1-\nu^2}{E} A(V) K_I^2 , \qquad (2)$$

where A(V) is a universal geometry-independent function that is unity at zero crack speed, and increases monotonically to become unbounded as $V \to c_R$, where c_R is the speed of Rayleigh waves in the material. For most practical situations, A(V) can be taken as equal to one.

In addition to the work reported by Kanninen, et al (1), other applications which illustrate the necessity of a dynamic approach have been given by Hahn, et al (2,3). Specifically, a series of thermal shock experiments performed on axially-cracked thick-walled cylinders at the Oak Ridge National Laboratory (4) were analyzed. It was found that the predictions were in quite good agreement with the measured distances of crack propagation prior to arrest. These experiments produced only short crack jump lengths (e.g., penetration to 14% of the wall thickness) and for these a quasi-static approach would also be acceptable. However, for conditions which would produce much larger penetrations, a significant difference was found. Specifically, for a postulated reduced fracture toughness in which a quasi-static calculation would predict crack arrest at a penetration equal to 71% of the wall thickness, the dynamic fracture mechanics calculation of Reference 3 revealed that the crack would completely penetrate the wall.

The growth of a part-through wall crack is generally a three-dimensional problem. An effective simplifying approach is to assume a plane strain idealization; e.g., considering an initial part-through wall flaw to have a much greater length in the direction parallel to the surface of the wall than in the thickness direction. This approach was successfully taken in the finite-difference computation for a run-arrest event in a thermally shocked pressure vessel with an internal part-through wall crack reported in Reference (3). This method has been extended here to take account of rapidly applied loading for application to structures under impact loading.

The following analyses have two primary purposes. The work reported in Reference (1) has demonstrated that the elastodynamic crack propagation and crack arrest methodology can be applied to impact-loaded dynamic tear test specimens. It is therefore desirable to study rapid fracture and crack arrest in an impulsively loaded component that is more realistic than a simple laboratory specimen. Second, because there is a lack of information on stress intensity factors for impulsively loaded structures, these analyses will provide useful quantitative predictions of the magnitude of the impulsive loading required to initiate crack propagation in a precracked or flawed cylindrical vessel. It is expected that this information can be used to design a critical test of the methodology.

ANALYSIS AND RESULTS

The Computational Model

The objectives of immediate interest are to determine the magnitude of the impulsive loading that will initiate propagation of a part-through crack in the wall of a cylindrical vessel and to determine whether or not this crack will arrest before it penetrates the wall. The particular loading envisioned here is an intense pressure spike. The duration of the spike will be much smaller than the fundamental period of oscillation of the cylinder to constitute an impulsive or a shock loading.

The cylindrical vessel to be addressed in the following is depicted in Figure 1. It consists of a

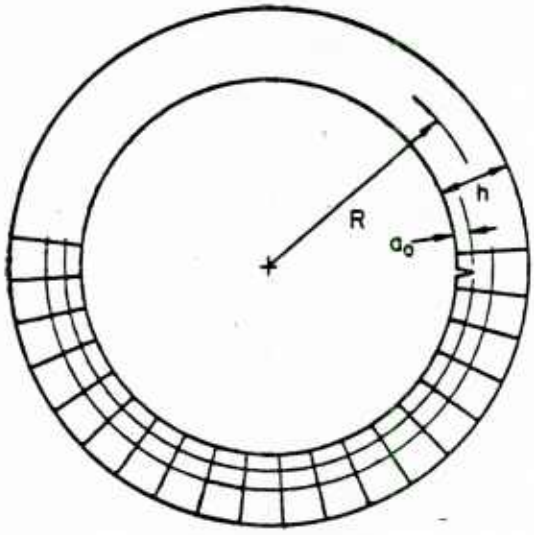

Figure 1. Cracked Cylinder with Finite Difference Grid

very long circular cylinder of mean radius R and wall thickness h. A part-through wall crack of depth a_o is assumed to exist at the inside surface of the cylinder. The length of the crack, like the cylinder, is taken to be long enough for plane strain conditions to be valid. This type of crack clearly poses a more severe condition than one with a finite axial length. An internal flaw is considered.

The loading is a uniform internal impulsive pressure. The reason for selecting an internal pressure over an external pressure is also one of convenience. The internal loading immediately causes the crack to open. By contrast, if an external impulse were applied, the cylinder would have to experience half an oscillation before any crack opening would occur. Hence, the internal loading requires less computer time. Also, the danger of buckling the cylinder is reduced.

This analysis is restricted to conditions where the time required for a longitudinal wave to propagate through the wall is small compared to the fundamental period of oscillation of the cylinder. Hence, it applies when the thickness of the cylinder is small compared to its radius. However, even though the cylinder is a thin shell, it does not follow that classical shell theory is applicable to the present problem.

The net effect of an impulsive loading on a thin cylinder is to impart a nearly uniform radial velocity v_o to its walls. (This condition is frequently assumed when analyzing impulsive loading of thin shells.) Under such a loading, the cylinder will respond by oscillating in essentially the breathing mode with superimposed low frequency flexural modes. Had an initial velocity imparted only to the inside surface been considered, then higher frequency modes would have been excited. Computations for the latter case showed that the period of these higher modes is small compared to the fracture event. While they can be included, they do little more than cloud the understanding of the fracture phenomenon. Furthermore, these high frequency modes would be the first to be damped out and, hence, can also be neglected on this basis.

The Solution Procedure

In common with the work presented in Reference (1), the approach is within the confines of LEFM with inertia effects included. The finite difference method is used to integrate the equations of motion expressed in terms of the nodal displacements[1]. The finite difference grid is depicted in Figure 1. It can be seen that, because of the symmetry with respect to the diametrical plane containing the crack, only half the cylinder need be analyzed. The faces of the crack may open up but they are prevented from penetrating each other. The stress intensity factor is determined from (2) using the energy release rate calculated from the displacements at the nodes in the near vicinity of the crack tip.

At time t = 0, each node is given only a radial initial velocity v_o. The impulse per unit of surface area is

$$I = \rho h v_o \tag{3}$$

where ρ is the density of the material. The equations of motion are solved with stepwise increasing time with the fracture criterion, Equation (1), being tested in each time step. When the fracture criterion is satisfied, the crack is permitted to advance one half of the radial nodal spacing. For the computations described herein, the number of nodes through the thickness was kept constant at thirteen. The number of nodes in the circumferential direction was selected to keep the aspect ratio (the ratio of the radial grid dimension to the circumferential grid dimension) of the grid at approximately 0.04. Favorable results have been obtained previously for this aspect ratio.

[1] A detailed description of the method appears in Reference (2) with an abbreviated account given in (3).

Computational Results for a Stationary Crack

Figure 2 shows the variation of the calculated

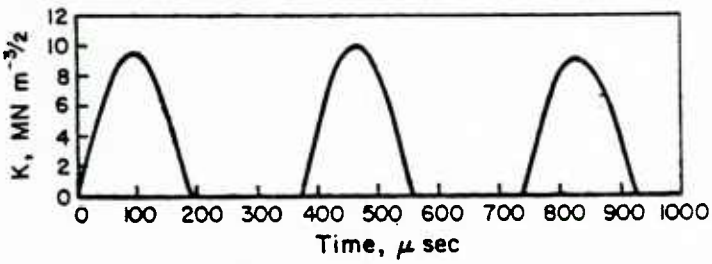

Figure 2. Stress Intensity Factor Versus Time For A Stationary Crack

stress intensity factor with time for an impulsively loaded steel cylinder for a stationary crack. These results are for R = 305-mm, h = 26-mm, a_o = 6-mm, and v_o = 1m/s. Note that the intervals where K = 0 correspond to the closing of the crack. Of most importance is the maximum stress intensity factor (K_{max} = 9.5 MNm$^{-3/2}$ in this instance) determined in this way. This value is required in order to determine the minimum load necessary to initiate crack propagation.

The period T of oscillation in the breathing mode of an unflawed cylinder is

$$T = \frac{2\pi R(1 - \nu^2)^{1/2}}{C_o} \tag{4}$$

where $C_o = \sqrt{E/\rho}$ is the bar wave speed which is 5000 m/s for steel. For ν = 0.3, the period for R = 305-mm is 365μs. This is very nearly equal to the period of the stress intensity factor in Figure 2. It is also apparent from this figure that, while the amplitude varies slightly, it can be taken as essentially constant. Therefore, subsequent analyses of the stationary crack need only consider the first half period of oscillation to determine reasonable values of K_{max}.

The maximum stress in an unflawed cylinder subjected to a uniform impulsive loading is readily shown to be

$$\sigma_o = \frac{E v_o}{C_o(1 - \nu^2)^{1/2}} \tag{5}$$

which is independent of R/h. The maximum stress intensity factor can be related to σ_o by a relation valid in quasi-static conditions. This is

$$K_{max} = \sigma_o \sqrt{\pi a_o}\, f(a_o/h, R/h) \tag{6}$$

where f is a function of the geometry of the flawed cylinder. In Table 1 the computed K_{max} values for various geometries are shown. These have also been

Table 1. Computational Results For A Stationary Crack In An Impulsively Loaded Radially Cracked Cylinder

R/h	K_{max} [MN/m$^{3/2}$]	σ_{max} [N/mm^2]	$\frac{K_{max}}{\sigma_o\sqrt{\pi a_o}}$	$\frac{\sigma_{max}}{\sigma_o}$
		$a_o/h = 0.23$		
11.7	9.44	50.1	1.70	1.24
30.	9.40	49.5	1.69	1.22
60.	9.42	49.4	1.70	1.22
		$a_o/h = 0.46$		
11.7	14.0	62.5	1.78	1.54
30.	14.5	62.7	1.85	1.55

normalized with respect to $\sigma_o\sqrt{\pi a_o}$. It appears from these results that the normalized stress intensity factor is virtually independent of R/h for these thin walled cylinders. Hence, for design purposes, it could be considered that

$$K_{max} = 1.75 \frac{E}{(1-\nu^2)^{1/2}} \frac{v_o}{C_o} (\pi a_o)^{1/2} \qquad (7)$$

where the result given in Table 1 has been used.

The maximum stress intensity factor also appears to be nearly independent of a_o/h. However, only relatively small values of a_o/h were used here and it is likely that the edge effect is small in this range. Results for steady state vibrations of center-crack plates and an infinite plane with a periodic system of cracks--see Reference (5)--also indicate that edge effects do not become significant until $a_o/h > 0.6$. For larger values of a_o/h, $K_{max}/\sigma_o\sqrt{\pi a_o}$ would be expected to be greater than the value found here.

Table 1 also shows the maximum stress attained at the point two nodes (4-mm) ahead of the crack tip. This value is denoted as σ_{max}. Here again, there is only a slight dependence on R/h. But, σ_{max} does depend upon a_o/h. By comparing σ_{max} to the yield stress, these results can be used to predict the maximum impulse that would satisfy the conditions of LEFM.

Computational Results for Unstable Crack Propagation

For the same initial loading, the computations for a stationary crack show that K_{max} increases with increasing crack depth. If crack propagation were to initiate, it would therefore appear that the crack would be propagating in an increasing K field. Under such circumstances the crack would not arrest, but would certainly penetrate the wall. On the other hand, the impulsive loading only imparts a finite amount of energy to the cylinder. And, as the crack propagates, it must consume some of this energy in the fracture process. Hence, there is a question as to whether or not this energy loss is sufficient to reduce the amplitude of the stress intensity factor sufficiently to arrest the crack. This question can be properly addressed only with a dynamic analysis.

A quarter-through-wall crack is frequently taken to be minimum identifiable crack length. If, for reasons of safety, cracks exceeding half the wall thickness are deemed not permissible, a question of concern is whether or not a quarter-through wall crack which initiates will arrest before it propagates half way through the wall. To study this question, assume that the material has a speed independent toughness $K_{ID} = K_{Ic}$ and the amplitude of the final stress intensity factor is K_{ID}; i.e., the crack just arrests. A balance of energy per unit length requires that

$$U_o - U_f = \frac{K_{ID}^2(1-\nu^2)}{E} (a_f - a_o) \qquad (8)$$

where U denotes the total energy per unit length and the subscripts o and f are used to denote initial and final quantities. Using (2), the energies can be written as

$$U_o = \pi\rho v_o^2 Rh = \frac{(K_o)_{max}^2 (1-\nu^2)\, Rh}{3.2\, E\, a_o}$$

$$U_f = \frac{K_{ID}^2(1-\nu^2)\, Rh}{3.2\, E\, a_f} \; ; \; \frac{a_f}{h} < 1/2 \; . \qquad (9)$$

Substituting Equations (9) into (8) with $a_o/h = 1/4$ and $a_f/h = 1/2$ gives

$$\frac{(K_o)_{max}}{K_{ID}} = (0.20 \frac{h}{R} + .5)^{1/2} < 1. \qquad (10)$$

But, for the crack to initiate, $K_{ID} < (K_o)_{max}$. However, this is inconsistent with (10)and the hypothesis that the crack arrests. Therefore, this contradiction implies that the crack will not arrest before it propagates half-way through the wall. Because of the impact loading, the crack might initiate with $K_{Id} \leq (K_o)_{max} < K_{ID}$ and no inconsistency would appear. Also, as noted earlier, viscous damping, which could have a significant effect under certain circumstances, is not included.

In order to determine the character of crack propagation in a cylinder under impulsive or shock loading, computations were performed for a steel cylinder of radius R = 305-mm and thickness h = 26-mm having an initial radial crack of depth a_o = 6-mm ($a_o/h = 0.23$). An initial uniform radial velocity of 1m/s was imparted to the cylinder. These are the same conditions upon which the results of Figure 2 are based. The fracture toughness was taken as a speed independent value equal to 98% of the maximum stress intensity factor experienced by a stationary crack for these same conditions; i.e., $K_{ID} = 9.25$ MN/m$^{3/2}$ per unit of initial velocity.

A plot of computed crack length versus time is shown in Figure 3. It can be seen that approximately 84 μ sec are required for the stress intensity to build up to the critical value and to initiate crack growth. During this interval, the variation of the stress intensity factor with time is depicted in Figure 2. After initiation, the crack propagates at a speed of approximately 300 m/s. As the crack tip propagated further into the wall, its speed increases. This reflects the unstable nature of the crack growth. Some 20 μ sec after initiation the crack tip finally penetrated the exterior surface. The speed of the crack tip during the final stages of the event was approximately 2200 m/s.

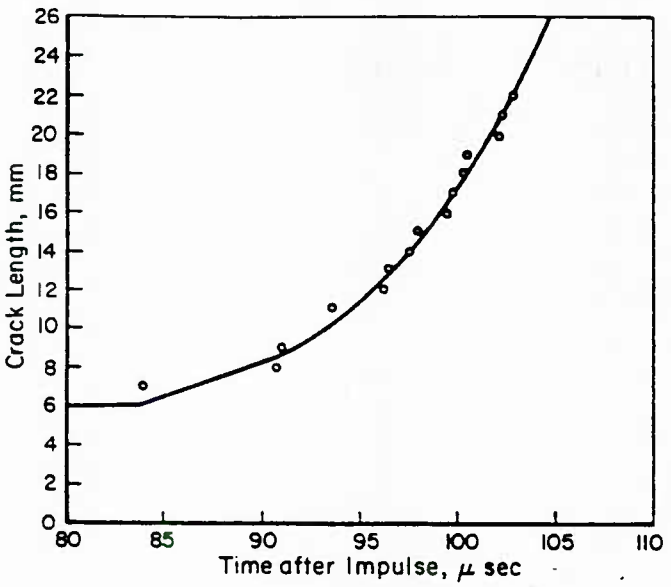

Figure 3. Crack Propagation in Impulsively Loaded Crack Cylinder

For all practical purposes this computation confirms the earlier suspicion that, if growth of an internal crack commences, the crack tip will eventually penetrate the exterior surface. This conclusion is predicated upon the assumption that the material is elastic-brittle and has a crack-speed-independent fracture toughness. In reality, as the remaining ligament becomes sufficiently small, inelastic behavior becomes important. Then, the fracture process is no longer K-dominated as required for LEFM to be applicable. While such inelastic behavior is important and of interest, its consideration is beyond the scope of this paper and is reserved for further research.

CONCLUSIONS

Elastodynamic crack propagation calculations have been performed for a part-through cracked circular cylinder subjected to a uniform impulsive loading. These calculations have demonstrated that, while actual crack-structure geometries are more complicated than are the simple laboratory test specimens previously analyzed, they can be treated effectively with dynamic fracture mechanics. Specifically, for the particular geometry considered in this paper:

1. The minimum impulse required to initiate unstable crack propagation for a given crack depth has been determined in terms of material, mechanical, and fracture properties.
2. Once initiated, crack propagation in the through-wall direction will continue until the crack penetrates the wall--crack arrest within the wall does not appear to be possible.
3. Crack length time predictions can be made for comparison with experimentally measured times of crack growth initiation and of crack penetration.

It is clear that more complicated geometries can be addressed with this analysis procedure (with a corresponding increase in computer costs). However, it should be recognized that the specific conclusions cited are restricted to LEFM conditions and for a material with a relatively constant dynamic fracture toughness.

ACKNOWLEDGEMENT

The work reported in this paper was supported by the Office of Naval Research, Structural Mechanics Division, under Contract Number N00014-77-C-0576. The authors would like to thank Dr. Nicholas Perrone of the ONR for his personal support and encouragement of their work in this area. The authors would also like to thank Dr. Melvin Baron and his colleagues at Weidlinger Associates for providing useful background information on the general problem area.

REFERENCES

1. Kanninen, M. F., Gehlen, P. C., Barnes, C. R., Hoagland, R., Hahn, G. T., and Popelar, C. H., "Dynamic Crack Propagation Under Impact Loading". Nonlinear and Dynamic Fracture, S. Atluri and N. Perrone, editors, ASME publication AMD - Vol. 35, p. 195, 1979.

2. Hahn, G. T., et al, "Critical Experiments, Measurements and Analyses to Establish a Crack Arrest Methodology for Nuclear Pressure Vessel Steels", Progress Report for U.S. Nuclear Regulatory Commission, NUREG/CR - 0057, BMI-1975, May, 1978.

3. Cheverton, R. D., Gehlen, P. C., Hahn, G. T., and Iskander, S. K., "Application of Crack Arrest Theory to a Thermal Shock Experiment", Proceedings ASTM Symposium on Crack Arrest Methodology and Application, Philadelphia, November 6-7, 1978.

4. Emery, A. F., Kobayashi, A. S., Love, W. J., and Jain, A., "Dynamic Propagation of Circumferential Cracks in Two Pipes with Large-Scale Yielding", J. Pressure Vessel Tech., in press, 1979.

5. Parton, V. Z., and Marozov, E. M., Elastic-Plastic Fracture Mechanics, Mir Publisher, Moscow, 1978.

DYNAMIC CRACK PROPAGATION UNDER IMPACT LOADING

by

M. F. Kanninen, P. C. Gehlen, C. R. Barnes,
R. G. Hoagland, G. T. Hahn

BATTELLE
Columbus, Ohio

and

C. H. Popelar
Ohio State University
Columbus, Ohio

June, 1979

Published in

Nonlinear and Dynamic Fracture Mechanics,
N. Perrone and S. N. Atluri, editors
ASME Publication AMD-Vol 35, 1979

REPORT DOCUMENTATION PAGE

READ INSTRUCTIONS BEFORE COMPLETING FORM

1. REPORT NUMBER

2. GOVT ACCESSION NO.

3. RECIPIENT'S CATALOG NUMBER

4. TITLE (and Subtitle)

DYNAMIC CRACK PROPAGATION UNDER IMPACT LOADING

5. TYPE OF REPORT & PERIOD COVERED

Interim

6. PERFORMING ORG. REPORT NUMBER

7. AUTHOR(s)

M.F. Kanninen, P.C. Gehlen, C.R. Barnes,
R.G. Hoagland, C.T. Hahn

8. CONTRACT OR GRANT NUMBER(s)

N00014-77-C-0576 - Battelle

9. PERFORMING ORGANIZATION NAME AND ADDRESS

Battelle Columbus Laboratories, Columbus, OH 43201
Ohio State University, Columbus, OH 43210

10. PROGRAM ELEMENT, PROJECT, TASK AREA & WORK UNIT NUMBERS

11. CONTROLLING OFFICE NAME AND ADDRESS

Office of Naval Research
Structural Mechanics Program
Dept. of the Navy, Arlington, VA 22217

12. REPORT DATE

June 1979

13. NUMBER OF PAGES

15

14. MONITORING AGENCY NAME & ADDRESS (if different from Controlling Office)

15. SECURITY CLASS. (of this report)

Unclassified

15a. DECLASSIFICATION/DOWNGRADING SCHEDULE

16. DISTRIBUTION STATEMENT (of this Report)

17. DISTRIBUTION STATEMENT (of the abstract entered in Block 20, if different from Report)

Approved for public release; distribution unlimited

18. SUPPLEMENTARY NOTES

Published in Nonlinear and Dynamic Fracture Mechanics
N. Perrone and S.N. Atluri, editors
ASME Publication AMD-Vol 35, 1979

19. KEY WORDS (Continue on reverse side if necessary and identify by block number)

dynamic crack propagation
dynamic fracture mechanics
AISI 4340 steel
A533B Steel
dynamic tear testing
ductile fracture
cleavage fracture
elastodynamic analysis

20. ABSTRACT (Continue on reverse side if necessary and identify by block number)

Dynamic crack propagation studies to date have been largely confined to simple laboratory test specimens under quasi-static applied loading conditions. Applications to crack propagation in structural components made of tough ductile materials under service loadings therefore require extension in three relatively unproven areas: when crack growth (1) is initiated under rapidly applied loading, (2) occurs in a geometrically complicated structure, and (3) is accompanied by extensive plastic deformation. As a first step, attention

was focused in this paper on crack initiation and propagation due to impact loading. For this purpose, dynamic tear test experiments on 4340 steel, a high-strength essentially rate-independent material, were performed. These tests were instrumented to determine crack length-time behavior after the dynamic initiation event. Two dimensional elastodynamic computations were performed for comparison with these results. Poor agreement was obtained using dynamic fracture toughness data from conventional quasi-static loading tests. It was instead found that a substantially elevated value of the dynamic toughness was needed to obtain reasonable agreement with the dynamic tear test results.

DYNAMIC CRACK PROPAGATION UNDER IMPACT LOADING

M. F. Kanninen, P. C. Gehlen, C. R. Barnes, R. G. Hoagland, G. T. Hahn
Battelle Memorial Institute
Columbus Laboratories
Columbus, Ohio

and

C. H. Popelar
Ohio State University
Columbus, Ohio

ABSTRACT

Dynamic crack propagation studies to date have been largely confined to simple laboratory test specimens under quasi-static applied loading conditions. Applications to crack propagation in structural components made of tough ductile materials under service loadings therefore require extension in three relatively unproven areas: when crack growth (1) is initiated under rapidly applied loading, (2) occurs in a geometrically complicated structure, and (3) is accompanied by extensive plastic deformation. As a first step, attention was focused in this paper on crack initiation and propagation due to impact loading. For this purpose, dynamic tear test experiments on 4340 steel, a high-strength essentially rate-independent material, were performed. These tests were instrumented to determine crack length-time behavior after the dynamic initiation event. Two dimensional elastodynamic computations were performed for comparison with these results. Poor agreement was obtained using dynamic fracture toughness data from conventional quasi-static loading tests. It was instead found that a substantially elevated value of the dynamic toughness was needed to obtain reasonable agreement with the dynamic tear test results.

INTRODUCTION

It is not always possible to absolutely preclude the initiation of crack growth in a structure containing a flaw. Dynamic fracture mechanics, which focuses on rapid unstable crack propagation, was developed in order to assess the possibility that, even if a crack begins to propagate, it can be arrested without complete severance of the structure. Current dynamic fracture mechanics techniques are somewhat restrictive, however. They are essentially a modest extension of conventional linear elastic fracture mechanics (LEFM) in which (1) inertia forces are included in the equations of motion for the structure, and (2) the fracture toughness property includes a crack-speed dependence. Furthermore, these extensions have been developed and verified only for simple test structure geometries under quasi-static loading conditions.

To be applicable to engineering materials and structural geometries under actual service conditions, further development and verification of dynamic fracture mechanics is needed. Specifically, the methodology must be made to cope with:

- complex flaw-structure geometries
- high-rate impact loading
- crack growth accompanied by extensive plastic yielding

As a step toward this goal, the work reported in this paper is focused on dynamic crack propagation under impact loading.

To minimize the complications involved in a study of impact loading--and to allow the conclusions to be drawn from the results to be as unequivocal as possible--this investigation was focused on a near ideal material and relatively simple specimen geometries. The primary material used was AISI 4340 steel--a well-characterized high strength material which exhibits little rate sensitivity. The approach was to (1) obtain dynamic fracture toughness data from the usual quasi-static initiation tests and (2) to assess the applicability of these data for the dynamic crack propagation in a dynamic tear test. Because 4340 steel satisfies the basic requirements of LEFM, this approach should clearly delineate the effects, if any, of high rate loading on dynamic crack propagation and arrest.

DYNAMIC FRACTURE MECHANICS BACKGROUND

Just as in ordinary fracture mechanics, for dynamic crack initiation and propagation, the remote stresses, the crack length, and the external geometry of the body are all contained in the parameter K_I--the mode I stress intensity factor. The fundamental role of K_I in dynamic fracture mechanics can be put on a rigorous basis provided certain essential conditions are met. This stems from the fact that, in an elastodynamic analysis, the stresses in the near vicinity of the crack tip can always be expressed as

$$\sigma_{ij} = \frac{K_I(\dot{a},t)}{\sqrt{2\pi r}} f_{ij}(\theta,\dot{a}) \qquad (1)$$

where r and θ are polar coordinates denoting the position of a generic point with respect to the moving crack tip and $\dot{a}$ is the crack speed [1].

Note that the omitted terms in Equation (1) are all of higher order in r. Consequently, within some distance R of the crack tip, the lowest order $r^{-1/2}$ term will give a sufficiently accurate estimate of the stresses. Because the elastodynamic strains are still connected to the stresses by the Hooke's law equations, the deformation state for $r < R$ is therefore essentially fixed by Equation (1).

Clearly, the deformation state in the inelastically deformed region that inevitably accompanies crack growth is inaccessible to an elastodynamic treatment. Nevertheless, because it must be directly controlled by the elastic behavior in the material surrounding it, an elastodynamic solution will provide a unique description of the events that accompany crack growth. Moreover, as can be seen from Equation (1), when the maximum size of the inelastic region is less than R, this description can depend only upon K_I and $\dot{a}$. As a direct consequence, when crack growth occurs at a given crack speed, it must do so because a critical value of K_I for that crack speed has been attained. By calling the critical value K_{ID}, this argument leads to the governing expression for elastodynamic crack propagation which, for a given loading and external geometry, can be written

$$K_I(\dot{a},t) = K_{ID}(\dot{a}) \qquad (2)$$

where t denotes time, and as above, $\dot{a}$ is the crack speed. Equation (2) represents the most general form of the governing relation for elastodynamic crack propagation that is now in use[1].

1 Dynamic plastic crack propagation computations are just being developed. For example, Emery, et al [2] have used a crack opening angle criterion for dynamic elastic-plastic crack propagation in a pipe.

A propagating crack must leave behind a wake of plastic deformation. Hence, while Equation (2) may be rigorously valid for initiation and some small amount of crack growth, its validity will certainly be lost in sustained crack propagation. Despite this fact, Equation (2) has been effectively used to describe extensive crack propagation using K_{ID} values that are, to a reasonable approximation, geometry-independent material properties [3]. However, the great bulk of the work that has been performed in this area has been confined to studying dynamic crack propagation initiated under quasi-static applied loads. The work reported in this paper was undertaken to test the effectiveness of this approach for a wider range of conditions via a combination of experimental and mathematical analysis of dynamic crack propagation initiated under impact loading.

Because of the virtual impossibility of devising closed-form elastodynamic solutions for finite sized bodies, numerical solution procedures must be used. In these, a difficulty currently exists in moving the crack tip with its accompaning singularity. To avoid this, a conventional (nonsingular) discrete representation can be used together with an energy release rate criterion for crack growth. This is possible because of the Freund-Niesson relation between K_I and G, the energy release rate parameter. For plane stress conditions, this relation is

$$EG = A(\dot{a})\, K_I^2 \tag{3}$$

where E is the elastic modulus and A is a universal function of crack speed whose value is approximately one for crack speeds of general interest [4]. Use of this approach has been proven in applications to many different kinds of testing conditions [5-7].

EXPERIMENTAL PROCEDURE

The experiments in this investigation primarily used quenched and tempered 4340 steel. For comparison, an A533B reactor steel was also used. The specimen blanks were prepared according to specifications in the ASTM E604-77, Standard Method for Dynamic Tear Testing, with the exception that the slot was prepared by Electric Discharge Machining. The dimensions of the specimen are shown in Figure 1.

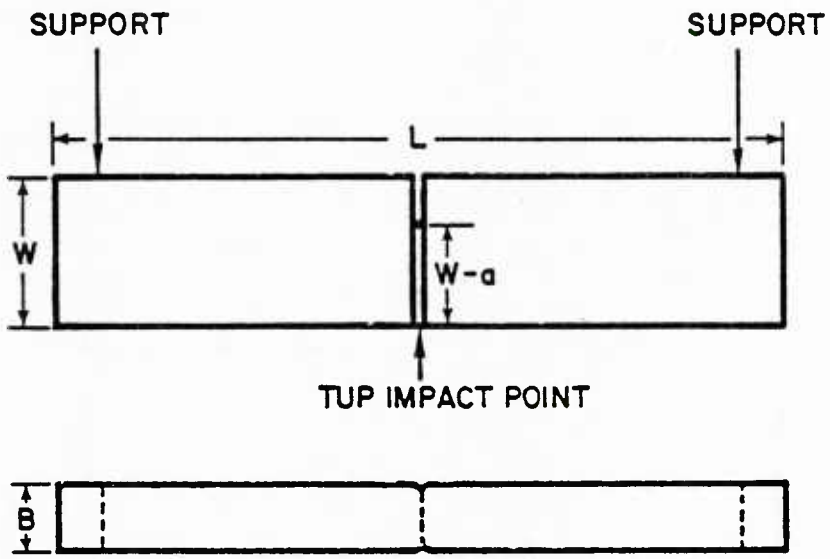

Fig 1. Dynamic tear test specimen geometry
L = 181 mm, W = 38 mm, B = 15.8 mm, W-a = 28.5 mm

Root diameters of .065 mm, 0.13 mm, and 1.27 mm were used to vary the amount of strain energy in the test piece at the instant of crack growth initiation. According to Hahn, et al [8] and to Lareim and Embury [9], the lowest of these root diameters should behave like a sharp fatigue crack[1]. Note also that some specimens had side grooves to a total depth of 25% of specimen thickness (12.5% each side) to control the crack path and to retard the formation of shear lips during crack extension.

To obtain data for comparison with the impact test results, initial dynamic crack propagation tests were performed with quasi-static loading. These tests were conducted using a 100,000 lb capacity Baldwin Universal Testing Machine. The specimens were tested in three point bending with supports as specified in ASTM Standard E604-77. The following parameters were measured with respect to load: (1) load point displacement, (2) crack opening displacement, (3) specimen arm displacement, and (4) strain 1/4 in. to the side and normal to the crack tip at crack initiation using strain gages. The results of these experiments are summarized in Table 1.

Table 1

Experimental Results for Dynamic Crack Propagation Initiated Under Quasi-Static Loading

Slot Root Diameter (mm)	Side Groove depth (%)	K_Q ($MPam^{1/2}$)	Absorbed Energy (Joules)	Crack Length at Arrest (mm)
		4340 Steel		
0.064	25	108	21.7	Complete fracture
0.13	0	191	23.1	15
1.27	0	215	37.8	20
		A533B Steel		
0.064	25	129	841	Complete fracture
0.13	0	112	1440	20

Two tests (one on 4340 steel and one on A533B steel) were interrupted at selected points on the load curve to replicate the notch using a silicon rubber compound (Kerr Citricone). These replicas were used to verify the reading of the clip gage monitoring the crack opening displacement. They also provided an accurate means of determining the load at crack initiation. Ordinarily, this point cannot be easily detected on the load displacement curve.

A machine designed and built by Battelle was used to conduct the impact tests. It is a multi-purpose pendulum-type machine similar in concept to a Charpy machine having a total impact energy of approximately 21,700 Joules. This machine will accommodate a variety of specimen geometries simply by changing the bolt-on supports. Figure 2 shows a photograph of the specimen arrangement used in these tests.

Specimens used in these tests had a grid vapor deposited upon a thin (.05 mm) insulating epoxy layer bonded to the specimen surface to measure the crack speed. Initially, the motion of the specimen was monitored using eddy-current type proximity gages. This feature was eliminated in later tests in favor of an electrical circuit that used the pendulum machine tup as a switch that closed upon contact with the specimen. This method provided the

1 The parameter K_Q is used to denote the apparent value of the stress intensity factor at the onset of crack growth for a blunted slot. If the slot root diameter is small enough, then $K_Q \approx K_{Ic}$ for larger diameters, $K_Q > K_{Ic}$.

time lapse from tup-specimen contact until crack initiation--see Figures 3 and 4. Additionally, some of the specimens had strain gages located 1/4 in. to the side of the notch with the active part of the gage normal to the slot tip. Figure 5 shows a photograph of a specimen ready for testing.

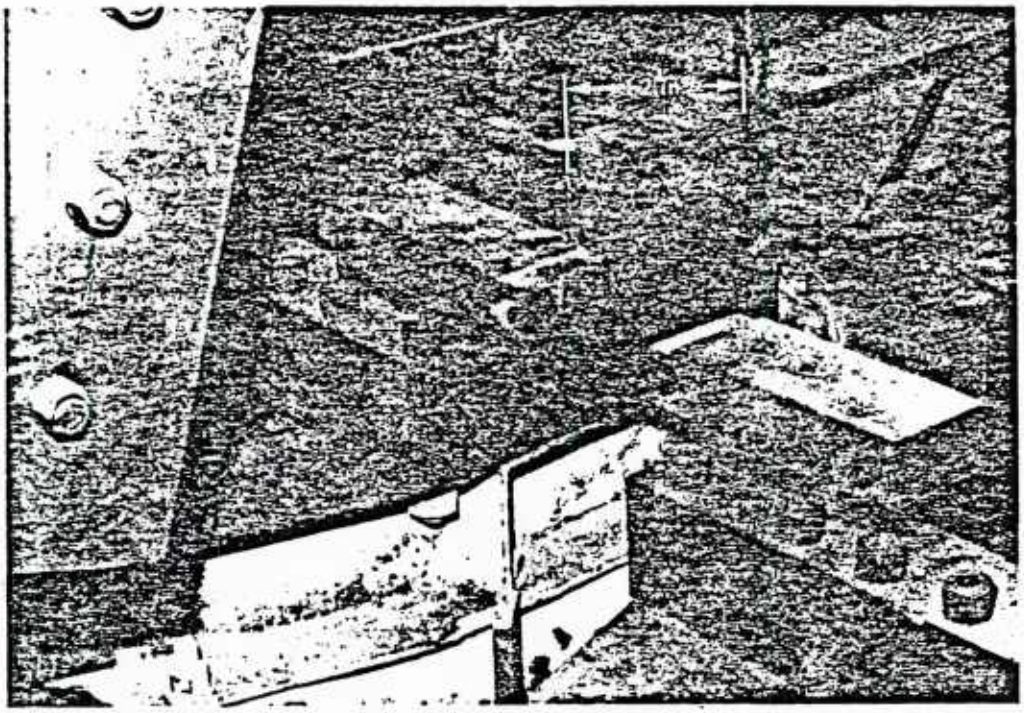

Fig 2. Specimen mounted in dynamic tear machine

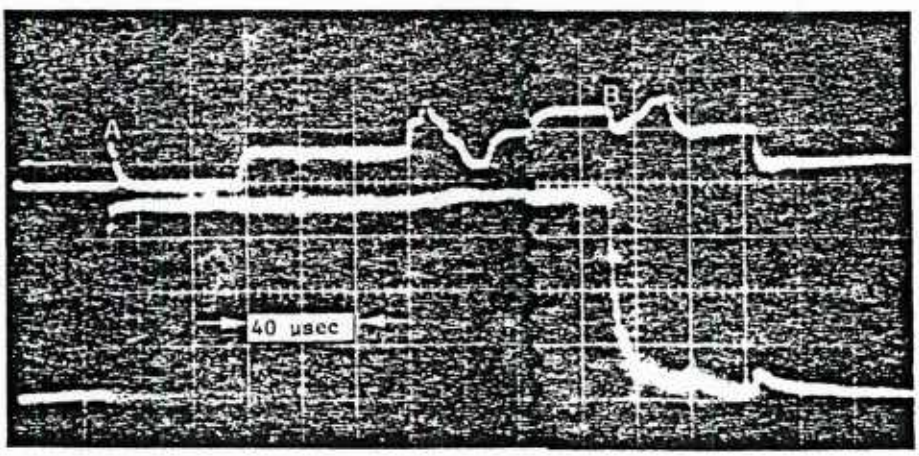

Fig 3. The top line represents the crack velocity grid while the bottom line represents tup contact time. Point A is the time of switch closure (tup contact); point B is the moment of switch opening (tup lost contact)

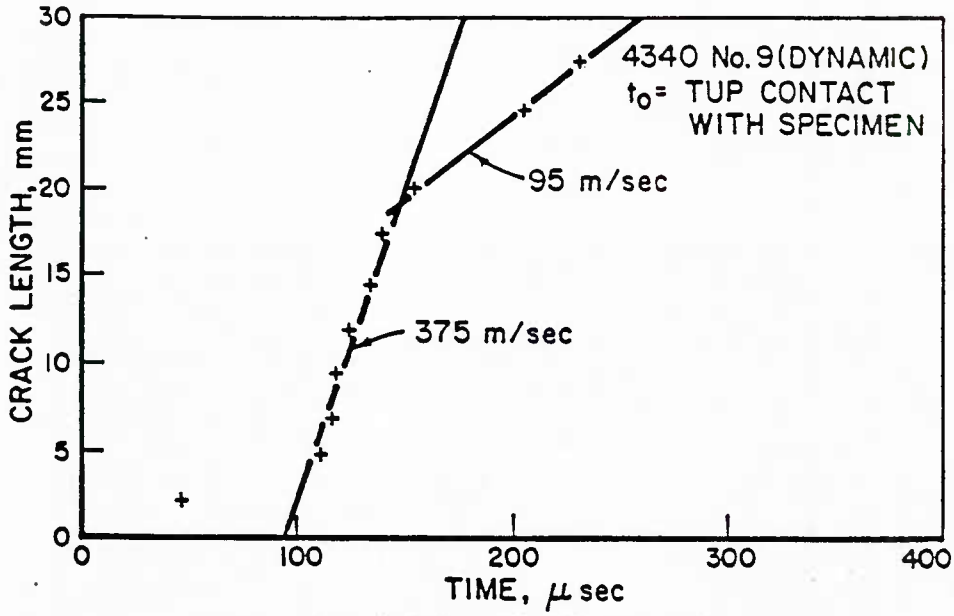

Fig 4. Crack extension deduced from Fig 2

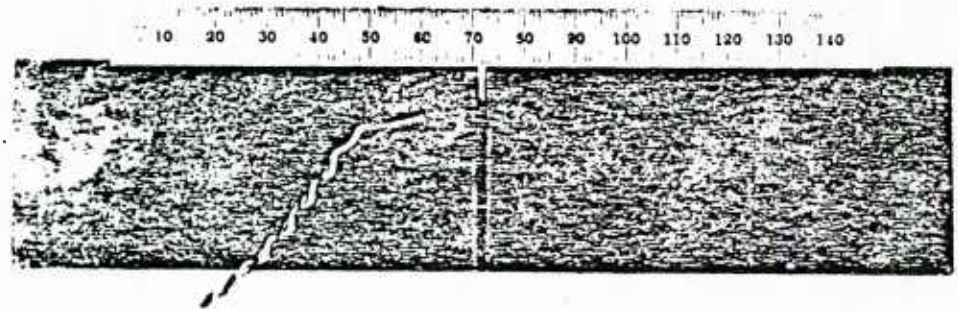

(a) Strain gage location

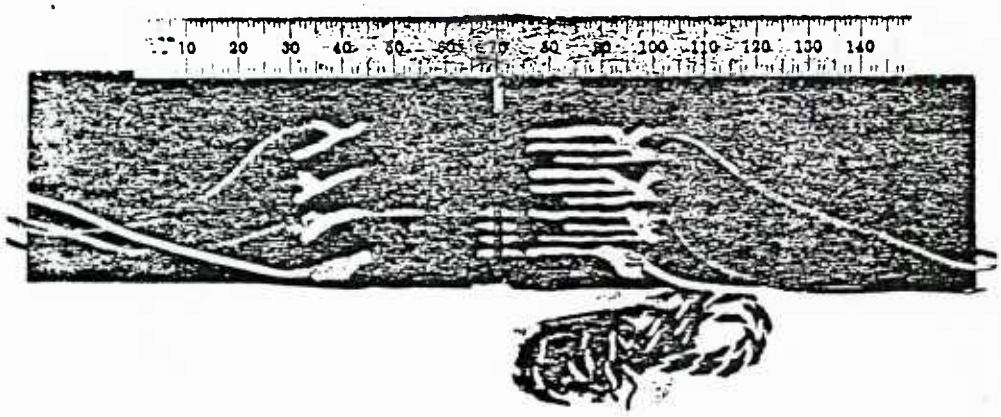

(b) Velocity grid deposted upon side opposite strain gage

Fig 5. Dynamic tear test Specimen Ready for Testing

Instrumentation for the impact experiments consisted of a dual channel transient recorder, a dual channel oscilloscope, a bridge amplifying meter, and a four channel high speed tape recorder, all monitoring the specimen simultaneously. The results from the tests in which the specimen was mounted as it normally is--i.e., with motion of the specimen restrained at the support points shown in Figure 1--are summarized in Table 2. For reasons discussed below, it was also desirable to perform a series of tests on unrestrained specimens. These results are summarized in Table 3.

Table 2

Experimental results for dynamic crack propagation initiated under impact loading in restrained specimens

Slot Root Diameter (mm)	Side Groove Depth (%)	Crack Speed (m/sec)	Absorbed Energy (Joules)
		4340 Steel	
0.064	25	291	130
0.064	25	375[a]	130
0.13	25	390	144
		A533B Steel	
0.064	25	measurement failed	532

(a) This specimen was struck off center. It exhibited an additional 50 μ sec delay in the onset of fast propagation.

Table 3

Experimental results for dynamic crack propagation initiated under impact loading in unrestrained specimens

Slot Root Diameter (mm)	Side Groove Depth (%)	Absorbed Energy (Joules)	Crack Growth (mm)
		4340 Steel	
0.064	25	79	~ 0.5[a]
0.064	25	79	none observed[b]
0.13	0	71	none observed
		A533B Steel	
0.13	0	62	none observed
		A533B Steel at -196 C[c]	
0.13	25	not recorded	complete fracture

(a) Revealed by heat-tinting
(b) Complete fracture occurred in a second test consuming 52 Joules
(c) Specimen was immersed in liquid nitrogen for 15 minutes before testing

The fracture mode in the 4340 steel was the same in both the quasi-static loading and the impact loading tests. The fracture surfaces were flat with a finely distributed array of ductile dimples. Crack extension occurred with no discernable geometrical distortion. This indicates that the amount of plasticity accompanying crack growth was minimal.

Crack extension in the A533B steel was accompanied by a large amount of plasticity with the plastic zone extending about 5 mm from the slot tip in all directions. Under quasi-static loading, the crack grew entirely by slow ductile tearing with large scale geometrical distortion of the specimen. Under impact loading, however, the fracture mode changed from ductile to cleavage--see Fig 6. The ductile portion of the fracture surface was about 10% of the total. As a result, the quasi-static test required about 37% more energy to fracture the specimen than did the impact test.

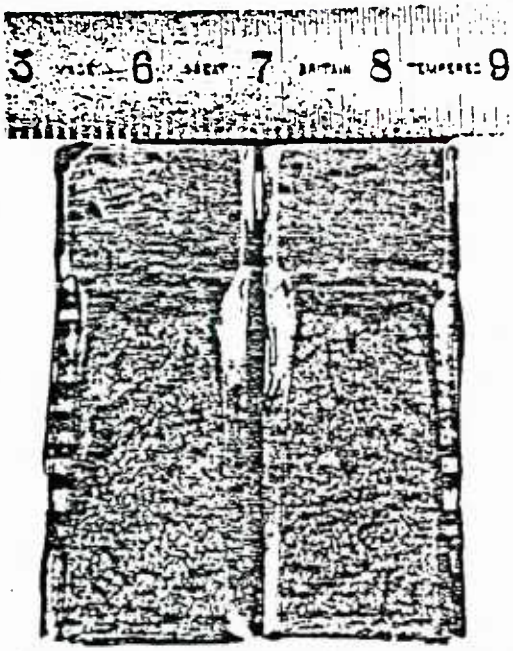

Fig 6. A533B Specimen showing fracture mode change. The ductile portion of fracture is the dark area at root of slot. The lighter area represents cleavage fracture (scale is in mm).

COMPUTATIONAL PROCEDURE

A two-dimensional finite difference method was used to analyze the experimental dynamic crack propagation events. In the finite difference method, the specimen is overlaid with a two-dimensional nodal grid with the displacements of the nodal points being the dependent variables in the time-integration of the elastodynamic equations. The node displacements in the proximity of the crack tip are used to evaluate the energy release rate parameter G which, in turn, is used to deduce K_I from Equation (3). Taken together with appropriate initial conditions and a prescribed relation for K_{ID} (which can be a function of the crack speed) the finite difference solution will generate crack growth versus time information that can be compared with the experimental results.

The value of G computed from the values of the displacements at the finite difference node points surrounding the crack tip will give a result such that the sum of the strain energy, the kinetic energy, and the fracture energy is always equal to the sum of the initial energy and external work done on the specimen. Nevertheless, G is sensitive to the node spacing. In specimens of various shapes, this dependence has been found to be primarily a function of the ratio $\eta = \Delta x/\Delta y$ where Δx and Δy respectively denote the finite difference

node spacings in the directions parallel to and normal to the direction of crack advance. For SEN and CT specimens it has been found that, if $\eta < 0.06$, the computed G value is in good agreement with reference values from static solutions. Hence, it is reasonable to assume that this holds for dynamic problems as well. Accordingly, a value of $\eta = 0.04$ was used in the work reported here. More detailed discussions of this effect and of the algorithm used to compute crack propagation and arrest are given in references [5-7].

In quasi-static loading conditions, the initial configuration must reflect the deflected shape under the load corresponding to the initiation of the propagation event. While both the load and deflection along the load line were determined experimentally, the load is more reliable. The reason is that the observed deflection is the sum of the actual specimen deflection and an unknown additional deflection resulting from the compliant testing machine. As a result, the initial configuration was obtained by minimizing the potential energy (for which the support position nodes were held in fixed positions) while a force equal to the experimentally observed load was applied at the load point nodes.

For an impact test, the initial configuration is simply the undeformed specimen. At time $t = 0$, the tup strikes the specimen on the midplane of the specimen at a point opposite the crack with a velocity $V_T = 6.88$ m/sec. Since in the finite difference representation used here, no nodes are placed on the plane of symmetry, it is considered that the tup strikes simultaneously at the two nodes nearest the impact point (see Fig 1). Consequently, at $t = 0$, these two nodes are displaced by $V_T \Delta t$ in the direction of the striker. Similarly, at each subsequent time step, the positions of these two nodes are moved to accommodate the motion of the tup. Note that, while the tup is never permitted to penetrate the specimen, the tup and the specimen can separate. This, in fact, occurs throughout the event.

Two types of support conditions are used in the calculation. In one, the nodes corresponding to the support points (see Fig 1) are held fixed. Alternatively, the elasticity of the supports can be represented by springs and some computations were performed in this way. But, it is difficult to deduce the appropriate spring constant. This suggested that, to circumvent this difficulty, some experiments and computations be performed with the specimen completely unrestrained. Accordingly, in the second type of support condition, the support points are taken to be stress-free.

RESULTS AND DISCUSSION

The immediate objective of this work was to examine the applicability of the dynamic fracture toughness property determined under conventional quasi-static loading when used in impact loading conditions. To minimize the complications due to extensive crack tip plasticity, 4340 steel, a material that was expected to satisfy the basic requirements of LEFM in a dynamic tear test was selected for this assessment. That small-scale contained yielding would be achieved was examined by calculating the plastically deformed regions with a finite element code for an equilibrium state corresponding to the load level achieved in the impact test at the initiation of crack growth. Because 4340 is essentially rate-insensitive, dynamic effects should not greatly affect these results. Consequently, the finite element results indicate that the LEFM requirements are probably well satisfied in these experiments. This finding was further confirmed by the elastodynamic finite difference solution which showed that, throughout the computation, the effective yield stress was exceeded only in regions comparable to those found in the finite element solution.

The next step in the research was to conduct and analyze a quasi-static loading experiment. The purpose was to determine if the established K_{ID} values for 4340 steel would be affected by either the particular specimen geometry used in this work or by heat-to-heat material and fracture property variations. A dynamic fracture toughness relation previously determined and verified for 4340 steel is given by

$$K_{ID} = 65 + .044\dot{a} \qquad (4)$$

where K_{ID} is in $MNm^{-3/2}$ and $\dot{a}$ is in m/sec [10][1]. Using this relation to predict crack growth as a function of time using the experimental K_Q value to set the initial configuration gave results shown in Figure 7. It is clear from this comparison that the experimental crack length-time results are well reproduced by the analysis using the previously determined K_{ID} values. Consequently, there need be no question of the appropriateness of these values for the material used in this research.

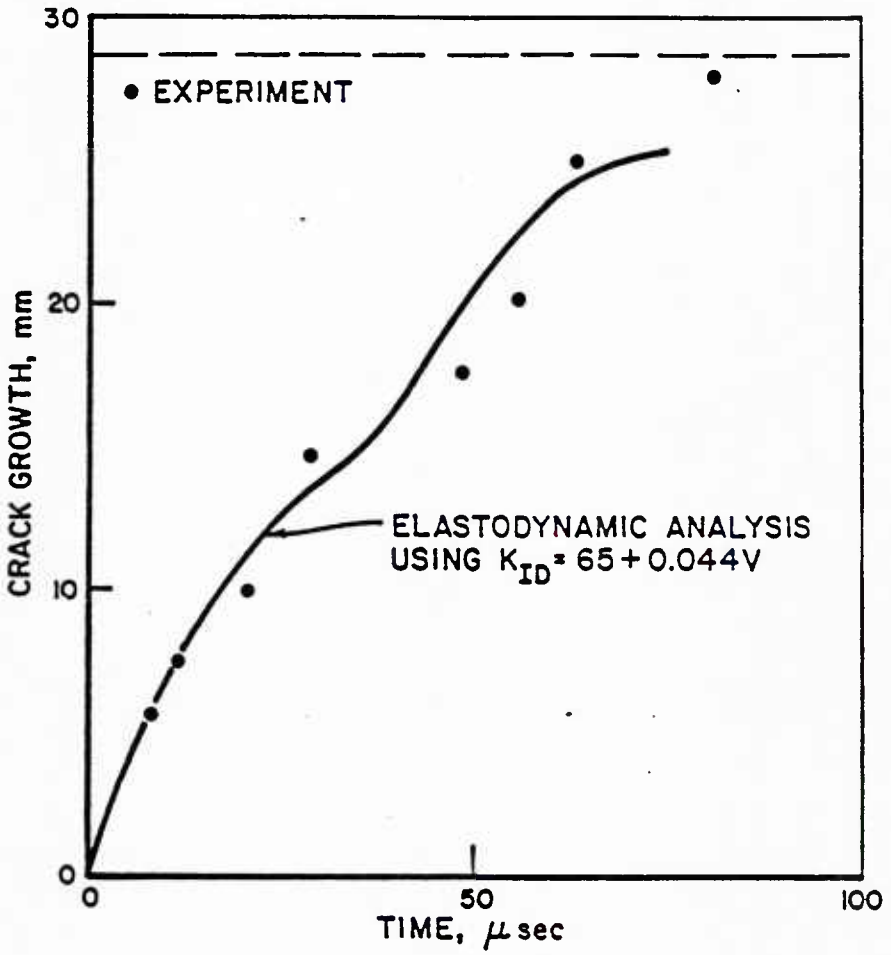

Fig 7. Comparison of measured and predicted dynamic crack propagation in 4340 steel initiated under quasi-static loading

The next step was to conduct impact tests. In these, the crack length could also be determined as a function of time for comparison with the analysis. A comparison using the same K_{ID} values that were used successfully in the quasi-static initiation test is shown in Fig 8. It can be seen that, with the quasi-static K_{ID} values, rather poor agreement is obtained, both for the time of initiation and for the speed of the subsequent propagation.

Further studies aimed at understanding the reasons for the discrepancy shown in Fig 8 revealed further anomalies. One of these was the fact that the measured amount of energy taken out of the pendulum by the impact process was roughly a factor of two greater than that determined in the analysis. While

1 Costin, et al [11], in comparing two different methods for dynamic crack initiation, found a value for K_{Ic} in good agreement with this result.

a part of the absorbed impact energy is the strain and kinetic energies left in the specimen after fracture, most of the difference between the measured and the calculated values is likely due to a discrepancy in the fracture energy. To see if this could account for the difference, a series of impact computations were made in which a hypothetical K_{ID} was postulated. These results suggested that the appropriate K_{ID} value may be much higher than that given by Equation (4).

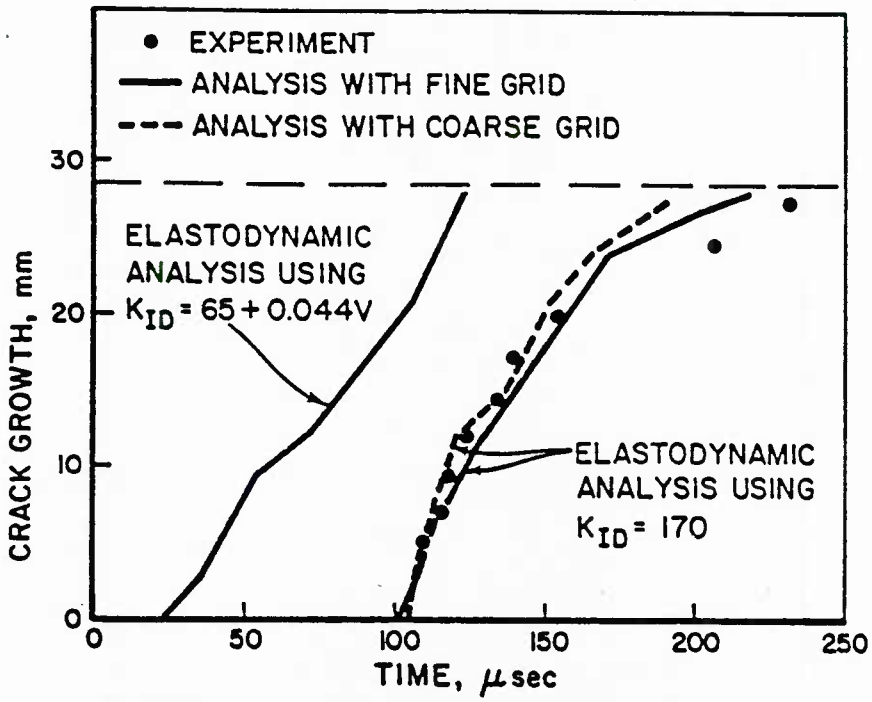

Fig. 8. Comparison of measured and predicted dynamic crack propagation in 4340 steel initiated under impact loading. Rigid supports—.064 mm initial slot diameter

The throw energy--the energy imparted to an unconstrained specimen from an elastic collision between the tup and specimen--was measured for an intact specimen and found to be 79 joules. This compares quite favorably with the 75 joules predicted by the analysis. The total energy absorbed during the impact fracture of the specimen shown in Fig 8 was 130 joules. This would indicate that, at least, some 51 joules were consumed as fracture energy. If this difference is assigned to fracture energy, the average fracture toughness would be 170 $MNm^{-3/2}$.

On the basis of this result, a K_{ID} value of 170 $MNm^{-3/2}$ was taken on a trial basis for reexamination of the impact test results. Note that, because the crack speed dependence of 4340 steel is not too great, these computations could neglect any speed dependence. This value led to the improved crack length—time prediction shown in Figure 8. It can be seen that these predictions are in excellent agreement with the observed results, both for a fine finite-difference grid and for a fairly coarse grid.

The quite satisfactory agreement demonstrated with an elevated K_{ID} value for the interpretation of the crack growth following an impact loading, while pleasing, is also somewhat disconcerting. Because 4340 steel appears to obey well the requirements of dynamic LEFM, there is no apparent reason why the K_{ID} values for impact loading should differ from those for quasi-static loading. In an effort to preclude the possibility that this may be simply an artifact of the experiment, two possible sources of error were examined. These are (1) the effect of the constraint exerted by the supports, and (2) the effect of the initial slot bluntness.

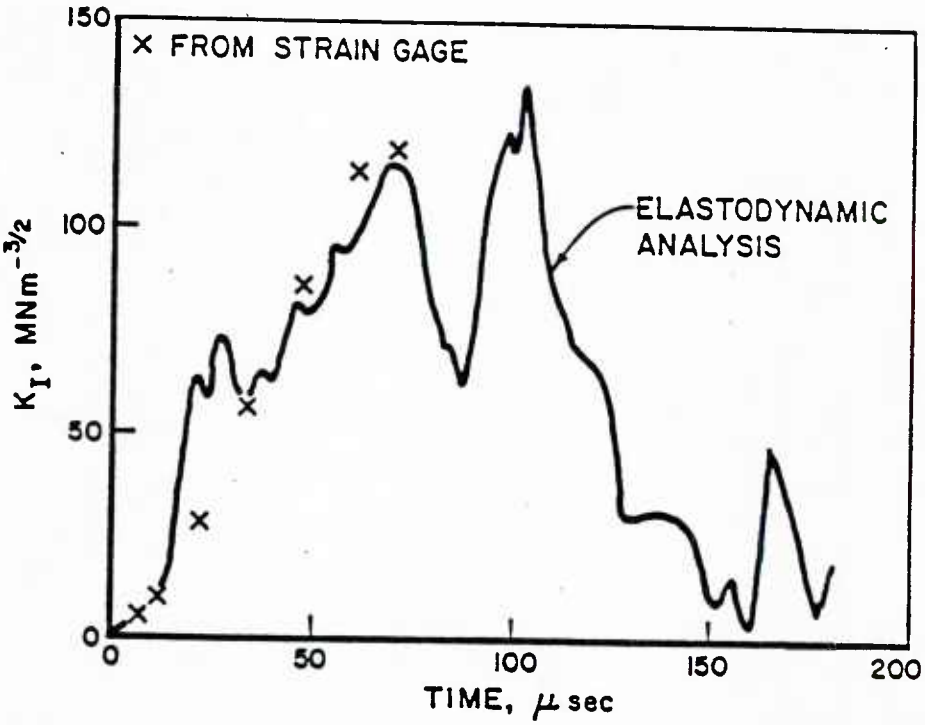

Fig 9. Calculated stress intensity factor for a stationary crack tip in an unrestrained dynamic tear test specimen.

A series of trial calculations were performed in which an elastic spring was substituted for the former rigid support condition in the impact tests. In this way, the support condition was quickly found to have only a modest effect and apparently could not account for the impact/quasi-static loading differences. To put this conclusion to a more rigorous test, experiments were performed in which the specimen was completely unconstrained after being struck by the pendulum. Figure 9 shows the $K_I = K_I(t)$ for the initial crack length under these conditions. It can be seen that a maximum predicted value of K_I of 135 $MNm^{-3/2}$ is reached. Consequently, if K_{ID} is less than this (i.e., as from the quasi-static loading), crack growth must occur. If K_{ID} is greater (i.e., as apparently it is in the impact loading), crack growth will not be possible. In the actual experiment, as illustrated in Fig 10, no crack growth was observed. This is further evidence for the correctness of the higher toughness in impact loading[1].

As an impact test on an unconstrained specimen may appear to be suspect, to demonstrate that fracture can be achieved in this way, an experiment using A533B steel at liquid nitrogen temperature, -196 C, was performed. At this temperature, the quasi-static dynamic fracture toughness is about 35 $MNm^{-3/2}$. Hence, referring to Figure 9, crack growth should be possible. This was, in fact, observed in the experiment[2].

The effect of the initial slot bluntness was addressed by performing an experiment with the relatively blunt slot diameter of 0.13 mm. While the slot tip diameter used in the work already described was small enough that the

1 An alternate explanation is that, because of a dynamic effect, K_Q is greater than 135 $MNm^{-3/2}$ in this experiment despite the fact that a small root diameter is used and 4340 steel is not rate sensitive.

2 It was also found that the unbroken 4340 steel specimen could be fractured in a second impact test. It is conceivable that the initial impact sharpened the slot tip to allow the crack to initiate more readily. But, it is difficult to understand why the dynamic propagation event thereby occurred at a lower toughness.

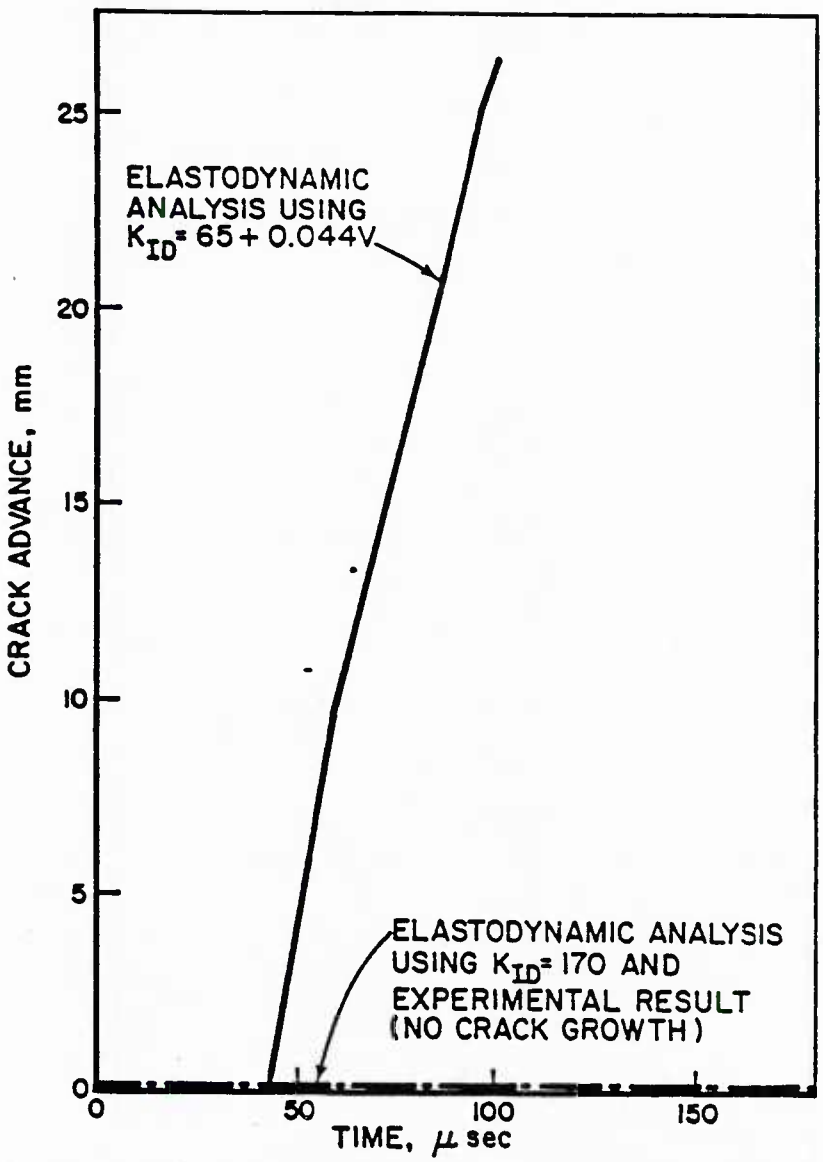

Fig 10. Comparison of measured and predicted dynamic crack propagation in 4340 steel initiated under impact loading. Unrestrained specimen--.064 mm initial slot diameter.

difference between K_Q and K_{ID} could (and was) neglected, this is not the case here. To circumvent the fact that K_Q is unknown, crack growth was initiated in this computation at the time dictated by the experiment. But, subsequently, crack propagation proceeded as before in accord with Equation (2). Comparisons between the measured values and the results of the analysis using K_{ID} as given by Equation (4) and K_{ID} = 170 $MNm^{-3/2}$ are shown in Figure 11. It can once again be seen that the K_{ID} value obtained in the impact tests provides substantially better agreement with the experiments than does the K_{ID} obtained under quasi-static loading.

A higher K_{ID} value is generally associated with a larger amount of energy absorption. For metals, this is in turn associated with a greater extent of plastic yielding around the crack plane. However, post mortem inspection of the fracture planes did not reveal a large difference between the results for the quasi-static and the impact loading conditions. These fracture surfaces are

shown in Figure 12. No explanation for the lack of a more decided difference commensurate with the apparently different K_{ID} values can be offered at this time.

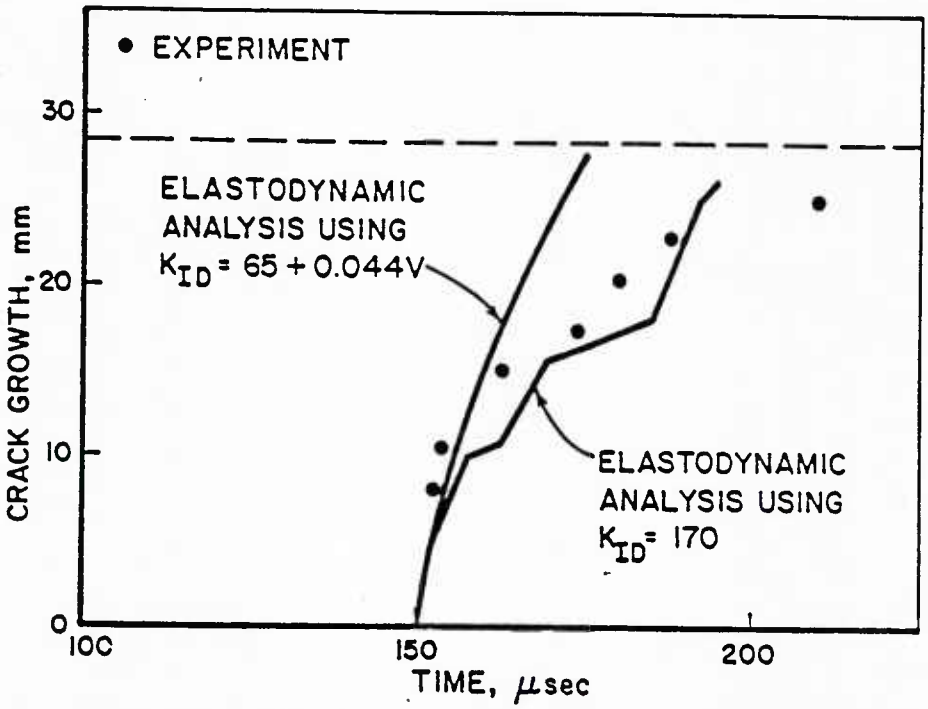

Fig 11. Comparison of measured and predicted dynamic crack propagation in 4340 steel initiated under impact loading. Rigid supports--.013 mm initial slot diameter.

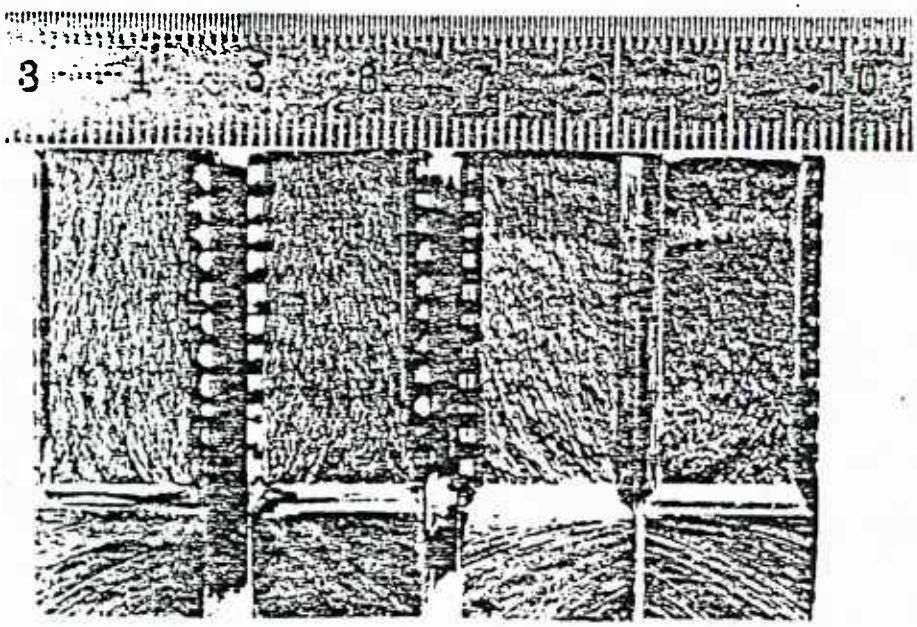

Fig 12. Fracture surfaces from quasi-static and impact loading on 4340 steel.

CONCLUSIONS

This investigation employed a material for which the basic assumptions of LEFM should be well satisfied. Hence, it would appear that the dynamic fracture toughness property obtained for this material under one type of loading condition should be applicable in any other. In contradiction to this intuitively reasonable expectation, the results of a coupled experimental and analysis approach instead suggests that the dynamic fracture toughness property governing crack propagation initiated from a blunted crack tip under impact loading may be significantly higher than when crack growth is initiated quasi-statically.

Clearly, if this finding is substantiated for other materials and testing conditions, it has profound implications--both practical and theoretical--for future work in this technology. However, because this finding is so at variance with previous experience--albeit not of the same type as in this work--it must be treated cautiously. Further work on dynamic crack propagation in impact loading conditions is needed to definitely establish whether the observations reported in this paper are widely valid or are simply an artifact of the experimental conditions selected for the work. This further work should also include tests on materials with sharp initial cracks rather than just the blunted cracks used in the work reported here.

One goal of this work was to investigate the possibility of extracting dynamic fracture toughness data from a measurement of the energy absorbed in a dynamic tear test. Through the use of a series of elastodynamic analyses of the test using hypothetical K_{ID} values, it does appear that a K_{ID} value giving good agreement with the crack growth-time measurements can be obtained by matching the measured energy only.

ACKNOWLEDGEMENT

The work reported in this paper was supported by the Office of Naval Research, Structural Mechanics Division, under contract number N00014-77-C-0576. The authors would like to thank Dr. Nicholas Perrone of the ONR for his personal support and encouragement of their work in this area.

REFERENCES

1 Achenbach, J. D. and Kanninen, M. F., "Crack Tip Plasticity in Dynamic Fracture Mechanics", Fracture Mechanics, N. Perrone, et al, editors, University of Virginia Press, Charlottesville, 1978, pp 649-670.

2 Emery, A. F., Kobayashi, A. S., Love, W. J., and Jain, A., "Dynamic Crack Propagation in Two Pipes With Large-Scale Yielding", J. Pressure Vessel Tech., in press, 1979.

3 Hahn, G. T., Rosenfield, A. R., Marschall, C. W., Hoagland, R. G., Gehlen, P. C., and Kanninen, M. F., "Crack Arrest Concepts and Applications", Fracture Mechanics, op cit, pp 205-228.

4 Kanninen, M. F., "A Critical Appraisal of Solution Techniques in Dynamic Fracture Mechanics", Numerical Methods in Fracture Mechanics, A. R. Luxmoore and D. R. J. Owen, editors, University College of Swansea Press, Swansea, U. K., 1978, pp 612-633.

5 Kanninen, M. F., Popelar, C. H., and Gehlen, P. C., "Dynamic Analysis of Crack Propagation and Arrest in the Double-Cantilever-Beam Test Specimen", Fast Fracture and Crack Arrest, ASTM STP 627, G. T. Hahn and M. F. Kanninen, editors, Philadelphia, 1977, pp 19-38.

6 Popelar, C. H. and Gehlen, P. C., "Modeling of Dynamic Crack Propagation: II Validation of Two-Dimensional Analysis", Int. J. Fracture, Vol. 15, 1979, pp 159-178.

7 Gehlen, P. C., Kanninen, M. F., Hahn, G. T., and Popelar, C. H., "Dynamic Fracture Analysis of Thermal Loading in Nuclear Pressure Vessels", Fifth International Conference on Structural Materials in Reactor Technology, Berlin, August, 1979.

8 Hahn, G. T., Hoagland, R. G., and Rosenfield, A. R., "Influence of Metallurgical Factors on the Fast Fracture Energy Absorption Rates", Met. Trans., Vol. 7A, 1976, pp 53.

9 Lerein, J. and Embury, J. D., "Some Aspects of the Process Zone Associated With the Fracture of Notched Bars", What Does the Charpy Test Really Tell Us, A. R. Rosenfield, et al, editors, ASM, 1978, pp 43.

10 Hahn, G. T., et al, Third Annual Report to U.S. Nuclear Regulatory Commission, Battelle's Columbus Laboratories, BMI 1995, May, 1978.

11 Costin, L. S., Server, W. L., and Duffy, J., "Dynamic Fracture Initiation: A Comparison of Two Experimental Methods", J. Eng. Mat. Tech., Vol. 101, pp 168-172, 1979.

CRACK TIP PLASTICITY IN DYNAMIC FRACTURE MECHANICS

by

J. D. Achenbach

Department of Civil Engineering
Northwestern University
Evanston, Illinois 60201

and

M. F. Kanninen

Applied Solid Mechanics Section
Battelle
Columbus, Ohio 43201

Office of Naval Research
N00014-76-C-0063 (Northwestern)
and
N00014-77-C-0576 (Battelle)

APRIL 1978

NU-SML-TR. No. 78-1

UNCLASSIFIED

SECURITY CLASSIFICATION OF THIS PAGE *(When Data Entered)*

REPORT DOCUMENTATION PAGE

READ INSTRUCTIONS BEFORE COMPLETING FORM

1. REPORT NUMBER: NU-SML TR No. 78-1

2. GOVT ACCESSION NO.:

3. RECIPIENT'S CATALOG NUMBER:

4. TITLE *(and Subtitle)*: CRACK TIP PLASTICITY IN DYNAMIC FRACTURE MECHANICS

5. TYPE OF REPORT & PERIOD COVERED: Interim

6. PERFORMING ORG. REPORT NUMBER:

7. AUTHOR(s): J. D. Achenbach and M. F. Kanninen

8. CONTRACT OR GRANT NUMBER(s): N00014-76-C-0063 (Northwestern)
N00014-77-0576 (Battelle)

9. PERFORMING ORGANIZATION NAME AND ADDRESS: Northwestern University, Evanston, Ill. 60201
and Battelle, Columbus, Ohio 43201

10. PROGRAM ELEMENT, PROJECT, TASK AREA & WORK UNIT NUMBERS:

11. CONTROLLING OFFICE NAME AND ADDRESS: Office of Naval Research
Structural Mechanics Program
Dept. of the Navy, Arlington, VA. 22217

12. REPORT DATE: April 1978

13. NUMBER OF PAGES: 22

14. MONITORING AGENCY NAME & ADDRESS *(if different from Controlling Office)*:

15. SECURITY CLASS. *(of this report)*: UNCLASSIFIED

15a. DECLASSIFICATION/DOWNGRADING SCHEDULE:

16. DISTRIBUTION STATEMENT *(of this Report)*

Approved for public release; distribution unlimited

17. DISTRIBUTION STATEMENT *(of the abstract entered in Block 20, if different from Report)*

18. SUPPLEMENTARY NOTES

To be presented at the Office of Naval Research International Symposium on Fracture Mechanics, George Washington University, Washington, DC. 20052, September 11-13, 1978.

19. KEY WORDS *(Continue on reverse side if necessary and identify by block number)*

plasticity
rapid crack propagation
dynamic effects
near-tip stress fields

20. ABSTRACT *(Continue on reverse side if necessary and identify by block number)*

The objective of this work is to develop a procedure by which crack tip plasticity can be taken directly into account in rapid crack propagation. To set the stage, a background description of linear elastic dynamic fracture mechanics is first given. Existing solutions for dynamic crack propagation and for quasi-static crack growth accompanied by crack tip plasticity are reviewed. It is found that existing dynamic plastic fracture solutions are essentially confined to strip yield (Dugdale model) plastic zones that are collinear with the crack.

DD FORM 1 JAN 73 1473 EDITION OF 1 NOV 65 IS OBSOLETE

UNCLASSIFIED

SECURITY CLASSIFICATION OF THIS PAGE *(When Data Entered)*

The ultimate goal of the research reported in this paper is to provide the basis of a computational procedure for plastic dynamic crack propagation in structures of engineering interest. The prerequisite for such a development is knowledge of the nature of the crack tip singularity, which can be obtained via an asymptotic analysis in which attention is focused on the very near crack tip region. Here we have considered the specific case of crack propagation in anti-plane strain (Mode III). The results suggest some interesting general conclusions, and the analysis has pointed the way to the solution of the Mode I problem.

The material model used in this work is based on Prandtl-Reuss incremental plasticity with a bilinear stress-strain relation. Irreversible material unloading behind the crack tip is specifically allowed. This formulation leads to a set of three first order ordinary differential equations that are nonlinear with variable coefficients. Therefore, a numerical solution was necessary. The results show that s, the order of the crack tip singularity, and θ_p, the angle defining the position of the plastic unloading interface, while highly dependent on the slope of the stress-strain curve in the plastic regime, are much less dependent on the crack speed. Specifically, for a given crack speed, both $|s|$ and θ_p increase with the slope of the plastic portion of the stress-strain curve. For a given bilinear relation, $|s|$ decreases modestly with crack speed while θ_p increases. Possibly of most significance, it appears that the change in the order of the singularity with crack speed may be considered to be negligible if the changes in the crack speed are not too large. If borne out by the analysis of the Mode I problem now in progress, this finding will greatly simplify the computation of dynamic crack propagation/arrest events.

CRACK TIP PLASTICITY IN DYNAMIC FRACTURE MECHANICS

J. D. Achenbach
Department of Civil Engineering
Northwestern University
Evanston, Illinois 60201

M. F. Kanninen
Applied Solid Mechanics Section
Battelle
Columbus, Ohio 43201

INTRODUCTION AND SUMMARY

Dynamic fracture mechanics encompasses all problems involving crack growth initiation, propagation, and arrest in which, for an acceptable solution, inertia forces must be included in the equations of motion of the cracked body. At present, dynamic fracture mechanics solutions are largely confined to conditions where linear elastic fracture mechanics (LEFM) is valid. These are appropriate when the plastic deformation attending the crack tip is small enough to be dominated by the elastic field surrounding it. Problems of crack growth initiation under impact loads and of rapid unstable crack propagation and crack arrest can be treated with LEFM by using dynamically computed stress intensity factors and experimentally determined dynamic fracture toughness values. However, as in static conditions, there are many tough, ductile materials for which LEFM cannot be confidently applied. Currently, there is little alternative: a dynamic plastic fracture methodology does not now exist. Indeed, work in developing a plastic fracture mechanics treatment of the slow stable crack growth under quasi-static monotonically increased loading has not yet come to maturity.

The objective of this work is to develop a procedure by which crack tip plasticity can be taken directly into account in rapid crack propagation. To set the stage, a background description of linear elastic dynamic fracture mechanics is first given. Then, existing solutions for dynamic crack propagation and for quasi-static crack growth accompanied by crack tip plasticity are reviewed. It is found that existing dynamic plastic fracture solutions are essentially confined to strip yield (Dugdale model) plastic zones that are collinear with the crack. In addition, such models do not contain the effect of material unloading. It has been concluded that more realistic treatments of crack tip plasticty via an incremental plasticity formulation for a propagating crack are needed.

The ultimate goal of the research reported in this paper is to provide the basis of a computational procedure for plastic dynamic crack propagation in structures of engineering interest. We envision that the results might be used to construct a special crack tip element in a finite element or other numerical analysis procedure. The prerequisite for such a development is knowledge of the nature of the crack tip singularity. This can be obtained via an asymptotic analysis in which attention is focused on the very near crack tip region. Previous solutions for a crack propagating dynamically with attendant plastic deformation have not been able to include

the singularity. This has been accomplished here with an asymptotic analysis in the specific case of antiplane shear (Mode III) crack propagation. While such calculations have little practical significance, the solution presented in this paper has allowed some important conclusions to be drawn and has pointed the way to the solution of Mode I problems.

In an asymptotic analysis, only the highly strained material in the near tip regime is considered. Hence, it is the stress-strain behavior at very large strains that is important. In fact, the limiting speed for crack propagation is dictated by the slope of the stress-strain curve at large strain. In this sense only a material model with a finite slope of the stress-strain curve at large strains offers a basis for such calculations; i.e., any other formulation will give either a zero or an infinite wave speed for large strain, neither of which are physically realistic.

The material model used in this work is based on Prandtl-Reuss incremental plasticity with a bilinear stress-strain relation. Irreversible material unloading behind the crack tip is specifically allowed. This formulation leads to a set of three first order ordinary differential equations that are nonlinear with variable coefficients. Therefore, a numerical solution was necessary. The results show that s, the order of the crack tip singularity, and θ_p, the angle defining the position of the plastic unloading interface, while highly dependent on the slope of the stress-strain curve in the plastic regime, are much less dependent on the crack speed. Specifically, for a given crack speed, both $|s|$ and θ_p increase with the slope of the plastic portion of the stress-strain curve. For a given bilinear relation, $|s|$ decreases modestly with crack speed while θ_p increases. Possibly of most significance, it appears that the change in the order of the singularity with crack speed may be considered to be negligible if the changes in the crack speed are not too large. If borne out by the analysis of the Mode I problem now in progress, this finding will greatly simplify the computation of dynamic crack propagation/arrest events.

STATUS OF DYNAMIC FRACTURE MECHANICS

There are two generic problems that fall into the domain of dynamic fracture mechanics. These are, (1) a cracked body subjected to a rapidly varying loading, and (2) a body containing a rapidly propagating crack. The first type has wide applicability. Several laboratory test specimens (e.g., Charpy, Drop Weight Tear Test) and virtually all structural components subjected to impact loading fall into this category. The second type of problem, while having a much narrower field of applicability, is no less important. There are several kinds of engineering structures in which unchecked unstable crack growth would have catastrophic consequences. These include gas transmission pipelines, ship hulls, and nuclear reactor components. In these structures, it is essential to go beyond the normal fracture mechanics design philosophy of simply attempting to preclude crack growth initiation. Specific attention must be given to the arrest of unstable crack propagation. This second line of defense requires direct consideration of rapid crack propagation preceding arrest.

Engineering structures requiring protection against the possibility of large-scale catastrophic crack propagation are generally constructed of ductile, tough materials. For the initiation of crack growth, LEFM procedures can give only approximately correct predictions for such materials. The elastic-plastic treatments required to give precise results have not yet been developed in a completely acceptable manner, even under static conditions. The following describes current progress in this area to provide a starting point for the development of the dynamic plastic propagating crack tip analysis that is the objective of this work.

Linear Elastodynamic Treatments

Under the assumption of linear elastic material behavior, the most prominent parameter is the elastodynamic stress intensity factor. This parameter, which enters in the computed elastodynamic stress field in the immediate vicinity of a crack tip, depends on time t and on the speed of the crack tip, v. It is given the symbol $k = k(t,v)$ to distinguish it from the stress intensity factor for the corresponding quasi-static problem (when inertia terms are ignored in the computations), indicated by $K = K(t)$. Although not explicity indicated, both $k(t,v)$ and $K(t)$ also depend on the crack length, on the external geometry of the cracked body, on material constants, and of course on the external loads.

The general form of the elastodynamic near-tip fields for a crack propagating rapidly along a rather arbitrary but smooth trajectory is well known. Let us consider a crack propagating in its own plane with a time-varying crack-tip speed v(t). The two-dimensional geometry with a system of moving polar coordinates centered at the crack tip is shown in Fig. 1.

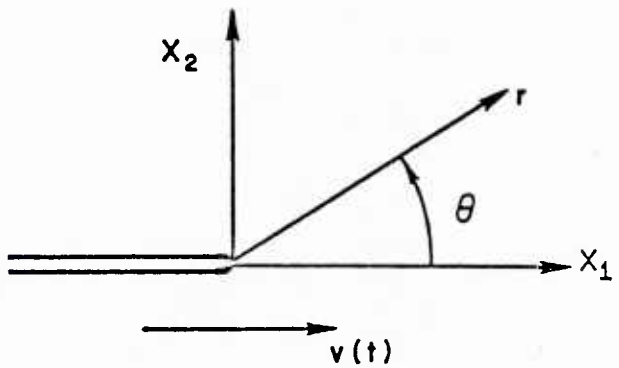

Fig. 1

For symmetric opening up of the crack (Mode I), the instantaneous hoop stress near the crack tip may be expressed as

$$\tau_\theta \sim \frac{1}{(2\pi)^{\frac{1}{2}}} \frac{1}{r^{\frac{1}{2}}} k_I(t,v)\, T_\theta^I(\theta,v) \quad , \tag{1}$$

where $T_\theta^I(0,v) = 1$, and $k_I(t,v)$ is the Mode I elastodynamic stress intensity factor. The function $T_\theta^I(\theta,v)$ is universal in that it is independent of the overall geometry and the loading. It is of note that the maximum value of $T_\theta^I(\theta,v)$ moves out of the plane $\theta = 0$ (the plane of crack propagation) as v(t) increases beyond a certain value. Generally $k_I(t,v)$ is much more difficult to compute than the corresponding quasi-static stress intensity factor.

The conditions governing crack motion can be expressed in terms of $k_I(t,v)$ and an experimentally determined critical value that is assumed to be a property of the material. In conventional (quasi-static) LEFM one has $K_I = K_c$ as the condition for crack instability. In the dynamic generalization of LEFM, K_c has two counterparts. First, for the initiation of crack growth

$$k_I(t,0) = K_d(\dot{\sigma}) \tag{2}$$

where $\dot{\sigma}$ represents the loading rate. For perfectly brittle fracture $K_c = K_d$. Similarly, for a propagating crack

$$k_I(t,v) = K_D(v) \quad , \tag{3}$$

where K_D is known as the dynamic fracture toughness.[1] A third such relation is sometimes used for crack arrest. This is expressed in terms of K_I and an "arrest toughness" parameter, K_a. However, while the concept can be useful as an approximation, clearly, for a propagating crack, arrest can only occur when Equation (3) cannot be satisfied. That is, a crack will arrest at a time t_a when $k_I < K_D$ for all $t > t_a$. Thus, crack arrest is properly viewed as the termination of a general dynamic crack propagation process, not as a unique event governed solely by material properties as suggested by the static crack toughness K_a approach. While there are circumstances where such a simplistic point of view gives an adequate engineering approximation, its limitations can only be determined via a rigorous, fundamentally correct approach.

Applications of LEFM can be made either in terms of the stress intensity factor or the strain energy release rate parameter G. The equivalence between these two quantities extends to the dynamic situation as well. Thus, the LEFM criterion for crack propagation can be generalized to the dynamic situation as an equality between G and its critical value R, the energy dissipation rate required for crack growth. Then, for given structural geometry, applied loads, and operating temperature, an alternative dynamic crack propagation condition to Equation (3) is

$$G = R(v) \quad . \tag{4}$$

In terms of Equation (4), a dynamic extension of LEFM can be viewed as one which delineates the structural contribution to a propagating crack--the driving force--from the material's fracture property--the resistance. The material property represents the energy dissipated in flow into the crack tip and the fracture processes accompanying crack extension. The crack driving force includes three individual contributions. A net change in these three components, per unit area of crack extension, is called the dynamic energy release rate, or, equivalently, the driving force for crack extension. Formally,

$$G = \frac{1}{b}\left\{\frac{dW}{da} - \frac{dU}{da} - \frac{dT}{da}\right\} = \frac{1}{bv}\left\{\frac{dW}{dt} - \frac{dU}{dt} - \frac{dT}{dt}\right\} \quad , \tag{5}$$

where U is the strain energy, T is the kinetic energy, W is the work done on the structure by external loads, a is the crack length, and b is the thickness of the body at the crack tip.

Although Equation (5) apparently represents a global quantity that must be evaluated by integrating over the entire structure, G can always be given a local crack tip interpretation. In particular, it can be directly connected to the dynamic stress intensity factor. For plane strain conditions we have

$$G = \frac{1-\nu^2}{E} A(v)\, k_I^2 \quad , \tag{6}$$

---

[1] In this paper, a crack tip parameter with a letter subscript always denotes a material property. Because the basic definitions are just the same in dynamic LEFM as in conventional static LEFM, there is no reason to put a subscript on the computational quantities as some authors have done, except for I, II, and III to indicate the fracture mode. In fact, because of the confusion between material properties and computed entities that then arises, there is good reason not to do so.

where E and ν, as usual, are the elastic modulus and Poisson's ratio, respectively, and A is a geometry independent function of the crack speed given by

$$A(v) = \frac{(v/c_T)^2(1-v^2/c_L^2)^{\frac{1}{2}}}{(1-\nu)[4(1-v^2/c_L^2)^{\frac{1}{2}}(1-v^2/c_T^2)^{\frac{1}{2}}-(2-v^2/c_T^2)^2]} \quad . \qquad (7)$$

Here c_L and c_T are the longitudinal and shear wave speeds, respectively. The function A(v) is unity at zero crack-tip speed, and increases monotonically to become unbounded as $v \to c_R$, where c_R is the speed of Rayleigh waves in the material. As $v \to c_R$ the elastodynamic stress intensity factor vanishes, and we find $G \to 0$ as $v \to c_R$. Consequently, without an external driving mechanism right at the crack tip, cracks cannot propagate faster than Rayleigh surface waves.[2]

Calculational procedures to evaluate k values are well advanced. Comprehensive review articles are available for further background--see Refs. [1-4]. The experimental determination of dynamic fracture toughness values is also well advanced--see Ref. [5]. More recent information on the application of linear elastic dynamic fracture mechanics to crack arrest predictions are contained in the paper by Hahn, et al in this volume. We now move on to consider solutions giving direct attention to the plastic deformation attending a moving crack tip.

Dynamic Strip Yield Plasticity Treatments

The basic postulate of LEFM is that all inelastic irreversible energy dissipation processes that accompany crack extension can be included in a single material property. This property may depend on thickness and temperature, but is independent of the crack length, the applied loads, and the external geometry of the body. This also applies to dynamic fracture mechanics with a dependence on crack speed being allowed to take account of strain rate effects in the intensely deformed region ahead of a propagating crack. This will be valid when the plastic zone at the crack tip is small relative to other dimensions of the cracked body. But, for ductile tough materials, crack tip plasticity can be quite large. For such materials, it becomes necessary to improve on the LEFM autonomous crack tip plastic zone assumption.

In ductile fracture, crack growth takes place by the nucleation and coalescence of voids accompanied by substantial plastic deformation. When the dominant mode of this deformation is shear on 45° planes through-the-thickness, crack growth occurs under conditions which approximate plane stress [6]. A useful model for this situation is the strip yield model given by Dugdale [7] in which the plastic zone is taken to be simply an extension of the crack. In essence, the Dugdale crack model is obtained by superposing two elastic solutions. The first is that for a stress free

---

[2] The four relations (2), (3), (4), and (6) can be used to establish a theoretical relation between K_D and K_c

$$K_D = \left[\frac{1}{A(v)}\,\frac{R(v)}{R(0)}\right]^{\frac{1}{2}} K_c \ ,$$

where $R(0)$ corresponds to the static critical energy release rate.

crack of length $2a$ in an infinite plate under a uniform tension σ. The second is for a crack loaded over intervals of length $\ell = a-c$ ($2c$ is the physical crack length) at each of its ends by a tensile stress equal to the yield stress Y of the material.[3]

Dugdale recognized that the stress singularities in each solution not only occur at the same point but have exactly the same character. The singularities can be made to exactly cancel by adjusting the plastic zone lengths such that

$$\frac{c}{a} = \cos \frac{\pi\sigma}{2Y} \quad . \tag{8}$$

A more direct way of deducing Eqn. (8) was given by Goodier and Field [8]. Because the singular terms in the stress functions for each subproblem differ by only a multiplicative constant, the singularities can be abolished by simply setting the coefficient of this term in the combined stress function to zero. In an equally expeditious manner, Goodier and Field were able to determine the normal displacements along the crack line for the Dugdale model. In particular, they found δ, the crack opening displacement at the tip of the crack, to be

$$\delta = \frac{(\kappa+1)}{\pi} \frac{Yc}{G} \log \left[\sec\left(\frac{\pi}{2} \frac{\sigma}{Y}\right)\right] \quad , \tag{9}$$

where $\kappa = (3-\nu)/(1+\nu)$ for plane stress, $3-4\nu$ for plane strain (ν is Poisson's ratio) and G is the shear modulus. The importance of this result is in the connection that exists between δ and other crack tip fracture parameters. As shown by Rice [9]

$$G = J = Y\delta \tag{10}$$

for the Dugdale model. Here, G is the LEFM energy release rate defined above, J denotes the value of the J integral, and Y is the yield stress. Clearly, the equivalence of the various different parameters arises because the Dugdale model solution is completely within the confines of linear elasticity.

Turning now to rapid crack propagation, Goodier and Field [8] appear to have been first to use the Dugdale model in a dynamic solution. They considered a semi-infinite crack with a finite length strip yield zone propagating at a constant speed in an infinite medium. For this situation, the yield zone length (determined as in the static case by abolishing the singularity) and the crack tip opening displacement are found to be independent of the crack speed. Kanninen, et al [10-11] extended this approach by taking a constant length Dugdale model crack propagating at a constant speed as the basis of a strain rate dependent crack tip plastic zone calculation. In this case, the plastic zone length also is independent of crack speed and, consequently, is just identical to Eqn. (8). The crack tip opening displacement, in contrast, does exhibit a crack speed dependence. This result can be written

---

[3] It is often incorrectly assumed that plastic deformation like that of the Dugdale model is always obtained if the material is thin enough that plane stress conditions hold. However, 'thinness' is not enough to assure this kind of deformation. Aluminum foil, for example, does not exhibit plastic enclaves of this kind. In addition to the specimen being thin, the material must work harden very little. Then, it will neck as soon as it yields giving through-the-thickness relaxation and, consequently, narrow elongated zones that extend along the prolongation of the crack line.

$$\delta(v) = A(v)\ \delta(0) \quad , \tag{11}$$

where $A(v)$ is the function given by Eqn. (7) and $\delta(0)$ denotes the value of the crack tip opening displacement in the static case; i.e., as given by Eqn. (9).

The idea motivating Kanninen, et al [10,11] was that the strain gradient ahead of a crack tip is so steep that the plastically deformed material is fractured at enormous strain rates. To take this into account, linear superposition was used to obtain a model in which the flow stress varied arbitrarily along the length of the strip yield zone. The flow stress values were assigned in accord with a known strain rate dependent constitutive relation using the crack line displacements in the strip yield zone to determine the local strain rates. In this way, predictions of the limiting speed of ductile crack propagation were made--the limiting speed being governed by the high strain rate dependence of the crack tip flow stress.

Glennie [12,13] has also adopted a model based on a crack propagating with a thin plastic zone and a strain rate dependent yield stress. He similarly concluded that the increased yield stress at high strain rates near the crack tip is the major factor limiting the crack speed. In addition, by comparing with a small-scale yielding calculation, he found that the LEFM stress intensity factor can be used for dynamic behavior even when there is considerable plastic yielding. However, because of the uncertainty of the constitutive relation at high strain rates, no qualitative connection with fracture toughness was made.

While some useful qualitative conclusions can be drawn from these calculations, it is not possible to obtain precise results. There are several shortcomings causing this. First, steady-state crack growth in an infinite medium is an obviously poor approximation to reality. Second, the strain rates that are predicted in these models (and, hence, for which constitutive relations are required) are several orders of magnitude greater than can be measured in any conventional test procedure. Third, this kind of model cannot take account of material unloading in the wake of the crack. Fourth and finally, there is a definite lack of correspondance between a <u>continuum</u> strip yield model and the actual fast fracture mechanisms.

As described by Hoagland, et al [14], the morphology of the plastic deformation attending crack propagation largely consists of highly segmented, but interconnected, regions arising from isolated high toughness zones that are bypassed and remain unbroken even at relatively large distances behind the crack front. They concluded that much of the energy absorbed in unstable crack propagation can be traced to the plastic stretching of these ligaments and, hence, that these are the principal source of the fracture resistance. These experimental observations were supported by computational results obtained with a quasi-static segmented (discontinuous) strip yield zone model. This model is somewhat similar to one proposed by Dvorak [15] to investigate crack growth accompanied by weakened ductile links within a discrete crack zone. This zone, which is supposed to form as a result of selective microcrack propagation in the elastic material ahead of the main crack, is connected with the energy absorption rate and fracture toughness.

All of the models discussed so far in this section suffer from the steady-state assumption which forces the propagating crack to maintain a constant length. A more realistic solution was obtained by Atkinson [16]. He considered a crack expanding at a uniform speed (Broberg model) with collinear strip yield zones, cancelling the singularity to obtain the length of these zones. In contrast to the steady-state solutions, the plastic zone size depends on the crack speed in this problem. In fact, it appears to decrease with crack speed. Unfortunately, the result is quite complicated and

no simple dependence can be extracted. Also, although it appears to be possible, no expression for the crack tip opening displacement was given that could be used to assess the applicability of Eqn. (11).

In short, while quite attractive from an analytical point of view, strip yield models suffer from a number of shortcomings when viewed from a physical mechanisms standpoint. Consequently, other more physically plausible models seem to be required for a realistic assessment of crack tip plasticity in dynamic crack propagation.

Dynamic Crack Propagation with Large-Scale Yielding

The strip yield models described in the preceding section were all of the Dugdale type; i.e., with a thin plastic zone ahead of and collinear with the crack. Other types of strip yield models do exist. Models employing dislocation pileups on slip planes inclined to the crack plane to represent crack tip plasticity have been developed. A particularly tractable model employing a superdislocation on an inclined slip plane used by Atkinson and Kanninen [17] has been found to give highly reasonable results for static conditions. Riedel [18] has used a similar picture to address dynamic loading in a strain rate sensitive material. However, it has not so far been possible to incorporate this type of strip yield zone plasticity into a model for a rapidly propagating crack tip.

At present, calculations for unstable crack growth in elastic-plastic materials can only be carried out using numerical methods. There generally are two deficiencies in all these approaches. First, the work is addressed to very specific applications; e.g., pipe fracture. Second, the crack growth criterion used is overly simplistic. Nevertheless, it is useful to briefly review the work that has been done in order to properly assess the directions for future progress. In doing so, attention will be put on the fracture mechanics aspects only. Computational procedures are well covered elsewhere--for example, see Ref. [19].

Current results in elastic-plastic dynamic crack propagation seem to be focused on one of two specific applications: analysis of the Charpy impact test [20-21] and crack propagation in pressurized pipes [22-24]. Ayres [20] performed a two-dimensional (plane strain) elastic-plastic finite element analysis of a precracked Charpy V-notch specimen. Attention was focused on the value of the J integral for the initiation of crack growth. This is given by

$$J = \int_{\Gamma} W dy - T \frac{du}{dx} ds \quad , \tag{12}$$

where x and y are Cartesian coordinates (y normal to the crack line), ds is an increment of arc length along a contour Γ, T is the stress vector on the contour, u is the displacement vector, and W is the strain energy density. He further defines a corresponding stress intensity factor K_J given by

$$K_J = \left[JE/(1-\nu^2) \right]^{\frac{1}{2}} \quad . \tag{13}$$

Recognizing that path independence of J cannot be expected in the dynamic situation, Ayres used a contour that included only the node points closest to the crack tip to minimize the error involved. He concluded that values of J and K_J computed in this way offer reasonable candidate criteria for dynamic elastic-plastic fracture.

Norris [21] has taken a different point of view in his analysis of the initiation of crack growth in a Charpy V-notch specimen. He has used a three-dimensional finite difference method and the semi-empirical crack growth criterion developed by Wilkins [25]. Wilkins' criterion stems from

a ductile fracture model and contains material dependent parameters that are adjusted (by trial and error) to fit the experimentally determined fracture initiation in several different geometries. It takes the form

$$D(t) = \int_0^t f(\sigma_m)\, d\bar{\varepsilon}_p \qquad (14)$$

with fracture occurring when $D > D_c$ over a specified region. In Eqn. (14), σ_m denotes the mean stress while $d\bar{\varepsilon}_p$ is the increment of equivalent plastic strain. It can be seen that the parameter D can be interpreted as an integrated damage with the critical damage being roughly the strain required for crack initiation. In particular, Norris found that fracture initiation in a Charpy test is associated with net section yielding and notch root strains of about 100 percent. In contrast to Ayres, he concludes that a calculation of K is therefore not relevant.

A complication existing in all realistic dynamic fracture problems is that the boundary conditions are generally time-dependent and, arising from an interaction between the cracked body and the agency supplying the driving force for fracture, they are somewhat uncertain. Thus, in the Charpy specimen, the forces arising from the striking tup must be known in some way. For laboratory tests, the interaction between the test specimen and the loading machine must be taken into account. Lastly, for pipelines, a relation between crack speed and the pressurizing medium must be considered.

In the work of Emery, et al [22], an axial-through-wall crack was suddenly introduced in the wall of a pipe pressurized by either hot water or air. A finite difference solution procedure was used with the leakage of fluid through the crack taken into account. In their elastic-plastic calculations, the crack tip was advanced according to a critical crack tip strain criterion of 2 percent. Of some interest, their results suggest that the simpler models for crack propagation in ductile pipes using essentially LEFM concepts devised by Popelar, et al [26] and by Freund, et al [24] may be reasonably accurate.

The flow area from a postulated pipe break is an important parameter in the design of nuclear reactor steam supply systems. This problem was addressed by Ayres [23]. He determined the largest stable crack that could suddenly appear during normal operating conditions using an elastic-plastic finite element analysis. The J integral ductile fracture criterion--see Eqn. (12)--was used to predict the stability of the hypothetical cracks.

Some progress has been made on elucidating the effects of crack tip plasticity in dynamic crack propagation, both theoretically [27] and semi-empirically [28]. Broberg [27] concludes from a study of the morphology of material separation that energy dissipation accompanying rapid crack propagation can be separated into two components: that dissipated in a process region in the neighborhood of the crack tip and that dissipated in the plastic region outside the process region. His investigations indicate that the plastic energy dissipation decreases with increasing crack speed while the converse is true for the process zone. The net effect can be a decrease of the total energy dissipation with increasing speed to a minimum followed by a rapid increase at higher speeds. This is consistent with the character of the bulk of the experimentally determined $K_D = K_D(v)$ curves that have been reported.

In contrast to Broberg's continuum level approach, Shockey, et al [28] have developed a micromechanical computational capability for fast fracture. Their approach is to directly simulate the events occurring in the process zone and, by computing the energy dissipation rates, determine the fracture toughness of a propagating crack. This is done by considering crack growth to occur by the nucleation, growth, and coalescence of microfractures in the plastically deforming material at the crack tip. Input is

taken from measurements on specimens fractured under stress wave loads. In this way, they hope to be able to derive fracture toughness values directly from micromechanical flow and fracture processes.

To close this section of the paper, it might be concluded that current analyses are clearly unable to ascribe elastoplastic dynamic crack propagation to a basic condition at the crack tip. Thus, the delineation of a proper fracture criterion may be the most critical outstanding problem in the field. The next section describes recent progress in the static case as a prelude to direct consideration of this problem for dynamic fracture.

Plastic Fracture Criteria for Stable Crack Growth

While the preponderance of all fracture mechanics applications at the present time are based on LEFM concepts, it is fast becoming clear that there are situations where LEFM-based predictions are so conservative that an inordinate penalty is exacted on the design. An application which has perhaps motivated a more intense research effort than any other is the assessment of the margin of safety of flawed nuclear pressure vessels and piping near and beyond general yielding conditions [29]. A general background on plastic fracture mechanics can be obtained from Ref. [30]. Here, recent work by Kanninen, et al [31,32] on the development of a plastic fracture methodology for stable crack growth under monotonically increasing loading is briefly summarized.

The research reported in Refs. [31,32] proceeds through three main stages. First, laboratory test pieces of pressure vessel steel and of two "toughness-scaled" materials are tested to obtain data on crack growth initiation and stable growth.[4] Next, "generation-phase" analyses are performed. In these, the experimentally observed applied stress versus stable crack growth data are used as input to a finite element model. Critical values for each of a number of candidate crack initiation and stable growth criteria are then generated from the particular test results. Comparison of results obtained for different initial crack sizes and overall test piece geometries provide a basis for an objective appraisal. Finally, in the third stage, "application-phase" finite element analyses are performed. These analyses apply a specific fracture criterion to predict the applied stress versus crack growth behavior for a new set of conditions. The accuracy of the predictions then offers a further basis for appraising the various candidate fracture criteria.

A number of different fracture criteria have been examined. These include the J integral, an elastic-plastic energy release rate G^{Δ}, the crack tip opening angle CTOA, the average crack opening angle COA, and a generalized energy release rate G. Another is the crack tip force F which acts at the crack tip nodes in a finite element model during the stable crack growth process.

Computationally, the generalized energy release rate is the sum of two terms. That is, $G = G^{\Delta} + G_Z$ where G^{Δ} is the work done in separating the crack faces and G_Z is the change in the energy contained in the computational process zone (CPZ). Crack growth then proceeds such that

$$R = G \equiv G^{\Delta} + G_Z \tag{15}$$

---

[4] Toughness-scaled materials (e.g., aluminum alloys) exhibit essentially the yield/crack growth character of full thickness pressure vessel steel but in reduced thicknesses. This simplifies the testing requirements and thereby allows a wider range of conditons to be examined than would otherwise be possible.

in this approach. Crack instability (fracture) will then occur when $G > R$ for the prescribed loads or displacements at some crack length. It might be noted that the use of a process zone also circumvents the difficulty associated with a crack tip energy release rate alone. As pointed out by Rice [33], G^{Δ} has a very strong step size dependence, approaching zero in the limit of vanishing crack advance length.

As described in Refs. [31,32], generation-phase computations were made for three aluminum-center cracked panels, an aluminum compact tension specimen, and a steel compact tension specimen. Computational results for the different fracture parameters during stable crack growth show that the quantities that reflect the toughness of the material in the locale of the crack tip--G_c, R, G_{Zc}, $(CTOA)_c$, and F_c--are relatively invariant during stable crack growth. Of these quantities, F_c and the $(CTOA)_c$ appear to be most nearly constant. All of the local quantities reflect a loss in crack growth resistance at the beginning of crack extension, but are then constant. In contrast, the parameters that sample large portions of the elastic and plastic strain field--$(COA)_c$ and J_c--vary monotonically with stable crack extension. But, within the precision of the analyses, the comparison of the center cracked panel and compact specimen results indicate that only $(COA)_c$ is independent of geometry. The quantity J_c shows geometry dependence after a small amount of stable crack growth.

The findings of this research illuminate the basic cause of stable growth in elastic-plastic materials. In the cases analyzed, crack growth stability cannot be attributed to an increase of the toughness of the material. Rather, an increasing load during stable crack growth means that the portion of the energy flow reaching the crack tip region diminishes with crack extension. The reduced energy flow can be thought to result from the "screening" action of the plastic zone accompanying the growing crack in the sense described by Broberg [27].

ANALYSIS OF THE NEAR TIP FIELD FOR ANTI-PLANE STRAIN DYNAMIC CRACK PROPAGATION IN AN ELASTIC-PLASTIC MATERIAL

As described in the preceding portion of this paper, crack tip plasticity in dynamic crack propagation has been taken into account in two simplistic ways. The first is by assuming that the plastic region is a small autonomous region controlled by the surrounding elastic stress field. The second is that the plastic deformation is confined to a strip ahead of the crack tip. In both approaches the techniques are essentially those of linear elasticity. Thus, these models do not account for nonlinear elasto-plastic constitutive behavior, nor do they account for different stress-strain paths in loading and unloading. The importance of these effects can only be examined with an incremental plasticity model. Due to the difficulty of performing such calculations, it is appropriate for a preliminary appraisal to consider the anti-plane strain case, and to restrict the attention to the general nature of the near-tip field. An analysis of the near-tip field is presented in this section, by extending a corresponding quasi-static solution given by Amazigo and Hutchinson [35] to the dynamic case.

Mode III Crack Propagation

The system of moving coordinates (x_1,x_2,x_3) shown in Fig. 1 is oriented such that the crack lies in the (x_1x_3)-plane, x_3 coincides with the crack front and x_1 is the direction of crack advance. Motion in anti-plane strain is defined by a displacement distribution $w(x_1,x_2,t)$ where w is the displacement in the x_3-direction. Here t is a time consistent with the moving coordinate system. For future reference we introduce the following notation for material derivatives with respect to time

$$\frac{d(\ )}{dt} = (\dot{\ }) \quad . \tag{16}$$

If the speed of the crack tip is v, where $v = v(t)$ is an arbitrary function of time subject to the conditions that $v(t)$ and dv/dt are continuous, we have relative to the moving coordinate system

$$(\dot{\ }) = \frac{\partial}{\partial t} - v(t)\,\frac{\partial}{\partial x_1} \tag{17}$$

so that

$$(\ddot{\ }) = \frac{\partial^2}{\partial t^2} - \dot{v}(t)\,\frac{\partial}{\partial x_1} - 2\,v(t)\,\frac{\partial^2}{\partial t \partial x_1} + [v(t)]^2\,\frac{\partial^2}{\partial x_1^2} \quad . \tag{18}$$

For anti-plane strain the only nonvanishing strain components are ε_{13} and ε_{23}. The corresponding stresses are σ_{13} and σ_{23}. The notation can be simplified somewhat by the definitions

$$\tau_i = \sigma_{i3} \qquad i = 1,2 \tag{19}$$

$$\gamma_i = 2\varepsilon_{i3} = \frac{\partial w}{\partial x_i} \qquad i = 1,2 \quad . \tag{20}$$

Relative to the moving coordinates the equation of motion can then be written as

$$\tau_{i,i} = \rho\,\ddot{w} \quad , \tag{21}$$

where $i = 1,2$ and ρ is the density. Notice that $\ddot{w}$ follows from Eqn. (18).

The system of governing equations must be completed by constitutive relations. In the following we examine the near-tip fields for the various different constitutive behaviors shown in Fig. 2. First, for linear elasticity--Fig. 2(a)--the constitutive equation is $\tau_i = G\,\gamma_i$. The solution for this case with a near-tip field of the form

$$w = C\,W(\theta)\,r^s \tag{22}$$

has been obtained by Achenbach and Bazant [36]. The result is $s = \frac{1}{2}$ and

$$W(\theta) = \Psi_1 \cos\theta - (1-\beta^2)^{\frac{1}{2}}\,\Psi_2 \sin\theta \quad , \tag{23}$$

where $\beta = v/c_T$, $c_T = (G/\rho)^{\frac{1}{2}}$ and

$$\Psi_{1,2} = \left\{\frac{(1-\beta^2\sin^2\theta)^{\frac{1}{2}} \pm \cos\theta}{1-\beta^2\sin^2\theta}\right\}^{\frac{1}{2}} \quad . \tag{24}$$

Notice that the stresses show the familiar square root singularity of LEFM.

For bilinear elasticity--Fig. 2(b)--an effective shear stress τ for a simple shearing history can be defined as

$$\tau = (\tau_1^2 + \tau_2^2)^{\frac{1}{2}} \quad . \tag{25}$$

It is assumed that loading and unloading takes place along the same curve. The generalization to anti-plane shear deformation is then

$$G\,\gamma_i = \tau_i \qquad \tau < \tau_o \tag{26}$$

and

$$G\gamma_i = \tau_i + \left(\frac{G}{G_t} - 1\right)\left(1 - \frac{\tau_o}{\tau}\right)\tau_i \qquad \tau > \tau_o \tag{27}$$

For a near-tip solution of the form (22), the strength of the singularity and the general form of $W(\theta)$ are just the same as for classical elasticity. The relevant elastic constant is, however, the slope of the stress-strain curve in the high strain region, G_t, since this value applies at the large stresses and strains which pertain at the crack tip. The flattening of the stress-strain curve has important consequences for the significance of dynamic effects in rapid crack propagation. Although the speed of the crack tip may be small as compared to $(G/\rho)^{\frac{1}{2}}$, it may be significant compared to $(G_t/\rho)^{\frac{1}{2}}$, and it is the latter comparison which counts. In fact, if the fracture process is essentially brittle, the magnitude of $(G_t/\rho)^{\frac{1}{2}}$ presents an upper limit for the crack propagation speed.

Next we consider small strain nonlinear elasticity which is based on a power law relation of the kind illustrated in Fig. 2(c). For proportional loading the power hardening can be used to represent elastic-plastic material behavior in what is known as the deformation theory of plasticity. For anti-plane shear deformation we have

$$G\gamma_i = \tau_i \qquad \tau \leq \tau_o \tag{28}$$

$$G\gamma_i = \left(\frac{\tau}{\tau_o}\right)^{n-1}\tau_i \qquad \tau \geq \tau_o \tag{29}$$

where $n > 1$, and τ is defined by Eqn. (25).

For a propagating crack the loading near the crack tip is not proportional; in fact there is a zone of unloading. Thus, deformation theory cannot represent plastic deformation near a rapidly propagating crack tip. Even if Eqn (29) is interpreted as a nonlinear stress-strain relation for an elastic material, it is not possible to obtain a solution of the kind given by Eqn. (22). The reason is that for $n > 1$ the slope of the stress-strain curve vanishes as $\gamma_i \to \infty$, and the characteristic wave speed becomes zero. Thus, a crack tip moving at any speed is propagating supersonically, and asymptotic solutions of the kind (22) do not apply. On the other hand, if $n < 1$ the slope of the stress-strain curve becomes unbounded as $\gamma_i \to \infty$. Consequently, the characteristic wave speed of the material becomes unbounded and dynamic effects disappear altogether for a crack tip moving at a bounded velocity.

Finally, we consider rapid crack propagation in strain hardening elastic-plastic materials characterized by J_2 flow theory and a bilinear effective stress-strain curve as shown in Fig. 2(d). For deformation in anti-plane strain the incremental stress-strain relations for loading into the plastic regime ($d\tau \geq 0$) are

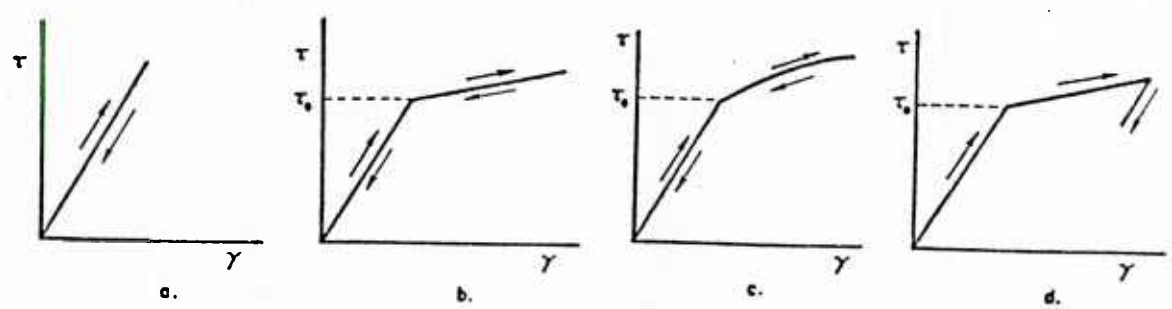

Figure 2

$$G_t \, d\gamma_i = \alpha \, d\tau_i + (1-\alpha) \, \tau^{-1} \, \tau_i \, d\tau \tag{30}$$

while for elastic unloading ($d\tau < 0$)

$$G_t \, d\gamma_i = \alpha \, d\tau_i \quad . \tag{31}$$

Here, $\alpha = G_t/G$. For the problem at hand the stress and strain increments can be replaced by the material derivatives with respect to time, as defined by Eqn. (16). We have

$$G_t \, \dot{\gamma}_i = \alpha \, \dot{\tau}_i + (1-\alpha) \, \tau^{-1} \, \tau_i \, \dot{\tau} \qquad (\dot{\tau} \geq 0) \tag{32}$$

and

$$G_t \, \dot{\gamma}_i = \alpha \, \dot{\tau}_i \qquad (\dot{\tau} \leq 0) \quad . \tag{33}$$

Some useful insight on the influence of strain hardening and unloading on the near-tip fields can be obtained on the basis of Eqns. (32) and (33) by an asymptotic analysis of the near-tip fields. This analysis is carried out in the next section, following the quasi-static treatment of Ref. [35].

Dynamic Near-Tip Fields According to J_2 Flow Theory

Analogously to Eqn. (22), we seek an asymptotically valid solution for $\dot{w}$ of the general form

$$\dot{w} = C \, v \, \dot{W}(\theta) \, r^s \quad , \tag{34}$$

where C is an amplitude factor, while $\dot{W}(\theta)$ and s are to be determined. By employing Eqn. (20), the strain rates corresponding to Eqn. (34) are obtained as

$$\dot{\gamma}_i = C \, v \, \frac{\partial}{\partial x_i} \left[\dot{W}(\theta) \, r^s \right] \qquad i = 1,2 \quad . \tag{35}$$

Now

$$\frac{\partial}{\partial x_1} = \cos\theta \, \frac{\partial}{\partial r} - \frac{\sin\theta}{r} \, \frac{\partial}{\partial \theta} \tag{36}$$

and

$$\frac{\partial}{\partial x_2} = \sin\theta \, \frac{\partial}{\partial r} + \frac{\cos\theta}{r} \, \frac{\partial}{\partial \theta} \tag{37}$$

so that Eqn. (35) yields

$$\dot{\gamma}_1 = C \, v \left[s \, \dot{W} \cos\theta - \dot{W}' \sin\theta \right] r^{s-1} \tag{38}$$

and

$$\dot{\gamma}_2 = C \, v \left[s \, \dot{W} \sin\theta + \dot{W}' \cos\theta \right] r^{s-1} \quad , \tag{39}$$

where $(\,)' = d/d\theta$. For an asymptotic analysis only the lowest orders in r need to be retained. This, in turn, means that $\partial/\partial t$ can be neglected as compared to $-v(t) \, \partial/\partial x_1$ in Eqn. (17). Thus

$$(\dot{}) \sim - \, v(t) \, \frac{\partial}{\partial x_1} \quad . \tag{40}$$

Expressions for the stress components can be written as

$$\tau_i = C\ G\ T_i\ r^s \qquad i = 1,2 \tag{41}$$

and

$$\tau = C\ G\ T\ r^s \qquad i = 1,2 \quad , \tag{42}$$

where Eqn. (25) implies

$$T = (T_1^2 + T_2^2)^{\frac{1}{2}} \quad . \tag{43}$$

We also define

$$\dot{\tau}_i = C\ G\ v\ \dot{T}_i\ r^{s-1} \tag{44}$$

and

$$\dot{\tau} = C\ G\ v\ \dot{T}\ r^{s-1} \quad . \tag{45}$$

It follows from (40) and (35) that

$$\dot{T}_i = -\ s\ T_i \cos\theta + T' \sin\theta \tag{46}$$

$$T = -\ s\ T \cos\theta + T' \sin\theta \quad . \tag{47}$$

Now, turning to the equation of motion, substitution of Eqns. (41) and (34) into (21) yields

$$s\ T_1 \cos\theta - T_1' \sin\theta + s\ T_2 \sin\theta + T_2' \cos\theta = \beta^2\ (-s\ \dot{W} \cos\theta + \dot{W}' \sin\theta) \ , \tag{48}$$

where $\beta = v/c_T$, and $c_T = (G/\rho)^{\frac{1}{2}}$. Substitution of Eqns. (38) to (45) into (32) yields

$$\alpha\ (s\ \dot{W} \cos\theta - \dot{W}' \sin\theta) = \alpha\ \dot{T}_1 + (1 - \alpha)\ T^{-1}\ T_1\ \dot{T} \tag{49}$$

and

$$\alpha\ (s\ \dot{W} \sin\theta + \dot{W}' \cos\theta) = \alpha\ \dot{T}_2 + (1 - \alpha)\ T^{-1}\ T_2\ \dot{T} \ . \tag{50}$$

The corresponding equations for elastic unloading can be obtained by extending the work of Achenbach and Bazant [36]. The solution is

$$\dot{W}_e = (1 - \beta^2 \sin^2\theta)^{s/2} \cos\ [s(\omega-\pi)] \quad , \tag{51}$$

where $\tan\omega = (1-\beta^2)^{\frac{1}{2}} \tan\theta$. In the sequel we will need $\dot{W}_e'$. This takes the form

$$\dot{W}_e' = -\ s\ \left\{\beta^2 \sin\theta \cos\theta \cos\ [s(\omega-\pi)] + (1-\beta^2)^{\frac{1}{2}} \sin\ [s(\omega-\pi)]\right\}(1-\beta^2 \sin^2\theta)^{s/2-1} \tag{52}$$

Because of antisymmetry relative to $\theta = 0$, only the domain $0 \leq \theta \leq \pi$ need be considered. The boundary conditions on the crack face and in the plane ahead of the crack tip must reflect a stress-free condition and a condition of antisymmetry, respectively. These can be expressed as

$$\dot{W} = 0 \qquad \text{on } \theta = 0 \tag{53}$$

and

$$\dot{W}_e' = 0 \qquad \text{on } \theta = \pi \quad . \tag{54}$$

As in the quasi-static solution of Ref. [35], the boundary between the loading and unloading zones surrounding the crack tip is assumed to be a radial line emanating from the crack tip at an angle $\theta = \theta_p$, see Fig. 3. The field in the loading zone $0 \leq \theta \leq \theta_p$ is governed by Eqns. (48) - (50). The solutions in the unloading zone $\theta_p \leq \theta \leq \pi$ are given by Eqns. (51) and (52).

It remains to determine the conditions at the interface $\theta = \theta_p$. One condition at $\theta = \theta_p$ is that $\dot{t}$ vanishes. This implies that $\dot{T} = 0$ or, from (47), that

$$- s\, T \cos\theta + T' \sin\theta = 0 \qquad \text{at } \theta = \theta_p \ . \tag{55}$$

In addition, the particle velocity and the stresses must be continuous. Consequently

$$[\dot{W}] = [\dot{W}'] = 0 \qquad \text{at } \theta = \theta_p \ , \tag{56}$$

where the following notation has been used

$$[\ ] = \lim_{\theta \to \theta_p^+} (\ ) - \lim_{\theta \to \theta_p^-} (\ ) \ . \tag{57}$$

The first of Eqns. (56) is automatically satisfied by writing the solution in the elastic unloading region in the form

$$\dot{W}_e = \dot{W}(\theta_p^-)\, \dot{W}_e(\theta)\, \dot{W}_e^{-1}(\theta_p) \ . \tag{58}$$

Here $\dot{W}(\theta_p^-)$ is the solution in the loading region evaluated at $\theta = \theta_p$. It then follows from continuity of $\dot{W}'$ at $\theta = \theta_p$ that

$$\dot{W}'(\theta_p^-) = \dot{W}(\theta_p^-)\, \dot{W}_e'(\theta_p)\, \dot{W}_e^{-1}(\theta_p) \ , \tag{59}$$

where $\dot{W}_e(\theta_p)$ and $\dot{W}'_e(\theta_p)$ follow from Eqns. (51) and (52). Using Eqns. (51) and (52) this can be expressed in the more convenient form

$$\dot{W}' + s \left\{ \frac{\beta^2 \sin\theta \cos\theta}{1 - \beta^2 \sin^2\theta} + \frac{(1-\beta^2)^{\frac{1}{2}}}{1 - \beta^2 \sin^2\theta} \tan\left[s(\omega - \pi)\right] \right\} \dot{W} = 0 \qquad \text{at } \theta = \theta_p \ , \tag{60}$$

where ω is evaluated at θ_p. This completes the formulation of the problem.

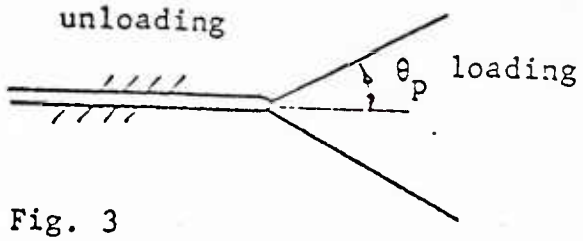

Fig. 3

Solution Procedure and Results

The problem has now been reduced to determining a solution for the plastic loading region; i.e., a solution that satisfies the field equations for the region $0 \leq \theta \leq \theta_p$ given by Eqns. (48) - (50), the boundary condition at $\theta = 0$ given by (53), and the boundary conditions at $\theta = \theta_p$ given by Eqns. (55) and (60). The quantities to be determined are $\dot{W}(\theta)$, $T_1(\theta)$, $T_2(\theta)$, θ_p, and s. This is a nonlinear eigenvalue problem which must be solved numerically.

The first step in the numerical procedure is to obtain expressions for the derivatives of the unknown functions. From Eqns. (49) and (50) we have

$$T_1' = -\dot{W}' + \alpha s \dot{W} \cos\theta + \frac{s}{\alpha} T_1 \cot\theta - \frac{1-\alpha}{\alpha} \frac{T_1 T'}{T} \tag{61}$$

and

$$T_2' = \dot{W}' \cot\theta + s\dot{W} + \frac{s}{\alpha} T_2 \cot\theta - \frac{1-\alpha}{\alpha} \frac{T_2 T'}{T} \quad , \tag{62}$$

where (47) has been used to obtain a slight simplification. Next, solving Eqn. (48) and using (61) and (62) gives

$$\dot{W}' = -\frac{\sin\theta}{1-\beta^2\sin^2\theta} \left\{ s\beta^2 \dot{W}\cos\theta - \frac{1-\alpha}{\alpha} s T_1 \cos\theta + \frac{s}{\alpha}(\alpha + \cot^2\theta) T_2 \sin\theta \right.$$
$$\left. + \frac{1-\alpha}{\alpha}(T_1 \sin\theta - T_2 \cos\theta) \frac{T'}{T} \right\} \quad . \tag{63}$$

Now, by multiplying (61) by T_1, (62) by T_2, and adding the results, making use of Eqn. (43) and the fact that $TT' = T_1T_1' + T_2T_2'$, gives

$$TT' = \alpha (T_2 \cot\theta - T_1)\dot{W}' + \alpha s (T_2 + T_1 \cot\theta)\dot{W} + s T^2 \cot\theta \quad . \tag{64}$$

By combining Eqns. (63) and (64), a recursion formula can be obtained for $\dot{W}$. This is

$$\dot{W}' = -s \left\{ T_2 + \beta^2 \dot{W} \sin\theta\cos\theta - (1-\alpha)\left(\frac{T_2\cos\theta - T_1\sin\theta}{T}\right)\left(\frac{T_2\sin\theta + T_1\cos\theta}{T}\right)\dot{W} \right\} \cdot$$
$$\cdot \left\{ 1 - \beta^2\sin^2\theta - (1-\alpha)\left(\frac{T_2\cos\theta - T_1\sin\theta}{T}\right)^2 \right\}^{-1} \quad . \tag{65}$$

The numerical procedure used is simply to replace $\dot{W}'$ by the difference formula $[\dot{W}(\theta + \Delta\theta) - \dot{W}(\theta - \Delta\theta)]/2\Delta\theta$ in Eqn. (65). Having a solution at an angle θ, $\dot{W}(\theta+\Delta\theta)$ can therefore be determined since all quantities on the right-hand side of (65) are known. To obtain T_1' and T_2', Eqn. (64) can be combined with (61) and (62) to get

$$T_1' = -\left[1 + (1-\alpha)(T_2 \cot\theta - T_1)\frac{T_1}{T^2}\right]\dot{W}' +$$
$$+ s\left[\cot\theta - (1-\alpha)(T_2 + T_1\cot\theta)\frac{T_1}{T^2}\right]\dot{W} + s T_1 \cot\theta \tag{66}$$

and

$$T_2' = \left[\cot\theta - (1-\alpha)(T_2\cot\theta - T_1)\frac{T_2}{T^2}\right]\dot{W} +$$
$$+ s\left[1 - (1-\alpha)(T_2 + T_1\cot\theta)\frac{T_2}{T^2}\right]\dot{W} + s T_2 \cot\theta \quad . \tag{67}$$

Then, replacing T_1' and T_2' by similar difference formulas, Eqns (66) and (67) can also be used as recursion relations.

In common with the numerical procedure used by Amazigo and Hutchinson [35], for given values of α and β, a trial value of s is selected and values of $\dot{W}$, T_1 and T_2 determined from Eqns. (65) to (67) as functions of θ. The

integration proceeds (with a normalization condition that $T_2(0) = 1$) until Eqn. (55) is satisfied. If Eqn. (60) is also satisfied, then θ_p has been found and the trial value of s is the correct one. If not, the estimate of s is improved and the computation repeated. In this way, the values of θ_p and s given in Tables 1 and 2, respectively, were determined[5]. These data are also shown in Figures 4 and 5. Values of the tangential stress component T_θ taken from these results are shown in Figs. 6 and 7.

TABLE 1. CALCULATED VALUES OF θ_p FOR DYNAMIC PLASTIC ANTI-PLANE SHEAR CRACK PROPAGATION

	θ_p				
α	β=0	β=0.1	β=0.25	β=0.5	β=0.75
1.0	1.571	1.576	1.602	1.690	1.786
0.7	1.522	1.528	1.554	1.643	1.731
0.5	1.473	1.478	1.505	1.595	
0.3	1.393	1.398	1.427	1.519	
0.2	1.328	1.334	1.363		
0.1	1.217	1.225	1.259		

TABLE 2. CALCULATED VALUES OF s FOR DYNAMIC PLASTIC ANTI-PLANE SHEAR CRACK PROPAGATION

	s				
α	β=0	β=0.1	β=0.25	β=0.5	β=0.75
0.1	-0.500	-0.500	-0.500	-0.500	-0.500
0.7	-0.444	-0.444	-0.442	-0.434	-0.396
0.5	-0.395	-0.394	-0.391	-0.375	
0.3	-0.325	-0.324	-0.319	-0.288	
0.2	-0.277	-0.276	-0.269		
0.1	-0.208	-0.206	-0.194		

[5] Results for $\beta = 0$ given in Tables 1 and 2 are in essential agreement with the quasi-static results given in Ref. [35]. However, it was not possible to verify the results of Ref. [35] for $\alpha < 0.1$.

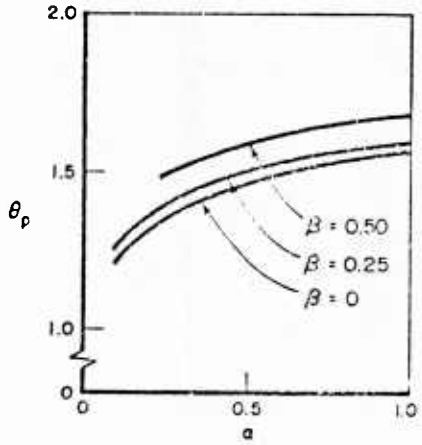

Fig. 4

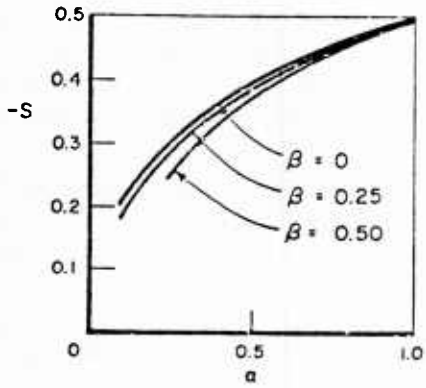

Fig. 5

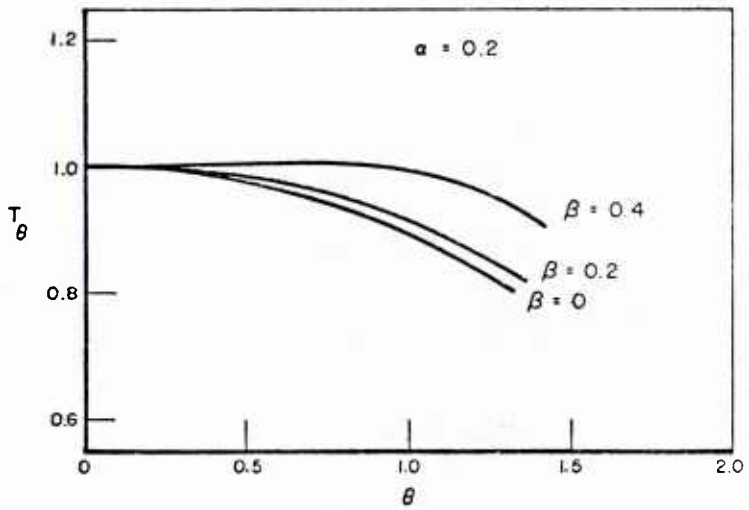

Fig. 6

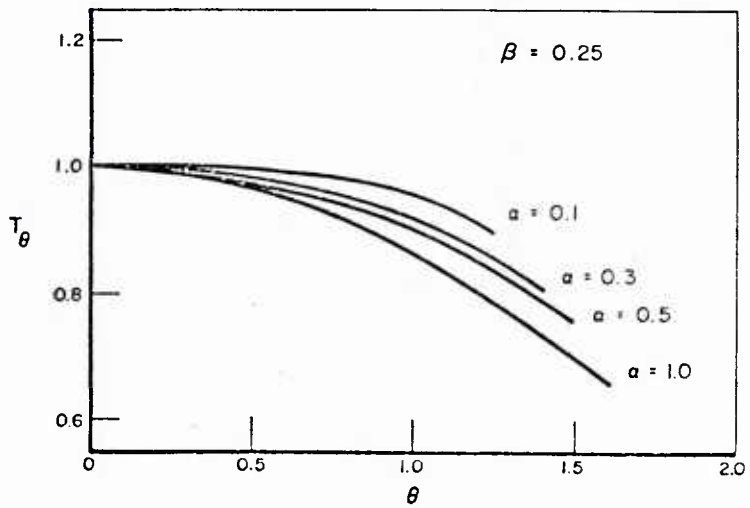

Fig. 7

DISCUSSION

There are several points that warrant further comment. First, the fact that the yield stress does not appear in the result might possibly be viewed as an inadequacy of this work. But, it is instead a natural consequence of the asymptotic analysis procedure followed here. In such an approach attention is focused exclusively on the highly deformed material at the crack tip; material that is already deformed beyond the yield point. It should also be noted that the asymptotic approach does not provide a complete description of the deformation state--it is known only to within a multiplicative factor. This factor must be determined from the interaction of the crack tip region and the material surrounding it; e.g., in a finite element analysis. In this way, the yield stress (together with the applied load and component geometry) will enter into the result. In such computations the well known effect of strain rate on yielding can then be taken into account. The effect of strain rate on the slope of the stress-strain curve beyond the yield point is less well established. However, it can be seen from the results of this paper that this effect could have a substantial influence on dynamic crack growth.

The preceding comments focus attention on a further key feature of the results. This is that the limiting speed of subsonic crack propagation is dictated by the slope of the stress-strain curve at very large strains where it likely is least accurately known. The extent to which this dominance will be mitigated by consideration of the full field is an open question at this point in the research.

Lastly, although a number of crack growth criteria for dynamic plastic fracture have been identified in this paper, it has not yet been possible to make even a tentative selection. On the basis of the success of the energy release rate parameter in both elastodynamic problems and in quasi-static plastic fracture, together with the theoretical considerations elucidated by Broberg, the energy criterion might be regarded as the leading candidate. To definitely establish the usefulness of such a criterion requires further progress in the course of research initiated in this paper. Specifically, an asymptotic solution for the Mode I case is needed. (This work is already in progress by the present authors.) Next, the asymptotic solution must be incorporated into a complete analysis; e.g., as a special crack tip finite element as in Ref. [37]. The first step is to use experimental results in conjunction with the analysis procedure so devised to appraise various candidate parameters and their formulations. This must be done in both the "generation" and "application" phases as in the quasi-static plastic fracture research described above. The present work is clearly just the first step in such a research effort.

ACKNOWLEDGMENT

This work was conducted for the Office of Naval Research, Structural Mechanics Program. The first author (J.D.A.) was supported under contract number N00014-76-C-0063, the second author (M.F.K.) under contract number N00014-77-C-0576. The authors would like to express their gratitude to Dr. Nicholas Perrone for his encouragement of their efforts in this area.

REFERENCES

1 Erdogan, F., "Crack Propagation Theories", in Fracture, ed. H. Liebowitz, Academic Press, New York, Vol. 2, 1968, pp 497-590.

2 Achenbach, J. D., "Dynamic Effects in Brittle Fracture", in Mechanics Today, ed. S. Nemat-Nasser, Pergamon, New York, Vol. 1, 1972, pp 1-57.

3 Freund, L. B., "Dynamic Crack Propagation", in The Mechanics of Fracture, ed. F. Erdogan, ASME AMD, Vol. 19, American Society of Mechanical Engineers, New York, 1975, pp 105-134.

4 Kanninen, M. F., "A Critical Appraisal of Solution Techniques in Dynamic Fracture Mechanics", in Numerical Methods in Fracture Mechanics, ed. A. R. Luxmoore and D.R.J. Owen, University College of Swansea, Swansea, U.K., 1978, pp 612-633.

5 Hahn, G. T. and Kanninen, M. F., ed., Fast Fracture and Crack Arrest, ASTM STP 627, American Society for Testing Materials, Philadelphia, 1977.

6 Hahn, G. T., Kanninen, M. F., and Rosenfield, A. R., "Fracture Toughness of Materials", in Annual Review of Materials Science, Vol. 2, 1972, pp 381-404.

7 Dugdale, D. S., "Yielding of Steel Sheets Containing Slits", Journal of the Mechanics of Physics of Solids", Vol. 8, 1960, pp 100-104.

8 Goodier, J. N. and Field, F. A., "Plastic Energy Dissipation in Crack Propagation", in Fracture of Solids, D. C. Drucker and J. J. Gilman, ed., Gordon and Breach, New York, 1963, pp 103-118.

9 Rice, J. R., "A Path Independent Integral and the Approximate Analysis of Strain Concentration by Notches and Cracks", Journal of Applied Mechanics, Vol. 35, 1968, pp 379-386.

10 Kanninen, M. F., Mukherjee, A. K., Rosenfield, A. R., and Hahn, G. T., "The Speed of Ductile Crack Propagation and the Dynamics of Flow in Metals", in Mechanical Behavior of Materials Under Dynamic Loads, ed. U.S. Lindholm, Springer-Verlag, New York, 1968, pp 96-133.

11 Kanninen, M. F., "An Estimate of the Limiting Speed of a Propagating Ductile Crack", Journal of the Mechanics and Physics of Solids, Vol. 16, 1968, pp 215-228.

12 Glennie, E. B., "A Strain-Rate Dependent Crack Model", Journal of the Mechanics and Physics of Solids, Vol. 19, 1971, pp 255-272.

13 Glennie, E. B., "The Unsteady Motion of a Rate-Dependent Crack Model", Journal of the Mechanics and Physics of Solids, Vol. 19, 1971, pp 329-338.

14 Hoagland, R. G., Rosenfield, A. R., and Hahn, G. T., "Mechanisms of Fast Fracture and Arrest in Steels", Metallurgical Transactions, Vol. 3, 1972, pp 123-136.

15 Dvorak, G. J., "Formation of Plastic Encloves at Running Brittle Cracks", International Journal of Fracture Mechanics, Vol. 7, 1971, pp 251-267.

16 Atkinson, C., "A Simple Model of a Relaxed Expanding Crack", Arkiv För Fysik, Vol. 35, 1967, pp 469-476.

17 Atkinson, C and Kanninen, M. F., "A Simple Representation of Crack Tip Plasticity: The Inclined Strip Yield Model", International Journal of Fracture, Vol. 13, 1977, pp 151-163.

18 Riedel, H., "Dynamically Loaded Cracks in Strain Rate Sensitive Materials", in Fracture 1977, ed. D.M.R. Taplin, Vol. 2, 1977, pp 553-559.

19 Belytschko, T., "A Survey of Numerical Methods and Computer Programs for Dynamic Structural Analysis", Nuclear Engineering and Design, Vol. 37, 1976, pp 23-34.

20 Ayres, D. J., "Dynamic Plastic Analysis of Ductile Fracture-The Charpy Specimen", International Journal of Fracture, Vol. 12, 1976, pp 567-578.

21 Norris, D. M., Jr., "Computer Simulation of the Charpy V-Notch Toughness Test", Report No. UCRL-79762, Lawrence Livermore Laboratory, Livermore, California, 1977.

22 Emery, A. F., Love, W. J., and Kobayashi, A. S., "Dynamic Finite Difference Analysis of an Axially Cracked Pressurized Pipe Undergoing Large Deformations", in Fast Fracture and Crack Arrest, ed. G. T. Hahn and M. F. Kanninen, ASTM STP 627, 1977, pp 142-158.

23 Ayres, D. J., "Determination of the Largest Stable Suddenly Appearing Axial and Circumferential Through Cracks in Ductile Pressurized Pipe", in Transactions of the 4th International Conference on Structural Mechanics in Reactor Technology, ed. T. A. Jaeger and B. A. Boley, Commission of the European Communities, Brussels, 1977, Paper No. F7/1.

24 Freund, L. B., Parks, D. M., and Rice, J. R., "Running Ductile Fracture in a Pressurized Line Pipe", in Mechanics of Crack Growth, ASTM STP 590, 1976, pp 243-260.

25 Wilkins, M. L., "Fracture Studies with Two- and Three-Dimensional Computer Simulation Programs", Report No. UCRL-78376, Lawrence Livermore Laboratory, Livermore, California, 1977.

26 Popelar, C., Rosenfield, A. R., and Kanninen, M. F., "Steady-State Crack Propagation in Pressurized Pipelines", Journal of Pressure Vessel Technology, Vol. 99, 1977, pp 112-121.

27 Broberg, K. B., "On Effects of Plastic Flow at Fast Crack Growth", in Fast Fracture and Crack Arrest, ed., G. T. Hahn and M. F. Kanninen, ASTM STP 627, 1977, pp 243-256.

28 Shockey, D. A., Seaman, L., and Curran, D. R., "Computation of Crack Propagation and Arrest by Simulating Microfracturing at the Crack Tip", Fast Fracture and Crack Arrest, ed. G. T. Hahn and M. F. Kanninen, ASTM STP 627, 1977, pp 274-285.

29 Marston, T. U., ed., EPRI Ductile Fracture Research Review Document, NP-701-SR, Special Report of the Electric Power Research Institute, Palo Alto, California, February, 1978.

30 Rice, J. R., "Elastic-Plastic Fracture Mechanics", in The Mechanics of Fracture, ed., F. Erdogan, ASME AMD, Vol. 19, Amerian Society of Mechanical Engineers, New York, 1975, pp 22-54.

31 Kanninen, M. F., Broek, D., Hahn, G. T., Marschall, C. W., Rybicki, E. F., and Wilkowski, G. M., "Towards an Elastic-Plastic Fracture Mechanics Predictive Capability for Reactor Piping", Nuclear Engineering and Design, in press, 1978.

32 Kanninen, M. F., Rybicki, E. F., Stonesifer, R. B., Broek, D., Rosenfield, A. R., Marschall, C. W., and Hahn, G. T., "Elastic-Plastic Fracture Mechanics for Two-Dimensional Stable Crack Growth and Instability Problems", ASTM Symposium on Elastic-Plastic Fracture, Atlanta, November 16-18, 1977. (To appear in an ASTM-STP, 1978.)

33 Rice, J. R., "An Examination of the Fracture Mechanics Energy Balance from the Point of View of Continuum Mechanics", Proceedings of the First International Conference of a Fracture, T. Yokoboro, ed, Japanese Society for Strength and Fracture, Tokyo, 1966, pp 43-60.

34 Hutchinson, J. W. and Paris, P. C., "Stability Analysis of J-Controlled Crack Growth", ASTM Symposium on Elastic-Plastic Fracture Mechanics, Atlanta, November 16-18, 1977. (To appear in an ASTM-STP, 1978.)

35 Amazigo, J. C. and Hutchinson, J. W., "Crack-Tip Fields in Steady Crack Growth with Linear Strain-Hardening", Journal of the Mechanics of Physics and Solids, Vol. 25, 1977, pp 81-97.

36 Achenbach, J. D. and Bazant, Z. P., "Elastodynamic Near-Tip Stress and Displacement Fields for Rapidly Propagating Cracks in Orthotropic Materials", Journal of Applied Mechanics, Vol. 42, 1975, pp 183-189.

37 Hilton, P. D. and Hutchinson, J. W., "Plastic Intensity Factors for Cracked Plates", Engineering Fracture Mechanics, Vol. 3, 1971, pp 435-451.

Battelle
Columbus Laboratories
505 King Avenue
Columbus, Ohio 43201
Telephone (614) 424-6424